NASA CR-72453
PWA FR-2832

DEVELOPMENT OF AN ADVANCED ANNULAR COMBUSTOR

By

J. P. RUSNAK and J. H. SHADOWEN

PRATT & WHITNEY AIRCRAFT
FLORIDA RESEARCH AND DEVELOPMENT CENTER

RECEIVED
NASA STI FACILITY
INPUT BRANCH
JUN 1969

Prepared for

National Aeronautics and Space Administration

Contract NAS3-9403

NASA Lewis Research Center
Cleveland, Ohio
J. D. Wear, Project Manager

N69-27411
(ACCESSION NUMBER)
220
(PAGES)
(NASA CR OR TMX OR AD NUMBER)
1
(THRU)
(CODE)
28
(CATEGORY)
FACILITY FORM 602

NOTICE

This report was prepared as an account of Government-sponsored work. Neither the United States, nor the National Aeronautics and Space Administration (NASA), nor any person acting on behalf of NASA:

A.) Makes any warranty or representation, expressed or implied, with respect to the accuracy, completeness, or usefulness of the information contained in this report, or that the use of any information, apparatus, method, or process disclosed in this report may not infringe privately owned rights; or

B.) Assumes any liabilities with respect to the use of, or for damages resulting from the use of, any information, apparatus, method, or process disclosed in this report.

As used above, "person acting on behalf of NASA" includes any employee or contractor of NASA, or employee of such contractor, to the extent that such employee or contractor of NASA or employee of such contractor prepares, disseminates, or provides access to any information pursuant to his employment or contract with NASA, or his employment with such contractor.

Requests for copies of this report should be referred to:

National Aeronautics and Space Administration
Scientific and Technical Information Facility
P.O. Box 33
College Park, Md. 20740

NASA CR-72453
PWA FR-2832

FINAL REPORT
FOR
DEVELOPMENT OF AN ADVANCED ANNULAR COMBUSTOR

By

J. P. RUSNAK and J. H. SHADOWEN

PRATT & WHITNEY AIRCRAFT
FLORIDA RESEARCH AND DEVELOPMENT CENTER
BOX 2691, WEST PALM BEACH, FLORIDA 33402

Prepared for
National Aeronautics and Space Administration

30 MAY 1969

Contract NAS3-9403

NASA Lewis Research Center
Cleveland, Ohio
J. D. Wear, Project Manager
Air Breathing Engines Division

PRECEDING PAGE BLANK NOT FILMED.

FOREWORD

This summary report was prepared by the Pratt & Whitney Aircraft Division of United Aircraft Corporation under Contract NAS3-9403.

The contract was administered by the Air-Breathing Engine Procurement Section of the National Aeronautics and Space Administration, Lewis Research Center, Cleveland, Ohio.

The report summarizes the technical effort that was conducted during the period 30 June 1966 through 24 April 1968.

ABSTRACT

The objective of the effort described in this report was to determine the structural durability of a full-scale advanced annular turbojet combustor using ASTM A-1 type fuel and operating at conditions typical of advanced supersonic aircraft.

A full-scale annular combustor of the ram-induction type was fabricated and subjected to a 325-hour cyclic endurance test at conditions representative of operation in a Mach 3.0 aircraft.

The combustor exhibited extensive cracking and scoop burning at the end of the test program. But these defects had no appreciable effect on combustor performance, as performance remained at a high level throughout the endurance program. Most performance goals were achieved with pressure loss values near 6% and 8%, and temperature rise variation ratio (ΔTVR) values near 1.25 and 1.22 at takeoff and cruise conditions, respectively. Combustion efficiencies approached 100% and the exit radial temperature profiles were approximately as desired.

CONTENTS

SECTION		PAGE
I	INTRODUCTION AND SUMMARY	1
	A. Introduction	1
	B. Summary	3
II	TEST APPARATUS	5
	A. Major Component Description	5
	B. Instrumentation	17
	C. Test Rig Modifications	27
III	COMBUSTOR	33
	A. Combustor Selection.	33
	B. Initial Combustor Design Modifications	33
	C. Combustor Modifications During Test	45
	D. Aerodynamic Analysis of the Model 1-1F Combustor	51
IV	TASK III - PRELIMINARY PERFORMANCE EVALUATION	59
	A. Objective	59
	B. Discussion of Testing and Results	59
	C. Summary	113
V	TASK IV - ENDURANCE TESTING	115
	A. Test Requirements	115
	B. Test Results	116
VI	CONCLUSIONS AND RECOMMENDATIONS	189
	A. Conclusions	189
	B. Recommendation	190
	APPENDIX	191

ILLUSTRATIONS

FIGURE		PAGE
1	Advanced Annular Combustor, Major Assembly, Test Rig.	6
2	Test Rig Assembly Installation at NASA Lewis Research Center (View 1).	7
3	Test Rig Assembly Installation at NASA Lewis Research Center (View 2).	7
4	Diffuser Inlet Duct Showing Inlet Dome.	8
5	Diffuser Assembly (Side View)	9
6	Diffuser Assembly (End View).	9
7	Exit Probe Shield	10
8	OD Distortion Plate After Testing	10
9	ID Distortion Plate After Testing	11
10	Schematic of Water-Cooled Exit Section.	12
11	Five-Point Total Temperature and Total Pressure Probe Head (View 1)	13
12	Five-Point Total Temperature and Total Pressure Probe Head (View 2)	13
13	Water-Cooled Exit Assembly.	14
14	Water-Cooled Exit Section with Actuator Assembly Installed	15
15	Actuator Cover.	16
16	Strut Spraybar.	16
17	Diffuser Inlet Pressure Probe	18
18	Diffuser Inlet Instrumentation Looking Downstream . . .	18
19	Chromel-Alumel Temperature Probe.	19
20	Actuator Assembly	21
21	Fuel Skid Installation.	22
22	Location of Diffuser and Combustor Instrumentation. . .	24
23	Control Panel of NASA ECRL Test Cell No. 1 (View 1).	25
24	Control Panel of NASA ECRL Test Cell No. 1 (View 2).	26
25	Location of Dowel Pins Used to Pin Rotating Drum to Actuator Shaft (Looking Downstream, Drum in Zero Degree Position)	28

ILLUSTRATIONS (Continued)

FIGURE		PAGE
26	Coupling.	28
27	Modification to Annular Traverse Drive (See Figure 26 for Coupling Detail.)	28
28	Model 1-1E Diffuser	30
29	Fuel Manifold Purge System.	31
30	Centerbody Modification A	32
31	Quench Water System Schematic	32
32	Conceptual Diffuser Streamline and Definition of Equivalent Conical Angle.	35
33	Diffuser and Combustor Pressure Distribution.	39
34	Combustor Flow Area Distribution.	40
35	Experience Curve of Diffuser Area Ratio vs Equivalent Conical Angle.	43
36	Flow Area to Weight Flow Ratio vs Diffuser Length . . .	44
37	Combustor Assembly Model 1-1A (View 1).	45
38	Combustor Assembly Model 1-1A (View 2).	46
39	Combustor Assembly Model 1-1A (View 3).	46
40	Advanced Annular Combustor Model 1-1B	47
41	Modification to Alternate No. 5 Scoops, OD Liner Combustor Model 1-1B.	47
42	Advanced Annular Combustor Model 1-1C	48
43	Modification to Scoop No. 5, OD Secondary Liner, Model 1-1C.	48
44	Model 1-1E Combustor.	49
45	Dome Modification, Model 1-1E	50
46	Model 1-1F Combustor.	51
47	Flow Area to Weight Flow Ratio vs Diffuser Length . . .	53
48	Model 1-1A Combustor and Diffuser Assembly.	60
49	Average Radial Pressure Profile at Diffuser Inlet . . .	60
50	Combustor Average Radial Exit Profile, Test No. 28. . .	62
51	Diffuser Inlet Velocity Head Profile, Test No. 48 . . .	63
52	Diffuser Inlet Velocity Head Profile, Test No. 52 . . .	63
53	Combustor Average Radial Exit Temperature Profile, Test No. 61	64

ILLUSTRATIONS (Continued)

FIGURE		PAGE
54	Advanced Annular Combustor, Model 1-1B.	65
55	Modifications to Alternate No. 5 Scoops - OD Liner Combustor Model 1-1B.	65
56	Diffuser Inlet Velocity Head Profile, Test No. 69 . . .	67
57	Diffuser Inlet Velocity Head Profile, Test No. 71 . . .	67
58	Combustor Dome Thermocouple Locations	70
59	Combustor Skin Temperature vs Fuel/Air Ratio.	70
60	Skin Temperature vs Diffuser Inlet Temperature.	71
61	Diffuser Inlet Velocity Head Profile, Test No. 95 . . .	71
62	Combustor Average Radial Exit Temperature Profile, Test No. 97	72
63	Combustor Average Radial Exit Temperature Profile, Test No. 72	72
64	Combustor Average Radial Exit Temperature Profile, Test No. 127.	73
65	Combustor Outlet Temperature Distribution, Test No. 159.	77
66	Combustor Outlet Temperature Distribution, Test No. 28	78
67	Combustor Average Radial Exit Temperature Profile, Test No. 159.	79
68	Combustor Outlet Temperature Distribution, Test No. 160.	80
69	Combustor Average Radial Exit Temperature Profile, Test No. 160.	81
70	Combustor Outlet Temperature Distribution, Test No. 167.	82
71	Combustor Outlet Temperature Distribution, Test No. 168.	83
72	ID Liner After Testing, View 1.	84
73	ID Liner After Testing, View 2.	84
74	ID Liner After Testing, View 3.	85
75	Model 1-1E Diffuser	87
76	Combustor Outlet Temperature Distribution, Test No. 173.	88

ILLUSTRATIONS (Continued)

FIGURE		PAGE
77	Combustor Average Radial Exit Temperature Profile, Test No. 173.	89
78	Model 1-1E Combustor, View 1.	89
79	Model 1-1E Combustor, View 2.	90
80	Combustor Outlet Temperature Distribution, Test No. 179.	91
81	Combustor Average Radial Exit Temperature Profile, Test No. 179.	92
82	Combustor Outlet Temperature Distribution, Test No. 180.	93
83	Combustor Dome Thermocouple Location and Test Results	94
84	Model 1-1F Combustor.	96
85	Combustor Outlet Temperature Distribution, Test No. 190.	97
86	Combustor Average Radial Exit Temperature Profile, Test No. 190.	98
87	Combustor Outlet Temperature Distribution, Test No. 191.	100
88	Combustor Outlet Temperature Distribution, Test No. 192.	101
89	Combustor Average Radial Exit Temperature Profile, Test No. 191.	102
90	Combustor Average Radial Exit Temperature Profile, Test No. 192.	103
91	Model 1-1F Combustor After Testing (View 1)	104
92	Model 1-1F Combustor After Testing (View 2)	104
93	Combustor Outlet Temperature Distribution, Test No. 197.	106
94	Combustor Average Radial Exit Temperature Profile, Test No. 197.	107
95	Combustor Outlet Temperature Distribution, Test No. 198.	108
96	Combustor Average Radial Exit Temperature Profile, Test No. 198.	109
97	Combustor Outlet Temperature Distribution, Test No. 199.	110

ILLUSTRATIONS (Continued)

FIGURE		PAGE
98	Combustor Average Radial Exit Temperature Profile, Test No. 199.	111
99	Model 1-1F Combustor After Testing (View 3)	112
100	Model 1-1F Combustor After Testing (View 4)	112
101	Combustion Time	116
102	ΔTVR vs Combustor Time.	117
103	Combustion Efficiency and Combustor Pressure Loss vs Combustor Time	117
104	Combustor Outlet Temperature Distribution, Test No. 250.	118
105	Combustor Outlet Temperature Distribution, Test No. 208.	119
106	Combustor Average Radial Exit Temperature Profile, Test No. 250.	120
107	Combustor Average Radial Exit Temperature Profile, Test No. 208.	120
108	Combustor Outlet Temperature Distribution, Test No. 207.	122
109	Combustor Outlet Temperature Distribution, Test No. 252.	123
110	Combustor Average Radial Exit Temperature Profile, Test No. 207.	124
111	Combustor Average Radial Exit Temperature Profile, Test No. 252.	124
112	Combustor After Test Condition 1 (View 1)	125
113	Combustor After Test Condition 1 (View 2)	125
114	Combustor After Test Condition 1 (View 3)	126
115	Combustor Outlet Temperature Distribution, Test No. 254.	127
116	Combustor Outlet Temperature Distribution, Test No. 273.	128
117	Combustor Outlet Temperature Distribution, Test No. 294.	129
118	Combustor Outlet Temperature Distribution, Test No. 315.	130
119	Combustor Outlet Temperature Distribution, Test No. 337.	131
120	Combustor Outlet Temperature Distribution, Test No. 357.	132

ILLUSTRATIONS (Continued)

FIGURE		PAGE
121	Combustor Average Radial Exit Temperature Profile. . .	133
122	Combustor Average Radial Exit Temperature Profile. . .	133
123	Combustor Average Radial Exit Temperature Profile. . .	134
124	Combustor Average Radial Exit Temperature Profile. . .	134
125	Combustor Average Radial Exit Temperature Profile. . .	135
126	Combustor Average Radial Exit Temperature Profile. . .	135
127	Combustor Outlet Temperature Distribution, Test No. 361	137
128	Combustor Average Radial Exit Temperature Profile, Test No. 361	138
129	Combustor After 40 Hours Testing at Test Condition 2 (View 1)	138
130	Combustor After 40 Hours Testing at Test Condition 2 (View 2)	139
131	Combustor After 40 Hours Testing at Test Condition 2 (View 3)	139
132	No. 1 Scoop Cap Broken Loose	140
133	Burned No. 3 ID Liner Scoop.	140
134	Combustor After 100 Hours of Condition 2 Testing . . .	141
135	Combustor Outlet Temperature Distribution, Test No. 370	142
136	Combustor Outlet Temperature Distribition, Test No. 391	143
137	Combustor Outlet Temperature Distribution, Test No. 406	144
138	Combustor Average Radial Exit Temperature Profile, Test No. 370	145
139	Combustor Average Radial Exit Temperature Profile, Test No. 391	145
140	Combustor Average Radial Exit Temperature Profile, Test No. 406	146
141	Inlet Velocity Head Profile, Test No. 370.	147
142	Inlet Velocity Head Profile, Test No. 391.	147
143	Inlet Velocity Head Profile, Test No. 370.	148
144	Inlet Velocity Head Profile, Test No. 391.	148

ILLUSTRATIONS (Continued)

FIGURE		PAGE
145	Combustor Outlet Temperature Distribution, Test No. 409.	150
146	OD Liner No. 1 Scoop Cap Missing.	151
147	OD Liner No. 5 Scoop Cap Missing.	151
148	OD Liner No. 4 and 5 Scoop Cap Missing.	152
149	Largest Combustor Crack After Condition 3 Testing . . .	152
150	Combustor After Condition 3 Testing (View 1).	153
151	Combustor After Condition 3 Testing (View 2).	153
152	Rotating Drum Cooling Water Leak.	154
153	Damaged Exit Probe.	154
154	Combustor Outlet Temperature Distribution, Test No. 411.	156
155	Combustor Outlet Temperature Distribition, Test No. 434.	157
156	Combustor Outlet Temperature Distribution, Test No. 454.	158
157	Combustor Outlet Temperature Distribution, Test No. 478.	159
158	Combustor Outlet Temperature Distribution, Test No. 498.	160
159	Combustor Outlet Temperature Distribution, Test No. 521.	161
160	Combustor Outlet Temperature Distribution, Test No. 542.	162
161	Combustor Outlet Temperatue Distribution, Test No. 563.	163
162	Combustor Outlet Temperature Distribution, Test No. 574.	164
163	Combustor Average Radial Exit Temperature Profile, Test No. 411.	165
164	Combustor Average Radial Exit Temperature Profile, Test No. 434.	165
165	Combustor Average Radial Exit Temperature Profile, Test No. 454.	166
166	Combustor Average Radial Exit Temperature Profile, Test No. 478.	166

ILLUSTRATIONS (Continued)

FIGURE		PAGE
167	Combustor Average Radial Exit Temperature Profile, Test No. 498.	167
168	Combustor Average Radial Exit Temperature Profile, Test No. 521.	167
169	Combustor Average Radial Exit Temperature Profile, Test No. 542.	168
170	Combustor Average Radial Exit Temperature Profile, Test No. 563.	168
171	Combustor Average Radial Exit Temperature Profile Test No. 574.	169
172	Burner Outlet Temperature Distribution, Test No. 578.	170
173	Two No. 5 Scoop Caps Missing.	171
174	No. 5 Scoop Cap Missing	171
175	Burned No. 3 Scoops (View 1).	172
176	Burned No. 3 Scoops (View 2).	172
177	Burned No. 3 Scoops (View 3).	173
178	Combustor After 98 Hours of Condition 4 Testing (View 1).	173
179	Combustor After 98 Hours of Condition 4 Testing (View 2).	174
180	Combustor After 98 Hours of Condition 4 Testing (View 3).	174
181	Missing Scoop Caps.	175
182	Combustor Crack Schematic Before Condition 4 Testing	176
183	Combustor Crack Schematic After 45 Hours of Condition 4 Testing	177
184	Combustor Crack Schematic After 98 Hours of Condition 4 Testing	178
185	Combustor Crack Schematic After 150 Hours of Condition 4 Testing	179
186	ID Primary Liner After Test Program Completion (View 1).	180
187	ID Primary Liner After Test Program Completion (View 2).	180

FIGURE		PAGE
188	ID Primary Liner After Test Program Completion (View 3)	181
189	ID Primary Liner After Test Program Completion (View 4)	181
190	ID Primary Liner After Test Program Completion (View 5)	182
191	ID Primary Liner After Test Program Completion (View 6)	182
192	ID Primary Liner After Test Program Completion (View 7)	183
193	ID Primary Liner After Test Program Completion (View 8)	183
194	ID Primary Liner After Test Program Completion (View 9)	184
195	OD Liner After Test Program Completion (View 1)	184
196	OD Liner After Test Program Completion (View 2)	185
197	ID Transition Liner After Test Program Completion	185
198	OD Transition Liner After Test Program Completion	186
199	Firewall After Test Program Completion	186
200	Diffuser After Test Program Completion	187
201	Water-Cooled Exit Assembly After Test Program Completion	187
202	Igniter Plugs After Test Program Completion	188
203	Exit Probe Shield After Test Program Completion	188
204	Fuel Struts and Swirlers After Test Program Completion	188
205	Combustion Model-Main Burner	195

TABLES

TABLE		PAGE
1	Task IV - Endurance Test Conditions.	2
2	Flow Areas for the Advanced Annular Combustor, Model 1-1A	41
3	Dome Flow Passage Areas.	52
4	Advanced Annular Combustor, Task III Test Summary.	61
5	Flow Areas for the Advanced Annular Combustor, Model 1-1B	66
6	Flow Areas for the Advanced Annular Combustor, Model 1-1C	69
7	Flow Areas for the Advanced Annular Combustor, Model 1-1D	74
8	Flow Areas for the Advanced Annular Combustor, Model 1-1E	86
9	Flow Areas for the Advanced Annular Combustor, Model 1-1F	95
10	Task IV - Endurance Test Conditions.	115
11	Nomenclature	192

SECTION I
INTRODUCTION AND SUMMARY

A. INTRODUCTION

This report summarizes the work conducted under Contract NAS3-9403 for the Development of an Advanced Annular Combustor. It covers the entire program from 1 June 1966 through 24 April 1968. The program consisted of the design and fabrication of an advanced annular combustor and test rig and the conduct of long-duration tests at operating conditions typical of advanced supersonic aircraft.

To meet these requirements, a modified version of the P&WA ram-induction combustor design of the first experimental supersonic transport engine, the JTF17, was selected. A considerable amount of rig and engine testing had been performed on this type combustor prior to the beginning of the program. These test results indicated that the combustor was ready for durability testing.

The program consisted of four tasks:

Task I - Rig Design, Fabrication, Installation, and Combustor Selection

Task II - Combustor Design, Fabrication, and Installation

Task III - Preliminary Performance Evaluation

Task IV - Endurance Testing

Tasks III and IV were conducted at the NASA Lewis Research Center at Cleveland, Ohio.

Several problems encountered during the preliminary performance evaluation resulted in a reduction of the original endurance program. The problems encountered included front firewall overheating, ID primary liner scoop burning, and diffuser stall. Five modifications were made to the original combustor before these problems were corrected and endurance testing could begin. The endurance program was reduced from 510 to 325 hours to provide the additional developmental testing required for elimination of these problems.

Endurance testing was subsequently conducted at the test conditions shown in table 1.

Table 1. Task IV - Endurance Test Conditions

TEST CONDITION	INLET TOTAL PRESSURE, (psia)	INLET TOTAL TEMP. (^{o}F)	OUTLET AVERAGE TOTAL TEMP. (^{o}F)	REFERENCE VELOCITY, (ft/sec)
1	60±2	1050±15	1900±25	150±5
2	60±2	1050±15	2200±25	140±5
3	90±2	1150±15	1900±25	160±5
4	90±2	1150±15	2200±25	150±5
5	90±2	600±15	1900±25	108±5
6	90±2	600±15	2200±25	100±5

Combustor Test Conditions 1, 2, 3, and 4 were tested in sequence for 35, 100, 30, and 150 hours, respectively. Before the start of Test Condition 1, and after the completion of Test Conditions 1, 2, 3, and 4, the combustor was run for one hour at Test Condition 5 and for one hour at Test Condition 6.

The combustor was operated in a cyclic manner, with four steps, as follows:

1. Increase combustor exit temperature to the specified test condition within 10 seconds after ignition.
2. Maintain the specified test conditions for 1 hour.
3. Reduce fuel flow to zero within a 10-second interval.
4. Wait a minimum of 5 minutes before commencing the next operating cycle.

Detailed discussions of the program are in the following sections:

Section II - General description including design and analysis of the test rig

Section III - General description of combustor design and modifications

Section IV - Preliminary performance evaluation

Section V - Endurance testing

B. SUMMARY

A full-scale ram-induction type annular combustor was designed, fabricated, and subjected to endurance testing at simulated flight conditions of a supersonic aircraft.

A total of 26.8 hours of testing, involving 5 modifications to the combustor (including 1 diffuser modification), was accomplished during the preliminary performance evaluation. The final configuration, Model 1-1F, was endurance tested for a total of 325 hours.

Most of the performance goals were accomplished with an overall combustor pressure loss of less than 6% at takeoff and 8% at the cruise conditions. Combustor efficiency approached 100% (within instrumentation accuracy), and the exit radial temperature profile very closely matched the desired profile at the cruise conditions and was acceptable at the takeoff conditions.

The overall combustor appearance was fair at the end of the endurance testing. An extensive number of cracks had developed and a number of scoops were slightly to severely burned, but no deterioration in combustor performance resulted from these deficiencies.

SECTION II
TEST APPARATUS

A. MAJOR COMPONENT DESCRIPTION

The purpose of this section is to explain the function of the major test rig components and to describe these components through the use of photographs and drawings. A test rig assembly drawing identifying the major components is shown in figure 1. The test rig assembly installed in the NASA Lewis Research Center is shown in figures 2 and 3.

All rig ducting was designed to the 1965 ASME Boiler and Pressure Vessel Code, Section VIII, for a maximum pressure of 150 psi and at working metal temperatures in accordance with contract requirements.

The major test rig components are identified in the following paragraphs.

1. Inlet Adapter Assembly

The inlet adapter was designed to mate the test rig to the existing 54-inch flange on the air supply line in the NASA Lewis Research Center ECRL Test Cell No. 1.

2. Inlet Spool Section Assembly

The inlet spool section was designed as a small easily removable section to allow access to the inlet of the test section. The test section can be rolled forward into the area normally occupied by the spool section to provide access to the combustor and test section exit.

3. Diffuser Inlet Duct and Inlet Dome Section

These sections (figure 4) were designed to provide an undistorted accelerating airstream to the diffuser inlet. Ten total temperature probes were located circumferentially around the section and 9 inches from the face of the inlet flange. Data from 8 of these probes were used in the combustor computer performance program; one was used for the ΔT abort system, and one for monitoring diffuser inlet temperature in the control room. The dome section was designed for easy removal to gain access to internal instrumentation.

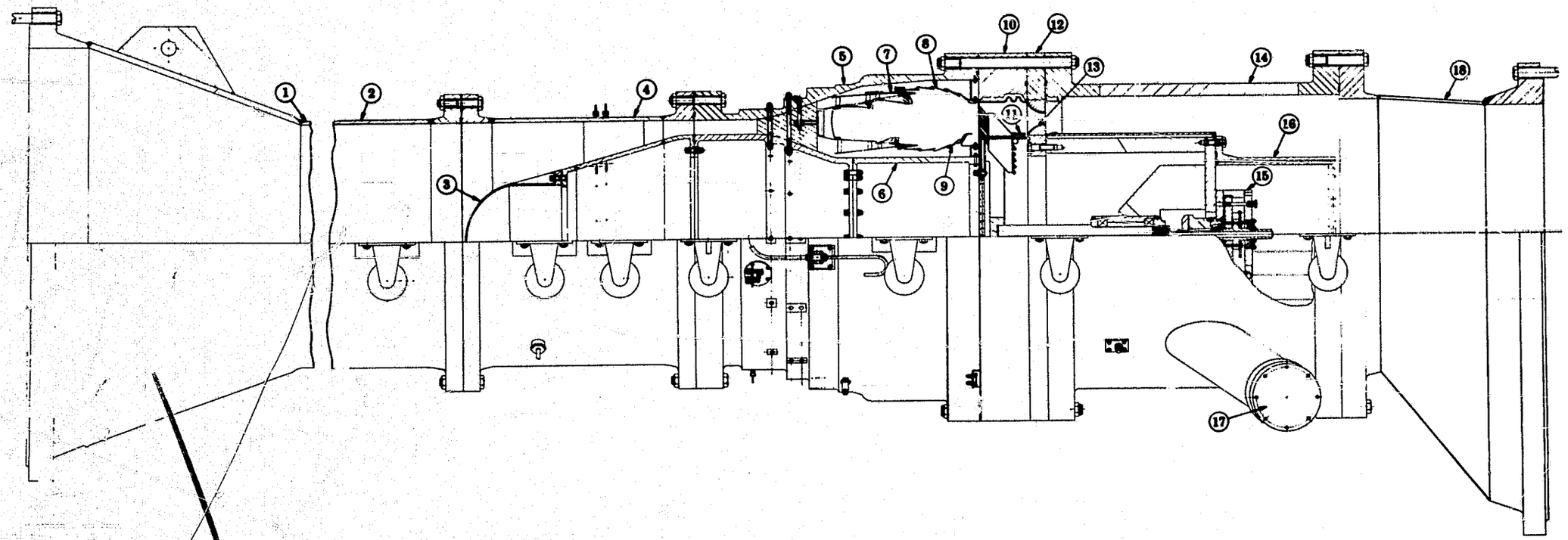

Item	Part Name
1.	Inlet Adapter Assembly
2.	Inlet Spool Section Assembly
3.	Dome Assembly
4.	Diffuser Inlet Duct Assembly
5.	Diffuser Assembly
6.	Inner Burner Case
7.	Combustor
8.	OD Transition Liner
9.	ID Transition Liner
10.	Water-Cooled Spacer
11.	5-Point Probe Traverse Assembly
12.	OD Nozzle
13.	ID Nozzle
14.	Water-Cooled Exit Assembly
15.	Actuator Assembly
16.	Actuator Cover Assembly
17.	Water-Cooled Strut Flange
18.	Exit Adapter Assembly

FD 24683

Figure 1. Advanced Annular Combustor, Major Assembly, Test Rig

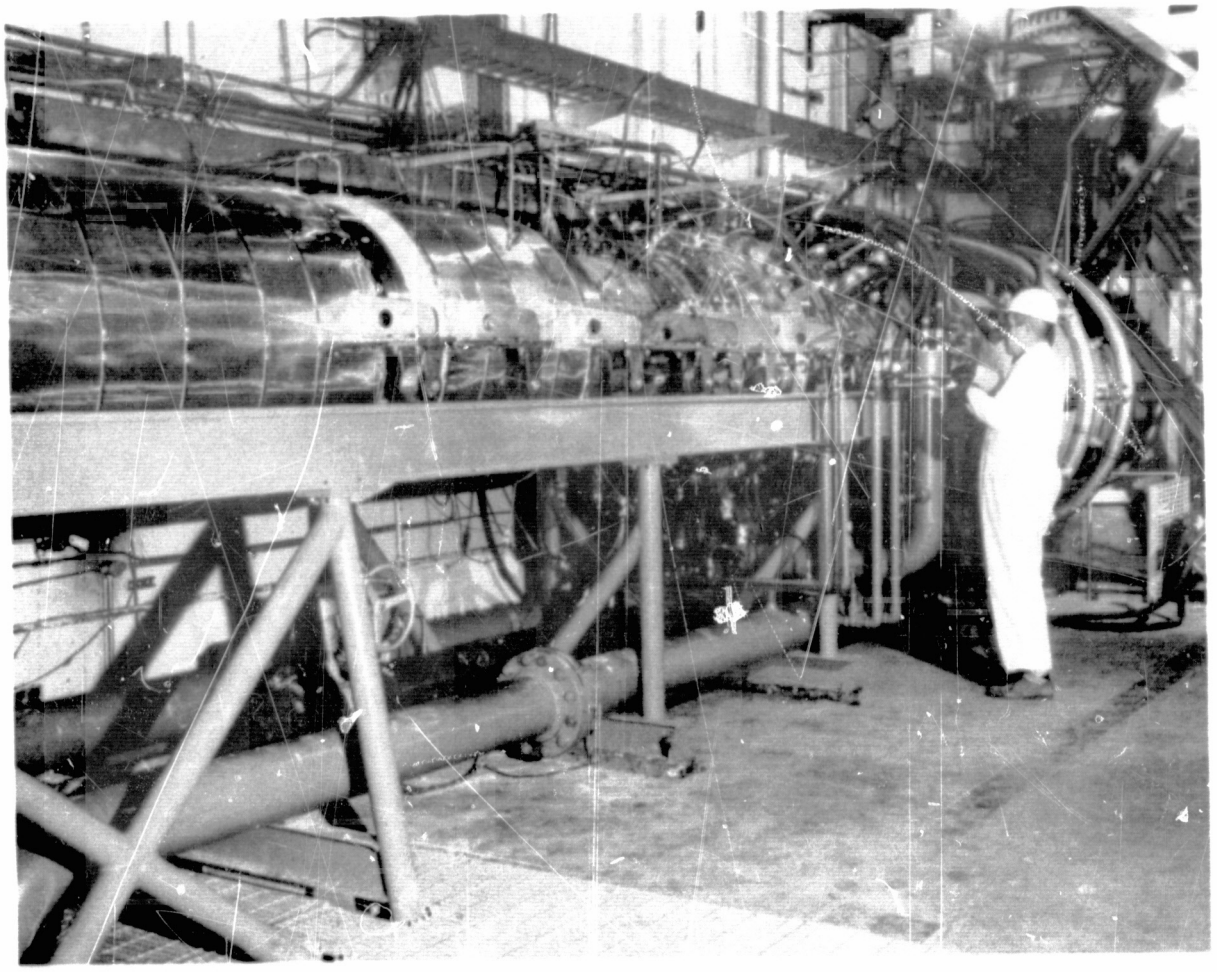

Figure 2. Test Rig Assembly Installation at NASA Lewis Research Center (View 1)

NASA C-67-1762

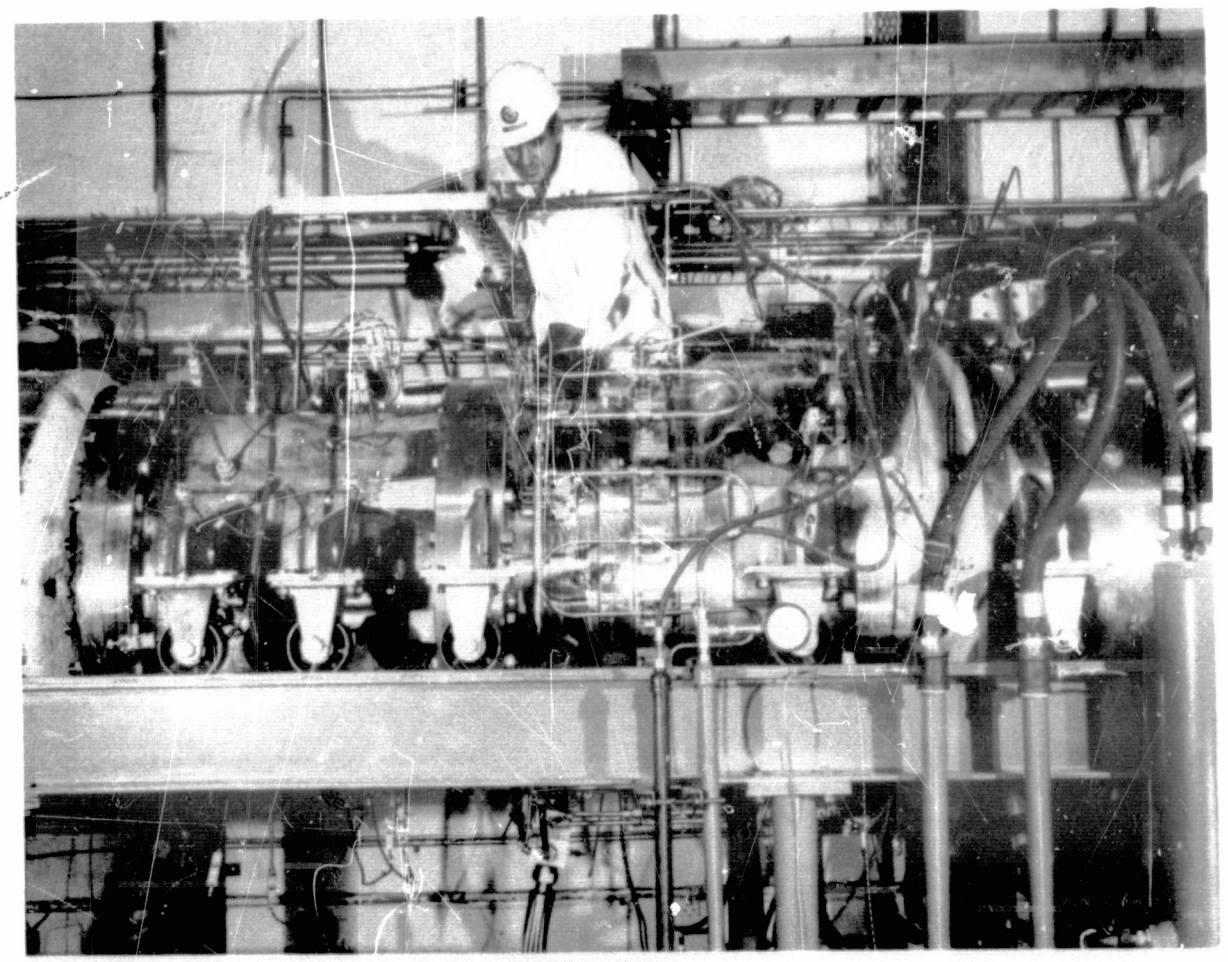

Figure 3. Test Rig Assembly Installation at NASA Lewis Research Center (View 2)

NASA C-67-1761

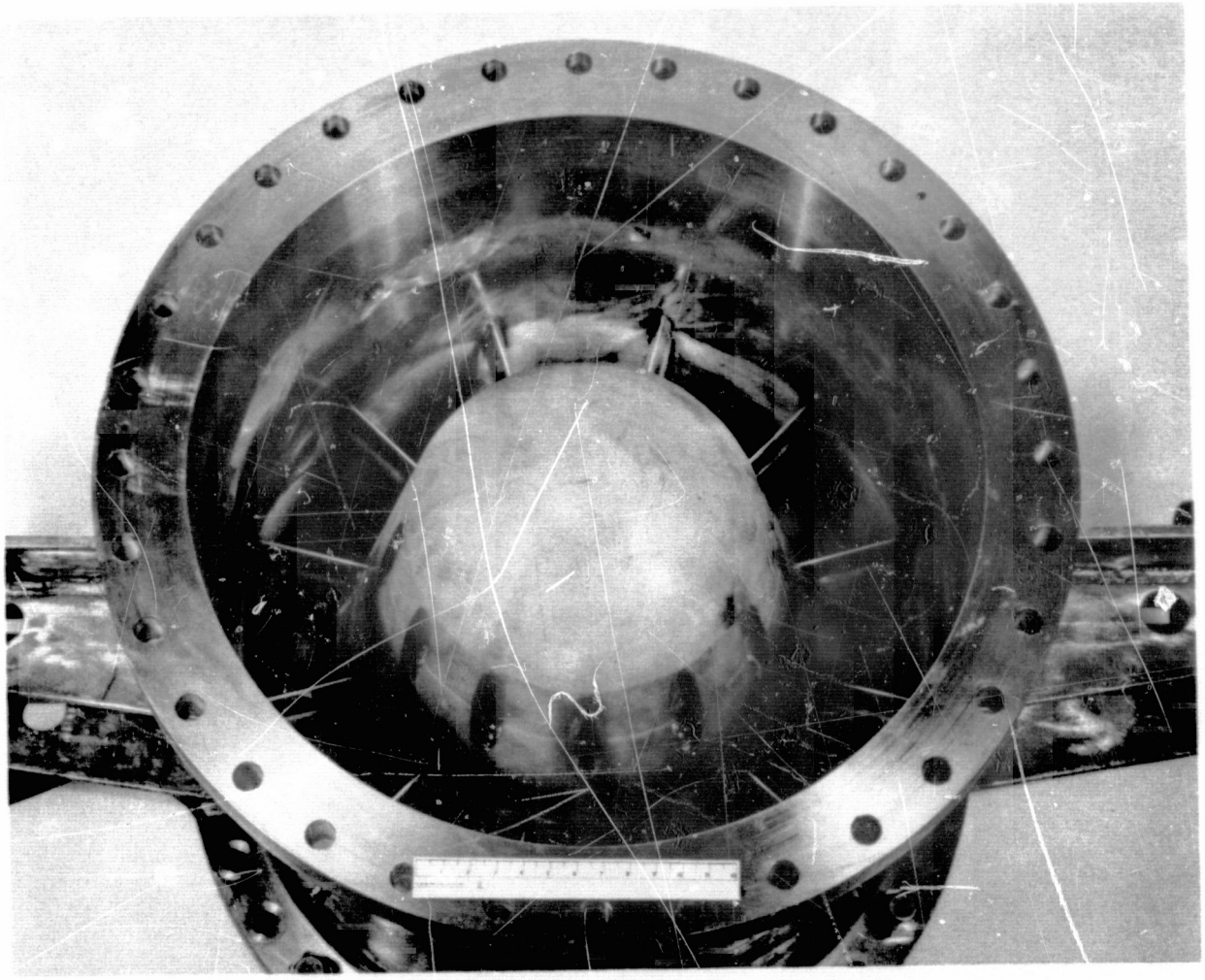

Figure 4. Diffuser Inlet Duct Showing Inlet Dome

FE 67667

4. Diffuser, Combustor Cases and Distortion Plates

The diffuser case (figures 5 and 6) was designed with inlet flow-path dimensions identical to those of the compressor discharge annulus of the Pratt & Whitney Aircraft JTF17A-20 Turbofan Engine. The outer combustor case was made integral with the diffuser to avoid the massive flanges required to comply with the ASME Boiler and Pressure Vessel Code. The cylindrical inner combustor case, which is subjected to a very small pressure load, was bolted to a light flange at the diffuser exit. Sixteen static pressure taps (8 on the OD and 8 on the ID) and 8 total pressure probes (each containing 5 pressure pickups) were located in the diffuser inlet in a plane simulating the trailing edge of the compressor exit guide vane. Three water-cooled probe shields (figure 7) were located in the rear flange of the outer combustor case. These sheltered the exit probe heads from the combustor exhaust during the testing period when data were not being taken.

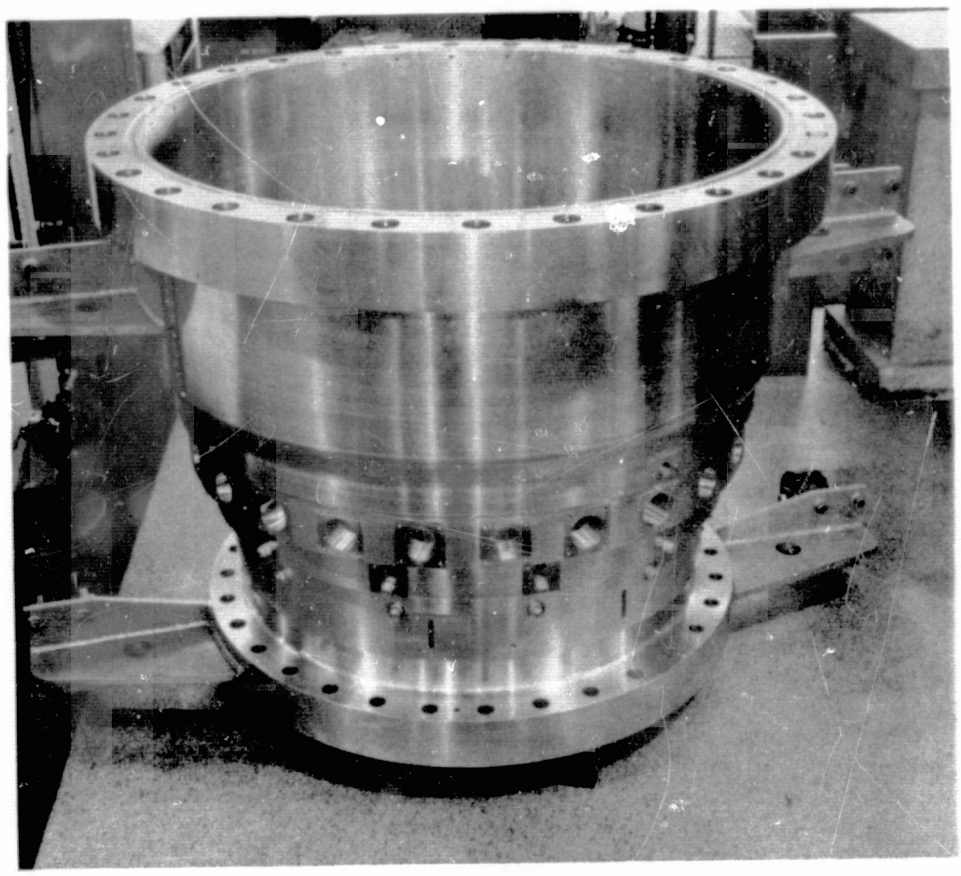

Figure 5. Diffuser Assembly (Side View) FE 66778

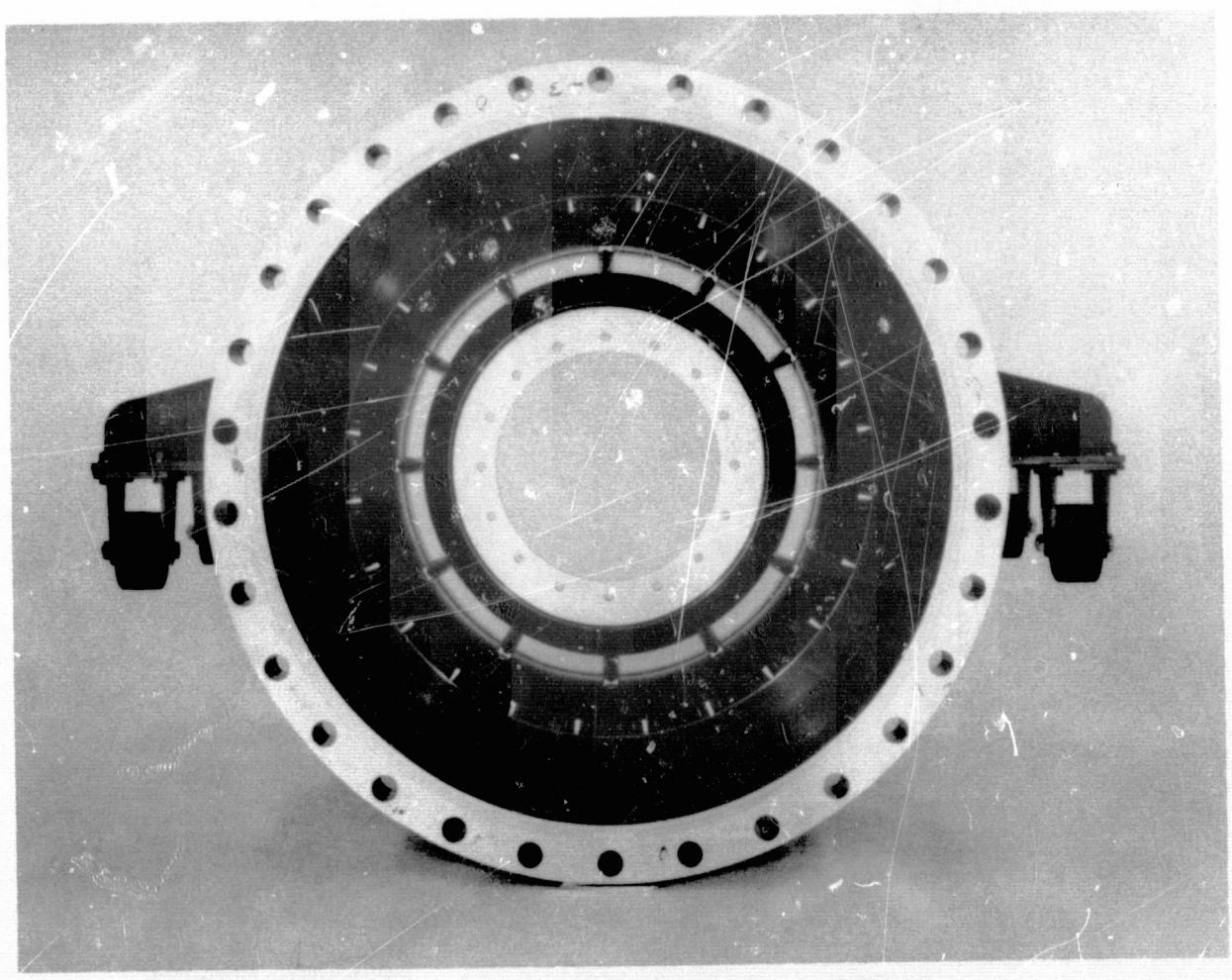

Figure 6. Diffuser Assembly (End View) FE 67032

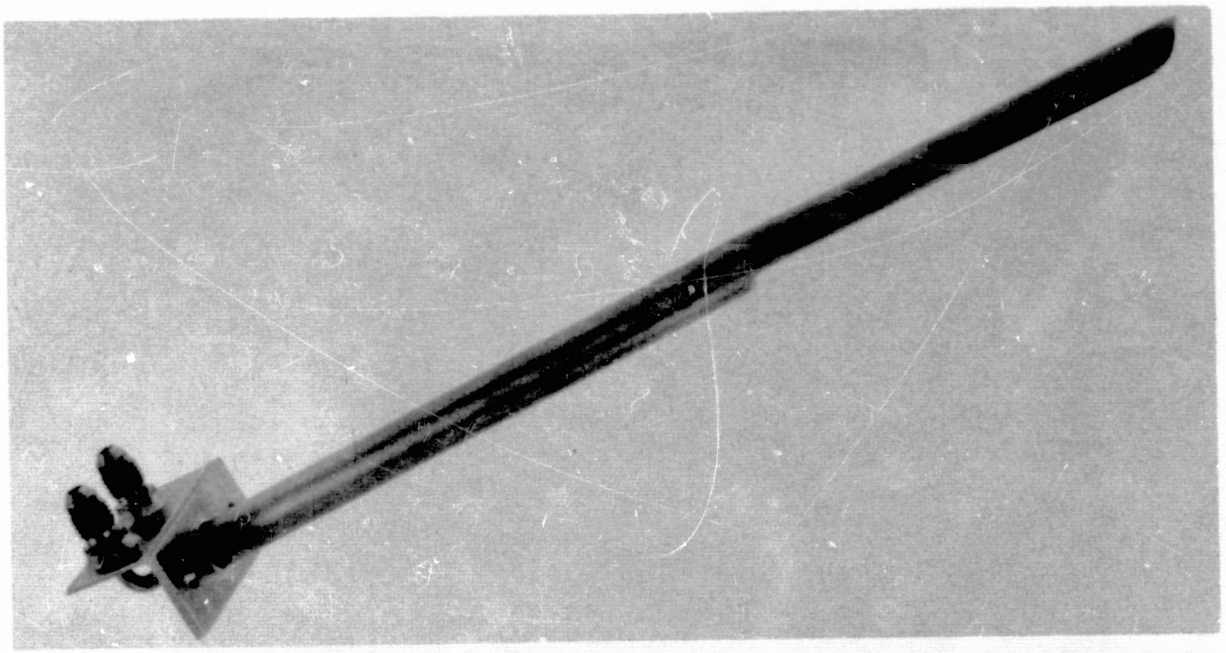

Figure 7. Exit Probe Shield FE 67680

The distortion plates (figures 8 and 9) were designed to restrict portions of the airflow to simulate the compressor exit velocity profile of the JTF17A-20 Pratt & Whitney Aircraft Turbofan Engine. These were installed between the diffuser inlet duct and diffuser case flanges.

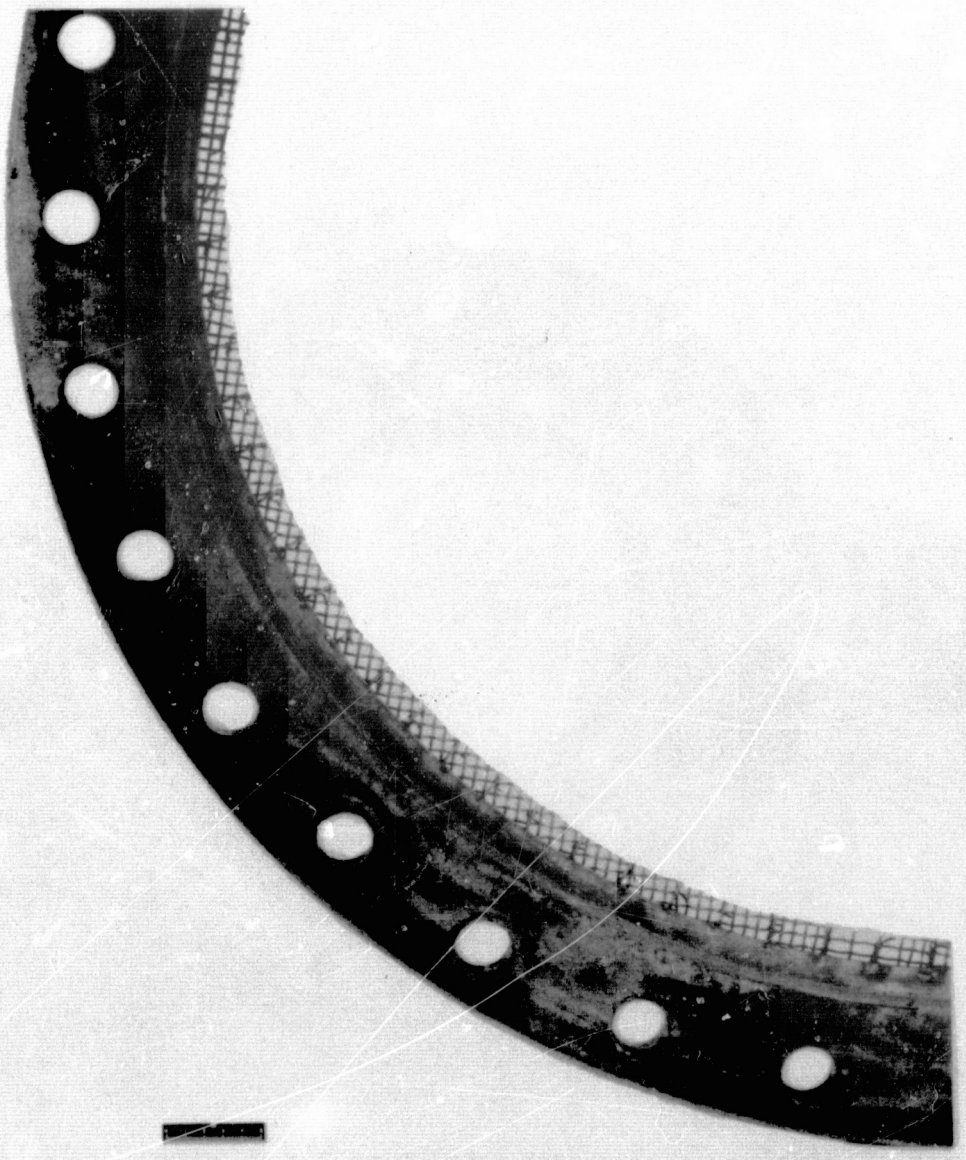

Figure 8. OD Distortion Plate After Testing NASA C-67-2648

Figure 9. ID Distortion Plate After Testing

NASA C-67-2649

5. Water-Cooled Exit Section (figure 10)

The water-cooled exit section contains the following test rig components: nozzle OD section, nozzle ID section, spacer, inspection plate, rotating drum, three thermocouple-total pressure probes, shaft, actuator, actuator cover, and the water-cooled exit assembly.

In accordance with contract requirements, three 5-point thermocouple and total pressure probe heads (figures 11 and 12), located 120 degrees apart and each traversing 120 degrees, were located in a plane simulating the leading edge of the first-stage turbine stator vane. The thermocouples were of the aspirating type with Pt 13% Rh - Pt inserts. A heat exchanger was provided on each probe to cool the aspiration gas before ducting it outside the rig in flexible hose.

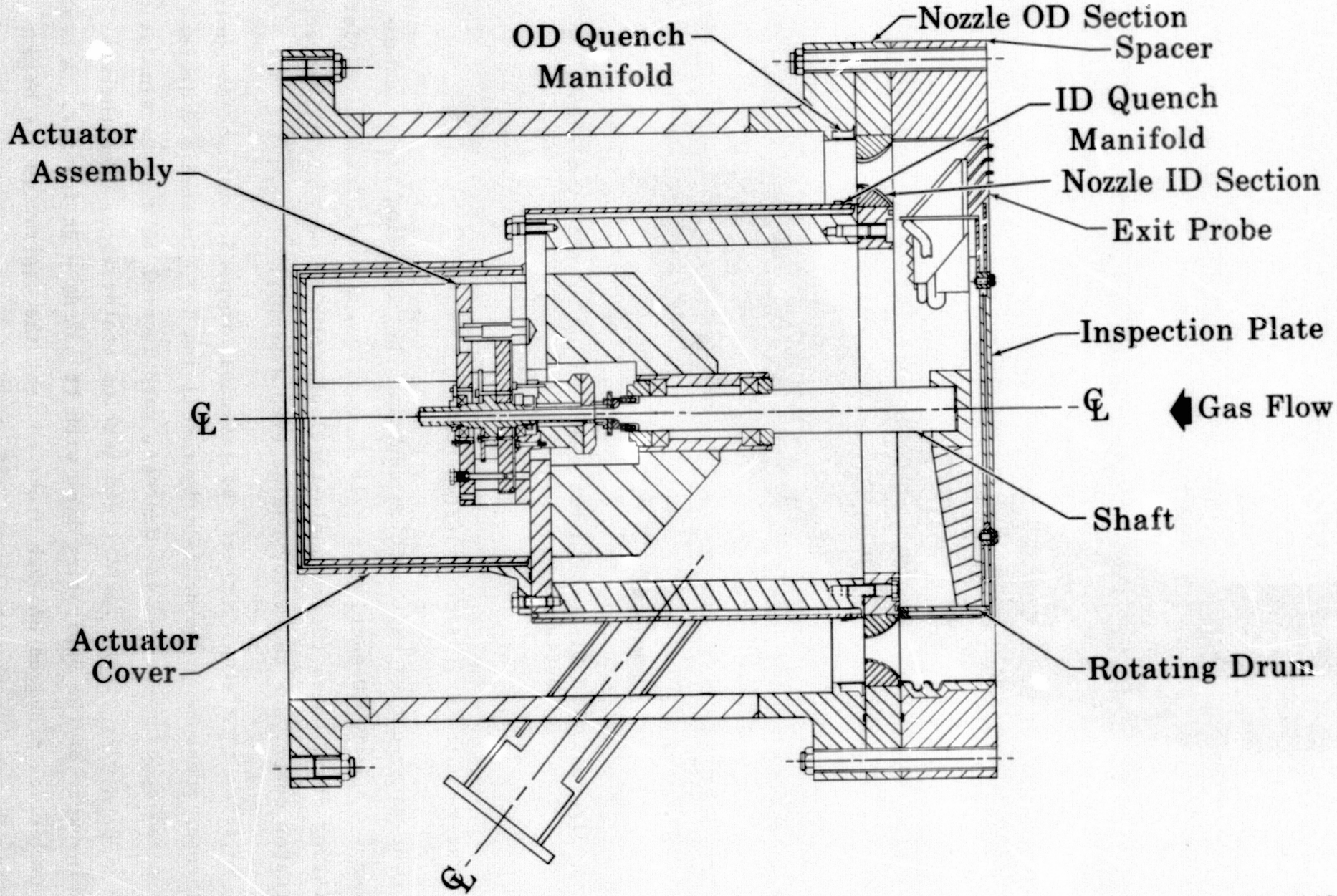

Figure 10. Schematic of Water-Cooled Exit Section

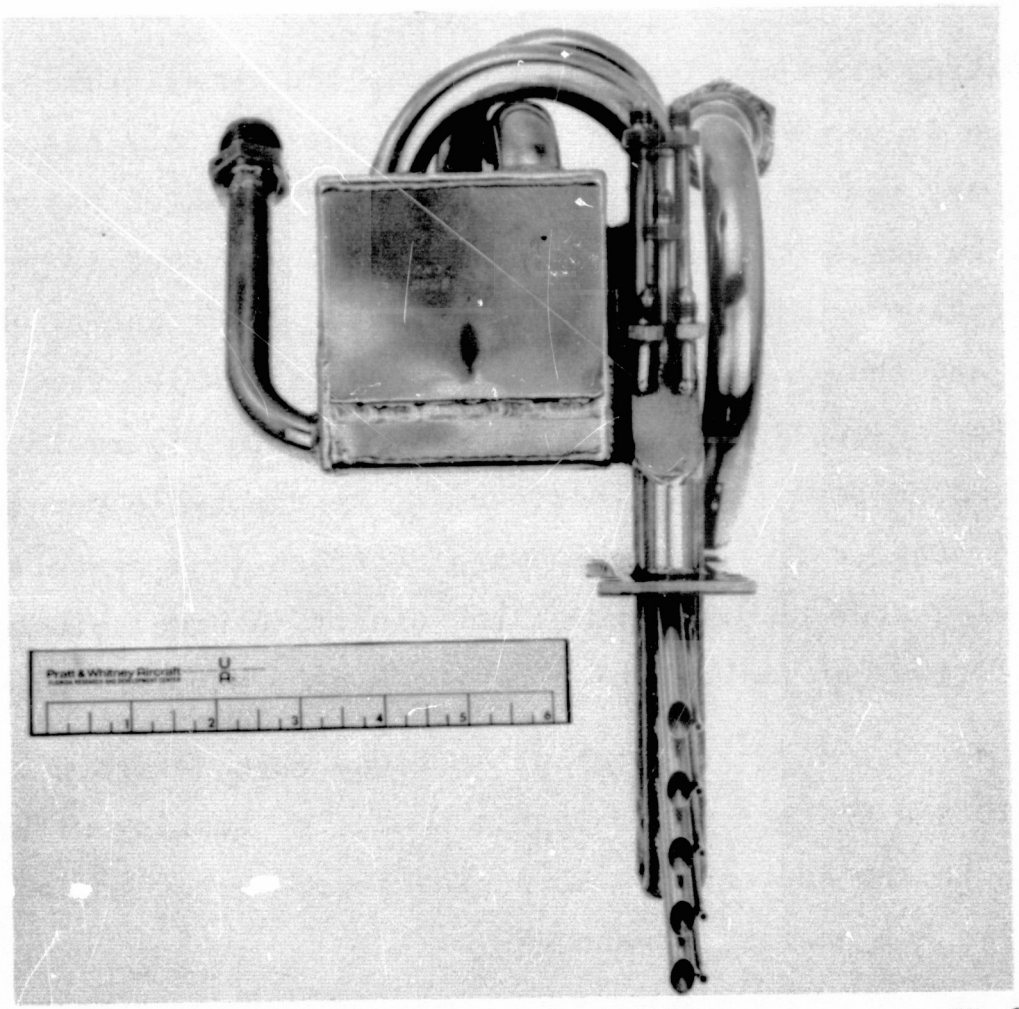

Figure 11. Five-Point Total Temperature and Total Pressure Probe Head (View 1)

FE 68347

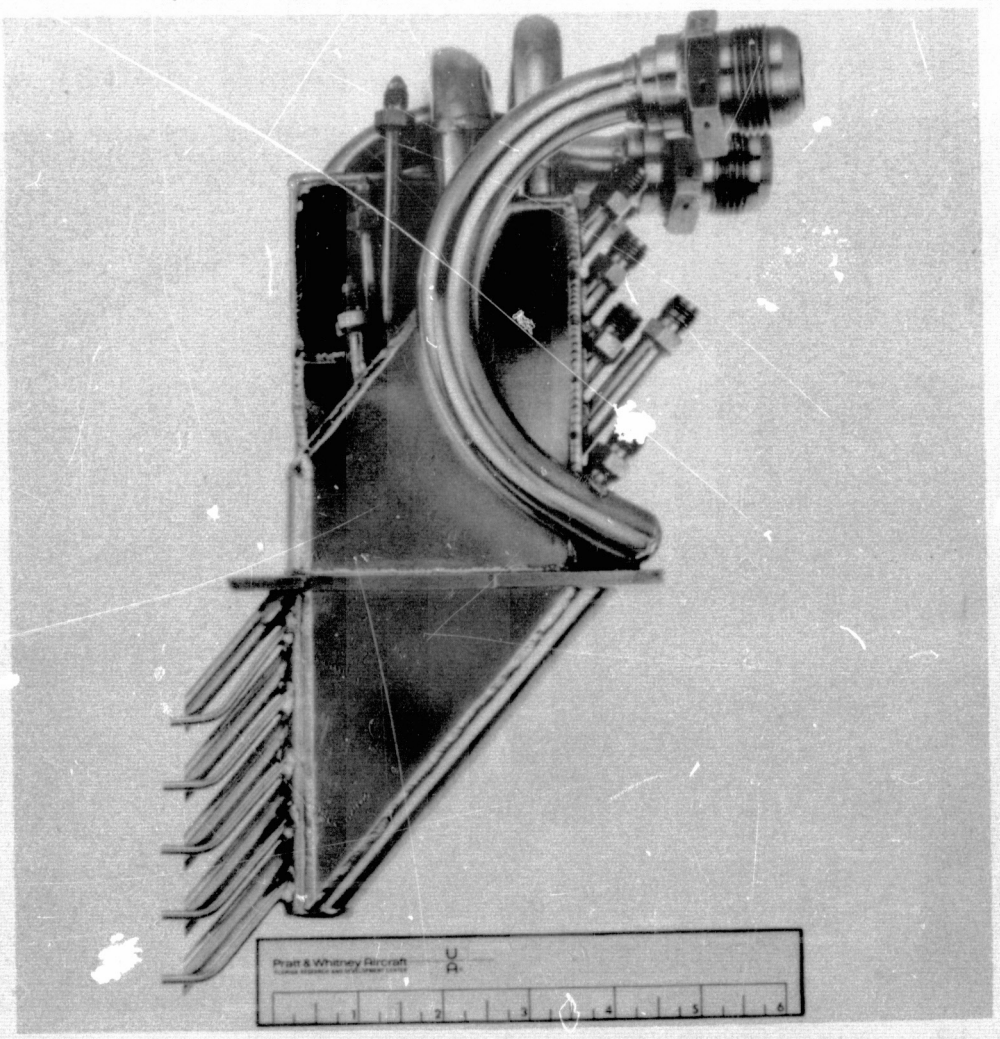

Figure 12. Five-Point Total Temperature and Total Pressure Probe Head (View 2)

FE 68346

The rotating drum was designed to house the three probes and was supported and driven by a shaft coupled to the actuator assembly. An inspection port was provided in the rotating drum which was covered by the inspection plate during testing. The port was used to provide access to the internal plumbing and instrumentation. The rotating drum, inspection plate, and the three exit probes were water-cooled through internal plumbing. The assembly of these parts is shown in figure 13. The nozzle ID section and OD section were designed to be removable and to obtain sonic flow at this station in accordance with contract requirements. The nozzle ID section was water-cooled through the use of internal plumbing and the nozzle OD section was water-cooled by the use of external plumbing.

The nozzle ID and OD replacement sections were designed to replace the nozzle ID and OD section to enable combustor testing without a flow constriction in the exit duct. Both pieces were water-cooled in the same manner as the nozzle components.

The spacer was water-cooled and was used to mate the diffuser outer case, nozzle OD section, and water-cooled exit assembly. This provided room for the rotating drum and probes on the ID of the exit section. The ID liner of the spacer was corrugated to allow for thermal expansion.

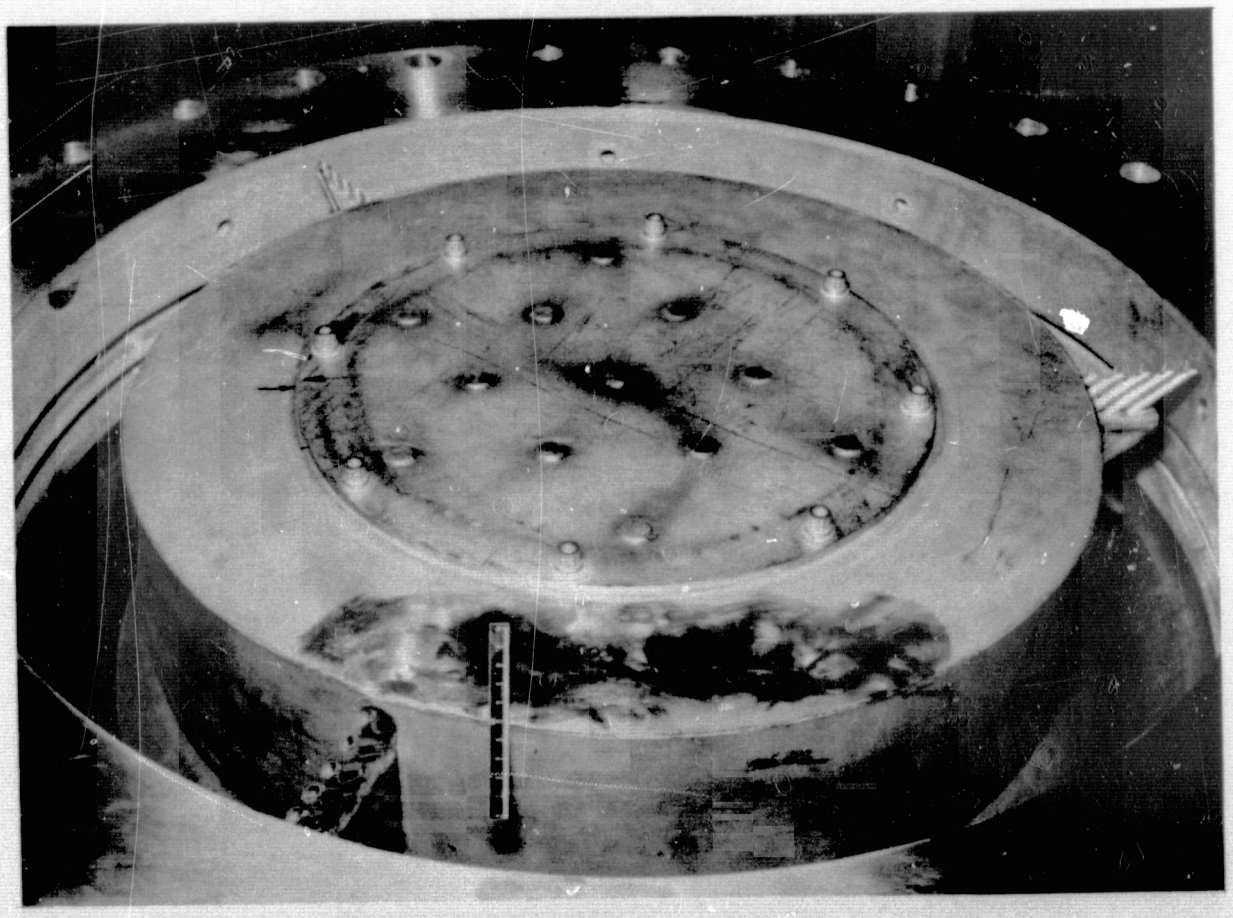

Figure 13. Water-Cooled Exit Assembly FE 69297

The quench water system used to cool the combustor exhaust gases was incorporated into the water-cooled exit assembly. Water was sprayed into the airstream through a series of holes around an annulus on both the ID and OD walls. The center section of the exit assembly is supported by four struts. These struts were also used for flowing the quench water to the ID wall and as passageways for internal plumbing, instrumentation, and actuator control cables. This section housed the bearings which mount the rotating drum support shaft. The traverse actuator engages the rotating drum support shaft through a spline located behind the shaft bearings. The actuator assembly is installed as shown in figure 14.

A water-cooled cover was used to protect the actuator assembly during testing. The actuator cover is shown in figure 15.

Four radial spraybars (figure 16), one located just upstream of each support strut, were provided to ensure adequate quench water flow in the vicinity of each support strut.

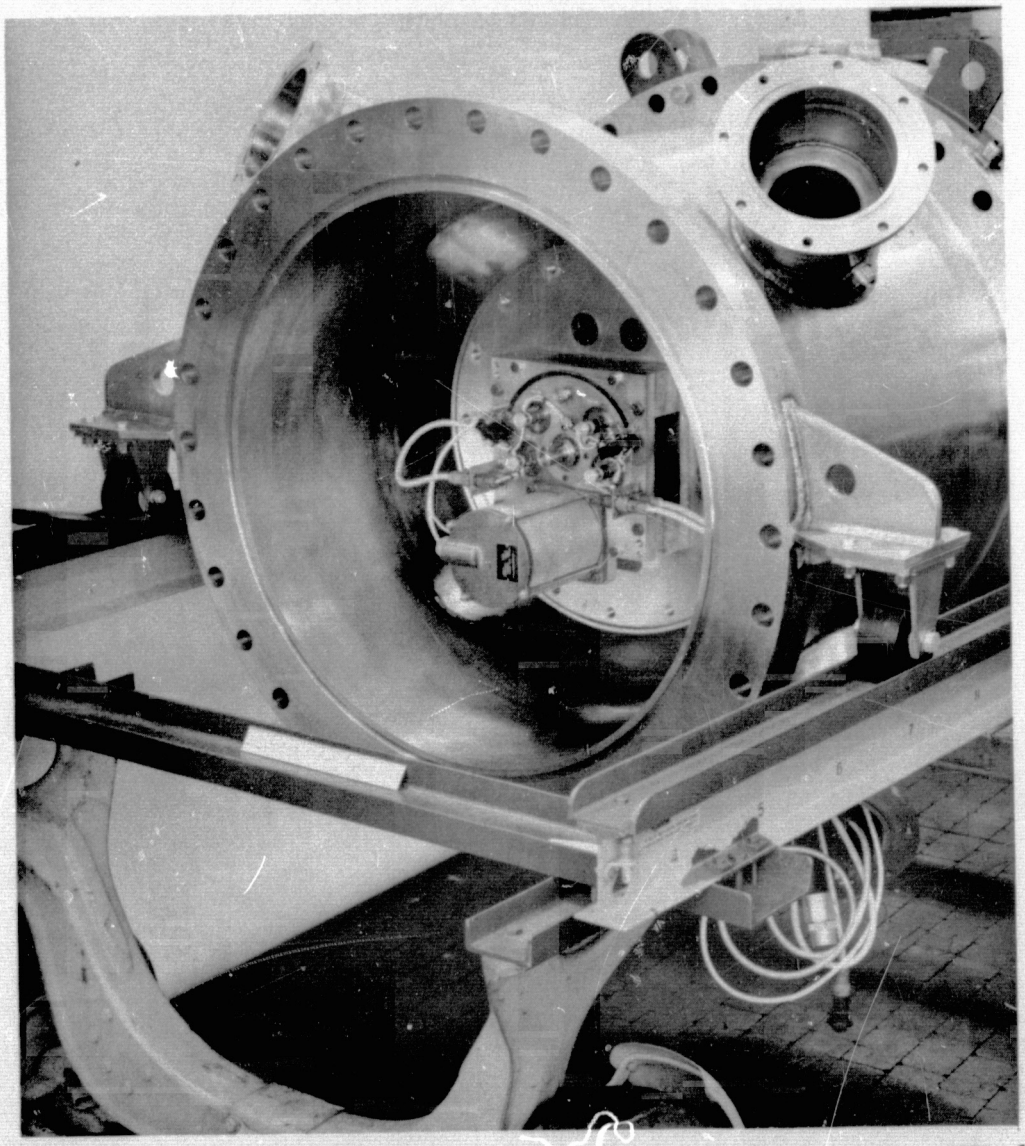

Figure 14. Water-Cooled Exit Section with Actuator Assembly Installed

FE 67665

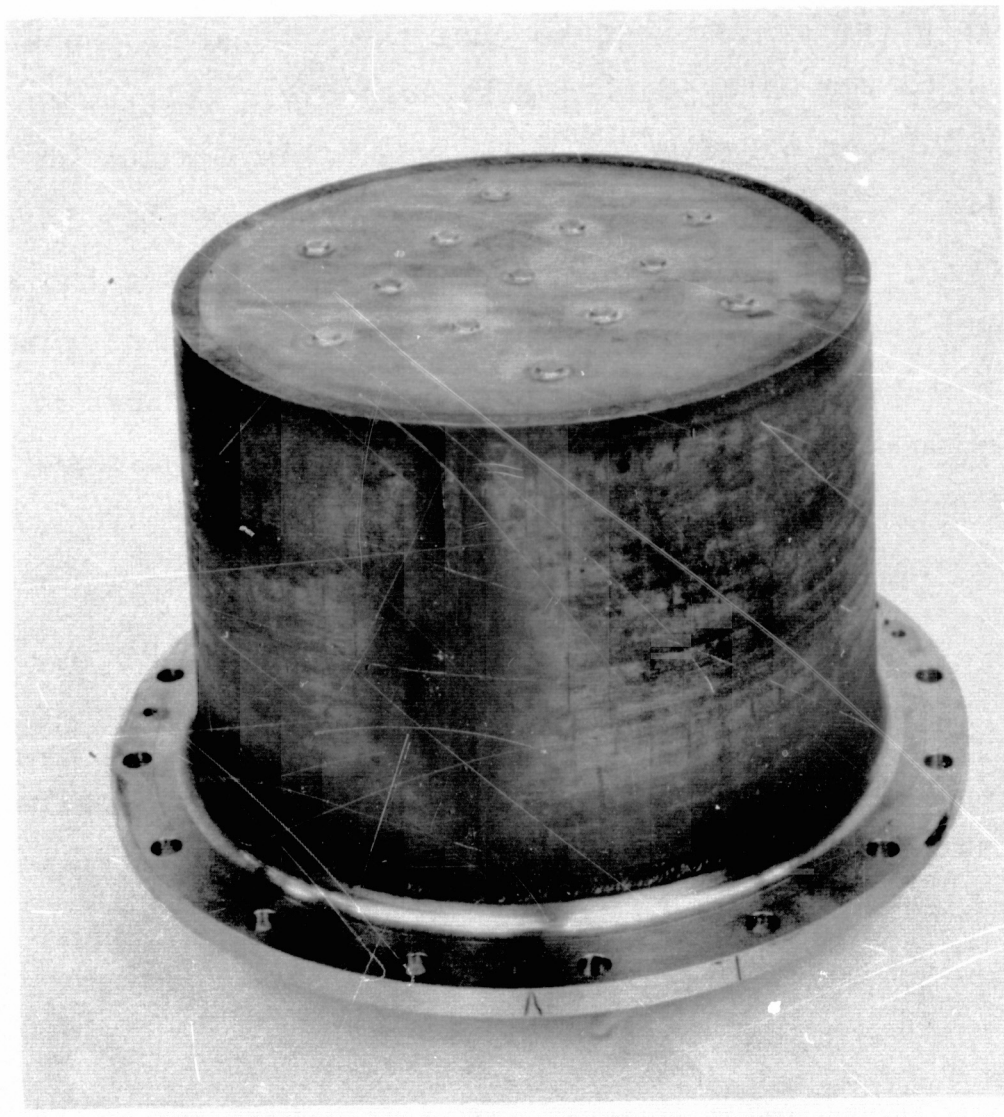

Figure 15. Actuator Cover FE 67769

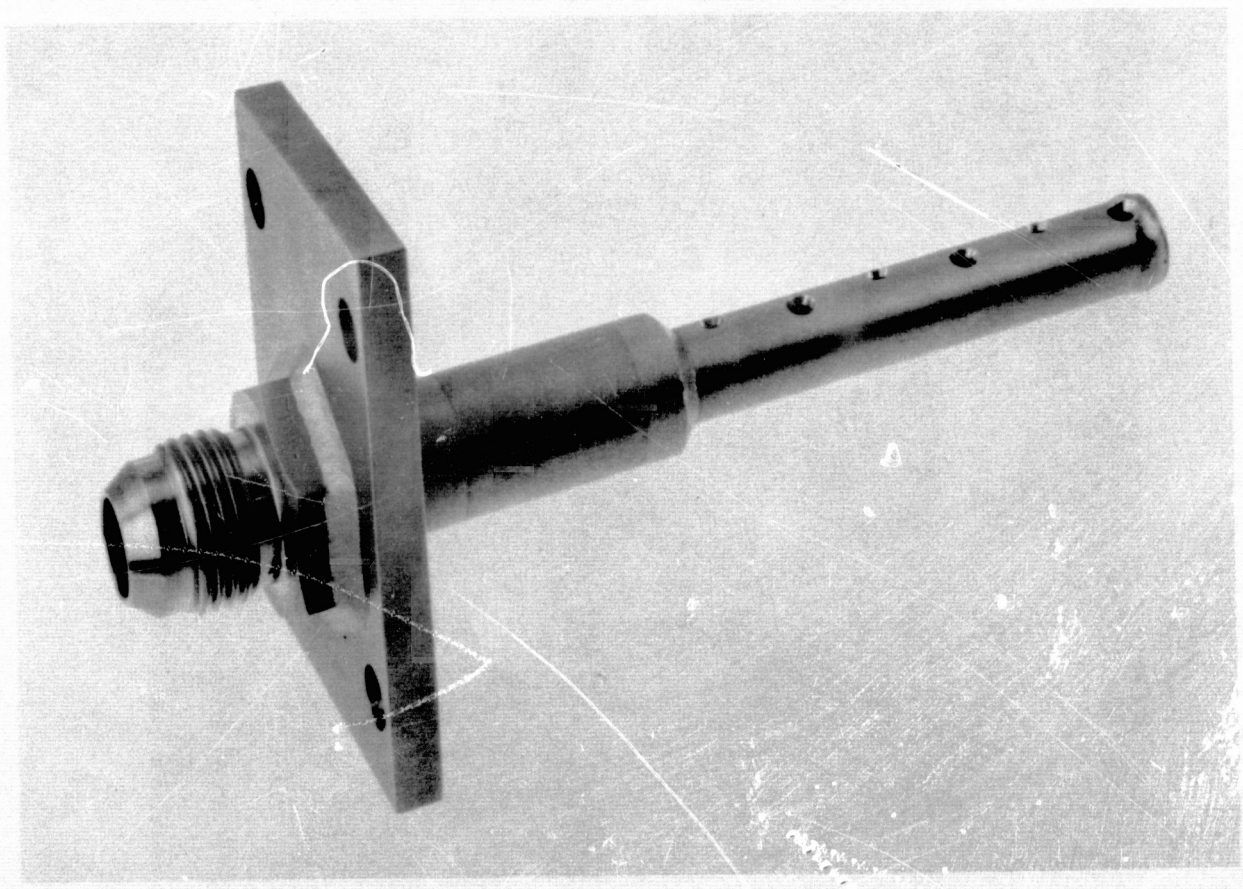

Figure 16. Strut Spraybar FE 67678

6. Exit Adapter

The exit adapter was designed to mate the test rig to the 54-inch flange of the exhaust ducting in the NASA Lewis Research Center ECRL Test Cell No. 1.

B. INSTRUMENTATION

Instrumentation was provided to monitor the following parameters: airflow; fuel flow; combustor inlet and exit total pressure and static pressure; combustor inlet and exit total temperature; fuel pressure; combustor liner and dome metal temperature at various locations; and fuel temperature.

The purpose of this section is to describe the instrumentation used to monitor and record the above parameters.

1. Airflow

The combustor airflow was measured by a sharp edged orifice fabricated to the ASME specifications. The orifice diameter is 17.875 inches and has an orifice diameter-to-pipe inner diameter ratio of 0.5069. The orifice is located in the rig ducting with 35 feet of straight pipe upstream of the orifice and 10 feet of straight pipe downstream of the orifice. The orifice upstream and downstream pressure was measured by flange taps and was recorded on the NASA DAMPR-CADDE system. The orifice temperature was measured by Iron Constantan (type J) thermocouples and is recorded on the NASA AVD-CADDE system.

2. Combustor Inlet Instrumentation

At the combustor inlet, the airflow total pressure, static pressure, and total temperature were sampled.

The combustor inlet total pressure was measured by eight 5-point rakes, figure 17, located circumferentially as shown in figure 18. The sampling probes on each rake were spaced so that each samples an equal area of the inlet. The data from each probe were recorded on the NASA DAMPR-CADDE system.

Two probes were monitored in the control room for setting the test point.

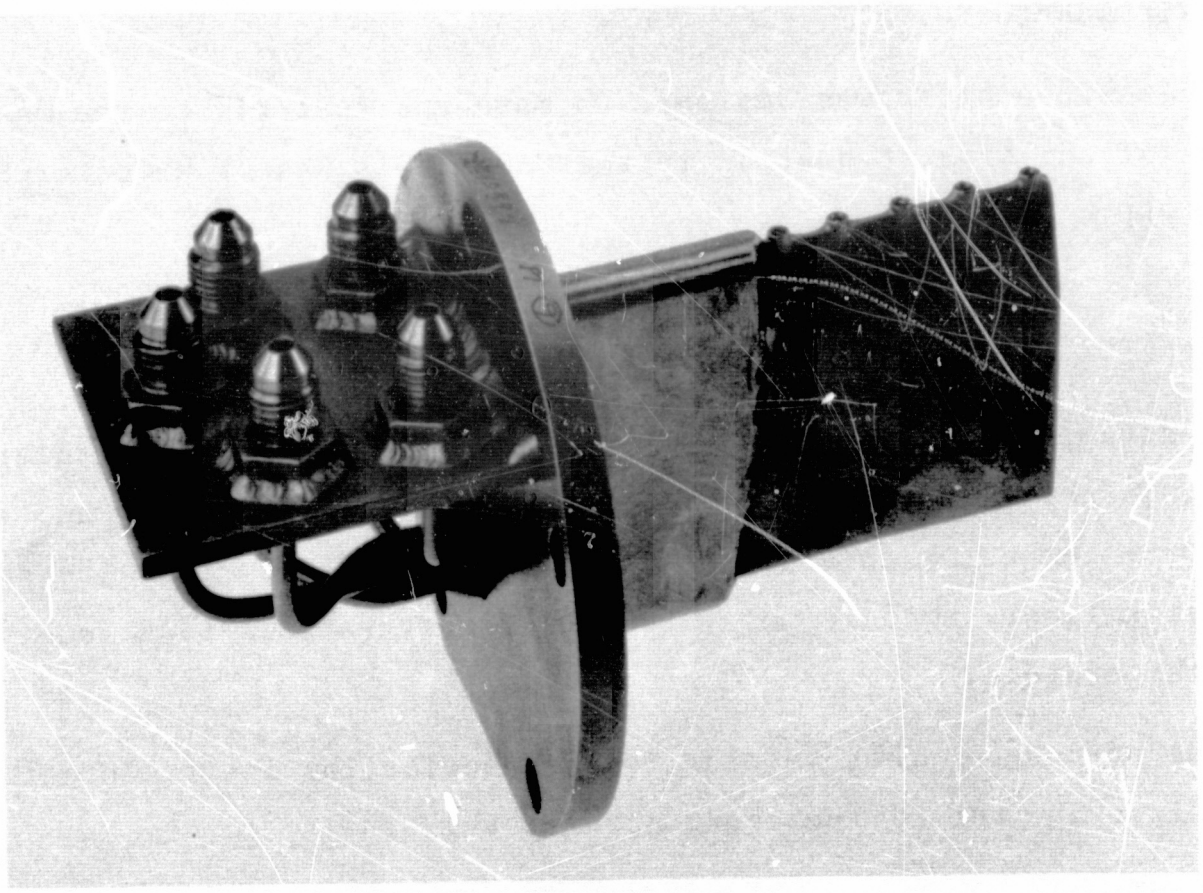

Figure 17. Diffuser Inlet Pressure Probe FE 67681

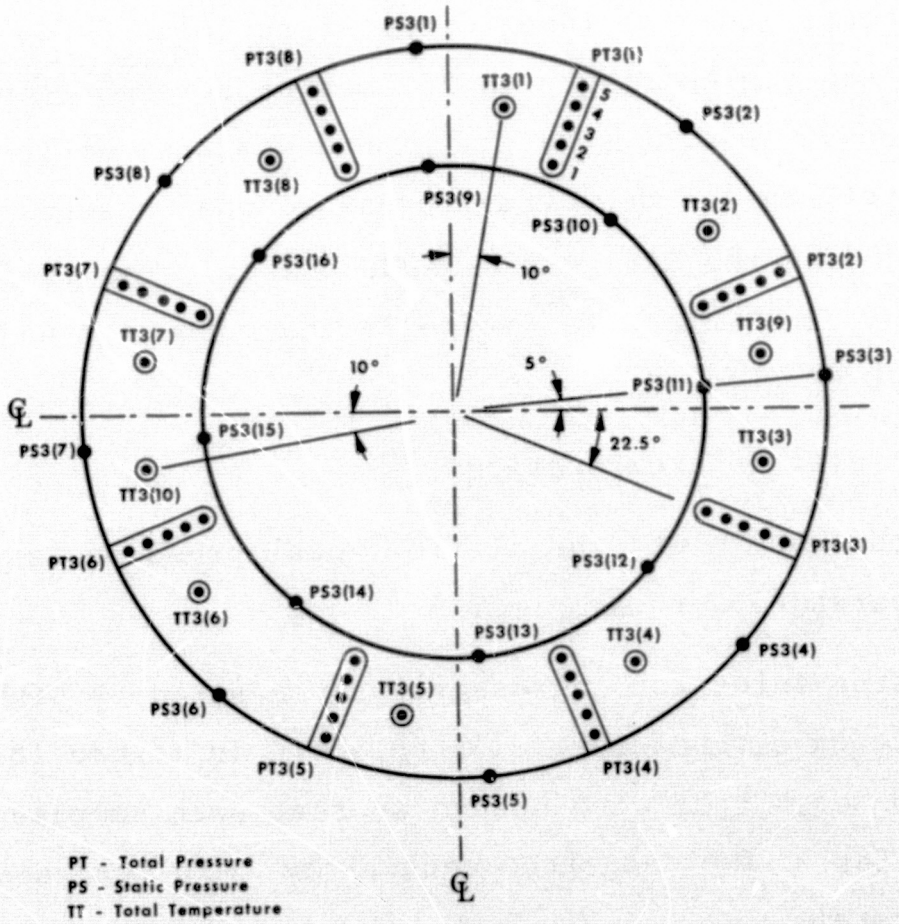

Figure 18. Diffuser Inlet Instrumentation Looking Downstream FD 24741A

That portion of the rake immersed in the airflow is contoured to the specifications of the NACA 16-015 airfoil cross section to reduce airflow disturbances behind the rake. The rake was designed to mount on a boss machined into the diffuser case so that the sampling probes were in a plane simulating the compressor exit guide vane trailing edge.

The combustor inlet total temperature was monitored by 10 venturi type, chromel-alumel thermocouple probes, figure 19, spaced circumferentially as shown in figure 18. Eight of these thermocouples were recorded on the NASA AVD-CADDE system; one was monitored in the control room for setting the test point and one was utilized in the ignition and combustor flameout abort sequence.

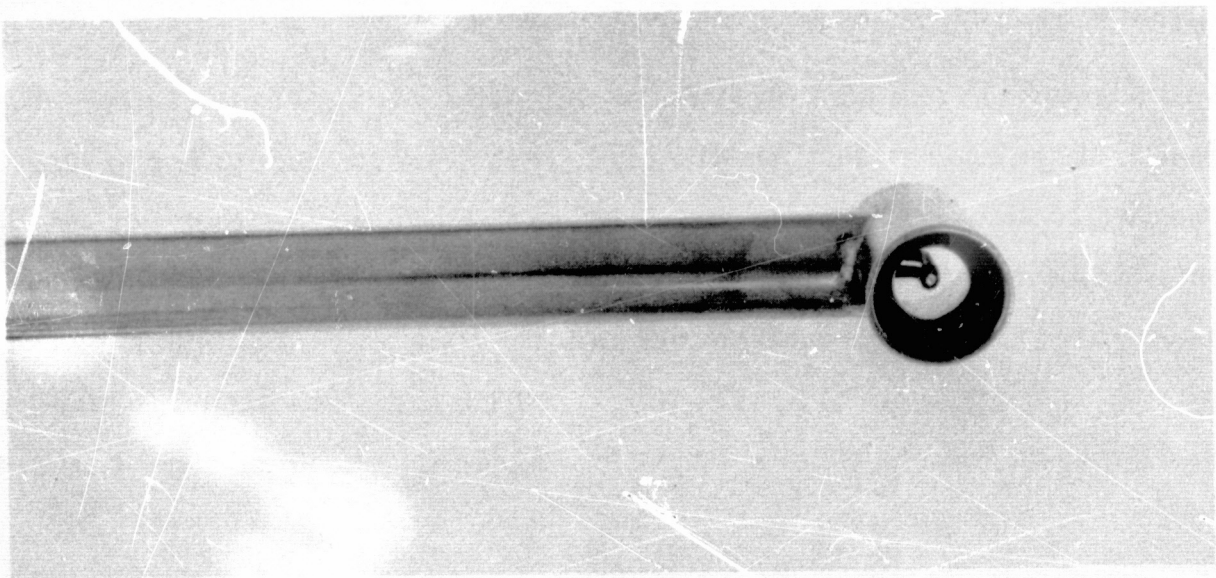

Figure 19. Chromel-Alumel Temperature Probe FE 77723

The combustor inlet static pressure was measured by 16 static pressure taps located circumferentially as shown in figure 18. All of the taps were placed to measure the static pressure in a plane simulating the compressor exit guide vane trailing edge. Two of the taps were also monitored in the control room for setting the test point. All 16 static pressure measurements were recorded on the NASA DAMPR-CADDE system.

3. Combustor Exit Instrumentation

The combustor exit total temperature and pressure were measured by a traversing rake, figure 13, which consisted of a water-cooled rotating drum equipped with three 5-point total temperature and total pressure probe heads, spaced 120° apart. The rotating drum was designed to traverse through a rotation of 120°.

The probe heads, figure 12, mounted on the rake were internally water-cooled except for the sampling probes which were made of platinum to withstand the high combustor exit temperatures.

The total pressure probes on each head were spaced radially on the head so that each sampled an equal area of the combustor exit. The data from each probe were recorded on the NASA AVD-CADDE system.

The thermocouples used were of the aspirating type with platinum 13% rhodium-platinum inserts. The probes were spaced at the same radial location on the head as the total pressure probes so that each sampled an equal area of the combustor exit. All of the exit temperature data were recorded on the NASA AVD-CADDE system.

The traversing rake was driven by a rotary actuator, figure 20. The actuator consisted of a stepping motor, a gear reduction unit, an electromagnetic brake, and various position potentiometers for measuring and controlling the angular position of the rake. There were a total of 8 position potentiometers on the actuator. One potentiometer was used as a control feedback to the actuator controller, and one was used as a position feedback to the probe position indicator mounted on the actuator control panel. The remaining 6 potentiometers were available for recording on the NASA AVD-CADDE system.

The actuator controller had provisions for either clockwise or counter-clockwise rotation in either a stepping mode or a continuous scanning mode. In the stepping mode, control could be either manual or automatic. In the Automatic Stepping Mode, the actuator was designed to traverse in 3° increments on command signals generated either internally by a time delay relay or externally by the NASA AVD-CADDE system.

The actuator and traversing rake were mounted in the centerbody of the water-cooled exit section (figure 10) so that the sampling probes were in a position simulating the leading edge of the first stage turbine stator. The centerbody was originally designed with a nitrogen purge to prevent the hot combustion gases from entering the centerbody. Initial testing proved this system to be inadequate. The system was then modified to incorporate a service air purge in conjunction with the nitrogen purge. This modification proved to be adequate.

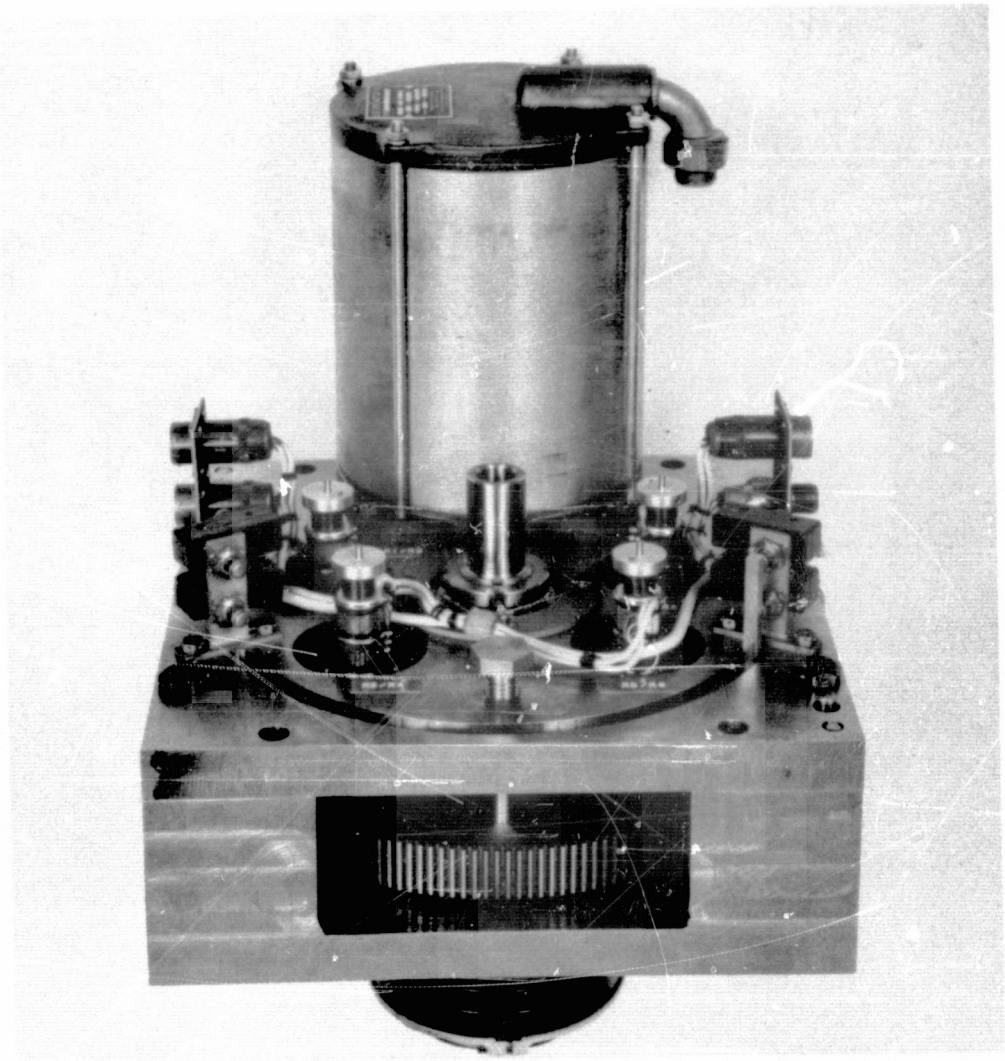

Figure 20. Actuator Assembly FE 67661

4. Fuel System Instrumentation

The fuel system, figure 21, was instrumented to allow for monitoring fuel temperature, fuel pressure at the combustor fuel manifold, and fuel flow. These data were recorded on the NASA AVD-CADDE system. In addition, the fuel pressure upstream and downstream of the fuel control valves was monitored in the control room to aid in positioning the control valves.

Fuel flow was measured by two turbine-type flowmeters which were capable of measuring flows up to 11,500 pph at pressures up to 1000 psig. The output from these meters was recorded on the NASA AVD-CADDE system and was also monitored in the control room.

The fuel temperature was measured by four iron-constantan thermocouples mounted in bosses just downstream of the fuel system control valves. Two of these thermocouples were recorded on the NASA AVD-CADDE system and the remaining two were monitored in the control room.

Figure 21. Fuel Skid Installation FE 70129

The rig fuel manifold pressure was measured by two strain gage transducers at the manifold main fuel block. The data were recorded on the NASA AVDCADDE system and also monitored in the control room.

5. Miscellaneous Instrumentation

Instrumentation was provided to measure rig jacket cooling water pressure and temperature. The jacket cooling water pressure was monitored for the following items:

a. Cooling water to the traversing rake probe heads.

b. Cooling water to the rig spacer.

c. Cooling water to the ID nozzle.

d. Cooling water to the OD nozzle.

e. Cooling water to the rotating drum inspection plate.

In addition the test rig quench water supply pressure was measured. The pressure taps for measuring the jacket water pressure were located on the inlet lines to the items mentioned above. The quench water pressure tap was located on the downstream side of the quench water orifice.

The jacket water temperature was monitored for the following items:

a. Cooling water return from the traversing rake probe heads.

b. Cooling water return from the rig spacer.

c. Cooling water return from the ID nozzle.

d. Cooling water return from the OD nozzle.

e. Cooling water return from the rotating drum of the traversing rake.

f. Cooling water return from the rotating drum inspection plate.

The jacket cooling water temperature was measured by iron-constantan immersion thermocouples located in the discharge lines of the above items.

Two static pressure taps were provided downstream of the combustor exhaust nozzle. The pressure at these taps was monitored in the control room to aid in determining if the exhaust nozzle was choked (sonic flow).

The internal air temperature of the water-cooled exit centerbody was measured by two iron-constantan immersion thermocouples, which were monitored in the control room, to avoid damage to the actuator stepping motor, the position potentiometers, and the internal plumbing due to excessive temperatures.

During testing conducted under Task III (performance eyaluation) of this contract, the combustor liners and dome were instrumented at various locations with chromel-alumel skin thermocouples to obtain information on metal temperatures. This information was recorded on the NASA AVD-CADDE system. During the early testing no control room readout was provided. After it was determined that the combustor dome was becoming excessively hot, the skin thermocouples were relocated to give more information on this section. Control room readout was then provided for those thermocouples attached to the dome.

During Task III testing the diffuser was instrumented, figure 22 to obtain data on the diffuser inlet and exit total pressure and static pressure and the total pressure and static pressure at the inlet to the combustor flowsplitter. This information was recorded on the NASA DAMPR-CADDE system; no provisions for control room monitoring were made.

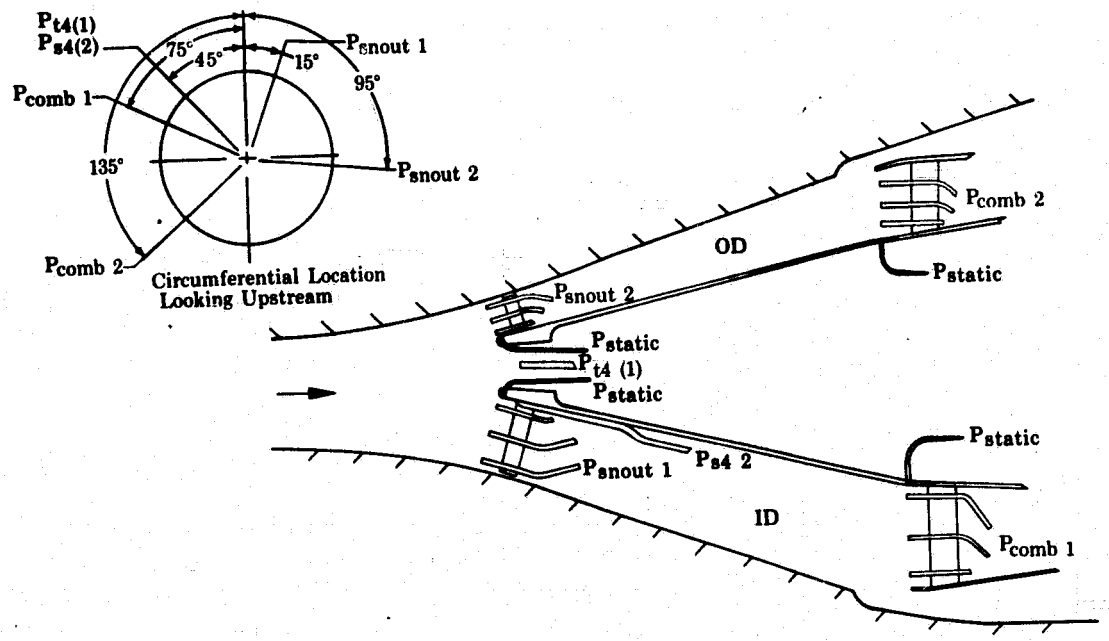

Figure 22. Location of Diffuser and Combustor Instrumentation FD 22259

During Task III and Task IV endurance testing, four static pressure taps, two upstream of the combustor dome and two downstream of the combustor dome, were provided for measuring the pressure drop across the dome. These data were recorded on the NASA CADDE system; no control room readout was provided.

6. Control Room Readout

Control room readouts were provided for monitoring the following parameters:

a. Rig cooling water pressure and flowrate.

b. Combustor inlet total pressure and static pressure.

c. Choke nozzle downstream static pressure.

d. Rig cooling water temperature.

e. Water-cooled exit section centerbody air temperature.

f. Combustor inlet total temperature.

g. Combustor exit total temperature.

h. Combustor fuel flow.

i. Rig airflow.

j. Fuel manifold pressure.

k. Fuel temperature.

The rig cooling water pressures, the combustor inlet total and static pressures, and the choke nozzle downstream static pressure were monitored on 0-150 psig gages mounted as shown in figure 23.

The rig-cooling water temperature and the exit-section centerbody air temperature were monitored on indicating pyrometers. The pyrometers were located on the control panel as shown in figure 23.

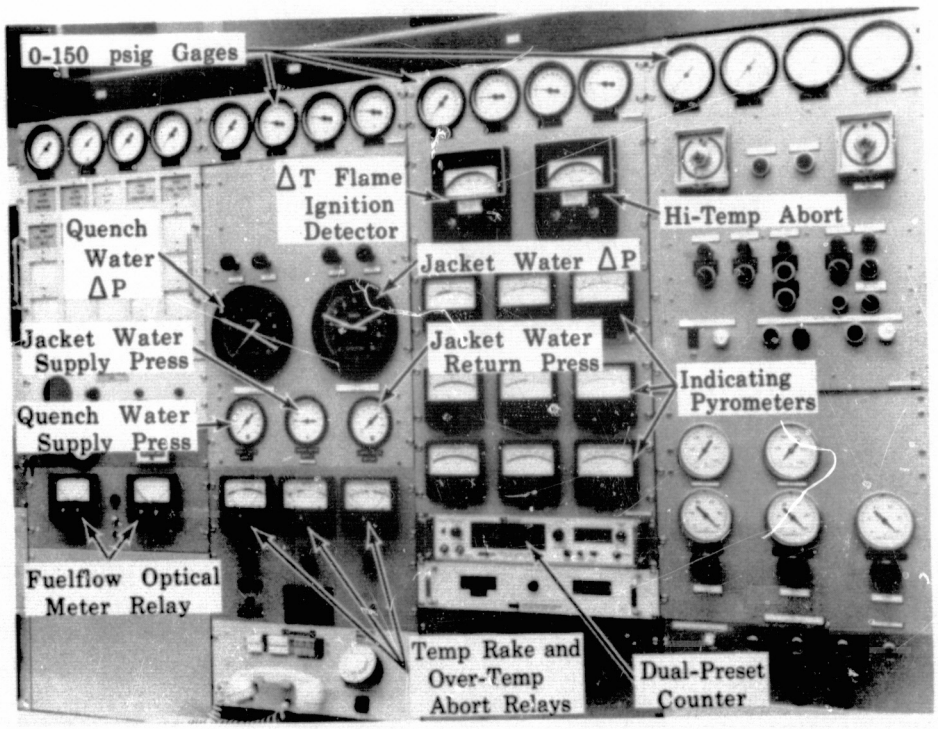

Figure 23. Control Panel of NASA ECRL Test Cell No. 1 (View 1) FD 24744A

The combustor inlet total temperature was monitored on a potentiometer indicator. The indicator was positioned on the NASA control panel to aid the NASA stand operator in setting the desired inlet temperature.

The combustor exit temperature was monitored on four X_1 X_2Y recorders mounted on the control panel as shown in figure 24. Since there are 15 exit temperature probes, a switch has been provided on the traversing rake overtemperature abort panel for selecting either a group of eight probes or the remaining group of seven probes to be monitored on the recorders.

The combustor fuel flow was monitored on a dual-preset counter located on the control panel as shown in figure 23.

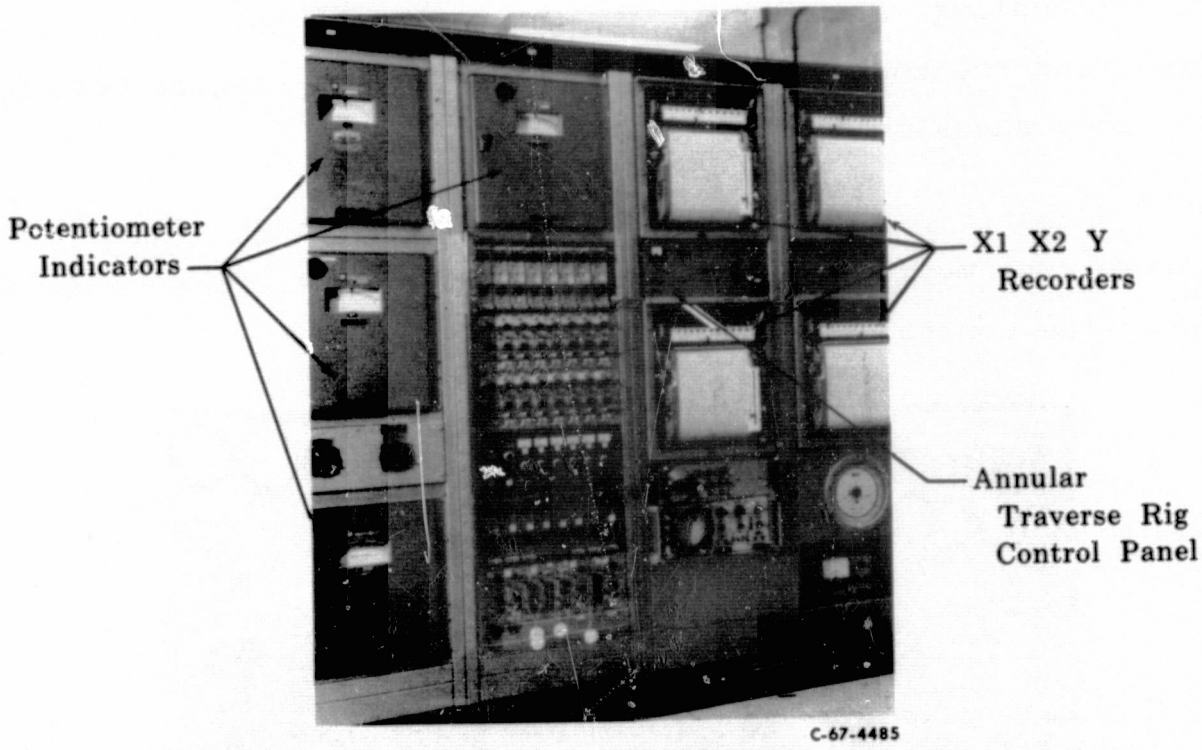

Figure 24. Control Panel of NASA ECRL Test Cell No. 1 (View 2)

FD 24745

The rig airflow was monitored on an orifice airflow computer which is located on the NASA control panel to aid the NASA stand operator in setting the test point. However, due to failure of the computer on several occasions, the orifice upstream pressure, the orifice temperature, and the orifice Δ pressure were monitored in the control room and the airflow read from a chart prepared for the orifice was used. This procedure was used as a check and as a backup for the computer. The orifice pressures were monitored on potentiometer indicators located on the control panel as shown in figure 24. The orifice temperature was monitored on an indicating pyrometer located on the NASA control panel.

The fuel manifold pressure and fuel temperature were monitored on potentiometer indicators located on the control panel as shown in figure 24.

7. Data Recording System

The following is a general description of the NASA central automatic digital data encoder (CADDE) system.

The CADDE system will automatically record as many as 300 pressures and 200 voltages in as little as 30 seconds to an accuracy of 0.15%, or better, of full scale range. All information is digitized, encoded, and recorded on magnetic tape for automatic insertion into a high-speed

general-purpose digital computer. Provisions for recording computer program modification instructions are incorporated. The computer accepts the encoded data produced by the recording system and automatically calibrates it, takes averages, forms ratios, and does terminal calculations. The performance program formulation is presented in Appendix A.

Pressures are taken from the combustor under test through copper tubing to the DAMPR system where they are transformed into electrical signals and retained in temporary storage for a 10-second measuring time. The data are then recorded onto magnetic tapes prepared by CADDE.

Voltages from equipment such as thermocouples, strain gages, potentiometers, and manual switches are measured and converted to digital form, one at a time, 20 readings per second, by an Automatic Voltage Digitizer (AVD) and recorded onto magnetic tape prepared by CADDE.

Having been recorded on magnetic tape, the data can be fed back to the control room on Flexowriters and/or facsimile plotters which type and plot the recorded data for examination during testing.

C. TEST RIG MODIFICATIONS

During Task III and Task IV testing, occasional problems occurred interfering with test rig operation and combustor testing. Each occurring problem and its correspondong corrective rig modification is listed chronologically as follows:

1. Prior to the start of Task III testing on 12 May, the rotating drum was pinned to the actuator shaft, as shown in figure 25, to prevent the rotating drum from slipping on the shaft.

2. Upon completion of testing on 26 May, it was found that the 3/16-inch drive pin connecting the actuator mechanism to the 3/4-inch rear portion of the rotating drum mounting shaft had sheared. A collar, shown in figure 26, was fabricated and installed as shown in figure 27. The collar transfers torque from the actuator directly to the 2-3/4-inch diameter forward portion of the actuator shaft

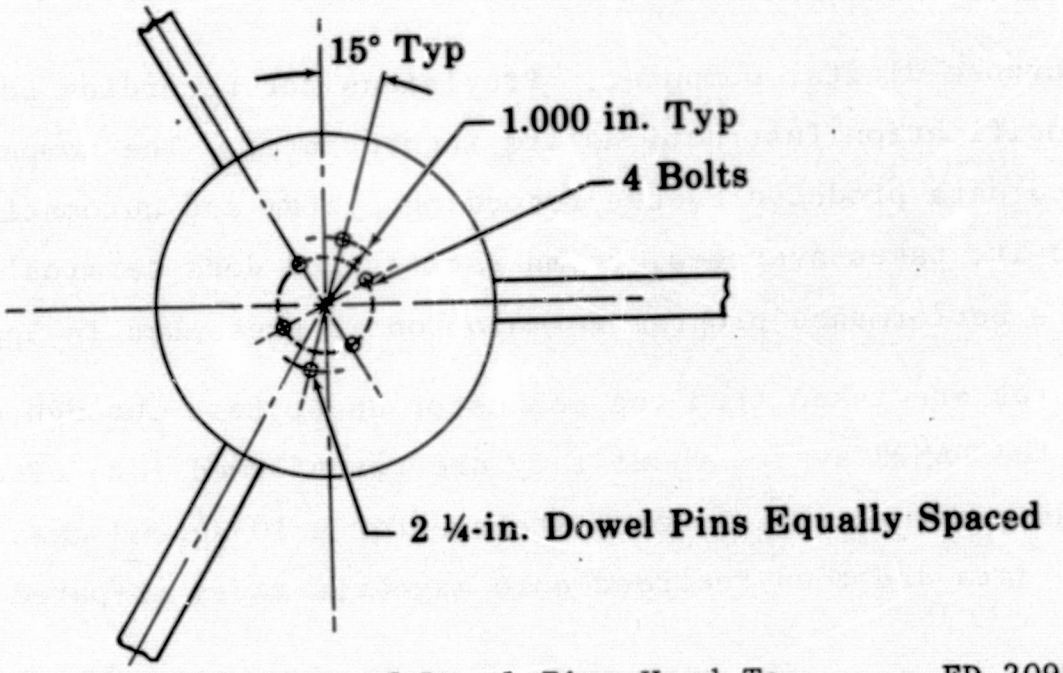

Figure 25. Location of Dowel Pins Used To Pin Rotating Drum To Actuator Shaft (Looking Downstream, Drum in Zero Degree Position)

FD 20920A

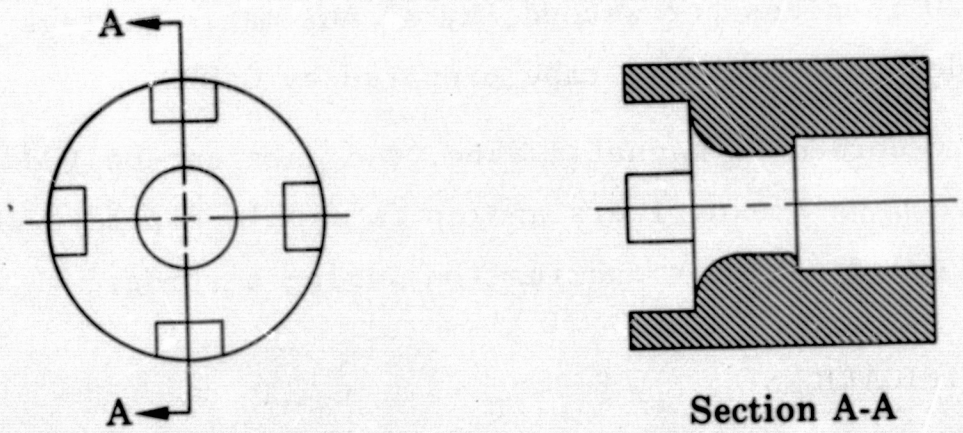

Figure 26. Coupling

FD 21848

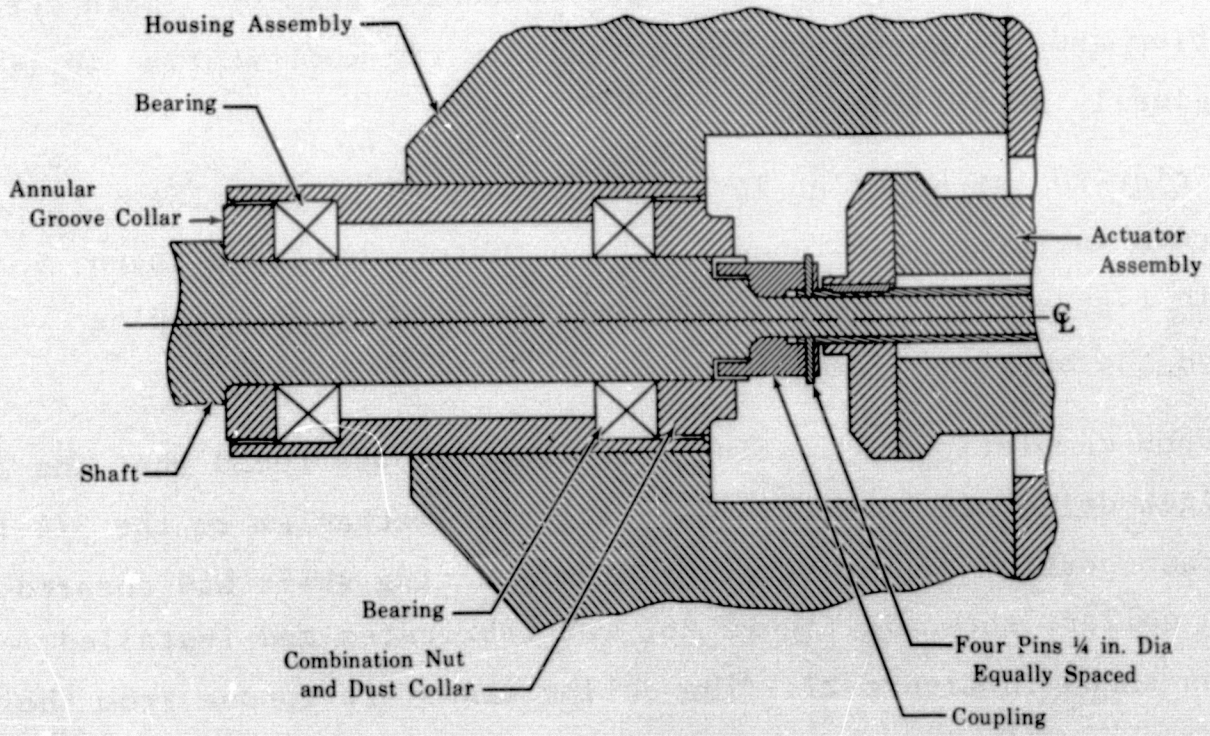

Figure 27. Modification to Annular Traverse Drive (See Figure 26 for Coupling Detail.)

FD 21849C

3. During initial testing, excessive centerbody temperatures were encountered. For this reason the discharge of the 0.25-inch nitrogen purge line was moved from the forward area of the traverse housing to the actuator housing behind the rear bulkhead to ensure cooling of the drive motor and of the potentiometers. An additional 0.5-inch nitrogen purge line, with throttle valve, was installed in the forward area of the traverse housing to provide increased purge flow, if needed.

4. Upon completion of testing on 23 June, the test rig was again disassembled. It was found that the rotating drum seal lip was extending into the seal groove on the ID nozzle only about 0.010 inch, and the rotating drum was found to be dragging in certain areas as it was rotated. To move the drum rearward and provide better seal engagement, the rotating drum mounting shaft was shortened by 0.050 inch. Light hand grinding on the seal lip eliminated the dragging problem.

5. The traverse unit operated satisfactorily during the next test sequence but the rotating drum was again found to be dragging during the post-test combustor inspection. Inspection of the seal lip of the rotating drum showed that it was warped 0.070 inch out of round. The drum and ID nozzle were sent to the machine shop and 0.020 inch was removed from the ID of the drum seal lip and 0.035 was removed from the ID of the mating groove on the nozzle.

6. While reassembling the cooling-water hoses in the actuator housing, it was determined that some of the hoses were weakening and binding on one another as the traverse drum was rotated. The one-inch diameter hoses to the inspection plate and the front face of the rotating drum were replaced with 5/8-inch diameter hoses and relocated to a more open area inside the housing to provide easier rotation of the traverse drum. No further traverse problems were encountered in subsequent testing.

7. Because excessive centerbody temperatures were again observed, the traverse housing purge system was again modified to include a service air purge in addition to the nitrogen purge system. The

nitrogen purge was used during combustor ignition to reduce the possibility of accumulating a combustible mixture inside the traverse housing when an unburned fuel/air mixture is passing through the rig. After ignition, the service air purge was substituted for the nitrogen purge to maintain a low temperature inside the traverse housing and to conserve nitrogen.

8. False walls were installed in the OD and ID passages of the diffuser (figure 28), to eliminate stall that had occurred with the original diffuser.

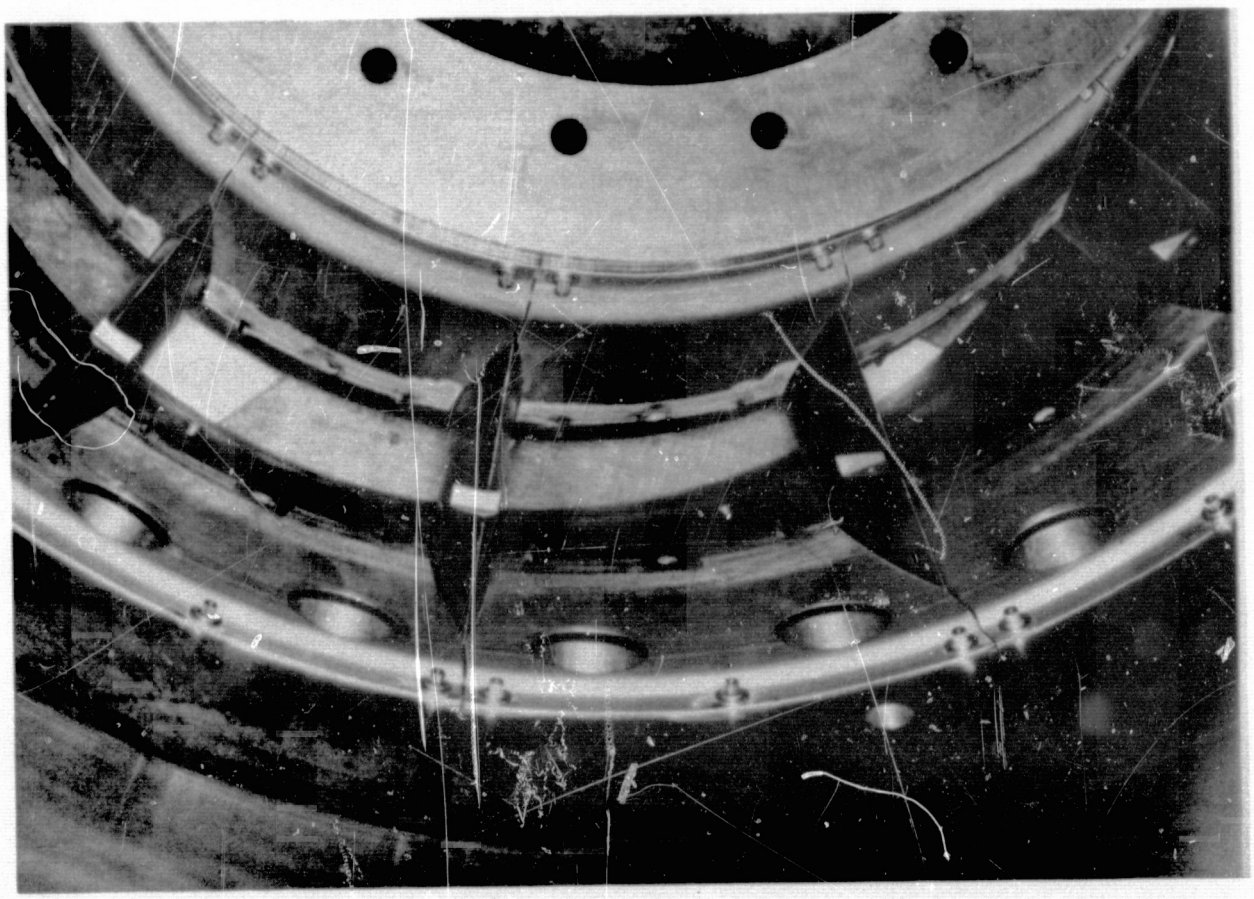

Figure 28. Model 1-1E Diffuser FE 72284

9. Originally the diffuser contained eight static pressure taps in the OD case located in a plane simulating the trailing edge of the compressor exit guide vane. Eight additional static pressure taps were installed in the ID case and located in the same plane as the original static pressure taps. This was done to obtain data that would give more complete information on the conditions at the diffuser inlet.

10. The fuel manifold nitrogen purge system was modified, as shown in figure 29. This modification included routing the purge

lines to the three fuel manifold junction blocks and installation of a drain line to drain the fuel between the shutoff valve and fuel nozzles prior to purging. The purpose of this modification was to prevent coking of the fuel nozzles and filter screens during the period of nonburning while flowing high temperature air through the rig, and also to more completely remove fuel from the fuel manifold after testing.

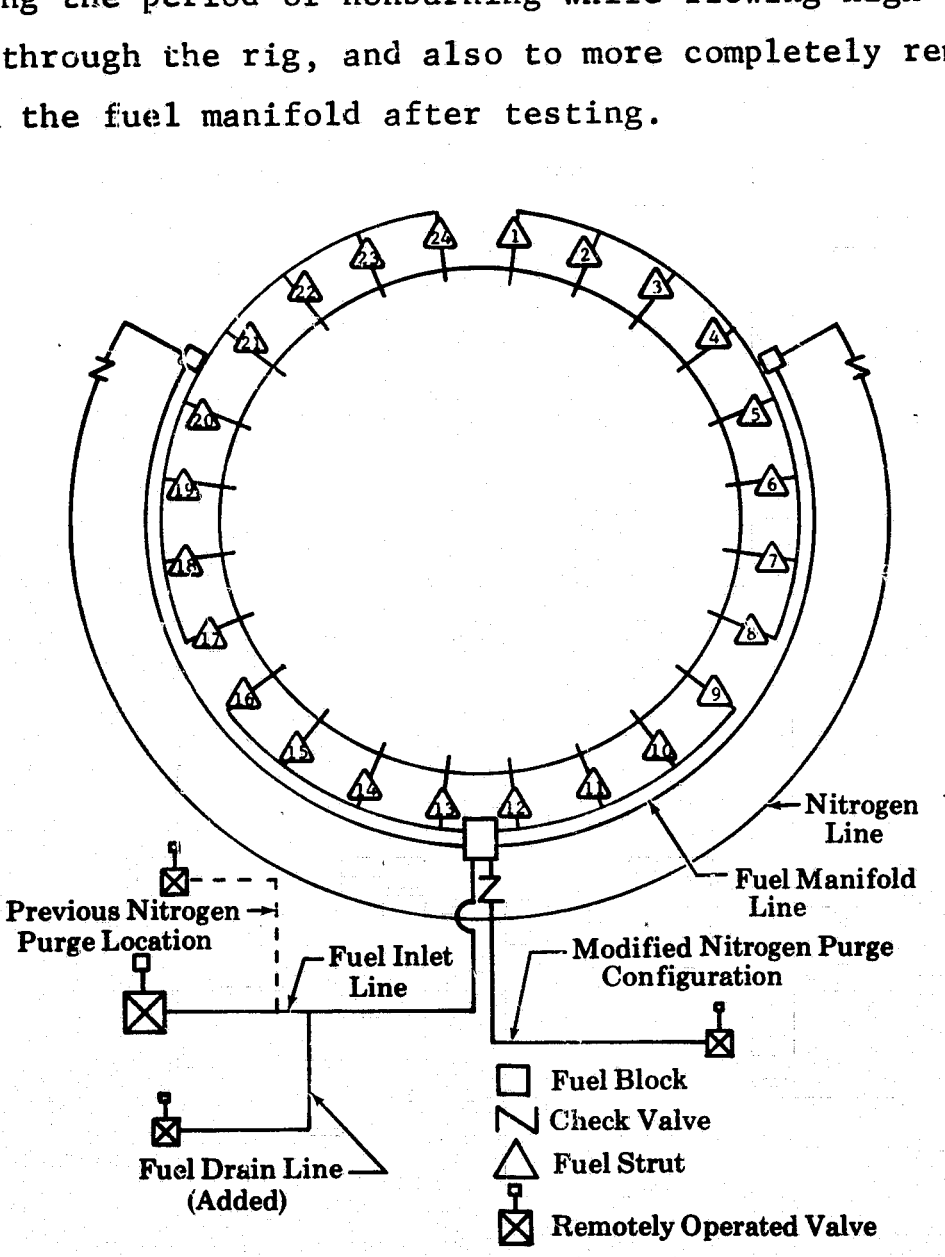

Figure 29. Fuel Manifold Purge System FD 23499

11. Several cracks developed in the welds holding the expansion tube located at the rear of the water-cooled exit assembly's ID water jacket. This was repaired by fabricating a new expansion tube and installing it on the exterior of the water jacket, as shown in figure 30. The actuator cover was modified for clearance of the new expansion tube.

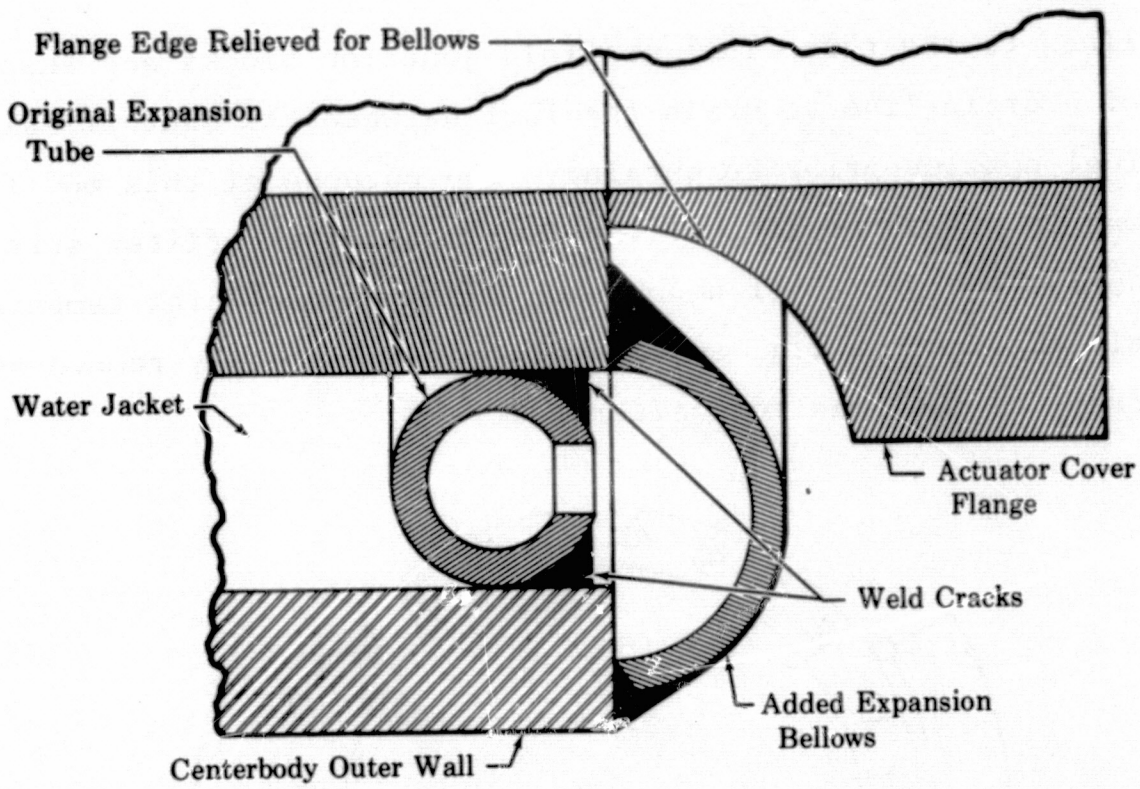

Figure 30. Centerbody Modification A FD 23632A

12. Filters were installed in all of the quench water lines, as shown in figure 31, to eliminate the problem of rust scale plugging the quench water holes and jackets.

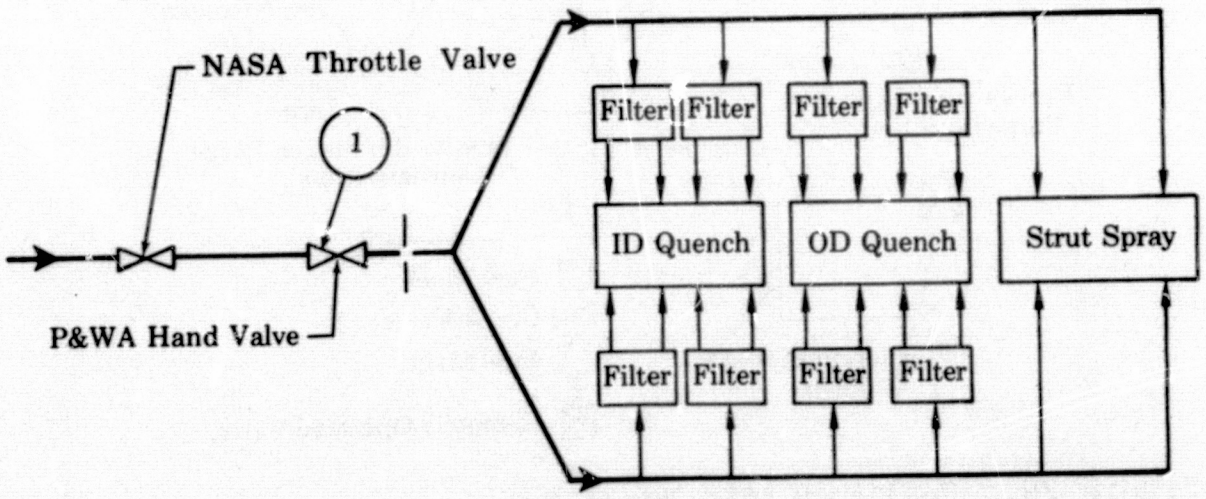

Figure 31. Quench Water System Schematic FD 24746

13. With the initiation of 1150°F inlet temperature testing, a serious warpage of the OD transition liner support ring was noted. The ring was sectioned into three parts and the bolt holes were elongated to allow for expansion. Additional support sections were then added to the ring and the problem was eliminated.

SECTION III
COMBUSTOR

A. COMBUSTOR SELECTION

The purpose of this section is to present the combustor aerodynamic design analysis performed under this contract. Because the contract called for a combustor design that had undergone sufficient prior testing to qualify for a full-scale endurance test, the ram induction primary combustor of the JTF17A-20 engine was selected for this program. This discussion is therefore limited to the modifications that were made to the basic JTF17A-20 combustor design.

B. INITIAL COMBUSTOR DESIGN MODIFICATIONS

Two major combustor design modifications were made prior to the fabrication of hardware for the preliminary performance evaluation.

First, the diffuser vanes used in the JTF17 were replaced with a combustor snout-type flow splitter to provide the combustor dome flow areas with higher pressure drop. Measurements on JTF17 configurations indicated this pressure drop to be 0.3% or less. A higher dome pressure drop was desirable to reduce carbon accumulation in the front of the combustor. This was accomplished by providing a reduction in fuel/air ratio in the front of the combustor and higher sweeping velocities on the combustor dome.

Secondly, the slots in the combustion dome at each fuel nozzle ID and OD tangency point were eliminated. These slots had been incorporated in the JTF17 combustor to prevent carbon accumulation and should no longer be necessary with the higher dome pressure drop. Their presence with the higher pressure drop could prove detrimental to combustor performance, as large quantities of air injected axially into a combustor usually produce cold areas in the exit temperature pattern.

These initial design modifications are covered in more detail in the following paragraphs.

1. Combustor Snout and Diffuser Design

The first step in the snout and diffuser redesign was to estimate the diffuser and combustor pressure distribution. The diffuser

pressure loss was assumed to equal a fraction of the theoretical velocity head change through the diffuser. The value was based on previous experience with diffusers of similar geometry. Calculation of the diffuser and combustor pressure distribution then required a reiterative calculation of diffuser pressure loss. A trial value of diffuser exit area/pound airflow/second was assumed to allow calculation of the diffuser theoretical velocity head change. The diffuser pressure loss was then calculated as 1/3 of the velocity head change to provide the diffuser exit, or combustor inlet, pressure level. The combustor pressure loss was obtained by correcting previous JTF17 combustor data to the conditions of this contract. The forward combustor internal static pressure was then assumed equal to the combustor exit total pressure, and the combustor dome supply pressure was set equal to the scoop supply pressure. The combustor dome, or snout inlet, airflow was then calculated to determine the quantity of flow remaining at the diffuser exit. The snout inlet area was calculated to provide the proper combustor dome supply pressure, and the snout geometry laid out to determine the snout wall radii at the diffuser exit. The diffuser case radii were then calculated to provide the assumed value of diffuser exit area/pound airflow/second $\left[\text{in.}^2/(\text{lb/sec})\right]$. If the calculated diffuser case radii could not be obtained from the forgings on hand (the diffuser forgings had been ordered for the wall contour of the JTF17 engine prior to the selection of a specific combustor design), or if the equivalent conical angle for the diffuser passage was undesirable, a new value of diffuser exit area/pound airflow/second was assumed and the procedure repeated.

The diffuser passages were designed with low equivalent conical angle (equivalent conical angle is defined in figure 32) and area ratio to provide the combustor with uniform, nonseparated flow and to provide maximum pressure recovery. The final design provided the lowest equivalent conical angle and area ratio that could be obtained with the diffuser forgings on hand.

The final set of calculations and a more extensive discussion of the assumptions involved follow.

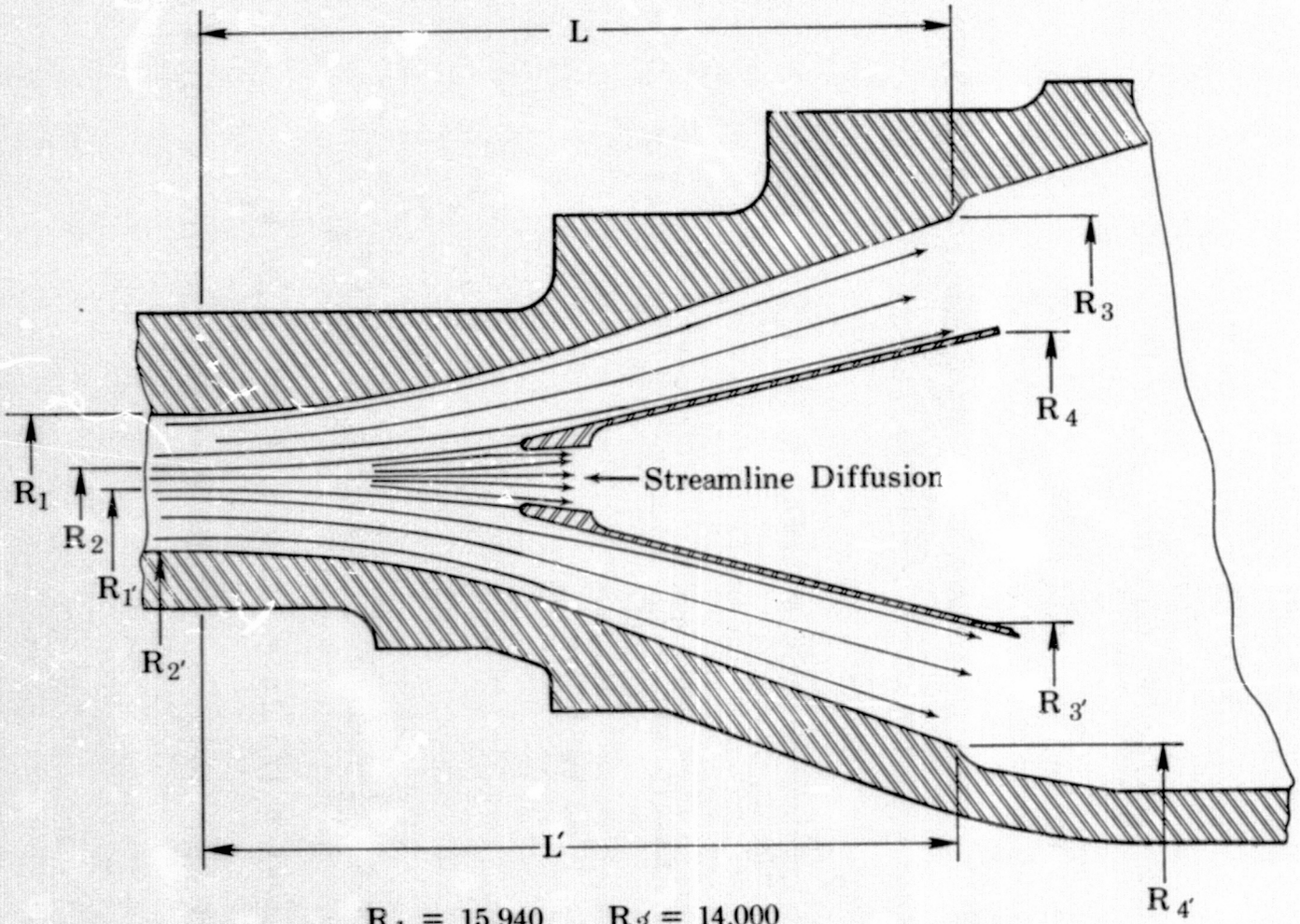

$R_1 = 15.940$ $R_{2'} = 14.000$
$R_2 = 15.181$ $R_{3'} = 13.246$
$R_3 = 18.478$ $R_{4'} = 11.290$
$R_4 = 17.135$ $L = 10.208$
$R_{1'} = 14.852$ $L' = 10.176$

The equivalent conical angle (ECA) is the included angle of a conical diffuser that has the same area ratio and wetted surface as the diffuser under investigation. It may be approximated by the following equation for annular diffusers:

$$ECA = 2 \tan^{-1}\left[\frac{\left(\frac{A_1}{A_2} - 1\right) A_1}{\pi L(R_1 + R_2 + R_3 + R_4)}\right]$$

With symbols as shown

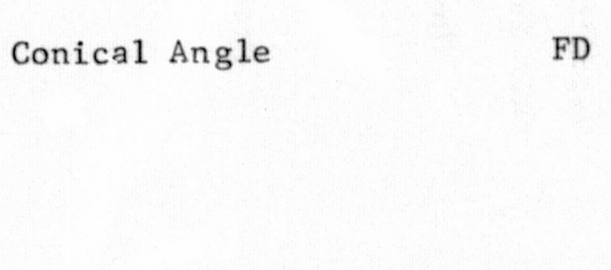

To apply this equation to diffusers with flow splitters the flow through the ID and OD passages is assumed to be divided at the diffuser inlet and the corresponding fictitious diffuser radii (R_2 and R_1') are used in the equation for ECA. The area between R_2 and R_1' is the same percentage of inlet area as percentage of total flow entering the snout. The remaining inlet area is divided equally between the ID and OD flow passages.

Figure 32. Conceptual Diffuser Streamline and Definition of Equivalent Conical Angle FD 20921

a. Diffuser Pressure Loss

The diffuser pressure loss was assumed to be 1/3 of the theoretical velocity head change, Δq, through the diffuser. Experience indicates this is a typical loss in diffusers of similar geometry.

The inlet q was obtained as follows:

$$\frac{W\sqrt{T}}{PA}\ \text{diffuser inlet} = \frac{110\sqrt{1060}}{90 \times 182.54} = 0.218$$

From compressible flow tables:

$$M = 0.248$$

$$\frac{P_s}{P_t} = 0.96$$

$$q = 4.13\ P_t$$

$$\frac{A}{A^*} = 2.43$$

The diffuser inlet area/pound airflow/second is:

$$\frac{182.54\ \text{in.}^2}{110\ \text{lb/sec}} = 1.66\ \text{in.}^2/(\text{lb/sec})$$

A trial value of diffuser exit area/pound airflow/second of 3.28 was assumed. The area ratio of the diffuser is therefore:

$$\frac{A_2}{A_1} = \frac{3.28\ \text{in.}^2/\text{pound/second}}{1.66\ \text{in.}^2/\text{pound/second}} = 1.97$$

$$\frac{A}{A^*}\ \text{for the diffuser exit} = \frac{A}{A^*}\ \text{inlet} \times \frac{A\ \text{exit}}{A\ \text{inlet}} = 2.43 \times 1.97 = 4.79.$$

From compressible flow tables:

$$M = 0.122$$

$$q = 1.02\ P_t$$

$$\Delta q = q_{inlet} - q_{exit} = 4.13\ P_t - 1.02\ P_t = 3.11\ P_t$$

$$\text{diffuser loss} = 1/3\ \Delta q = 1/3 \times 3.11\ P_t = 1.04\ P_t$$

$$\text{diffuser exit } P_t = \text{inlet } P_t - 1.04\ P_t = 90 - (0.0104 \times 90) = 89.1\ \text{psia}$$

The diffuser exit Mach number, corrected for diffuser pressure loss, may now be calculated:

$$\frac{W\sqrt{T}}{PA} = \frac{\sqrt{1060}}{89.1 \times 3.28} = 0.111$$

From compressible flow tables:

$$M = 0.122$$

$$\frac{P_s}{P_t} = 0.99$$

Therefore, P_s at diffuser exit = $P_t \times P_s/P_t$ = 89.1 x 0.99 = 88.1 psia.

b. Combustor Pressure Loss

The combustor pressure loss was obtained by correcting test results on similar configurations to the contract test condition. JTF17 combustors have demonstrated overall pressure losses of 6% when operating with reference velocities of 127 ft/sec. Of this overall loss, 3.5% is attributed to the combustor and the remaining 2.5% to the diffuser.

The combustor pressure loss for condition 6 was obtained by correcting the 3.5% JTF17 pressure loss by the ratio of the squares of the reference Mach numbers.

$$\frac{\Delta P}{P} = \frac{\Delta P}{P}_{JTF17} \left(\frac{M \text{ ref test condition 6}}{M \text{ ref JTF17}}\right)^2 = 3.5 \left(\frac{0.0715}{0.0876}\right)^2 = 2.33\%$$

The combustor inlet total pressure (diffuser exit pressure), as determined in the section on diffuser pressure loss, is 89.1 psia.

Combustor exit total pressure is therefore:

$$89.1 - (0.023 \times 89.1) = 87.1 \text{ psia}$$

If the effects of pressure loss due to heat addition are neglected, the total pressure throughout the length of the combustor may be considered constant since the mean velocity is relatively low. The magnitude of the pressure loss due to heat addition is on the order of 0.5% at maximum temperature rise conditions, and considered negligible for this analysis. Static pressure does vary down the length of the combustor as a function of local velocity, but may be assumed equal to

total pressure in the forward portion of the combustor where mean velocity is negligible.

Figure 33 shows the diffuser and combustor pressure distribution obtained from this analysis.

c. Snout Intake Area

The flow area distribution for the combustor is shown in figure 34. Table 2 (page 41) gives similar information in tabular form. The flow areas fed by the snout are as follows:

Item	Flow Area, $in.^2$
Swirlers	23.04
Cone Aligning Ring	8.86
Holes in Cone	7.08
ID Primary Liner Cooling	14.11
OD Primary Liner Cooling	14.79
Total	67.88

A flow coefficient of 0.62 was applied to these flow areas. The effective flow area is therefore, $A_{eff} = 67.88 \times 0.62 = 42\ in.^2$.

The snout inlet area was sized to provide a pressure drop across the combustor dome equal to the pressure drop across the forward liner scoops. With the pressure drop known, the flow through the snout-fed passages may be calculated as follows:

$$\frac{P_s}{P_t} \text{ for the flow passages} = \frac{P_s \text{ (inside combustor)}}{P_t \text{ (outside combustor)}} = \frac{871}{891} = 0.978$$

From compressible flow tables:

$$\frac{W\sqrt{T}}{PA} = 0.161$$

$$W = \frac{0.161 \times 89.1 \times 42}{1060} = 18.5 \text{ lb/sec or } 16.8\% \text{ of total airflow.}$$

The snout inlet area may now be sized to provide the desired combustor dome supply pressure. The following assumptions are involved:

1. No loss in total pressure has occurred in the flow from the diffuser inlet to the snout inlet.

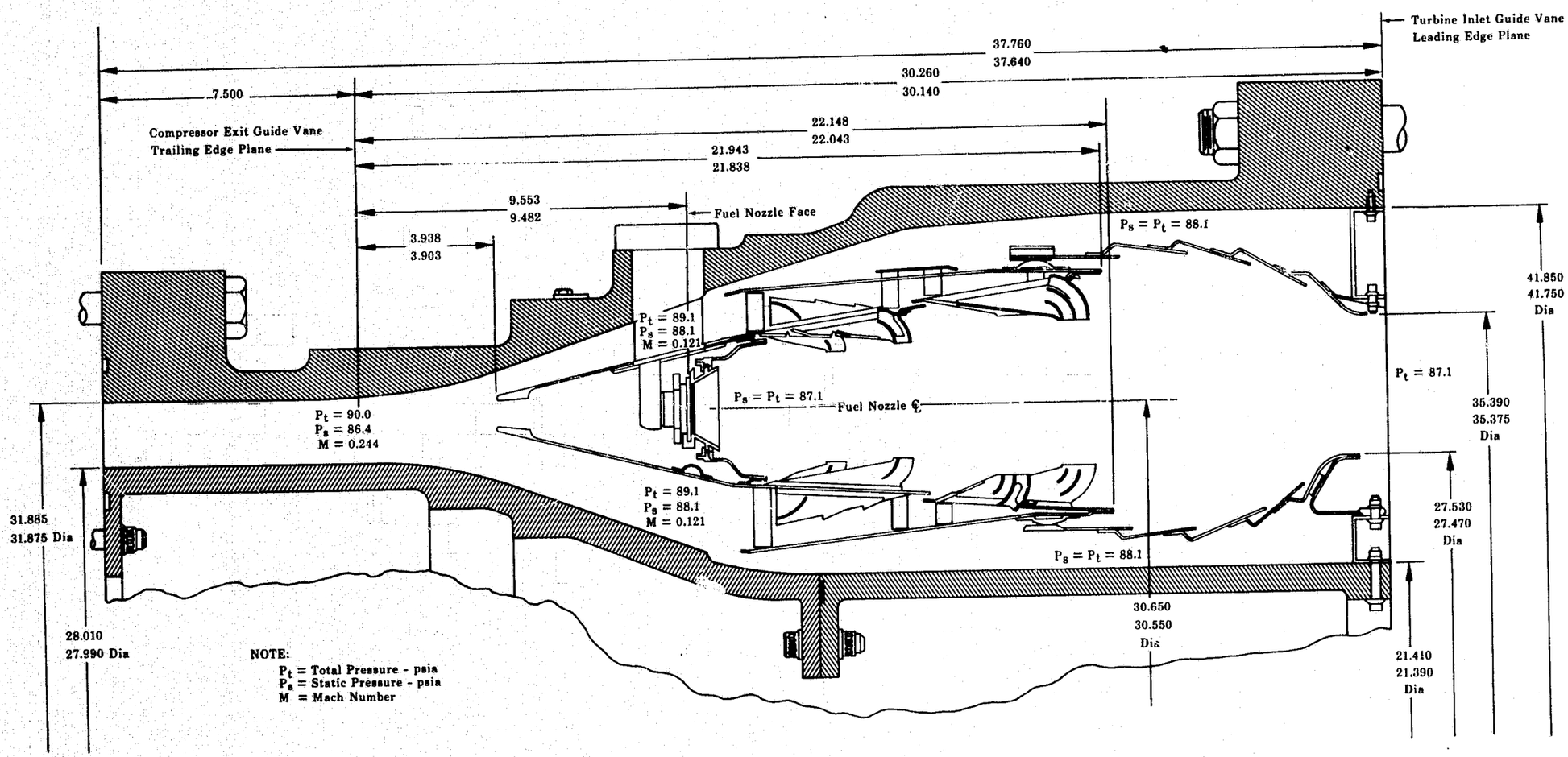

FD 20919

Figure 33. Diffuser and Combustor Pressure Distribution

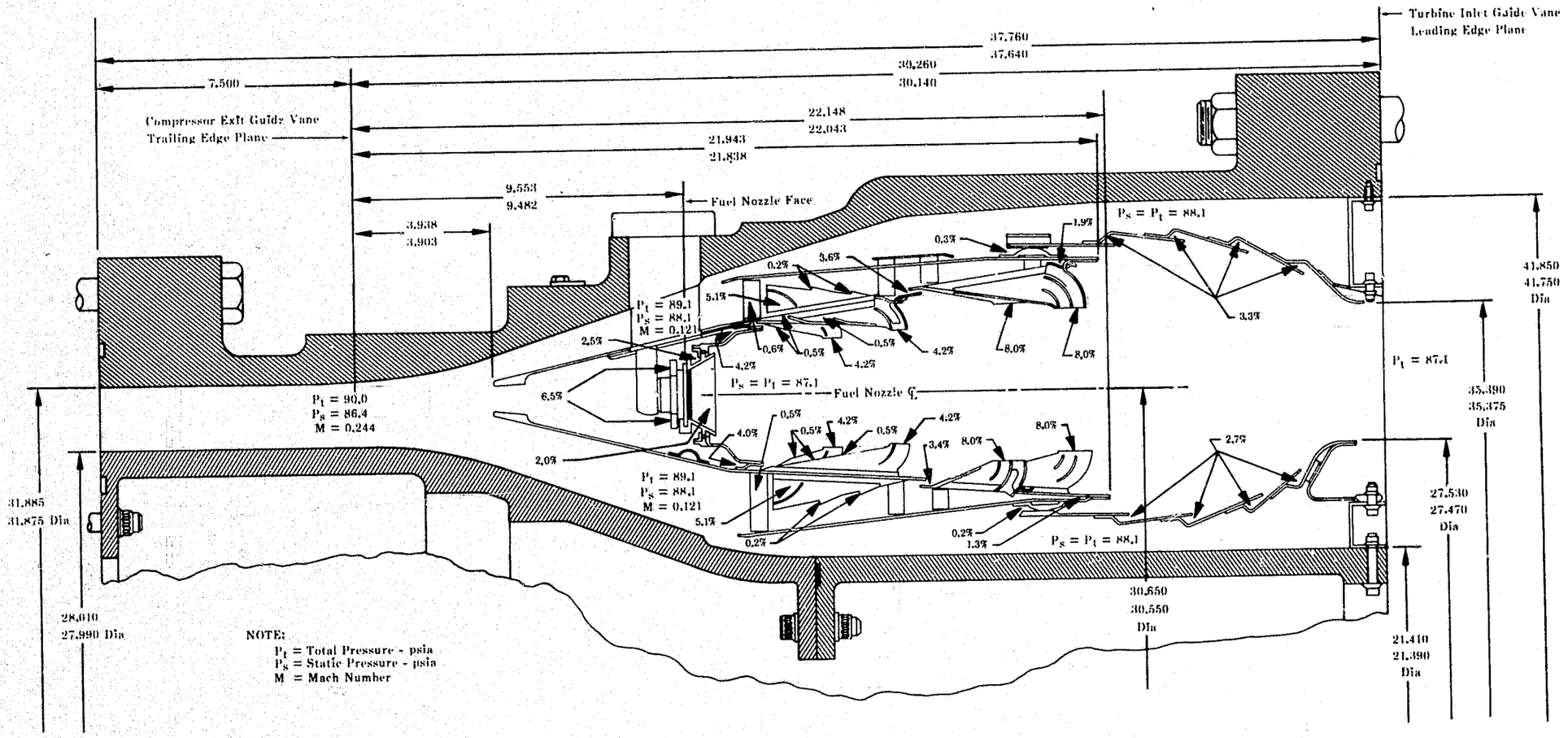

Figure 34. Combustor Flow Area Distribution

FD 24702

Table 2. Flow Areas for the Advanced Annular Combustor, Model 1-1A

ITEM	DESCRIPTION	% OF TOTAL AREA	LENGTH (in.)	WIDTH (in.)	AREA (in.^{2})	TOTAL AREA (in.^{2})
A	First Primary Scoop	10.16	0.953	0.800	0.745	35.760
B	Second Primary Scoop	8.38	0.801	0.800	0.614	29.472
C	Third Primary Scoop	8.38	0.801	0.800	0.614	29.472
D	First Secondary Scoop	16.10	1.121	1.120	1.180	56.640
E	Second Secondary Scoop	16.10	1.121	1.120	1.180	56.640
1	ID Primary Liner Cooling Holes	4.01	0.310 slots		0.217	14.105
2	ID Secondary Liner Cooling Gap	3.40	79.721	0.150	11.958	11.958
3	Cooling Film Gap	0.15	0.500	0.030	0.015	0.540
4	ID Transition Liner Film Cooling Gap	2.67	0.129, 0.183, & 0.104 dia			9.388
5	ID Rear Shroud Outlet	1.30	0.156 dia		0.0191	4.584
6	OD Primary Liner Cooling Holes	4.20	0.250 slots		0.145	14.790
7	OD Secondary Liner Cooling Gap	3.59	114.819	0.110	12.630	12.630
8	Cooling Film Gap	0.31	0.600	0.030	0.018	1.080
9	OD Transition Liner Film Cooling Gap	3.29	0.129, 0.120, & 0.166		0.094 dia	11.569
10	OD Rear Shroud Outlet	1.85	0.125 dia		0.0123	6.494
11	Holes in Cone	2.01	0.125 dia		0.0123	7.080
12	Holes in Cone Aligning Ring	2.52	0.125 dia		0.0123	8.856
13	First Primary Scoop Cooling Louver #1	0.40	0.575	0.050	0.029	1.392
14	First Primary Scoop Cooling Louver #2	0.40	0.575	0.050	0.029	1.392
15	Second Primary Scoop Cooling Louver	1.07	0.575	0.137	0.079	3.780
16	Third Primary Scoop Cooling Louver #1	1.07	0.575	0.137	0.079	3.780
17	Third Primary Scoop Cooling Louver #2	1.07	0.575	0.137	0.079	3.780
18	Louvers Between 2nd & 3rd ID Primary Scoops	0.48	0.600	0.117	0.070	1.680
19	Louvers Between 2nd & 3rd OD Primary Scoops	0.57	0.710	0.117	0.083	1.995
Swirlers		6.54			0.960	23.040
	Total	100.02				351.897

2. External streamline diffusion will occur isentropically from the main stream velocity to the flow velocity in the snout intake. A conceptual sketch of the streamline flow and the definition of equivalent conical angle is shown in figure 32.

3. Flow that has entered the snout inlet area incurs a 1-q dump loss. Therefore, the combustor dome supply pressure is equal to the static pressure in the snout inlet. The heavy reinforcing rings on the snout leading edges are contoured to form a diffusing path inside the snout with an area ratio of 1.14:1. This diffuser is neglected in the snout sizing calculations since the maximum possible static pressure rise through this diffuser is only 0.2%.

For the snout to provide the combustor dome supply pressure of 89.1 psia, which is the same as the scoop supply pressure, the flow must externally diffuse to a Mach number which provides a static pressure of 89.1 psia in the snout inlet area. The total pressure at the snout inlet is 90.0 psia, therefore

$$\frac{P_s}{P_t} = \frac{89.1}{90.0} = 0.99$$

From compressible flow tables:

$$\frac{W_1\sqrt{T}}{PA} = 0.1089$$

$$\text{Snout inlet area then} = \frac{18.5 \quad 1060}{0.1089 \times 90} = 61.5 \text{ in.}^2$$

The radial center of the snout inlet was then located approximately midway between the radial center of the diffuser inlet and the fuel nozzle radius. The leading edges of the snout were rounded to prevent separation of impacting flow. The snout inlet was located in the plane of maximum thickness of diffuser struts. The snout walls were made conical for economical fabrication, and blend smoothly into the ID and OD combustor walls, which are identical to those of the JTF17 combustor.

With the snout contour and inlet airflow so determined, the diffuser exit radii to provide the assumed value of diffuser exit area/pound airflow/second were calculated and compared with the existing diffuser

forgings. If the radii obtained fell outside the existing forgings, or gave excessive area ratio or equivalent angle, a new value of diffuser exit area/pound airflow/second was assumed and the procedure repeated. The calculations presented are for the final trial which gave the lowest diffuser area ratio and equivalent conical angle obtainable from the existing diffuser forgings. Figure 35 shows a comparison of diffuser area ratio versus equivalent conical angle for the initial diffuser design compared to a P&WA diffuser experience curve, and indicates the diffuser design was within good design practice.

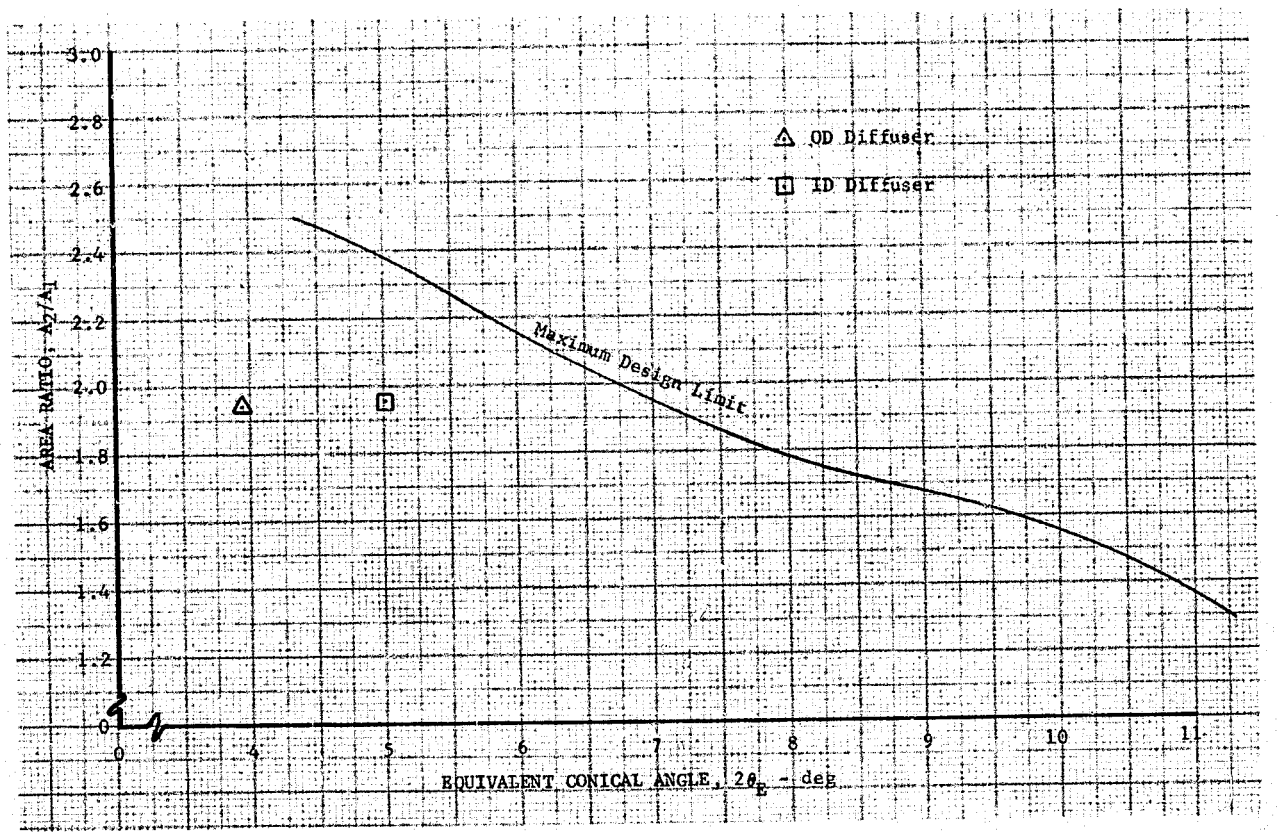

Figure 35. Experience Curve of Diffuser Area Ratio vs Equivalent Conical Angle DF 55793

The diffuser walls were then contoured to provide a smooth increase in area per unit flow down the length of the diffuser. Figure 36 shows a curve of area/pound airflow/second versus diffuser length for the initial configuration.

2. Combustor Flow Area Distribution

The combustor flow area distribution for this program was identical to that of the JTF17 combustor except for the elimination of slots in the dome as mentioned in the introduction. This modification was made on the basis of past experience and without theoretical analysis. The combustor flow area distribution is presented in figure 34 and table 2.

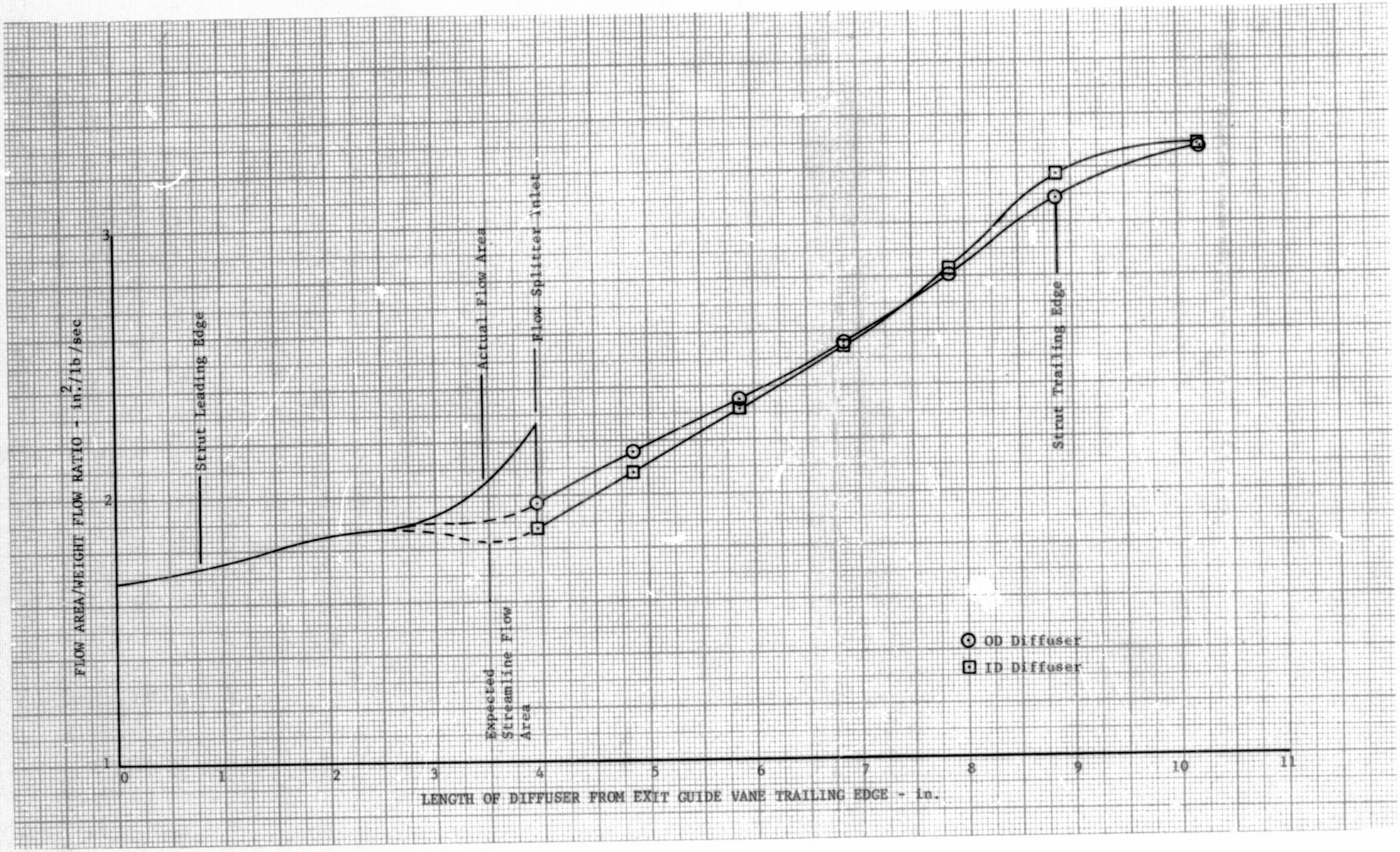

Figure 36. Flow Area to Weight Flow Ratio vs Diffuser Length

DF 64489

C. COMBUSTOR MODIFICATIONS DURING TEST

During the preliminary performance testing conducted under Task III of the contract (Section IV in this report) several modifications to the initial design combustor, designated Model 1-1A (shown in figures 37, 38, and 39), were made to improve combustor performance and to provide improved metal cooling. A description of each modification follows:

1. Model 1-1B

The Model 1-1B, as shown in figures 40 and 41, differed from the model 1-1A by the addition of slots and holes in the dome to provide improved metal cooling. The rear third of the No. 5 OD liner scoops that are circumferentially located between diffuser struts were capped off to provide a more uniform exit temperature pattern.

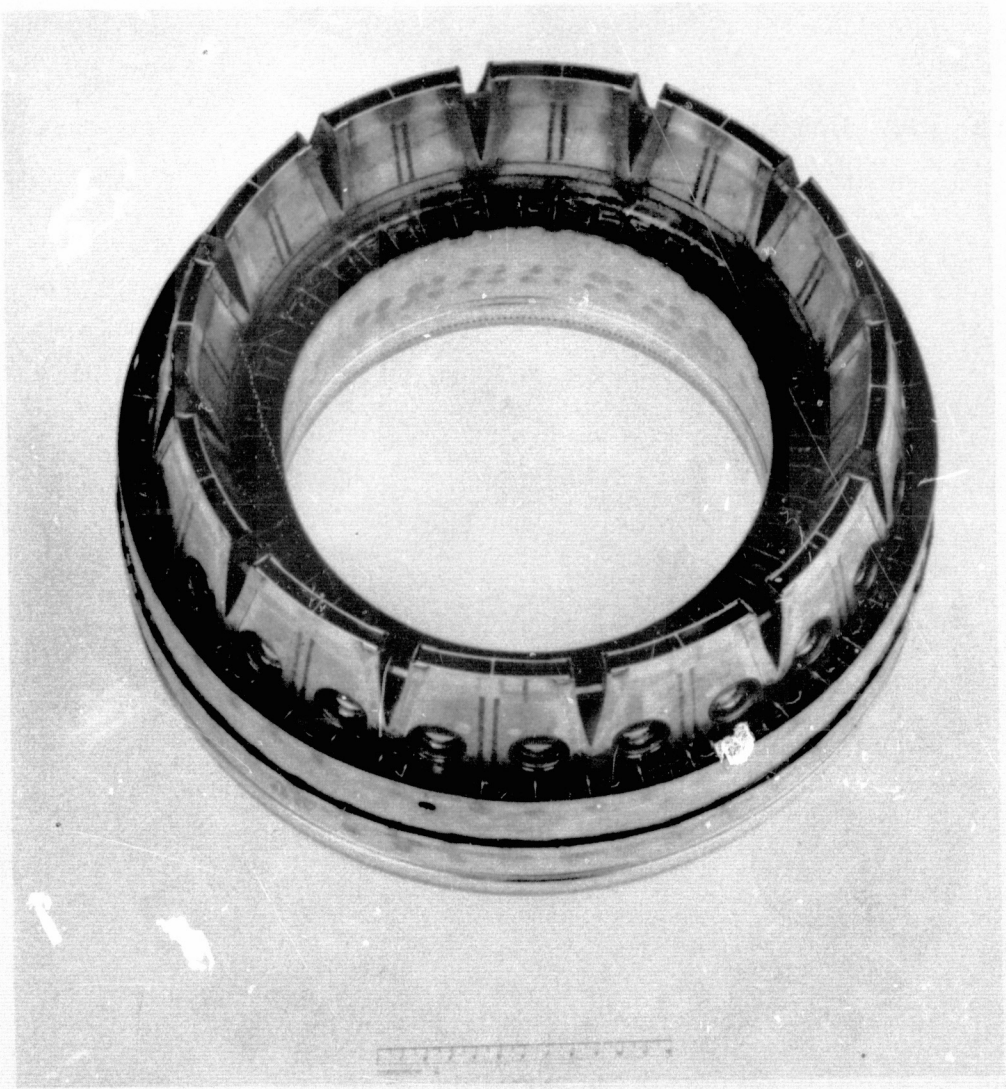

Figure 37. Combustor Assembly Model 1-1A (View 1) FE 68024

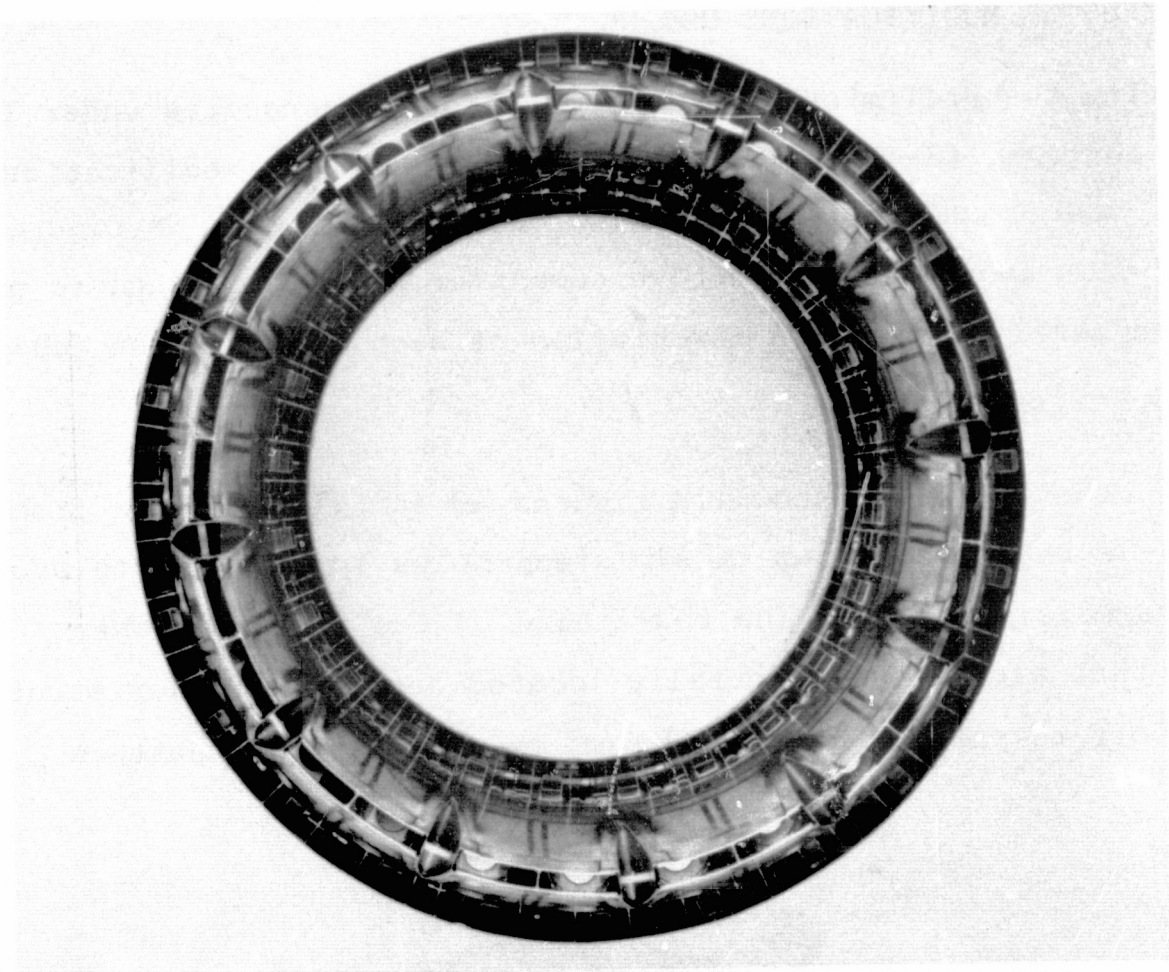

Figure 38. Combustor Assembly Model 1-1A (View 2)

FE 68026

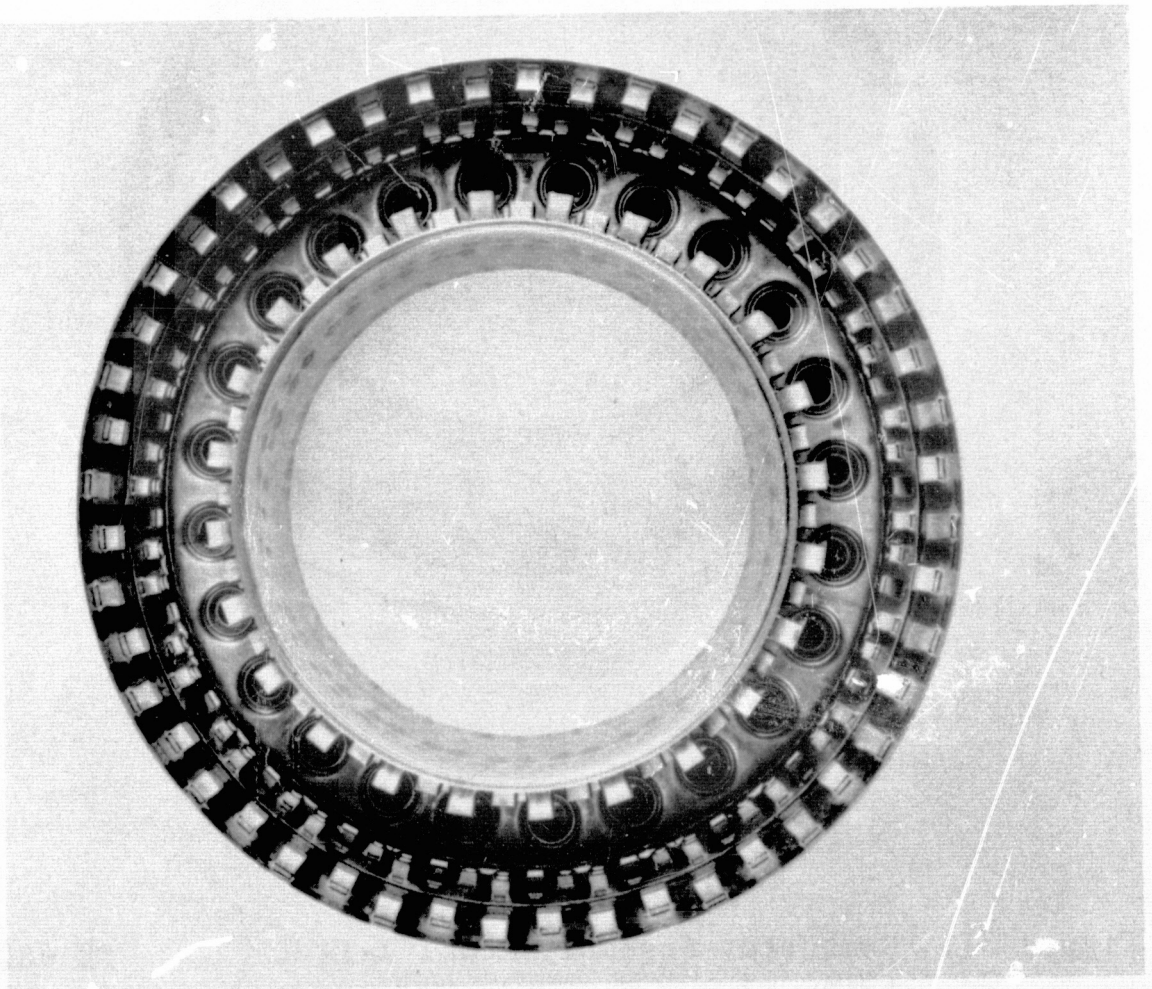

Figure 39. Combustor Assembly Model 1-1A (View 3)

FE 68025

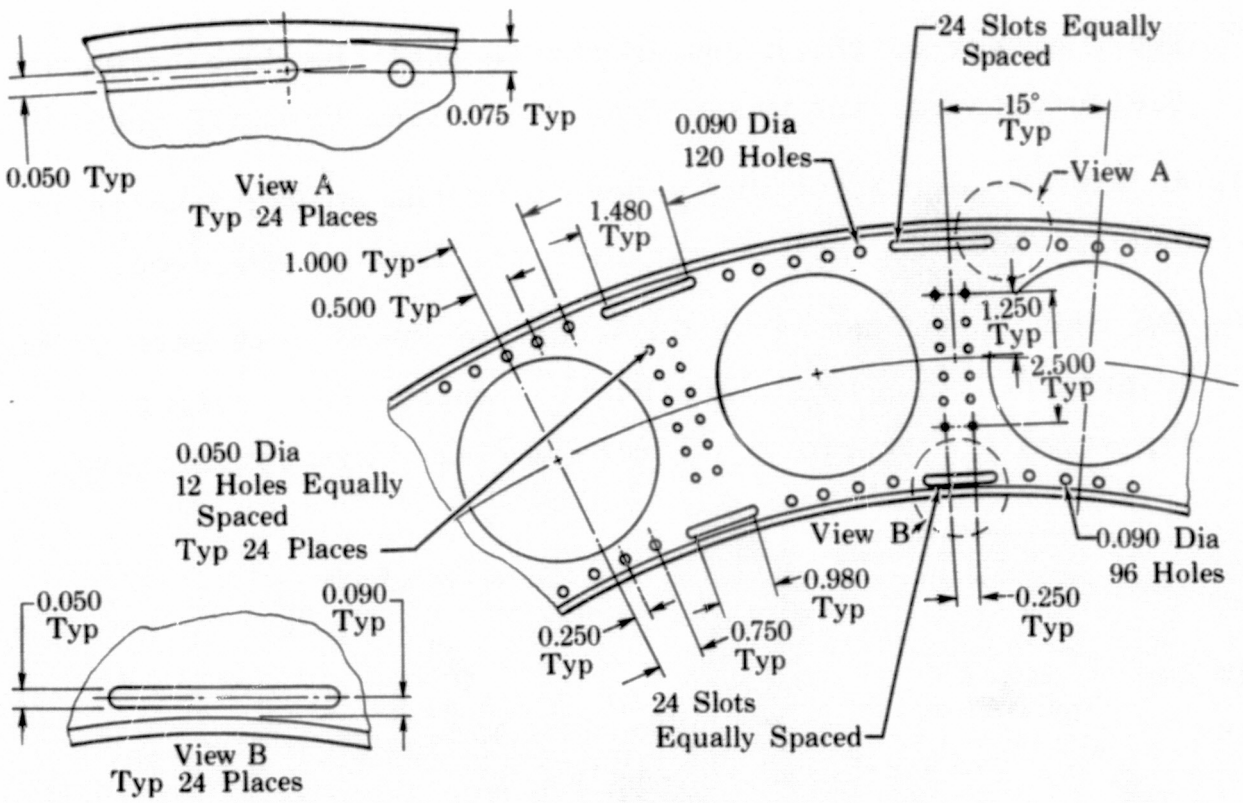

Figure 40. Advanced Annular Combustor Model 1-1B FD 21433

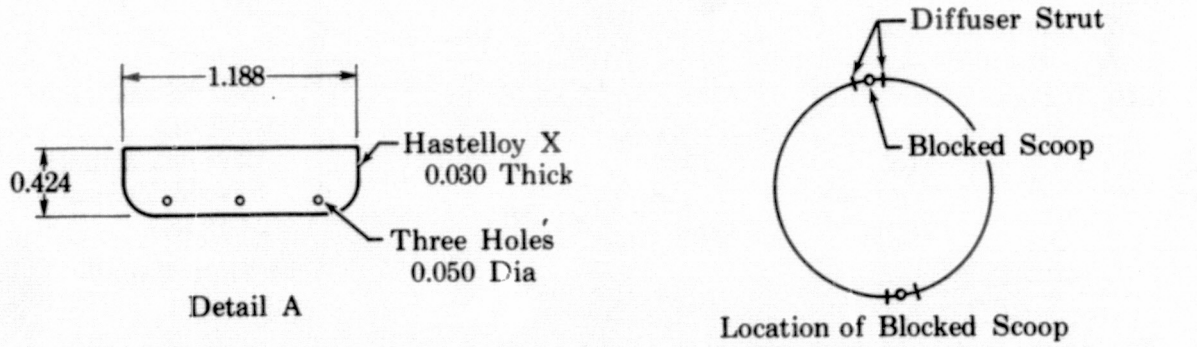

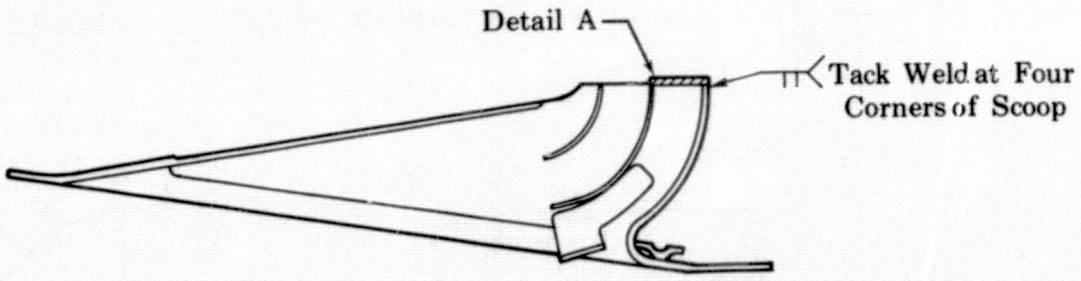

Figure 41. Modification to Alternate No. 5 Scoops, OD Liner Combustor Model 1-1B FD 22020A

2. Model 1-1C

The Model 1-1C, as shown in figures 42 and 43, is the same as the Model 1-1B except as follows:

1. The diameter of holes on the OD and ID edge of the dome were increased from 0.090 inch to 0.150 inch to increase the cooling air to the dome lip.

2. The diameter of the holes in the face of the dome between the fuel struts was increased from 0.050 inch to 0.175 inch.

3. An airflow deflector was placed over the enlarged holes in Item 2 above to deflect air over the face of the dome.

4. The caps on the number 5 OD scoops of Model 1-1B were trimmed to provide a gap of 0.120 inch to improve the cooling of the scoop and to provide a more uniform exit temperature.

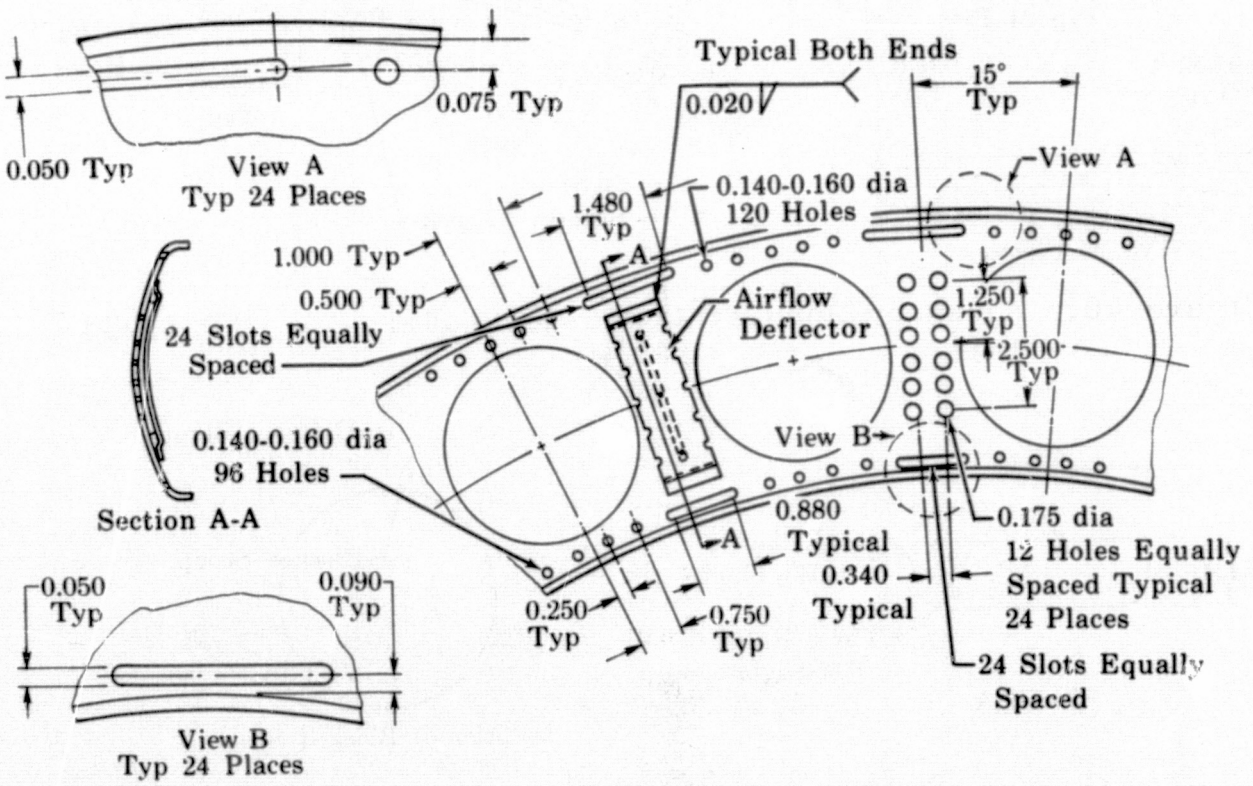

Figure 42. Advanced Annular Combustor Model 1-1C FD 22024A

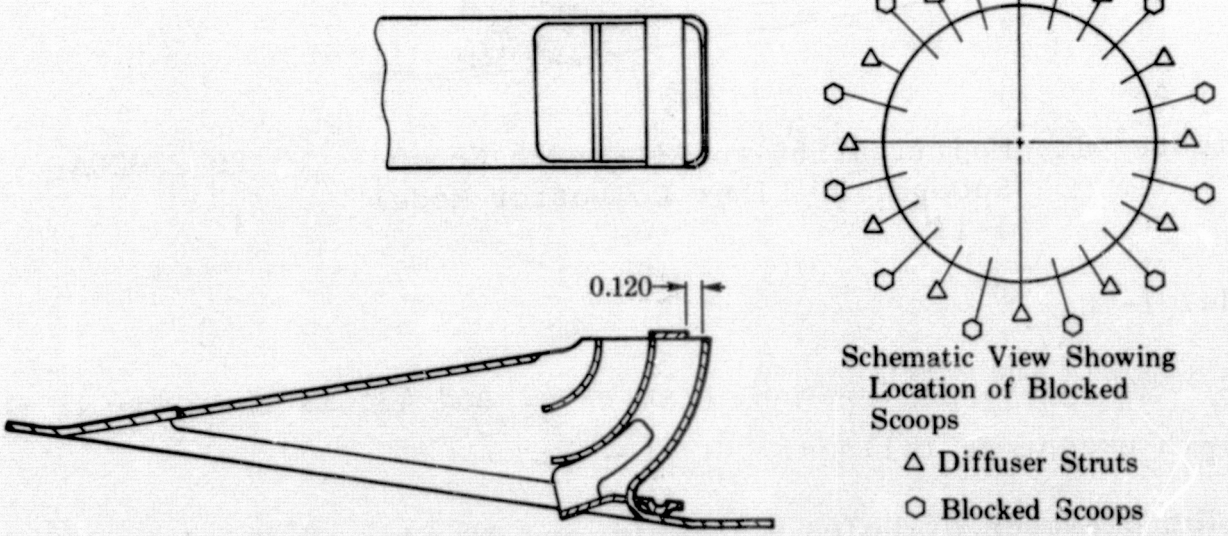

Figure 43. Modification to Scoop No. 5, OD Secondary Liner, Model 1-1C FD 22032

3. Model 1-1D

The caps were removed from the number 5 scoops of Model 1-1C, with the resulting configuration being designated Model 1-1D. This modification was made to increase the secondary airflow to improve the exit temperature profile.

4. Model 1-1E

The Model 1-1E combustor, as shown in figures 44 and 45, incorporated several major modifications to improve performance and to provide improved metal cooling of the dome and primary liners. These modifications included:

1. Replacing the original dome with a spare dome.
2. Adding cooling slots to the spare dome on the OD and ID edges midway between the swirl cups.
3. Removing 0.250 inch from the dome lips.
4. Adding airflow deflectors around each swirl cup to direct cooling air over the face of the dome. A ring of holes around each swirl cup was added to supply air to the deflectors.

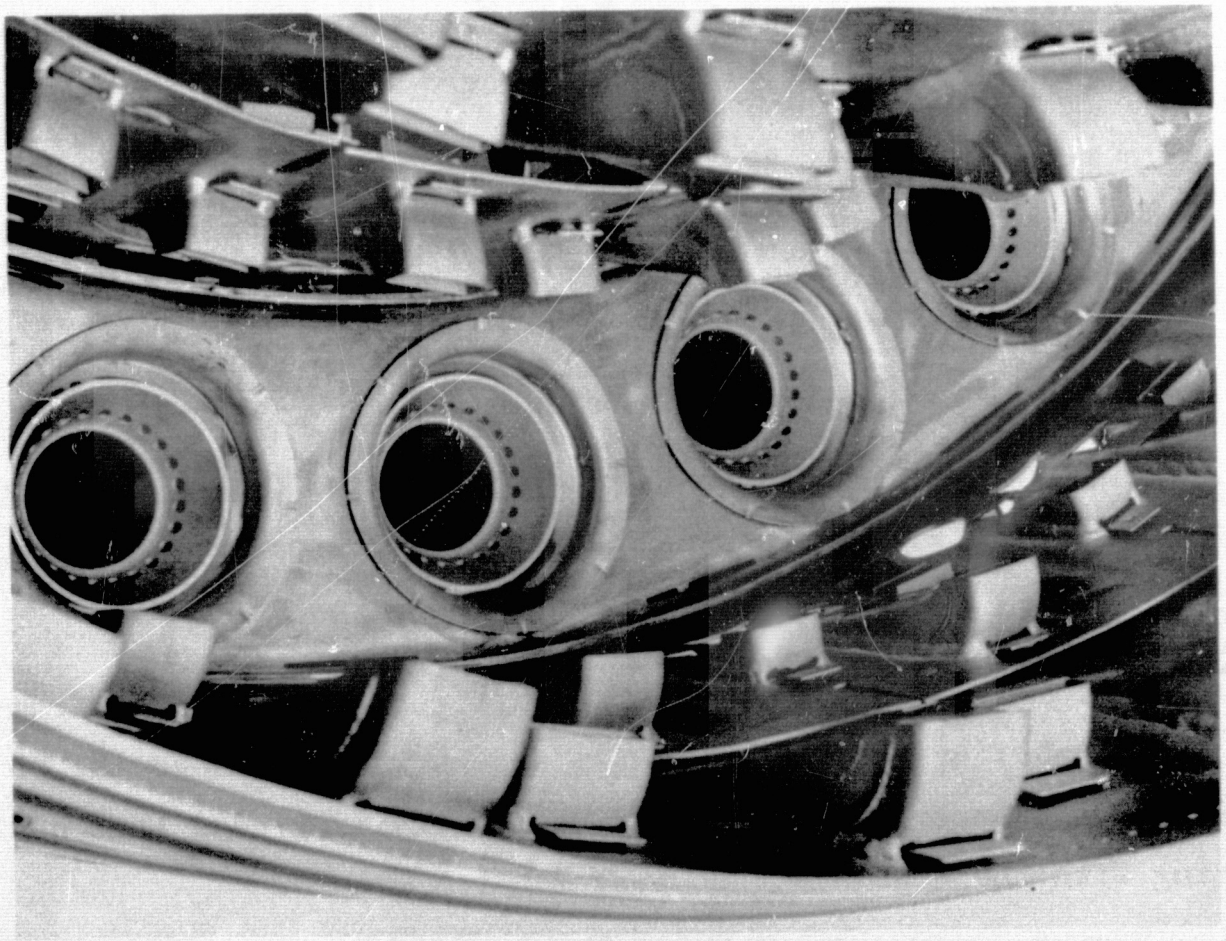

Figure 44. Model 1-1E Combustor FE 72430

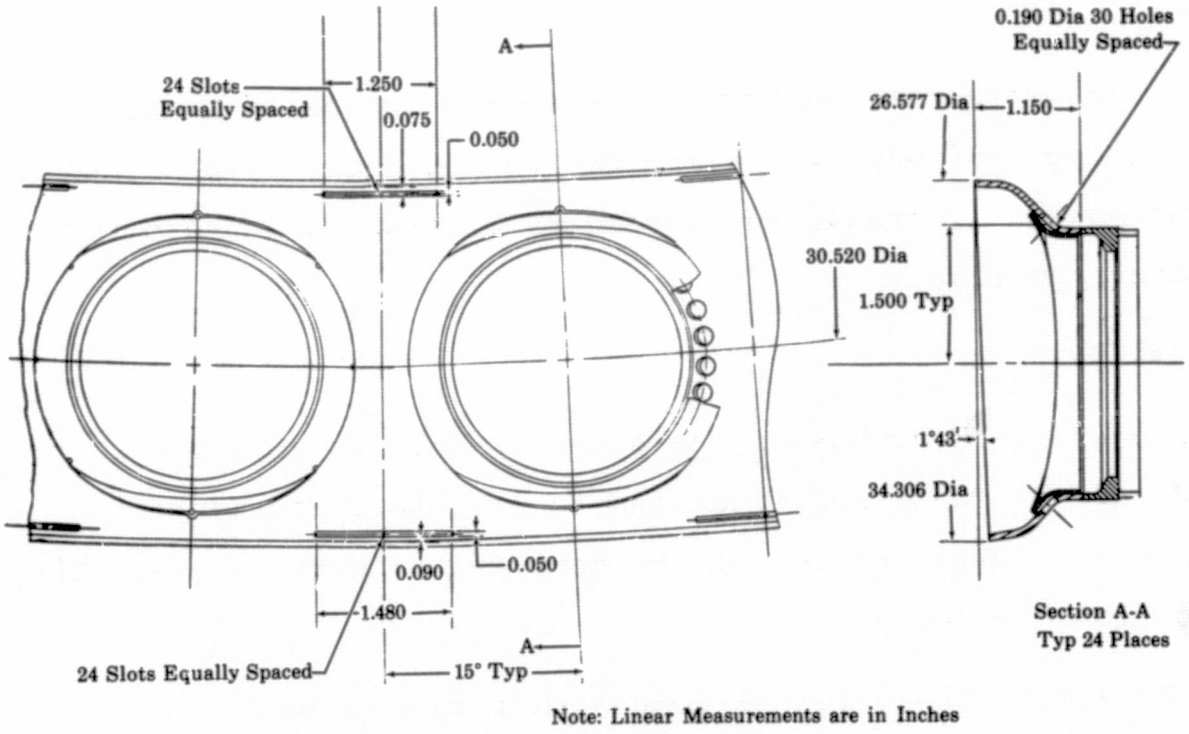

Figure 45. Dome Modification, Model 1-1E FD 22815

5. Replacing the original OD and ID primary liner support rings with redesigned rings to provide a more rigid structure preventing the primary liner cooling gaps from closing.

6. Replacing the ID primary liner with the spare liner since a number of scoops were severely damaged.

7. Blocking the center 1/3 of the number 4 and 5 ID and OD liner scoops and complete blockage of the number 1 ID and OD liner scoops, except for a small cooling gap, to increase the combustor pressure drop. This was done to correct the unbalanced airflow split between the ID and OD passages.

8. Adding false walls to the ID and OD passages of the diffuser to eliminate stall which had occurred with the original design.

5. Model 1-1F

The Model 1-1F combustor, as shown in figure 46, differed from the Model 1-1E combustor in that thumbnail scoops were added to the OD primary liner to prevent the warping of the trailing edge that had been occurring with the Model 1-1E combustor.

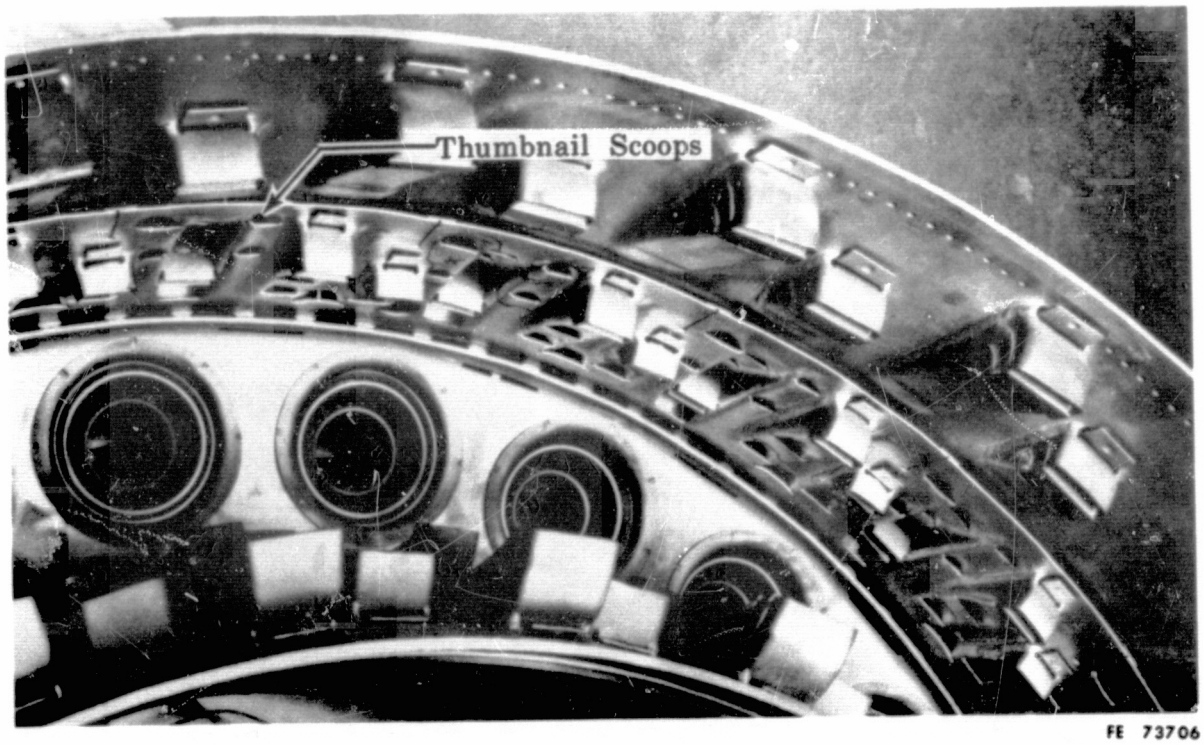

Figure 46. Model 1-1F Combustor FD 24686

D. AERODYNAMIC ANALYSIS OF THE MODEL 1-1F COMBUSTOR

The performance and structural cooling of the Model 1-1F were considered adequate to begin endurance testing. An aerodynamic analysis of the Model 1-1F combustor and diffuser to determine the theoretical pressure distribution for that configuration was made as follows:

1. Design Procedure

The design modifications (shown in figures 44 and 45) for cooling the combustor dome were based on results from combustor testing conducted at the NASA Lewis Research Center and on past experience with combustors of similar design. The resulting areas of the dome flow passages are summarized in table 3, page 52.

Although the original diffuser design was acceptable by the design standards (figure 35), test results and visual inspection of flow marking on the walls indicated that a stall problem existed. Recent experience with similar diffusers indicated a conservative modification was necessary. The false wall design was made to reduce the diffuser area by 10% (both OD and ID passages) in the plane of the snout leading edge and by 20% (both OD and ID passages) at the diffuser exit.

Table 3. Dome Flow Passage Areas

ITEM	AREA ($in.^2$)
Swirlers	23.040
OD Slots	1.824
ID Slots	1.488
Dome Air Deflector	10.248
OD Primary Liner Gap	11.016
ID Primary Liner Gap	8.970
Cone Aligning Rings	8.860
Holes in Cone	7.080
Total	72.526

The false walls were contoured to give a smooth increase in the area per unit flow down the length of the diffuser. Figure 47 shows the area/pound airflow/second versus length for the modified diffuser.

2. Diffuser and Combustor Pressure Distribution

To determine the diffuser and combustor pressure distribution, an iterative calculation on the dome airflow was required. A trial value of the snout airflow was assumed. The remaining airflow was considered to be divided equally between the ID and OD passages. A value of the diffuser exit area/pound airflow/second was calculated and the resulting theoretical diffuser velocity head change was determined. The diffuser pressure loss was then calculated as 1/3 of the velocity head change to provide the diffuser exit or combustor inlet pressure level. The forward combustor static pressure was then assumed to be equal to the combustor exit total pressure. The dome supply pressure was assumed to be equal to the snout inlet static pressure. The resulting dome airflow was calculated and then compared with the assumed airflow. If they did not agree, a new dome airflow was assumed and the procedure repeated.

The final set of calculations and a more extensive discussion of the assumptions involved follow:

a. Diffuser Pressure Loss

A total airflow of 110 pounds/sec at total temperature and pressure of $1060^{\circ}R$ and 90 psia was assumed. These are the airflow parameters of test condition 6.

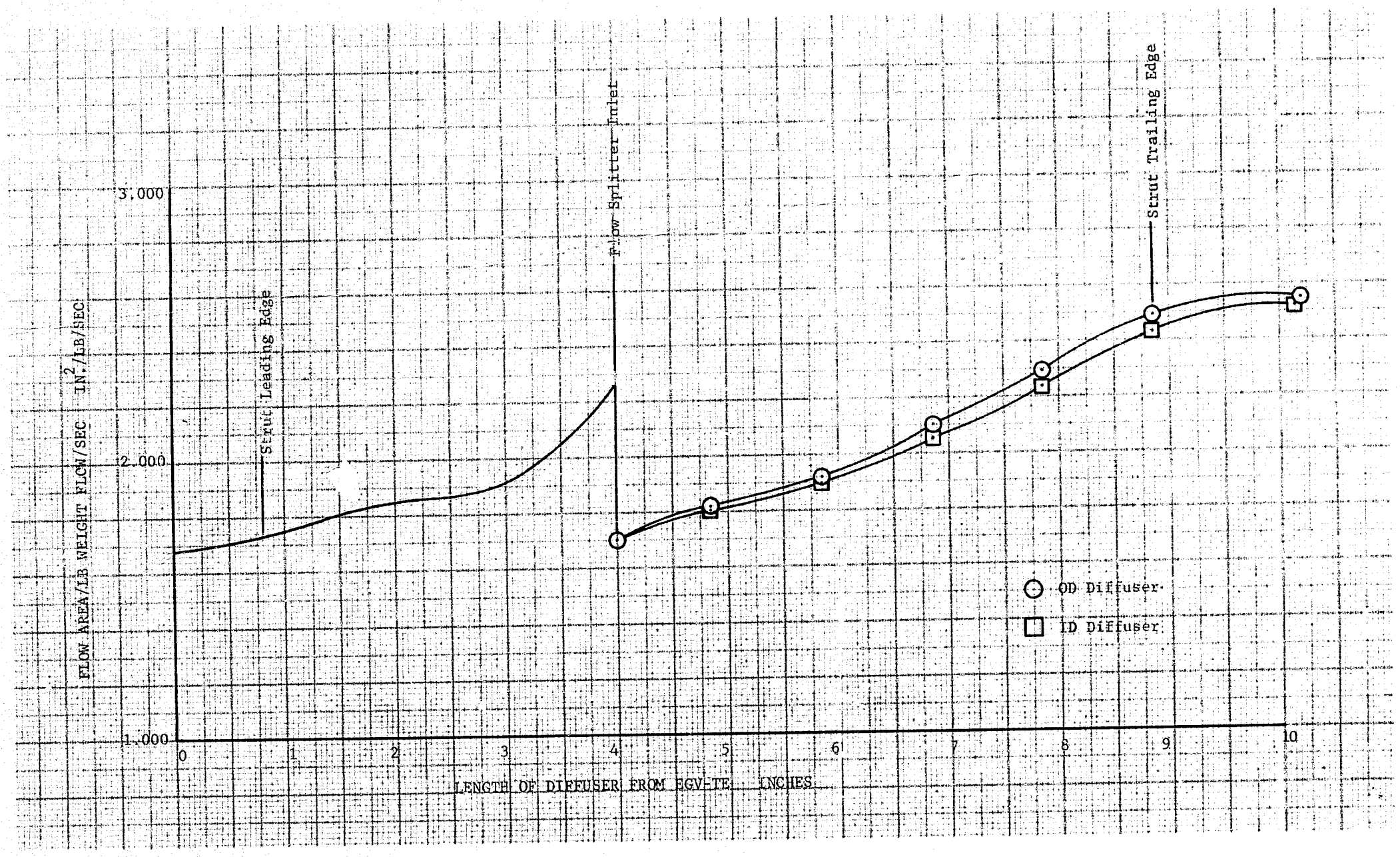

Figure 47. Flow Area to Weight Flow Ratio vs Diffuser Length

DF 64490

A trial value of the dome airflow of 22.52 pounds/second was assumed. The resulting diffuser exit area/pound airflow/second was calculated to be

$$\frac{121.5 \text{ in.}^2}{43.74 \text{ lb/sec}} = 2.78 \text{ in.}^2/\text{lb/sec}$$

The diffuser inlet area/pound airflow/second is:

$$\frac{182.54 \text{ in.}^2}{110 \text{ lb/sec}} = 1.66 \text{ in.}^2/\text{lb/sec}$$

The diffuser area ratio therefore is:

$$\frac{A_2}{A_1} = \frac{2.78 \text{ M}^2/\text{pound/second}}{1.66 \text{ M}^2/\text{pound/second}} = 1.66$$

The diffuser inlet q was obtained as follows:

$$\frac{W\sqrt{T}}{PA} = \frac{110\ \sqrt{1060}}{90\ (182.54)} = 0.218$$

From compressible flow tables:

$$M = 0.248$$

$$q = 4.13\ P_t$$

$$A/A^* = 2.43$$

$$P_s/P_t = 0.959$$

For the diffuser exit:

$$\frac{A}{A^*} \text{ Exit} = \frac{A}{A^*} \text{ Inlet} \times \frac{\text{A Exit}}{\text{A Inlet}} = 2.43\ (1.66) = 4.06$$

From compressible flow tables:

$$M = 0.145$$

$$q = 1.43\%\ P_t$$

$$\Delta q = q \text{ inlet} - q \text{ exit} = 4.13\ P_t - 1.43\ P_t = 2.70\ P_t$$

The diffuser loss was assumed to be 1/3 of the theoretical velocity head change, Δq, through the diffuser. Experience indicates this is a typical loss for diffusers of similar geometry - therefore:

$$\text{Diffuser loss} = 1/3\ \Delta q = 1/3 \times 2.70\ P_t = 0.899\%\ P_t$$

and

$$\text{Diffuser exit } P_t = \text{Inlet } P_t - 0.899\%\ P_t$$
$$= 90 - (0.00899 \times 90)$$
$$= 89.190 \text{ psia}$$

The diffuser exit Mach number, corrected for pressure loss may now be calculated:

$$\frac{W\sqrt{T}}{PA} = \frac{\sqrt{1060}}{(89.190)\ (2.78)} = 0.132$$

From compressible flow tables:

$$M = 0.146$$
$$P_s/P_t = 0.985$$

Therefore, P_s at the diffuser exit is:

$$P_s = P_t \times \frac{P_s}{P_t} = 89.190 \times 0.985$$

$$P_s = 87.893 \text{ psia}$$

b. Combustor Pressure Loss

Since the combustor flow area was changed, the pressure drop of the original design was multiplied by the square of the inverse flow area ratio to obtain the pressure loss of the modified combustor:

$$\frac{\Delta P}{P} \text{ modified combustor} = \frac{\Delta P}{P} \text{ original combustor} \times \left(\frac{A \times \text{original combustor}}{A \times \text{modified combustor}}\right)^2$$
$$= 2.33\% \left(\frac{351.9}{288.86}\right)^2 = 3.46\%$$

If the effects of pressure loss due to heat addition are neglected, the total pressure throughout the length of the combustor may be considered constant, since the mean velocity is relatively low. The magnitude of the pressure loss due to heat addition is on the order of 0.5% at maximum temperature rise conditions and considered negligible for this analysis. Static pressure does vary down the length of the combustor as a function of local velocity, but may be assumed equal to

total pressure on the forward portion of the combustor where mean velocity is negligible.

The combustor inlet total pressure (diffuser exit pressure), as determined in the preceding section on diffuser pressure loss, is 89.211 psia.

Combustor exit total pressure is therefore:

$$89.21 - (0.0346 \times 89.19) = 86.11 \text{ psia}$$

c. Dome Airflow

To calculate the dome supply pressure, the following assumptions are made:

1. No loss in total pressure has occurred in the flow from the diffuser inlet to snout inlet.

2. External streamline diffusion will occur isentropically from the mainstream velocity to the flow velocity in the snout intake.

3. Flow that has entered the snout incurs a 1-q dump loss. Therefore, the combustor dome supply pressure is equal to the static pressure in the snout inlet. The heavy reinforcing rings on the snout leading edges are contoured to form a diffusing path inside the snout with an area ratio of 1.14:1. This diffuser is neglected in the calculations since the maximum possible static pressure rise through this diffuser is only 0.2%.

The assumed dome airflow is used to calculate the snout inlet static pressure as follows:

$$\frac{W\sqrt{T}}{PA} = \frac{22.6\sqrt{1060}}{90\ (61.5)} = 0.132$$

From compressible flow tables:

$$M = 0.147$$

$$P_s/P_t = 0.985$$

Therefore, the snout inlet static pressure is:

$$P_s = P_t\ (P_s/P_t) = 90\ (0.985)$$

$$= 88.67 \text{ psia}$$

The dome airflow is calculated as follows:

$$P_s/P_t = 86.11/88.67$$

From compressible flow tables:

$$\frac{W\sqrt{T}}{PA} = 0.184$$

An overall discharge coefficient for the dome flow passages of 0.62 is assumed. The effective dome area is then:

$$72.5 \times 0.62 = 45 \text{ in.}^2$$

Therefore, the dome airflow is:

$$W = 0.184\ (88.67)\ (45)/\sqrt{1060}$$

$$W = 22.52 \text{ lb/sec}$$

which agrees with the assumed value of dome airflow.

SECTION IV
TASK III - PRELIMINARY PERFORMANCE EVALUATION

A. OBJECTIVE

The objective of the preliminary performance evaluation was to obtain a limited amount of data at the contract test conditions to:

1. Check out instrumentation and all required facility equipment.
2. Measure the isothermal pressure loss.
3. Measure the diffuser inlet airflow profile and correct, if required, to an airflow profile simulating the discharge of a JTF17A-20 compressor.
4. Establish the general combustor operating characteristics including efficiency, pressure loss, and temperature profile.
5. Achieve the desired temperature profile.

The combustor performance goals were as follows:

1. Combustion efficiency - 98%
2. Maximum combustor total pressure loss - 8%
3. At any radial position of the combustor outlet, the local peak temperature should not exceed the specified temperature at that position by more than 100°F.

B. DISCUSSION OF TESTING AND RESULTS

The Model 1-1A combustor (the original combustor scheme, figure 48), was tested for a total of 5.7 hours. The flow area distribution for this combustor is shown in table 2 (page 41). Test Points 1 through 5 of table 4 (page 61) were conducted with an undistorted diffuser inlet profile, as shown in figure 49. A ΔTVR value of 1.405 was recorded at an average exit temperature of 1848°F (Test Point 4 of table 4). A hot spot of 2350°F was located near top dead center of the rig, with lesser hot spots located downstream of the majority of the 12 diffuser struts. The combustor average radial exit temperature profile for this test is shown in figure 50. Higher exit temperature levels could have been attained, but it was not considered prudent at that time.

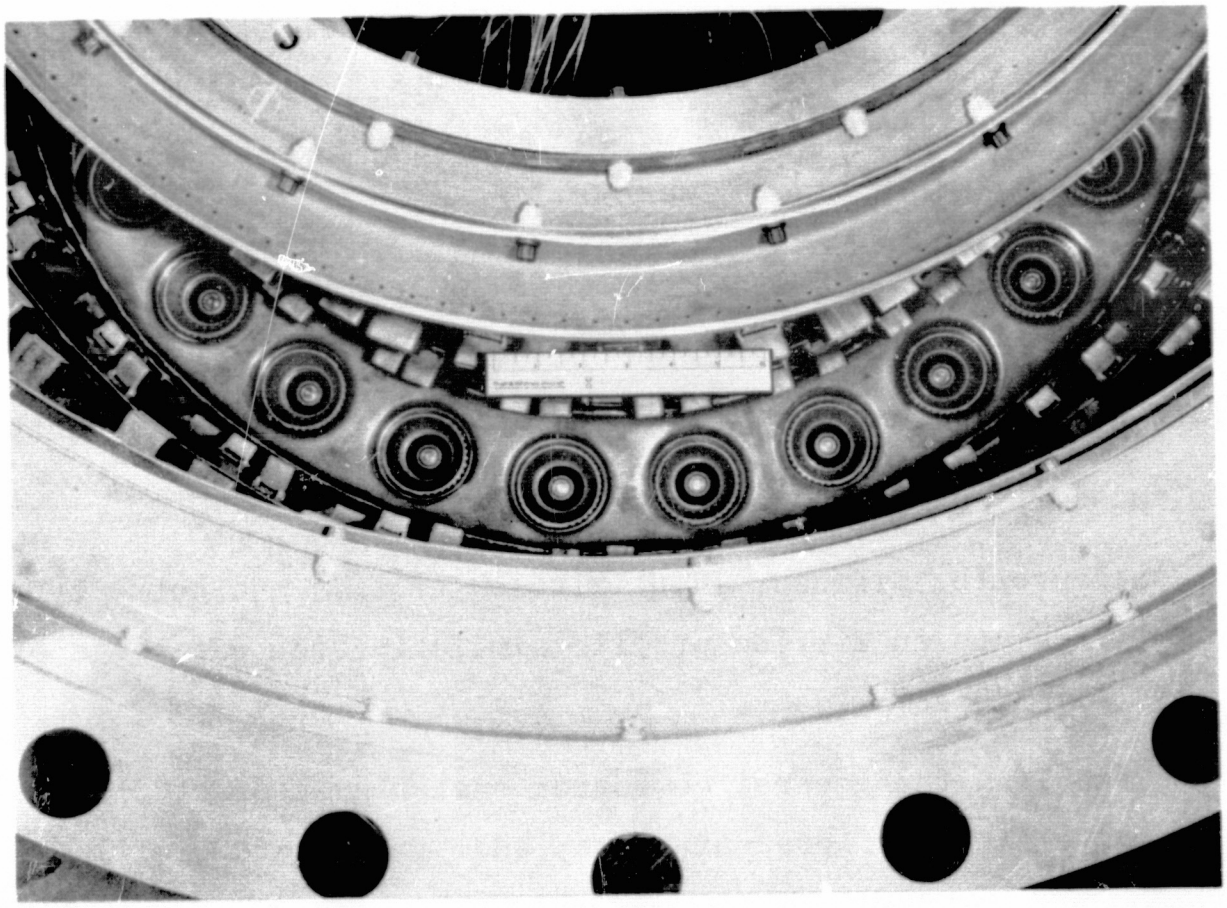

Figure 48. Model 1-1A Combustor and Diffuser Assembly FE 68320

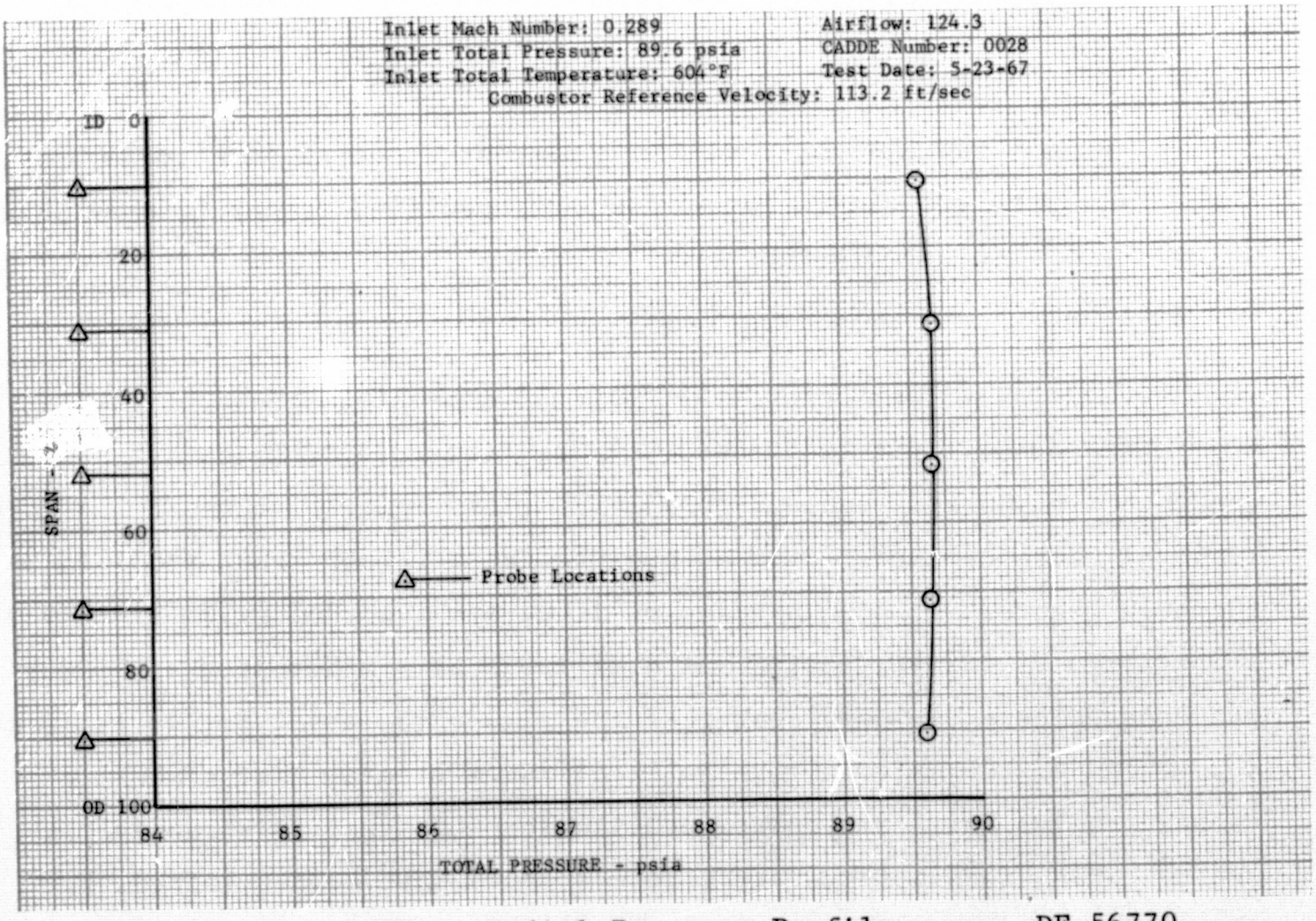

Figure 49. Average Radial Pressure Profile at Diffuser Inlet DF 56770

Table 4. Advanced Annular Combustor, Task III Test Summary

TEST POINT	DATE	AIRFLOW (lb/sec)	INLET TOTAL PRESSURE (psia)	INLET TEMPERATURE (°F)	COMBUSTOR REFERENCE VELOCITY (ft/sec)	DIFFUSER INLET MACH NUMBER	FUEL FLOW (lb/hr)	FUEL/AIR RATIO	AVERAGE EXIT TEMPERATURE (°F)	ΔTVR	COMBUSTION EFFICIENCY (%)	OVERALL COMBUSTOR PRESSURE LOSS (%)	CADDE NUMBER	CUMULATIVE COMBUSTOR TIME (hr)	COMBUSTOR MODEL NUMBER	CONTRACT TEST CONDITION NUMBER
1	5/16	119.0	87.5	522	102.5	0.261	----	---	----	---	-----	1.61	13	0	1-1A	
2	5/16	92.7	59.8	614	127.7	0.283	3660	0.010	1384	1.323	-----	3.31	15	0.5	1-1A	
3	5/19	182.9	89.8	590	162.6	0.463	----	---	----	---	-----	6.42	21	0.5	1-1A	
4	5/23	124.3	89.6	604	113.2	0.289	8239	0.0185	1848	1.405	105.6	2.93	28	1.8	1-1A	
5	5/25	125.9	90.3	603	113.6	0.290	7952	0.0175	1800	1.383	-----	4.20	40	3.3	1-1A	
6	5/26	125.0	89.4	603	114.8	0.292	7906	0.0176	1807	1.373	107.7	3.83	41	3.4	1-1A	
7	6/3	115.8	88.0	600	107.0	0.291	0	---	----	---	-----	4.14	48	3.4	1-1A	
8	6/6	109.3	89.1	604	100.0	0.297	0	---	----	---	-----	3.18	52	3.4	1-1A	
9	6/6	123.2	91.9	594	108.0	0.326	7717	0.018	1743	1.220	103.0	4.68	54	4.4	1-1A	
10	6/7	112.8	88.0	591	103.0	0.304	8850	0.022	2006	1.24	103.0	4.02	59	5.7	1-1A	
11	6/7	109.5	90.2	586	97.0	0.289	10194	0.026	2217	1.29	101.0	3.45	61	6.3	1-1A	6
12	6/23	99.1	89.2	598	90.0	0.252	0	---	----	---	-----	1.74	69	6.3	1-1B	
13	6/23	148.6	78.5	612	154.0	0.474	0	---	----	---	-----	7.96	71	6.3	1-1B	
14	6/23	109.2	87.7	602	101.0	0.286	7754	0.019	1852	1.31	99.0	3.59	72	6.6	1-1B	
15	6/23	102.3	88.9	598	93.4	0.265	7796	0.021	1923	1.36	99.0	3.17	73	6.9	1-1B	5
16	7/11	114.9	90.0	607	104.2	0.328	8204	0.020	1893	1.358	102.4	4.67	95	8.5	1-1C	5
17	7/11	114.1	91.3	607	102.1	0.299	8810	0.0216	1981	1.394	102.1	5.55	96	9.1	1-1C	
18	7/11	116.0	90.2	601	104.5	0.318	9488	0.0229	2059	1.437	104.5	5.14	97	9.4	1-1C	
19	7/13	117.8	91.7	1123	155.2	0.396	5072	0.0120	1878	1.330	102.8	7.69	110	10.1	1-1C	
20	7/13	108.2	90.8	1145	146.1	0.377	5391	0.0139	2002	1.293	102.0	6.09	111	10.4	1-1C	
21	7/13	110.9	90.7	1157	151.0	0.384	6111	0.0154	2092	1.282	101.4	6.20	112	11.5	1-1C	
22	7/13	110.9	91.1	1155	150.2	0.379	6787	0.0171	2194	1.341	102.3	6.39	113	12.65	1-1C	4
23	7/13	112.0	90.3	600	100.6	0.305	8685	0.0217	1995	1.425	103.1	4.51	116	12.95	1-1C	
24	7/14	118.9	90.6	603	106.6	0.329	8614	0.0203	1899	1.426	101.8	5.28	124	13.3	1-1D	
25	7/14	110.8	90.3	602	99.8	0.294	8697	0.0220	1983	1.400	100.9	5.20	126	13.6	1-1D	
26	7/14	112.1	91.0	602	100.2	0.296	9178	0.0229	2056	1.420	102.3	5.50	127	14.1	1-1D	
27	7/18	121.2	90.6	600	108.6	0.326	8594	0.0198	1885	1.427	102.9	5.71	132	14.3	1-1D	5
28	7/18	113.0	90.3	601	101.6	0.305	9384	0.0232	2078	1.516	102.6	4.78	133	14.7	1-1D	
29	8/1	116.8	91.0	608	105.1	0.291	8645	0.0207	1893	1.448	99.0	3.53	159	14.9	1-1D	5
30	8/1	108.9	90.9	602	97.5	0.267	8677	0.0223	1971	1.453	98.8	3.28	160	15.5	1-1D	
31	8/3	115.1	90.1	596	103.2	0.313	7985	0.0194	1852	1.366	102.5	5.93	167	16.2	1-1D	5
32	8/3	113.5	90.8	621	103.4	0.308	8688	0.0214	1977	1.406	101.6	5.47	168	16.8	1-1D	
33	10/17	113.8	89.6	604	103.5	0.259	-----	------	----	-----	-----	5.42	171	16.8	1-1E	
34	10/17	111.7	87.6	602	101.5	0.254	8012	0.0201	1891	1.231	102.2	5.57	172	17.2	1-1E	
35	10/17	111.3	89.8	603	100.9	0.252	9535	0.0240	2115	1.255	102.3	5.44	173	18.0	1-1E	
36	10/19	110.3	89.1	598	100.3	0.251	8045	0.0204	1915	1.250	102.8	5.21	179	18.4	1-1E	
37	10/19	108.7	90.1	603	98.3	0.245	10141	0.0261	2232	1.287	102.2	5.17	180	18.8	1-1E	6
38	10/19	116.8	91.2	1155	157.7	0.353	-----	------	----	-----	-----	8.00	181	18.8	1-1E	
39	11/13	115.0	[illegible]	604	105.2	0.264	7995	0.0195	1882	1.24	104.2	5.50	190	19.9	1-1F	5
40	11/13	112.7	[illegible]	603	99.6	0.249	10147	0.0252	2194	1.32	103.0	5.08	191	21.9	1-1F	6
41	11/13	109.2	[illegible]	608	97.9	0.243	10116	0.0257	2236	1.25	102.9	5.00	192	22.5	1-1F	6
42	11/15	111.4	[illegible]	602	98.8	0.246	10008	0.0251	2188	1.24	102.8	5.15	197	23.2	1-1F	6
43	11/15	115.9	[illegible]	1165	157.6	0.332	5098	0.0123	1936	1.18	103.5	8.09	198	24.1	1-1F	3
44	11/15	109.[illegible]	[illegible]	1155	148.2	0.310	6724	0.0172	2215	1.21	103.7	7.31	199	25.3	1-1F	4

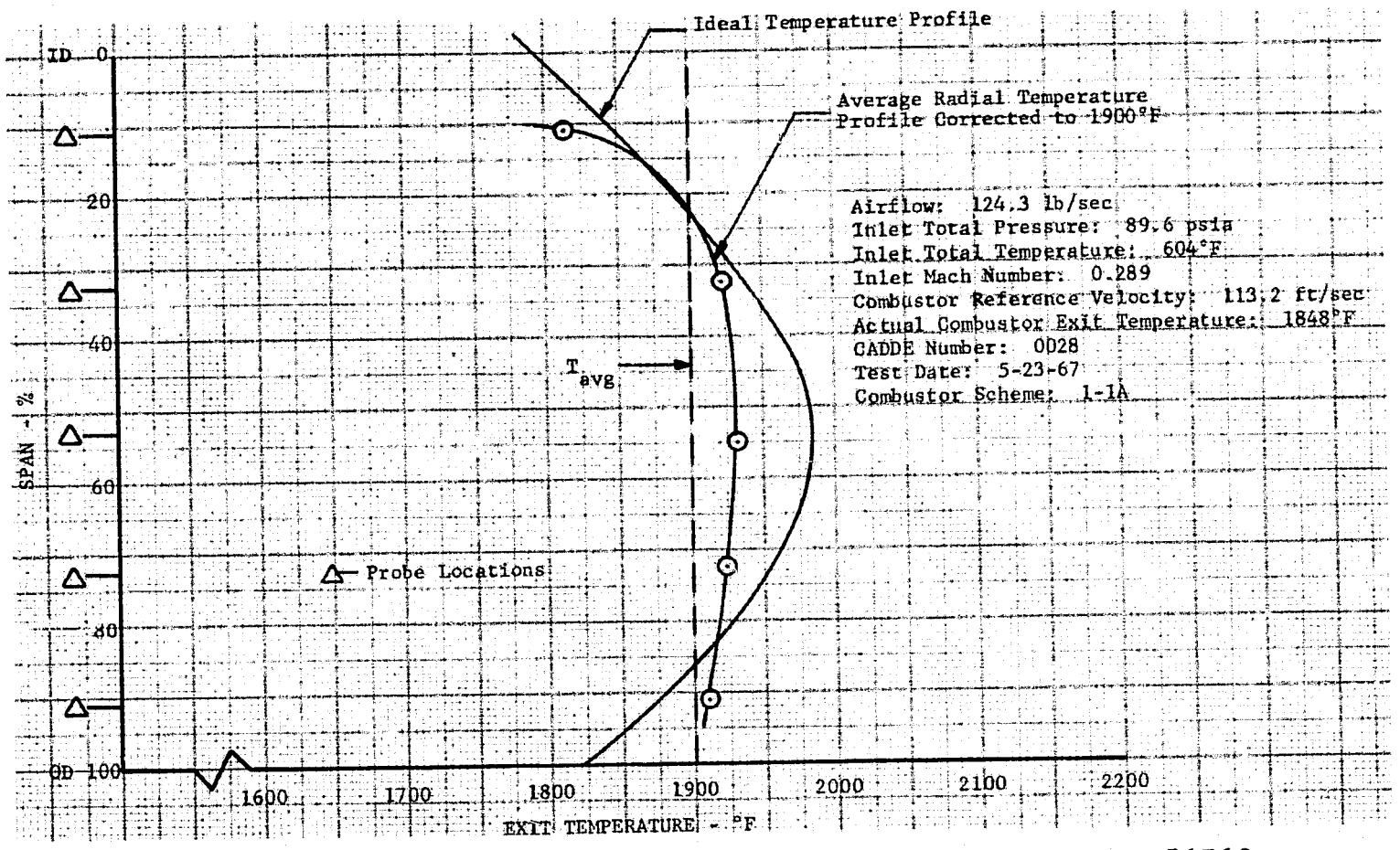

Figure 50. Combustor Average Radial Exit Profile, Test No. 28

DF 56769

The original diffuser inlet distortion plates (three screens on the OD and three on the ID) were then installed, and two cold flow points (Test Points 7 and 8 of table 4) were recorded to establish the non-burning inlet profile (figures 51 and 52). Test Points 9 through 11 of table 4 were combustion tests conducted with the distortion plates installed. Test Point 11 of table 4 (which is Contract Test Condition No. 6) was conducted at an average exit temperature of 2217°F. A hot spot of 2689°F was located near top dead center of the rig with lesser hot spots downstream of the diffuser struts as in previous testing. The average radial exit temperature profile (figure 53) was improved over the test results obtained with a flat diffuser inlet velocity profile. The ΔTVR value for this test was 1.29, as compared to 1.405 at an exit temperature of 1848°F with the flat inlet velocity profile. The overall combustor pressure loss had increased from 2.93 to 3.45%. Diffuser inlet mach number, as used for comparison of test data, was determined from air orifice mass flow, diffuser inlet area, and the mass weighted diffuser inlet total pressure. The total pressure measurement was made by instrumentation described on page 17, figures 17 and 18.

burned side walls on two of the No. 2 scoops and several small cracks and warped areas on the OD lip of the dome.

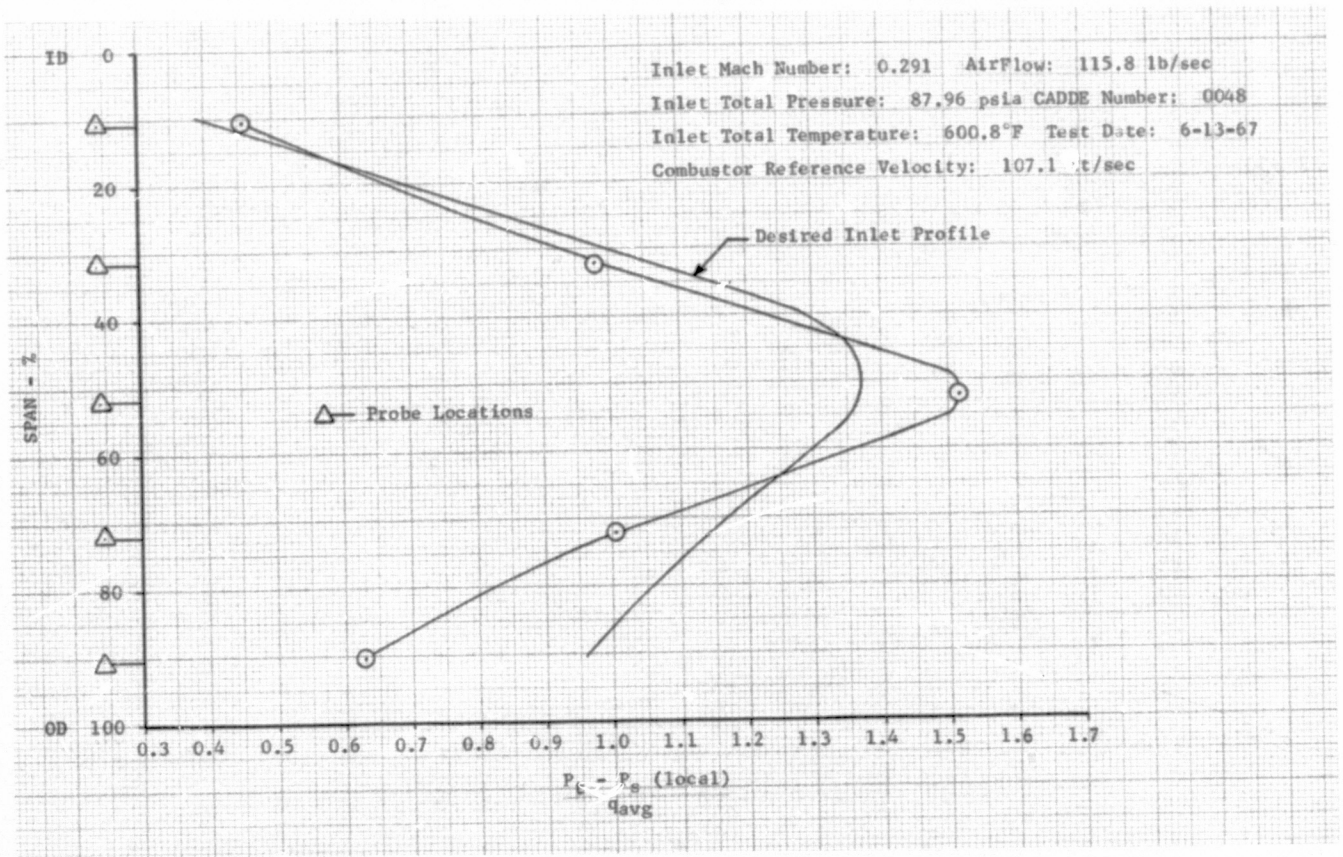

Figure 51. Diffuser Inlet Velocity Head Profile, Test No. 48 DF 57683

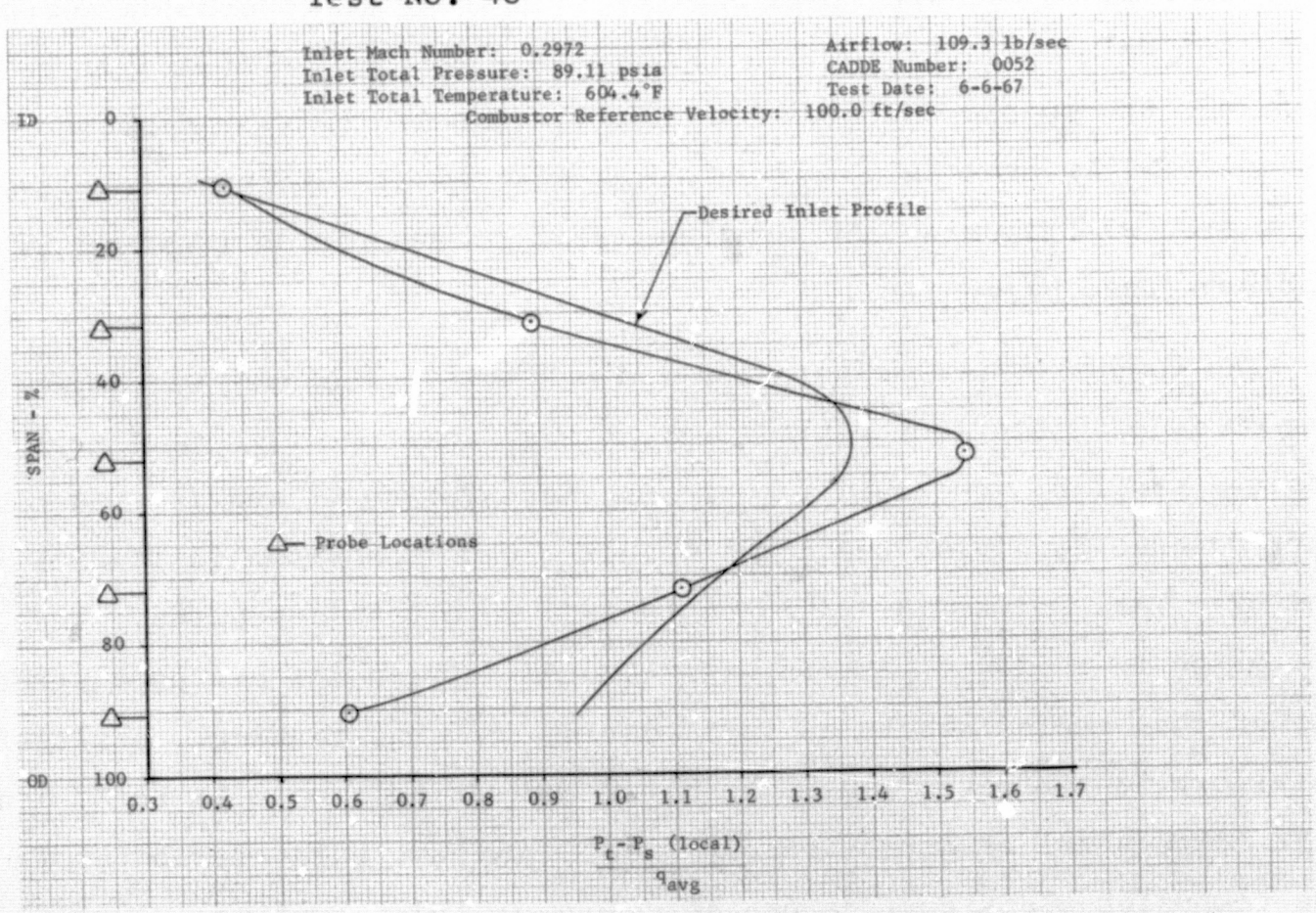

Figure 52. Diffuser Inlet Velocity Head Profile, Test No. 52 DF 57684

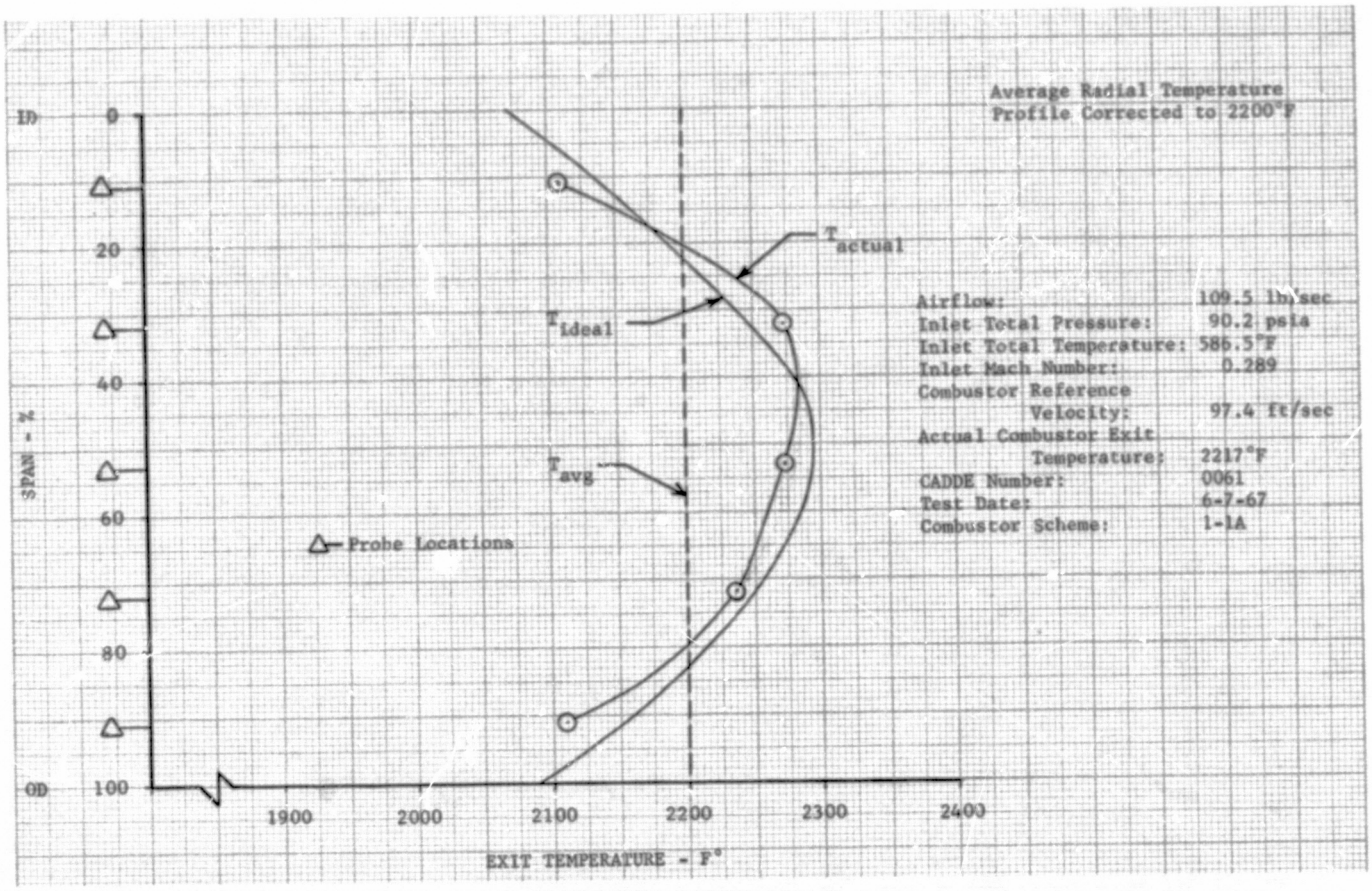

Figure 53. Combustor Average Radial Exit Temperature Profile, Test No. 61

DF 57693

The combustor was then modified to the Model 1-1B configuration by the addition of cooling slots and holes in the dome to provide additional dome and primary liner cooling (figure 54), and by the installation of partial caps on the No. 5 OD liner scoops located between diffuser struts (figure 55) to provide a more uniform exit temperature pattern. The flow area distribution for the Model 1-1B configuration is shown in table 5 (page 66).

The combustor was reinstalled and one layer of screen was removed from the OD inlet distortion plate to produce an inlet profile more near the desired profile. Two cold flow tests (Test Points 12 and 13 of table 4) were conducted, giving the inlet velocity profiles shown in figures 56 and 57. Test Points 14 and 15 of table 4 were then conducted. The hot areas in the exit pattern were located between the diffuser struts rather than behind struts as noted during previous testing. A slight deterioration in performance with ΔTVR increasing from 1.24 to 1.31 at an exit temperature of approximately 2000°F may have been attributed to either the combustor modifications or the change in inlet profile. A total of 1.2 hours of combustion time was accumulated on the Model 1-1B combustor.

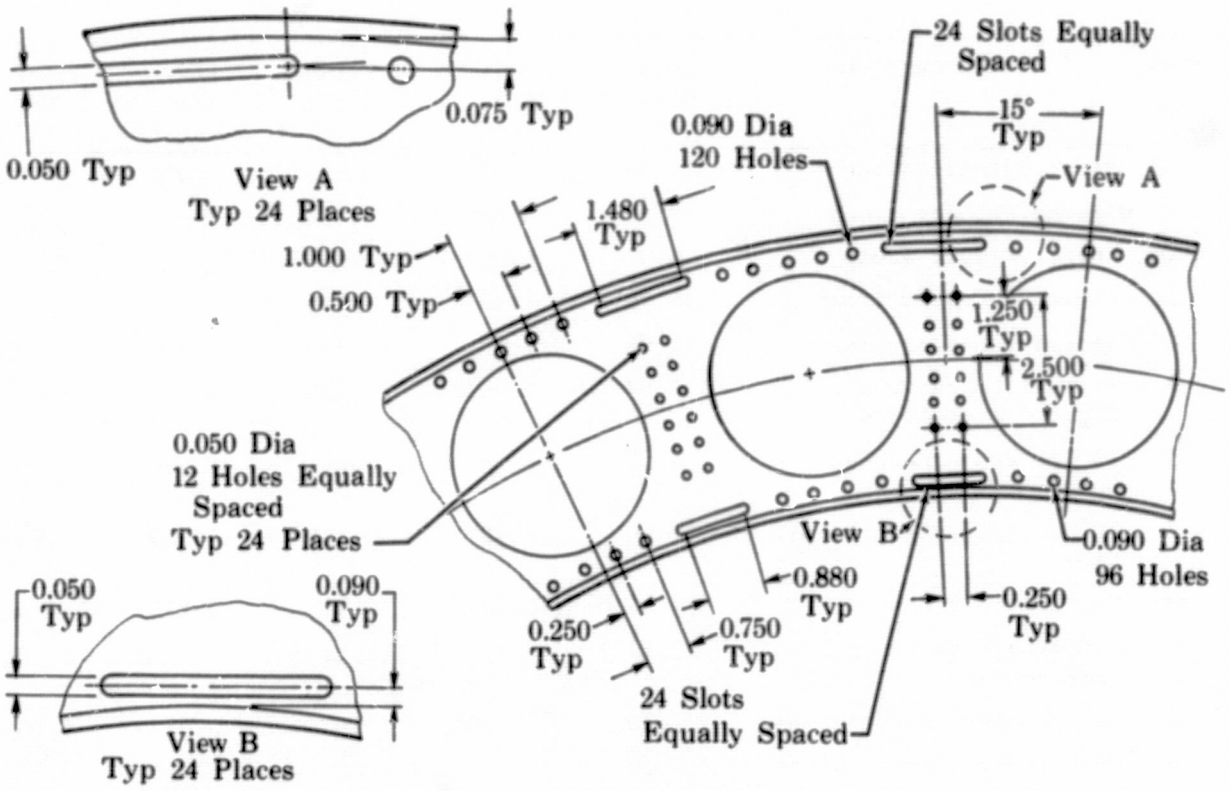

Figure 54. Advanced Annular Combustor, Model 1-1B

FD 21433A

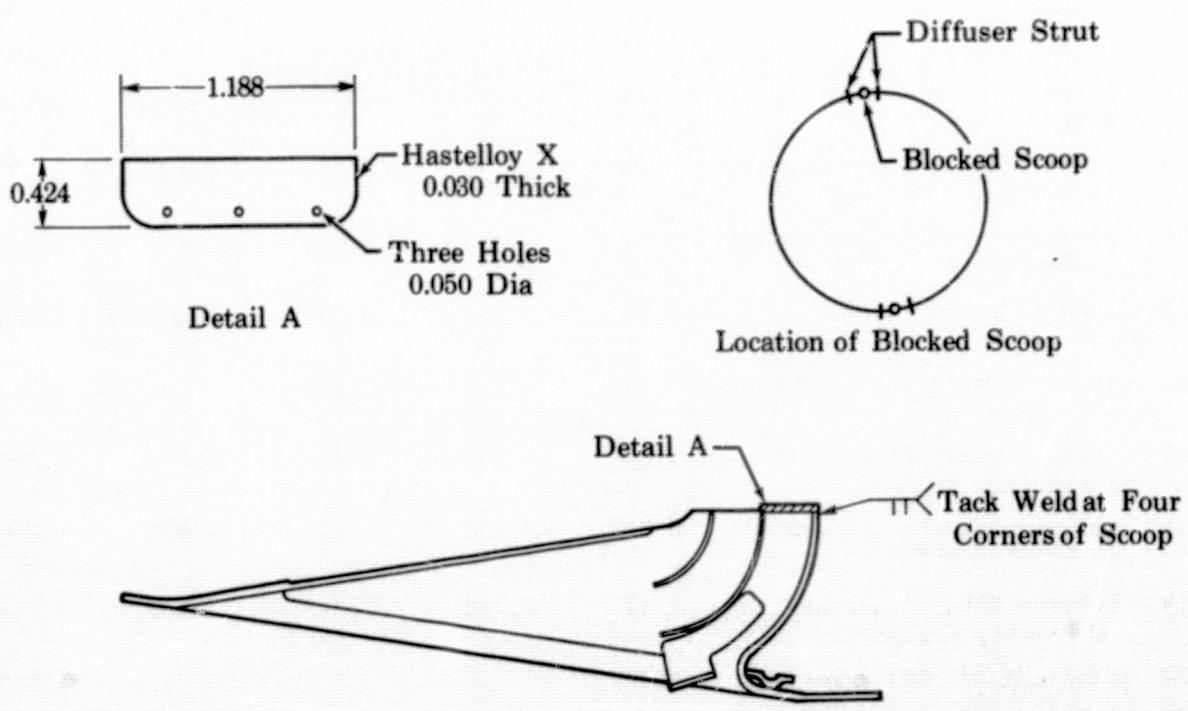

Figure 55. Modifications to Alternate No. 5 Scoops, OD Liner Combustor Model 1-1B

FD 22020A

Table 5. Flow Areas for the Advanced Annular Combustor, Model 1-1B

ITEM	DESCRIPTION	TOTAL AREA (%)	LENGTH (in.)	WIDTH (in.)	AREA (in.^{2})	TOTAL AREA (in.^{2})
A	First Primary Scoop	10.15	0.953	0.800	0.745	35.760
B	Second Primary Scoop	8.37	0.801	0.800	0.614	29.472
C	Third Primary Scoop	8.37	0.801	0.800	0.614	29.472
D	First Secondary Scoop	16.08	1.121	1.120	1.180	56.640
E	Second Secondary Scoop	12.06	1.121	1.120	1.180	42.480
F	Second Secondary Scoop Block Plates Added	2.67	0.767	1.120	0.785	9.420
1	ID Primary Liner Cooling Holes	4.01	0.310 slots		0.217	14.105
2	ID Secondary Liner Cooling Gaps	3.40	79.721	0.150	11.958	11.958
3	Cooling Film Gap	0.15	0.500	0.030	0.015	0.540
4	ID Transition Liner Film Cooling Gap	2.67	0.129, 0.183, and 0.104 dia			9.388
5	ID Rear Shroud Outlet	1.30	0.156 dia		0.0191	4.584
6	OD Primary Liner Cooling Gap	4.20	0.250 slots		0.145	14.790
7	OD Secondary Liner Cooling Gap	3.59	114.819	0.110	12.630	12.630
8	Cooling Film Gap	0.31	0.600	0.030	0.018	1.080
9	OD Transition Liner Film	3.29	0.129, 0.120, and 0.166 dia		0.094 in. dia	11.569
10	OD Rear Shroud Outlet	1.84	0.125 dia		0.0123	6.494
11	Holes in Cone	2.01	0.125 dia		0.0123	7.080
12	Holes in Cone Aligning Ring	2.51	0.125 dia		0.0123	8.856
13	First Primary Scoop Cooling Louver No. 1	0.40	0.575	0.050	0.029	1.392
14	First Primary Scoop Cooling Louver No. 2	0.40	0.575	0.050	0.029	1.392
15	Second Primary Scoop Cooling Louver	1.07	0.575	0.137	0.079	3.780
16	Third Primary Scoop Cooling Louver No. 1	1.07	0.575	0.137	0.079	3.780
17	Third Primary Scoop Cooling Louver No. 2	1.07	0.575	0.137	0.079	3.780
18	Louvers Between 2nd and 3rd ID Primary Scoops	0.48	0.600	0.117	0.070	1.680
19	Louvers Between 2nd and 3rd OD Primary Scoops	0.57	0.710	0.117	0.083	1.995
20	Swirlers P/N CKJ 2476	6.54			0.960	23.040
21	OD Slots in Dome	0.51	1.480	0.050	0.076	1.824
22	ID Slots in Dome	0.35	0.980	0.050	0.051	1.224
23	OD Holes in Dome	0.22	0.090 dia		0.0064	0.768
24	ID Holes in Dome	0.17	0.090 dia		0.0064	0.614
25	Holes in Dome Between Fuel Nozzles	0.16	0.050 dia		0.002	0.576
	Totals	99.99				352.163

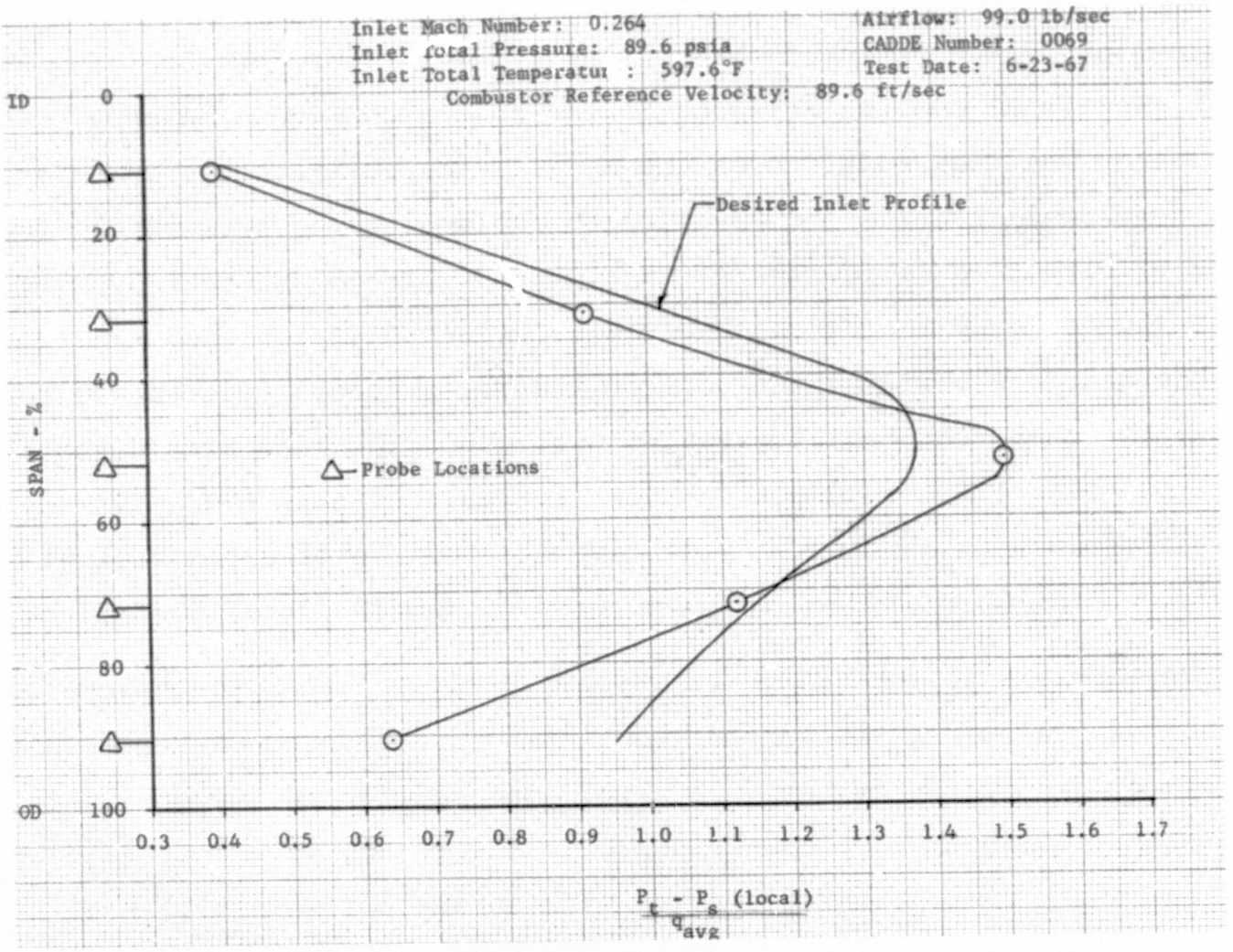

Figure 56. Diffuser Inlet Velocity Head Profile, Test No. 69

DF 57685

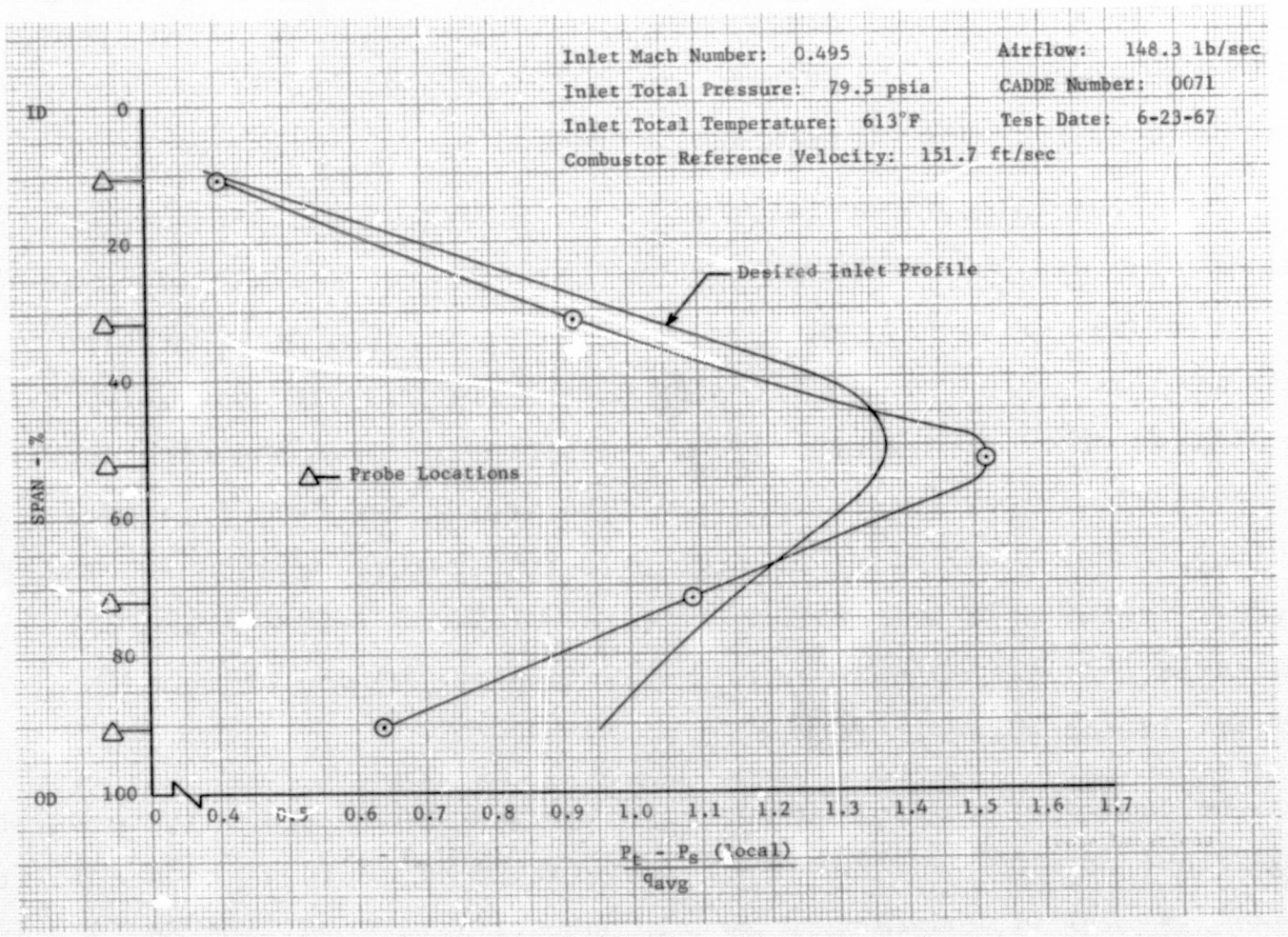

Figure 57. Diffuser Inlet Velocity Head Profile, Test No. 71

DF 57686

An inspection of the combustor showed no further metal burning but that additional cooling measures in the dome area were necessary. The combustor was then modified to the Model 1-1C configuration by enlarging the dome cooling holes and covering the holes located between the fuel nozzles with flow deflectors (figure 42) to improve the cooling airflow distribution over the dome. The modifications also included the removal of the rear one-third of the caps on the No. 5 scoops (figure 43) to improve the combustor exit temperature pattern. The flow area distribution for the Model 1-1C combustor is shown in table 6 (page 69). Testing was then resumed with the further modified inlet distortion plates (one screen on the OD plate and three screens on the ID plate) installed.

Test Points 12 through 22 of table 4 were conducted to measure the effect of fuel/air ratio and/or inlet temperature on combustor skin temperature, especially in the dome area. In addition to the original thermocouples, six thermocouples, as shown in figure 58, were installed on the combustor dome prior to testing. As shown in figure 59, an increase in fuel/air ratio at an inlet temperature of 600°F tended to raise dome skin temperatures in some areas and had little effect on skin temperatures in other areas. Figure 60 shows that an increase in combustor inlet temperature, while holding the fuel/air ratio constant, produces an almost equal increase in skin temperature.

The inlet velocity profile, as shown in figure 61, very closely matches the desired profile. Either the combustor modifications or the change of the distorted inlet profile had produced a deterioration in exit temperature pattern uniformity with a serious hot spot (2700°F at an average exit temperature of 2059°F) appearing near the right horizontal centerline looking upstream and ΔTVR increasing from 1.24 (Model 1-1A) to 1.39 (Model 1-1C) at an average exit temperature of 2000°F. The average radial exit temperature profile for Model 1-1C (figure 62) indicates that the ID had become hotter and the OD cooler than in Model 1-1B (as shown in figure 63).

The combustor was tested for 63 minutes at inlet and exit temperature conditions of 1155° and 2194°F (Test Point 22 of table 4) to accumulate a small amount of endurance time at Contract Test Condition No. 4. Test Point 23 was conducted to compare combustor performance after the 1150°F inlet temperature testing to that previously recorded (no change was noted).

Table 6. Flow Areas for the Advanced Annular Combustor, Model 1-1C

ITEM	DESCRIPTION	TOTAL AREA (%)	LENGTH (in.)	WIDTH (in.)	AREA ($in.^2$)	TOTAL AREA ($in.^2$)
A	First Primary Scoop	9.95	0.953	0.800	0.745	35.760
B	Second Primary Scoop	8.20	0.801	0.800	0.614	29.472
C	Third Primary Scoop	8.20	0.801	0.800	0.614	29.472
D	First Secondary Scoop	15.76	1.121	1.120	1.180	56.640
E	Second Secondary Scoop	11.82	1.121	1.120	1.180	42.480
F	Second Secondary Scoop Block Plates Added	3.07	0.887	1.120	0.919	11.028
1	ID Primary Liner Cooling Holes	3.93	0.310 slots		0.217	14.105
2	ID Secondary Liner Cooling Gaps	3.33	79.721	0.150	11.958	11.958
3	Cooling Film Gap	0.15	0.500	0.030	0.015	0.540
4	ID Transition Liner Film Cooling Gap	2.61	0.129, 0.183, and 0.104 dia			9.388
5	ID Rear Shroud Outlet	1.28	0.156 dia		0.0191	4.584
6	OD Primary Liner Cooling Holes	4.12	0.250 slots		0.145	14.790
7	OD Secondary Liner Cooling Gap	3.51	114.819	0.110	12.630	12.630
8	Cooling Film Gap	0.30	0.600	0.030	0.018	1.080
9	OD Transition Liner	3.22	0.129, 0.120, and 0.166		0.094 in dia	11.569
10	OD Rear Shroud Outlet	1.81	0.125 dia		0.123	6.494
11	Holes in Cone	1.97	0.125 dia		0.0123	7.080
12	Holes in Cone Aligning Ring	2.46	0.125 dia		0.0123	8.856
13	First Primary Scoop Cooling Louver No. 1	0.39	0.575	0.050	0.029	1.392
14	First Primary Scoop Cooling Louver No. 2	0.39	0.575	0.050	0.029	1.392
15	Second Primary Scoop Cooling Louver	1.05	0.575	0.137	0.079	3.780
16	Third Primary Scoop Cooling Louver No. 1	1.05	0.575	0.137	0.079	3.780
17	Third Primary Scoop Cooling Louver No. 2	1.05	0.575	0.137	0.079	3.780
18	Louvers Between 2nd and 3rd ID Primary Scoops	0.47	0.600	0.117	0.070	1.680
19	Louvers Between 2nd and 3rd OD Primary Scoops	0.56	0.710	0.117	0.083	1.995
20	Swirlers P/N CKJ-2476	6.41			0.960	23.040
21	OD Slots in Dome	0.51	1.480	0.050	0.076	1.824
22	ID Slots in Dome	0.34	0.980	0.050	0.051	1.224
23	OD Holes in Dome	0.59	0.150 dia		0.0177	2.124
24	ID Holes in Dome	0.47	0.150 dia		0.0177	1.699
25	Holes in Dome Between Fuel	1.03	2.75	0.028	0.077	3.696
	Totals	100.00				359.332

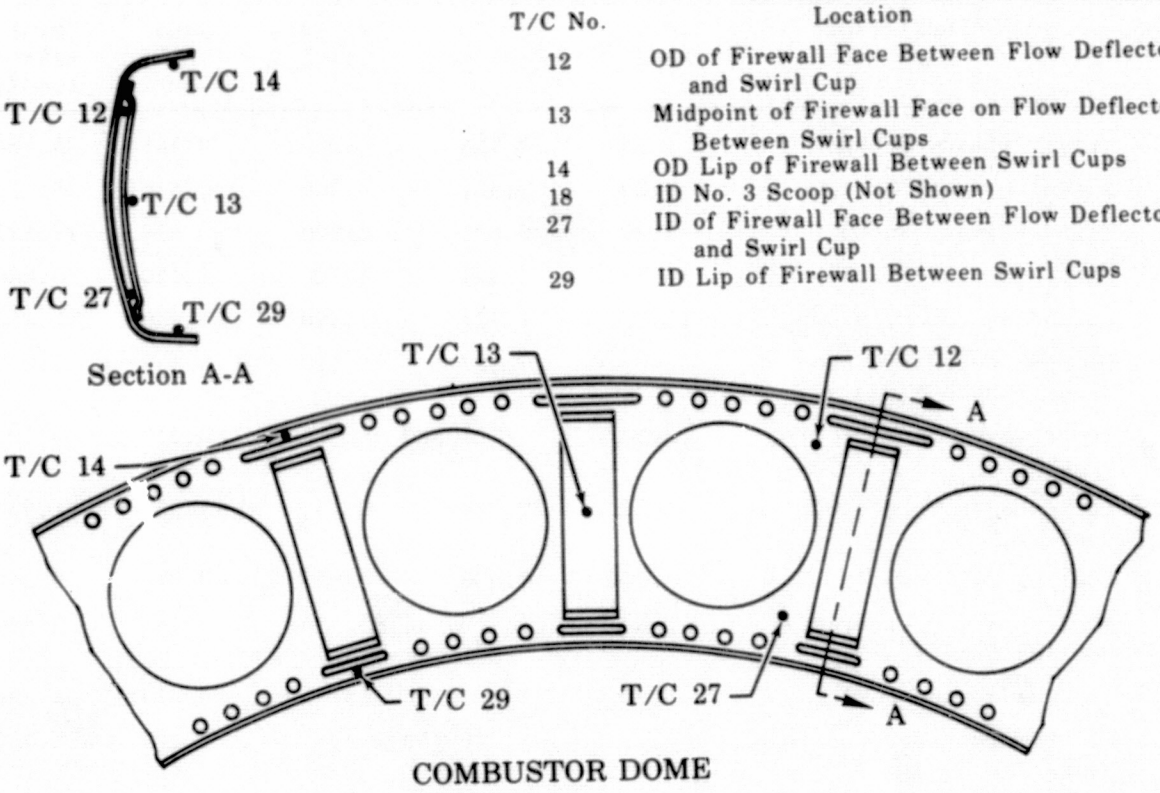

Figure 58. Combustor Dome Thermocouple Locations FD 22257A

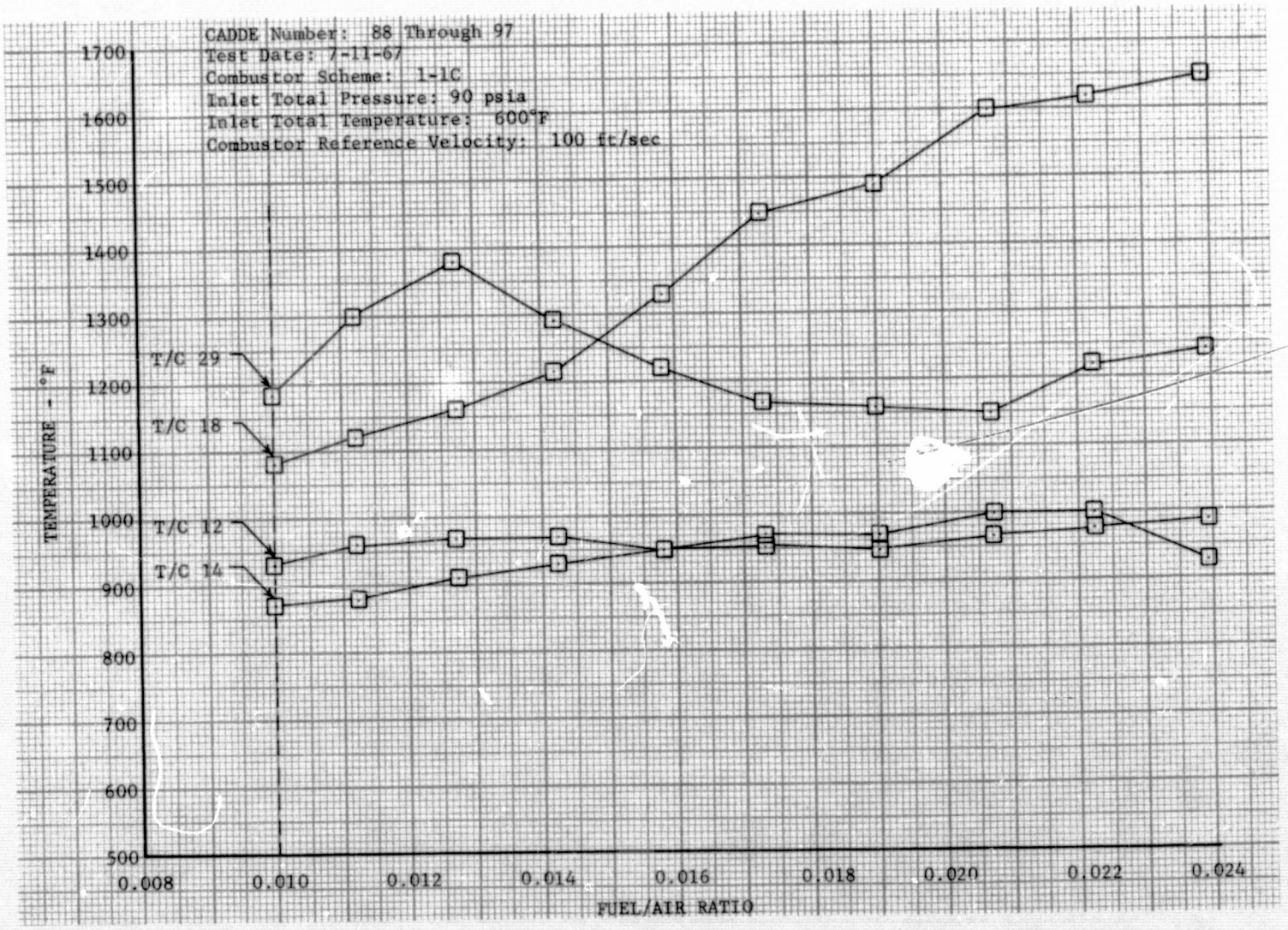

Figure 59. Combustor Skin Temperature vs Fuel/Air Ratio DF 58292

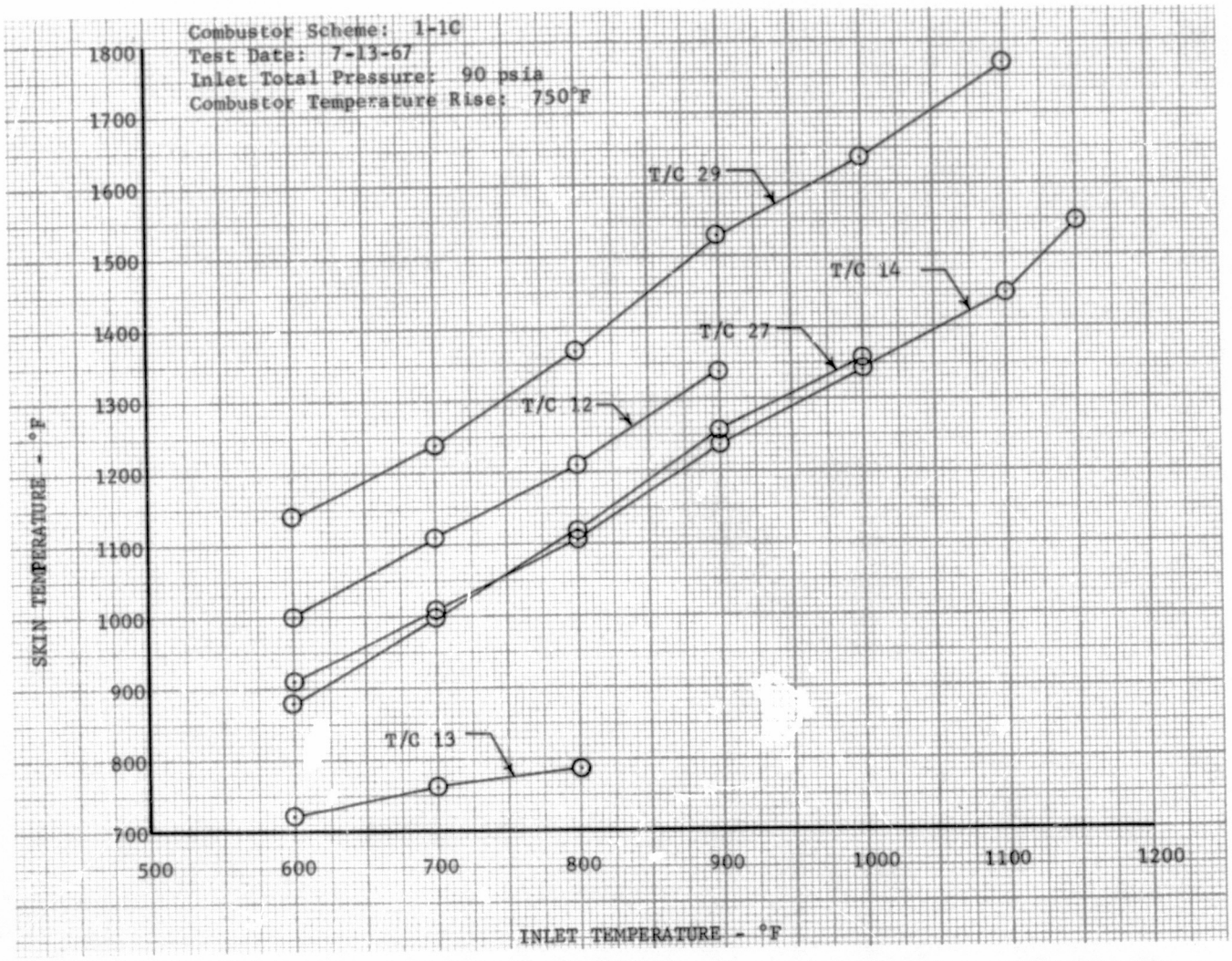

Figure 60. Skin Temperature vs Diffuser Inlet Temperature

DF 58296

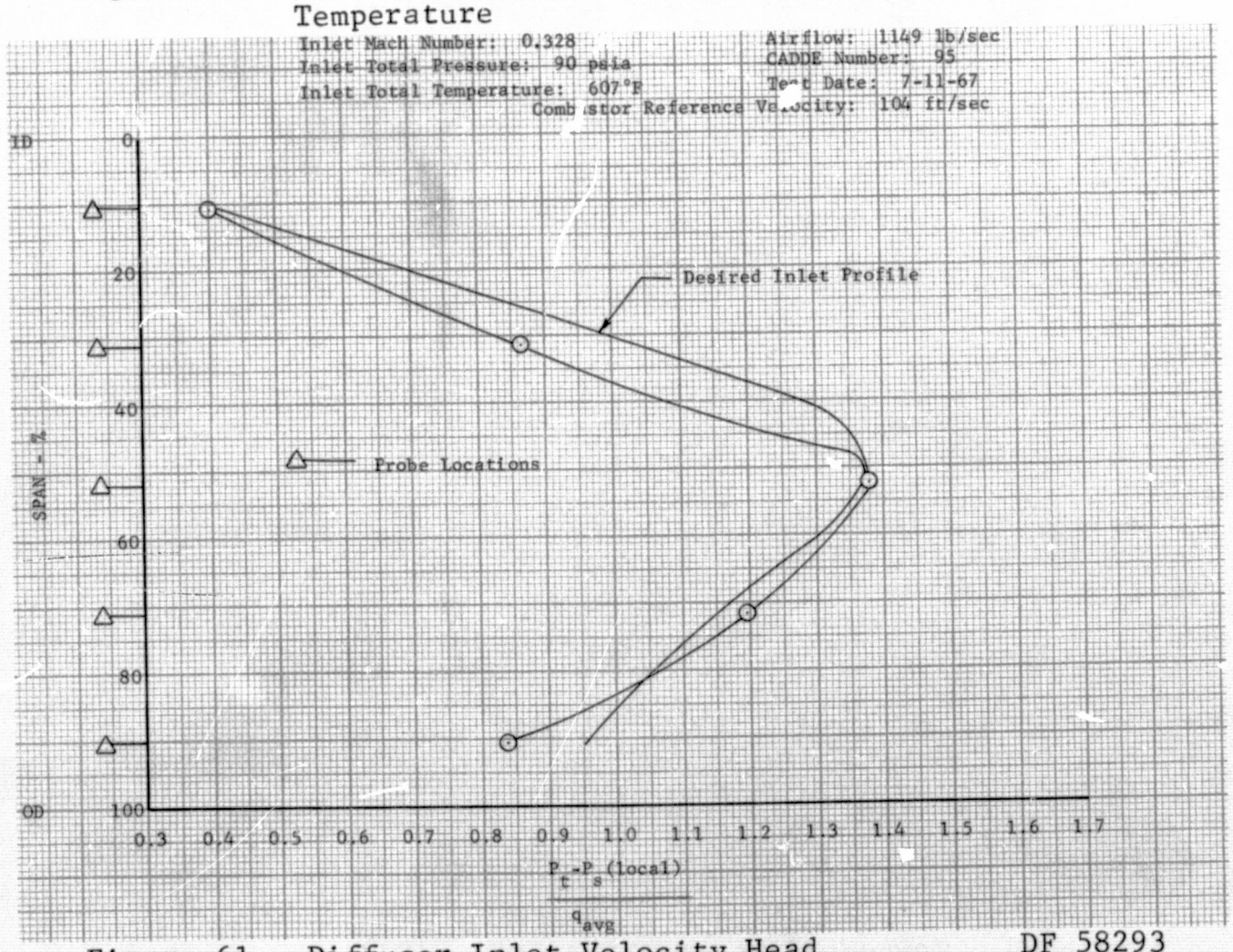

Figure 61. Diffuser Inlet Velocity Head Profile, Test No. 95

DF 58293

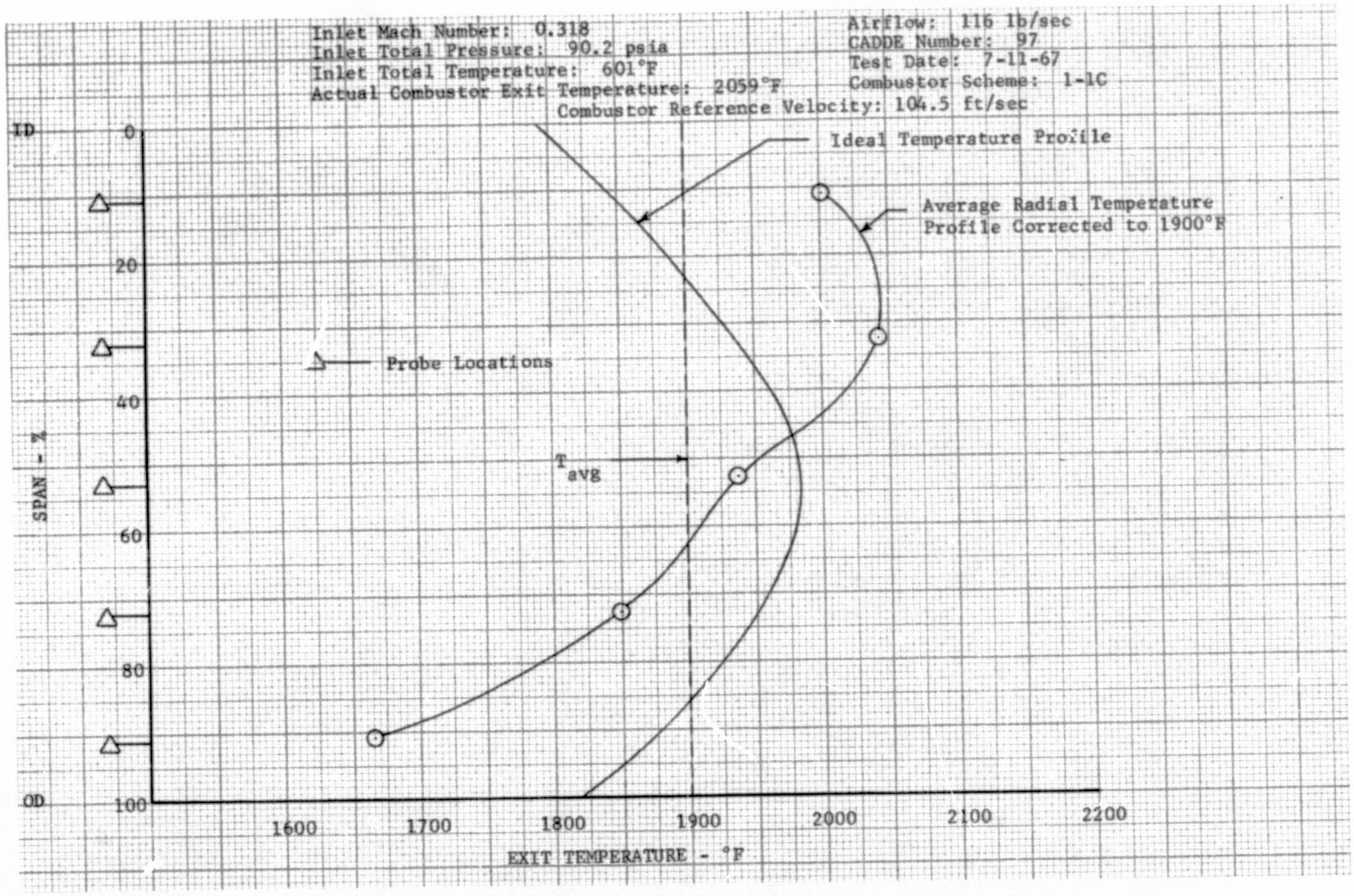

Figure 62. Combustor Average Radial Exit Temperature Profile, Test No. 97

DF 58295

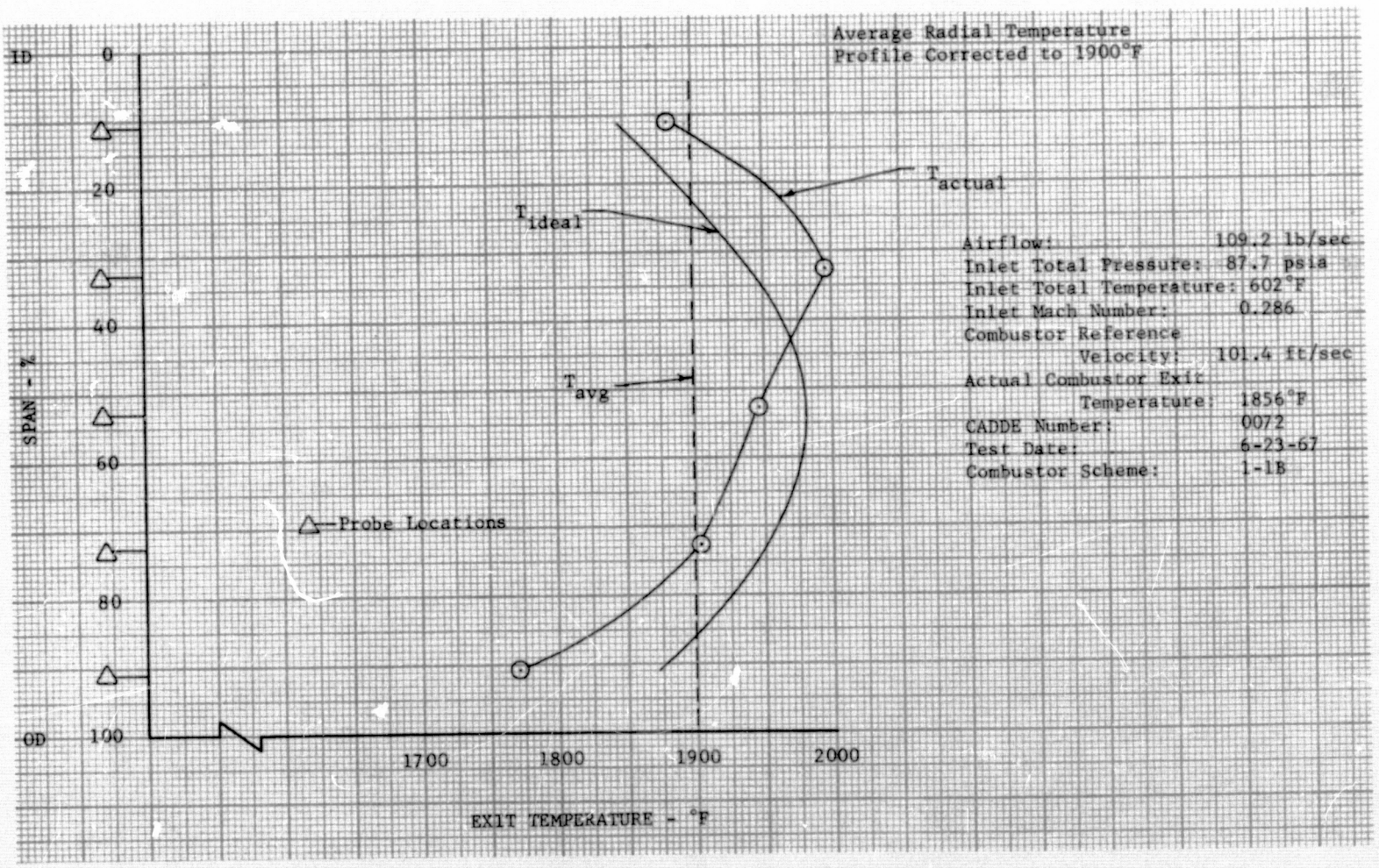

Figure 63. Combustor Average Radial Exit Temperature Profile, Test No. 72

DF 57695

At the end of this series of tests, the combustor showed a serious closing of the ID primary liner cooling gap, and an offset of the fuel nozzle openings in the dome to the point of swirler blockage. These problems were apparently caused by a dome shrinkage. Several No. 2 and No. 3 scoops on the ID primary liner showed slight to moderate burning, which is attributable to the closed ID primary liner cooling gap. A total of 6.05 hours of combustion time was accumulated on the Model 1-1C scheme for a total accumulated time to date of 12.75 hours.

The caps were then removed from the No. 5 OD liner scoops to separate the effect of the capping of the scoops from the dome changes. The modified combustor (Model 1-1D) with a flow area distribution, as shown in table 7, was then tested (Test Points 24 through 28 of table 4). The hot spot was in the same location reported in the previous model testing. As shown in figure 64, the average radial exit temperature profile improved over the test results obtained with the combustor Model 1-1C at the same test condition.

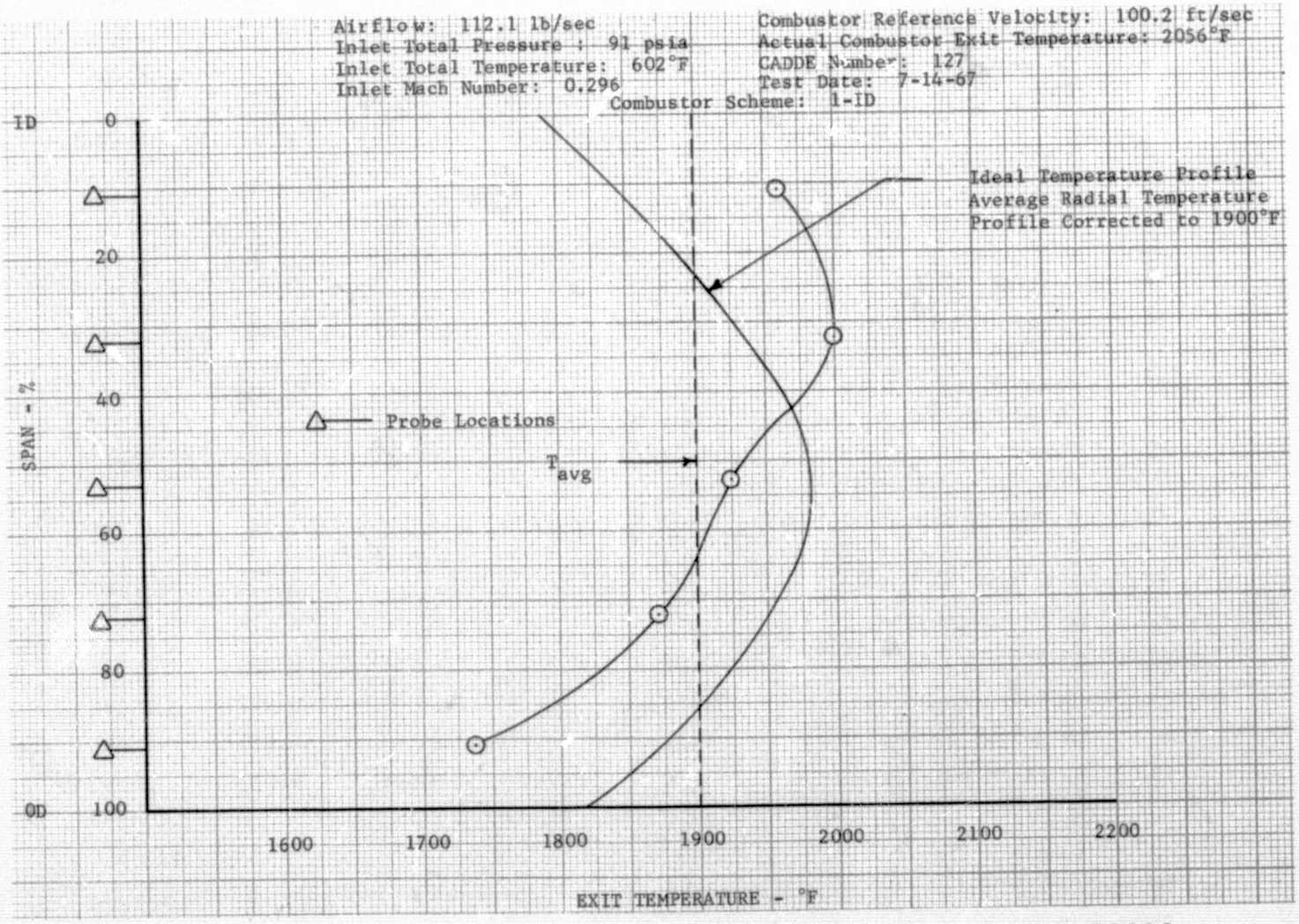

Figure 64. Combustor Average Radial Exit Temperature Profile, Test No. 127

DF 58298

Table 7. Flow Areas for the Advanced Annular Combustor, Model 1-1D

ITEM	DESCRIPTION	TOTAL AREA (%)	LENGTH (in.)	WIDTH (in.)	AREA ($in.^2$)	TOTAL AREA ($in.^2$)
A	First Primary Scoop	9.87	0.953	0.800	0.745	35.760
B	Second Primary Scoop	8.13	0.801	0.800	0.614	29.472
C	Third Primary Scoop	8.13	0.801	0.800	0.614	29.472
D	First Secondary Scoop	15.63	1.121	1.120	1.180	56.640
E	Second Secondary Scoop	15.63	1.121	1.120	1.180	56.640
1	ID Primary Liner Cooling Holes	3.89	0.310 slots		0.217	14.105
2	ID Secondary Liner Cooling Gaps	3.30	79.721	0.150	11.958	11.958
3	Cooling Film Gap	0.15	0.500	0.030	0.015	0.540
4	ID Transition Liner Film Cooling Gap	2.59	0.129, 0.183, and 0.104 dia			9.388
5	ID Rear Shroud Outlet	1.26	0.156 dia		0.0191	4.584
6	OD Primary Liner Cooling Holes	4.08	0.250 slots		0.145	14.790
7	OD Secondary Liner Cooling Gap	3.49	114.819	0.110	12.630	12.630
8	Cooling Film Gap	0.30	0.600	0.030	0.018	1.080
9	OD Transition Liner Film Cooling Gap	3.19	0.129, 0.120, and 0.166		0.094 in. dia	11.569
10	OD Rear Shroud Outlet	1.79	0.125 dia		0.123	6.494
11	Holes in Cone	1.95	0.125 dia		0.0123	7.080
12	Holes in Cone Aligning Ring	2.44	0.125 dia		0.0123	8.856
13	First Primary Scoop Cooling Louver No. 1	0.38	0.575	0.050	0.029	1.392
14	First Primary Scoop Cooling Louver No. 2	0.38	0.575	0.050	0.029	1.392
15	Second Primary Scoop Cooling Louver	1.04	0.575	0.137	0.079	3.780
16	Third Primary Scoop Cooling Louver No. 1	1.04	0.575	0.137	0.079	3.780
17	Third Primary Scoop Cooling Louver No. 2	1.04	0.575	0.137	0.079	3.780
18	Louvers Between 2nd and 3rd ID Primary Scoops	0.46	0.600	0.117	0.070	1.680
19	Louvers Between 2nd and 3rd OD Primary Scoops	0.55	0.710	0.117	0.083	1.995
20	Swirlers P/N CKJ 2476	6.37			0.960	23.040
21	OD Slots in Dome	0.50	1.480	0.050	0.076	1.824
22	ID Slots in Dome	0.33	0.980	0.050	0.051	1.224
23	OD Holes in Dome	0.59	0.150 dia		0.0177	2.124
24	ID Holes in Dome	0.47	0.150 dia		0.0177	1.699
25	Holes in Dome Between Fuel Nozzles	1.02	2.750 dia	0.028	0.077	3.696
	Totals	99.99				362.464

The combustor was then removed from the diffuser case and instrumented as shown in figure 22. A series of cold flow tests was then conducted.

The first test was conducted with the distortion plates installed. Results indicated an airflow split between the diffuser OD and ID passages of approximately 2.5:1. The inlet distortion plates were then removed and the test repeated. The results with the distortion plates removed showed an airflow split between the OD and ID passages of 2:1

It was now apparent that modifications and repairs to the combustor and diffuser were required before endurance testing could begin. Two final test series (Test Points 29 through 32 of table 4) were conducted and the combustor and diffuser were then sent to P&WA FRDC for modification. Test Point 29 of table 4 was conducted with the diffuser inlet distortion plates removed to compare the modified combustor (Model 1-1D) performance with that of the original combustor (Model 1-1A). Data were taken at an average combustor exit temperature of 1893°F. As shown in the combustor exit temperature pattern (figure 65), a hot spot of 2418°F was located approximately 3 degrees clockwise of top dead center looking upstream. This corresponds to the hot spot location of the Model 1-1A combustor as shown in figure 66. The combustor radial exit temperature profile for this test is shown in figure 67.

The fuel/air ratio was then increased until an average exit temperature of 1971°F was obtained. The hot spot of 2550°F (Test Point 30 of table 4), as shown in the combustor exit temperature pattern (figure 68), was located in the same position as the previous test. The average radial exit temperature profile for this test point is shown in figure 69.

To check the effect of the distortion screens on hot spot location, the diffuser inlet distortion plates were reinstalled and rotated 90 degrees from their original position. Testing was then resumed. The first data point taken (Test Point 31 of table 4) was at an average exit temperature of 1852°F. The hot spots of 2260° and 2270°F, as shown in combustor exit temperature pattern (figure 70), were located at approximately 78 degrees and 201 degrees, respectively, clockwise of

top dead center (both looking upstream). The first hot spot is at the same location reported in previous testing (in which the diffuser inlet distortion plates were installed in their original position), whereas the second was at a new location.

The fuel/air ratio was then increased until an average exit temperature of 1977°F was obtained (Test Point 32 of table 4). The hot spot of 2558°F, as shown in the combustor exit temperature pattern (figure 71), was located in the same position as the 2260°F hot spot of Test Point 31.

The combustor and diffuser were removed from the test cell and shipped to the P&WA FRDC for modification. These modifications were made during a test facility shutdown at the NASA-LeRC.

The combustor and diffuser arrived at FRDC on 11 August. The liners and dome were removed from the inlet flow splitter and measurements were taken. The dome diameter was found to be approximately 0.250 inch undersize. The inspection of the ID primary liner indicated that thirteen No. 2 and No. 3 scoops were slightly to moderately burned (figures 72 through 74). This liner was replaced with the spare liner. The original liner was retained for possible repair.

The original dome was not salvageable and was replaced with the spare dome, which was modified to include ID and OD cooling slots and flow deflectors around the swirler area (figure 45).

It was first believed that the shrinkage of the original dome was caused by a cold stretching during fabrication without subsequent heat-treating. However, the spare dome (which was fabricated in the same manner) was heat-treated at 1400°F for 1-1/2 hours and at 1800°F for 2 hours in a free state with no resulting shrinkage. It now appears that the shrinkage was caused by an overheating of the dome while it was being restrained by a cooler structure during combustor operation. This would result in a yielding of the dome as it attempted to expand during operation and a shrinkage as it cooled after testing.

Other combustor modifications included caps for the No. 1, 4, and 5 OD and ID liner scoops and false diffuser walls. These modifications were designed to increase combustor pressure drop and eliminate diffuser separation in order to improve combustor performance.

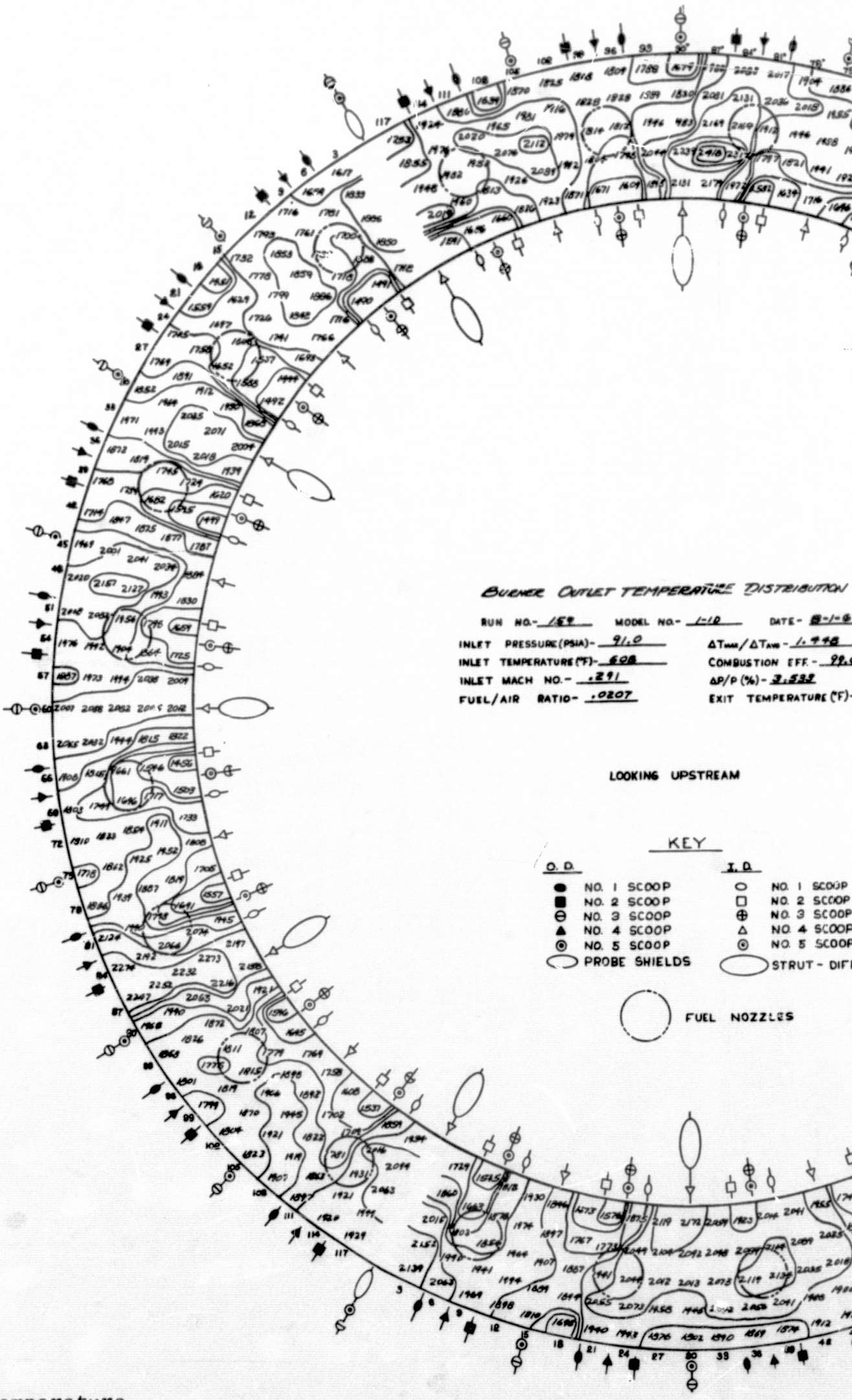

Figure 65. Combustor Outlet Temperature Distribution, Test No. 159

FOLDOUT FRAME 1

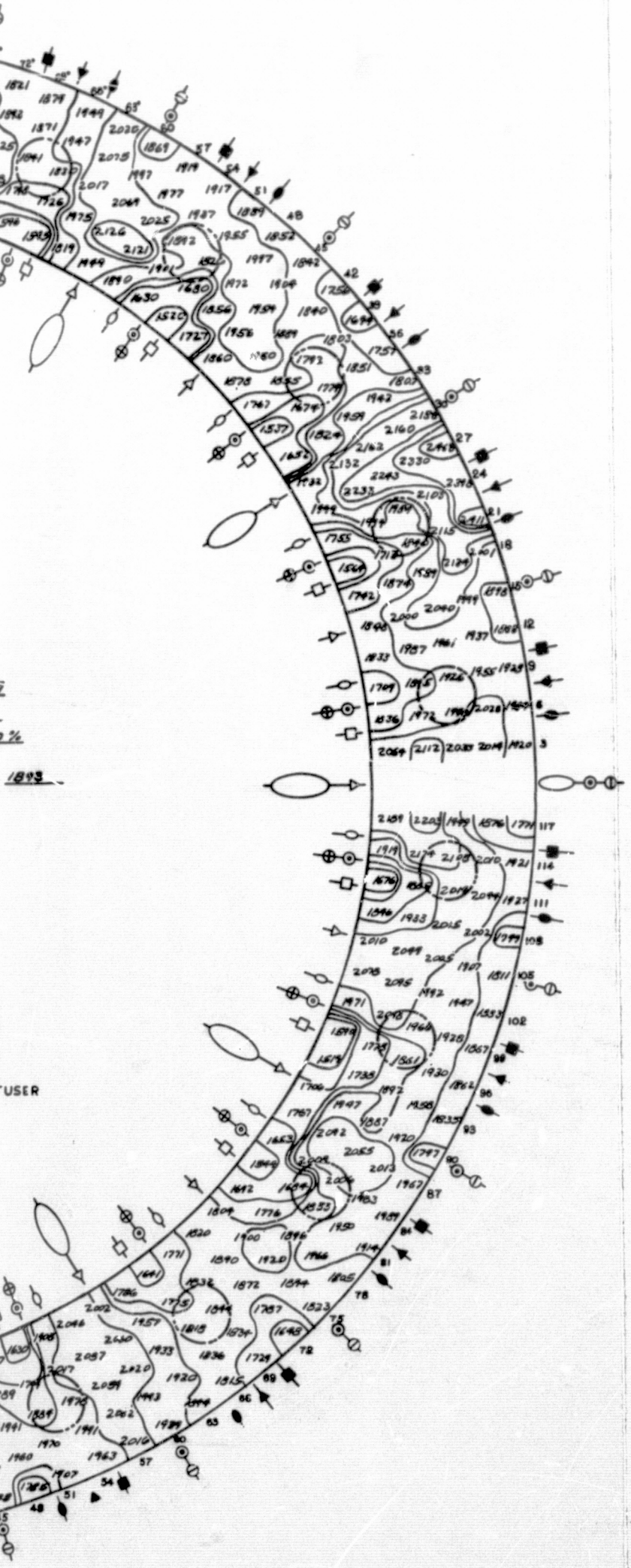

FD 22811

FOLDOUT FRAME 2

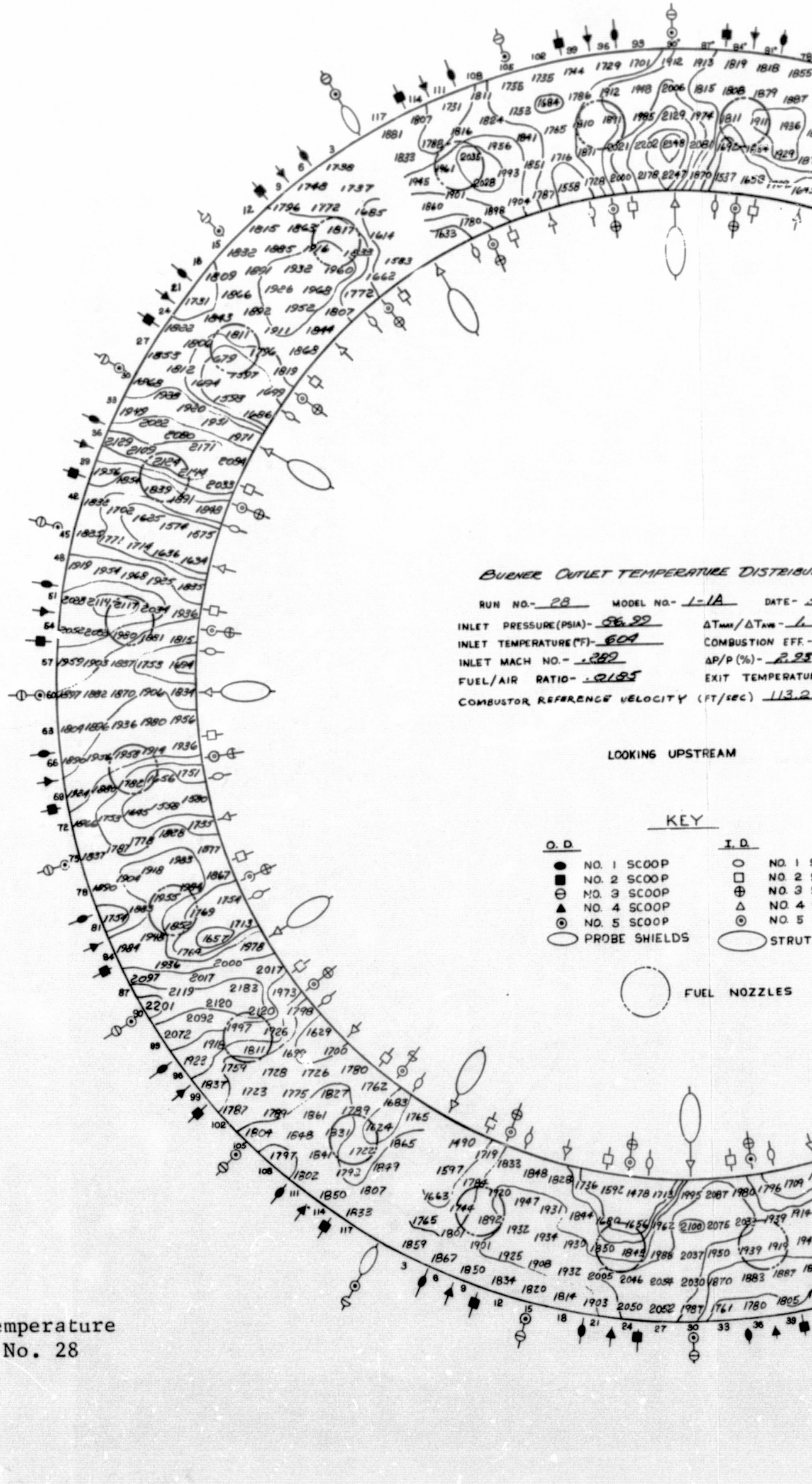

.gure 66. Combustor Outlet Temperature Distribution, Test No. 28

FOLDOUT FRAME |

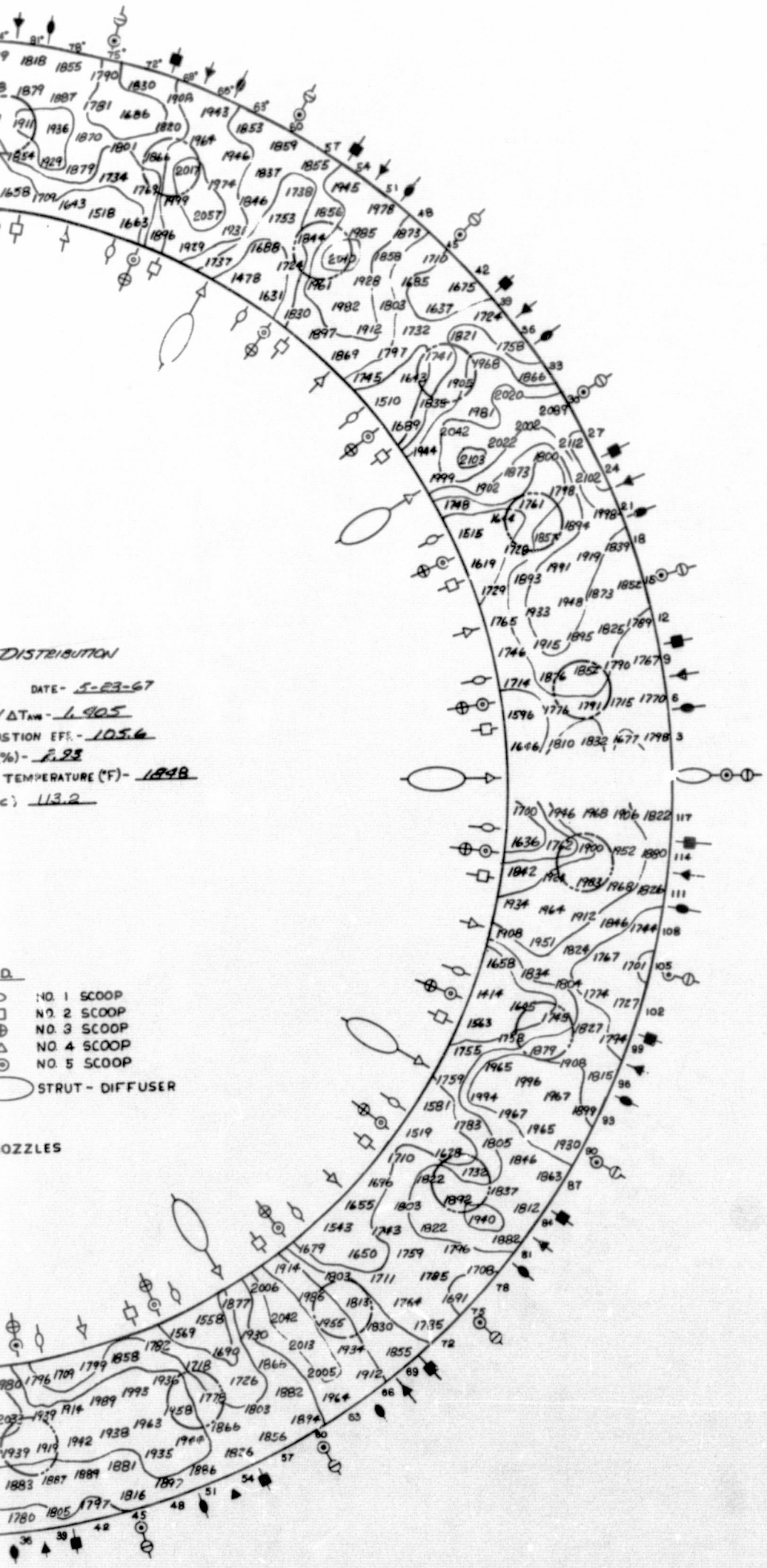

FD 21787

FOLDOUT FRAME 2

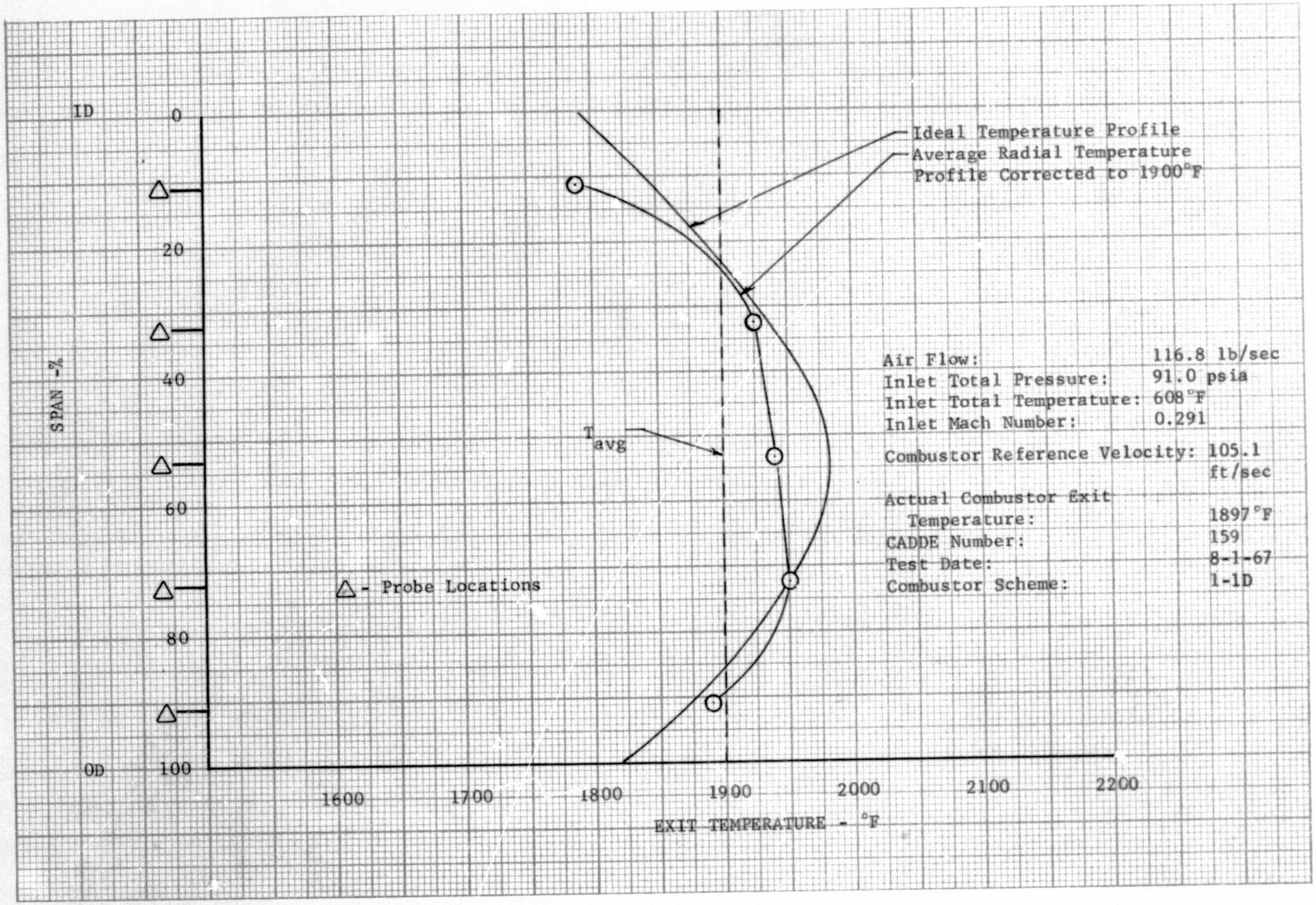

DF 58891

Figure 67. Combustor Average Radial Exit Temperature Profile, Test No. 159

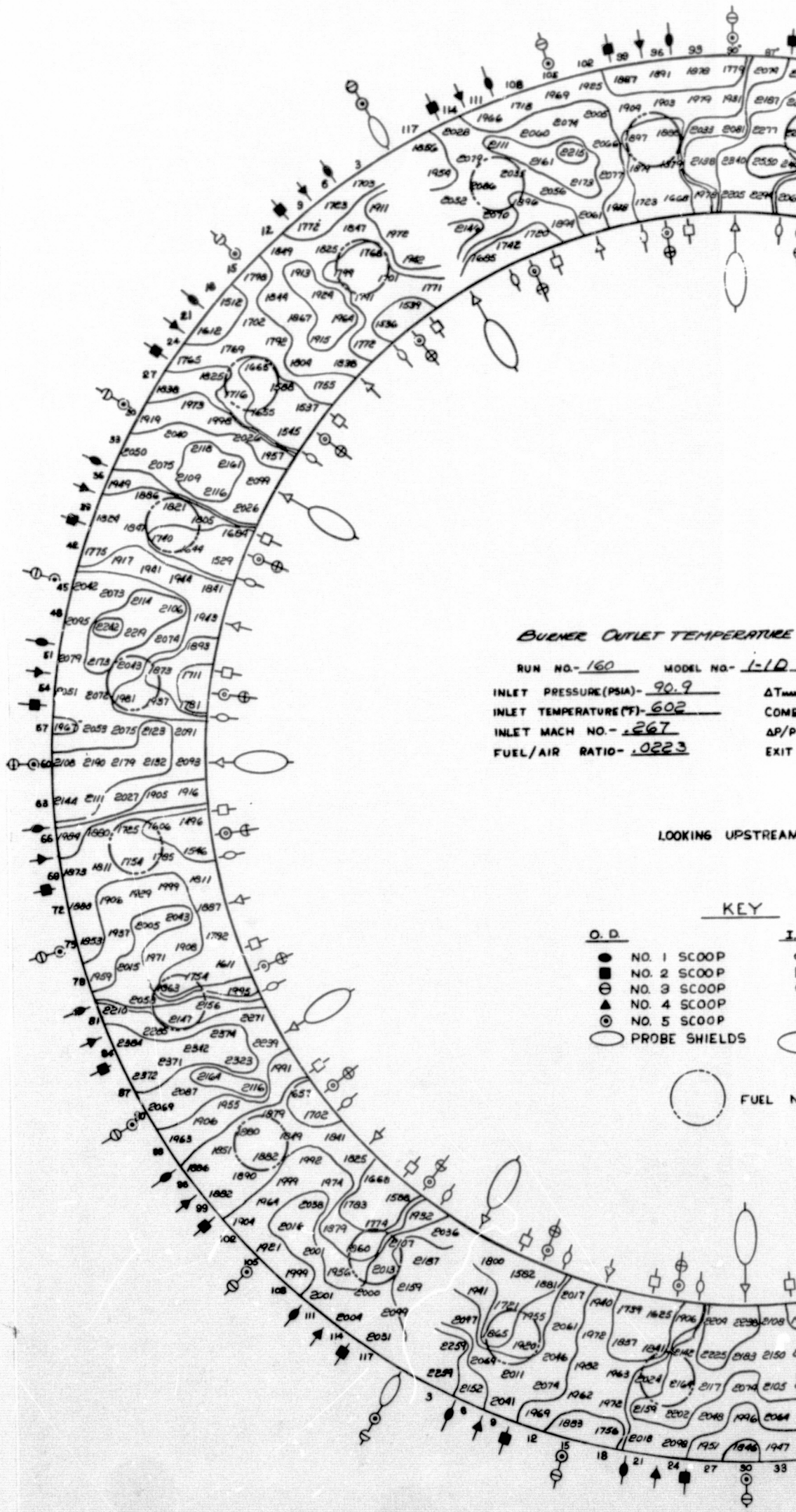

Figure 68. Combustor Outlet Temperature Distribution, Test No. 160

FOLDOUT FRAME 1

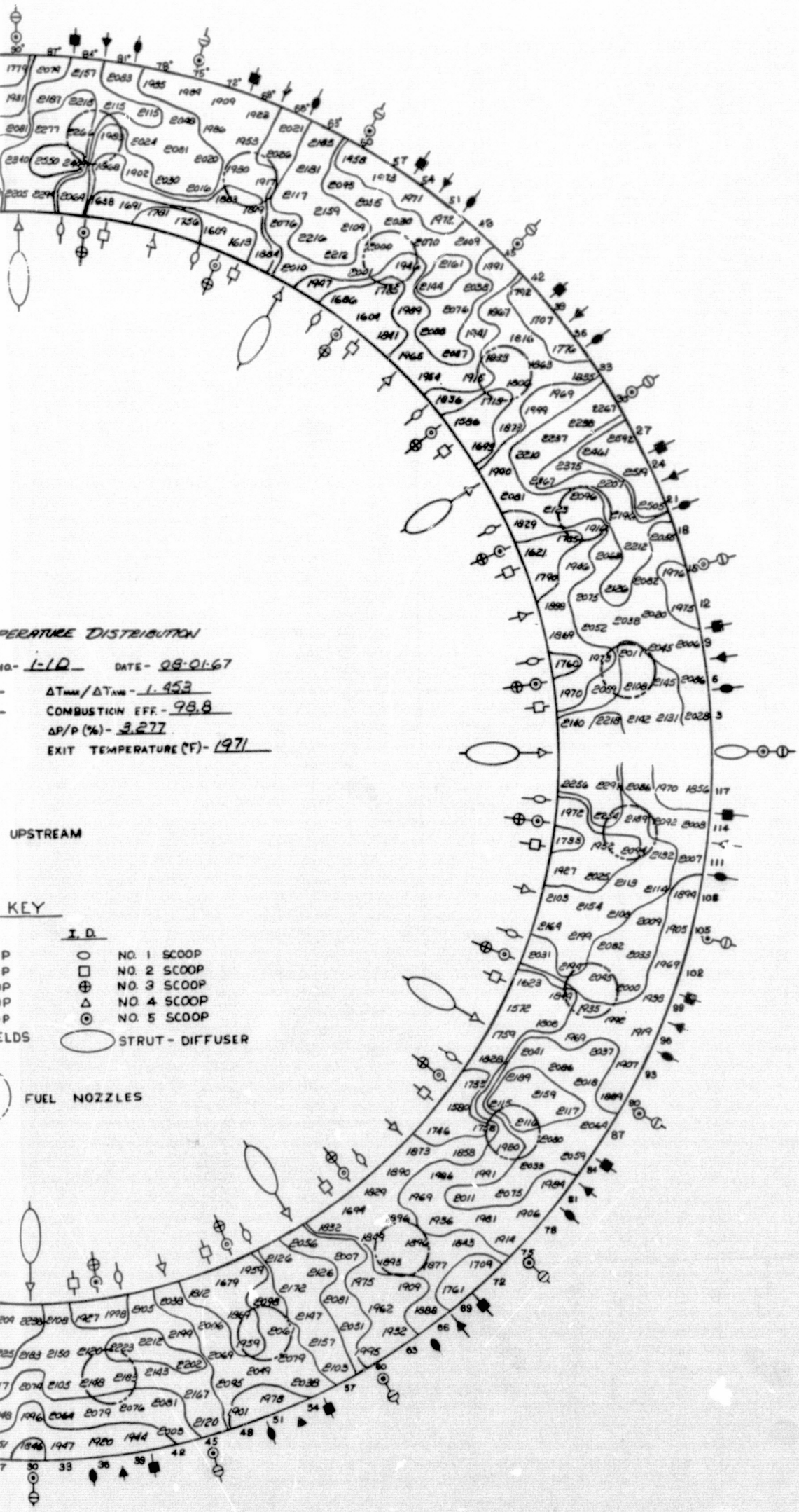

FD 22814

FOLDOUT FRAME 2

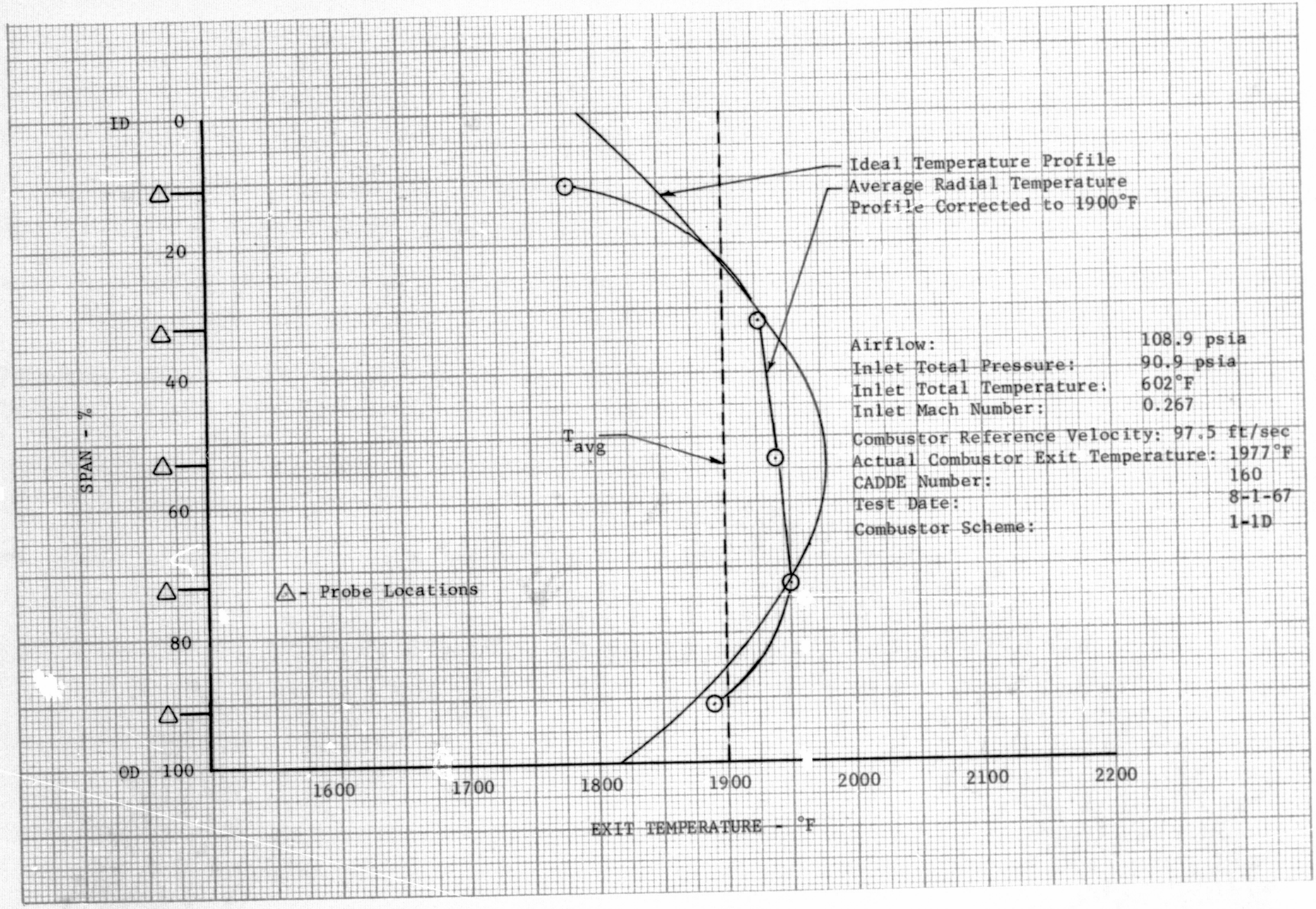

DF 58892

Figure 69. Combustor Average Radial Exit Temperature Profile, Test No. 160

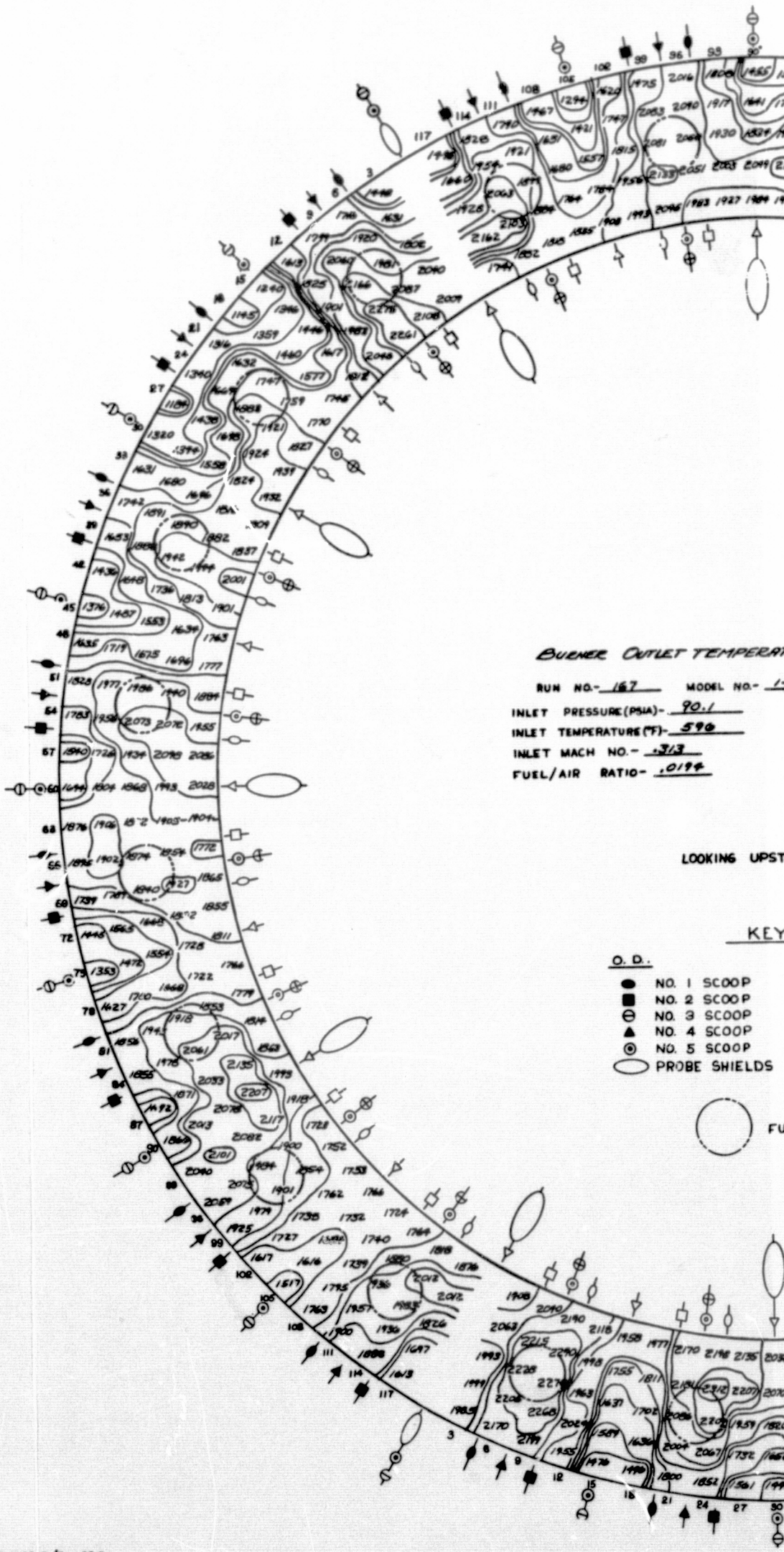

Figure 70. Combustor Outlet Temperature Distribution, Test No. 167

FOLDOUT FRAME 1

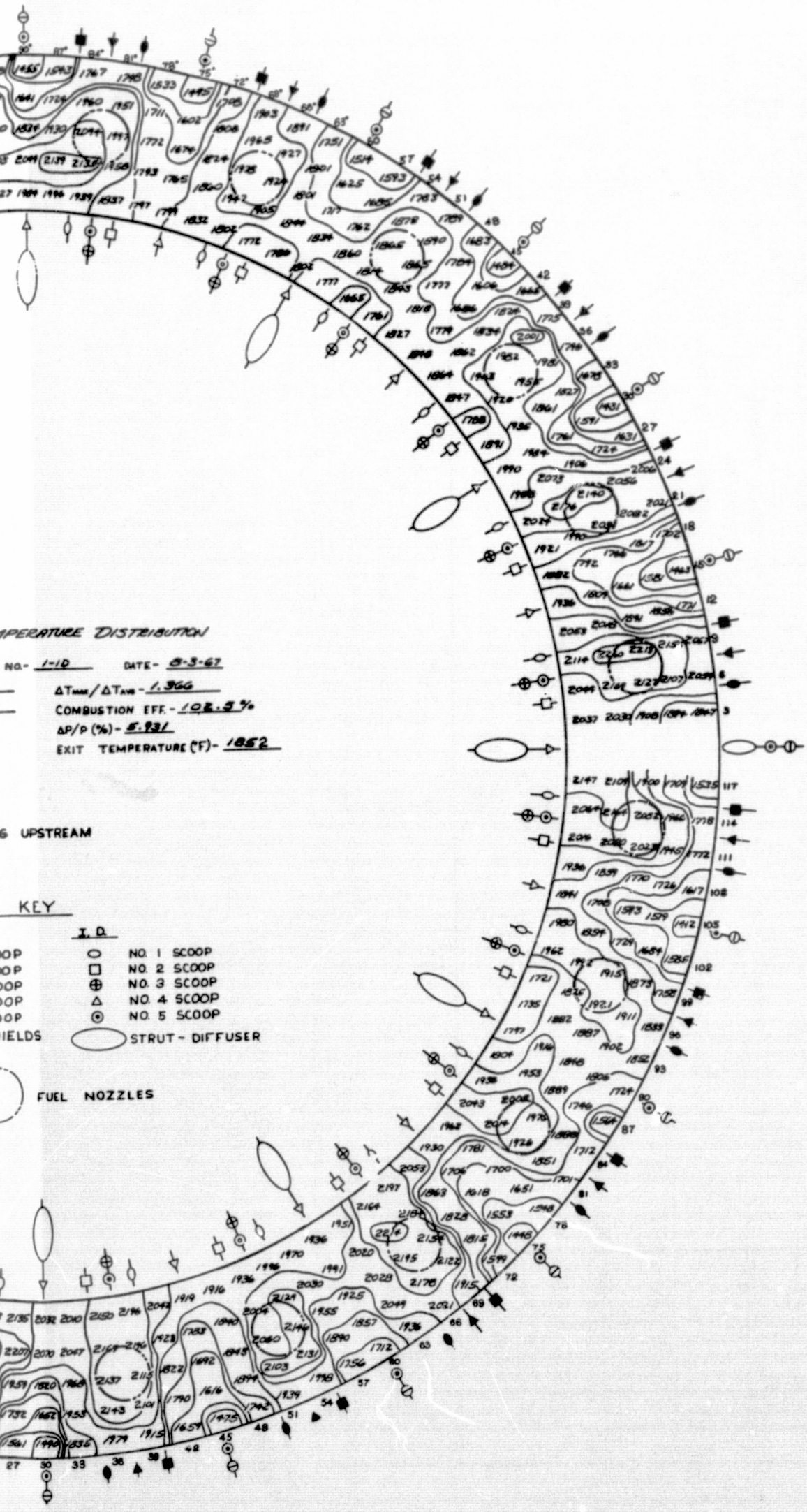

FD 22812

FOLDOUT FRAME 2

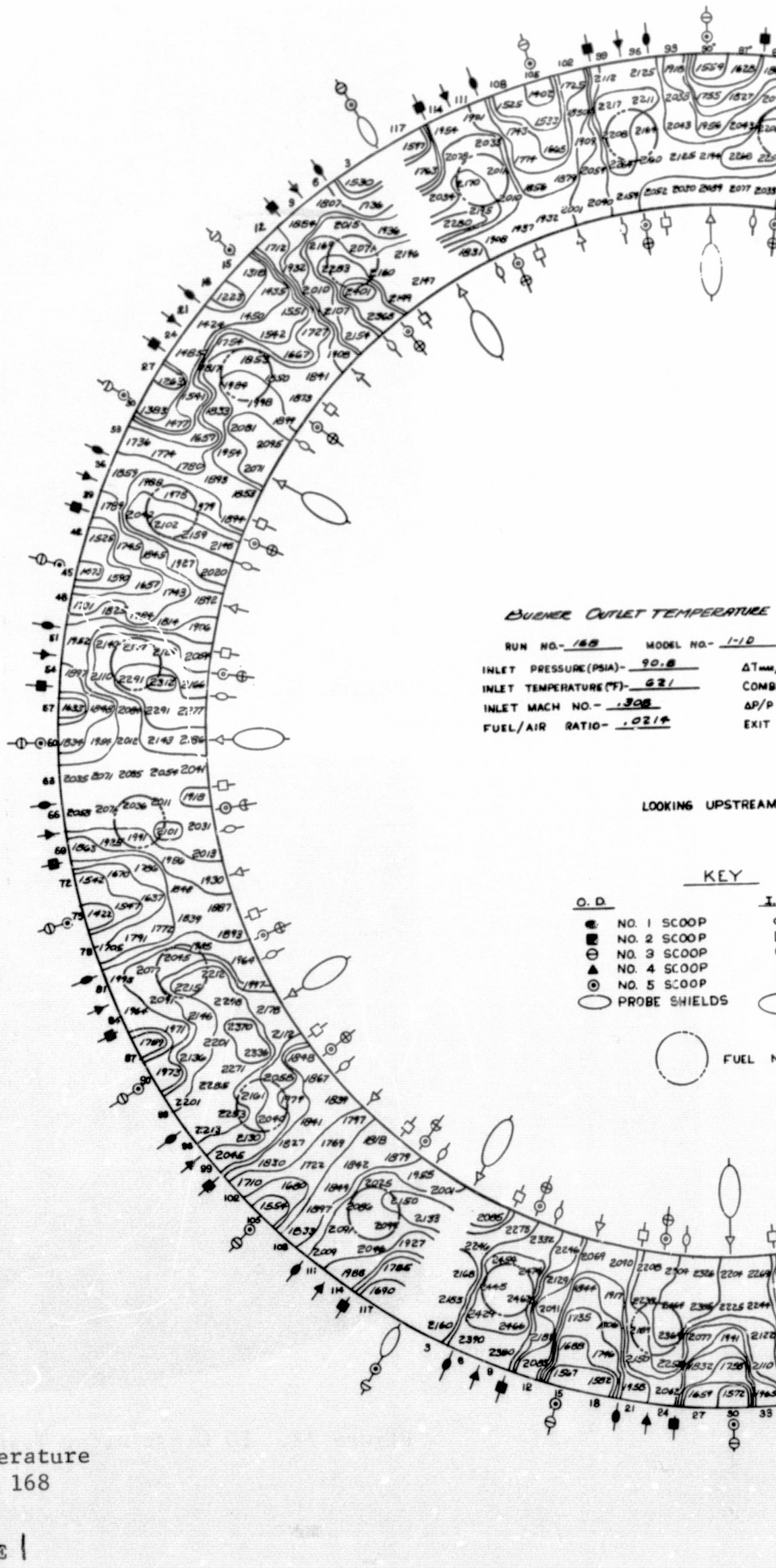

Figure 71. Combustor Outlet Temperature Distribution Test No. 168

FOLDOUT FRAME |

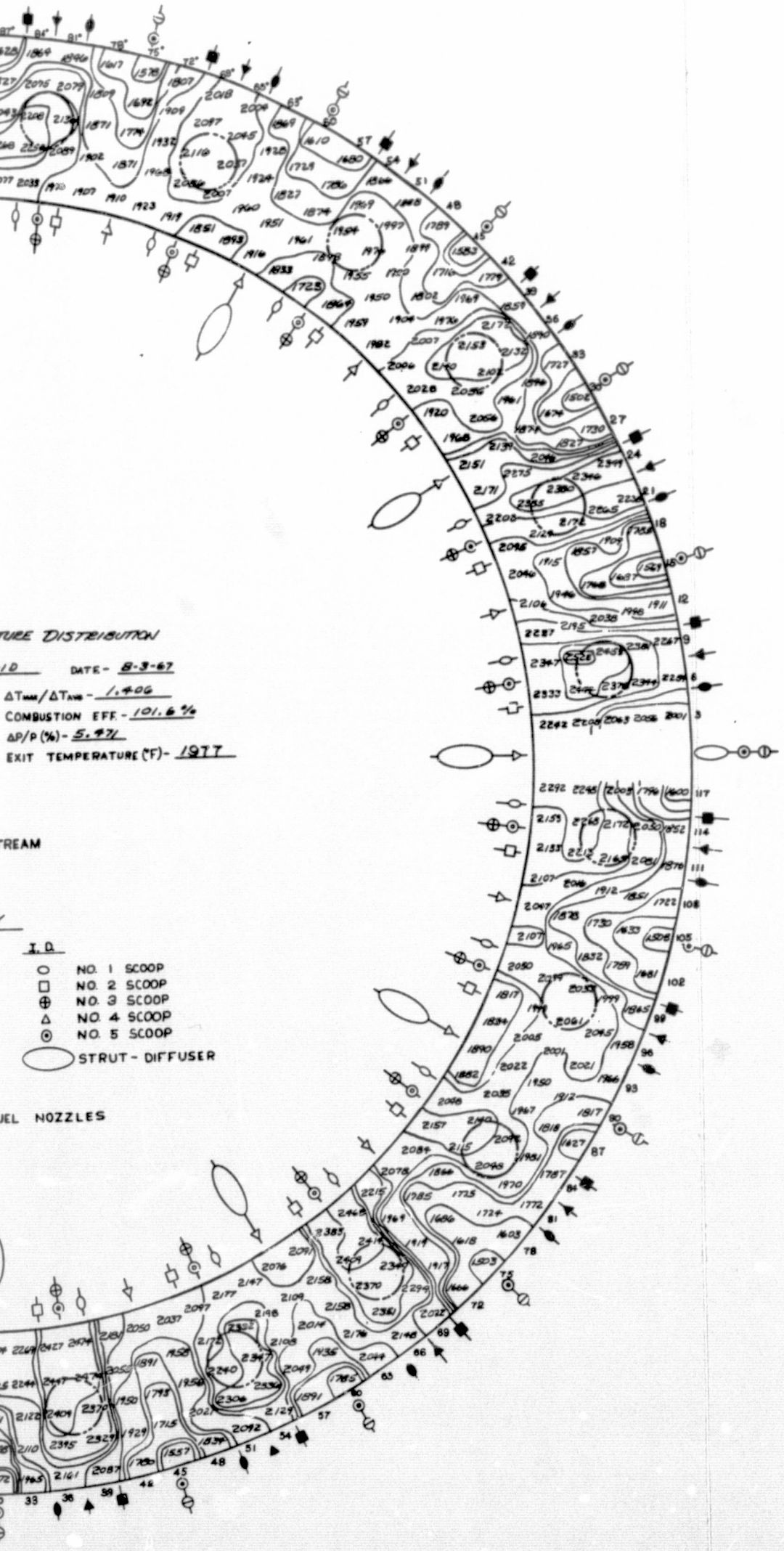

FD 22813

FOLDOUT FRAME 2

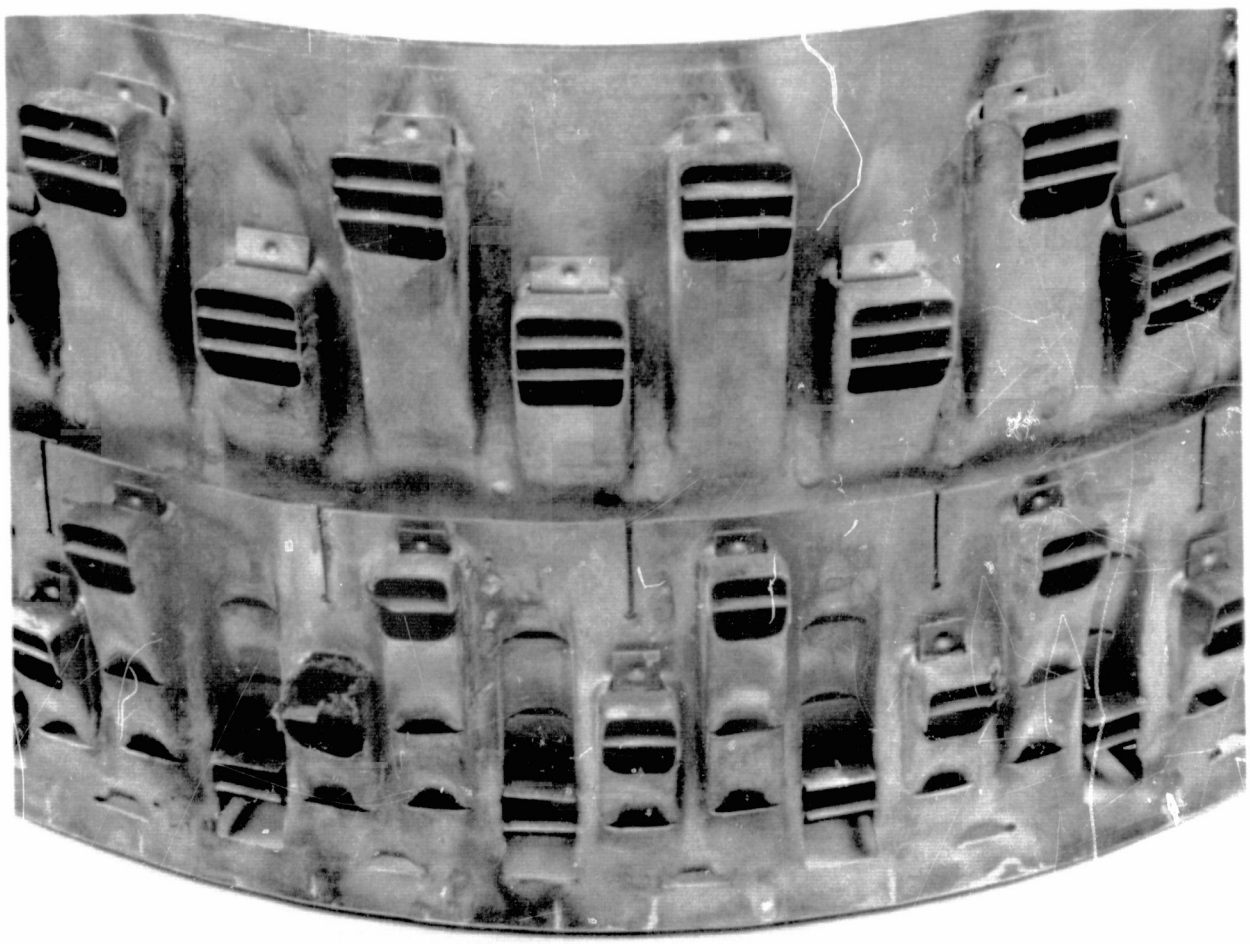

Figure 72. ID Liner After Testing, View 1 FD 71438

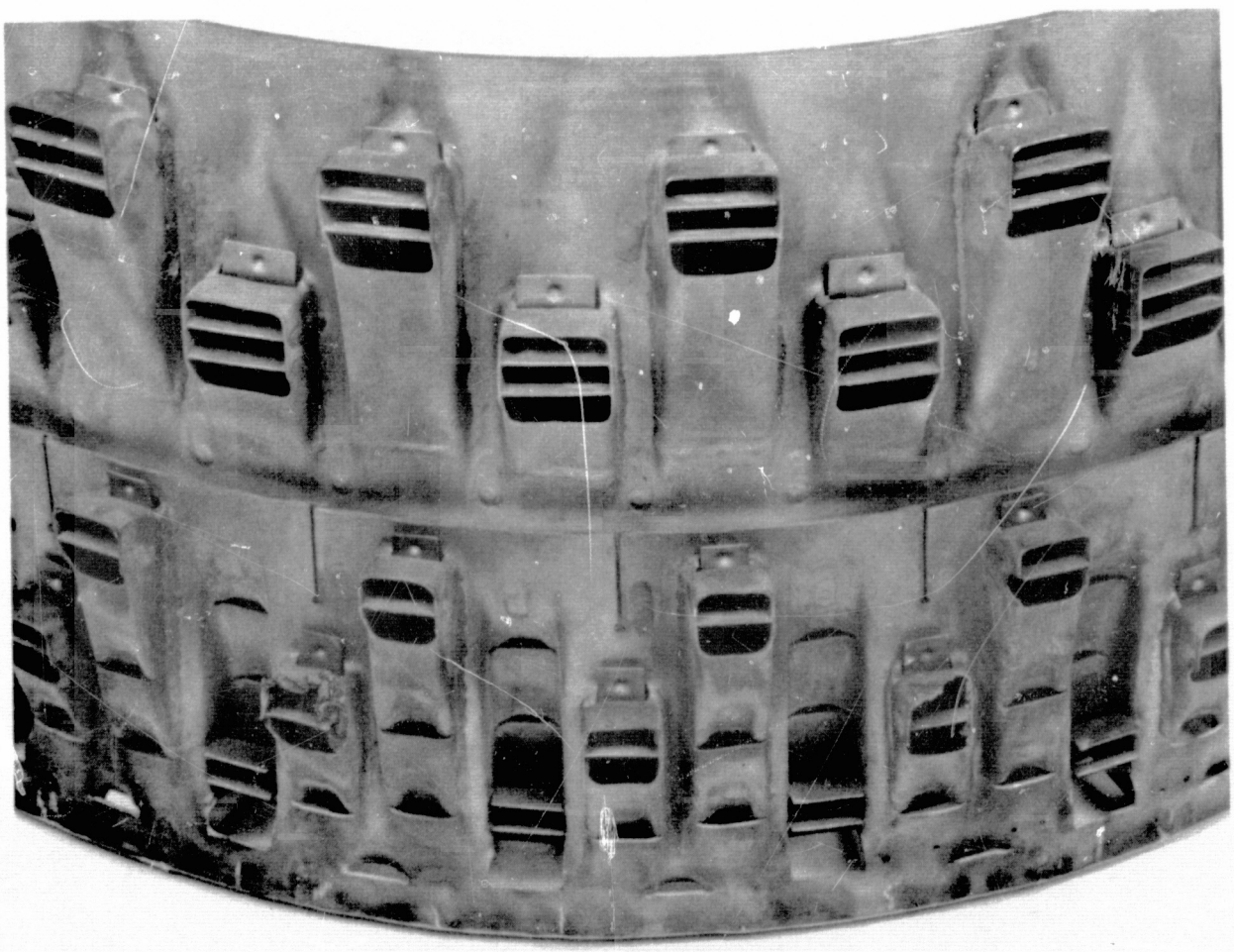

Figure 73. ID Liner After Testing, View 2 FD 71439

Figure 74. ID Liner After Testing, View 3 FE 71440

The ID and OD dome supports were also redesigned in an attempt to prevent closing of the OD and ID liner primary cooling gaps.

The flow area distribution for the Model 1-1E combustor (figures 44 and 75) is shown in table 8 (page 86).

The combustor and diffuser were returned to the NASA-LeRC on 29 September and on 1 October testing was resumed.

The first data point (Test Point 33 of table 4) was an isothermal test conducted to measure the combustor pressure loss of the Model 1-1E combustor. The overall combustor pressure loss had increased to a value of 5.42% as compared to 4.14% with the Model 1-1B combustor at essentially the same test condition.

The combustor was then ignited and a data point was taken when the exit temperature reached 1891°F (Test Point 34 of table 4). A cold area was noted at approximately 300° clockwise of top dead center, looking upstream. No hot spots were noted.

Table 8. Flow Areas for the Advanced Annular Combustor, Model 1-1E

ITEM	DESCRIPTION	TOTAL AREA (%)	LENGTH (in.)	WIDTH (in.)	AREA$_2$ (in.^{2})	TOTAL AREA (in.^{2})
A	First Primary Scoop	0.78	0.058	0.800	0.046	2.227
B	Second Primary Scoop	10.34	0.801	0.800	0.614	29.472
C	Third Primary Scoop	10.34	0.801	0.800	0.614	29.472
D	First Secondary Scoop	13.22	0.702	1.120	0.787	37.700
E	Second Secondary Scoop	13.22	0.702	1.120	0.787	37.700
1	ID Primary Liner Cooling Holes	3.14	0.135		0.138	8.970
2	ID Secondary Liner Cooling Gaps	4.19	79.721	0.150	11.958	11.958
3	Cooling Film Gap	0.19	0.500	0.030	0.015	0.540
4	ID Transition Liner Film Cooling Gap	3.29	0.129, 0.183, and 0.104 dia			9.388
5	ID Rear Shroud Outlet	1.61	0.156 dia		0.0191	4.584
6	OD Primary Liner Cooling Holes	3.86	0.145 slots		0.108	11.016
7	OD Secondary Liner Cooling Gap	4.43	114.819	0.110	12.630	12.630
8	Cooling Film Gap	0.38	0.600	0.030	0.018	1.080
9	OD Transition Liner Film Cooling Gap	4.06	0.129, 0.120, and 0.166		0.094 dia	11.569
10	OD Rear Shroud Outlet	2.28	0.125 dia		0.123	6.494
11	Holes in Cone	2.48	0.125 dia		0.0123	7.080
12	Holes in Cone Aligning Ring	3.10	0.125 dia		0.0123	8.856
13	First Primary Scoop Cooling Louver No. 1	0.49	0.575	0.050	0.029	1.392
14	First Primary Scoop Cooling Louver No. 2	0.49	0.575	0.050	0.029	1.392
15	Second Primary Scoop Cooling Louver	1.33	0.575	0.137	0.079	3.780
16	Third Primary Scoop Cooling Louver No. 1	1.33	0.575	0.137	0.079	3.780
17	Third Primary Scoop Cooling Louver No. 2	1.33	0.575	0.137	0.079	3.780
18	Louvers Between 2nd and 3rd ID Primary Scoops	0.59	0.600	0.117	0.070	1.680
19	Louvers Between 2nd and 3rd OD Primary Scoops	0.70	0.710	0.117	0.083	1.995
20	Swirlers P/N CKJ-2476	8.08			0.960	23.040
21	OD Slots in Dome	0.64	1.480	0.050	0.076	1.824
22	ID Slots in Dome	0.52	1.250	0.050	0.062	1.488
23	Dome Air Deflectors	3.59	0.040 Gap		0.427	10.248
	Totals	100.00				285.135

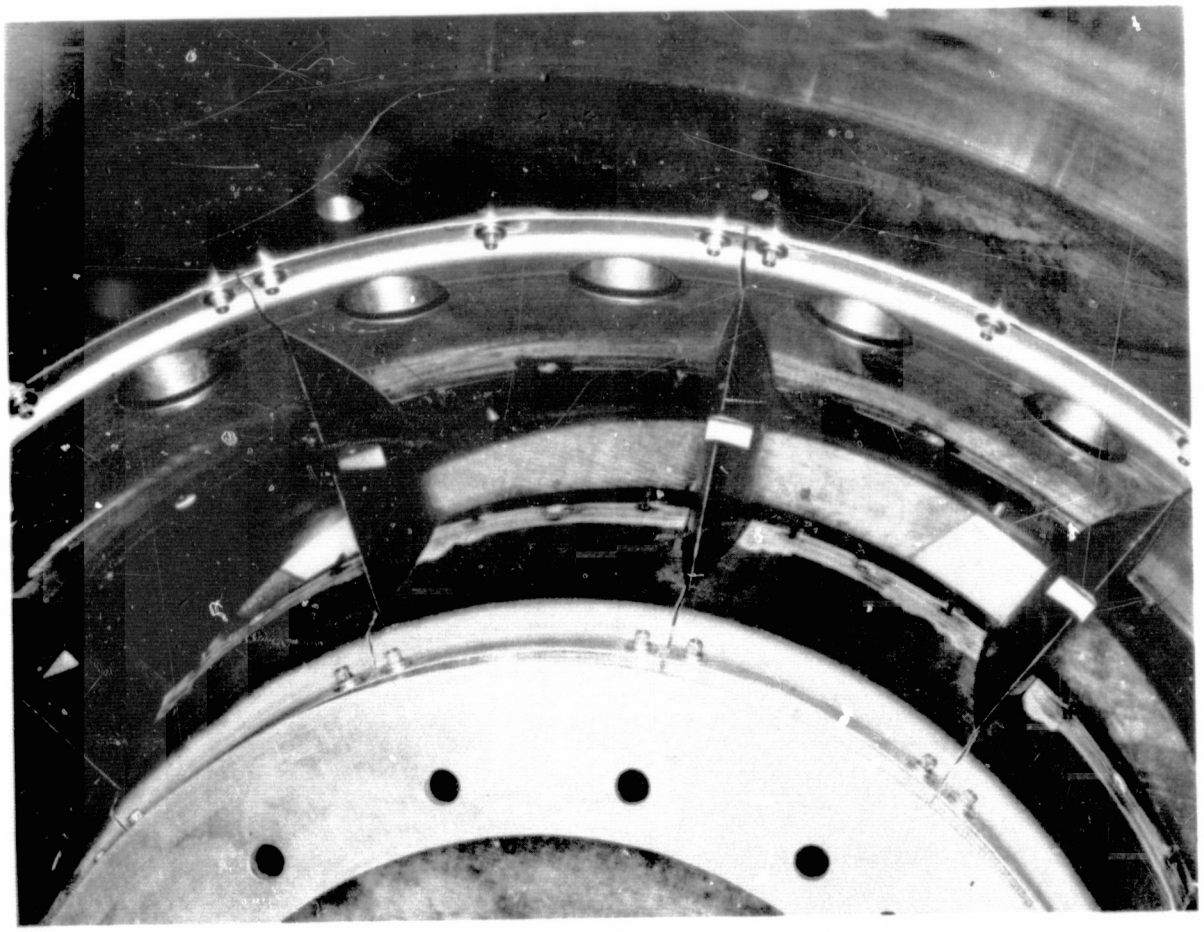

Figure 75. Model 1-1E Diffuser FE 72284

The fuel/air ratio was then increased until an average exit temperature of 2115°F was obtained (Test Point 35 of table 4). The desired test condition was an exit temperature of 2200°F but a malfunction in the fuel flow readout resulted in the setting of a slightly lower average exit temperature. The cold area, as shown in the combustor exit temperature pattern (figure 76), was in the same location as in the previous test condition. The combustor exit radial temperature profile for this test condition is shown in figure 77.

The rig was then disassembled for inspection. The combustor, as shown in figures 78 and 79, was in good condition. The dome area appeared to have been operating exceptionally cool. However, metal coloration indicative of high thermal gradients was noted on each side of the No. 1 scoops on the OD primary liner. A small hole in one of the turning vanes of a No. 1 scoop was also noted.

The four fuel struts in the area of the cold spot were removed and an inspection of the filter screens revealed one screen completely plugged and another screen partially plugged. The screens and corresponding fuel nozzles were replaced with spares and the rig reassembled.

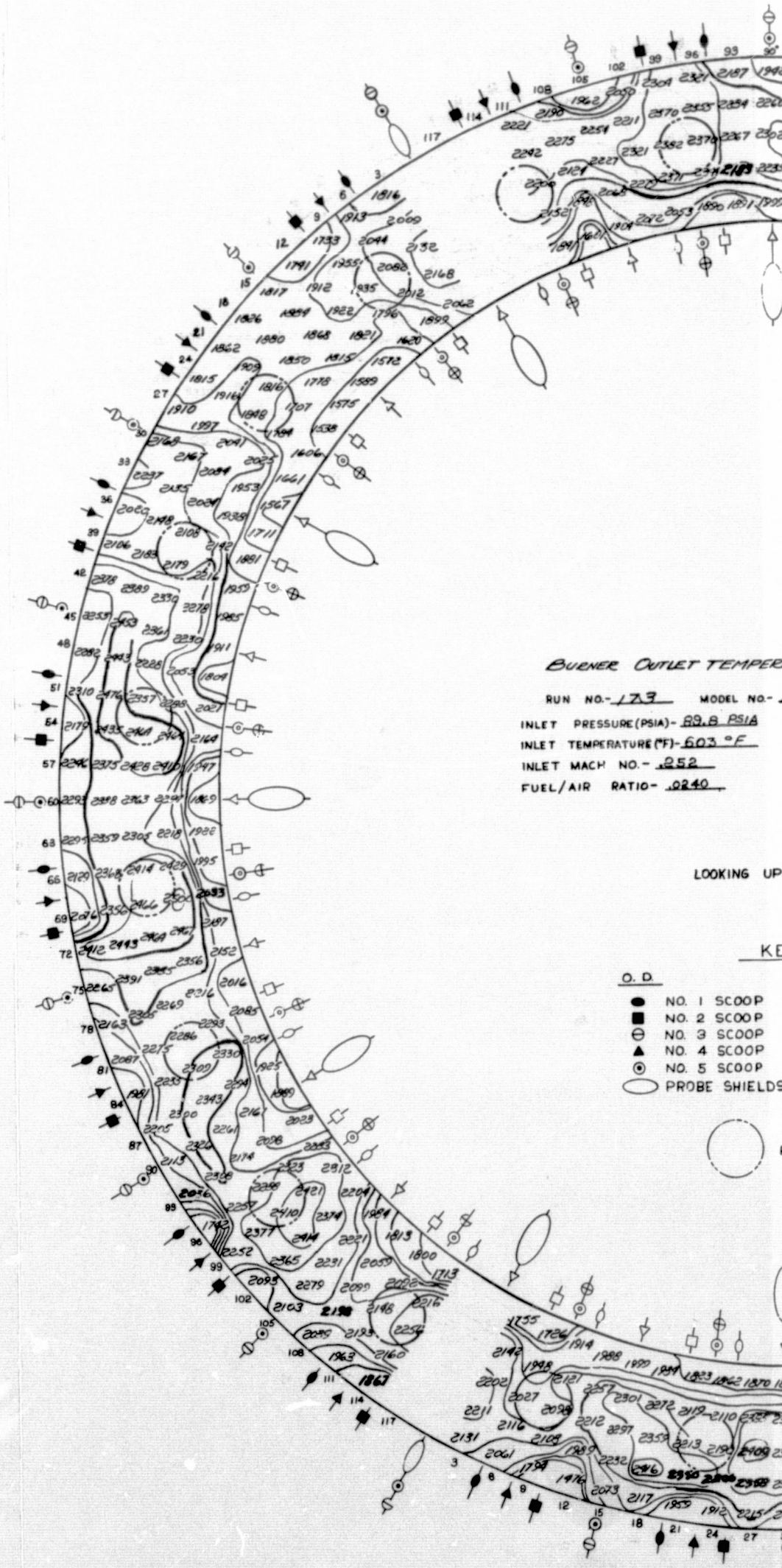

Figure 76. Combustor Outlet Temperature Distribution, Test No. 173

FOLDOUT FRAME 1

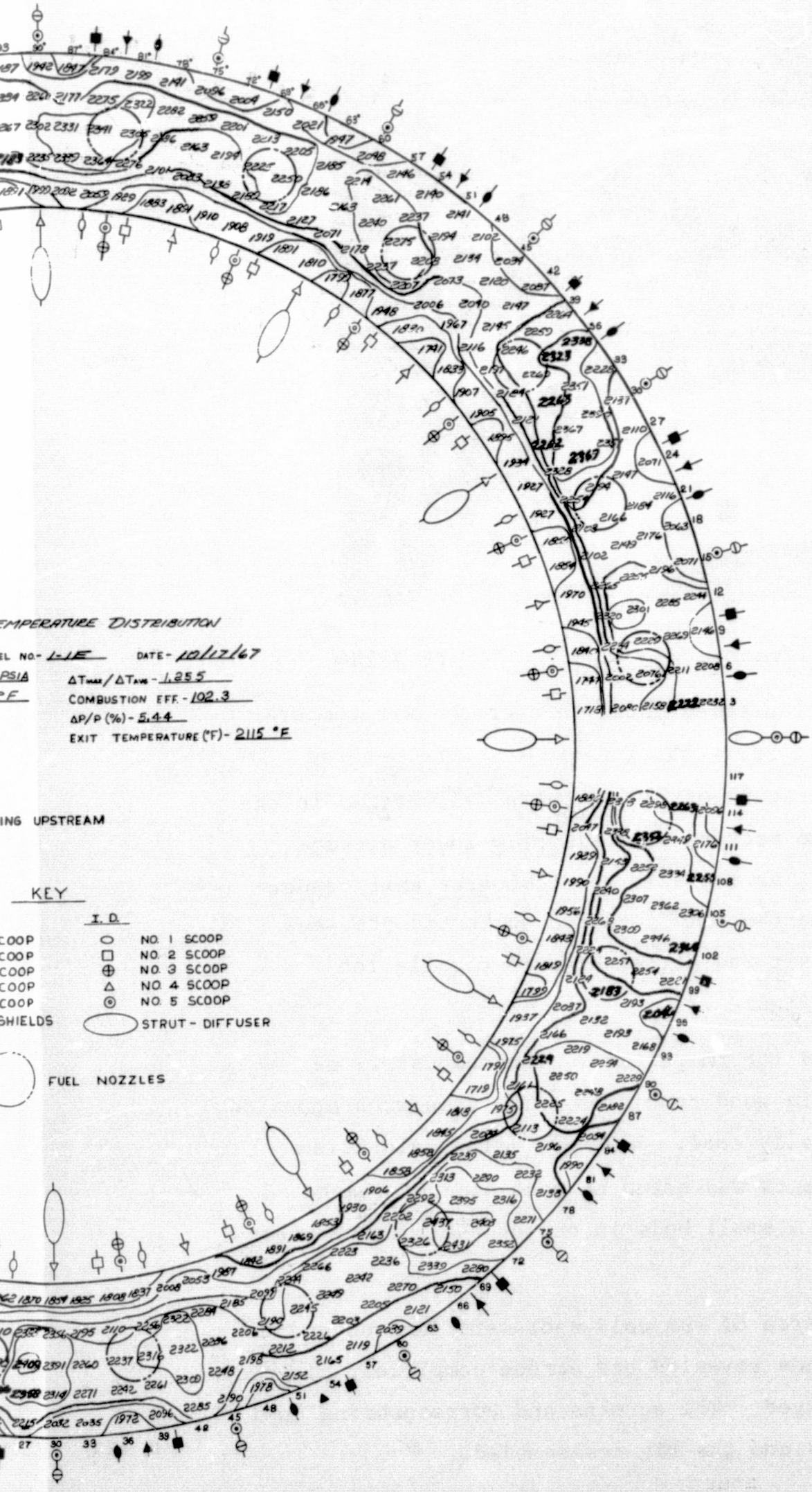

FD 23116

FOLDOUT FRAME 2

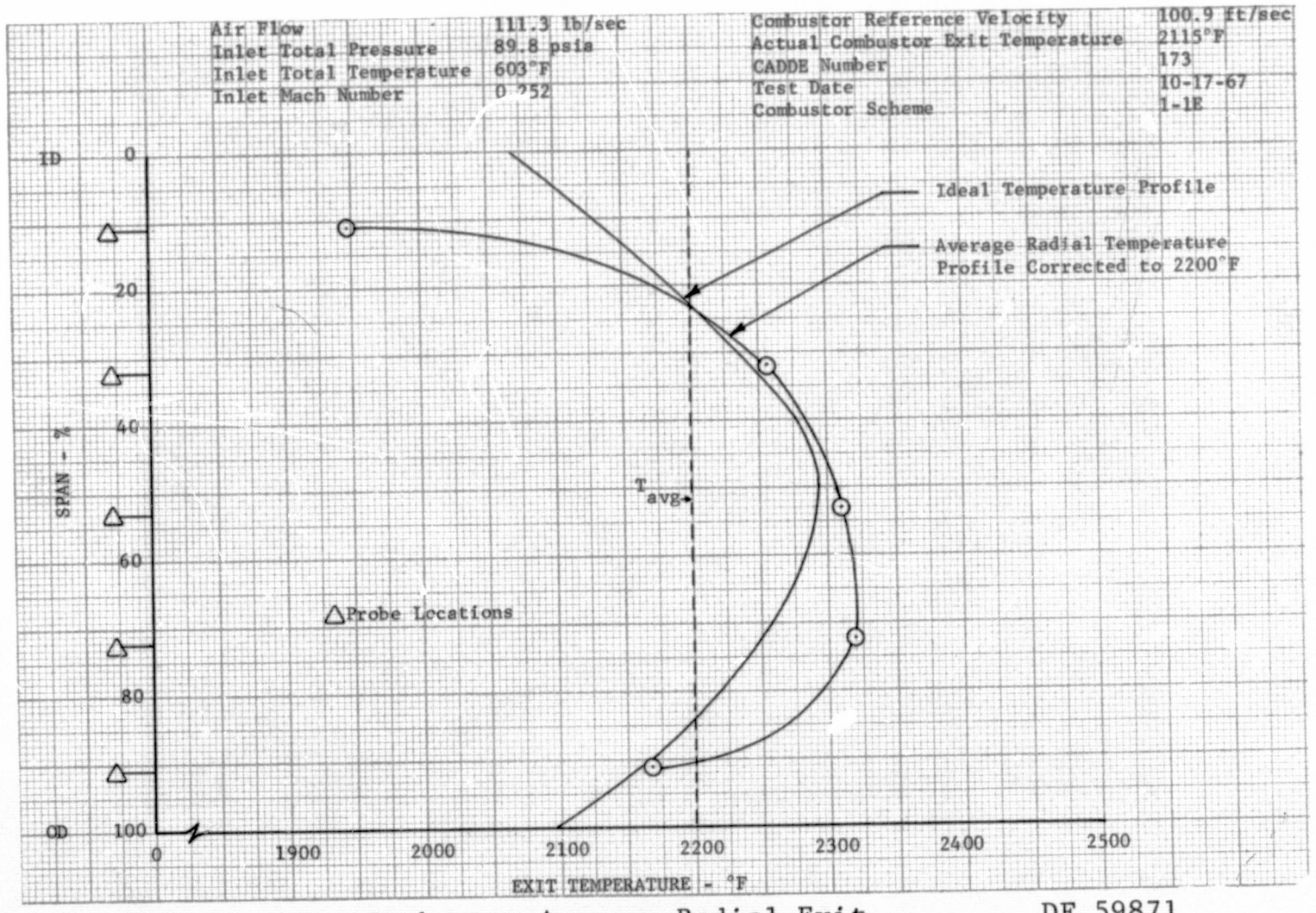

Figure 77. Combustor Average Radial Exit Temperature Profile, Test No. 173

DF 59871

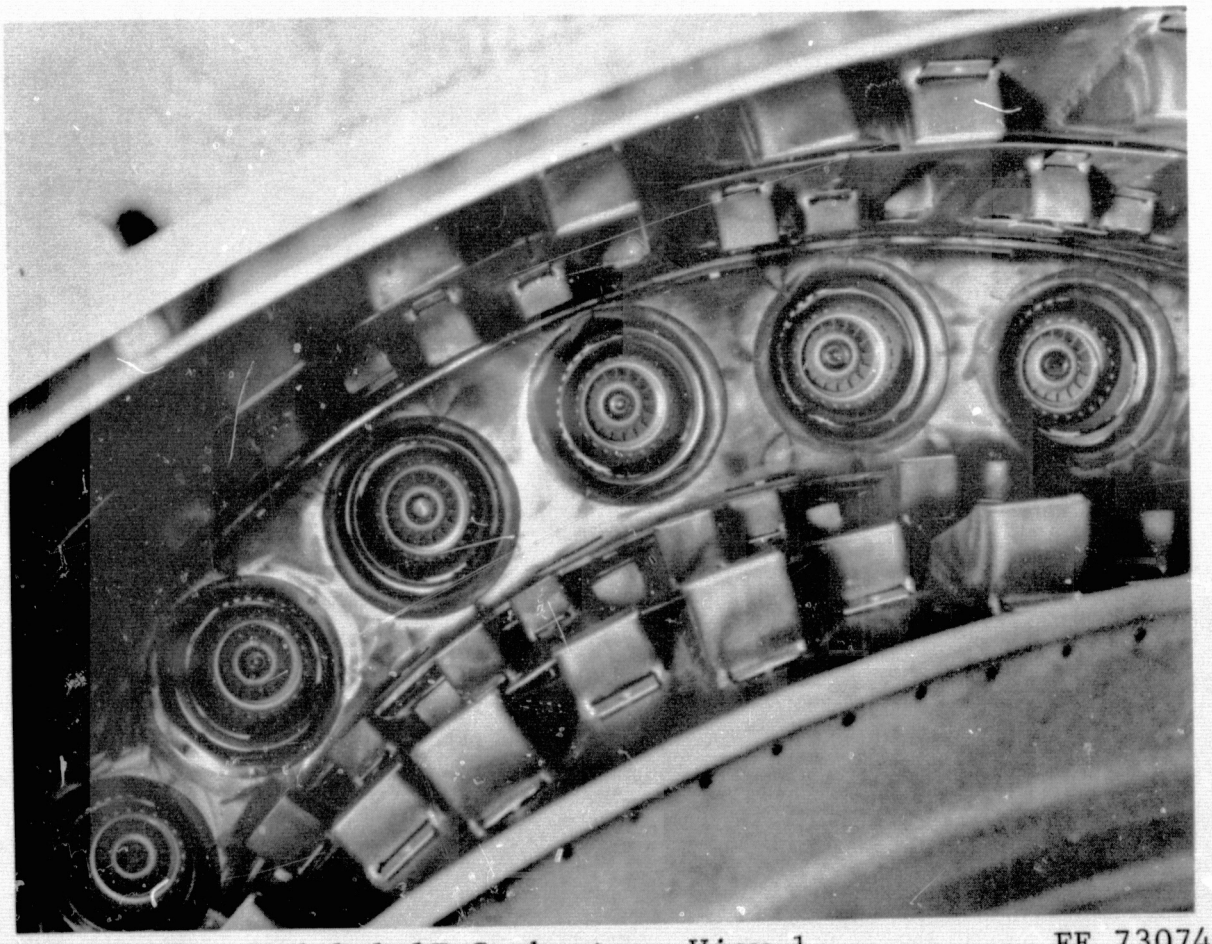

Figure 78. Model 1-1E Combustor, View 1

FE 73074

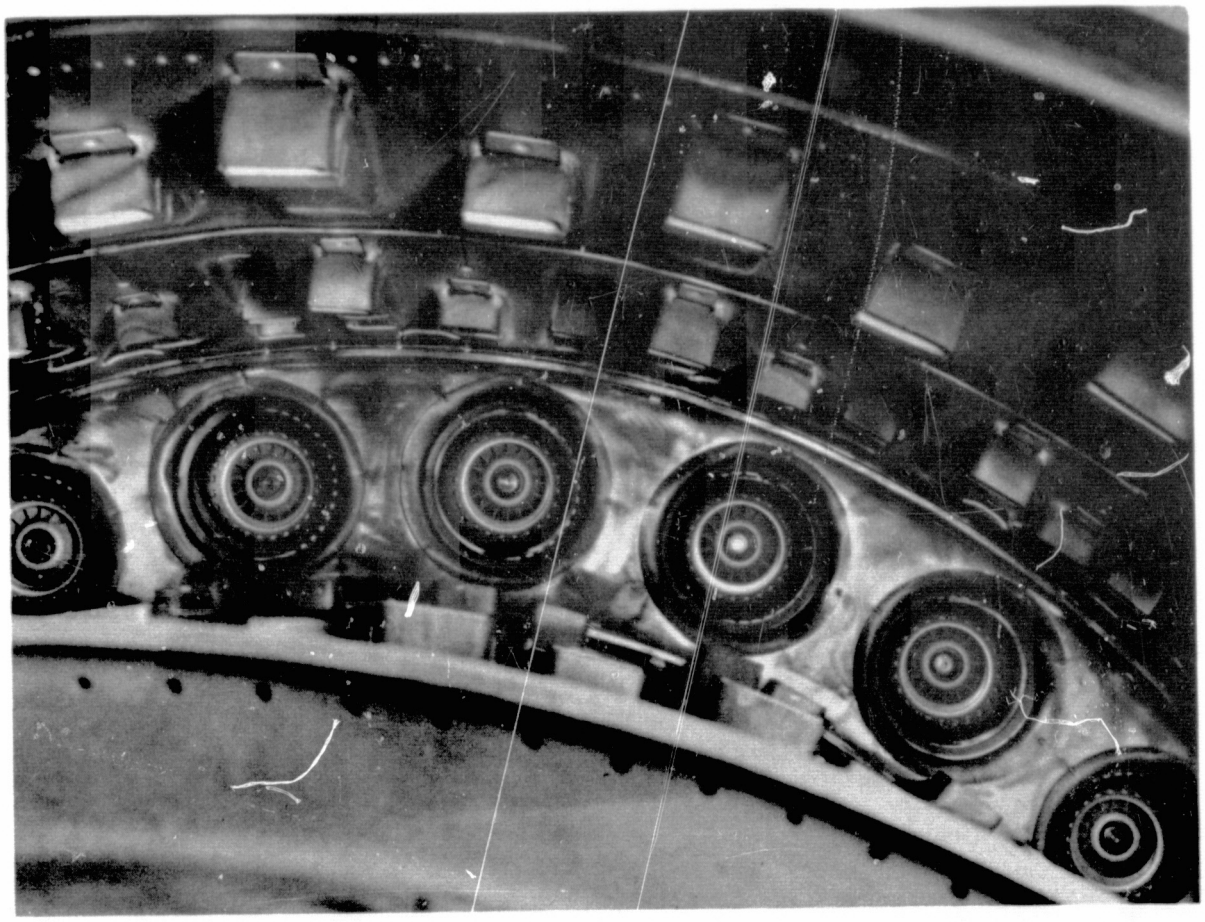

Figure 79. Model 1-1E Combustor, View 2 FE 73075

Testing was then resumed. The first data point taken (Test Point 36 of table 4) was at an average exit temperature of 1915°F. As shown in the combustor exit temperature pattern, figure 80, the cold area was no longer evident. The average radial exit temperature profile for this test point (which very closely matches the ideal profile) is shown in figure 81.

The fuel/air ratio was then increased until an average exit temperature of 2232°F (Test Point 37 of table 4) was obtained. A hot spot of 2706°F was located at 300 degrees clockwise of top dead center and three other hot areas in the 2600°F range were located at 180, 255, and 280 degrees from top dead center (all looking upstream) as shown in the combustor exit temperature pattern, figure 82.

Four skin thermocouples were located on the combustor dome during these tests. The readings obtained from these thermocouples during each of the four combustion tests are presented in figure 83. The highest temperature recorded during any of the previous test series was 871°F.

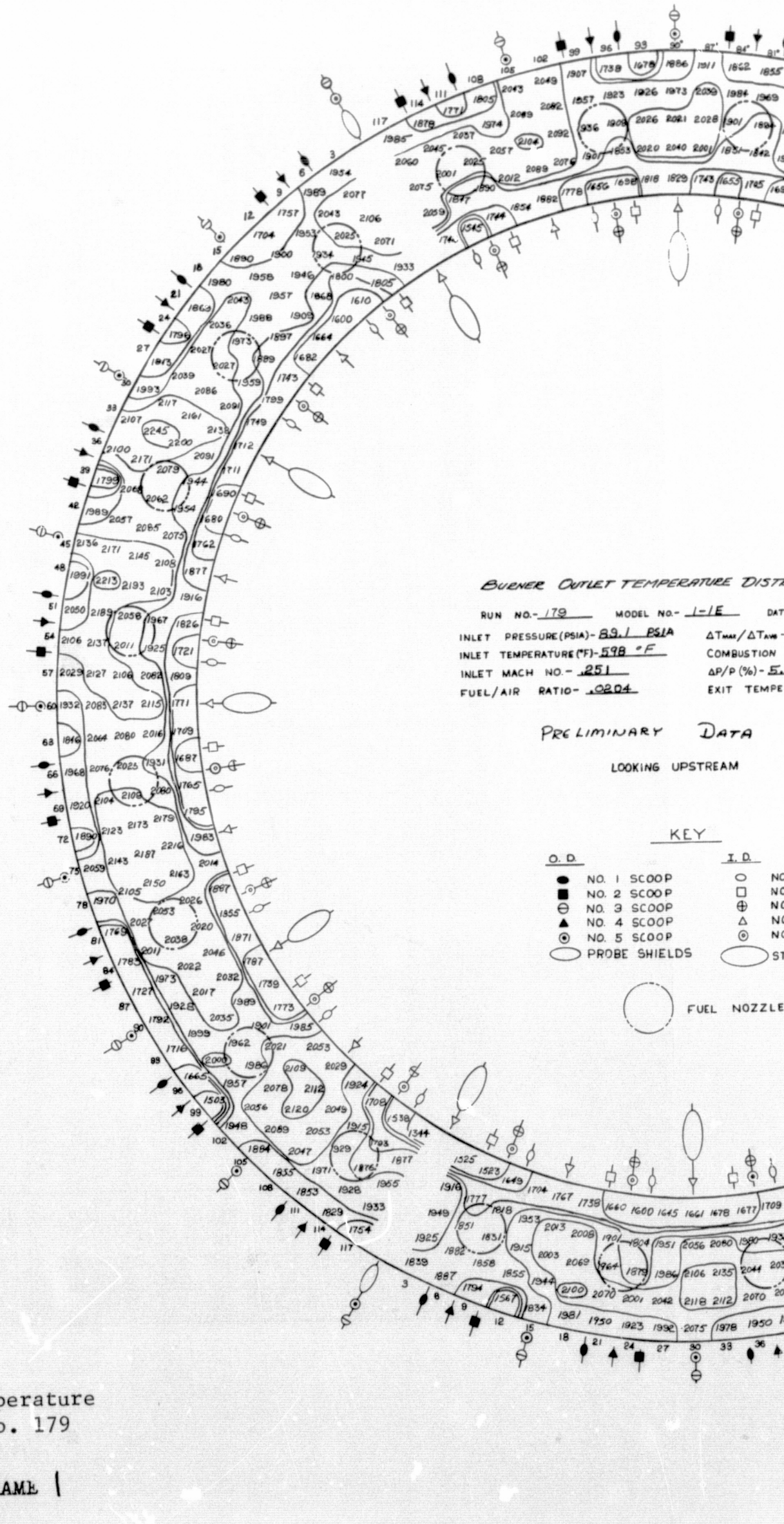

Figure 80. Combustor Outlet Temperature Distribution, Test No. 179

FOLDOUT FRAME 1

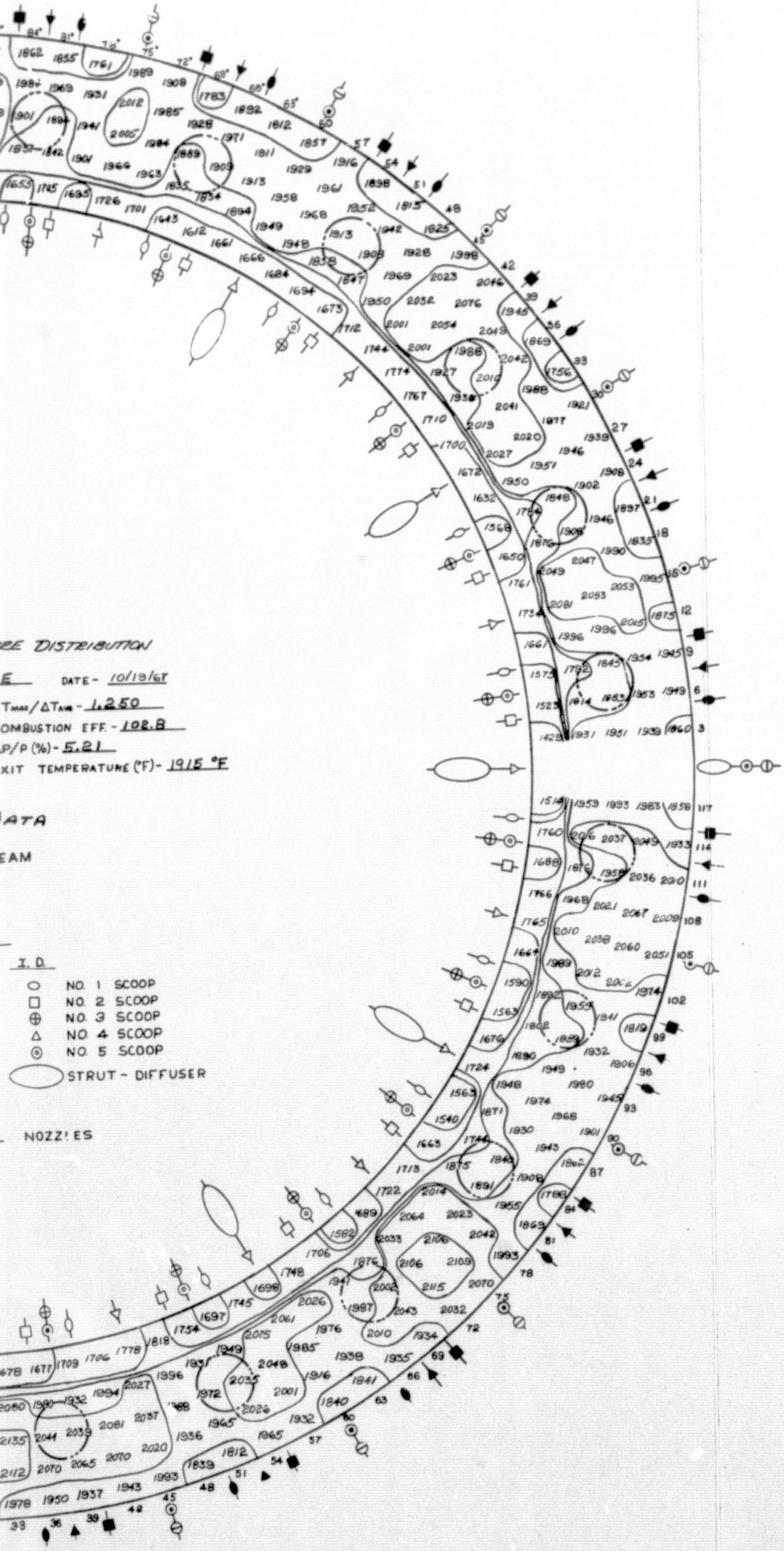

FD 23117

FOLDOUT FRAME 2

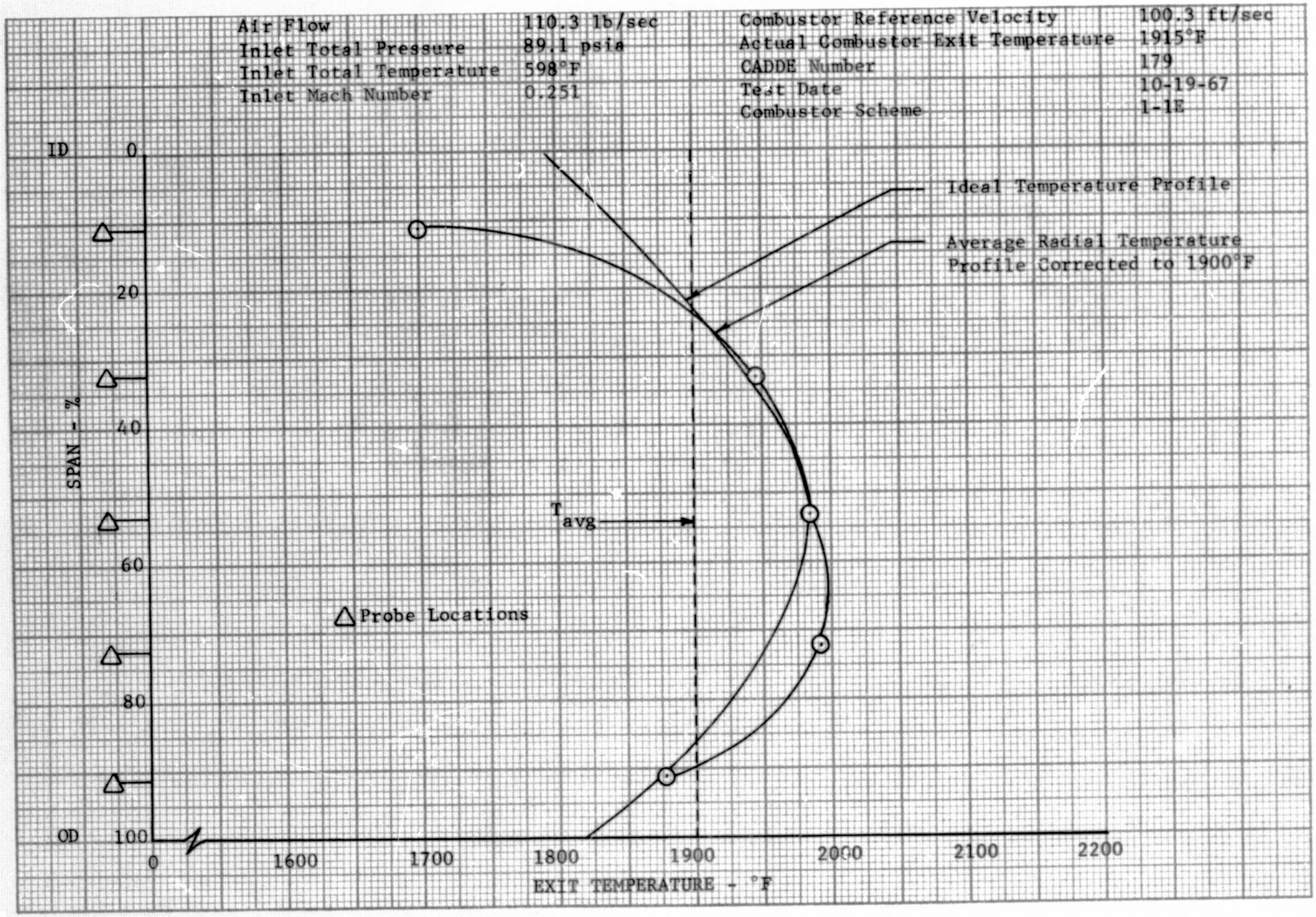

Figure 81. Combustor Average Radial Exit Temperature Profile, Test No. 179

DF 59872

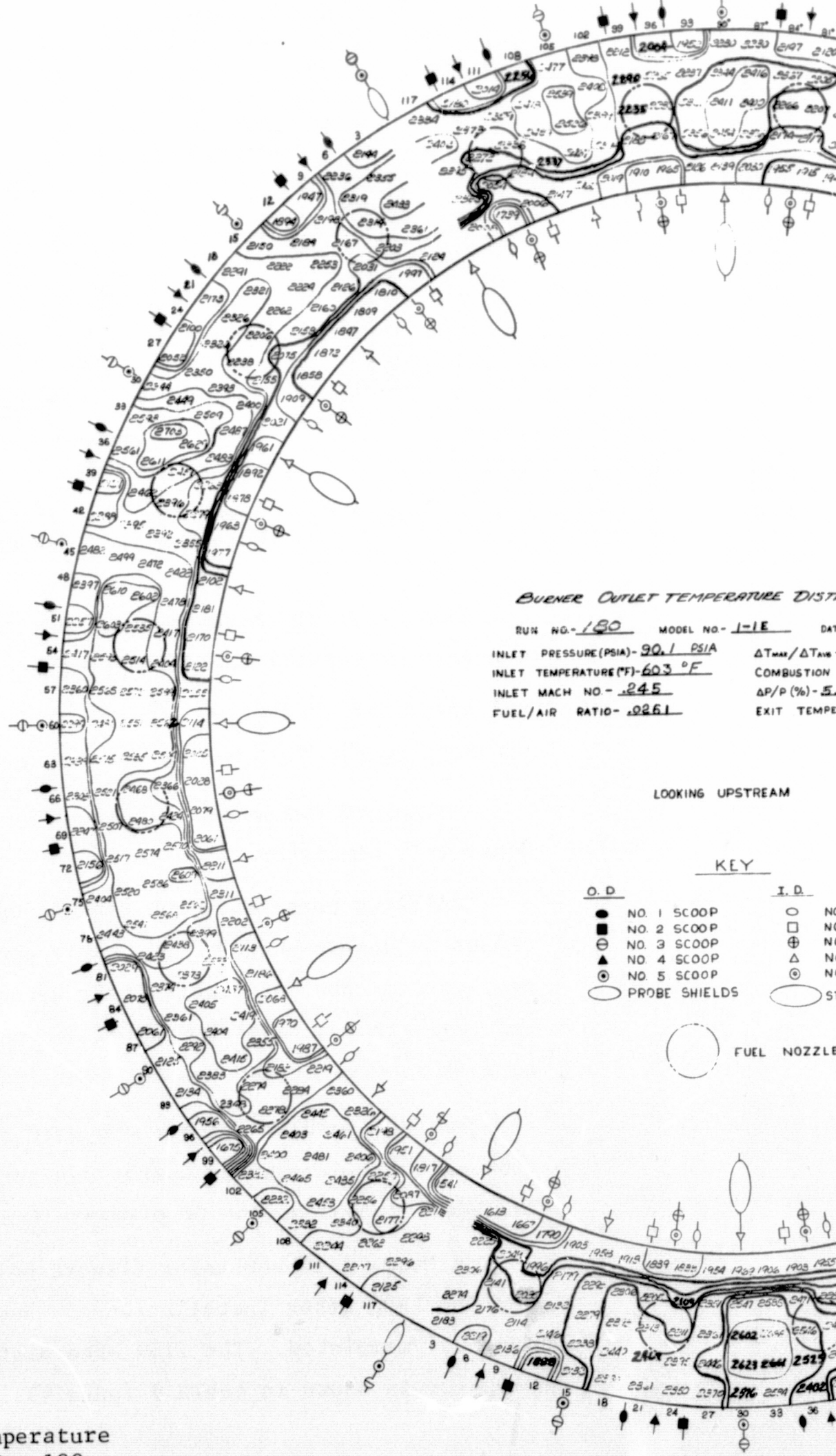

Figure 82. Combustor Outlet Temperature Distribution, Test No. 180

FOLDOUT FRAME |

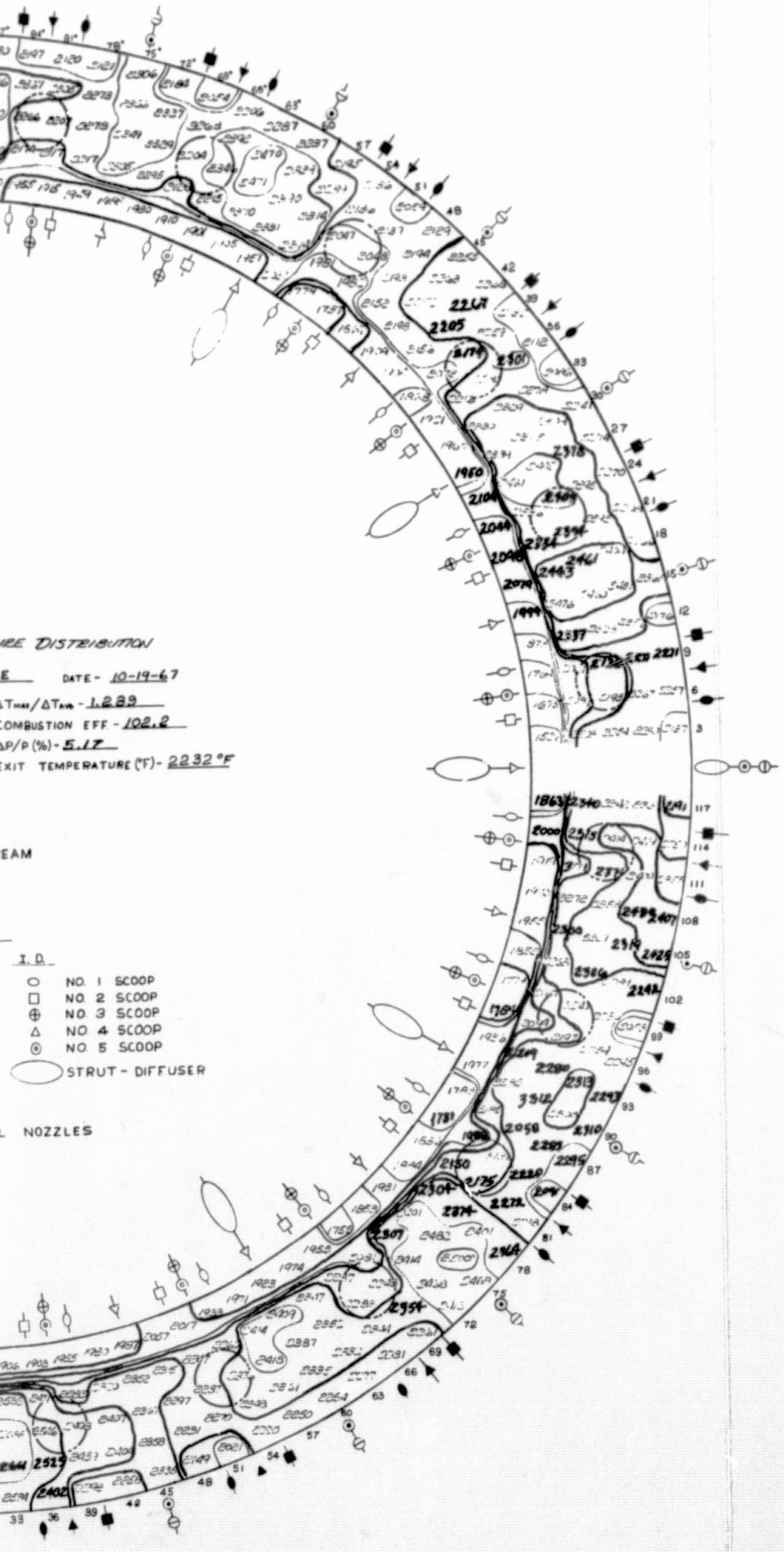

FD 23115

FOLDOUT FRAME 2

CADDE No.	TC Number 1	2	3	4
	TC Reading			
172	805	733	789	730
173	812	736	801	739
179	791	738	818	741
180	812	738	871	840

All Readings are in °F

Location	
TC: No. 1 and 4	OD of Firewall Face Between Swirl Cups Spaced 180 deg Apart
TC: No. 2 and 3	ID of Firewall Face Between Swirl Cups Spaced 180 deg Apart

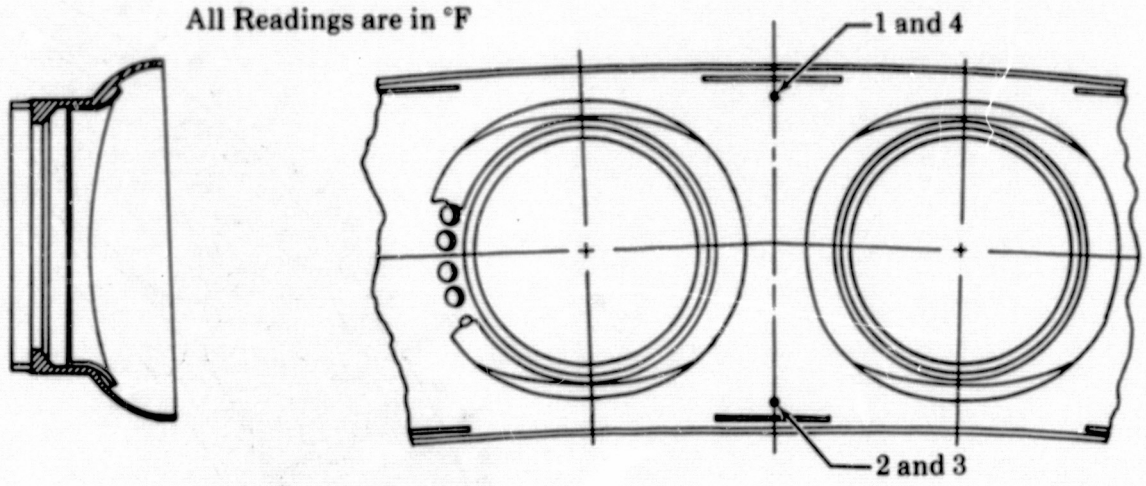

Figure 83. Combustor Dome Thermocouple Location and Test Results FD 23114

Test Point 38 of table 4 was an isothermal test conducted to measure the overall combustor pressure loss at the maximum reference velocity test condition. The 8% value obtained was an increase over previous models tested, but was still within the contract limitations.

A total of two hours of combustion time was accumulated on the Model 1-1E combustor for a total to date of 18.8 hours.

Following this test, the rig was opened for inspection. The overall combustor appearance was very satisfactory although the high thermal gradients on the OD primary liner were still evident. An inspection of the fuel strut screens indicated screen contamination that was believed to be the cause of the new hot spot appearance.

The fuel nozzles and screens were sent to be cleaned and the nozzles flow calibrated. The combustor was returned to FRDC for the addition of thumbnail scoops on the OD primary liner to provide additional cooling.

The Model 1-1F combustor (figure 84) was returned to NASA-LeRC from the FRDC after installation of thumbnail scoops on the OD primary liner was completed. The flow area distribution chart for the Model 1-1F combustor is shown in table 9 (page 95).

Table 9. Flow Areas for the Advanced Annular Combustor, Model 1-1F

ITEM	DESCRIPTION	TOTAL AREA (%)	LENGTH (in.)	WIDTH (in.)	AREA (in.^{2})	TOTAL AREA (in.^{2})
A	First Primary Scoop	0.77	0.059	0.800	0.046	2.227
B	Second Primary Scoop	10.20	0.801	0.800	0.614	29.472
C	Third Primary Scoop	10.20	0.801	0.800	0.614	29.472
D	First Secondary Scoop	13.05	0.702	1.120	0.787	37.700
E	Second Secondary Scoop	13.05	0.702	1.120	0.787	37.700
1	ID Primary Liner Cooling Holes	3.11	0.135		0.138	8.970
2	ID Secondary Liner Cooling Gaps	4.14	79.721	0.150	11.958	11.958
3	Cooling Film Gap	0.19	0.500	0.030	0.015	0.540
4	ID Transition Liner	3.25	0.129, 0.183, and 0.104 dia			9.388
5	ID Rear Shroud Outlet	1.59	0.156 dia		0.0191	4.584
6	OD Primary Liner Cooling Holes	3.81	0.145 slots		0.108	11.016
7	OD Secondary Liner Cooling Gap	4.37	114.819	0.110	12.630	12.630
8	Cooling Film Gap	0.37	0.600	0.030	0.018	1.080
9	OD Transition Liner Film Cooling Gap	4.01	0.129, 0.120, and 0.166 dia		0.094 dia	11.569
10	OD Rear Shroud Outlet	2.25	0.125 dia		0.123	6.494
11	Holes in Cone	2.45	0.125 dia		0.0123	7.080
12	Holes in Cone Aligning Ring	3.07	0.125 dia		0.0123	8.856
13	First Primary Scoop Cooling Louver No. 1	0.48	0.575	0.050	0.029	1.392
14	First Primary Scoop Cooling Louver No. 2	0.048	0.575	0.050	0.029	1.392
15	Second Primary Scoop Cooling Louver	1.31	0.575	0.137	0.079	3.780
16	Third Primary Scoop Cooling Louver No. 1	1.31	0.575	0.137	0.079	3.780
17	Third Primary Scoop Cooling Louver No. 2	1.31	0.575	0.137	0.079	3.780
18	Louvers Between 2nd and 3rd ID Primary Scoops	0.58	0.600	0.117	0.070	1.680
19	Louvers Between 2nd and 3rd OD Primary Scoops	0.69	0.710	0.117	0.083	1.995
20	Swirlers P/N CKJ-2476	7.98			0.960	23.040
21	OD Slots in Dome	0.63	1.480	0.050	0.076	1.824
22	ID Slots in Dome	0.52	1.250	0.050	0.062	1.488
23	Dome Air Deflectors	3.55	0.040 gap		0.427	10.248
24	Louvers Between 1st and 3rd OD Primary Scoops	0.70	0.375	0.113	0.042	2.016
25	Large Louvers Between 1st and 2nd OD Primary Scoops	0.24	0.575	0.050	0.029	0.696
26	Small Louvers Between 1st and 2nd OD Primary Scoops	0.35	0.375	0.113	0.042	1.008
	Totals	100.01				288.855

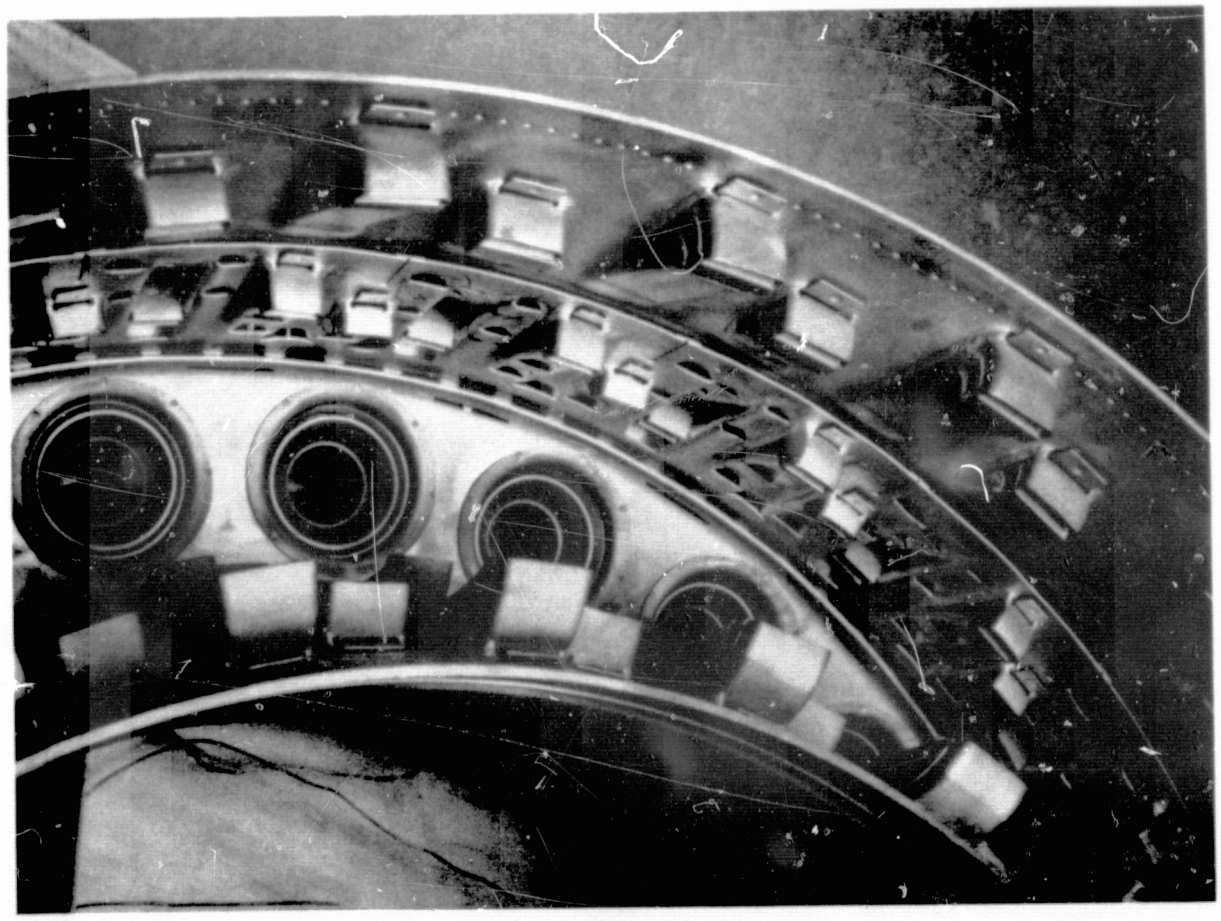

Figure 84. Model 1-1F Combustor FE 73706

Testing was then resumed. The first data point (Test Point 39 of table 4) was taken at an average exit temperature of 1882°F. The highest temperature recorded was 2191°F located on top dead center of the rig, as shown in the combustor exit temperature pattern (figure 85). Three other areas in the 2100°F temperature range were located 255°, 264°, and 288° clockwise from top dead center. The average exit radial temperature profile for this test point is shown in figure 86.

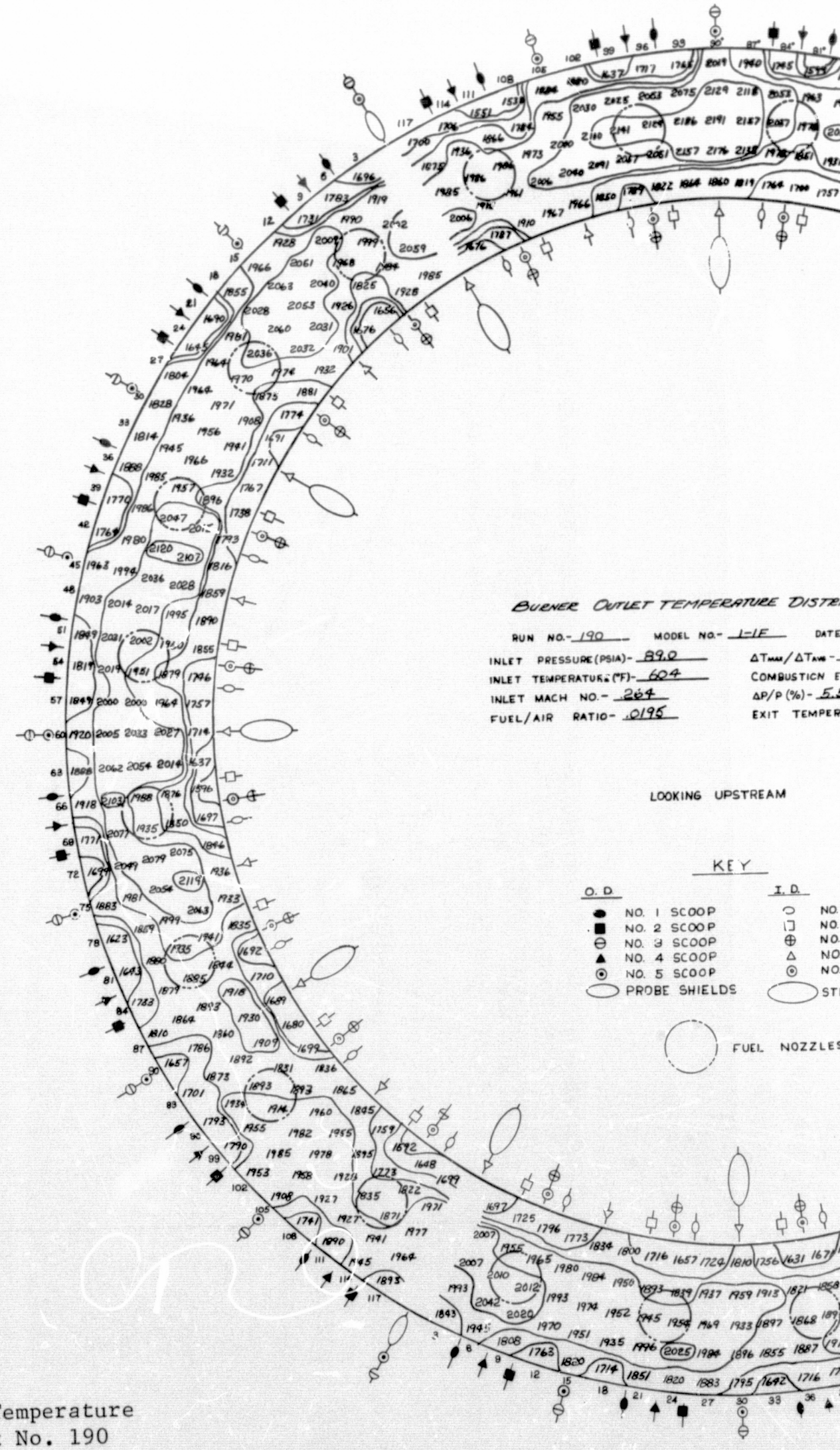

Figure 85. Combustor Outlet Temperature Distribution, Test No. 190

FOLDOUT FRAME 1

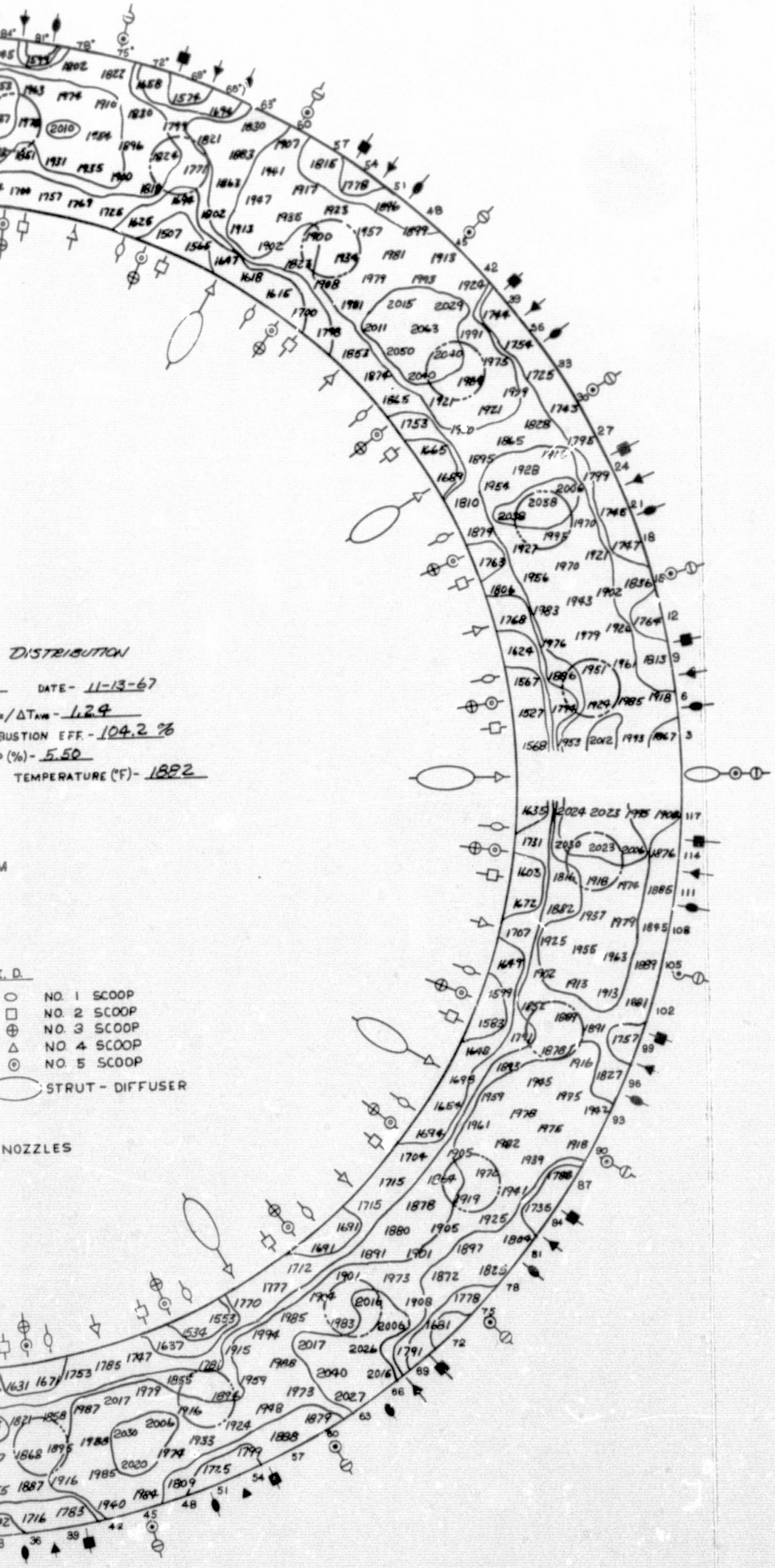

FD 23506

FOLDOUT FRAME 2

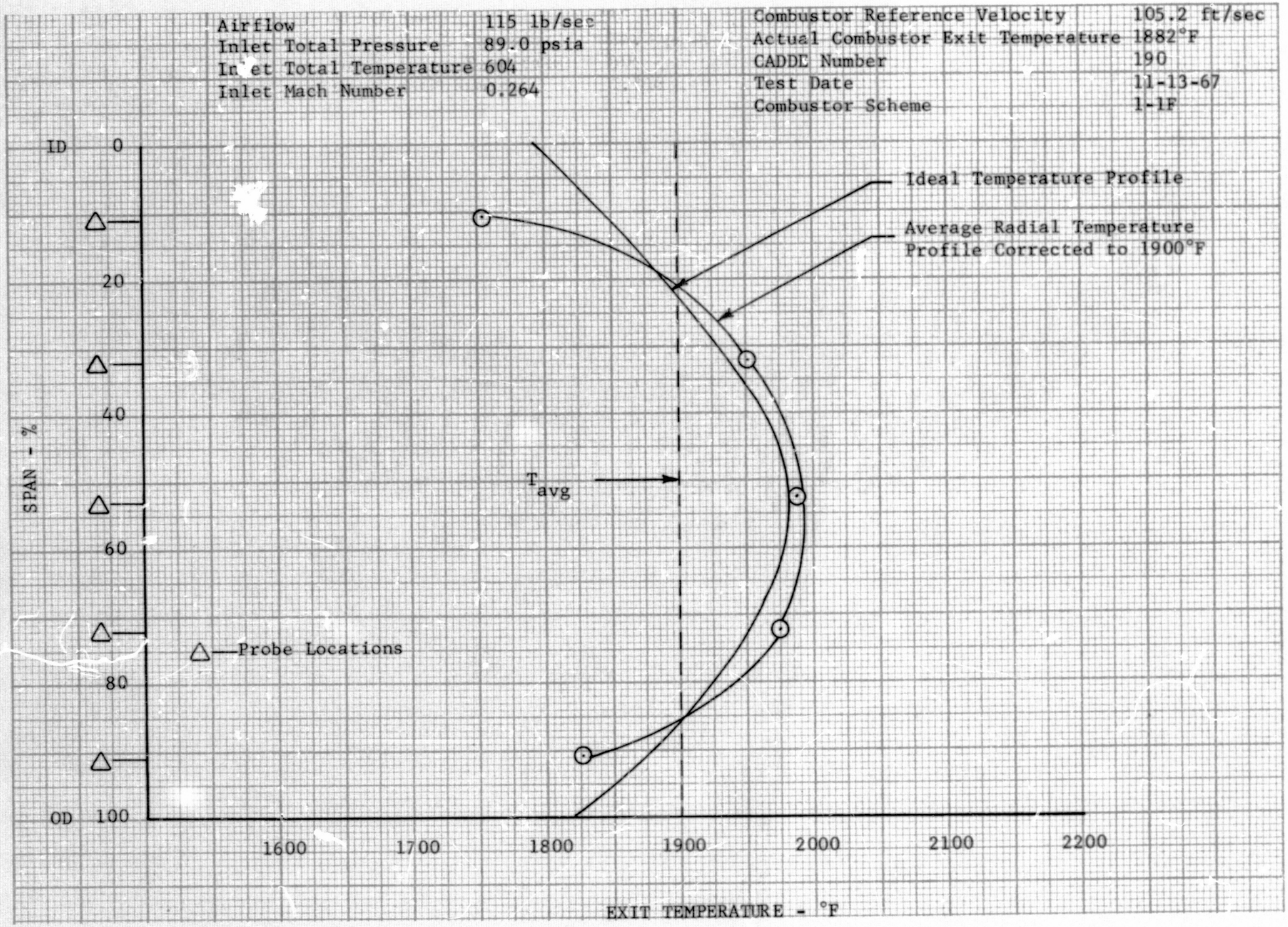

Figure 86. Combustor Average Radial Exit Temperature Profile Test No. 190

DF 60476

The fuel/air ratio was then increased until an average exit temperature of 2194°F was obtained (Test Point 40 of table 4). A hot spot of 2709°F was located on top dead center; as shown in the combustor outlet temperature distribution (figure 87). The fuel struts on each side of top dead center were then interchanged with the fuel struts on each side of the 240° (clockwise from top dead center looking upstream) position This was done to determine if a fuel nozzle was the cause of the hot spot. The combustor was again ignited and a second data point (Test Point 41 of table 4) was recorded at the same test condition, at an average exit temperature of 2236°F. Three hot spots of 2630°, 2619°, and 2647°F were located at approximately top dead center and at 255° and 264° clockwise from top dead center looking upstream, respectively, as shown in the combustor exit temperature pattern (figure 88). The combustor radial exit temperature profiles for Test Points 40 and 41 of table 4 are shown in figures 89 and 90, respectively.

Examination of the test data disclosed that the airflow had been fluctuating between 109 lb/sec and 115 lb/sec during the period in which Test Point 40 was recorded. This is believed to be the reason for the 2709°F hot spot. In Test Point 41, the hot spot had not moved; however, the hot spot was 79°F cooler at an average exit temperature which was 42°F hotter than recorded in Test Point No. 40.

The test rig was then disassembled for inspection. The overall appearance of the combustor was very satisfactory with no evidence of high thermal gradients on the OD primary liner in the area of the new thumbnail scoops (figures 91 and 92).

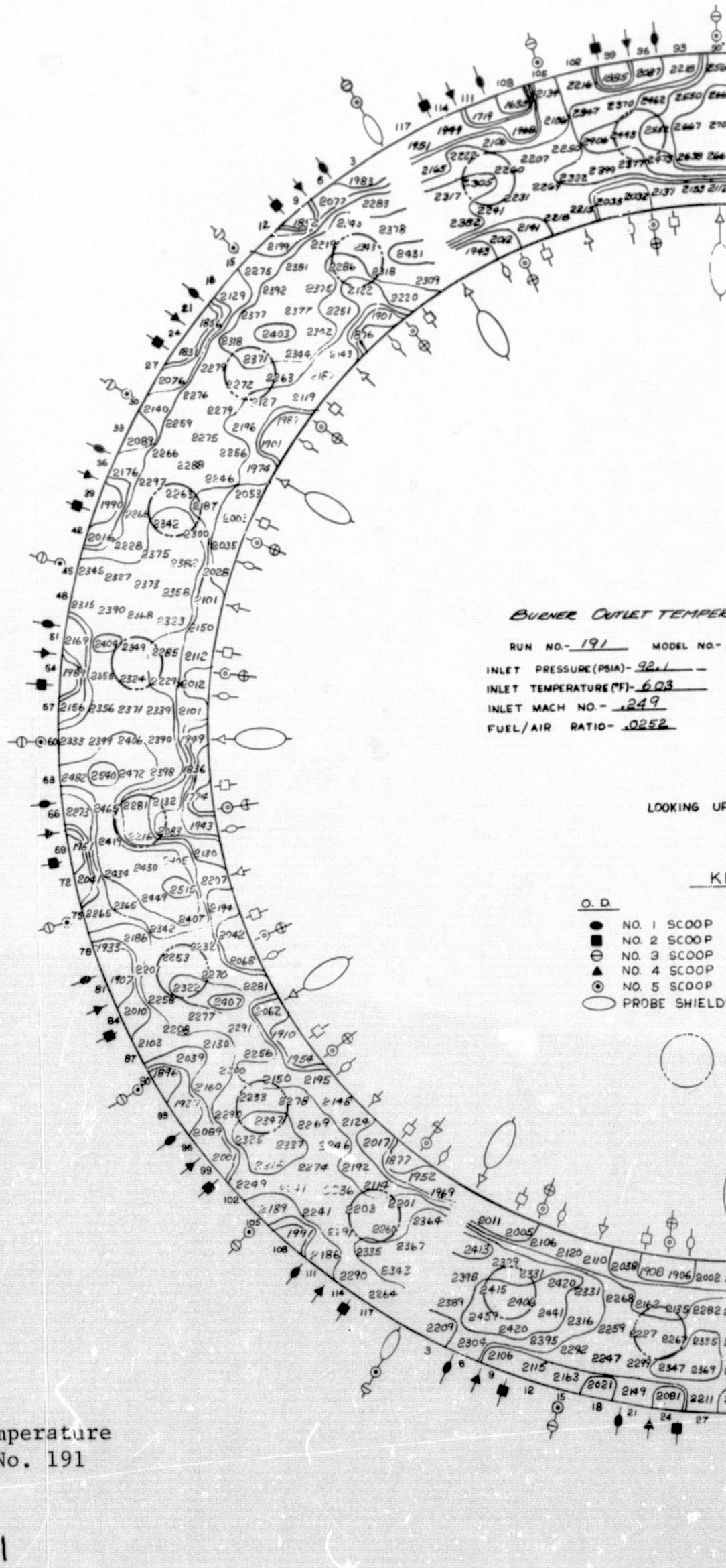

Figure 87. Combustor Outlet Temperature Distribution, Test No. 191

FOLDOUT FRAME 1

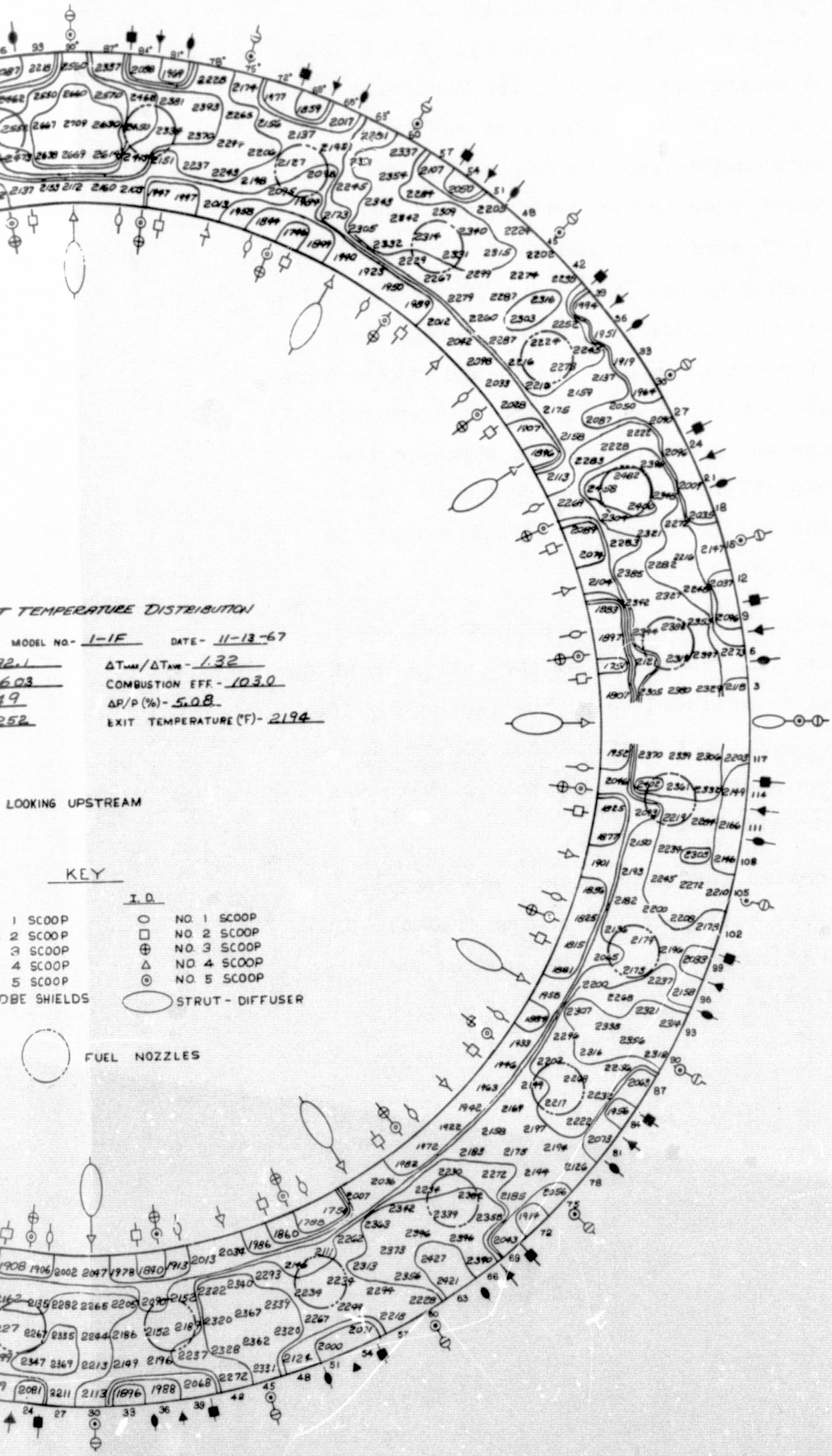

FD 23501

FOLDOUT FRAME 2

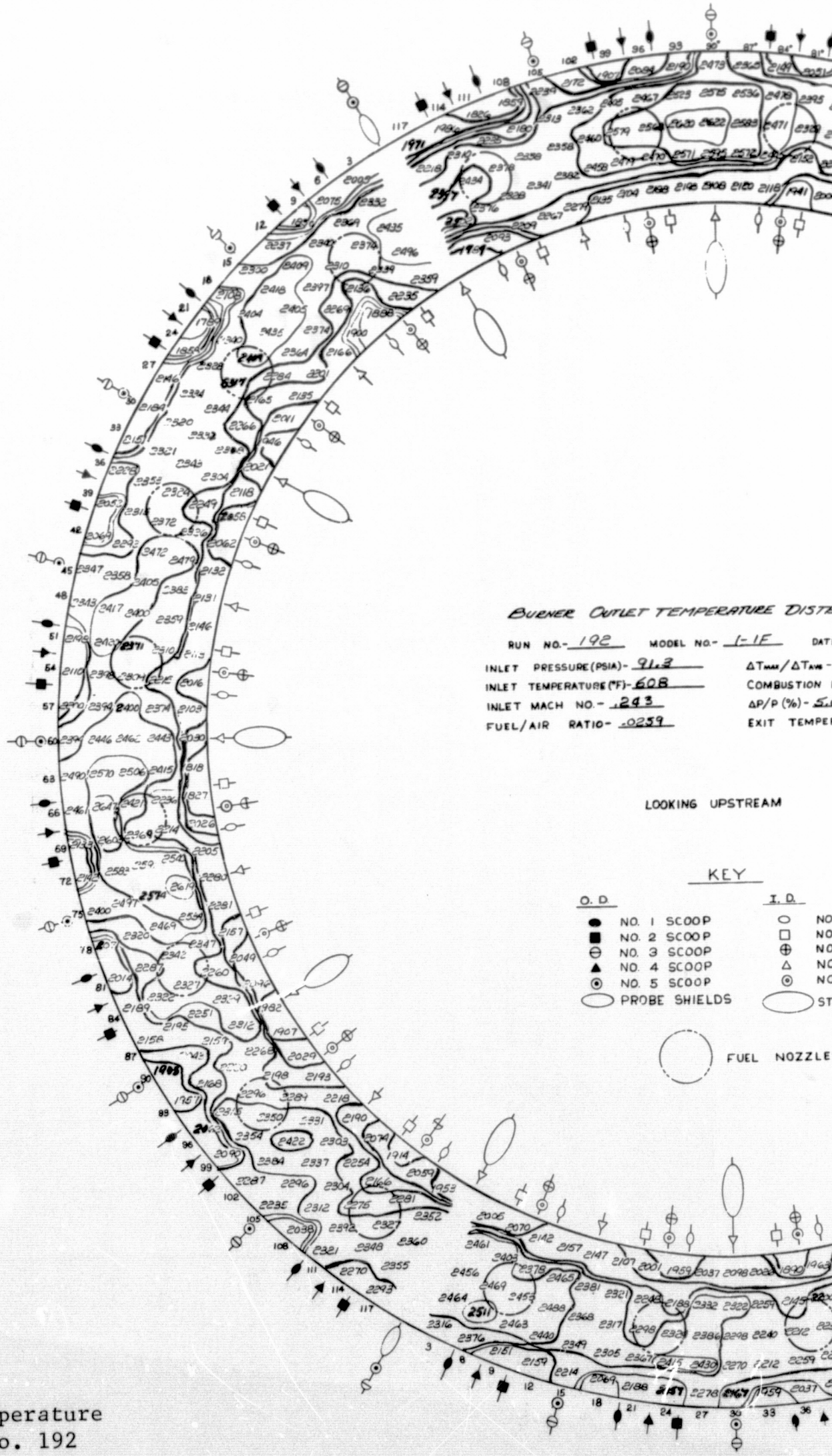

Figure 88. Combustor Outlet Temperature Distribution, Test No. 192

FOLDOUT FRAME 1

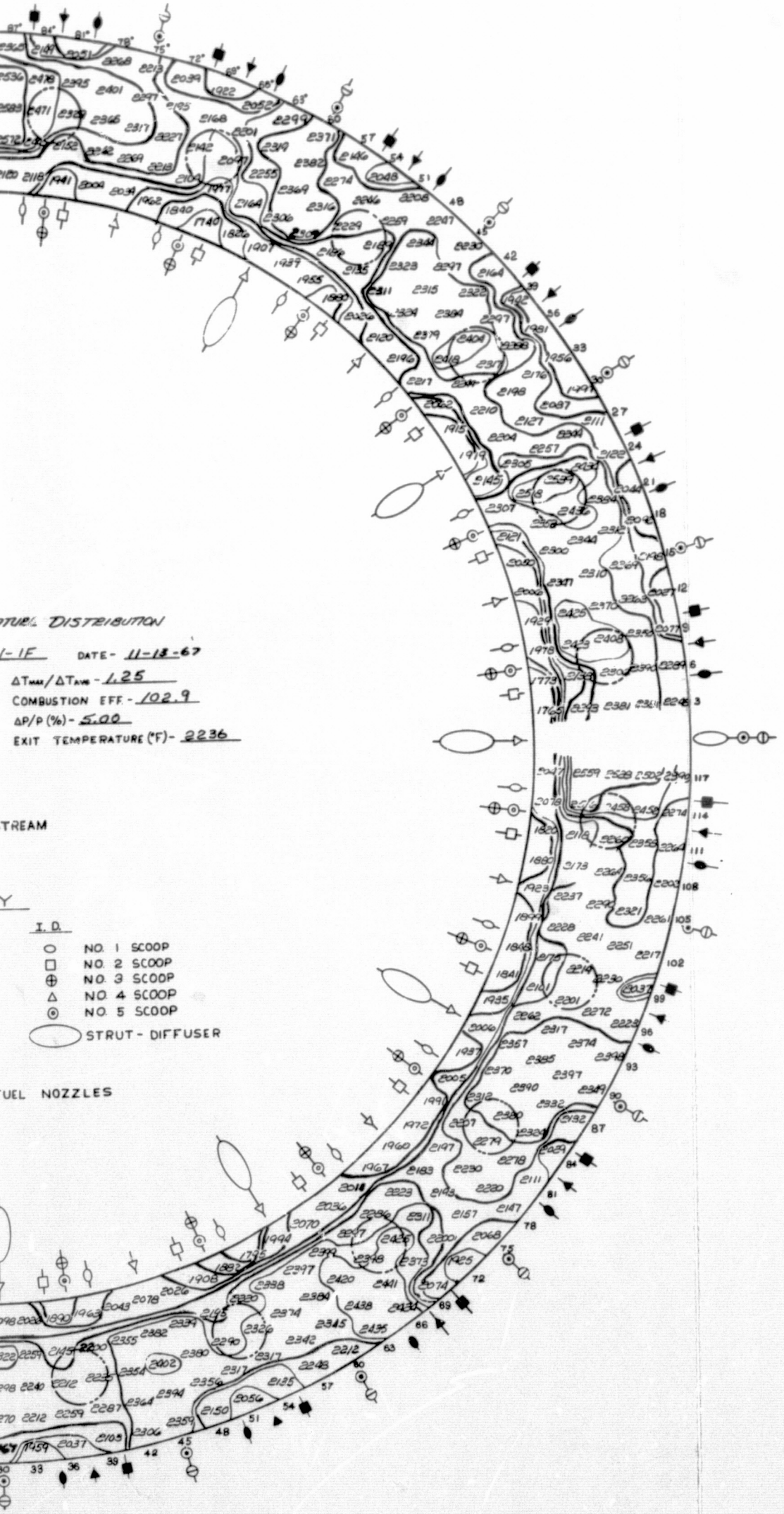

FD 23502

FOLDOUT FRAME 2

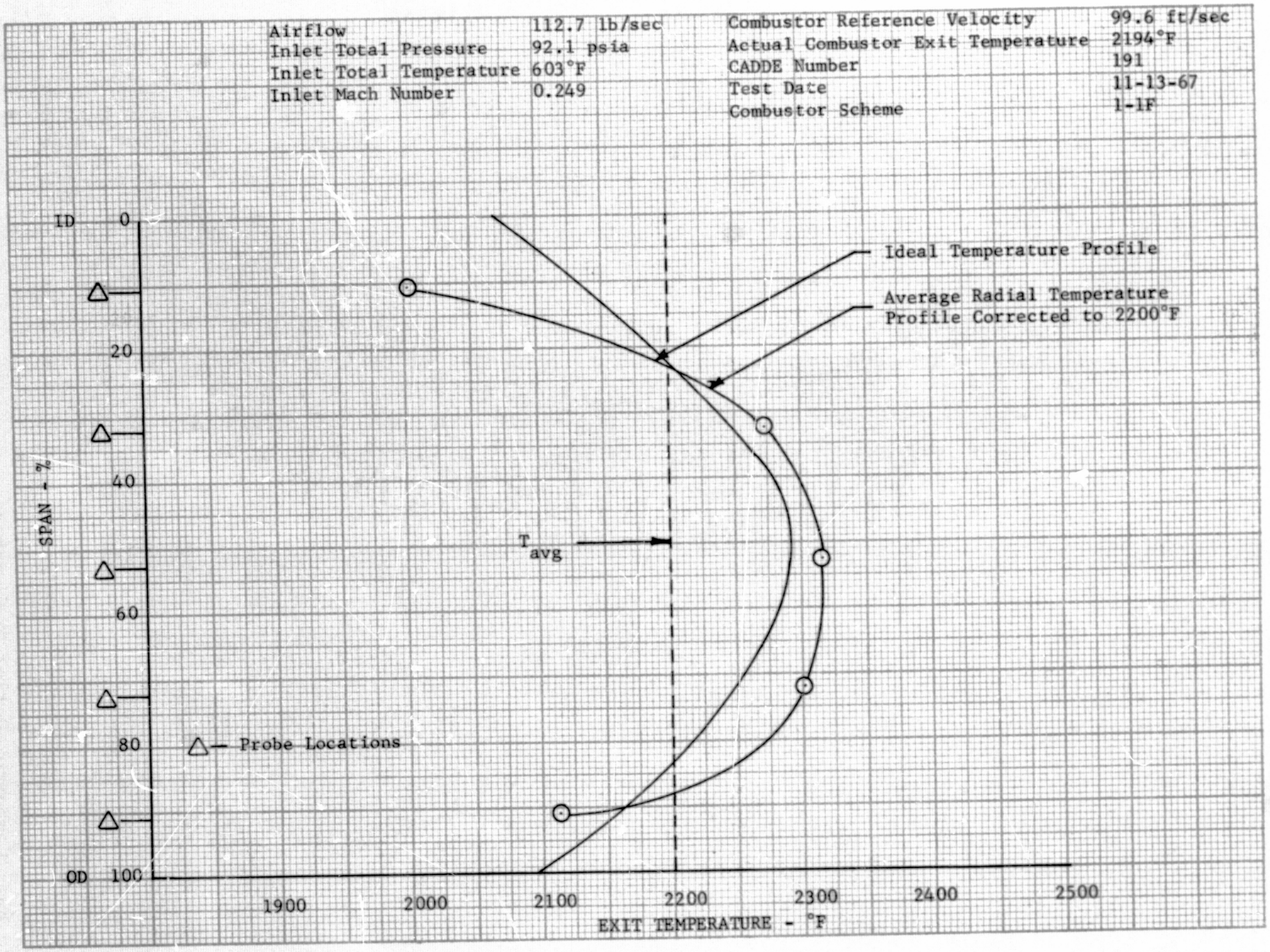

Figure 89. Combustor Average Radial Exit Temperature Profile, Test No. 191

DF 60477

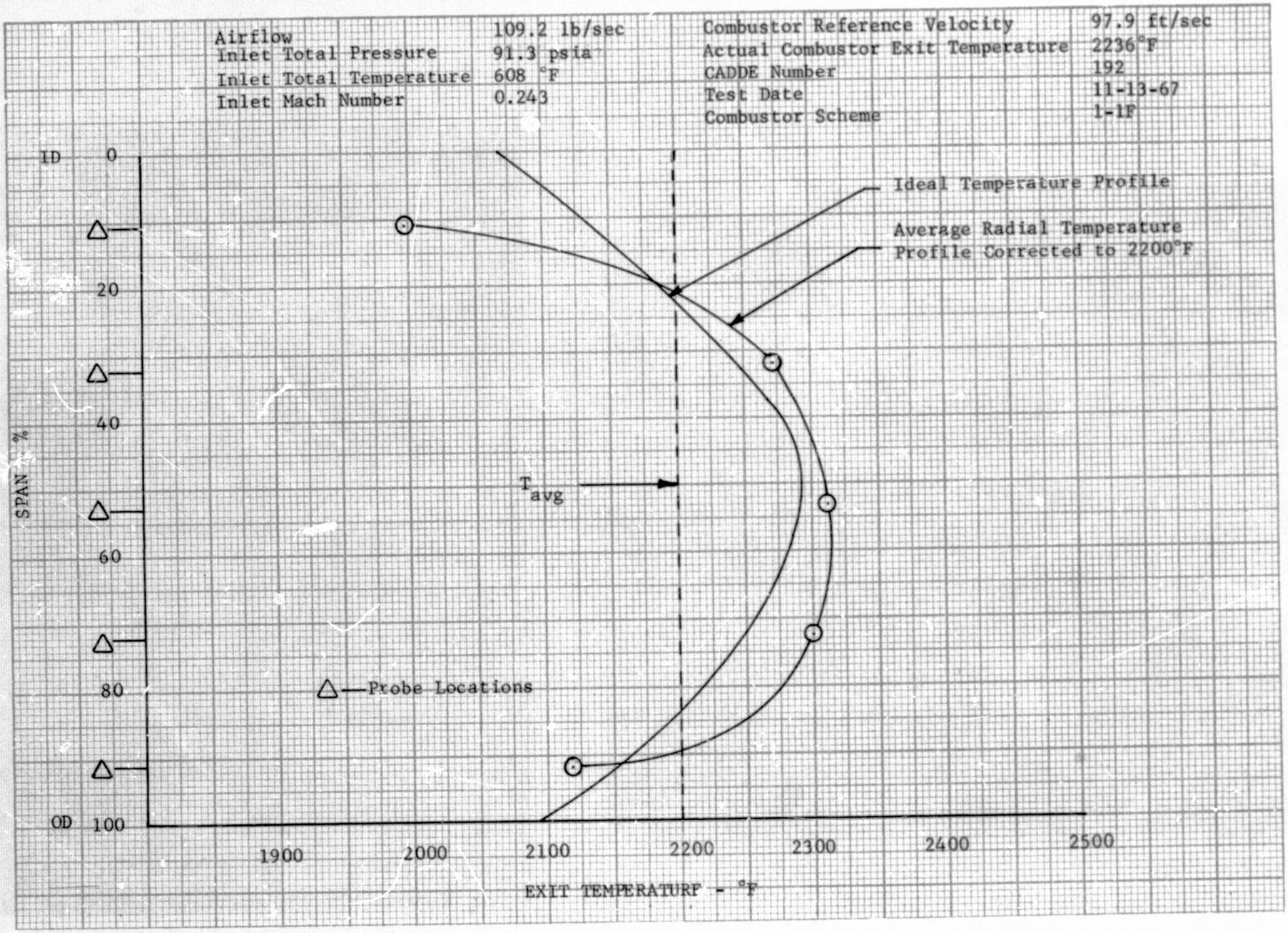

Figure 90. Combustor Average Radial Exit Temperature Profile, Test No. 192

DF 60478

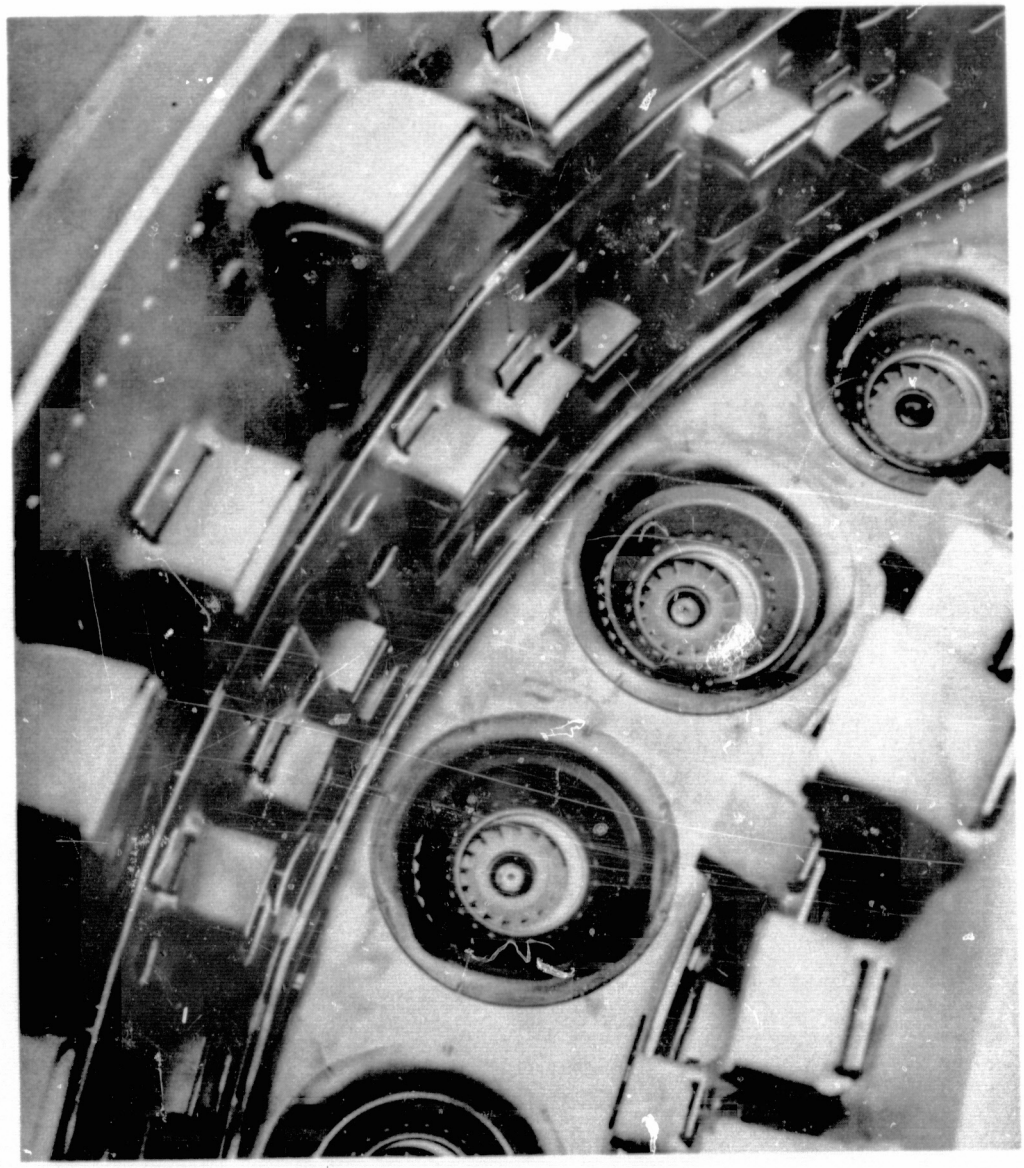

Figure 91. Model 1-1F Combustor After Testing (View 1) FE 73707

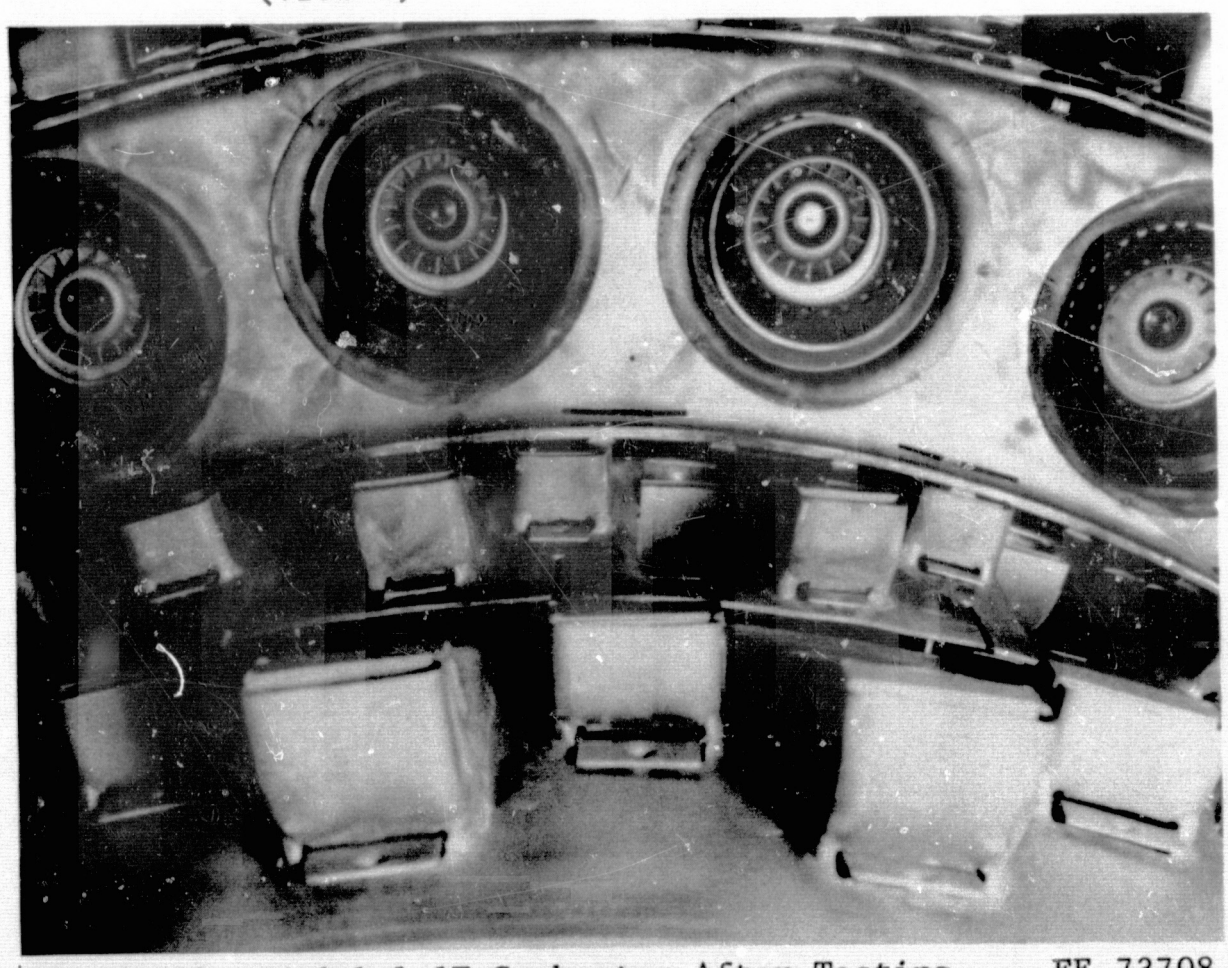

Figure 92. Model 1-1F Combustor After Testing (View 2) FE 73708

Testing was resumed and the first data point (Test Point 42 of table 4) was taken at an average exit temperature of 2188°F. There were no hot spots in the 2600°F temperature range. However, three hot spots in the 2500°F temperature range were located at top dead center, 96° and 255° clockwise from top dead center, looking upstream as shown in the combustor exit temperature pattern (figure 93). The average exit radial temperature for this test is shown in figure 94. The combustor inlet temperature was then increased to 1165°F and the fuel/air ratio was set to give an average exit temperature of 1936°F (Test Point 43 of table 4). As shown in the combustor exit temperature pattern (figure 95), there were no hot spot areas. The average radial exit temperature profile for this test point, which very closely matches the ideal profile, is shown in figure 96.

The fuel/air ratio was then increased until an average exit temperature of 2215°F was obtained (Test Point 44 of table 4). The hottest temperature recorded, 2436°F, was located 255° clockwise from top dead center looking upstream, as shown on the combustor exit temperature pattern (figure 97). Figure 98 shows that the average exit radial temperature profile for this test point very closely matches the ideal profile.

Test Point 44 concluded the testing conducted under Task III. A total of 6.5 hours of combustion time was accumulated on the Model 1-1F combustor for a total Task III combustion time of 25.3 hours.

The test rig was then disassembled for inspection. The inspection revealed a slight amount of nibbling on 6 or 7 No. 3 ID primary liner scoops (figure 99). However, the overall appearance of the combustor was very satisfactory (figure 100). There were no signs of high thermal gradients similar to those found on previous models of the combustor.

It was noted during the inspection that six fuel struts were not seating properly into the sealing collars on the OD flow splitter wall. This was corrected as much as possible with the combustor installed in the diffuser.

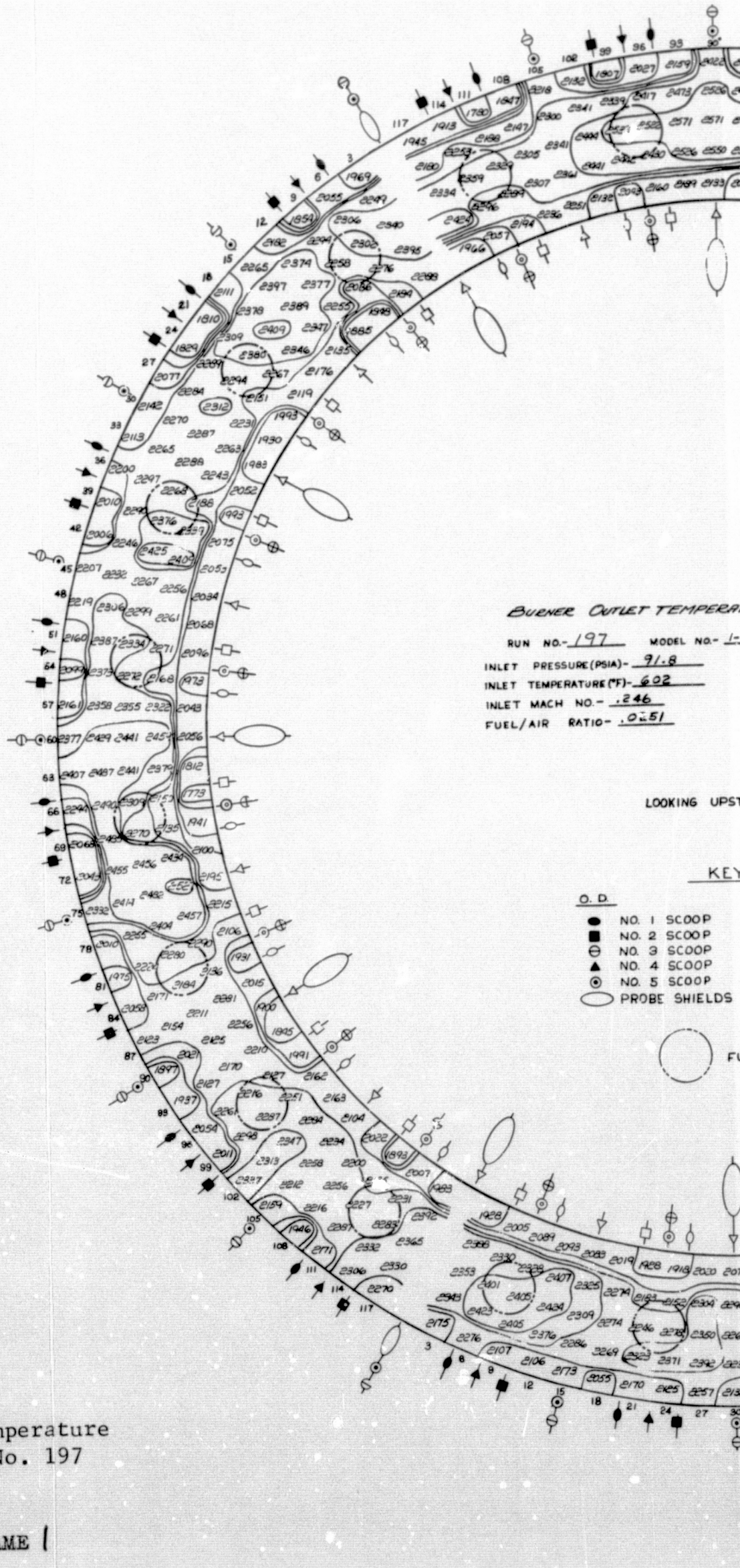

Figure 93. Combustor Outlet Temperature Distribution, Test No. 197

FOLDOUT FRAME 1

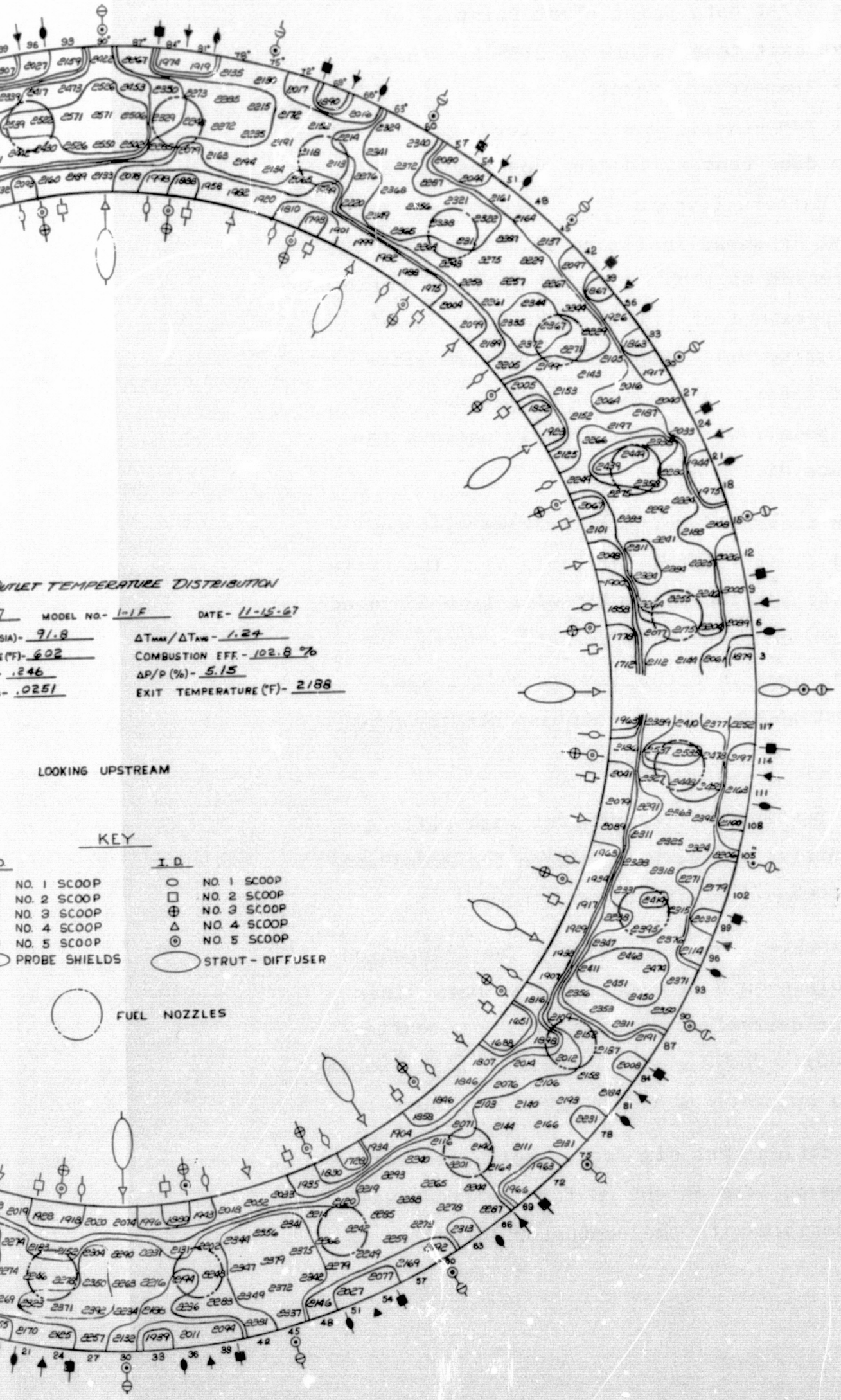

OUTLET TEMPERATURE DISTRIBUTION

7 MODEL NO.- I-1F DATE- 11-15-67

SIA)- 91.8 $\Delta T_{MAX}/\Delta T_{AVG}$ - 1.24

E (°F)- 602 COMBUSTION EFF. - 102.8 %

- .246 $\Delta P/P$ (%)- 5.15

)- .0251 EXIT TEMPERATURE (°F)- 2188

LOOKING UPSTREAM

KEY

	I.D.
NO. 1 SCOOP	NO. 1 SCOOP
NO. 2 SCOOP	NO. 2 SCOOP
NO. 3 SCOOP	NO. 3 SCOOP
NO. 4 SCOOP	NO. 4 SCOOP
NO. 5 SCOOP	NO. 5 SCOOP
PROBE SHIELDS	STRUT - DIFFUSER

FUEL NOZZLES

FD 23505

FOLDOUT FRAME 2

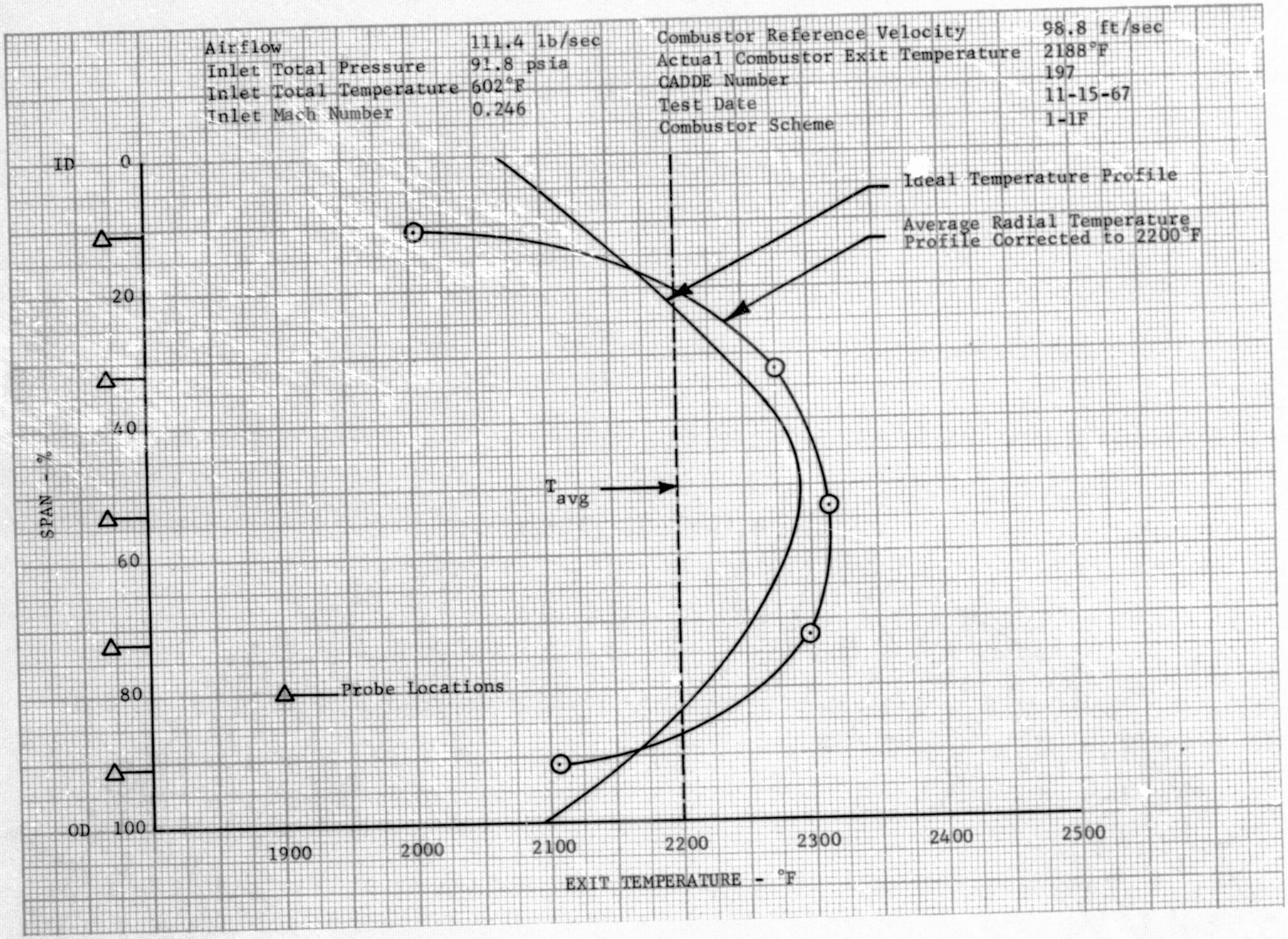

Figure 94. Combustor Average Radial Exit Temperature Profile, Test No. 197

DF 60479

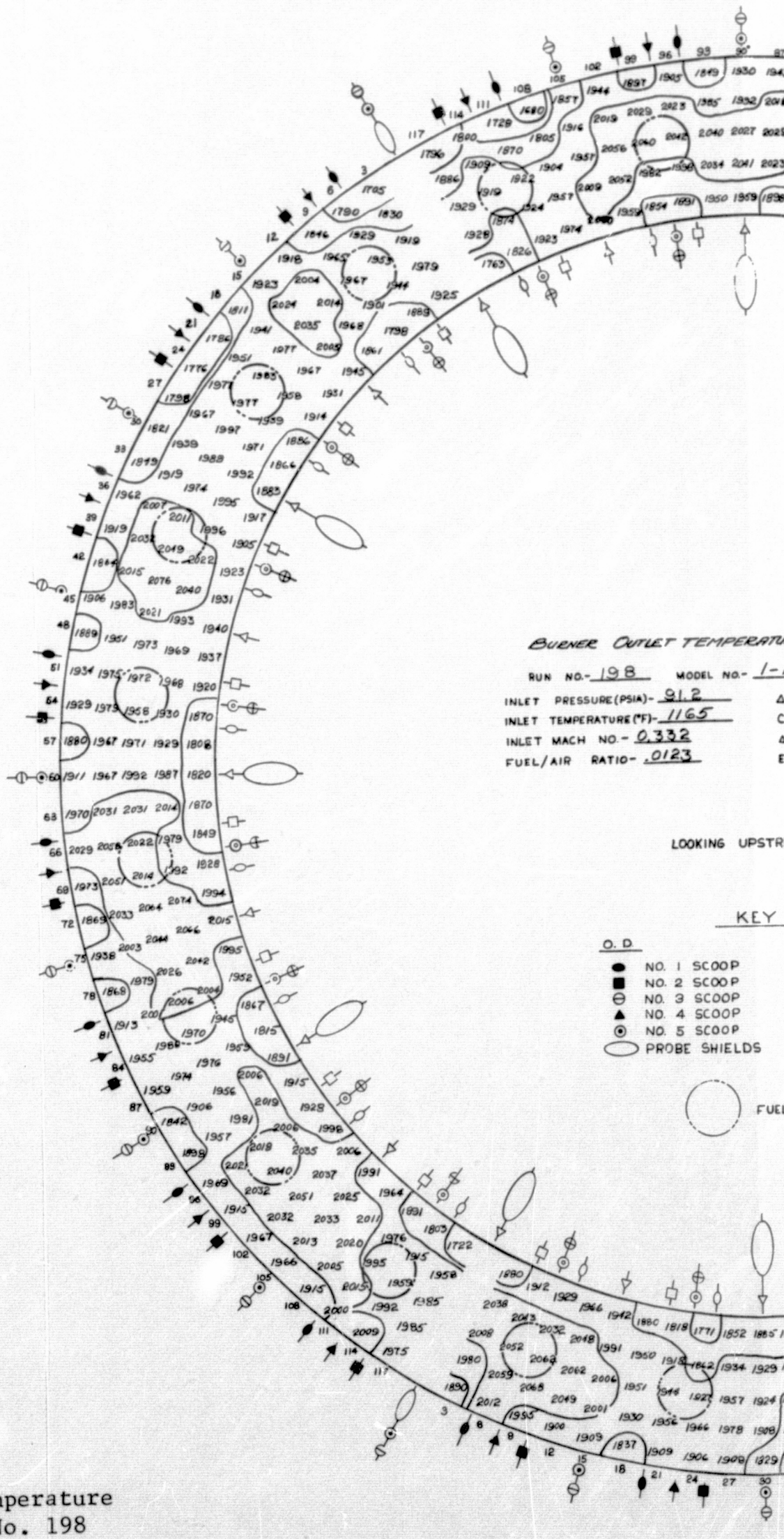

Figure 95. Combustor Outlet Temperature Distribution, Test No. 198

FOLDOUT FRAME |

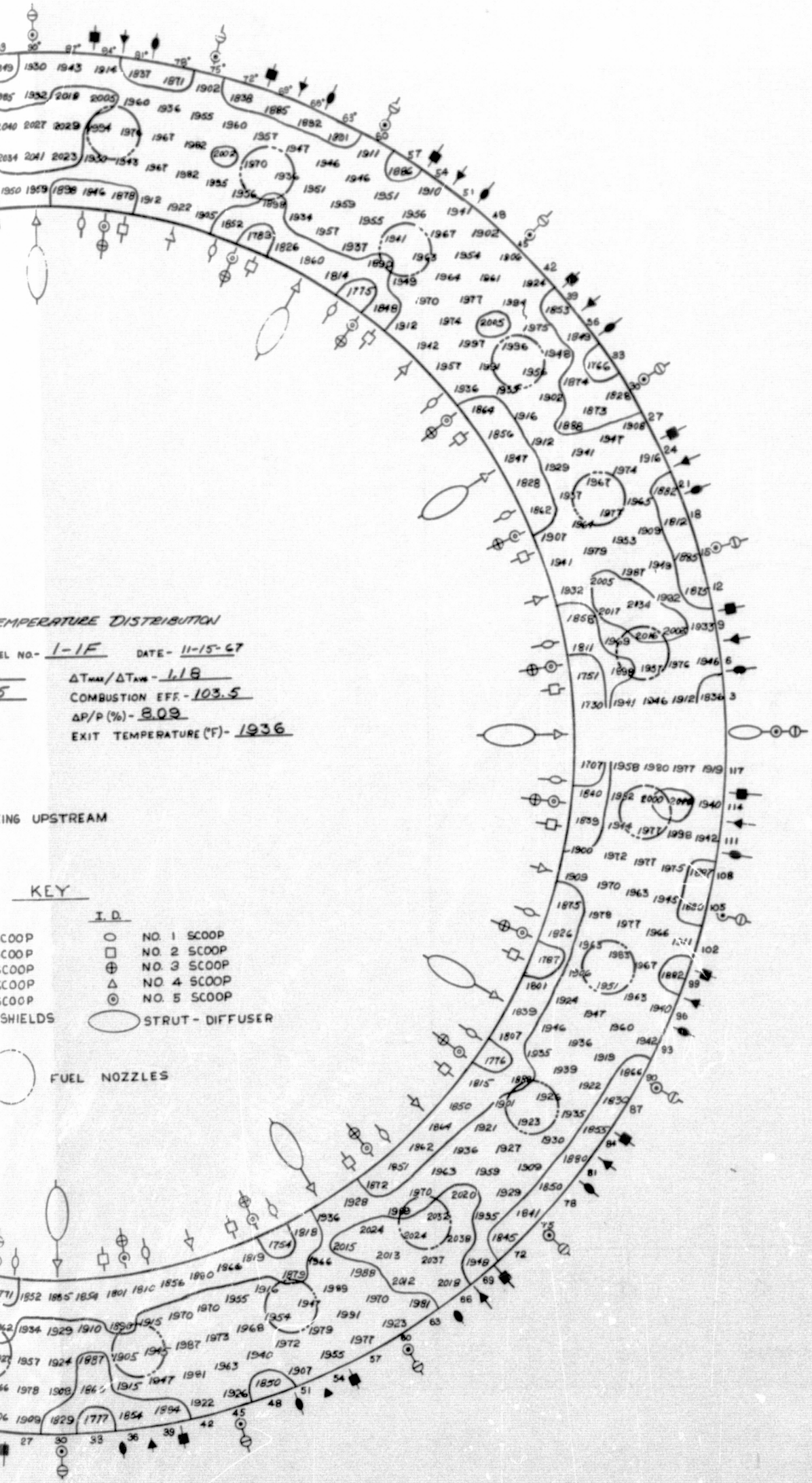

FD 23504

FOLDOUT FRAME 2

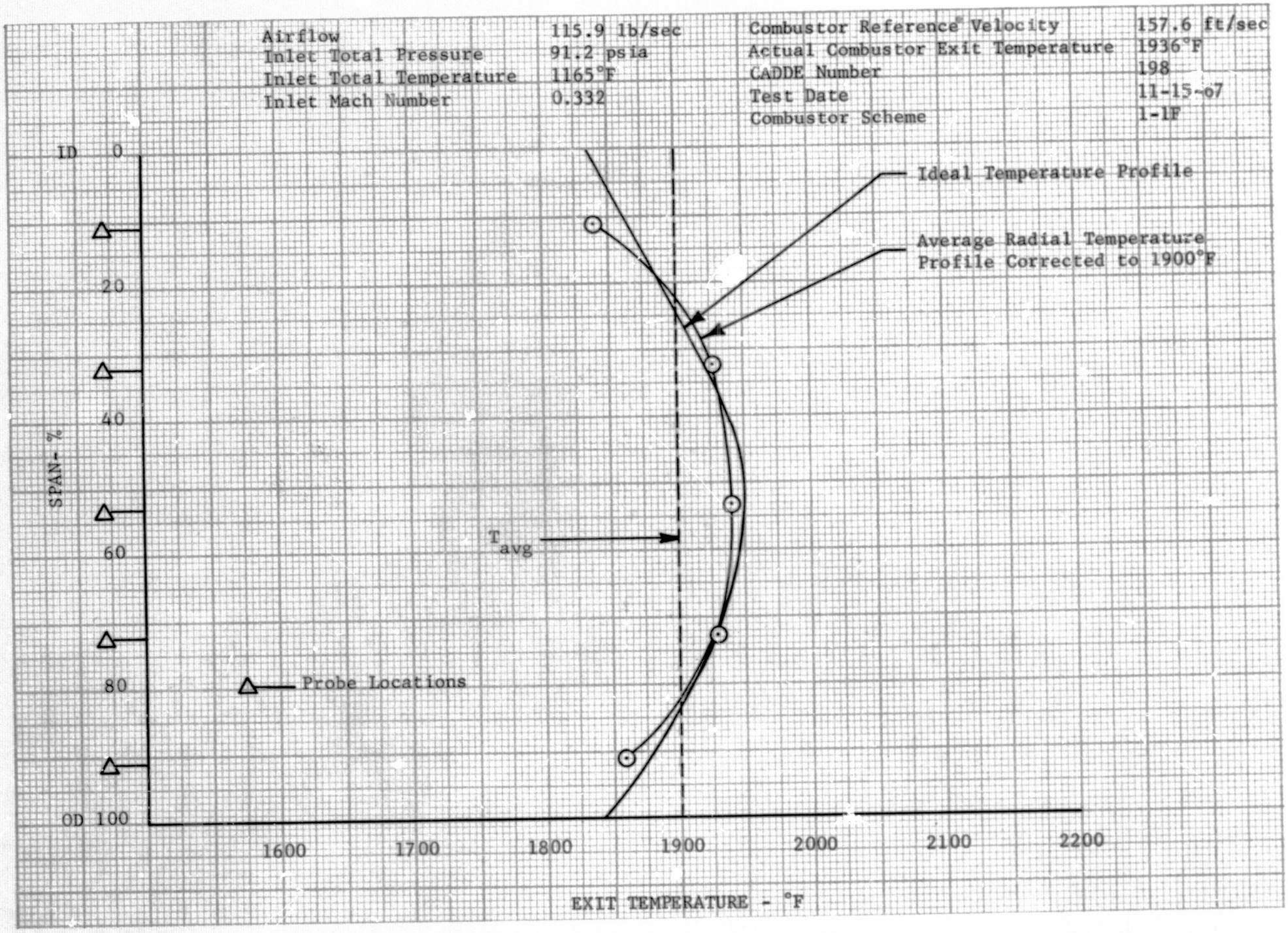

Figure 96. Combustor Average Radial Exit Temperature Profile, Test No. 198

DF 60480

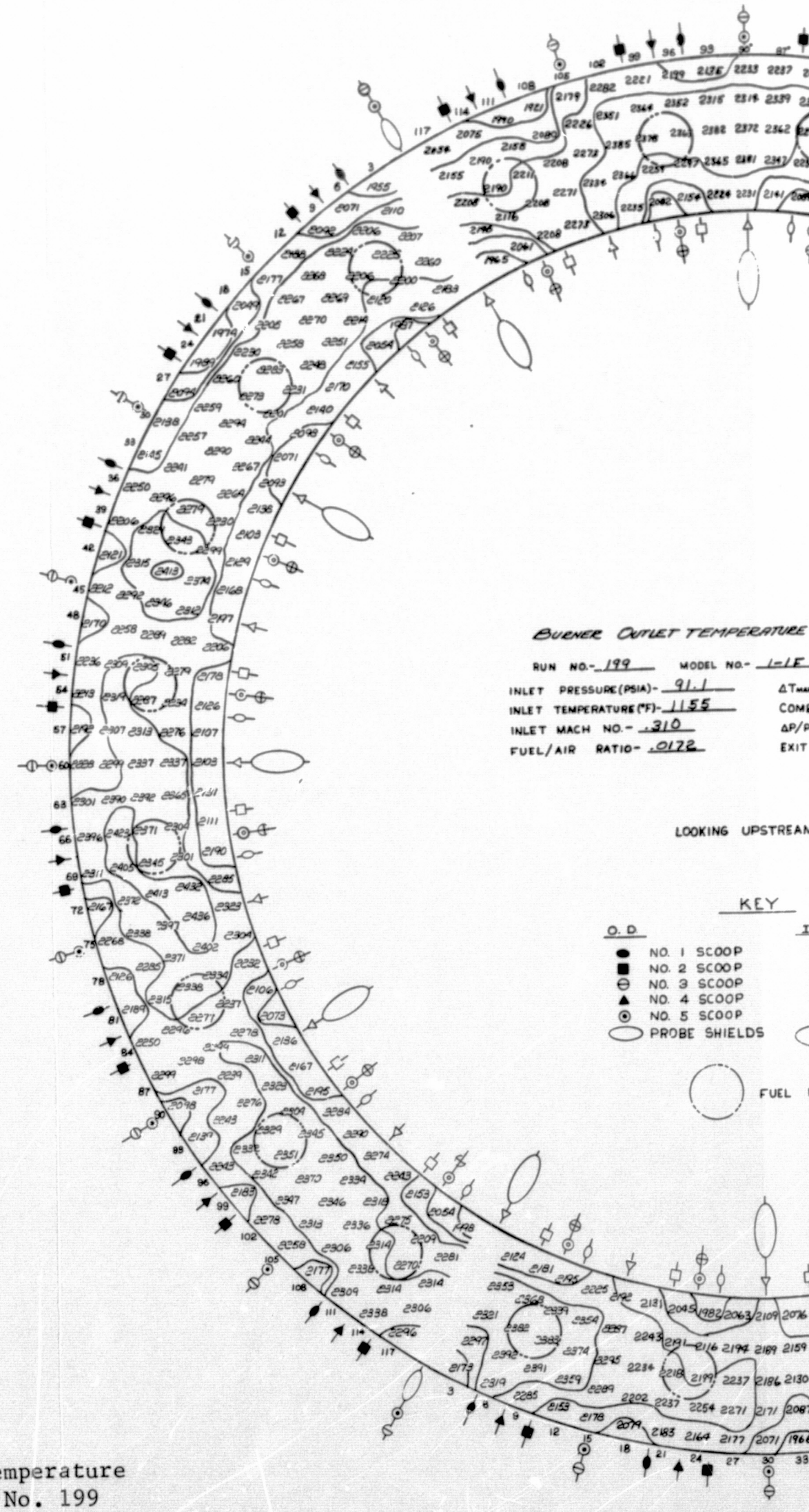

Figure 97. Combustor Outlet Temperature Distribution, Test No. 199

FOLDOUT FRAME 1

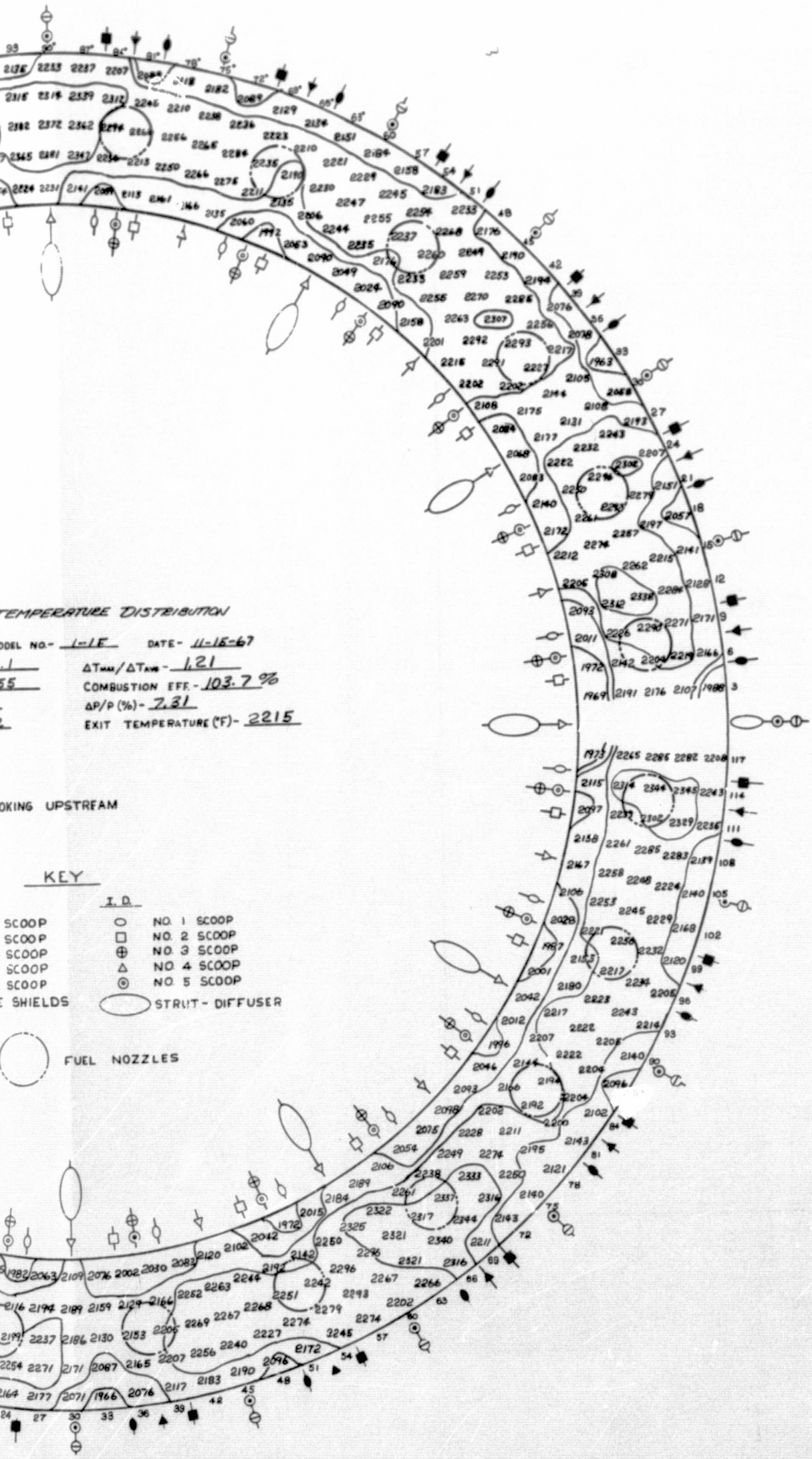

FD 23503

FOLDOUT FRAME 2

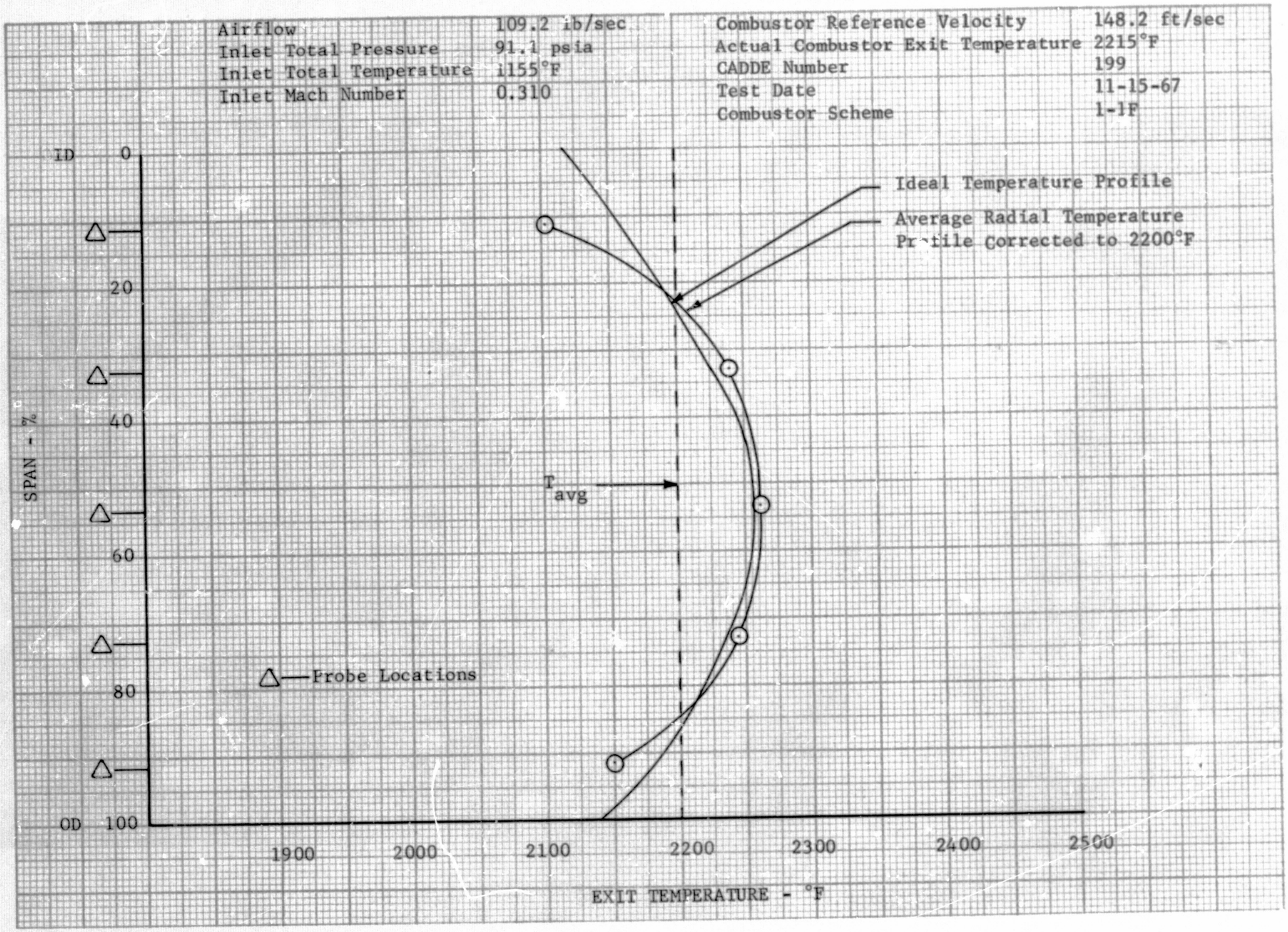

Figure 98. Combustor Average Radial Exit Temperature Profile, Test No. 199

DF 60481

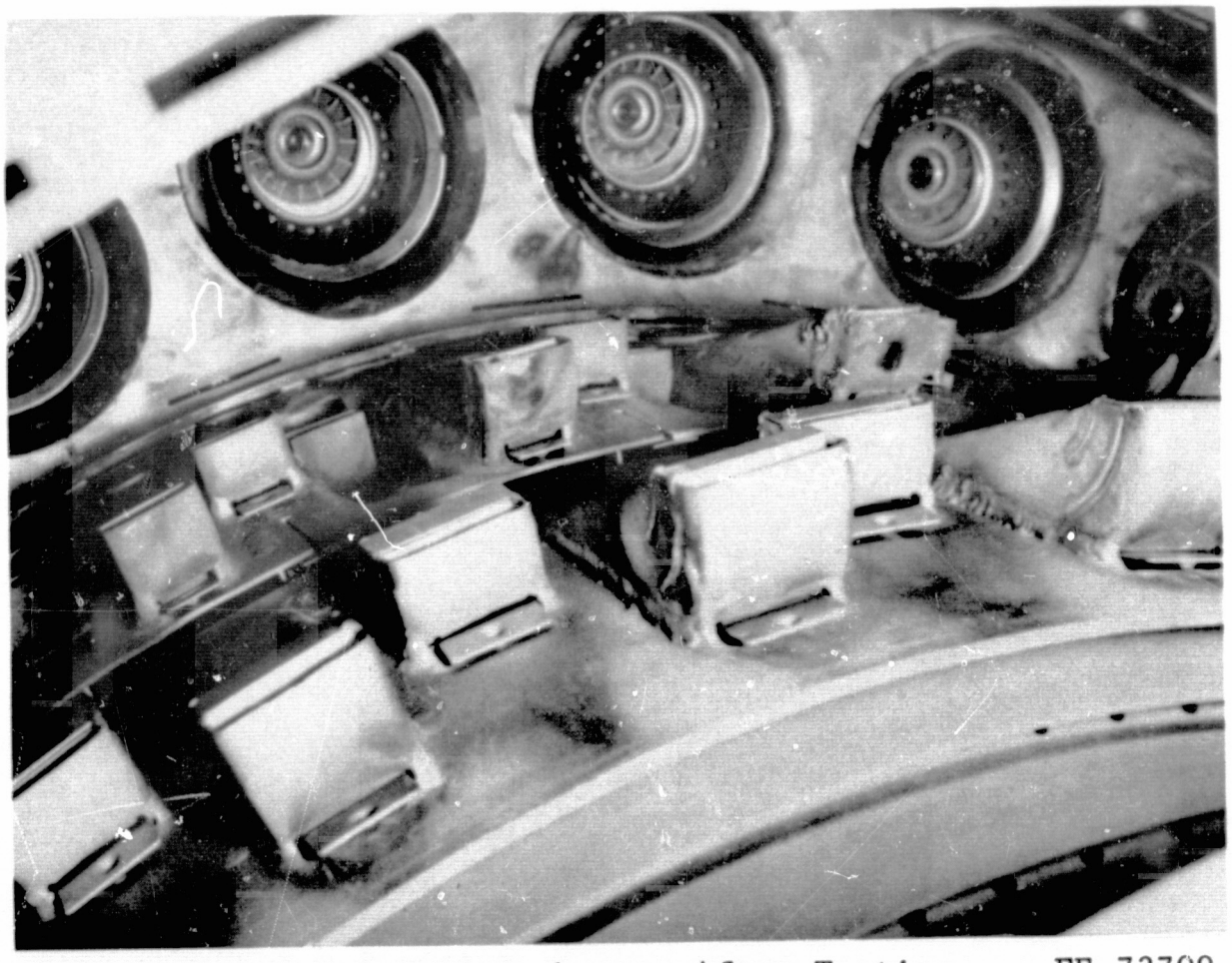

Figure 99. Model 1-1F Combustor After Testing (View 3) FE 73709

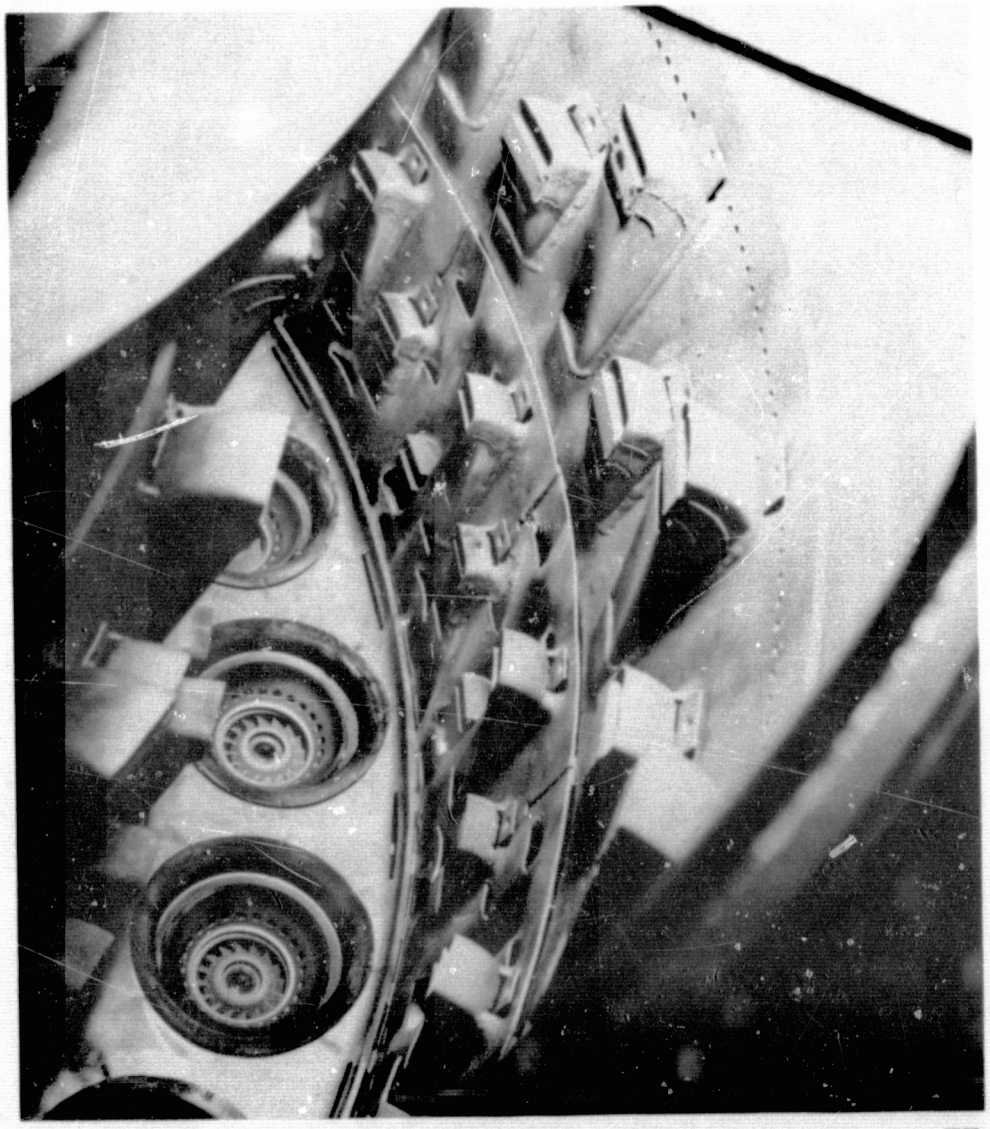

Figure 100. Model 1-1F Combustor After Testing (View 4) FE 73710

C. SUMMARY

The original combustor (Model 1-1A) was fair in overall performance with a flat inlet airflow profile and with a very center-peaked inlet profile. The performance values were good with a ΔTVR value of 1.29 and an overall pressure loss of 3.45% at an average exit temperature of 2217°F (Contract Test Condition No. 6), but the combustor definitely had shortcomings in dome cooling which in turn caused a shrinkage of the dome and closing of the ID primary liner cooling gap, resulting in an overheating of the liner.

Combustor Models 1-1B, 1-1C, and 1-1D were modifications to the original combustor, based on previous experience, in an attempt to correct the overheating problem and better the combustor performance. Although some of these schemes did help the cooling problem, the combustor dome and primary liner were in a serious overheated condition with the dome having shrunk to the point of nearly closing the ID primary liner cooling gap. This resulted in a number of burned No. 2 and 3 scoops and a misalignment of fuel swirlers with the dome.

This deterioration of the combustor was accompanied by a deterioration in performance with a ΔTVR value of 1.406 at an average exit temperature of 1977°F (inlet temperature of 621°F) obtained in the final test on the Model 1-1D combustor.

It was now apparent that modifications and repairs to the combustor and diffuser were required before endurance testing could begin. The combustor dome and ID primary liner were replaced with spares. The diffuser had apparently been separating. This was corrected by the addition of false walls to reduce the diffuser area ratio. The new dome was modified to include a cooling air deflector and slots to redistribute the cooling airflow. A number of scoops were blocked or partially blocked to increase the overall combustor pressure loss which would more evenly balance the ID and OD passage airflow split.

This combustor (Model 1-1E) showed a marked improvement in performance with a ΔTVR value of 1.29 at an average exit temperature of 2232°F (inlet temperature of 603°F). The improved temperature pattern was

accompanied by an increase in pressure loss to 5.47% as compared to the 3.45% with the Model 1-1A. The exit temperature pattern was somewhat distorted because of a fouled fuel nozzle problem.

The overall combustor appearance was very good, indicating that the latest modification had corrected the previous cooling problems.

There was evidence of high thermal gradients on the sides of the No. 1 scoops on the ID primary liner. This problem was corrected by the addition of thumbnail scoops in the liner, upstream of the hot areas. The fuel nozzles were cleaned and calibrated, and testing on this combustor (Model 1-1F) was resumed. The combustor was tested at Contract Test Conditions Nos. 3, 4, 5, and 6. A periodic inspection of the combustor indicated that it was in very good condition. The only evidence of deterioration was a slight burning on 6 or 7 No. 3 ID primary scoops, which was considered to be a minor problem.

The overall combustor performance was good with a ΔTVR value of 1.25 at Contract Test Condition No. 6 and 1.21 at Test Condition No. 4, which are the severest conditions for performance and endurance.

The radial exit temperature profiles very closely matched the ideal profiles. Although the pressure loss had increased over the previous models, it was still within the contract goals.

A meeting was held with the NASA project management and a decision was made, following a review of the combustor performance and overall appearance, to begin endurance testing.

SECTION V
TASK IV - ENDURANCE TESTING

A. TEST REQUIREMENTS

The following summary of the final contractual requirements for Task IV - Endurance Testing is presented for convenient reference during the discussion of the test results.

The combustor shall be operated at the conditions listed in table 10 for a cumulative time of approximately 315 hours:

Table 10. Task IV - Endurance Test Conditions

TEST CONDITION	INLET TOTAL PRESSURE (psia)	INLET TOTAL TEMPERATURE (^{o}F)	OUTLET AVERAGE TOTAL TEMPERATURE (^{o}F)	REFERENCE VELOCITY (ft/sec)
1	60 ± 2	1050 ± 15	1900 ± 25	150 ± 5
2	60 ± 2	1050 ± 15	2200 ± 25	140 ± 5
3	90 ± 2	1150 ± 15	1900 ± 25	160 ± 5
4	90 ± 2	1150 ± 15	2200 ± 25	150 ± 5
5	90 ± 2	600 ± 15	1900 ± 25	108 ± 5
6	90 ± 2	600 ± 15	2200 ± 25	100 ± 5

Combustor Test Conditions 1, 2, 3, and 4 shall be tested in sequence for 35, 100, 30, and 150 hours, respectively. Before the start of Test Condition 1, and after the completion of Test Conditions 1, 2, 3, and 4, the combustor shall be run for one hour at Test Condition 5 and for one hour at Test Condition 6.

The combustor shall be operated in a cyclic manner, with four steps, as follows:

1. Increase combustor outlet average temperature to the specified test condition within 10 seconds after ignition.
2. Maintain the specified test conditions for 1 hour.
3. Reduce fuel flow to zero within a 10-second interval.
4. Wait a minimum of 5 minutes before commencing the next operating cycle.

B. TEST RESULTS

A total of 325 hours of endurance testing was conducted in accordance with contract requirements. Figure 101 shows the entire endurance program in bar-graph form.

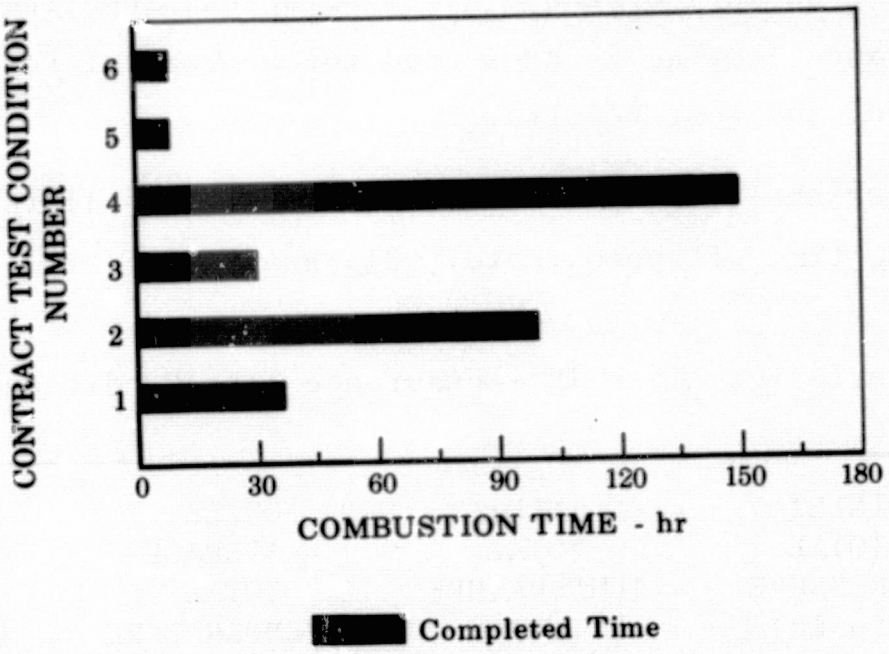

Test Condition	Inlet Total Pressure, psia	Inlet Total Temperature, °F	Outlet Average Total Temperature, °F	Reference Velocity, ft/sec
1	60 ± 2	1050 ± 15	1900 ± 25	150 ± 5
2	60 ± 2	1050 ± 15	2200 ± 25	140 ± 5
3	90 ± 2	1150 ± 15	1900 ± 25	160 ± 5
4	90 ± 2	1150 ± 15	2200 ± 25	150 ± 5
5	90 ± 2	600 ± 15	1900 ± 25	108 ± 5
6	90 ± 2	600 ± 15	2200 ± 25	100 ± 5

Figure 101. Combustion Time FD 23500G

The combustor exit temperature uniformity parameter (ΔTVR) remained fairly constant throughout Test Conditions 1 through 4 of the endurance testing at a value of 1.18 to 1.24, as shown in figure 102.

Figure 103 indicates that the combustor system pressure loss ($\Delta P/P$) and combustor efficiency $\left(\frac{\Delta T_{act}}{\Delta T_{ideal}}\right)$ remained fairly constant throughout endurance testing at values of 6 to 8% and 98 to 106%, respectively. (The excessive efficiency numbers are due to the method of measurement.)

The combustor exit temperature pattern for the last hour (35th) of Test Condition 1 is shown in figure 104. Comparison of this temperature pattern with the temperature pattern from the first hour of testing at this condition (figure 105) indicates that no significant performance change occurred throughout Test Condition 1. Comparison of the average

radial exit temperature profiles for these tests (figures 106 and 107) indicates little change in profile throughout Test Condition 1. These figures also show that the maximum peak temperatures closely approximated the desired goal of 100°F above the specified temperature at any radial position.

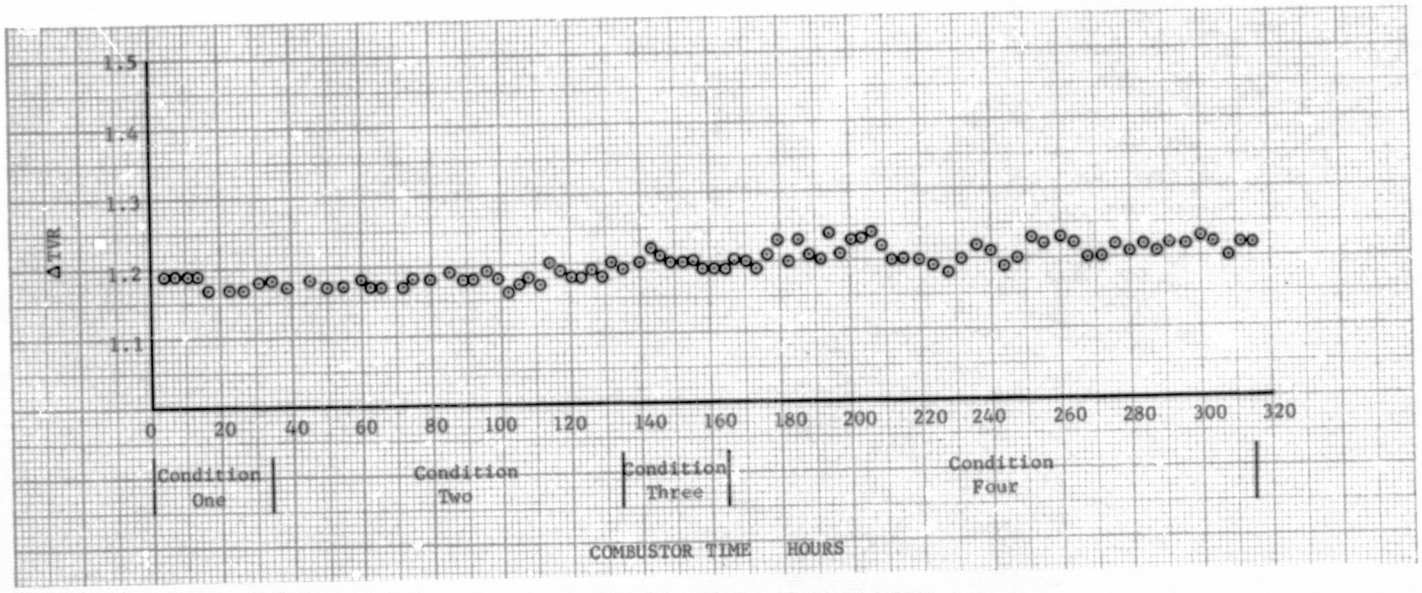

Figure 102. ΔTVR vs Combustor Time DF 64511

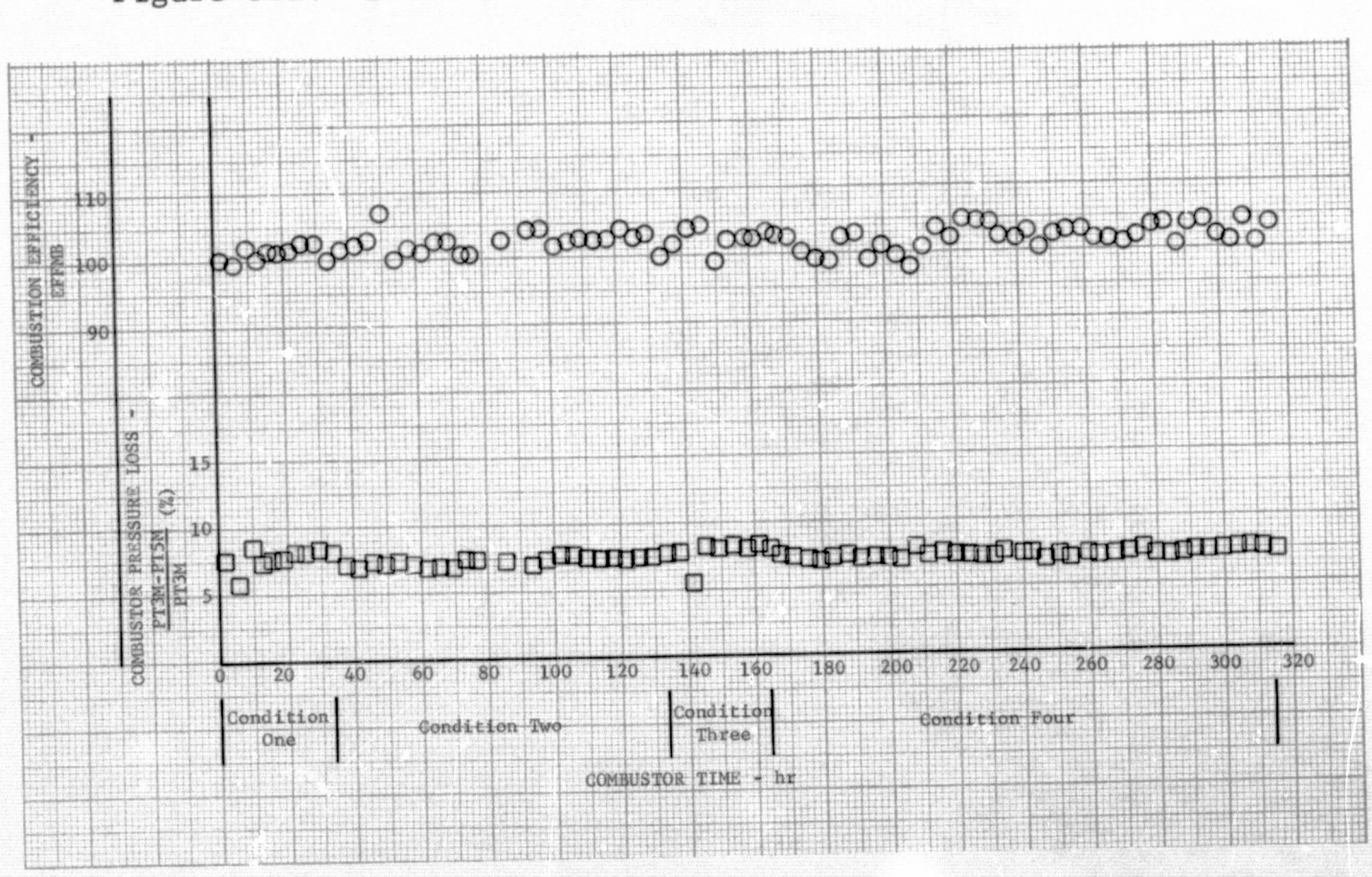

Figure 103. Combustion Efficiency and Combustor Pressure Loss vs Combustor Time DF 69436

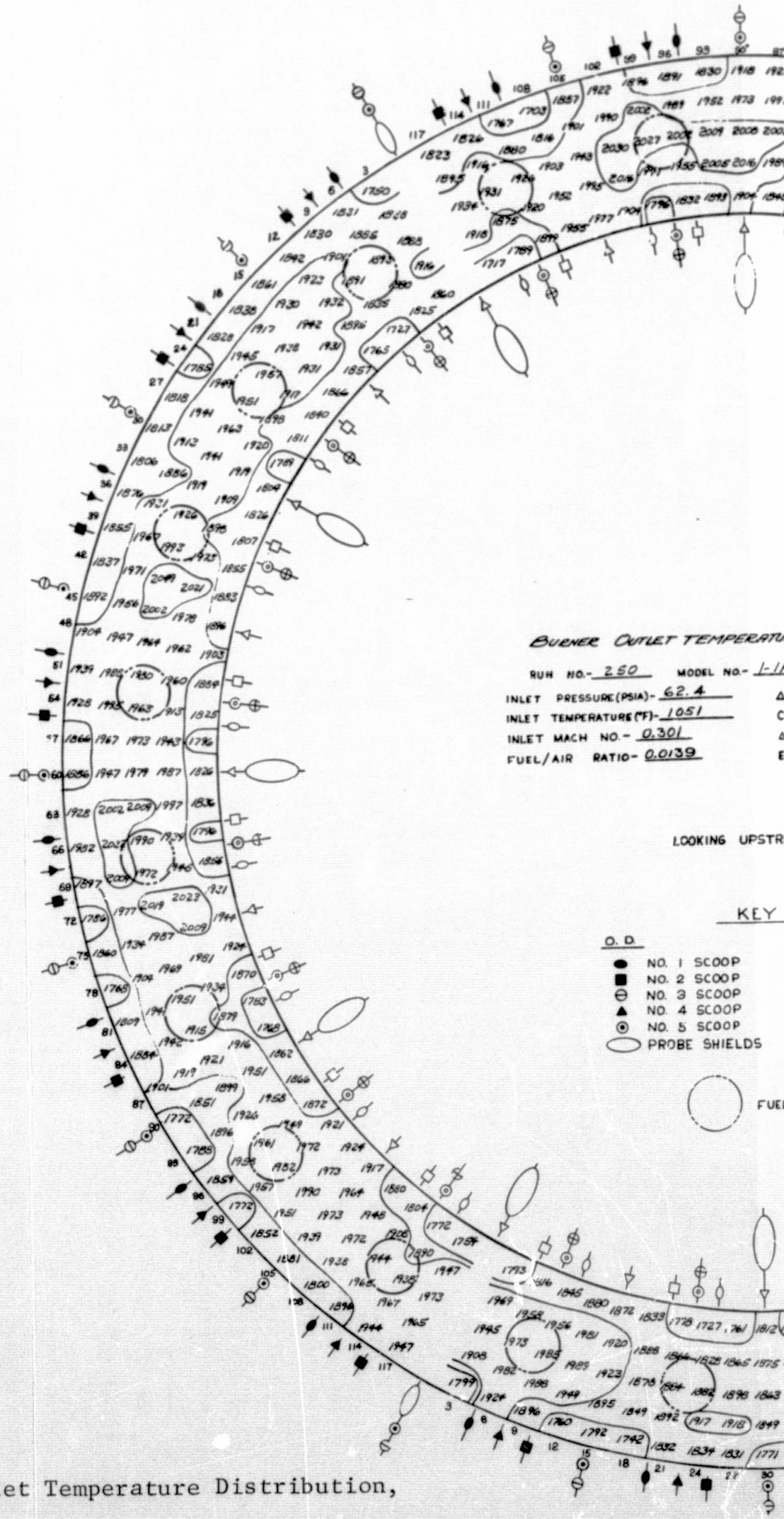

Figure 104. Combustor Outlet Temperature Distribution, Test No. 250

FOLDOUT FRAME 1

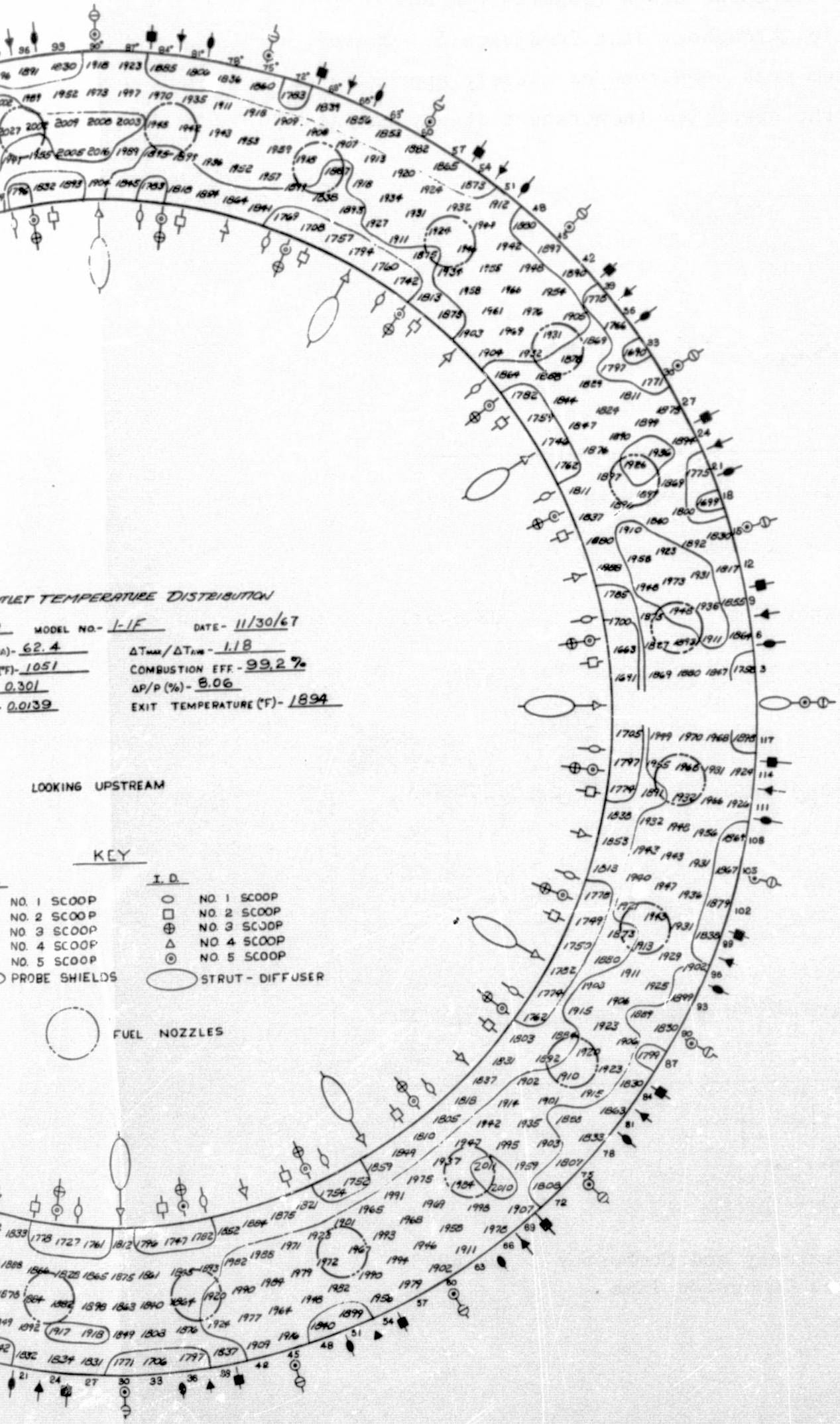

FD 24561

FOLDOUT FRAME 2

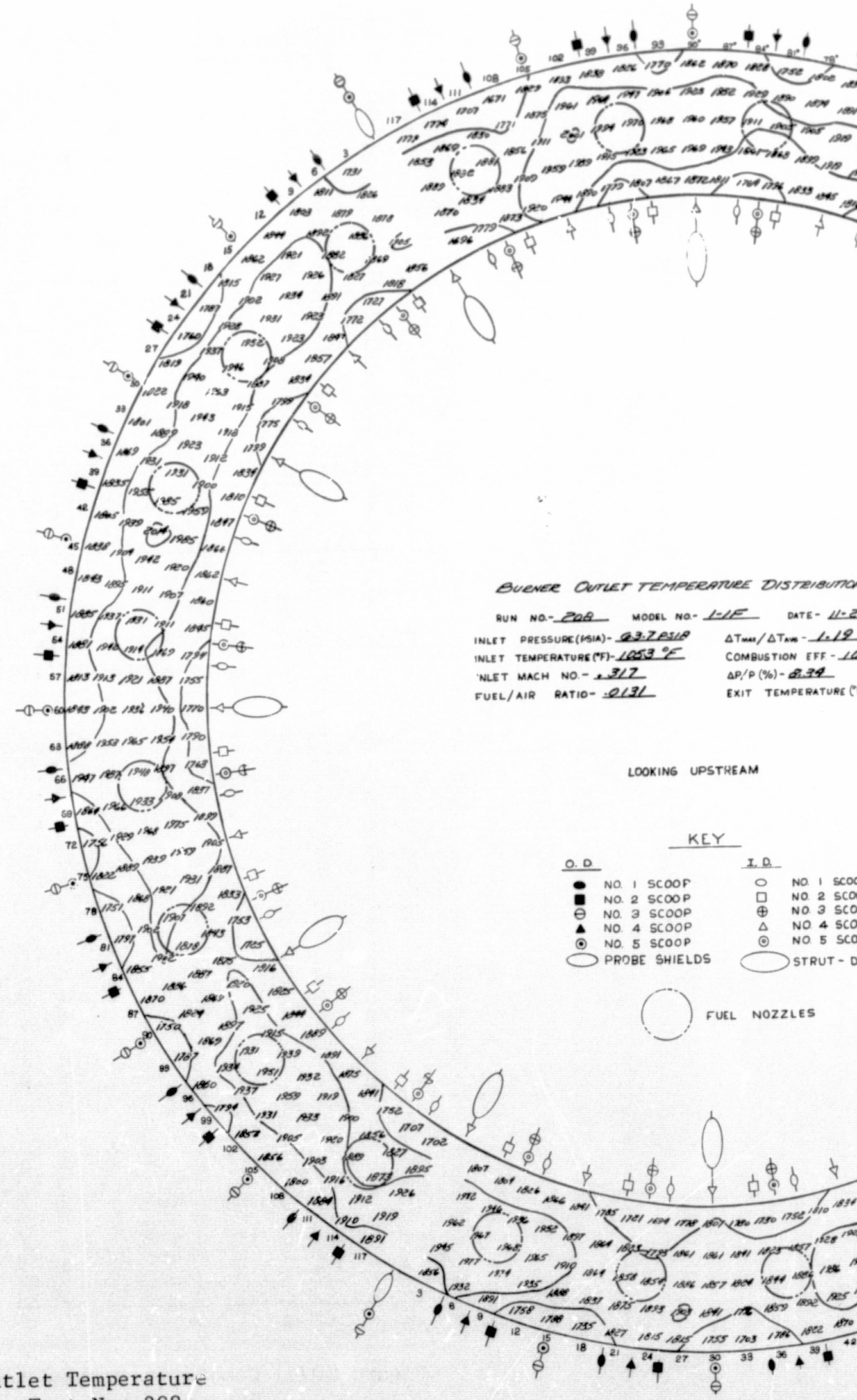

Figure 105. Combustor Outlet Temperature Distribution, Test No. 208

FOLDOUT FRAME 1

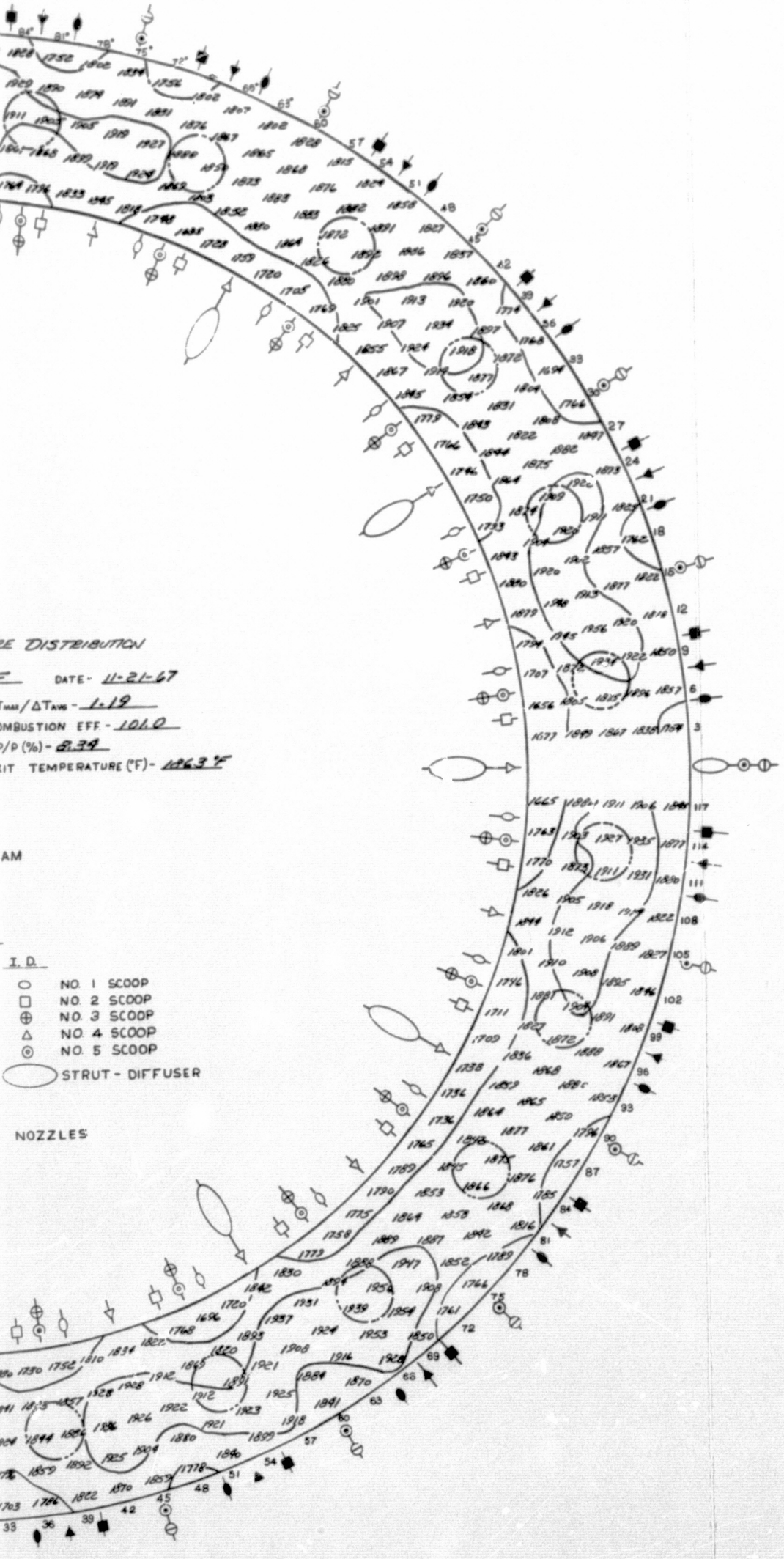

FD 23510

FOLDOUT FRAME 2

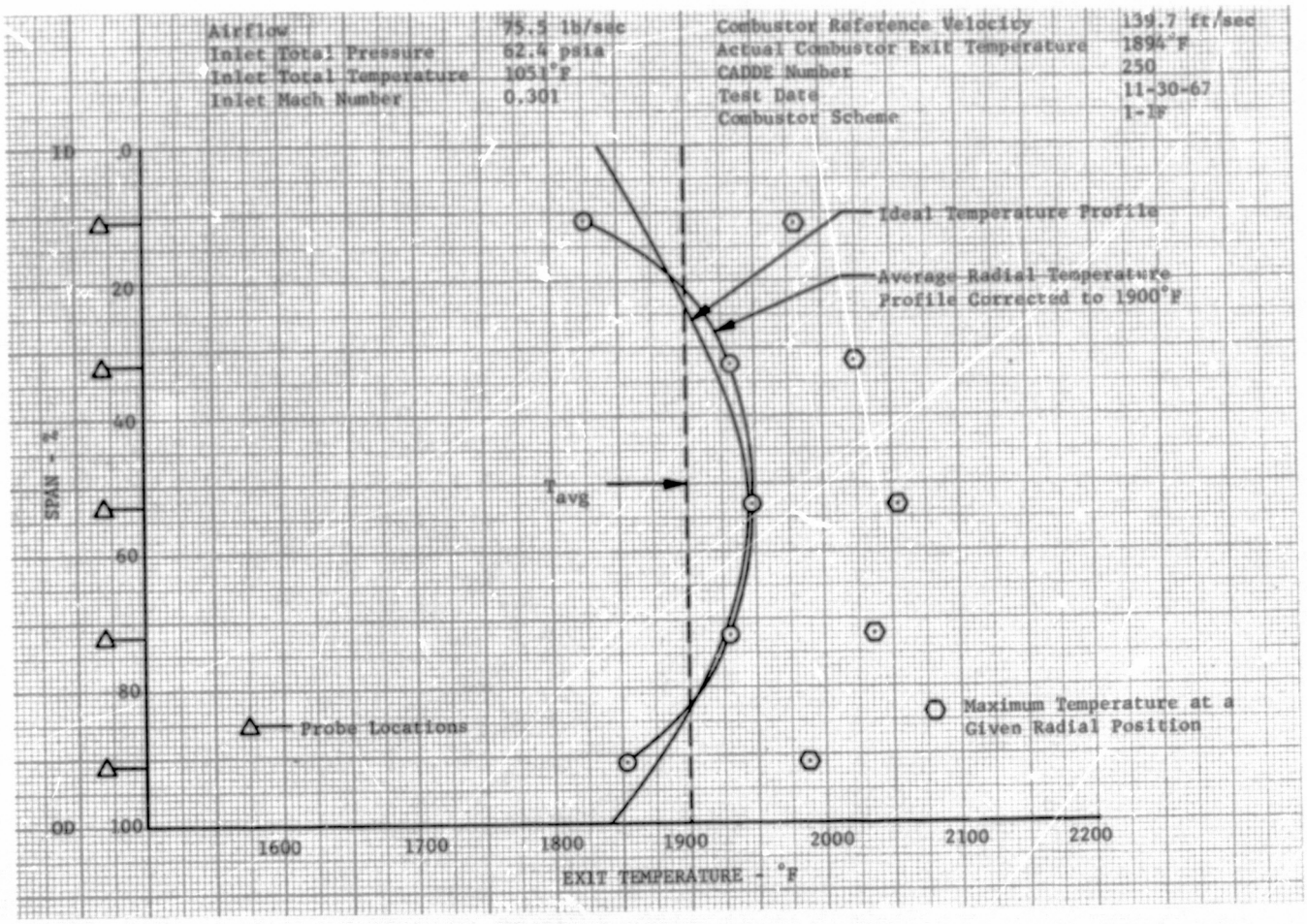

Figure 106. Combustor Average Radial Exit Temperature Profile, Test No. 250

DF 64491

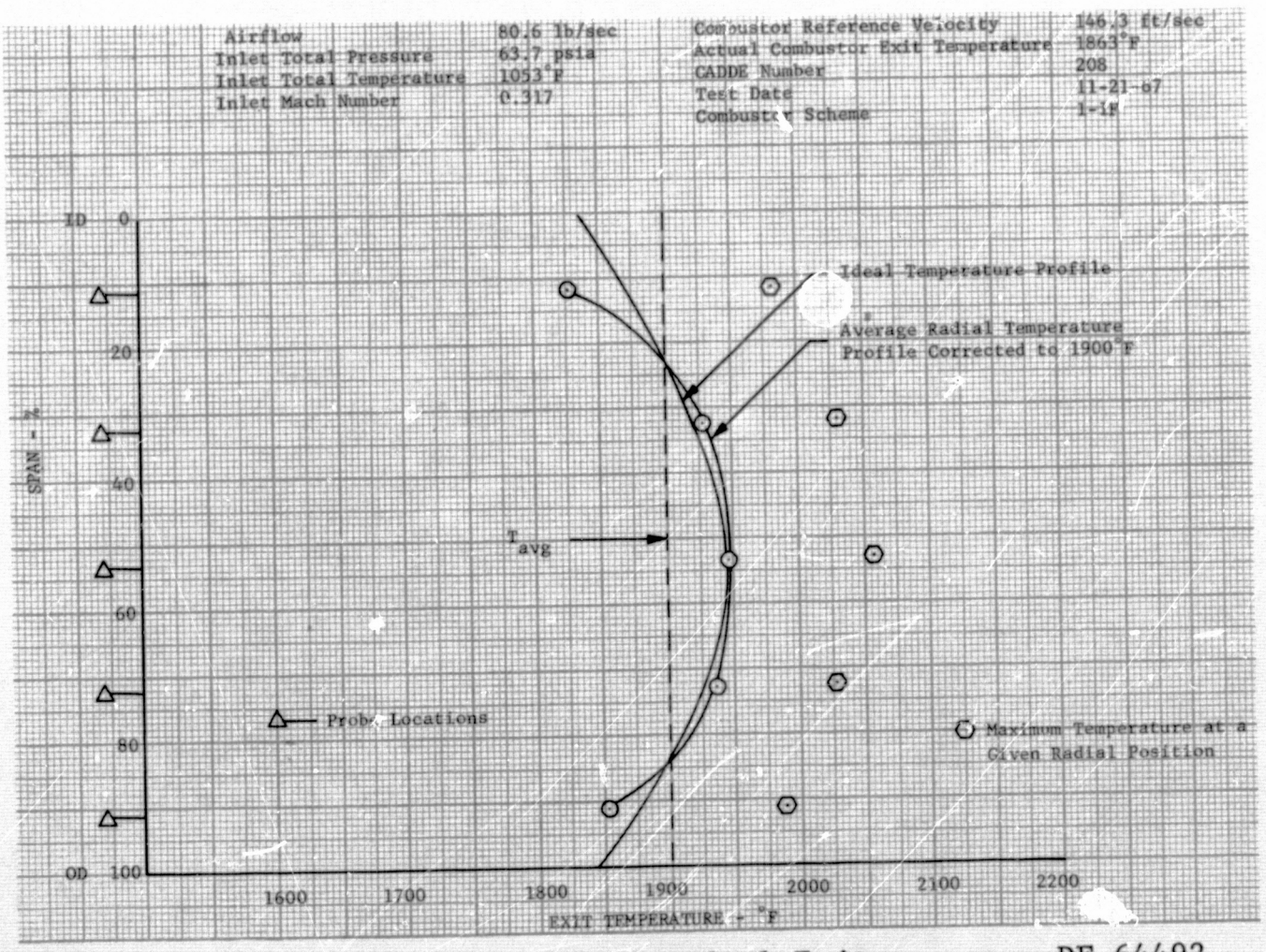

Figure 107. Combustor Average Radial Exit Temperature Profile, Test No. 208

DF 64492

The combustor exit temperature patter s for the tests at Test Condition 6, before and after the 35 hours of testing at Test Condition 1, are shown in figures 108 and 109. Comparison of these temperature patterns indicates no significant change in performance, although the uniformity parameter, ΔTVR, improved slightly from 1.26 to 1.23. The combustor average radial exit temperature profiles for these tests also show little change as seen by comparing figures 110 and 111.

Upon completion of Test Condition 1 testing, the test rig was opened for inspection. As shown in figures 112 through 114, the combustor was in very good condition. No metal burning or high thermal gradients were noted. An inspection of the test rig revealed slight metal burning on the exit section centerbody at bottom dead center, and a slight water leak on the rotating traverse drum. Further investigation revealed rust and scale deposits behind the exit section ID quench water holes (some of the holes upstream of the burned area were completely plugged), and in the filter screens of the exit probe cooling water supply lines. An acid solution (followed by flushing with water) was used to remove most of these particles. The cooling water supply lines were then modified to include filters as shown in the schematic (figure 31).

The inspection also revealed that the expansion joint at the rear of the water-cooled exit section centerbody, between the inner and outer wall, had cracked at the welds in several places. This failure was corrected by welding a sectioned 5/8-inch OD tube on the back side of the joint (figure 30). This also involved machining the actuator cover flange to allow room for this modification. Following these repairs and modifications endurance testing at Test Condition 2 was initiated.

The combustor exit temperature patterns for the 1st, 20th, 40th, 60th, 80th, and 100th hours of testing at Test Condition 2 are shown in figures 115 through 120, respectively. Comparison of these temperature patterns indicates that no significant change in performance occurred throughout the period of Test Condition 2. The combustor average radial exit temperature profiles for these tests also show little change as shown by comparing figures 121 through 126. The combustor exit temperature uniformity parameter (ΔTVR) remained fairly constant throughout Test Condition 2 testing at a value of 1.17 to 1.20 (see figure 102).

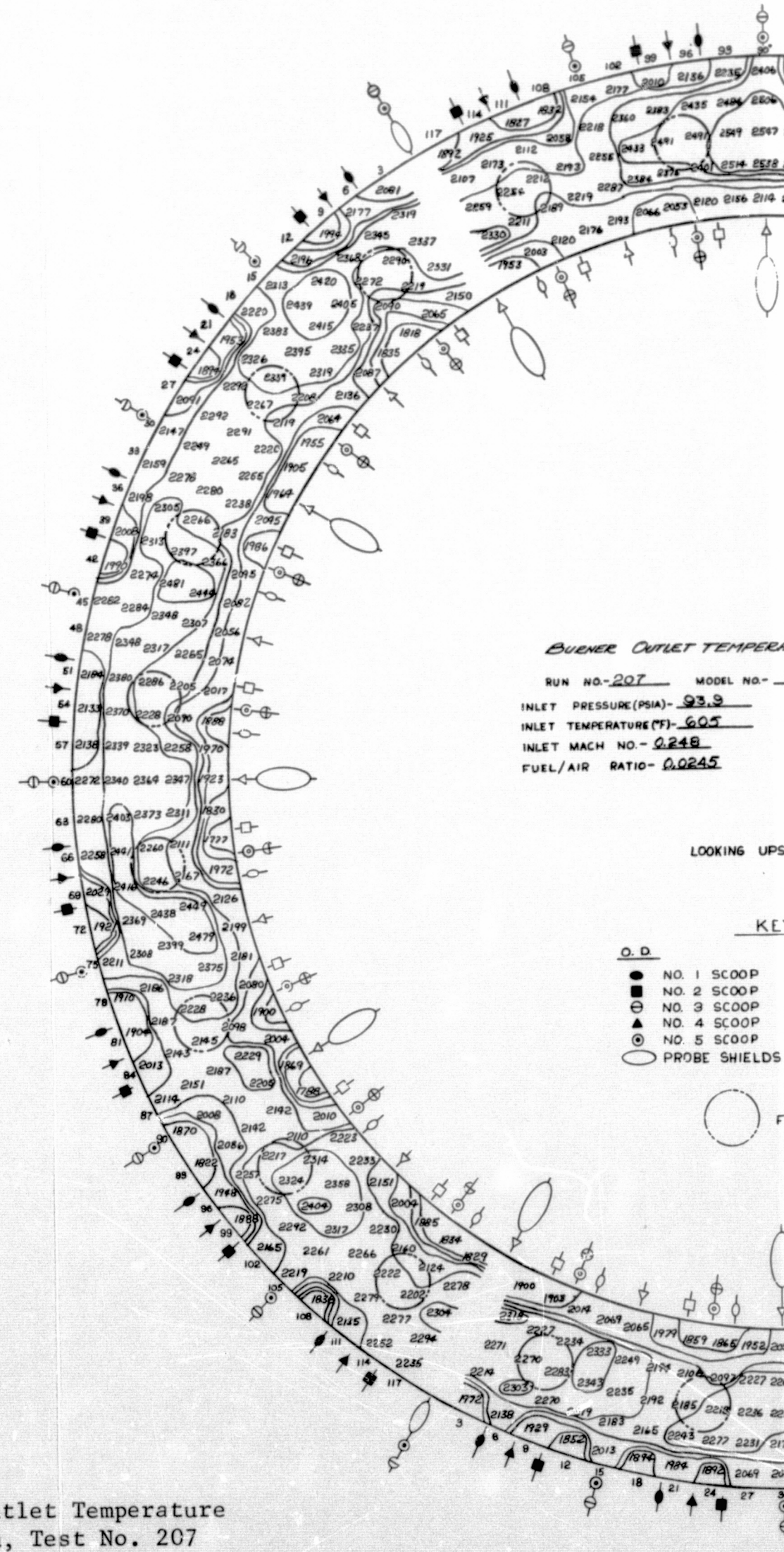

Figure 108. Combustor Outlet Temperature Distribution, Test No. 207

FOLDOUT FRAME |

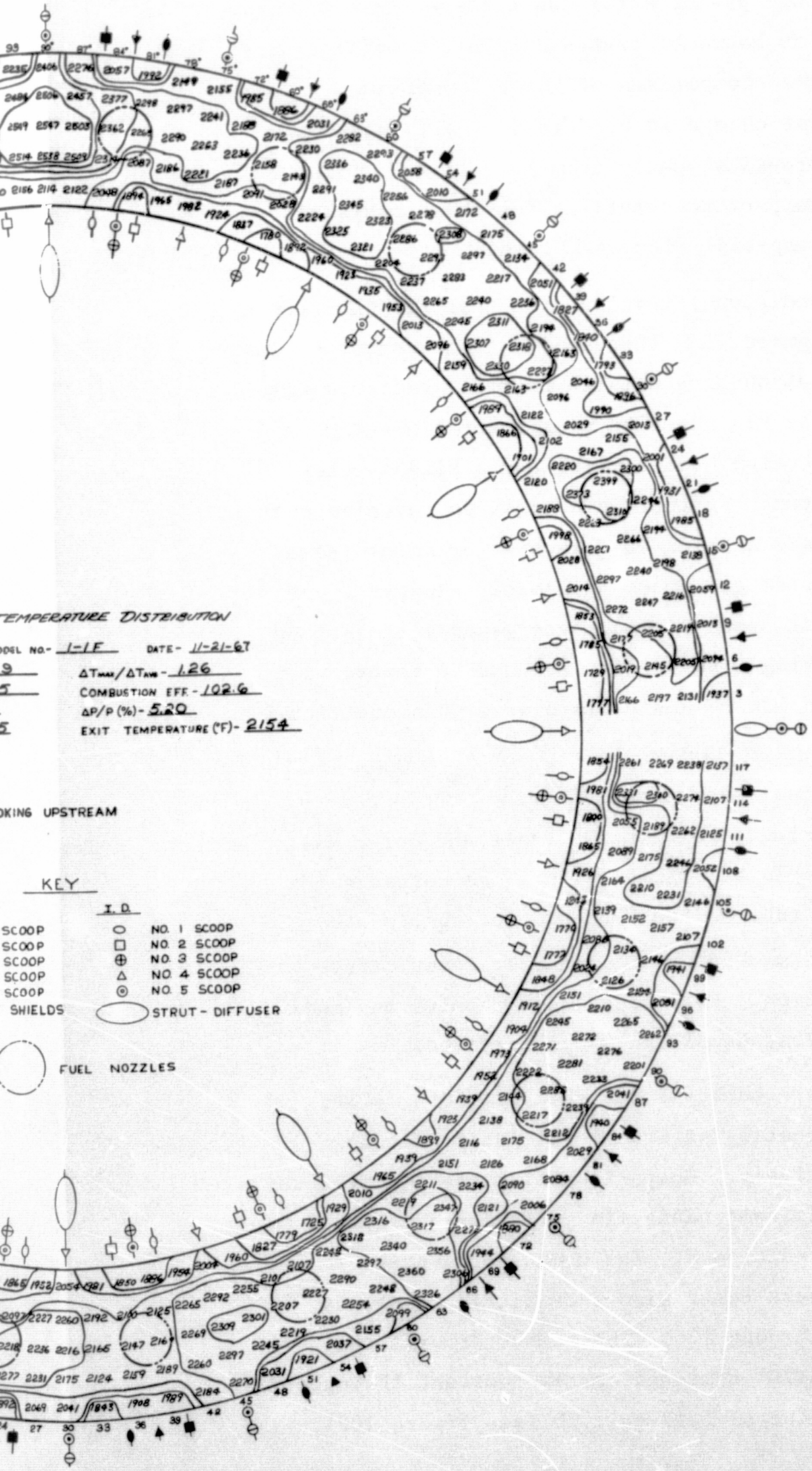

FD 23508

FOLDOUT FRAME 2

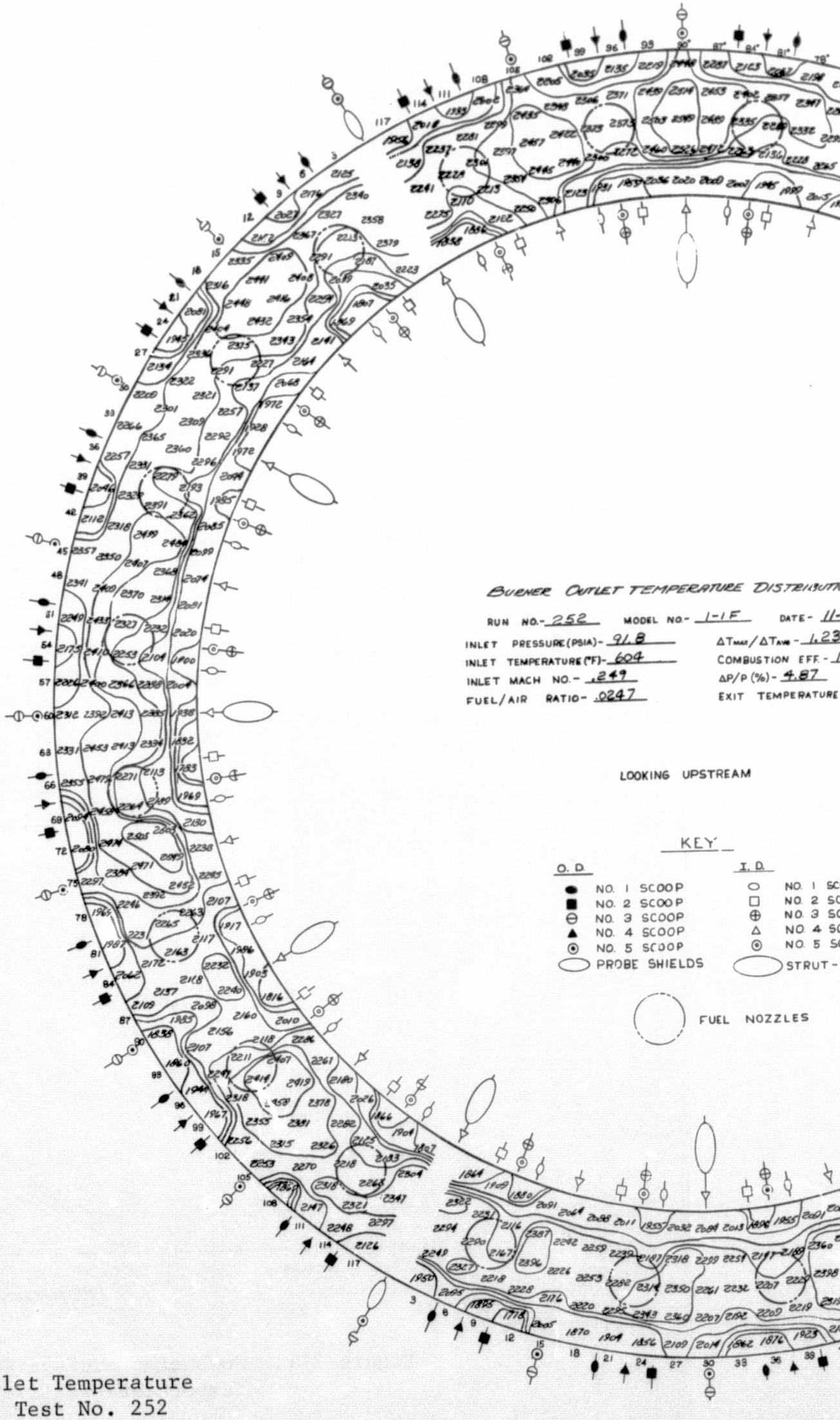

Figure 109. Combustor Outlet Temperature Distribution, Test No. 252

FOLDOUT FRAME 1

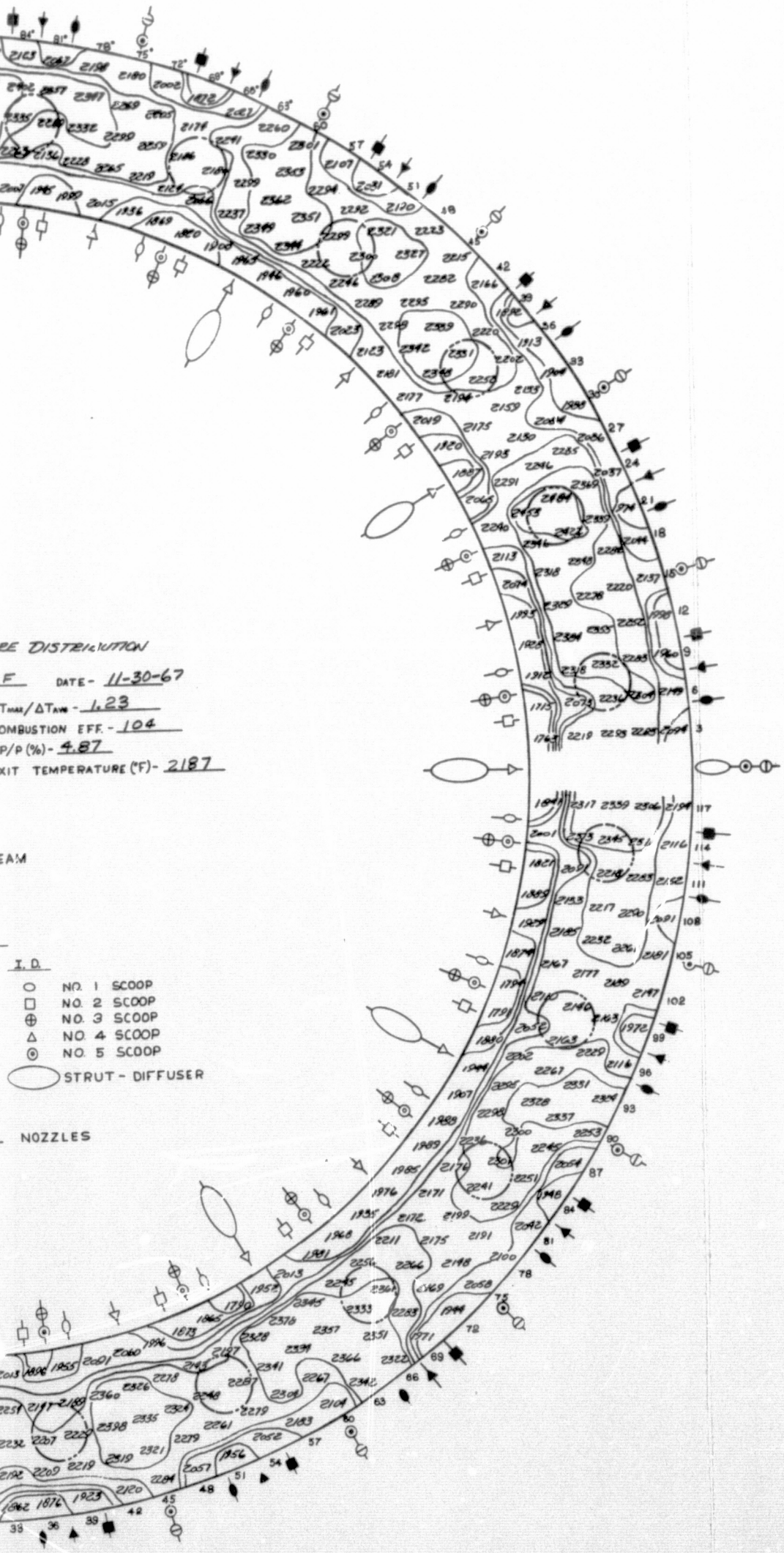

E DISTRIBUTION

F DATE - 11-30-67

$T_{MAX}/\Delta T_{AVG}$ - 1.23

OMBUSTION EFF. - 104

P/P (%) - 4.87

XIT TEMPERATURE (°F) - 2187

EAM

FD 23507

FOLDOUT FRAME 2

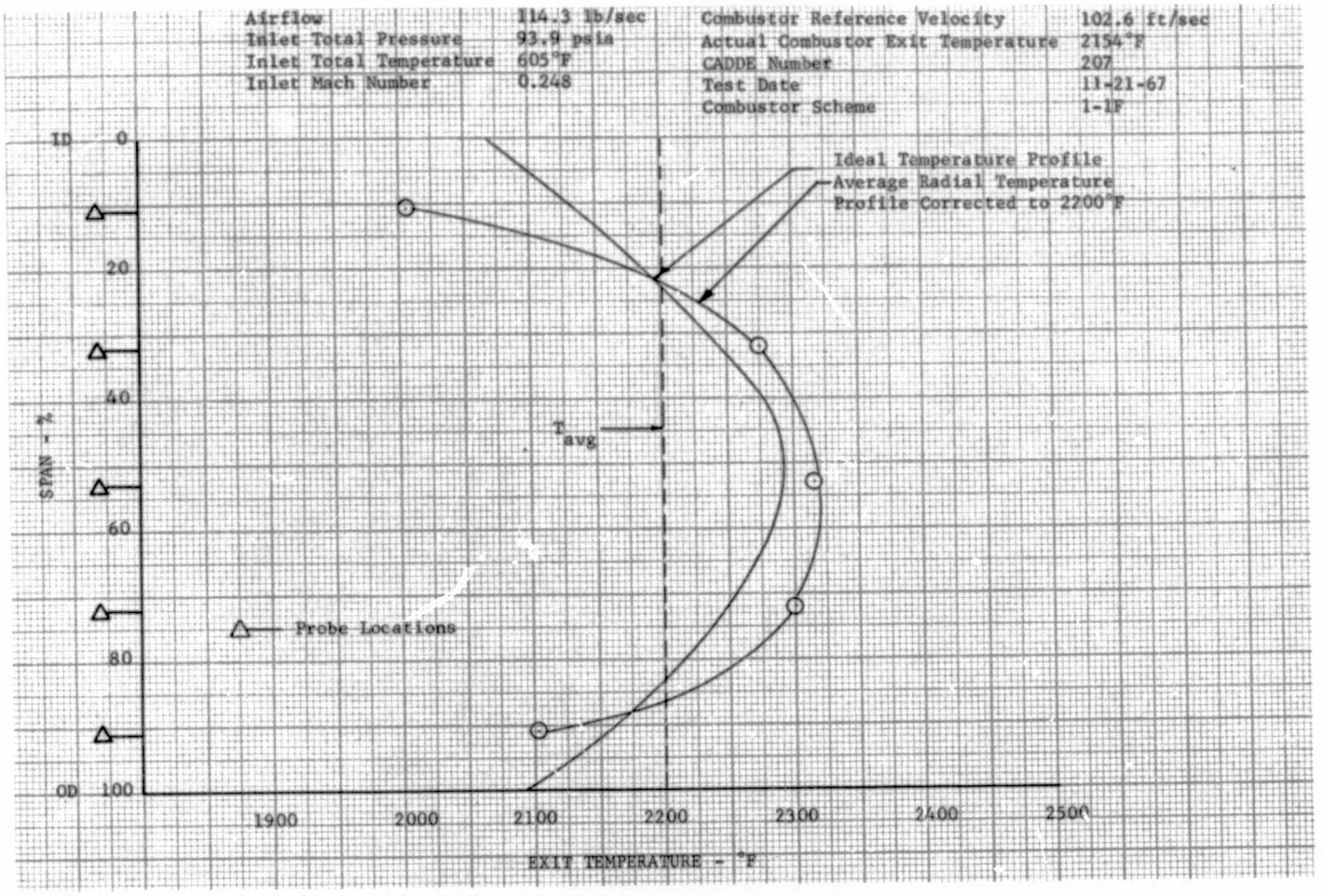

Figure 110. Combustor Average Radial Exit Temperature Profile, Test No. 207

DF 60483

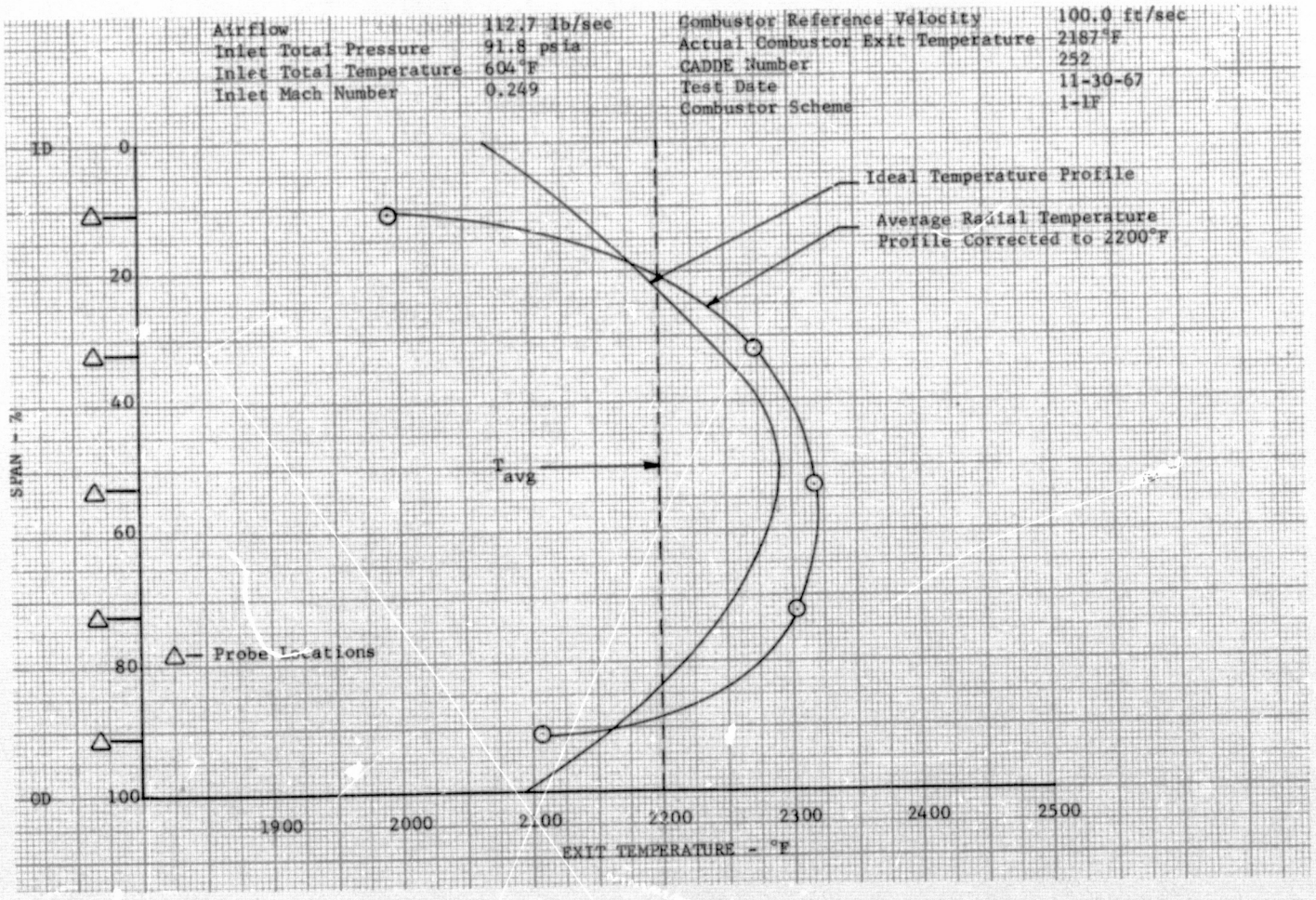

Figure 111. Combustor Average Radial Exit Temperature Profile, Test No. 252

DF 60598

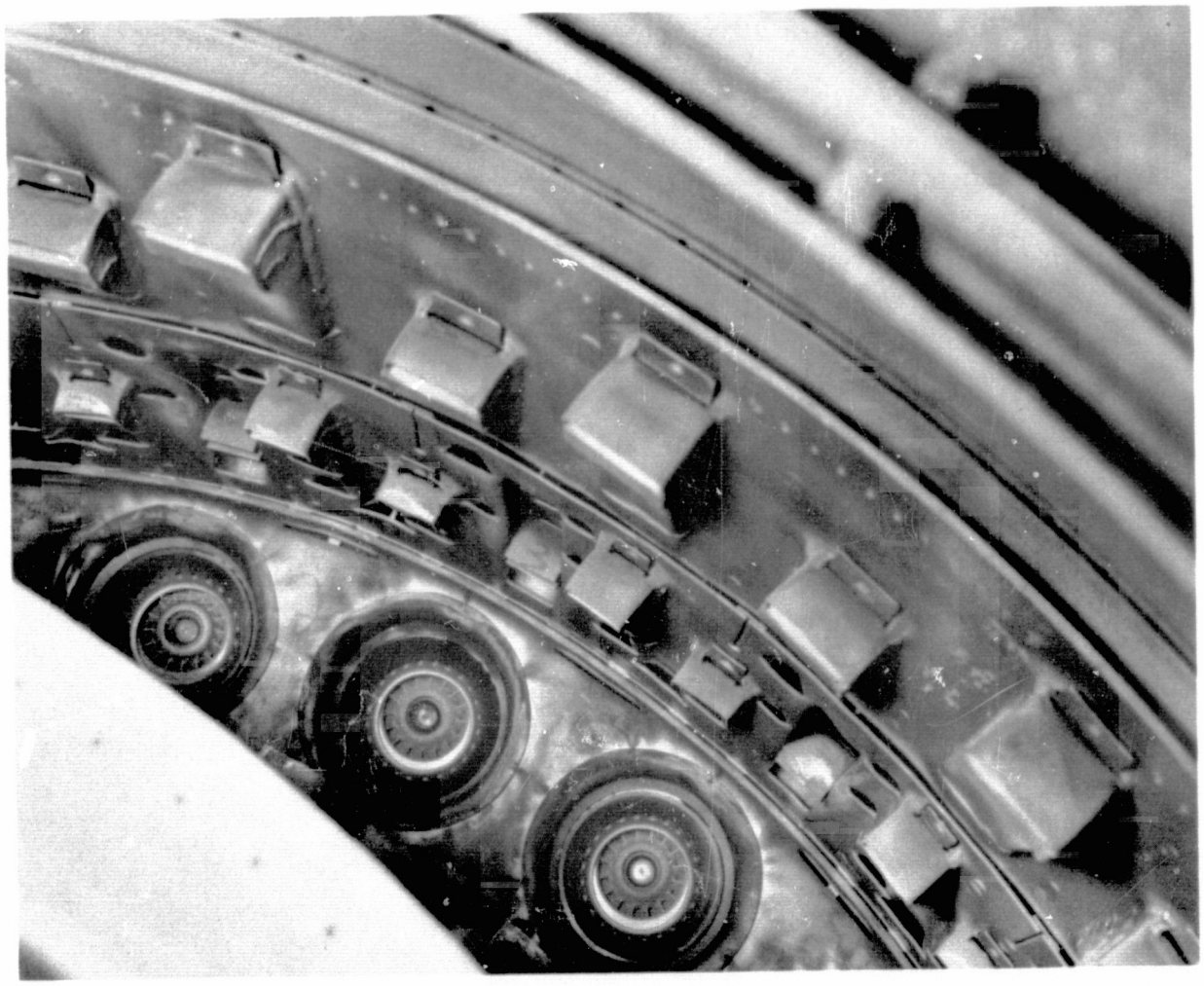

Figure 113. Combustor After Test Condition 1 (View 2) FE 73712

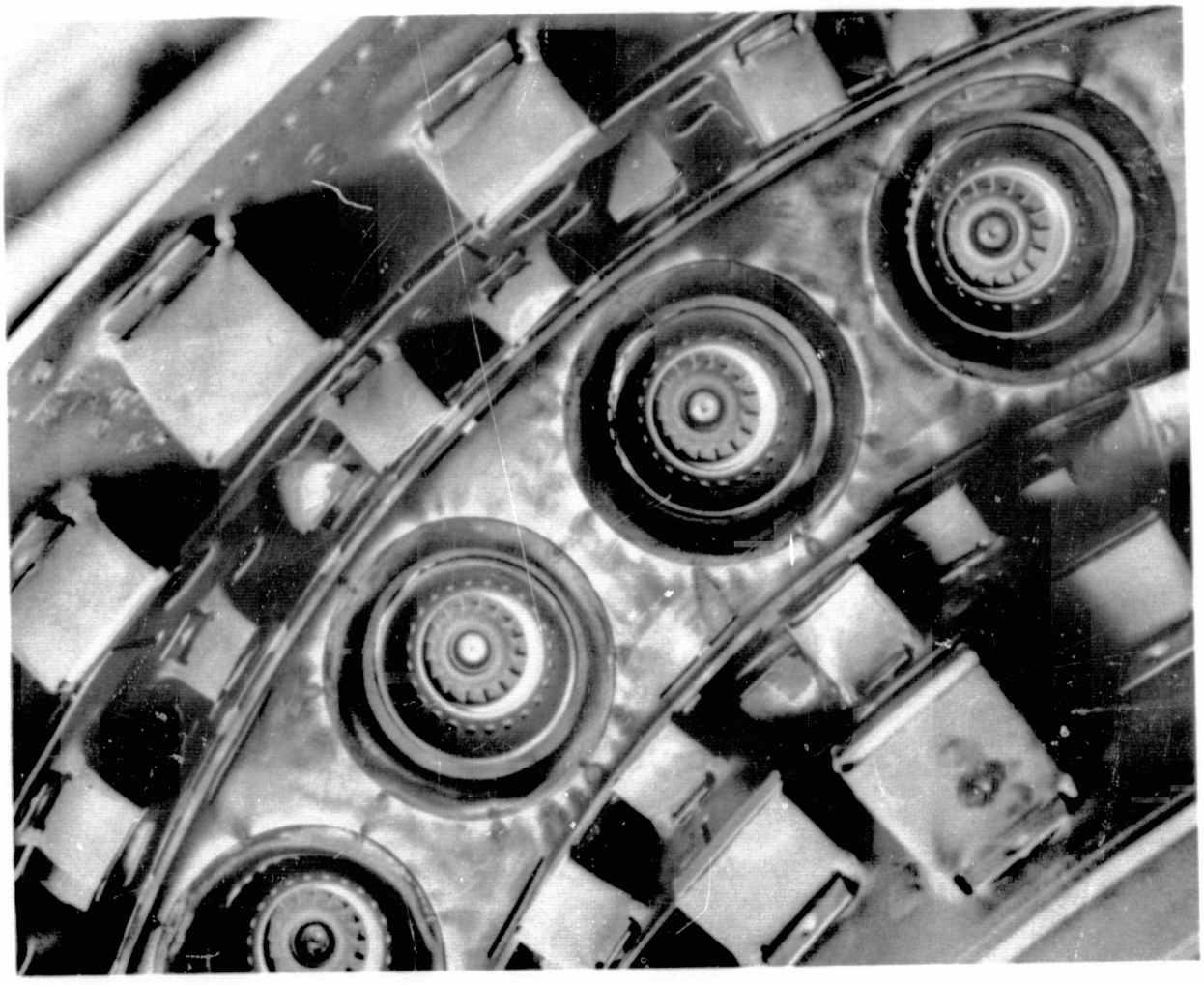

Figure 114. Combustor After Test Condition 1 (View 3) FE 73713

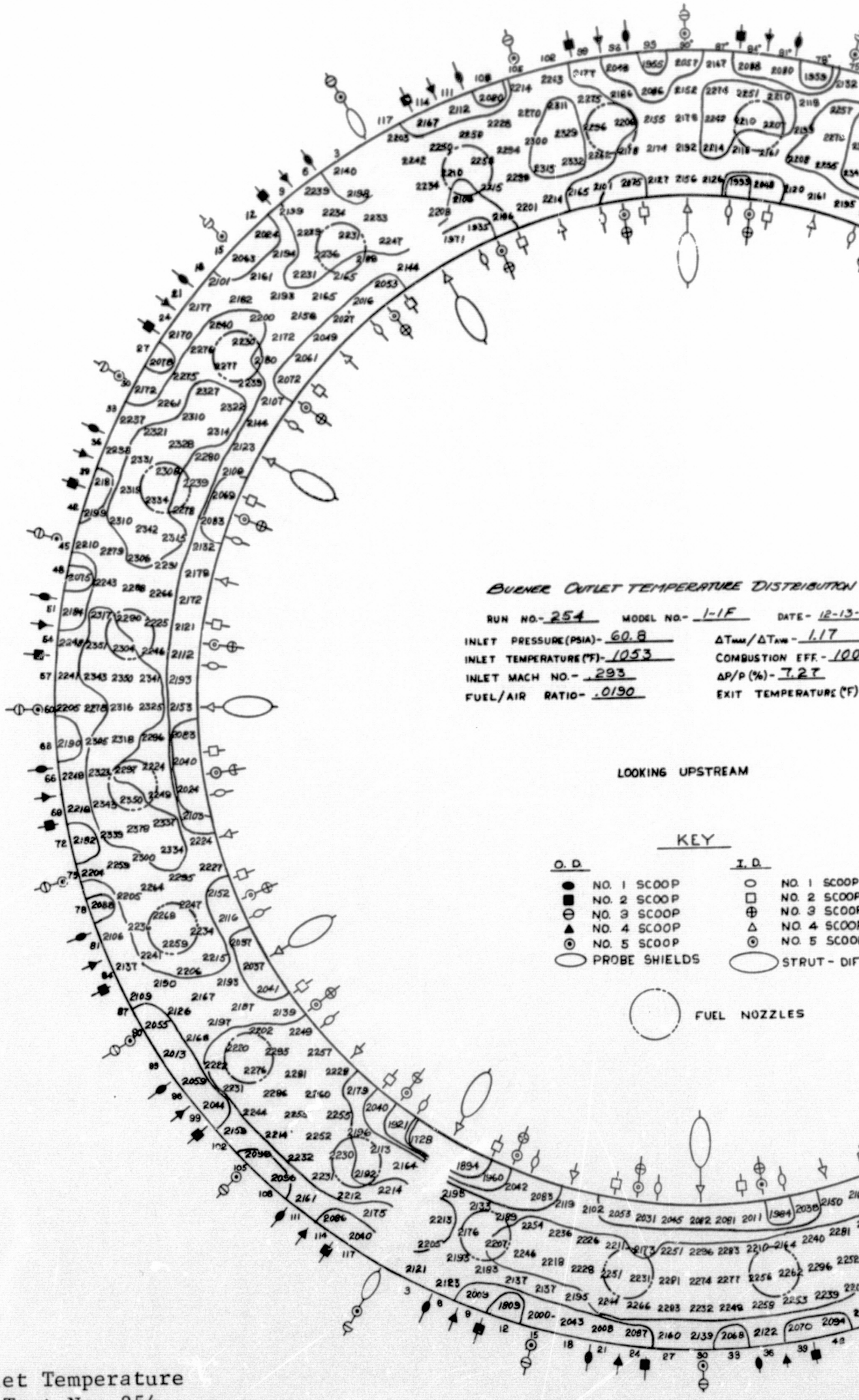

Figure 115. Combustor Outlet Temperature Distribution, Test No. 254

FOLDOUT FRAME 1

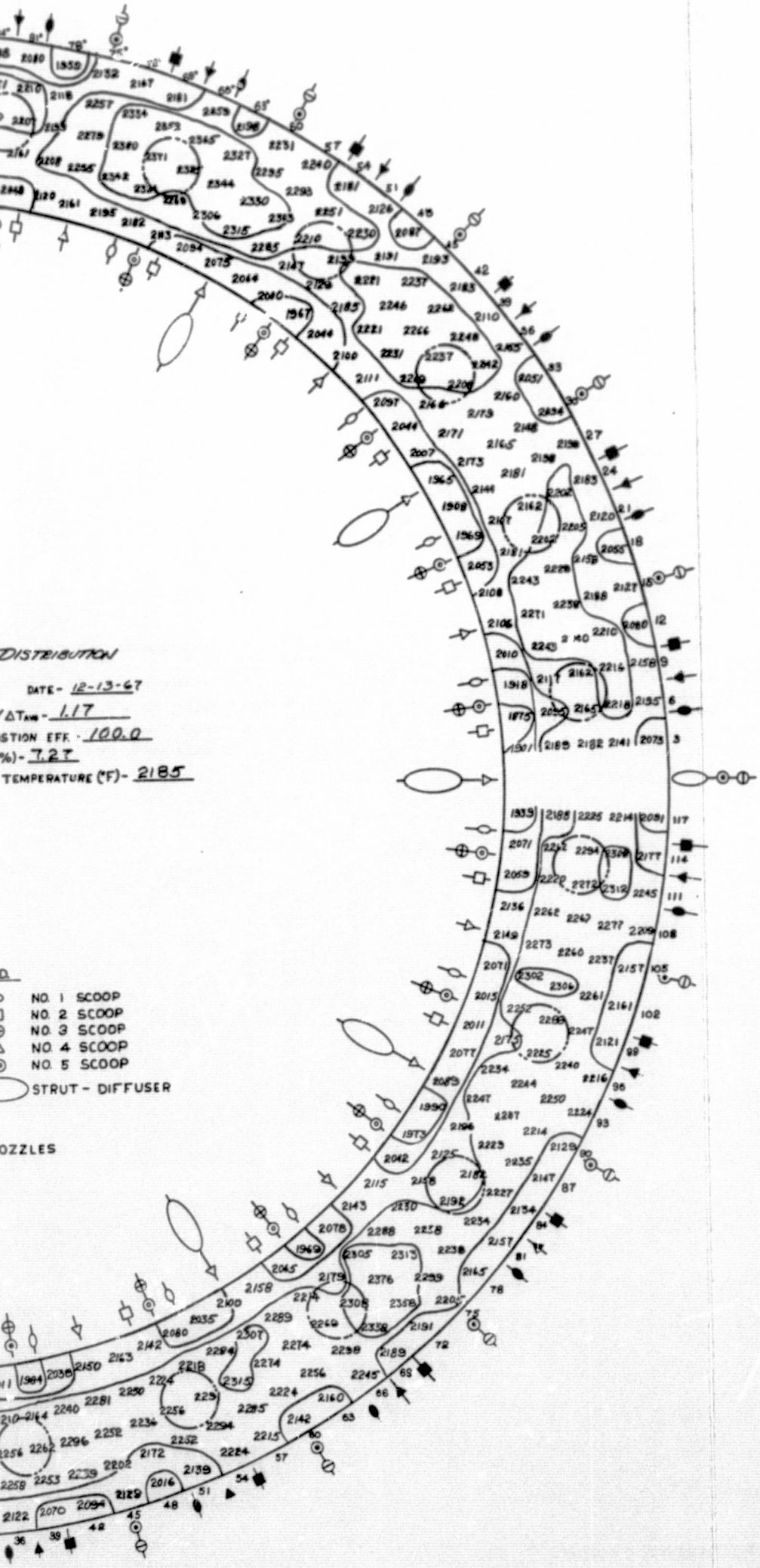
DISTRIBUTION
DATE- 12-13-67
ΔTAMB - 1.17
STION EFF. - 100.0
%)- 7.27
TEMPERATURE (°F)- 2185
D
NO. 1 SCOOP
NO. 2 SCOOP
NO. 3 SCOOP
NO. 4 SCOOP
NO. 5 SCOOP
STRUT - DIFFUSER
OZZLES

FD 23629

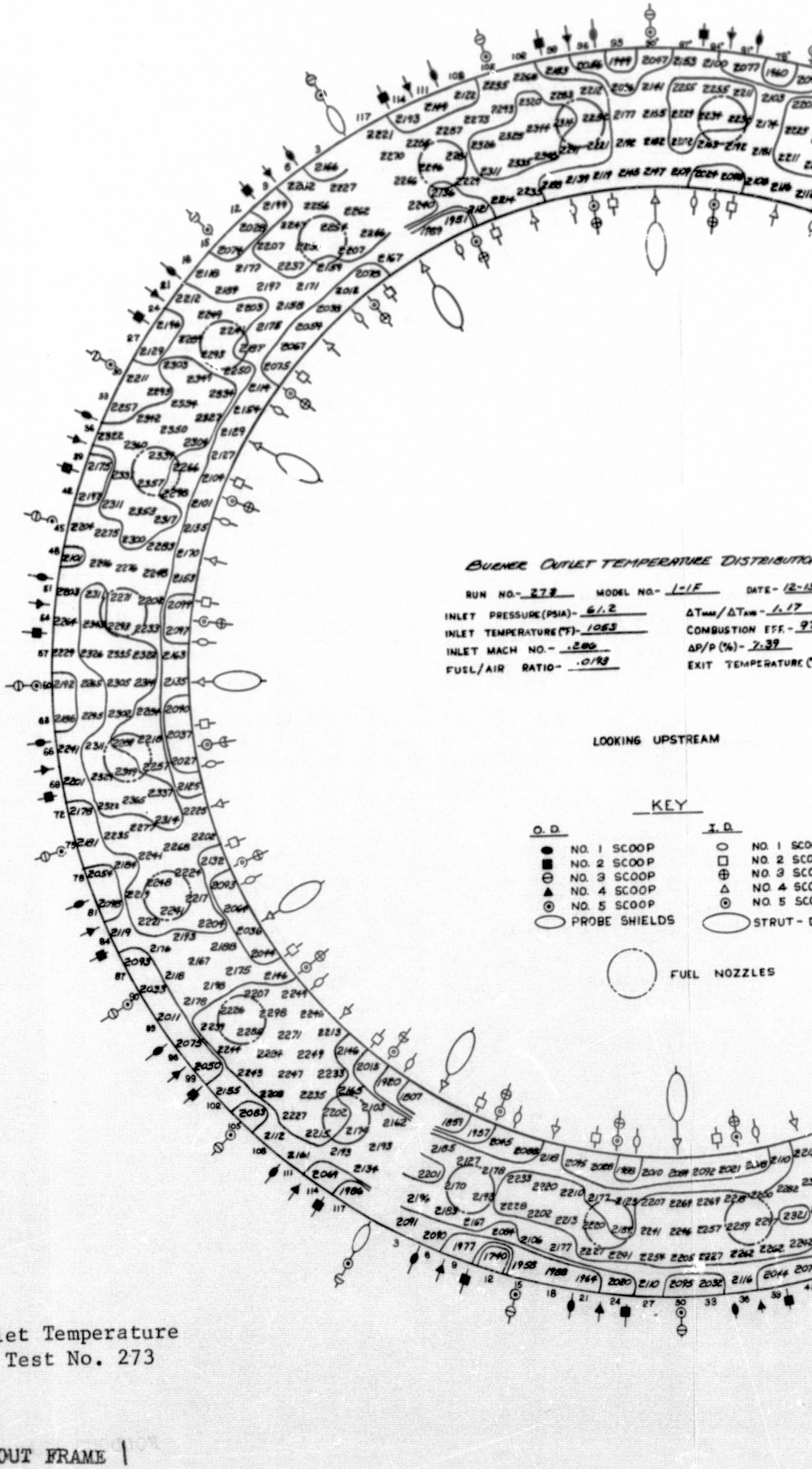

Figure 116. Combustor Outlet Temperature Distribution, Test No. 273

FOLDOUT FRAME 1

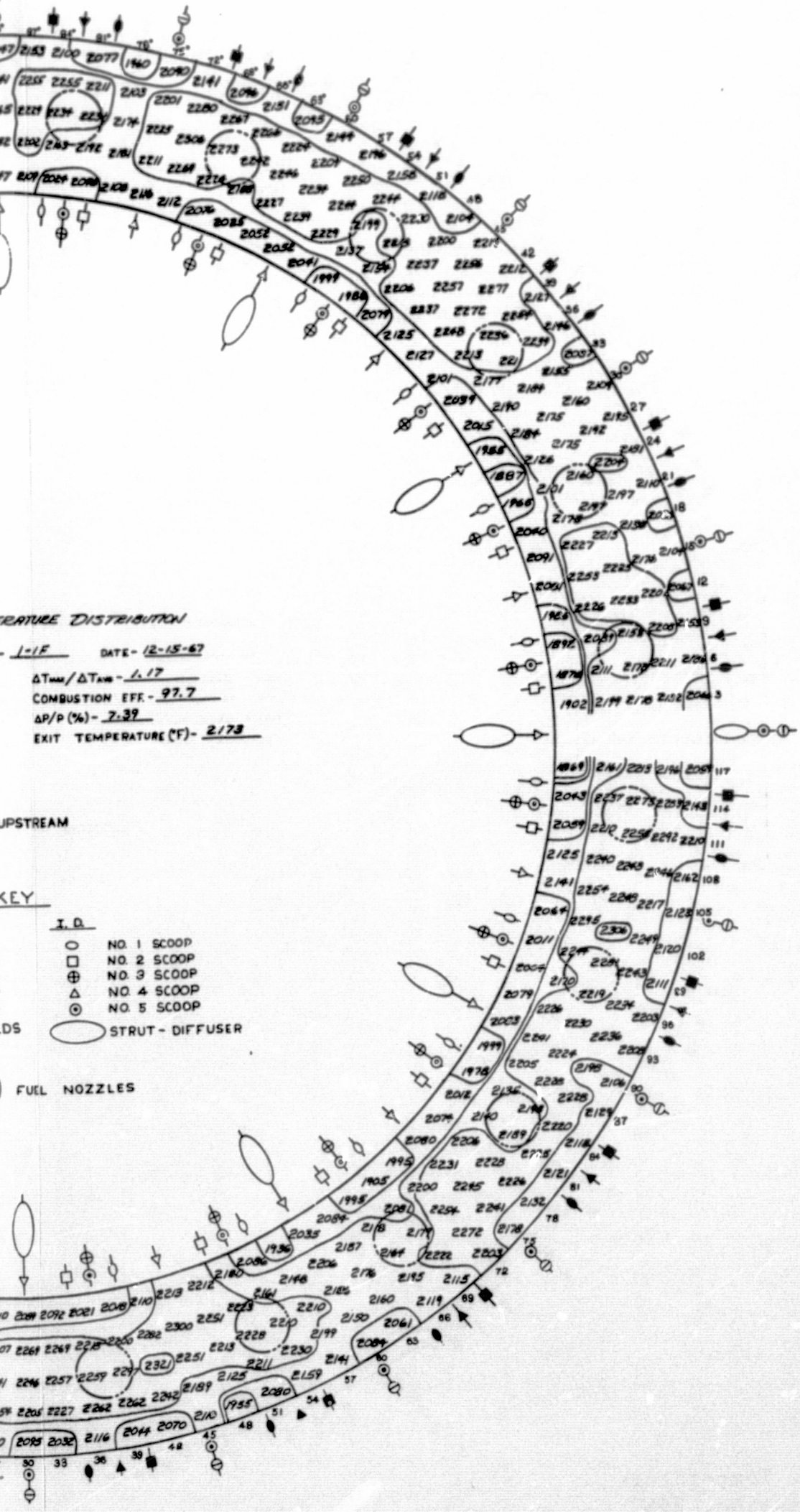

FD 23630

FOLDOUT FRAME 2

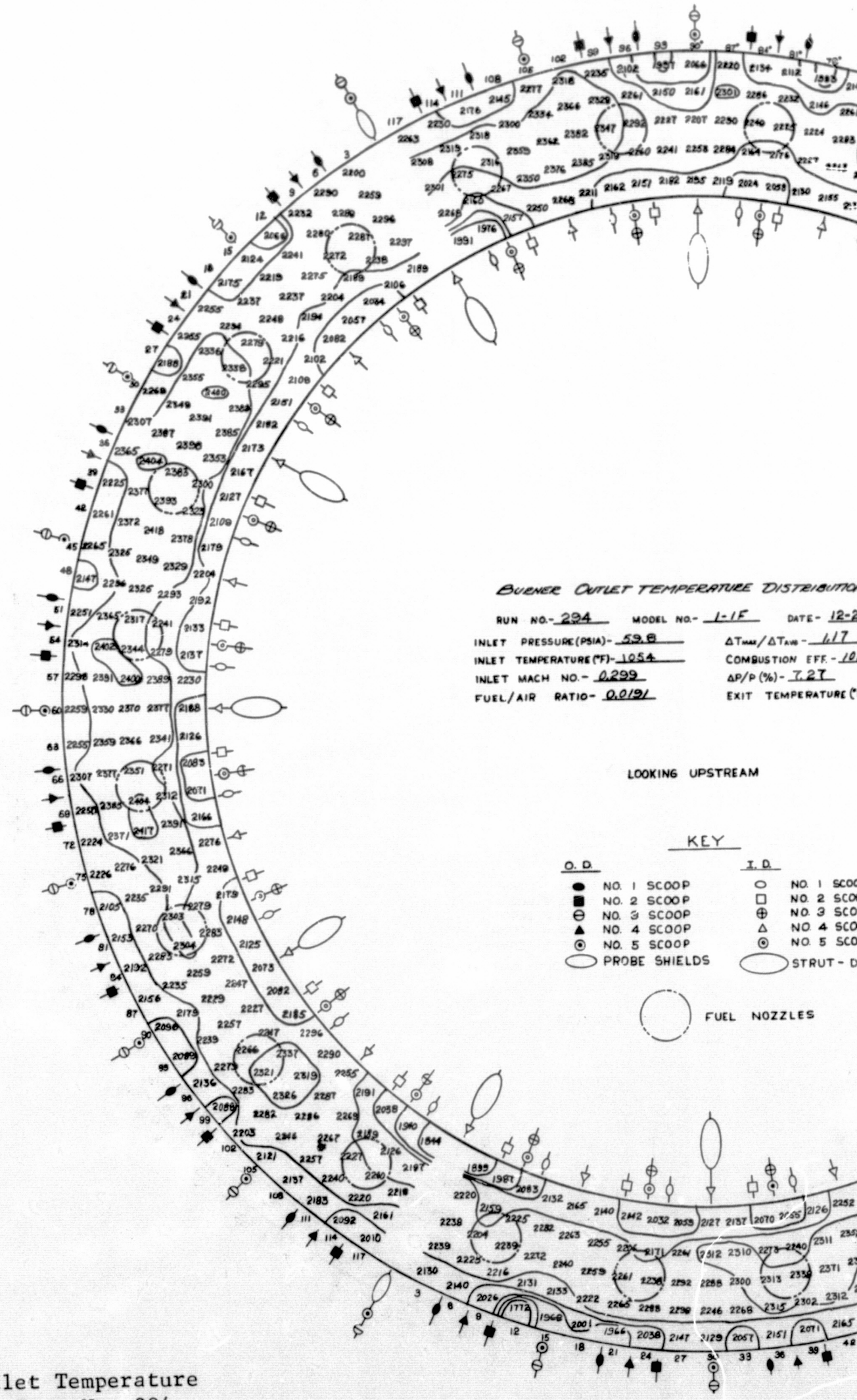

Figure 117. Combustor Outlet Temperature Distribution, Test No. 294

FOLDOUT FRAME 1

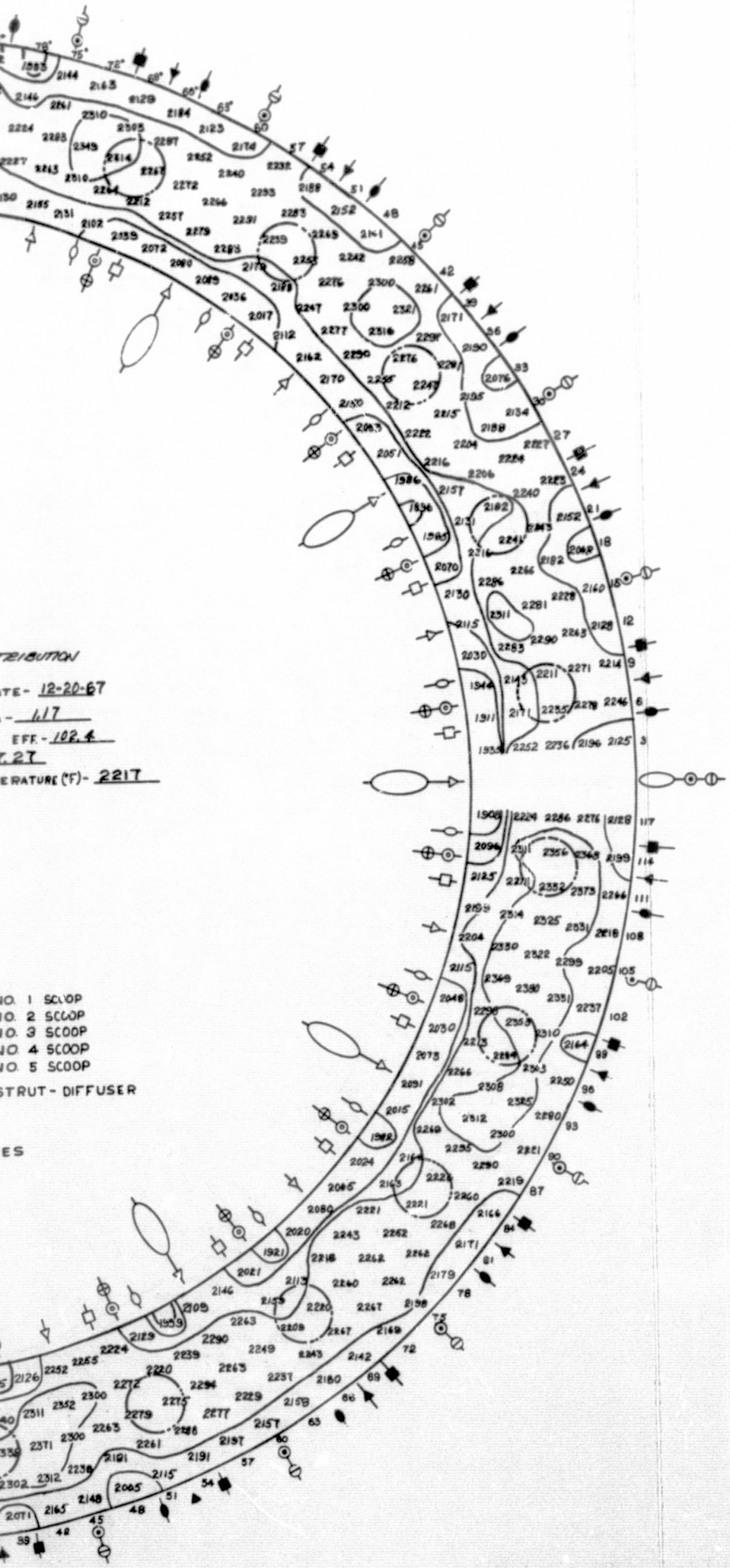

FD 23631

FOLDOUT FRAME 2

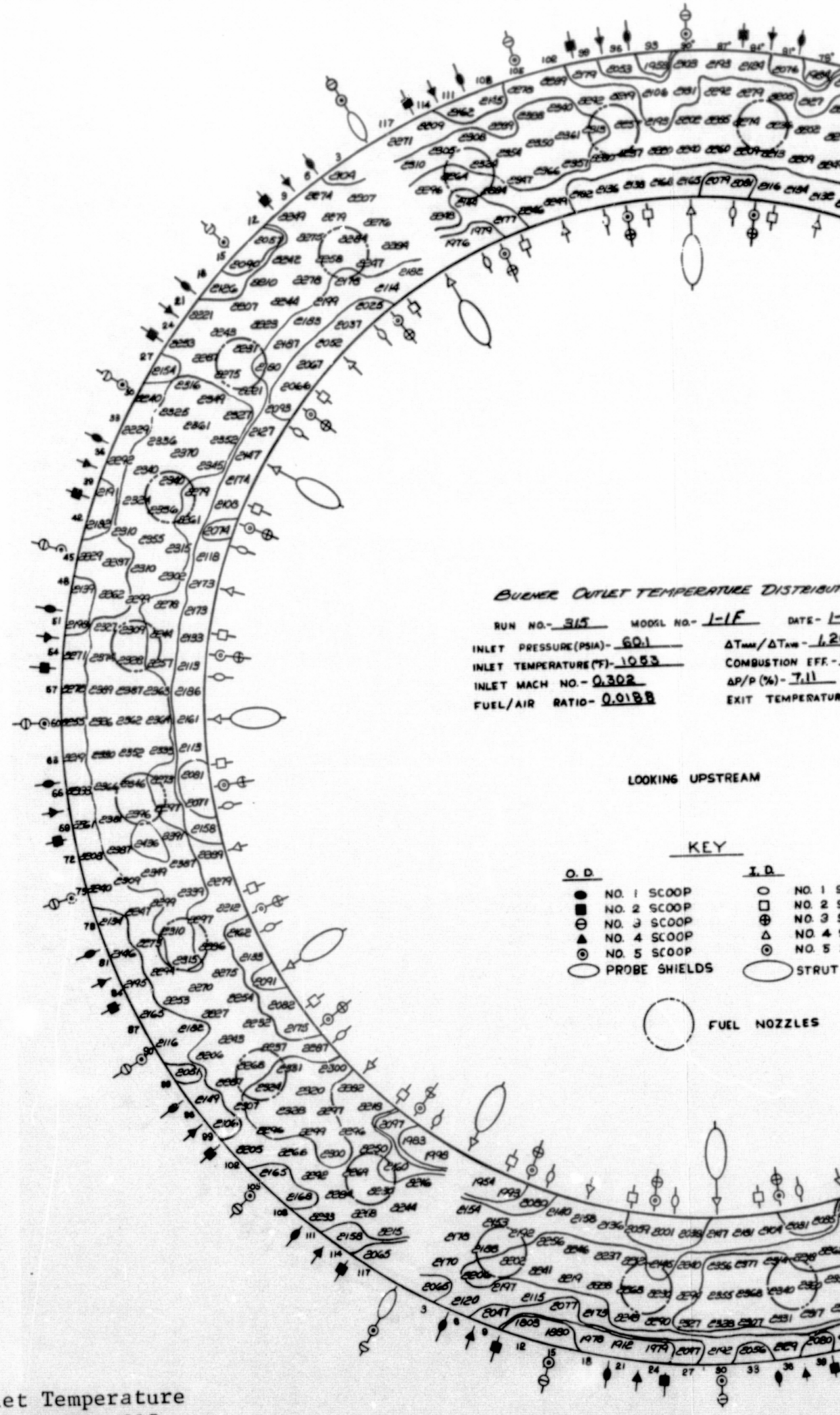

Figure 118. Combustor Outlet Temperature Distribution, Test No. 315

FOLDOUT FRAME 1

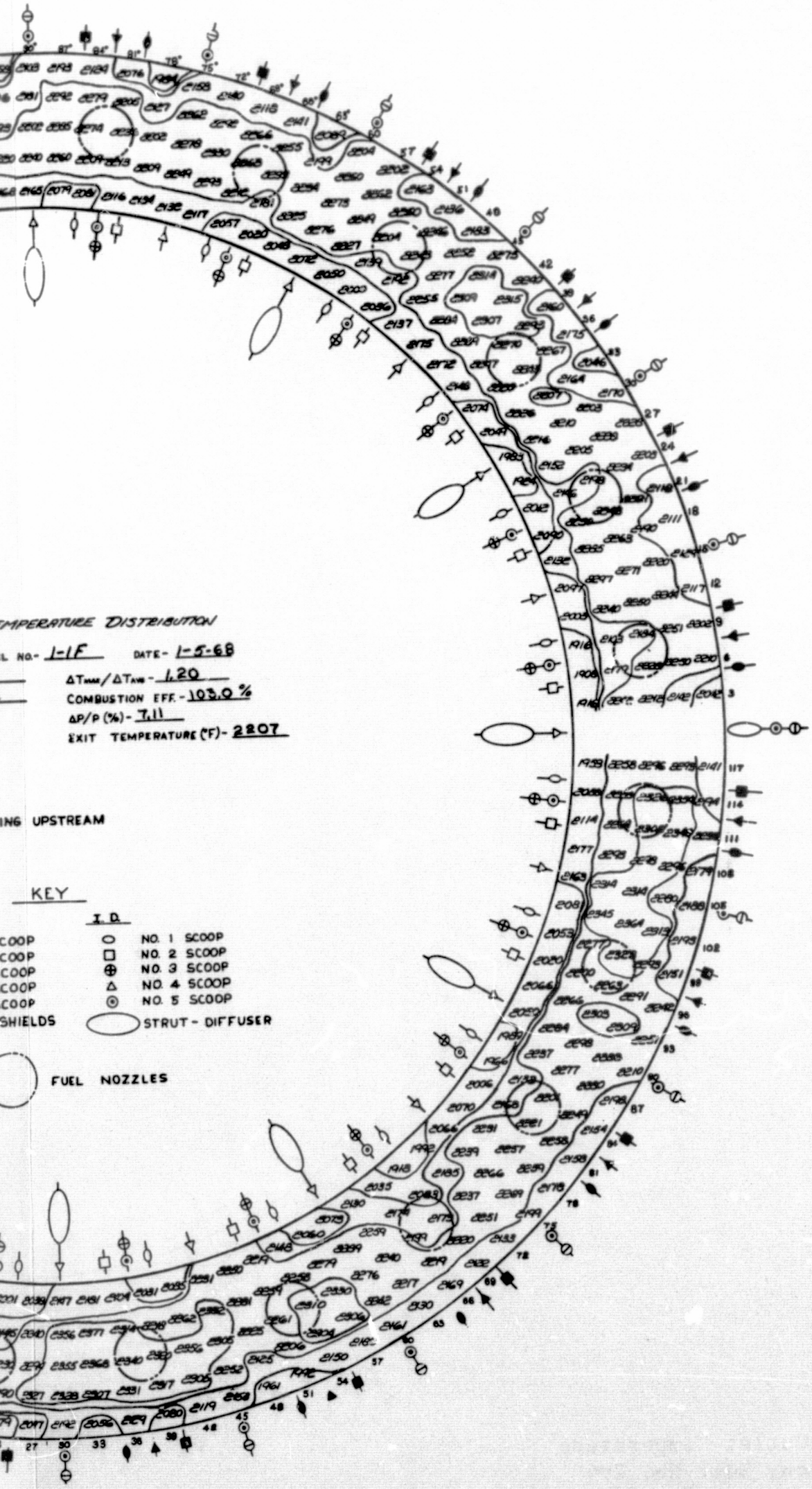

FD 23812

FOLDOUT FRAME 2

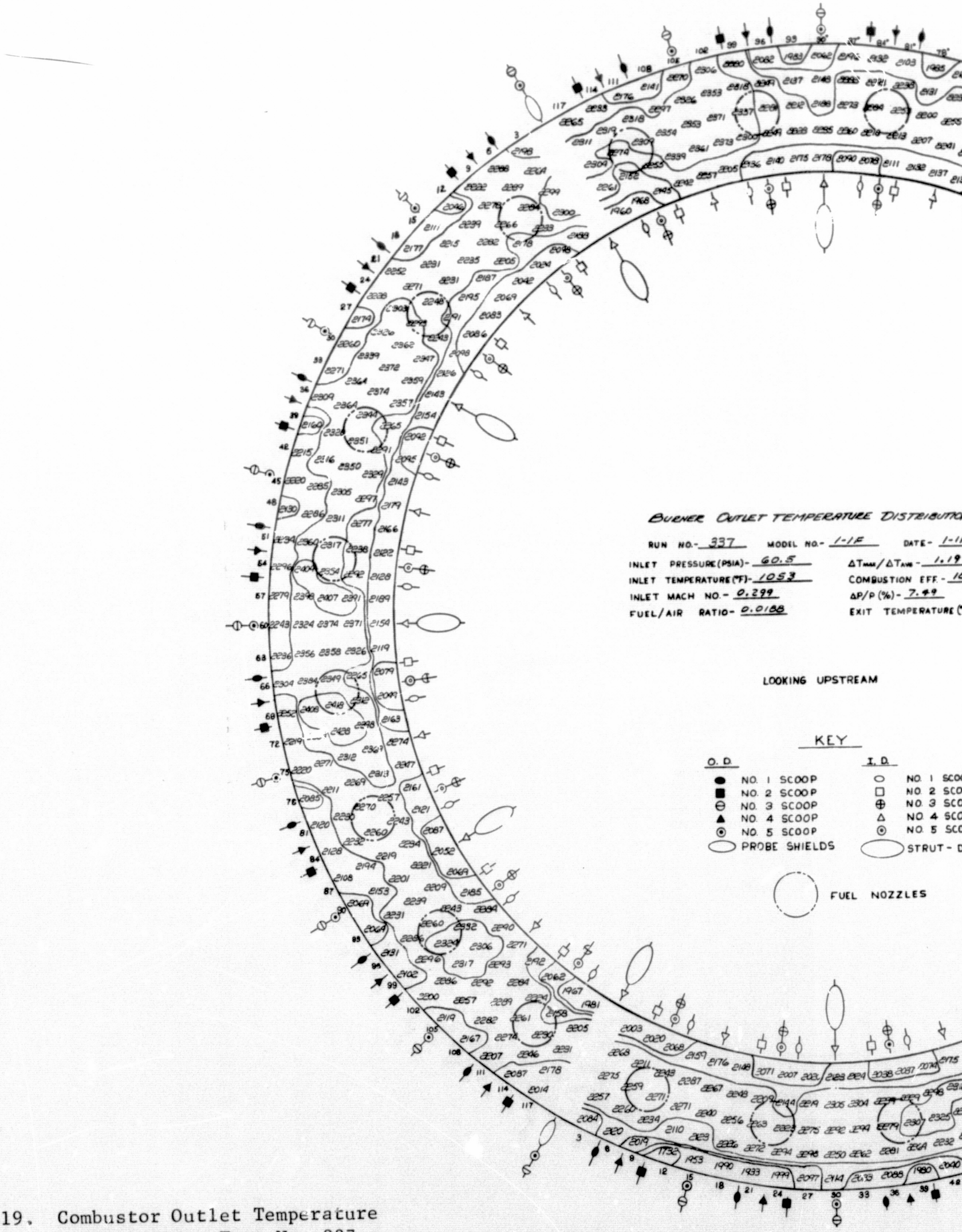

Figure 119. Combustor Outlet Temperature Distribution, Test No. 337

FOLDOUT FRAME 1

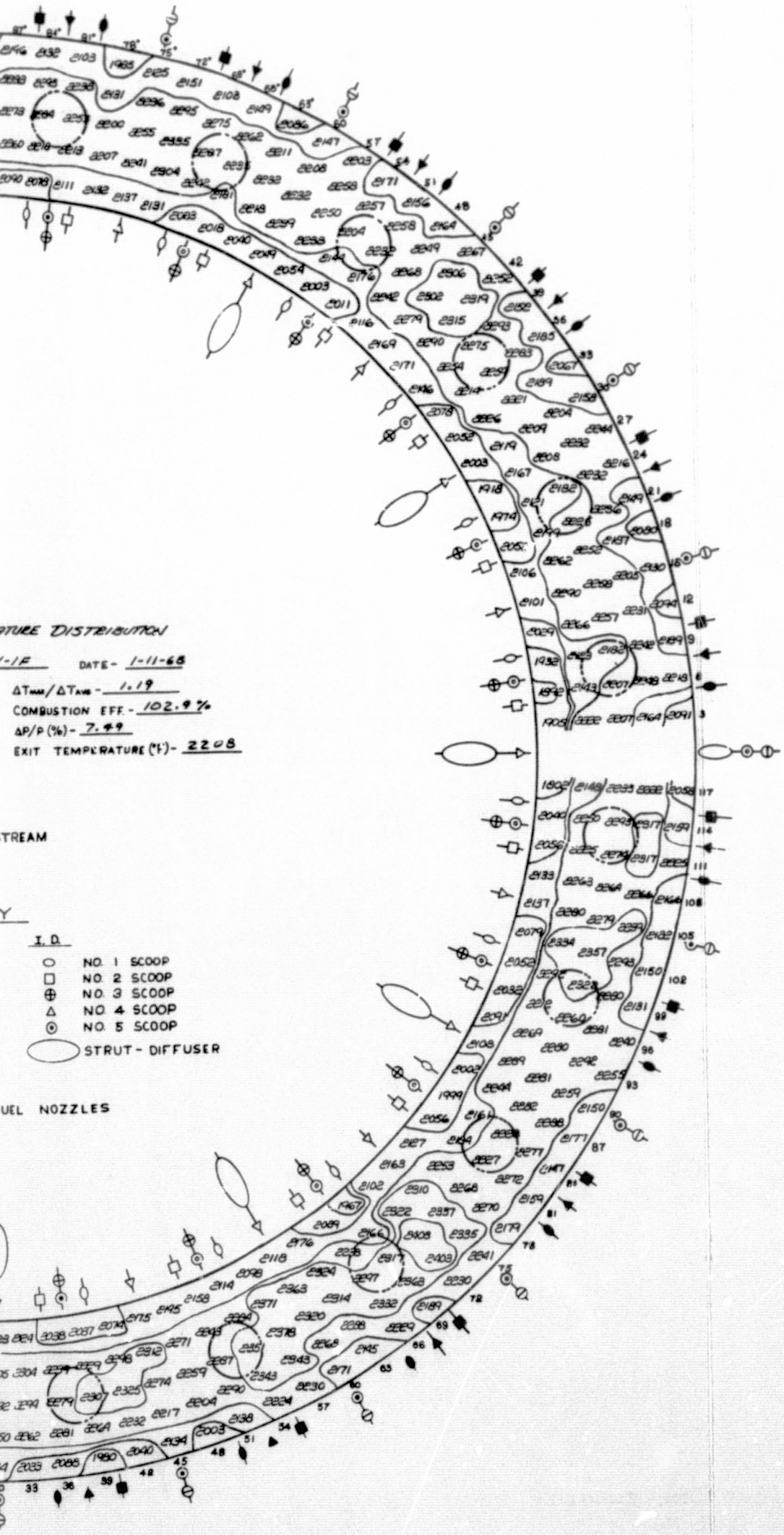

FD 23814

FOLDOUT FRAME 2

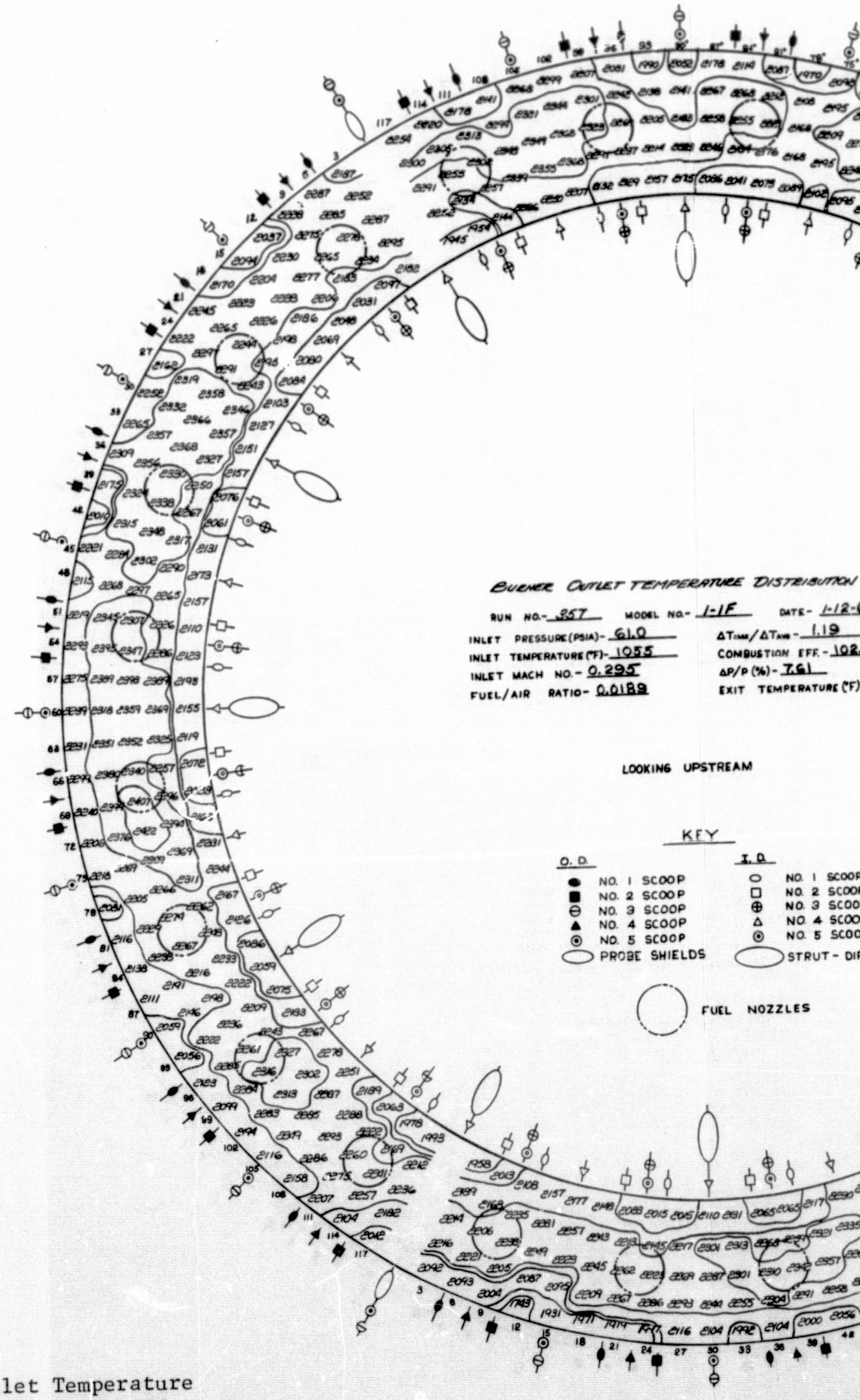

Figure 120. Combustor Outlet Temperature Distribution, Test No. 357

FOLDOUT FRAME 1

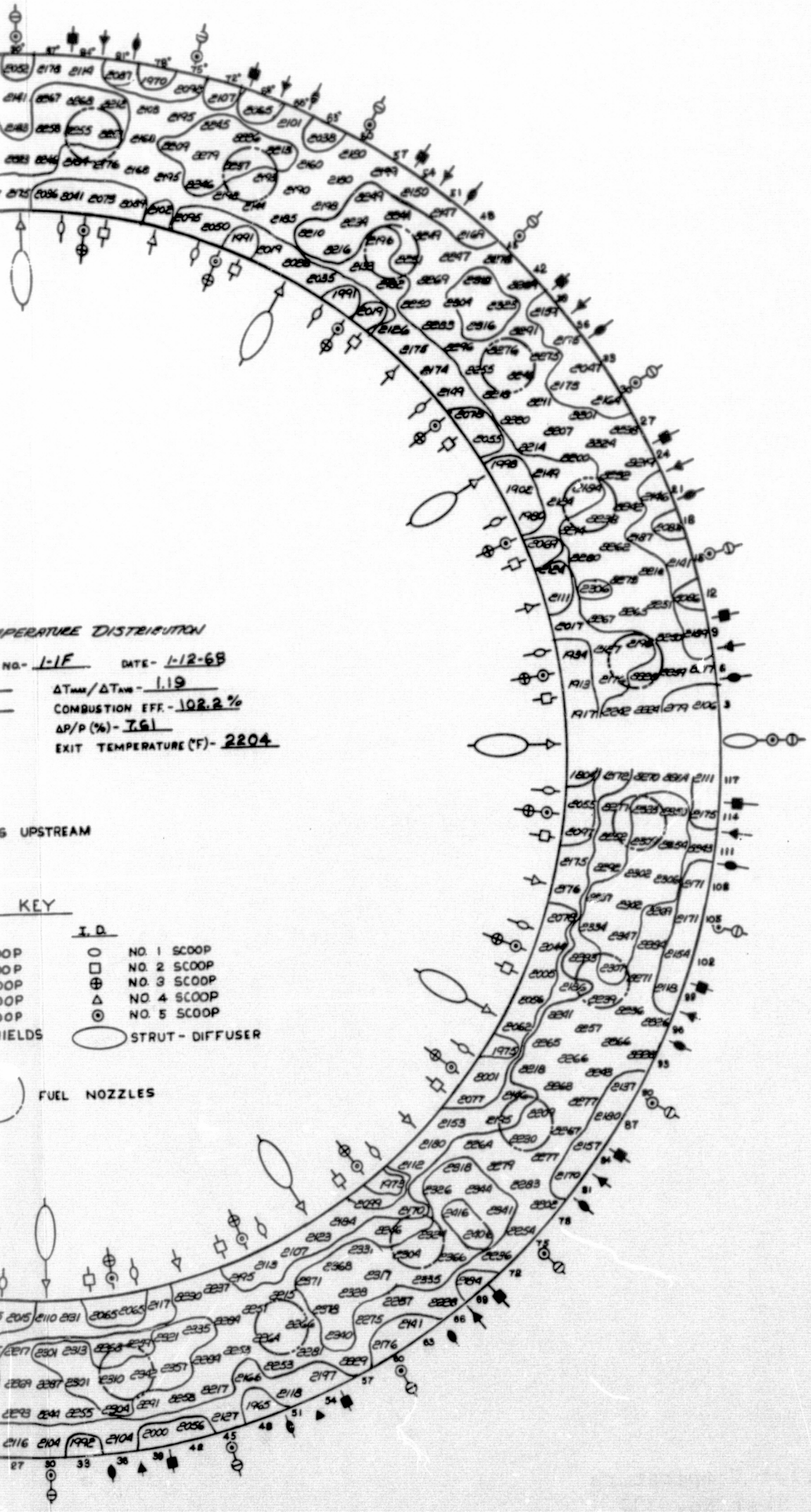

FD 23815

FOLDOUT FRAME 2

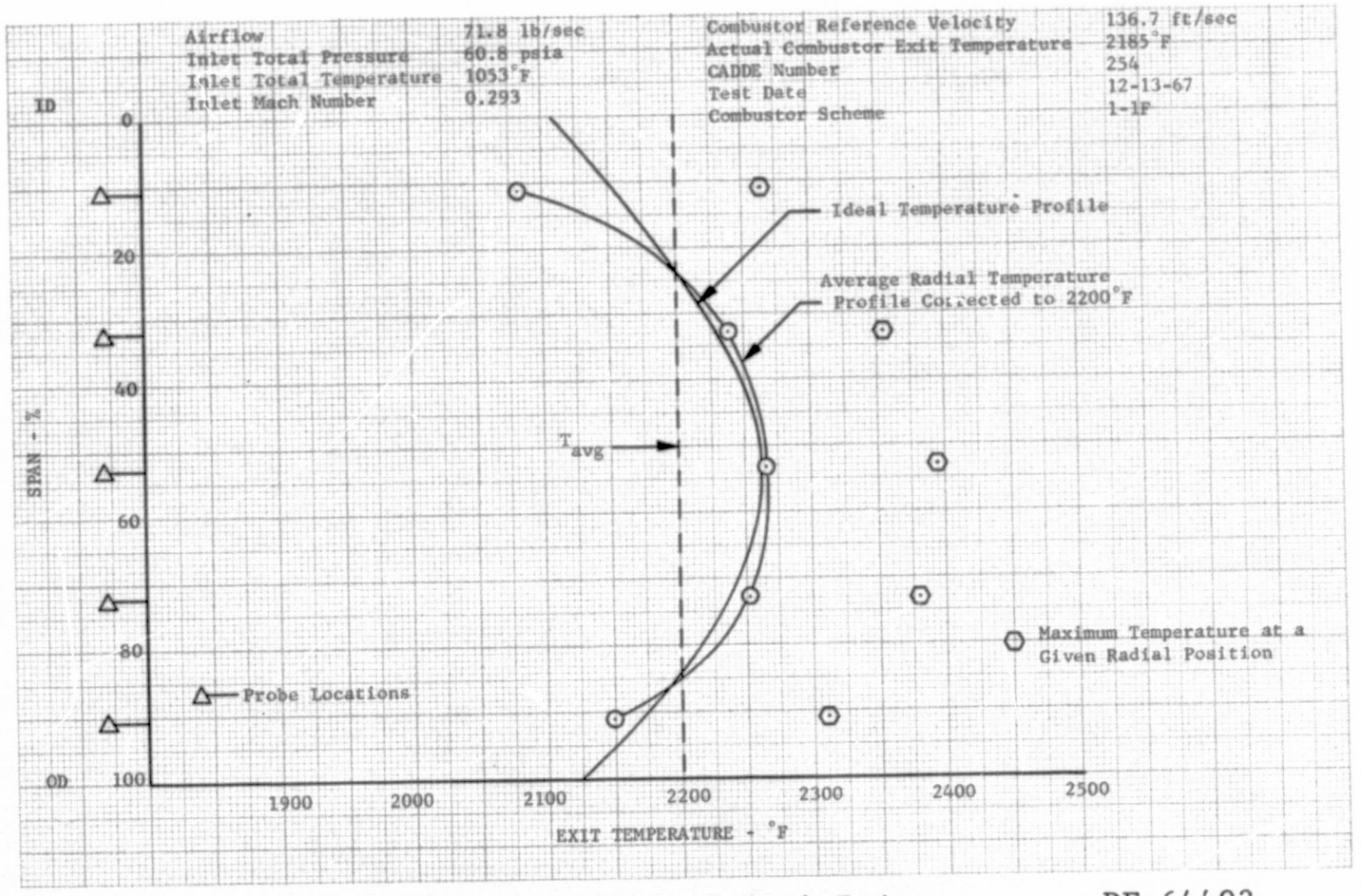

Figure 121. Combustor Average Radial Exit Temperature Profile, Test No. 254

DF 64493

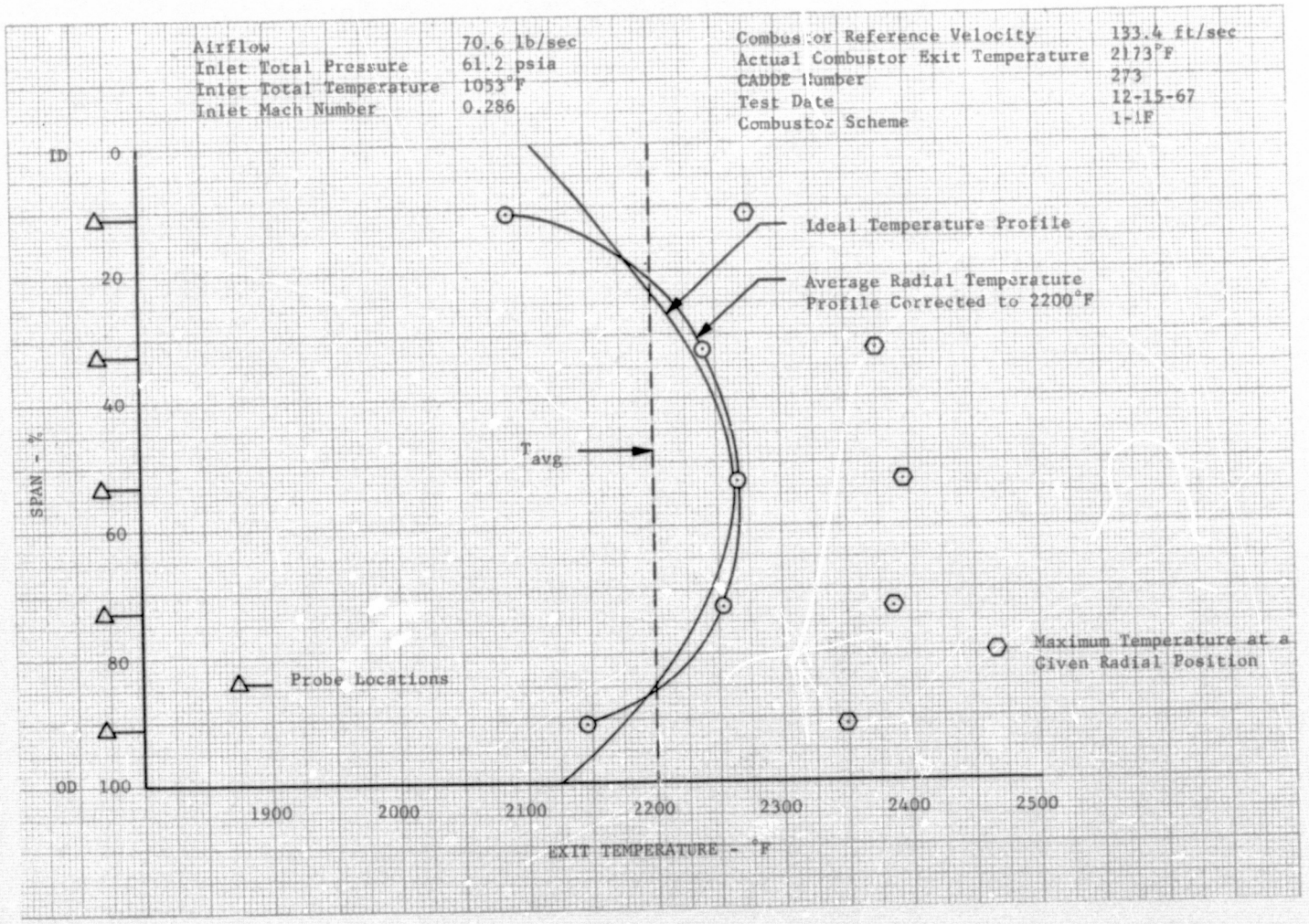

Figure 122. Combustor Average Radial Exit Temperature Profile, Test No. 273

DF 64494

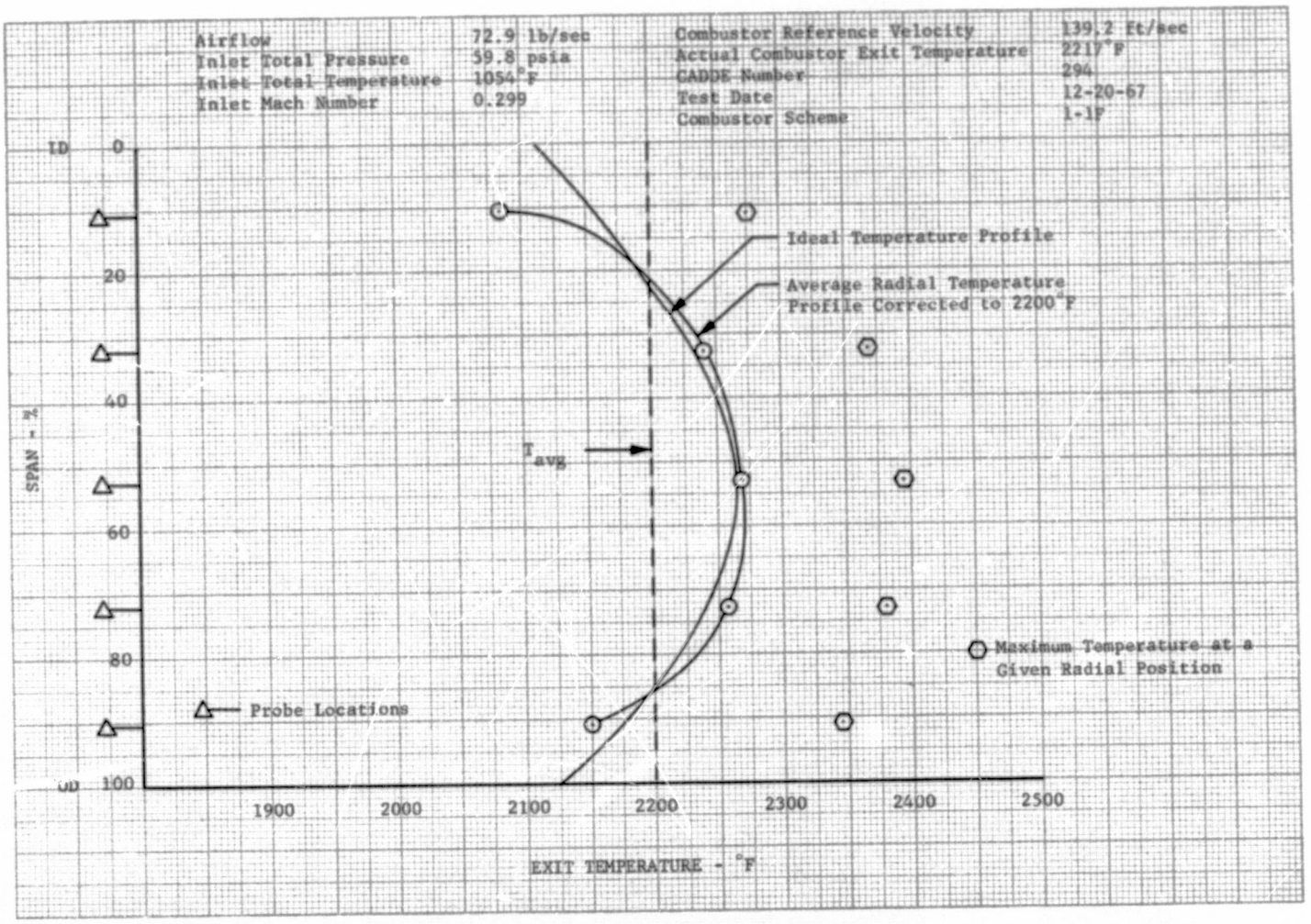

Figure 123. Combustor Average Radial Exit Temperature Profile, Test No. 294

DF 64495

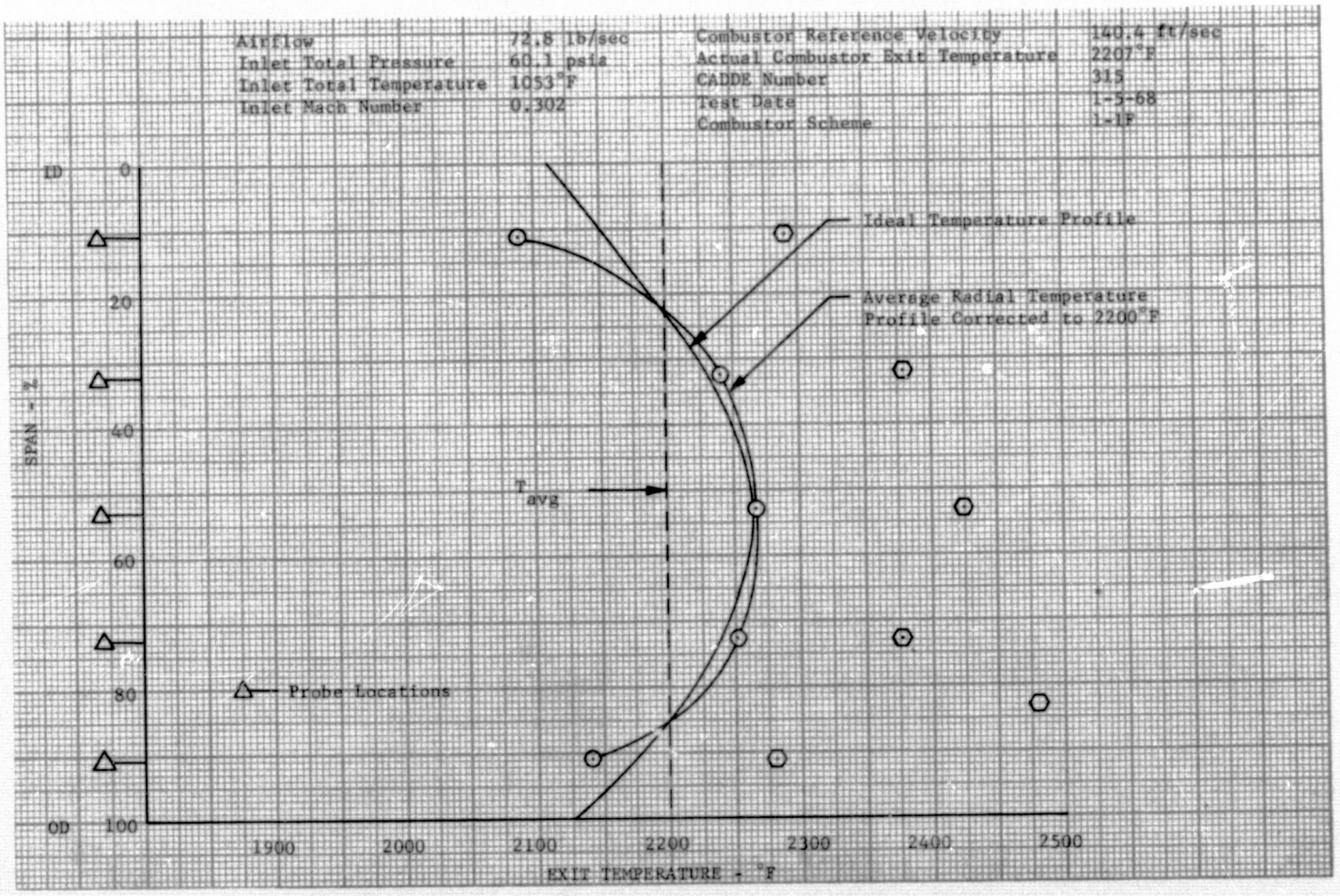

Figure 124. Combustor Average Radial Exit Temperature Profile, Test No. 315

DF 64496

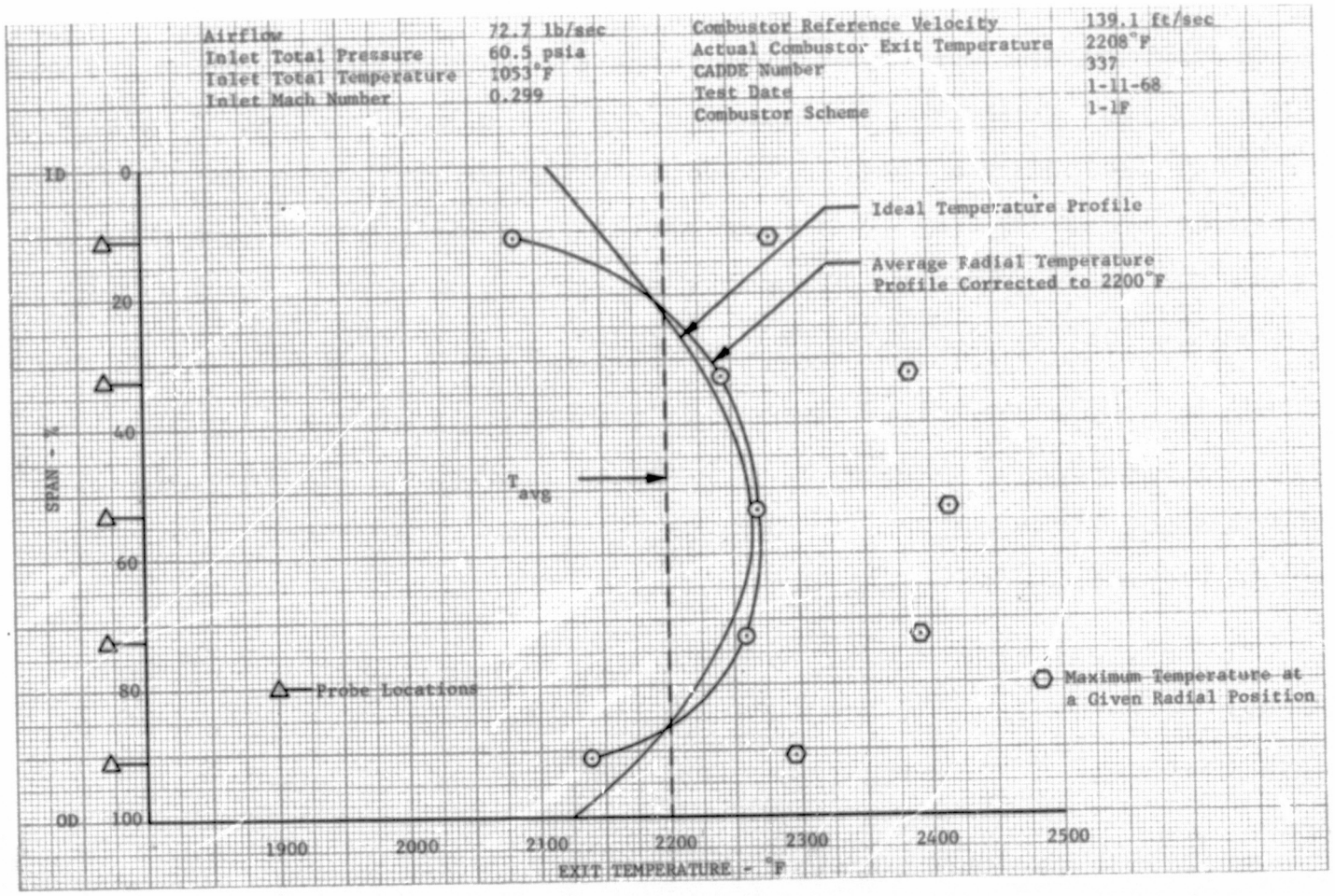

Figure 125. Combustor Average Radial Exit Temperature Profile, Test No. 337

DF 64497

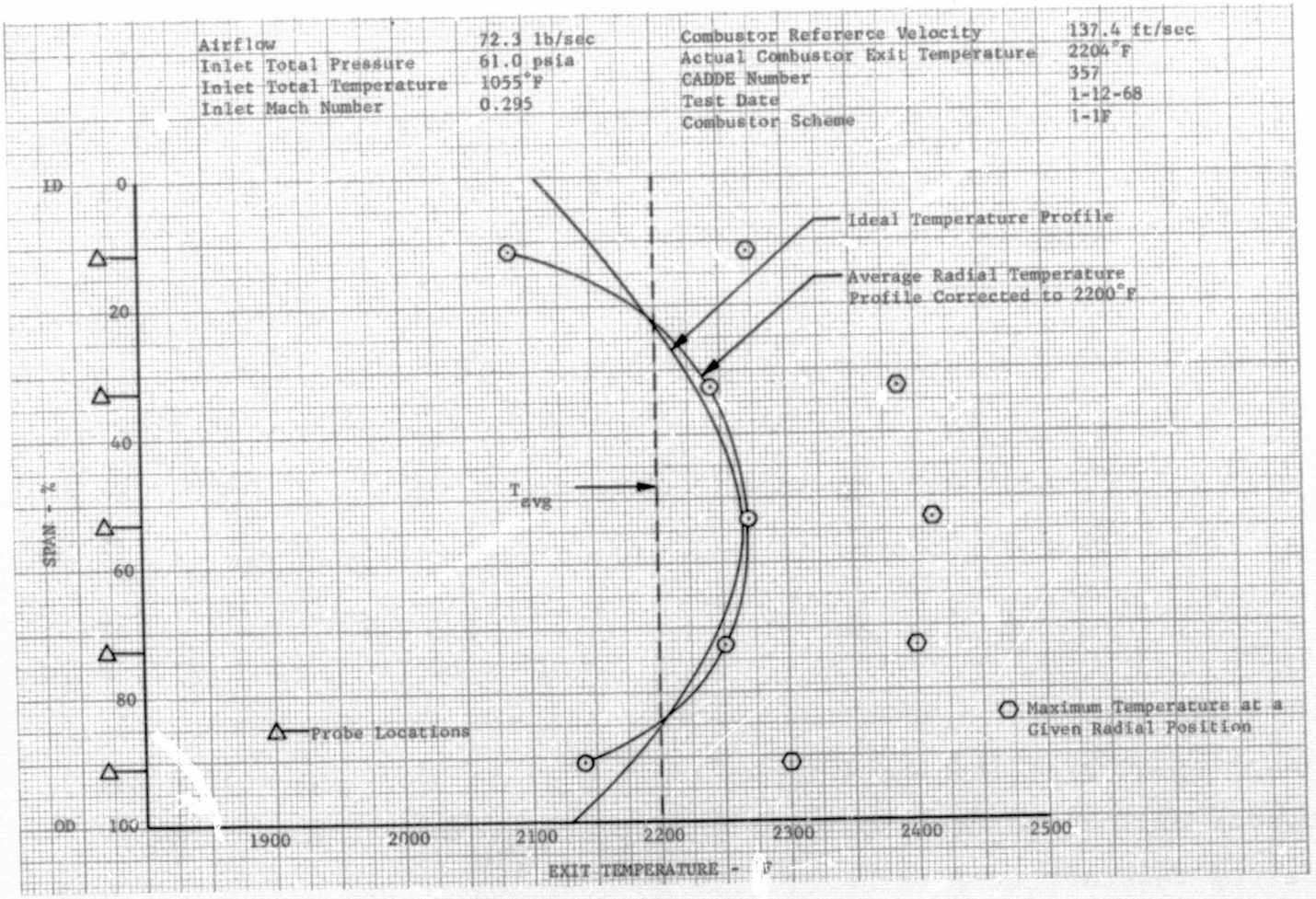

Figure 126. Combustor Average Radial Exit Temperature Profile, Test No. 357

DF 64498

Comparison of the combustor exit temperature patterns (figures 109 and 127) for Test Condition 6 tests, before and after the Test Condition 2 testing, indicates a deterioration in performance. This may also be shown by comparing the combustor radial exit temperature profiles for these two tests (figures 111 and 128). The combustor exit temperature uniformity parameter (ΔTVR) had increased from a value of 1.23 to 1.30.

Upon completion of 40 hours of Test Condition 2 testing, the test rig was opened for inspection. As shown in figures 129 through 131, the combustor was in very good condition. No metal burning or high thermal gradients were noted.

The rig was also opened for inspection upon completion of Test Condition 2 testing. As shown in figure 132, one of the No. 1 scoop caps on the ID liner had broken loose and was wedged between the scoop and a liner support. Also noted was a slight burning of a No. 3 ID liner scoop (shown in figure 133) and 5 or 6 cracks in the ID primary liner. All of the cracks had originated from the first row of thumbnail cooling scoops and extended from the thumbnail scoops toward the No. 1 scoops. The cracks varied in length from 0.125 to 0.750 inch. The scoop cap was repaired and holes (0.100-inch in diameter) were drilled at the end of the cracks in an attempt to stop propagation. As shown in figure 134, the overall combustor appearance was good.

Following the inspection and repairs, testing was resumed. A data point was taken at Test Condition 6 before the beginning of Test Condition 3 testing. The hot areas evident during the previous test were still present. Testing at Test Condition 3 was then initiated.

The combustor performance remained constant through Test Condition 3 testing, as shown by comparing the combustor exit temperature patterns after 1, 20, and 30 hours of testing (figures 135 through 137). Figures 138 through 140 show the constancy of the combustor exit radial temperature profiles and maximum local peak temperatures. The combustor exit temperature pattern uniformity parameter (ΔTVR) remained fairly constant at a value of 1.19 to 1.22, which was slightly higher than expected at this test condition (figure 102).

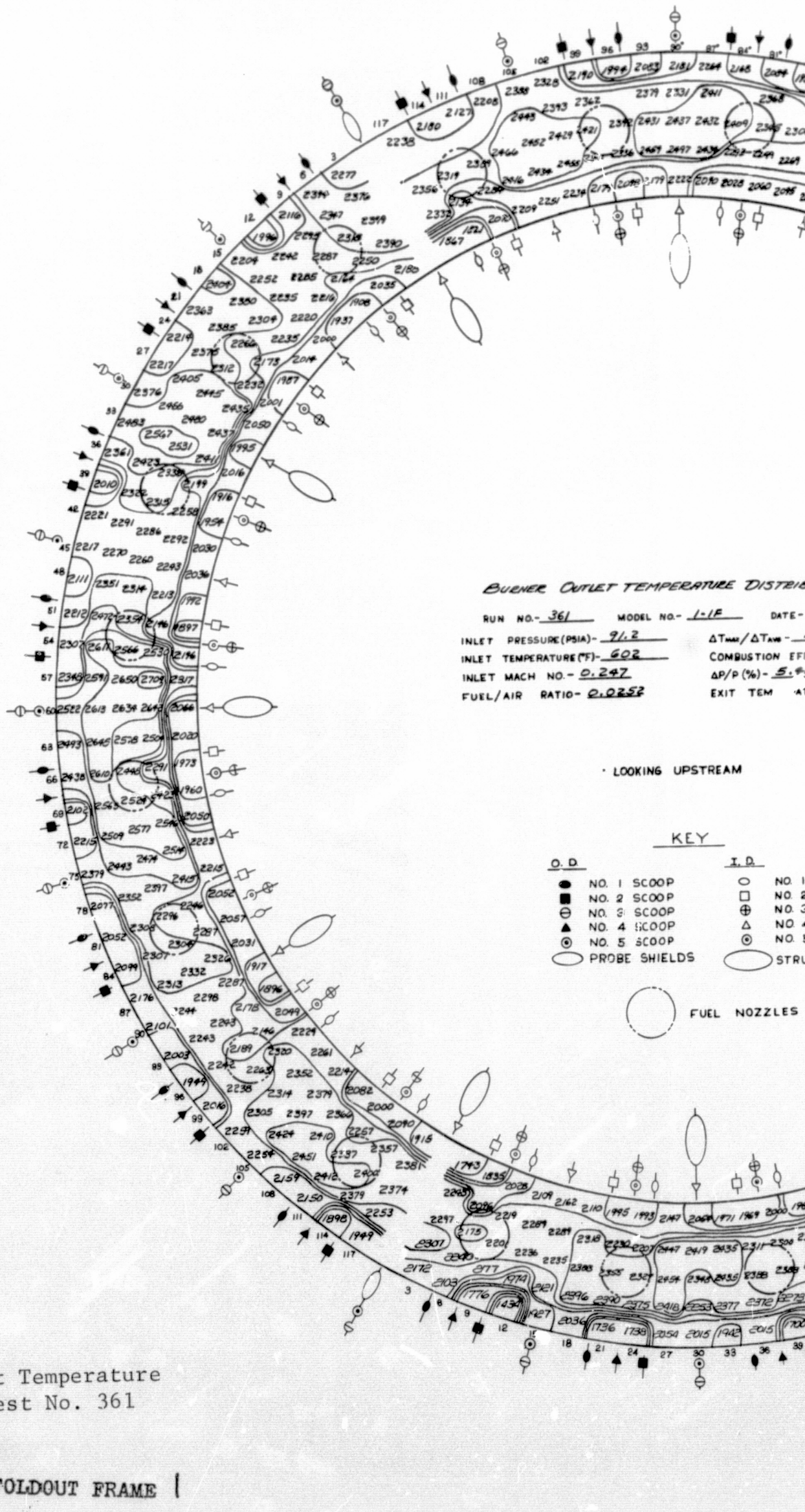

Figure 127. Combustor Outlet Temperature Distribution, Test No. 361

FOLDOUT FRAME |

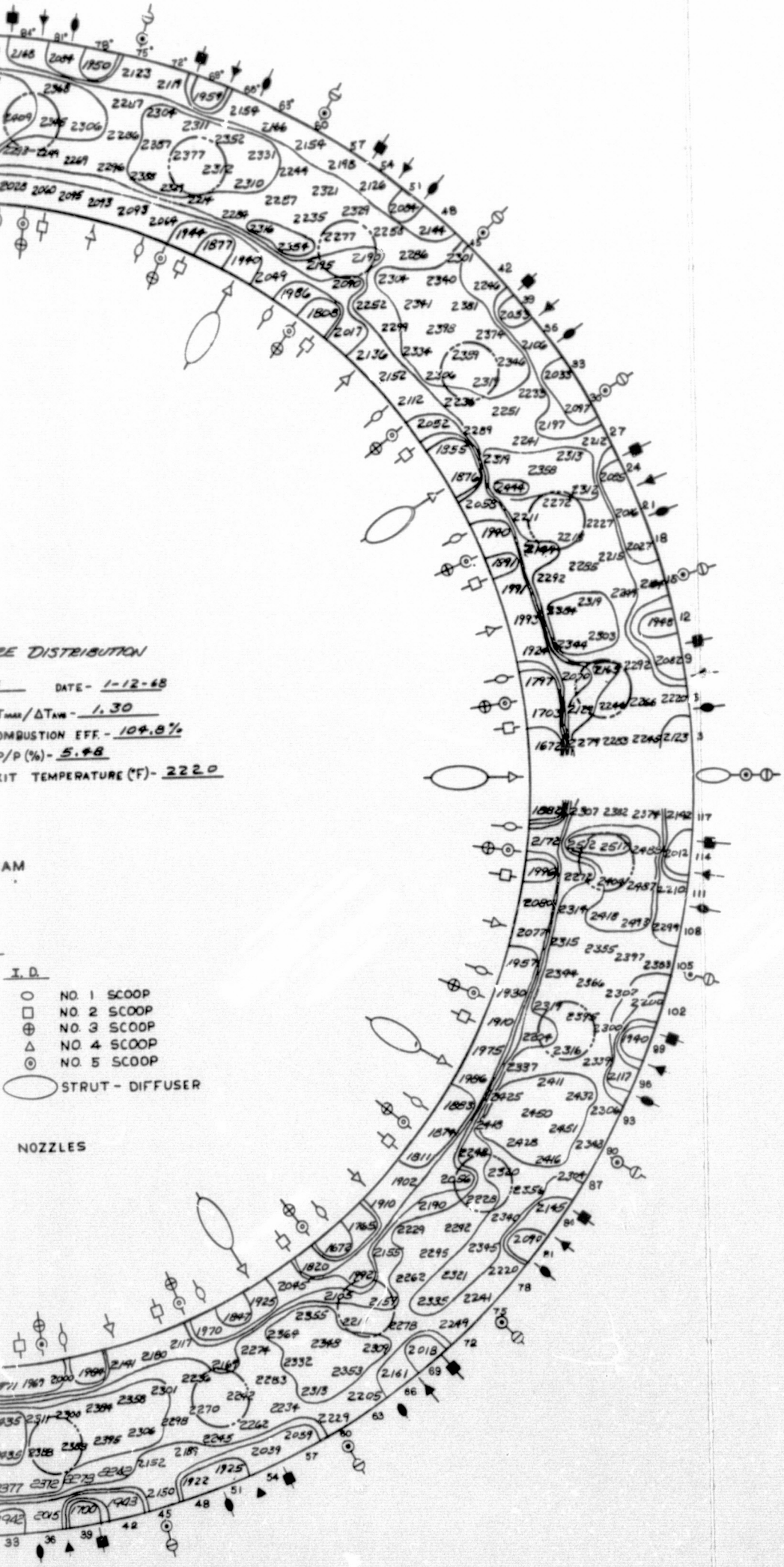

FD 23816

FOLDOUT FRAME 2

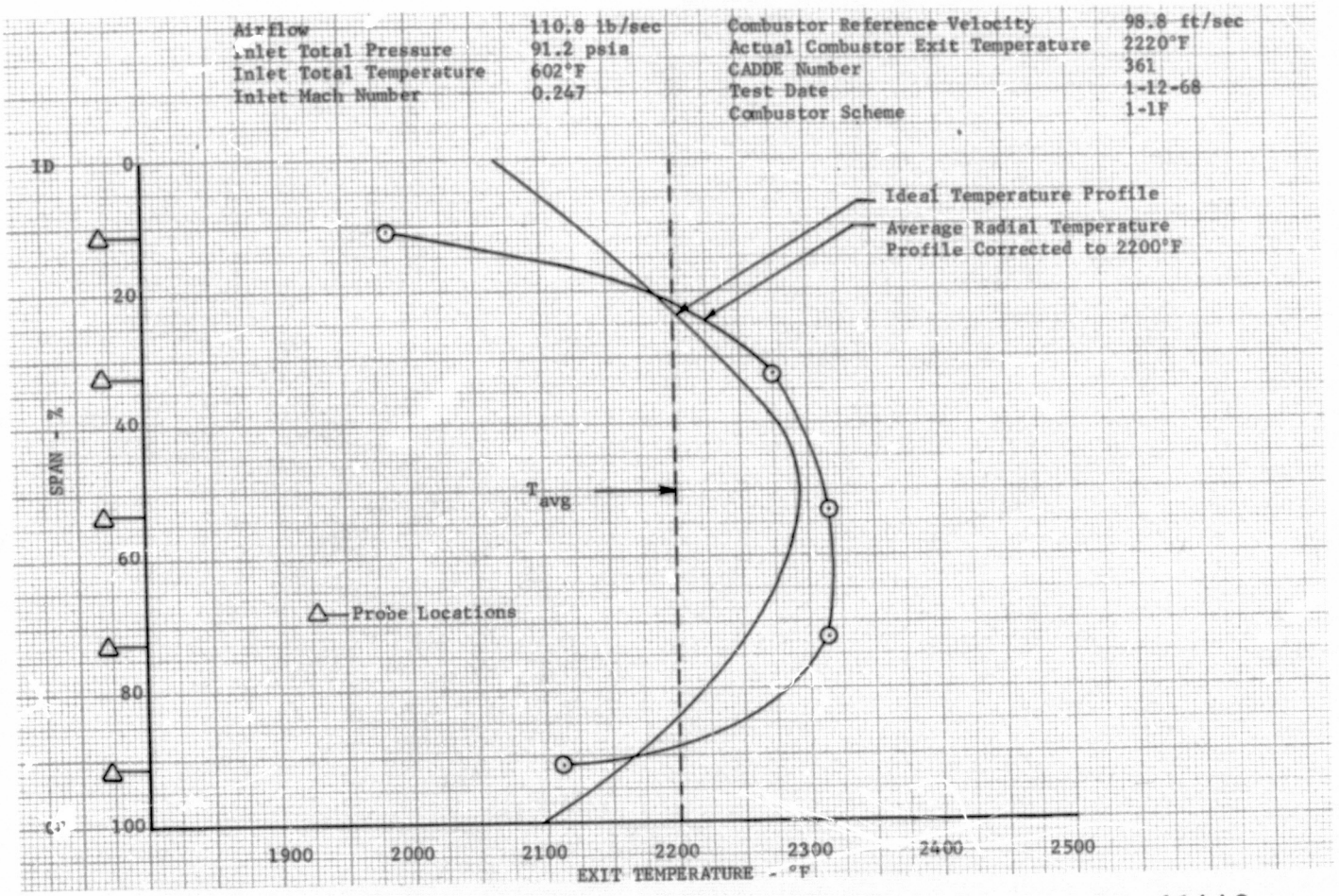

Figure 128. Combustor Average Radial Exit Temperature Profile, Test No. 361

DF 61440

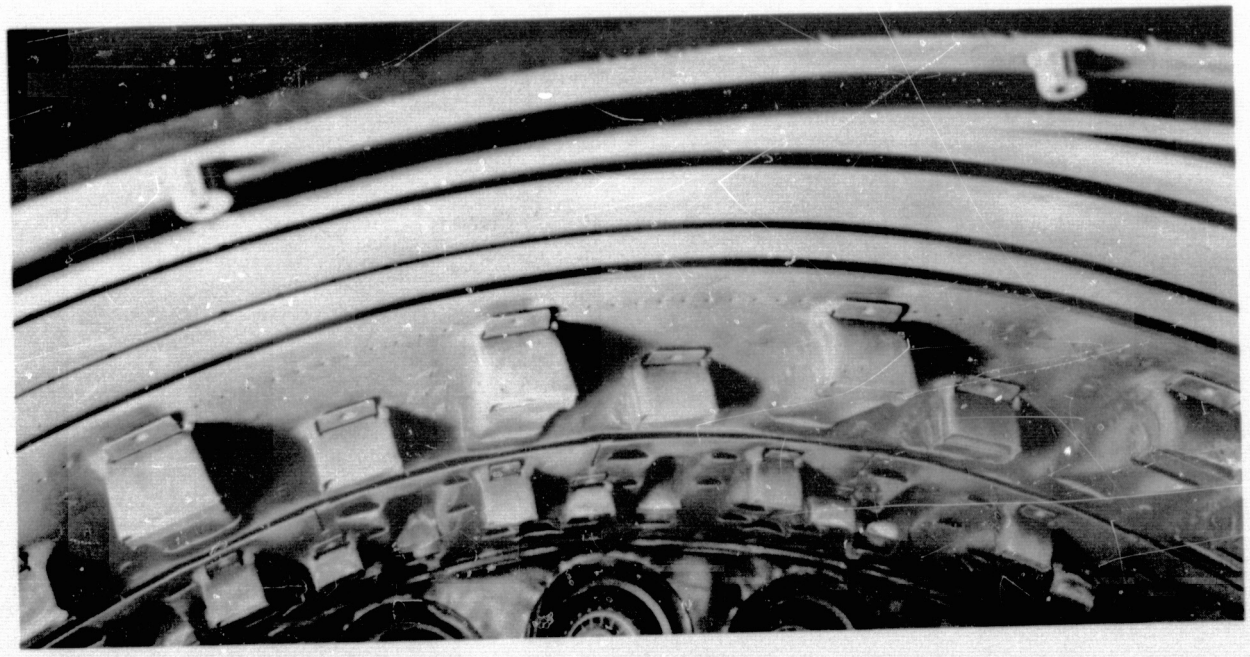

Figure 129. Combustor After 40 Hours Testing at Test Condition 2 (View 1)

FE 74060

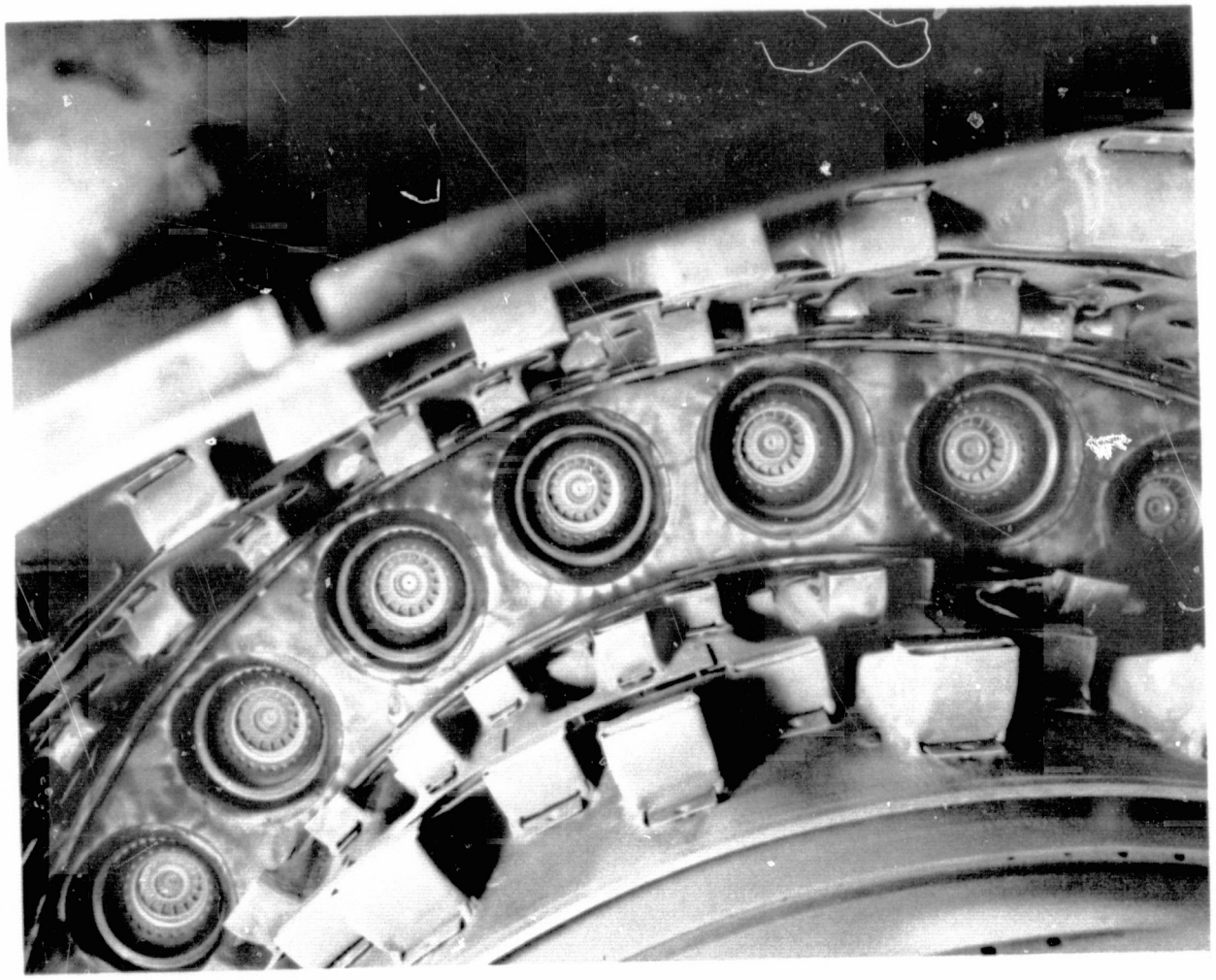

Figure 130. Combustor After 40 Hours Testing at Test Condition 2 (View 2) FE 74061

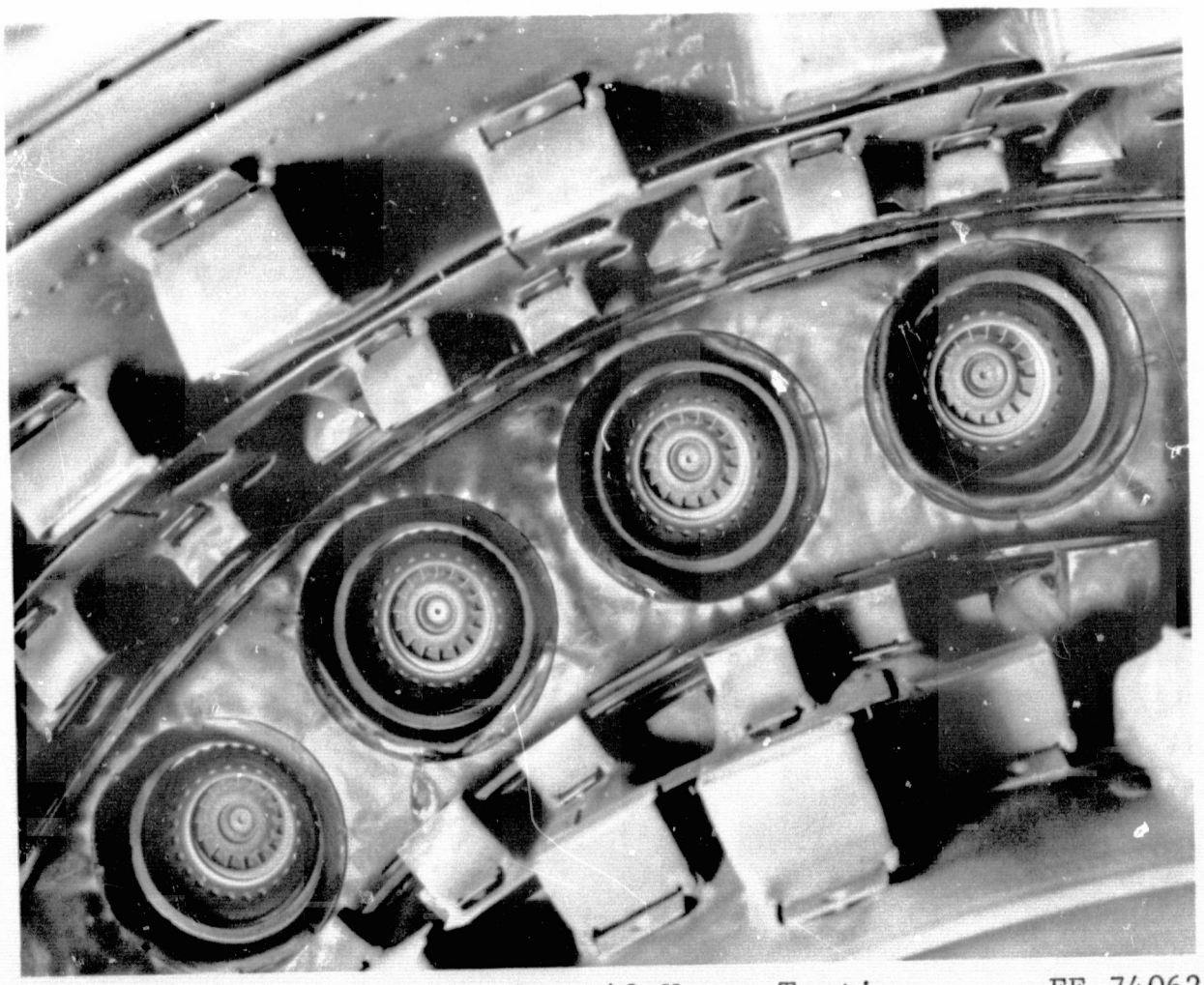

Figure 131. Combustor After 40 Hours Testing at Test Condition 2 (View 3) FE 74062

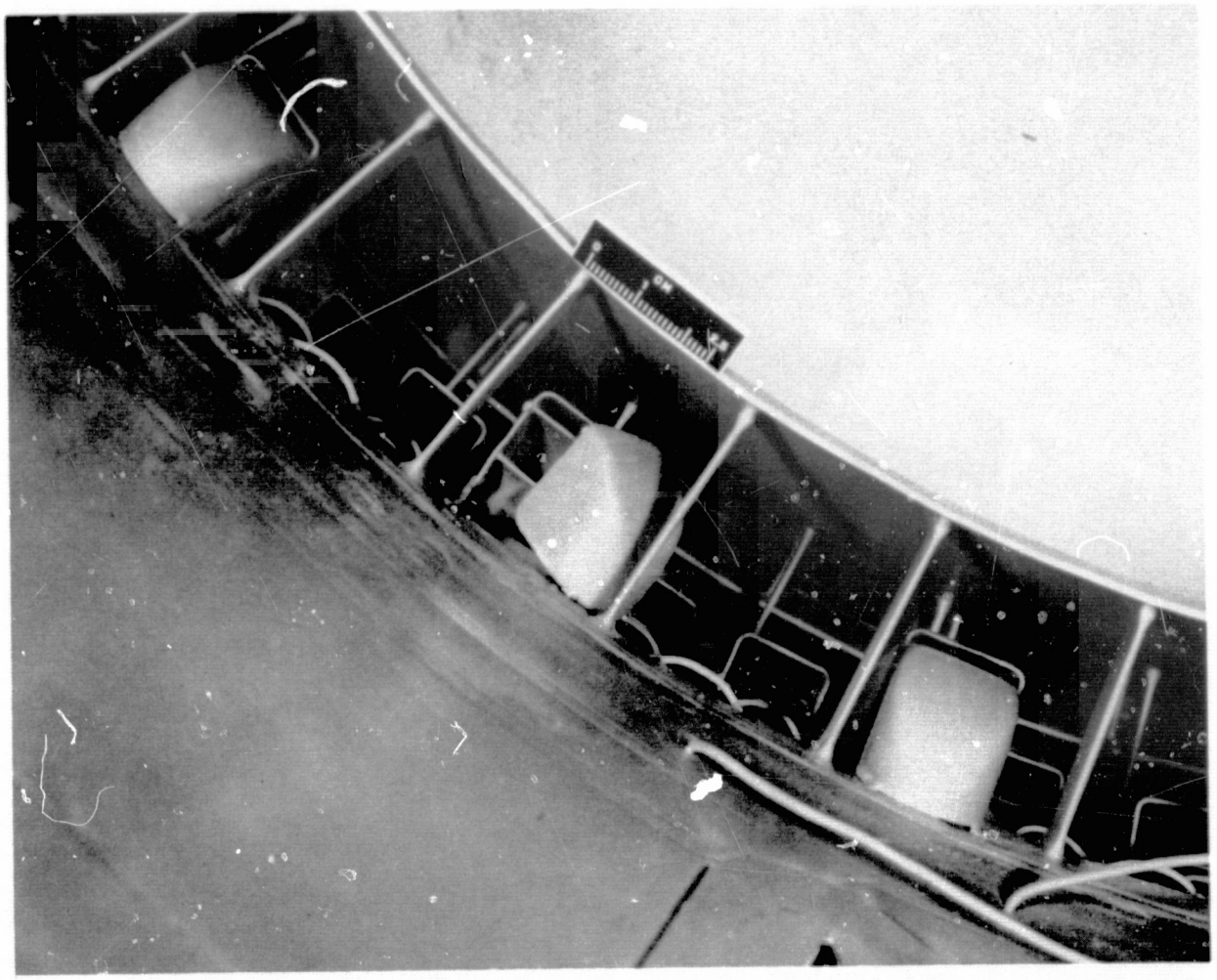

Figure 132. No. 1 Scoop Cap Broken Loose FE 75216

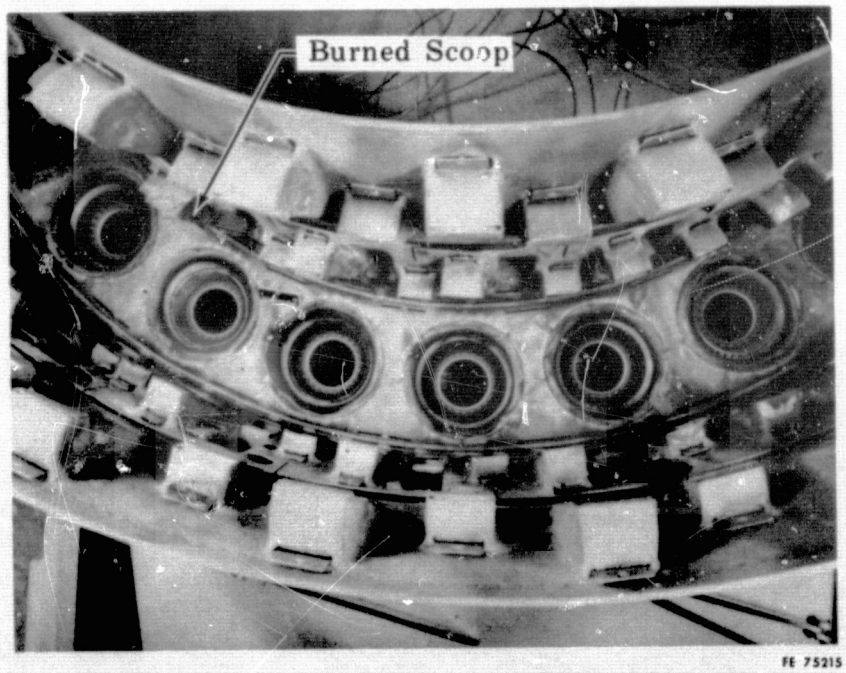

Figure 133. Burned No. 3 ID Liner Scoop FD 23825

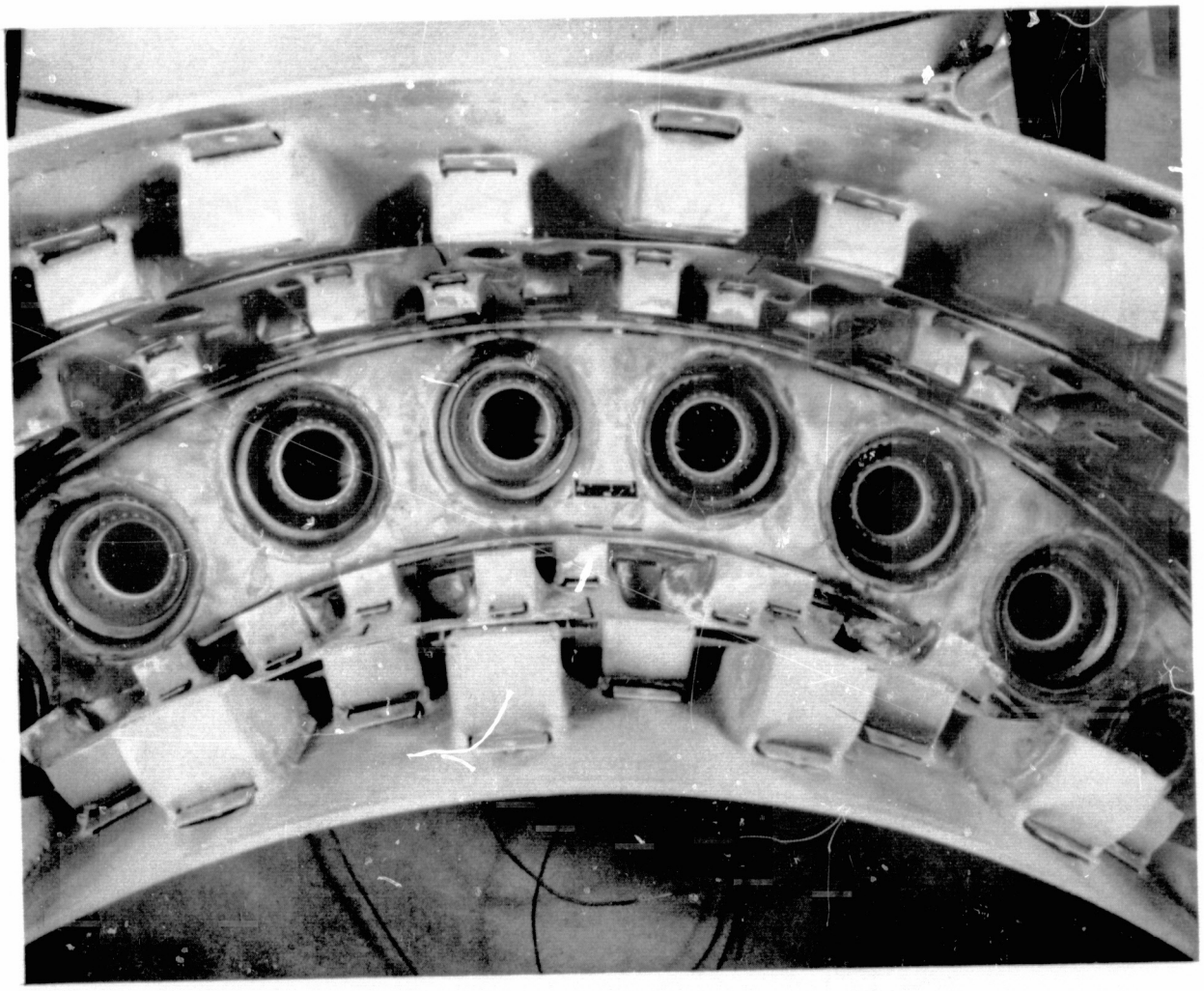

Figure 134. Combustor After 100 Hours of Condition 2 Testing

FE 75214

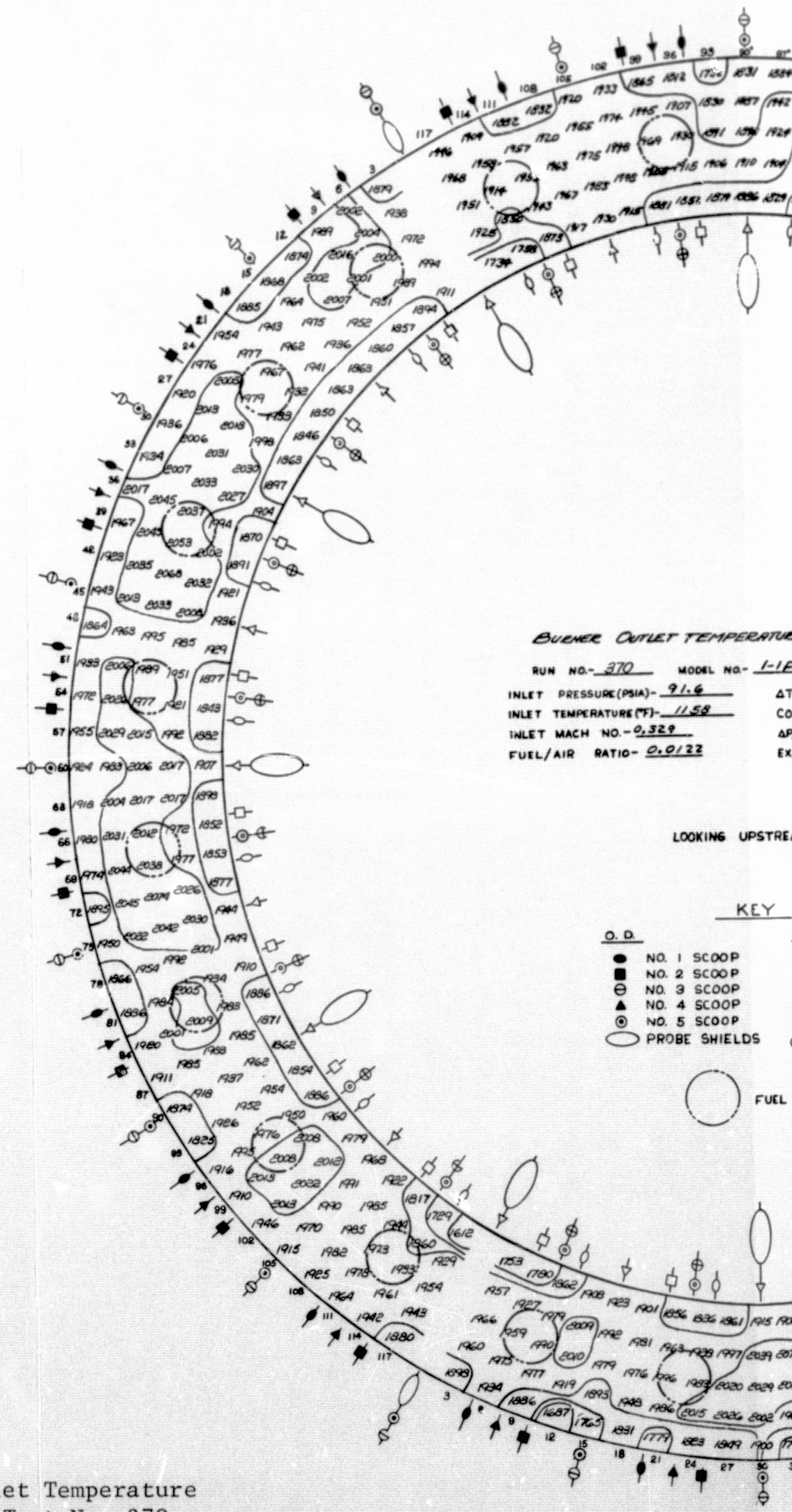

Figure 135. Combustor Outlet Temperature Distribution, Test No. 370

FOLDOUT FRAME |

e OUTLET TEMPERATURE DISTRIBUTION

370 MODEL NO.- 1-1F DATE- 1-18-68

URE (PSIA)- 91.6 $\Delta T_{MAX}/\Delta T_{AVG}$ - 1.19

IATURE (°F)- 1158 COMBUSTION EFF. - 103.6 %

NO. - 0.329 $\Delta P/P$ (%) - 8.58

RATIO- 0.0122 EXIT TEMPERATURE (°F)- 1925

LOOKING UPSTREAM

KEY

O. D.	I. D.
NO. 1 SCOOP	NO. 1 SCOOP
NO. 2 SCOOP	NO. 2 SCOOP
NO. 3 SCOOP	NO. 3 SCOOP
NO. 4 SCOOP	NO. 4 SCOOP
NO. 5 SCOOP	NO. 5 SCOOP
PROBE SHIELDS	STRUT - DIFFUSER

FUEL NOZZLES

FD 23817

FOLDOUT FRAME 2

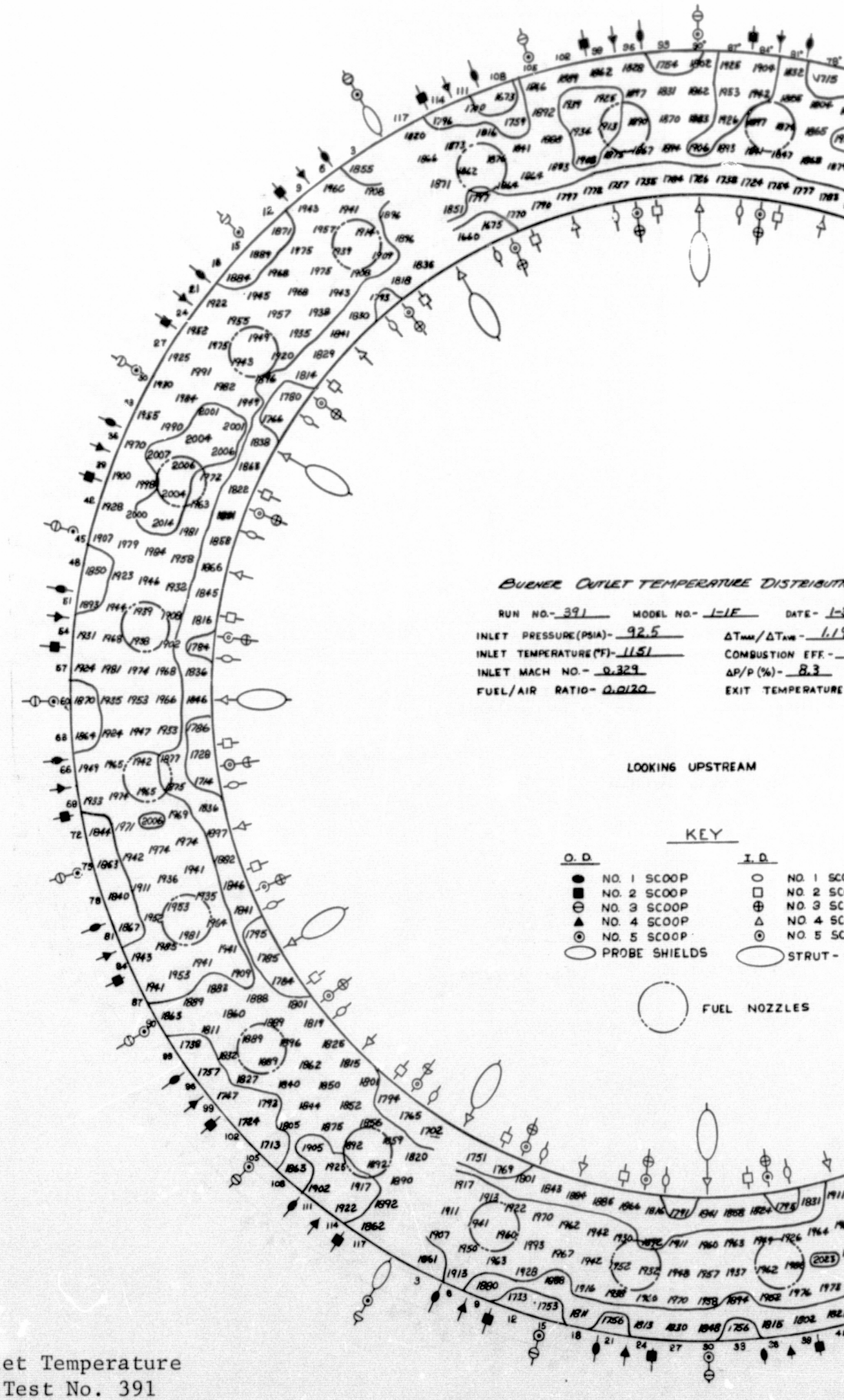

Figure 136. Combustor Outlet Temperature Distribution, Test No. 391

FOLDOUT FRAME 1

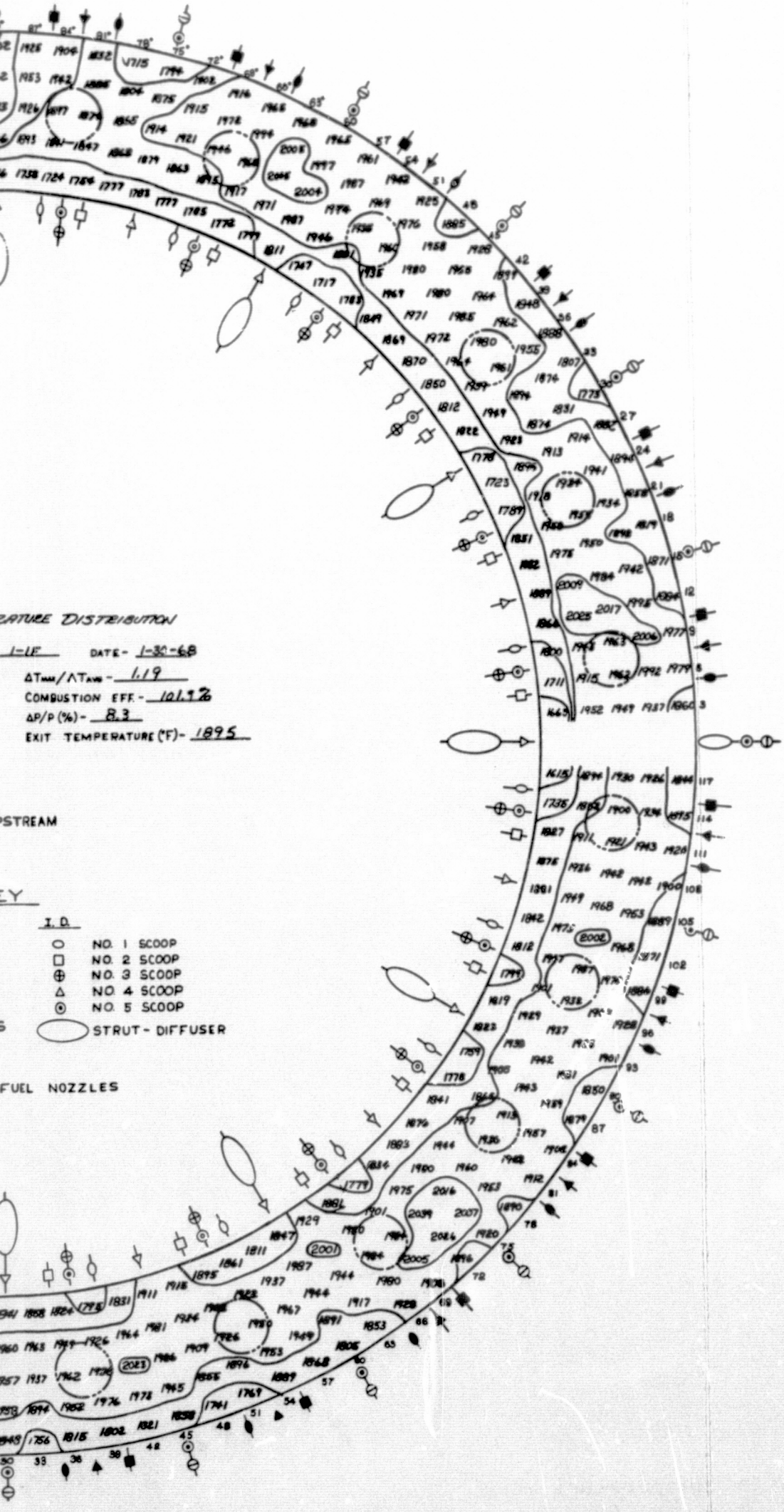

FD 23818

FOLDOUT FRAME 2

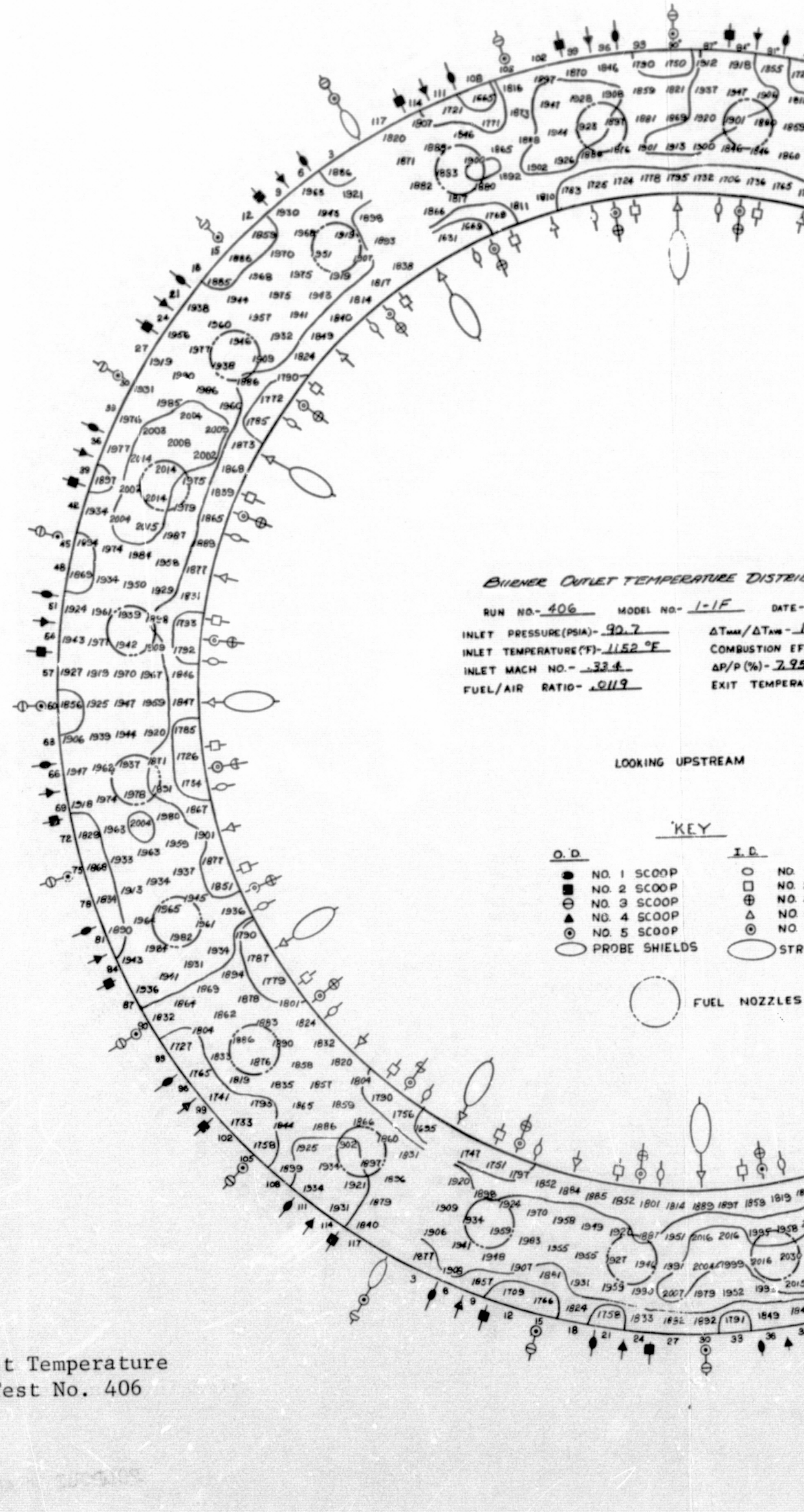

Figure 137. Combustor Outlet Temperature Distribution, Test No. 406

FOLDOUT FRAME 1

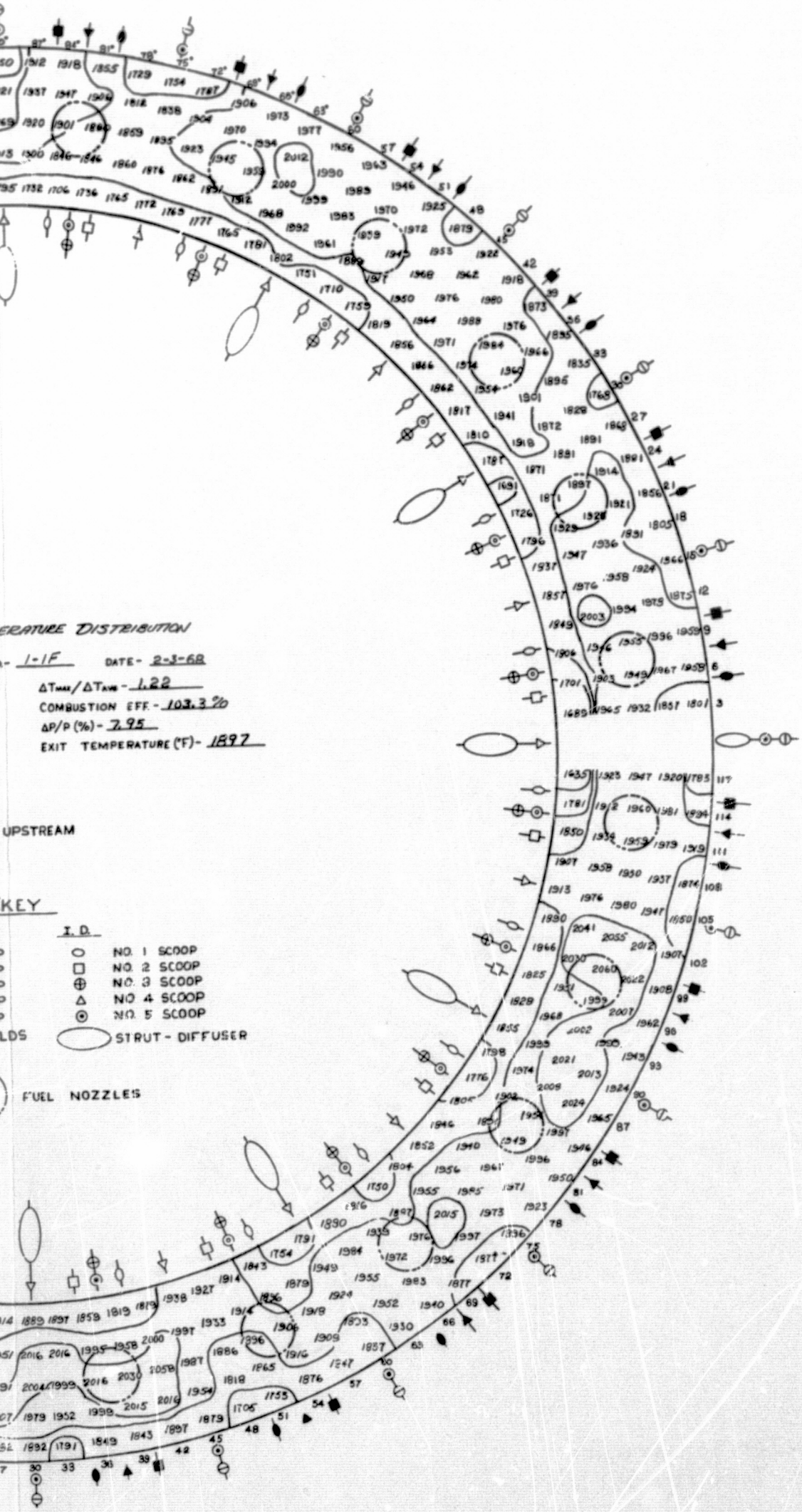

FD 23934

FOLDOUT FRAME 2

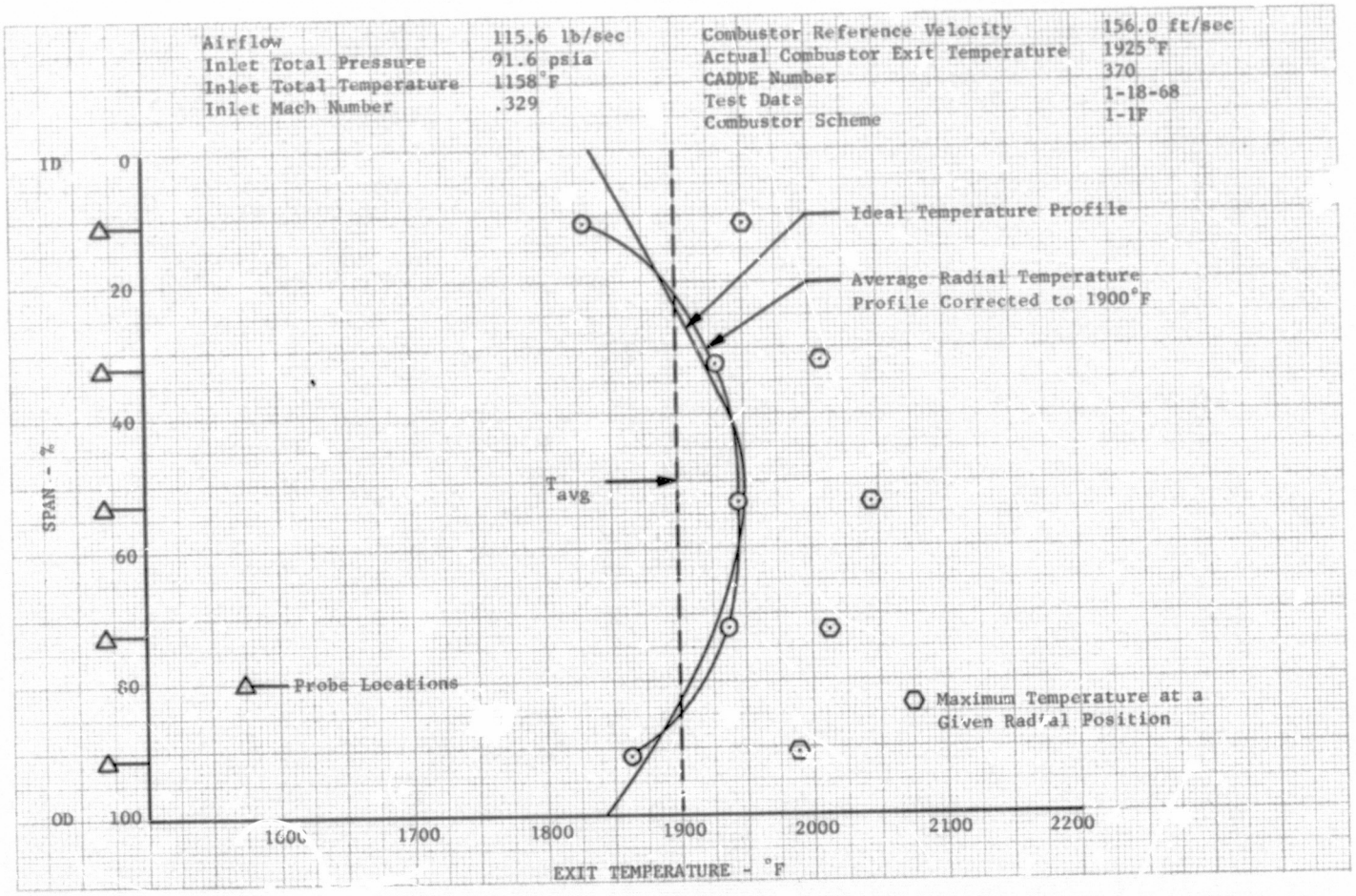

Figure 138. Combustor Average Radial Exit Temperature Profile, Test No. 370

DF 64499

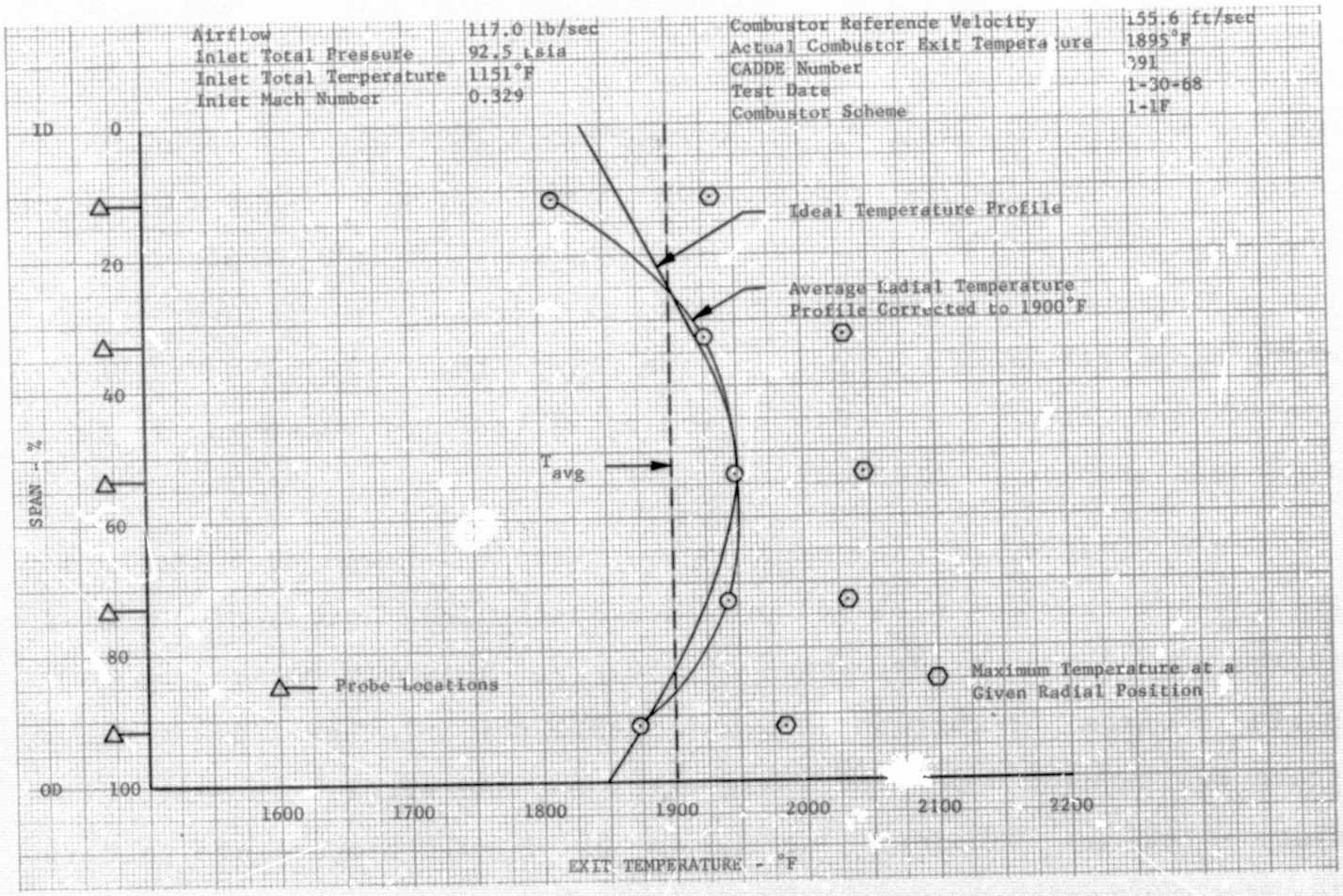

Figure 139. Combustor Average Radial Exit Temperature Profile, Test No. 391

DF 64500

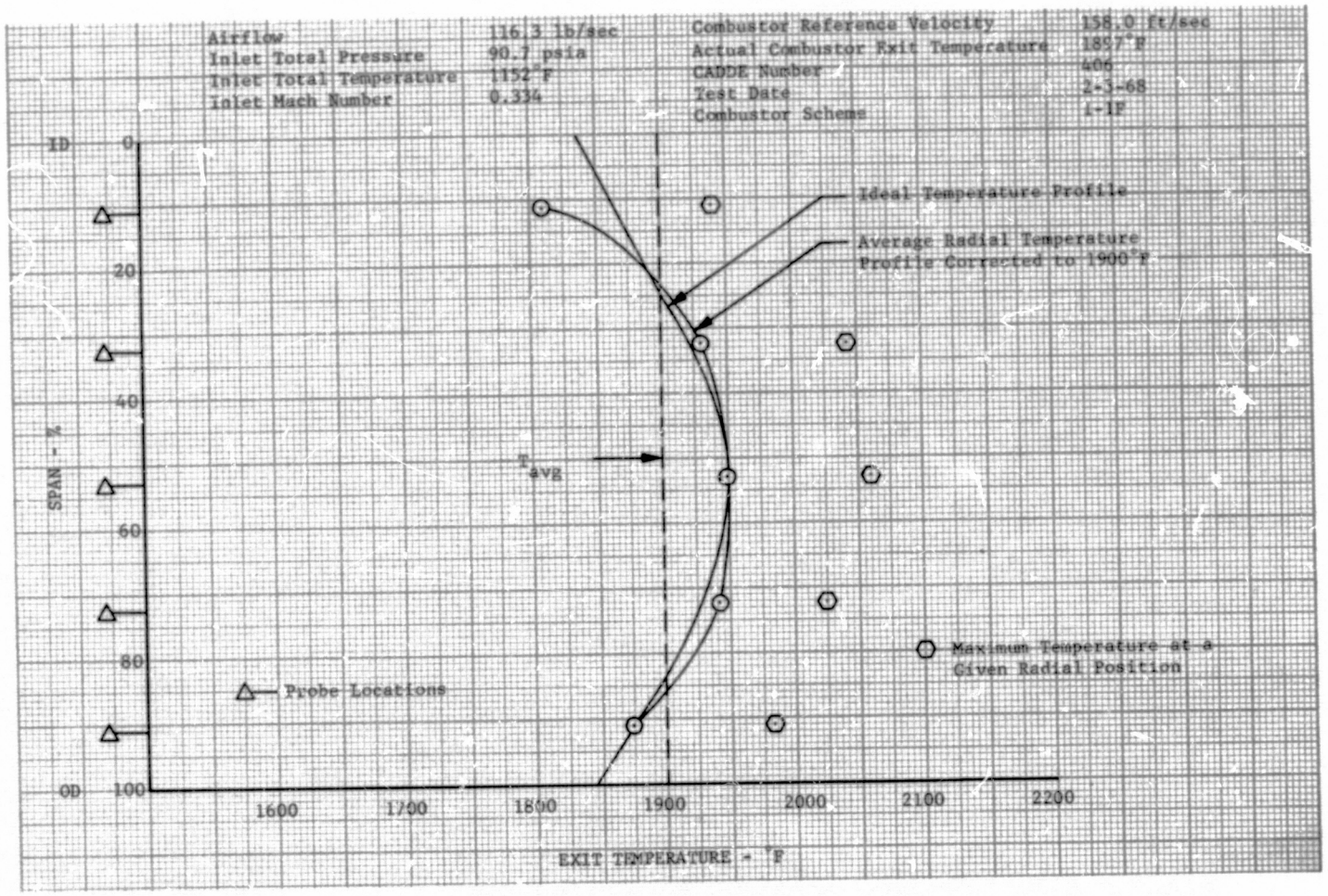

Figure 140. Combustor Average Radial Exit Temperature Profile, Test No. 406

DF 64501

During the shutdown periods of Test Condition 3 testing, two changes were made to check their effect on the hot areas that had recently appeared at Test Condition 6 testing. The changes were (1) interchanging the eight fuel struts in the hotter segment with eight struts from a cooler segment of the combustor, and (2) rotating the diffuser inlet distortion screens 180 degrees. Data points that were taken at Test Condition 6 after these changes indicated that the switching of the fuel nozzles had no effect.

An evaluation of the computed test results showed that the radial profile and flow distribution provided by the inlet distortion plates varied around the circumference of the rig. This may be seen by comparing figures 141 through 144, which show the inlet profile at two probe positions 180 degrees apart prior to, and after, the distortion plate rotation. Comparison of the combustor exit temperature patterns for the two tests (figures 135 and 136) shows no significant change, indicating that the combustor was tolerant of this degree of inlet non-uniformity.

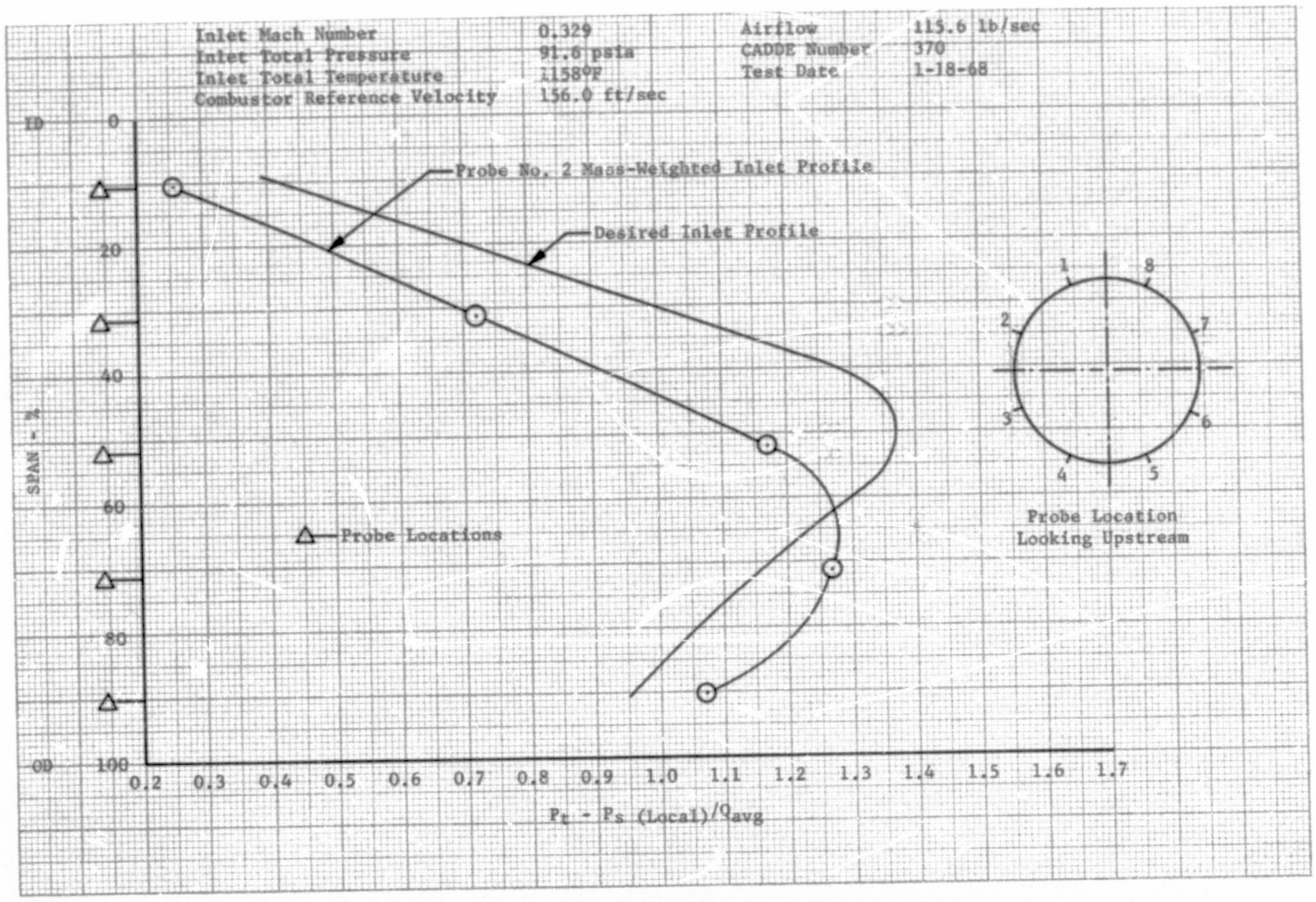

Figure 141. Inlet Velocity Head Profile, Test No. 370

DF 61793

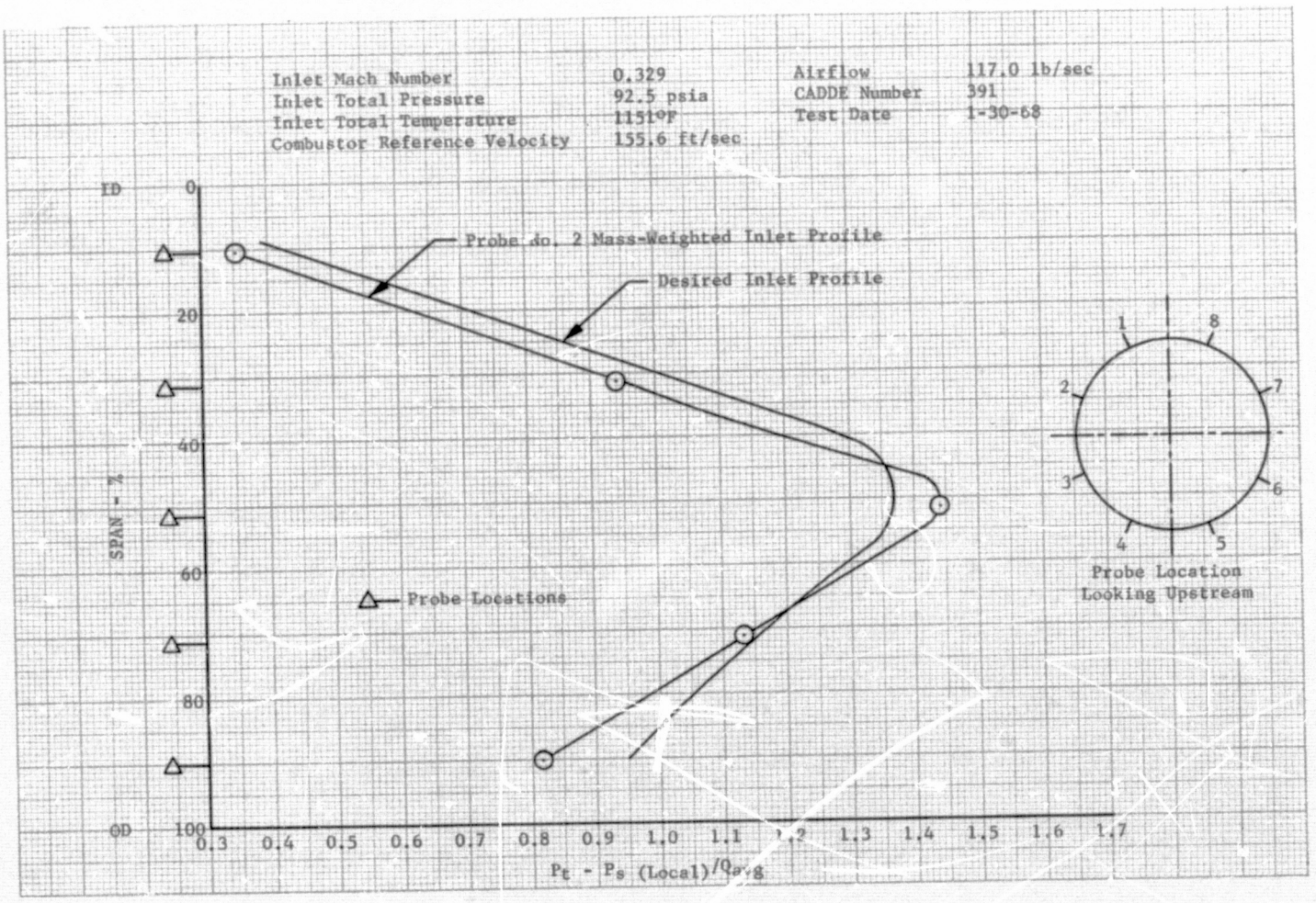

Figure 142. Inlet Velocity Head Profile, Test No. 391

DF 61794

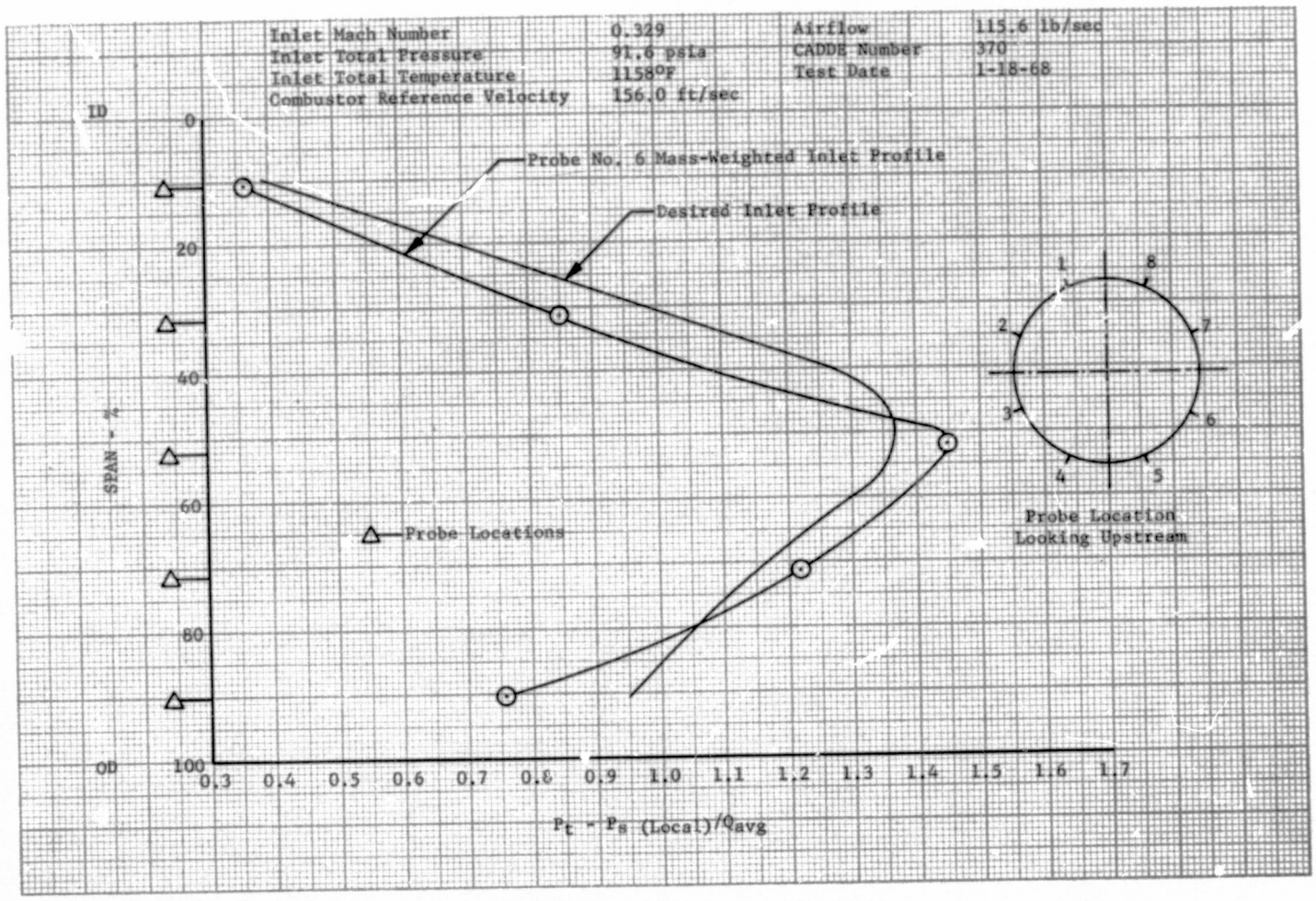

Figure 143. Inlet Velocity Head Profile, Test No. 370

DF 61795

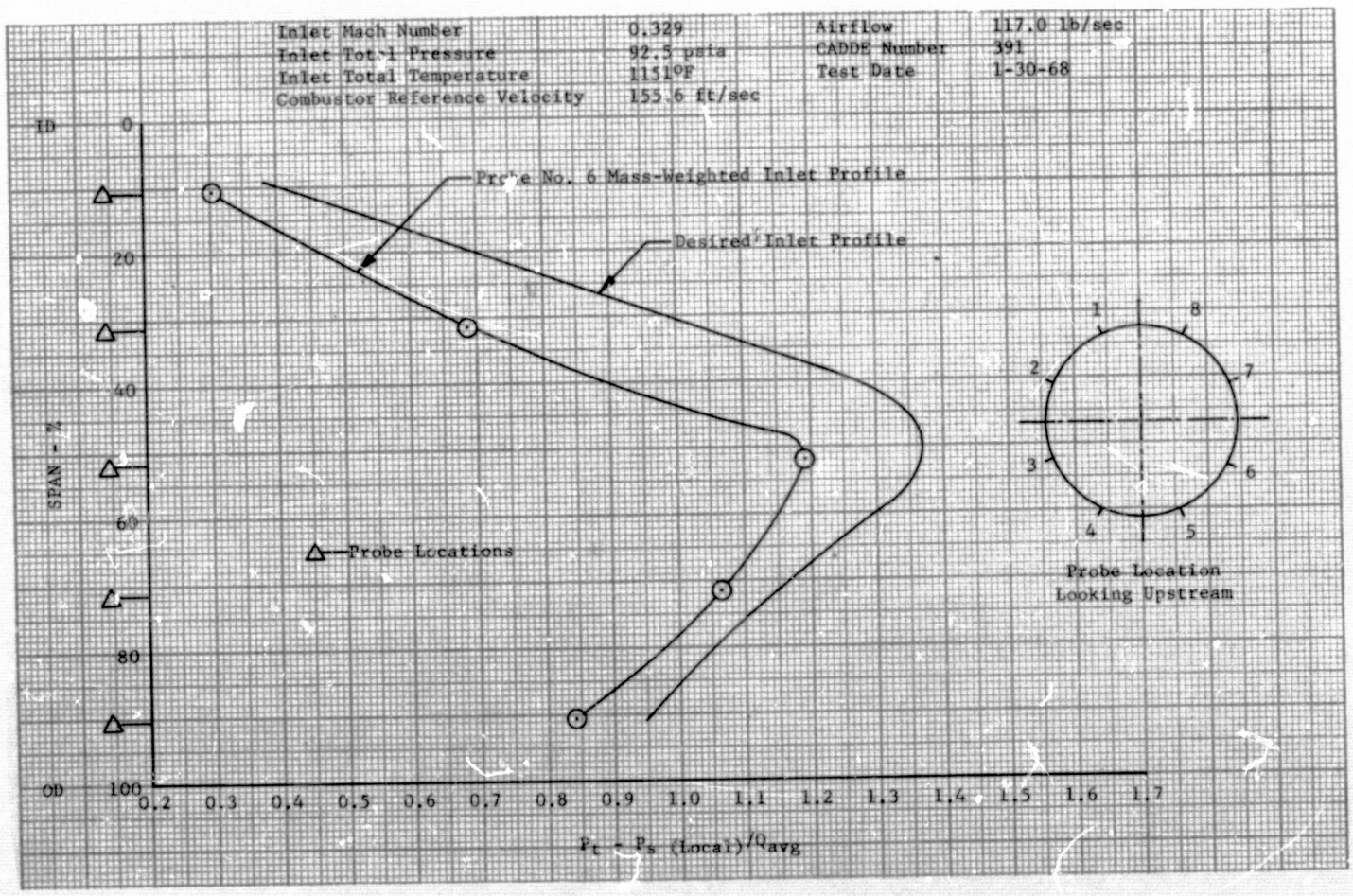

Figure 144. Inlet Velocity Head Profile, Test No. 391

DF 61796

Upon completion of Test Condition 3 testing, Test Conditions 5 and 6 were repeated as required. The combustor exit temperature pattern (figure 145) for Test Condition 6, when compared with the pattern obtained at Test Condition 6 prior to beginning Test Condition 3 testing (figure 127), indicates that little change in performance occurred. The combustor exit temperature pattern uniformity parameter (ΔTVR) was 1.30 prior to the first hour of Test Condition 3 testing as compared to 1.29 after the 30th hour of Test Condition 3 testing. Both of these test points had deteriorated slightly in performance when compared to the original test at Test Condition 6 which gave a ΔTVR value of 1.26.

Upon completion of testing, the rig was opened for inspection. As shown in figure 146, one of the OD liner No. 1 scoop caps had broken loose. One No. 4 and two No. 5 OD liner scoop caps were also missing, as shown in figures 147 and 148.

Also noted were a number of cracks in both the OD and ID primary liners. The largest of these cracks is shown in figure 149. Although these cracks were numerous, they did not appear to be causing a serious structural problem or have any effect on combustor performance. The overall combustor appearance is shown in figures 150 and 151. The scoop caps were repaired or replaced and the combustor was assembled in the test rig.

An inspection of the test rig revealed a cooling water leak in the rotating drum located in front of two of the exit probes, as shown in figure 152. A missing pressure tube from one of the exit probes (figure 153), and a leaking exit pressure hose were also noted. An inspection of the cooling water hoses inside the actuator housing revealed a number of worn and frayed hoses. The worn hoses and damaged exit probe were replaced. The rotating drum and exit pressure hose were repaired and the rig was assembled.

While pressure checking the rig prior to resuming testing, a leak in the facility air supply bellows was discovered. Repairs on the bellows required cancellation of testing for a period of one month.

Testing was resumed upon completion of the facility repair with initiation of Test Condition 4 testing.

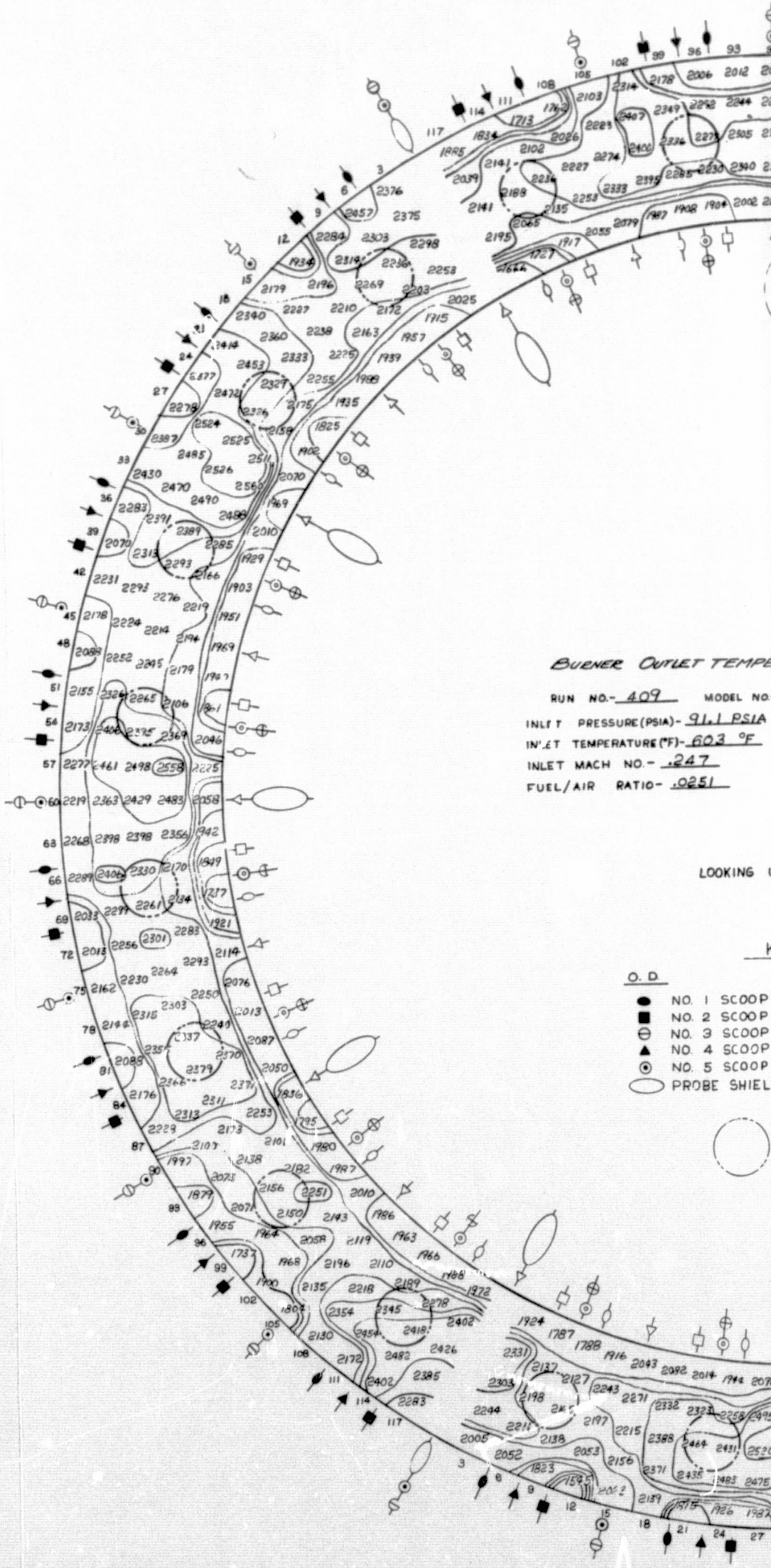

Figure 145. Combustor Outlet Temperature Distribution, Test No. 409

FOLDOUT FRAME 1

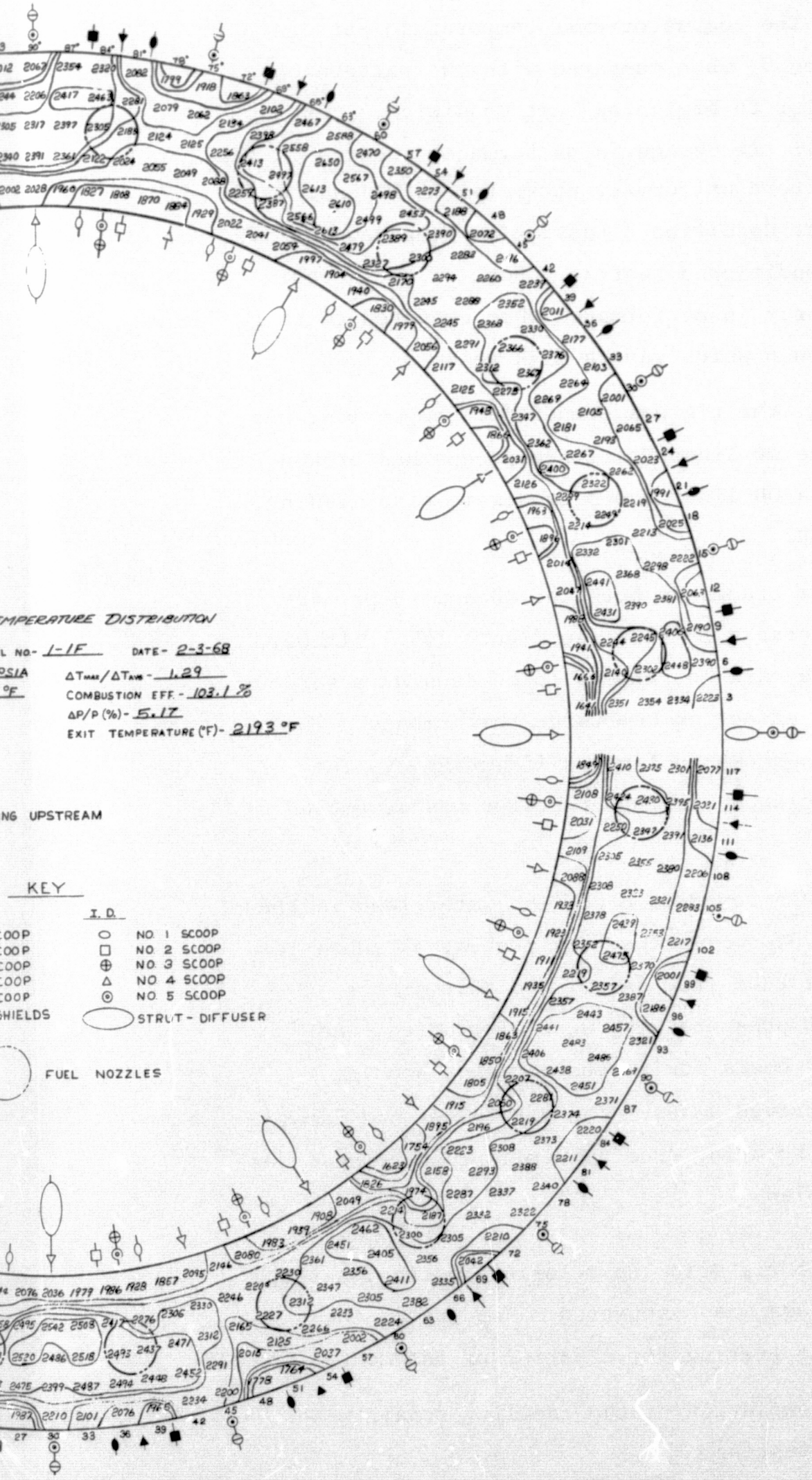

FD 23935

FOLDOUT FRAME 2

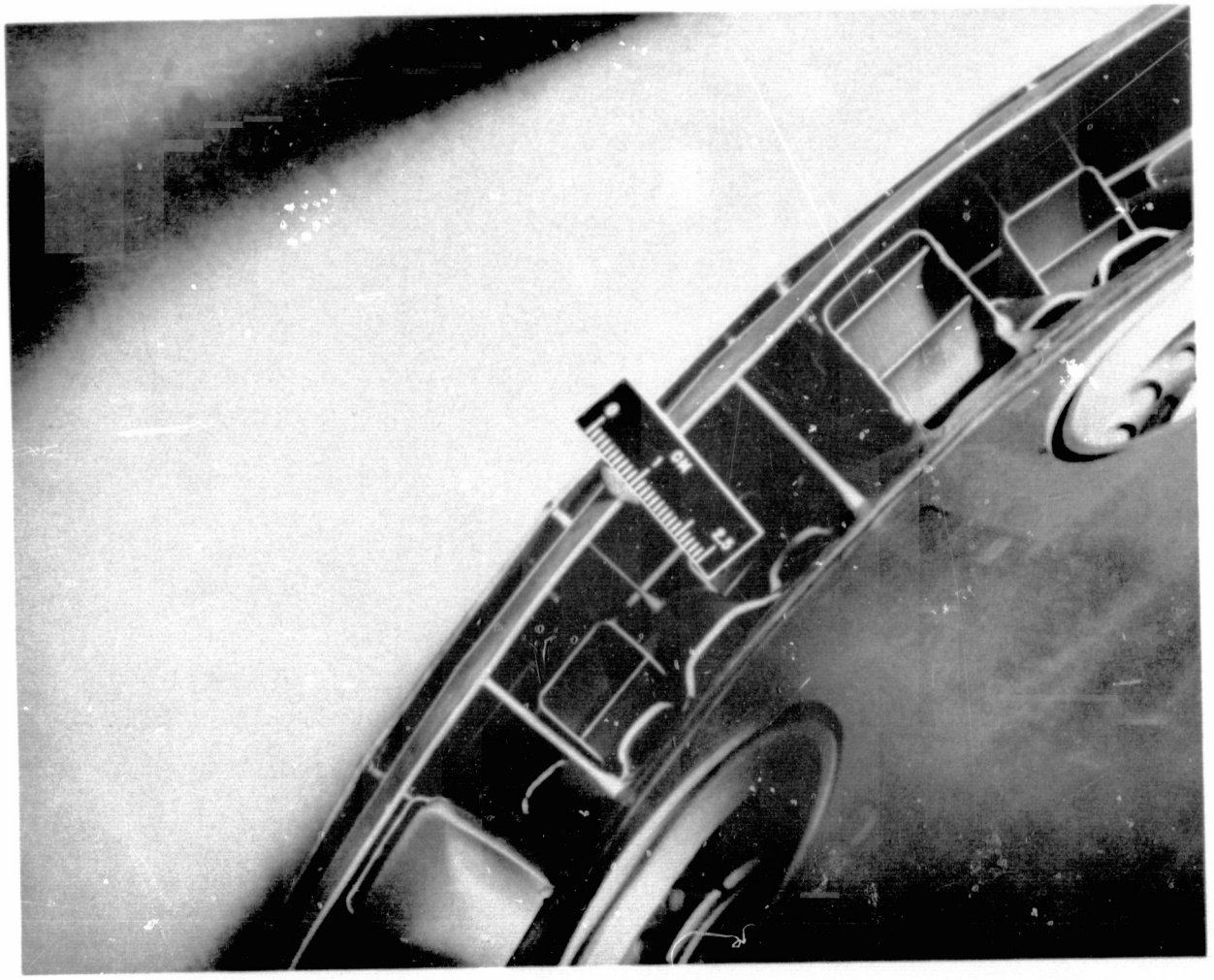

Figure 146. OD Liner No. 1 Scoop Cap Missing FE 75784

Figure 147. OD Liner No. 5 Scoop Cap Missing FD 23941

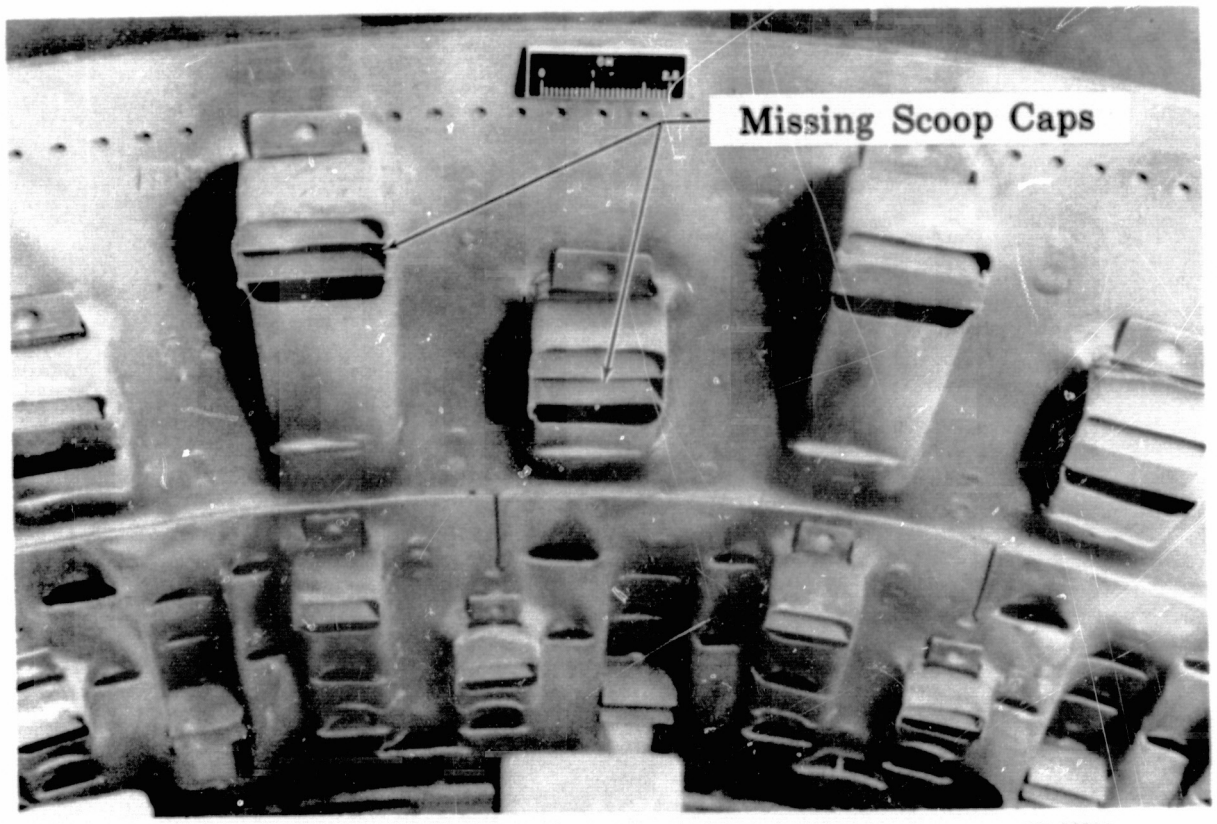

FE 75783
FD 23918

Figure 148. OD Liner No. 4 and 5 Scoop Cap Missing

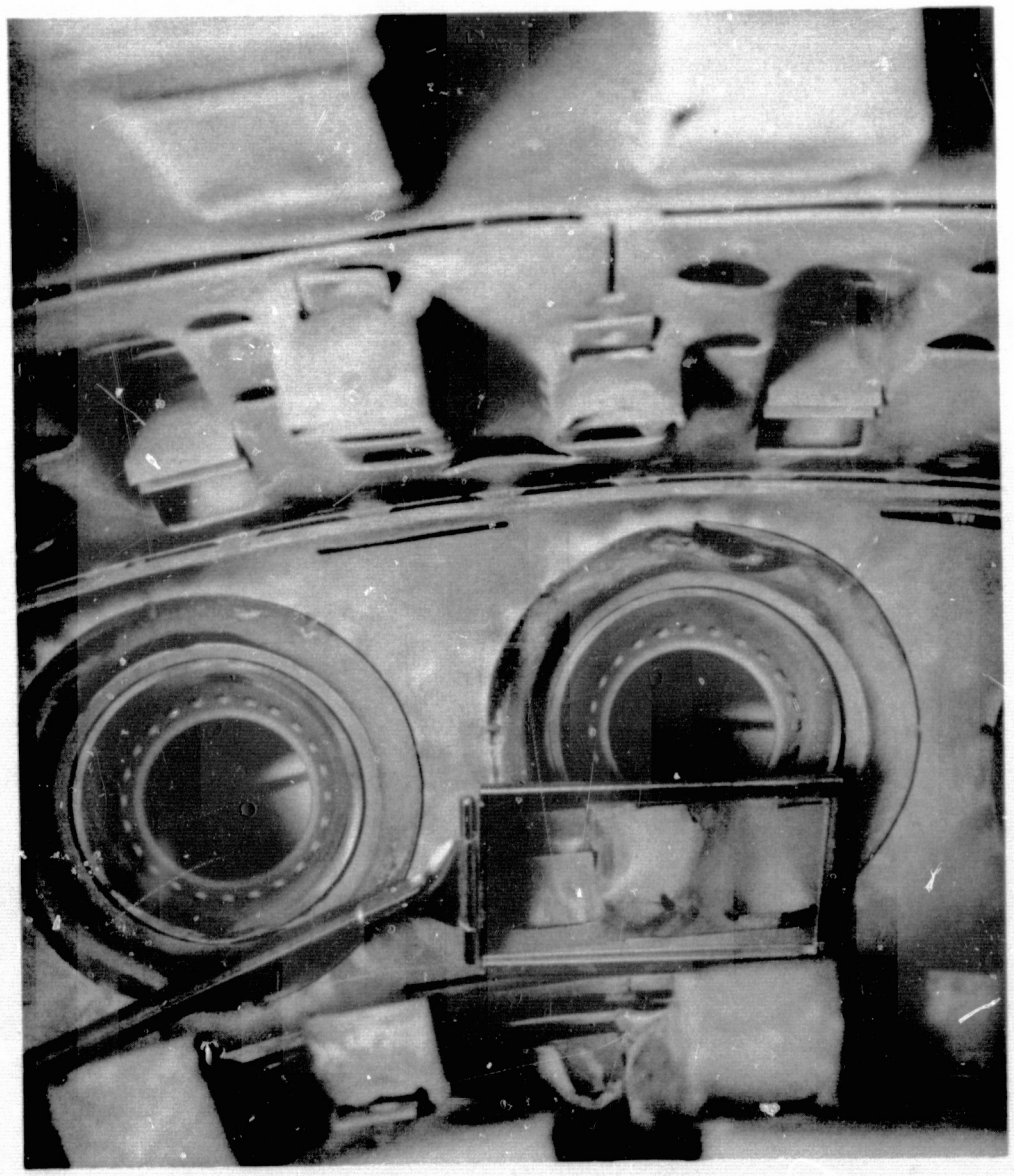

FE 75781

Figure 149. Largest Combustor Crack After Condition 3 Testing

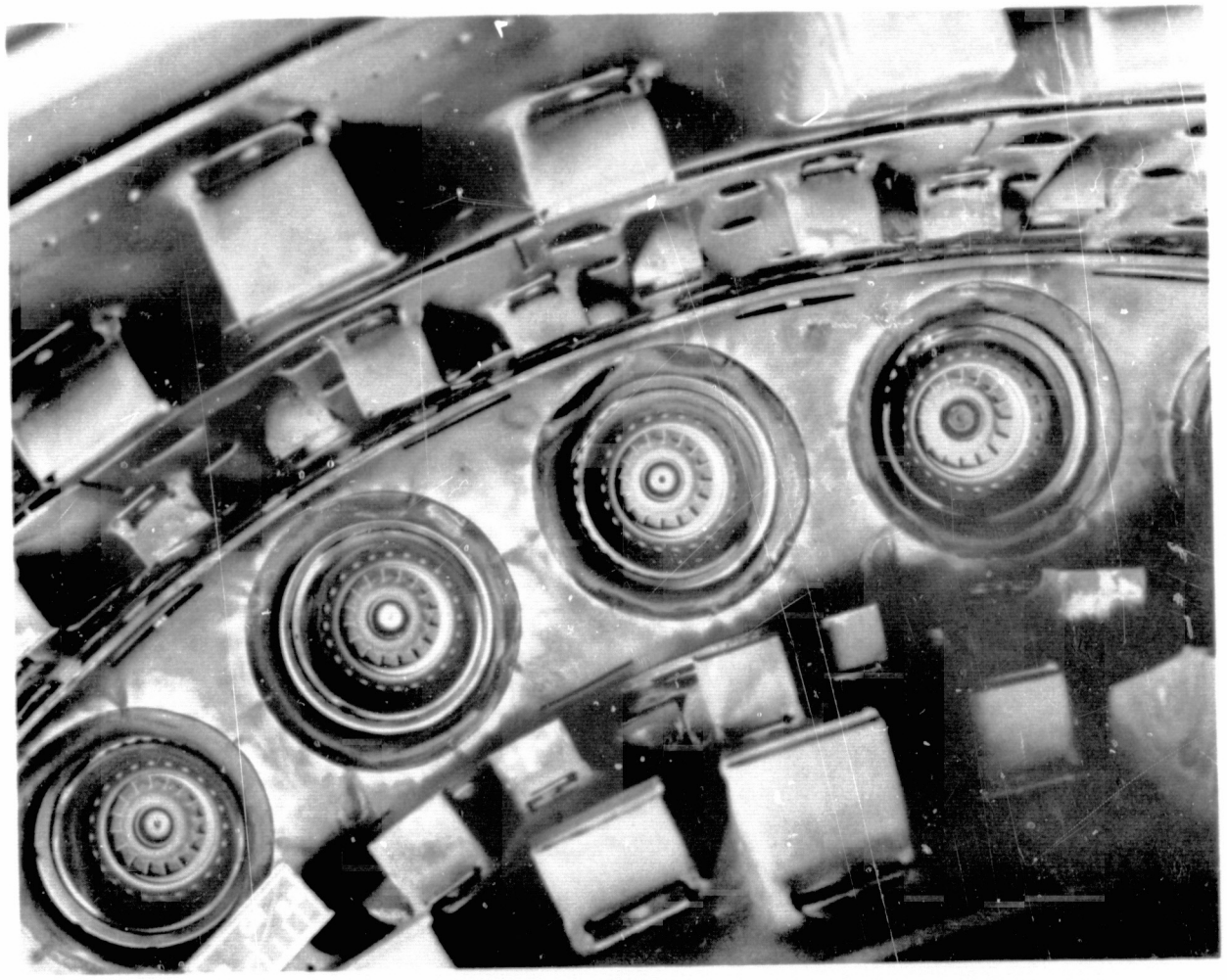

Figure 150. Combustor After Condition 3 Testing (View 1)

FE 75778

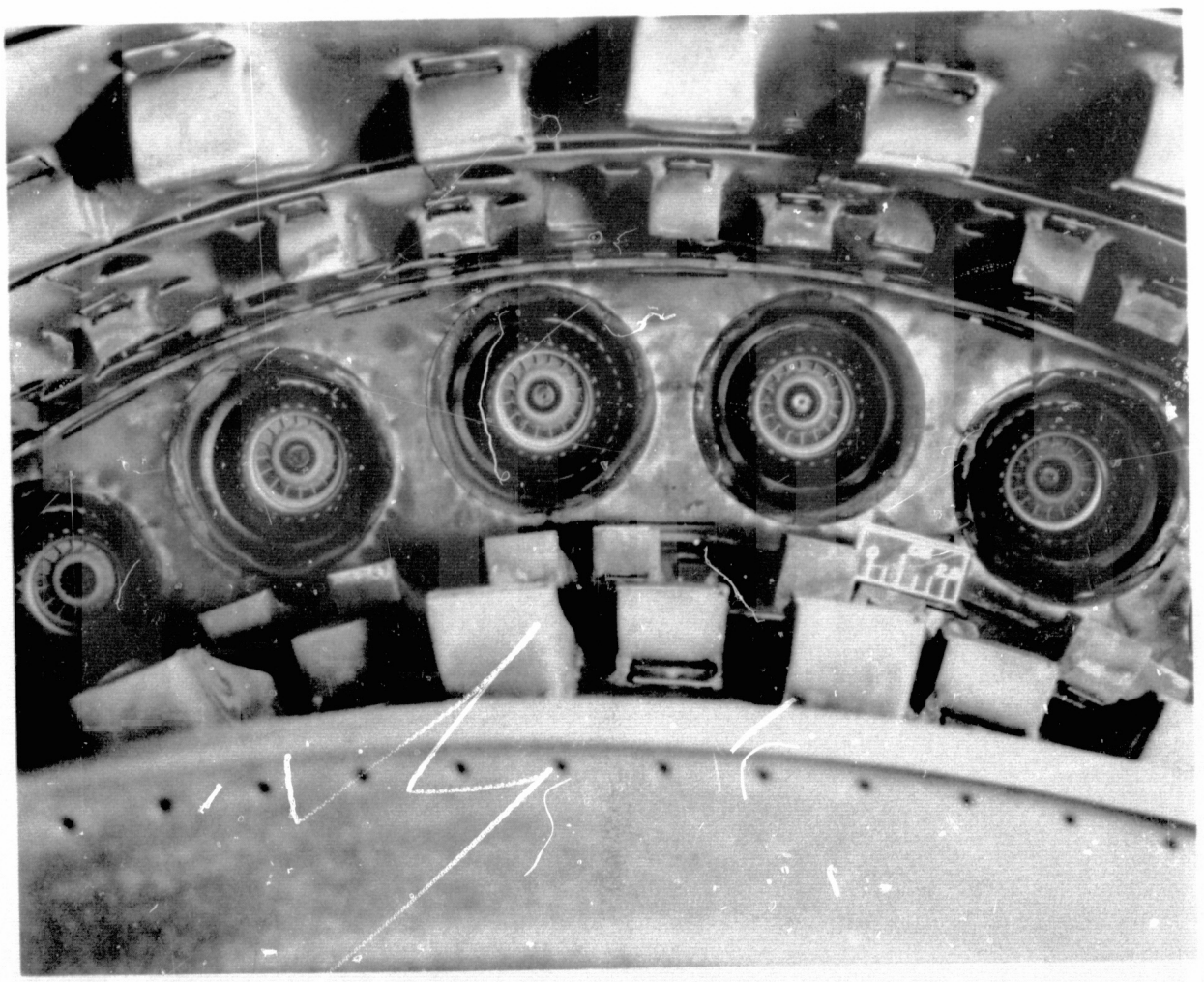

Figure 151. Combustor After Condition 3 Testing (View 2)

FE 75777

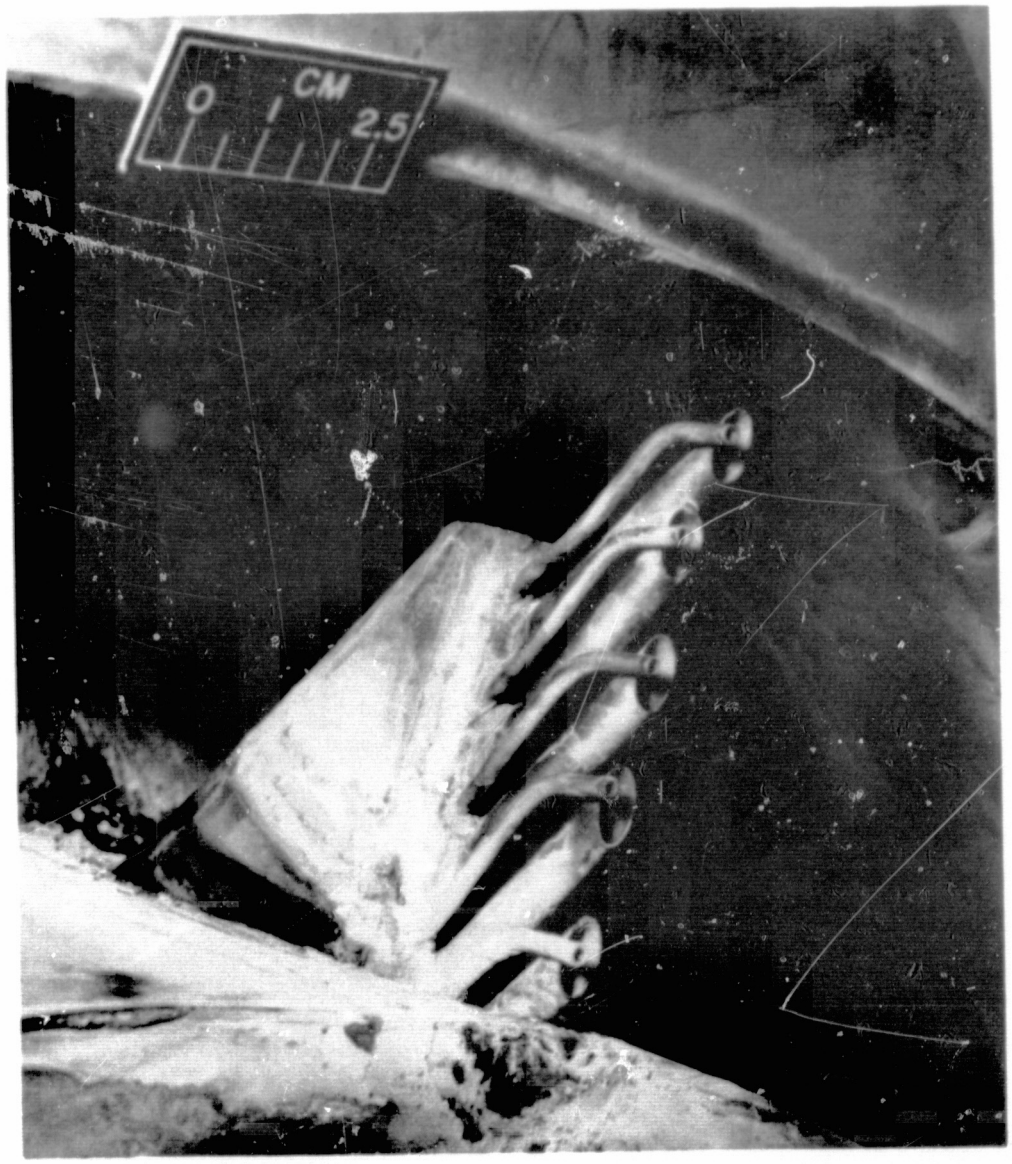

Figure 152. Rotating Drum Cooling Water Leak FE 75780

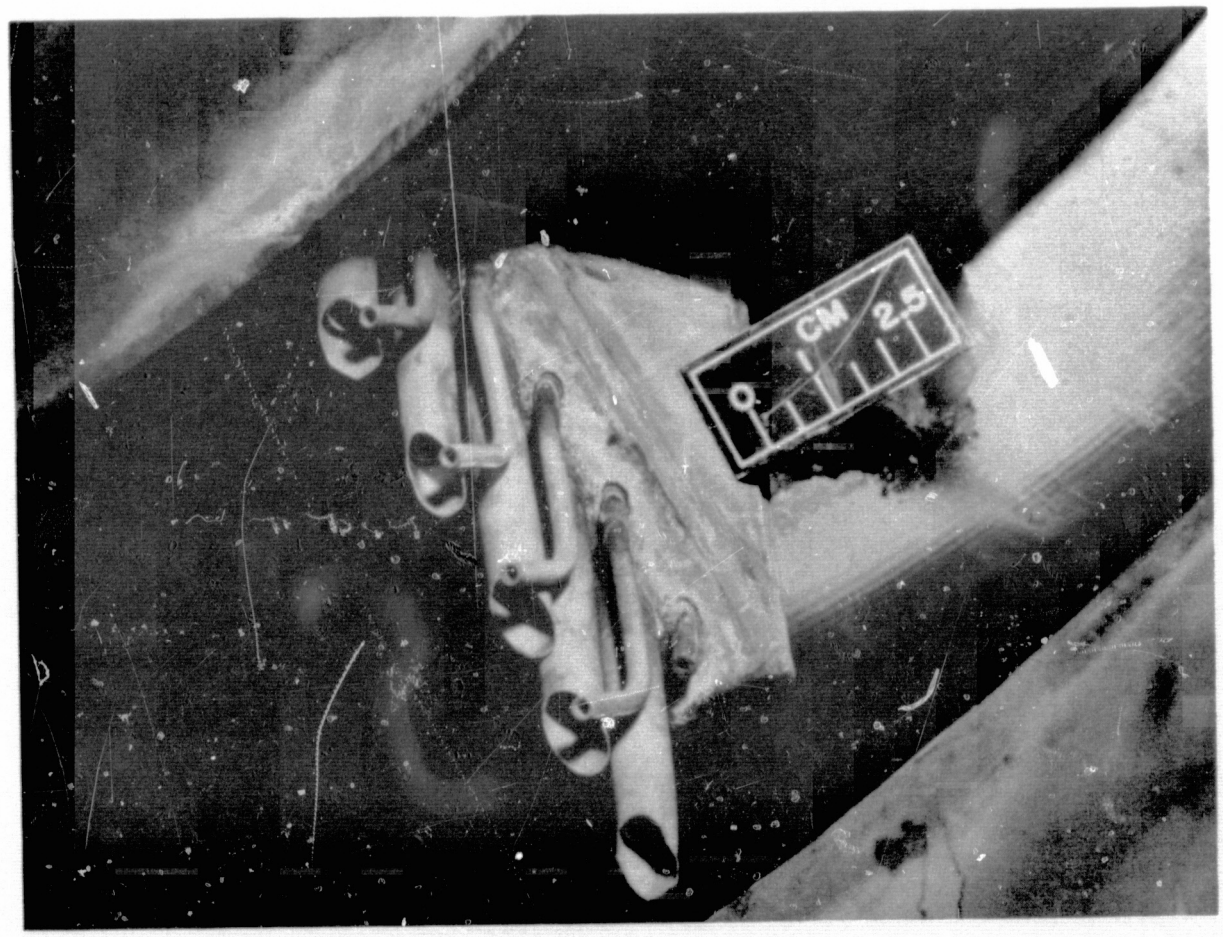

Figure 153. Damaged Exit Probe FE 75779

The combustor exit temperature patterns for the 1st, 20th, 40th, 60th, 80th, 100th, 120th, 140th, and 150th hours of testing at Test Condition 4 are shown in figures 154 through 162, respectively. Comparison of these temperature patterns indicates that no significant change in performance occurred throughout Test Condition 4 testing. The combustor average radial exit temperature profiles for these tests also show little change, as seen by comparing figures 163 through 171. The combustor exit temperature uniformity parameter (ΔTVR) remained fairly constant throughout Test Condition 4 testing at a value of 1.18 to 1.24 as shown in figure 102. Comparison of the combustor exit temperature patterns (figures 145 and 172) for Test Condition 6 tests, before and after Test Condition 4 testing, indicates that no change in performance occurred. The combustor exit temperature uniformity parameter (ΔTVR) had decreased from a value of 1.29 to 1.24.

Upon completion of 45 hours of testing, the rig was opened for inspection. As shown in figures 173 and 174, three No. 5 scoop caps had broken loose. Some burning of the No. 3 ID primary liner scoops was also evident. The most badly burned scoops are shown in figures 175 through 177. Also noted were a number of new cracks and a lengthening of some of the previous cracks in the primary liners and scoops. Most of the cracks were 3/8-inch or shorter in length. An inspection of the test rig, after 45 hours of Test Condition 4 testing, revealed cooling water leaks in the following parts: rotating traverse drum, rotating drum access plate, and the ID choke nozzele. Also noted were a leaking combustor exit pressure hose, a worn aspiration gas hose, and a plugged cooling water return hose for the rotating drum access plate. The necessary repairs and replacements were made and testing was resumed.

The rig was again opened for inspection after 98 hours of Test Condition 4 testing and several new cracks in the combustor, as well as an elongation of some of the previous cracks, were noted. Additional burning on several No. 3 ID primary liner scoops was also noted, as shown in figures 178 through 181. An inspection of the test rig revealed cooling water leakage in the rotating traverse drum and the ID choke nozzle. These two parts required repeated welding repair throughout the balance of the test program.

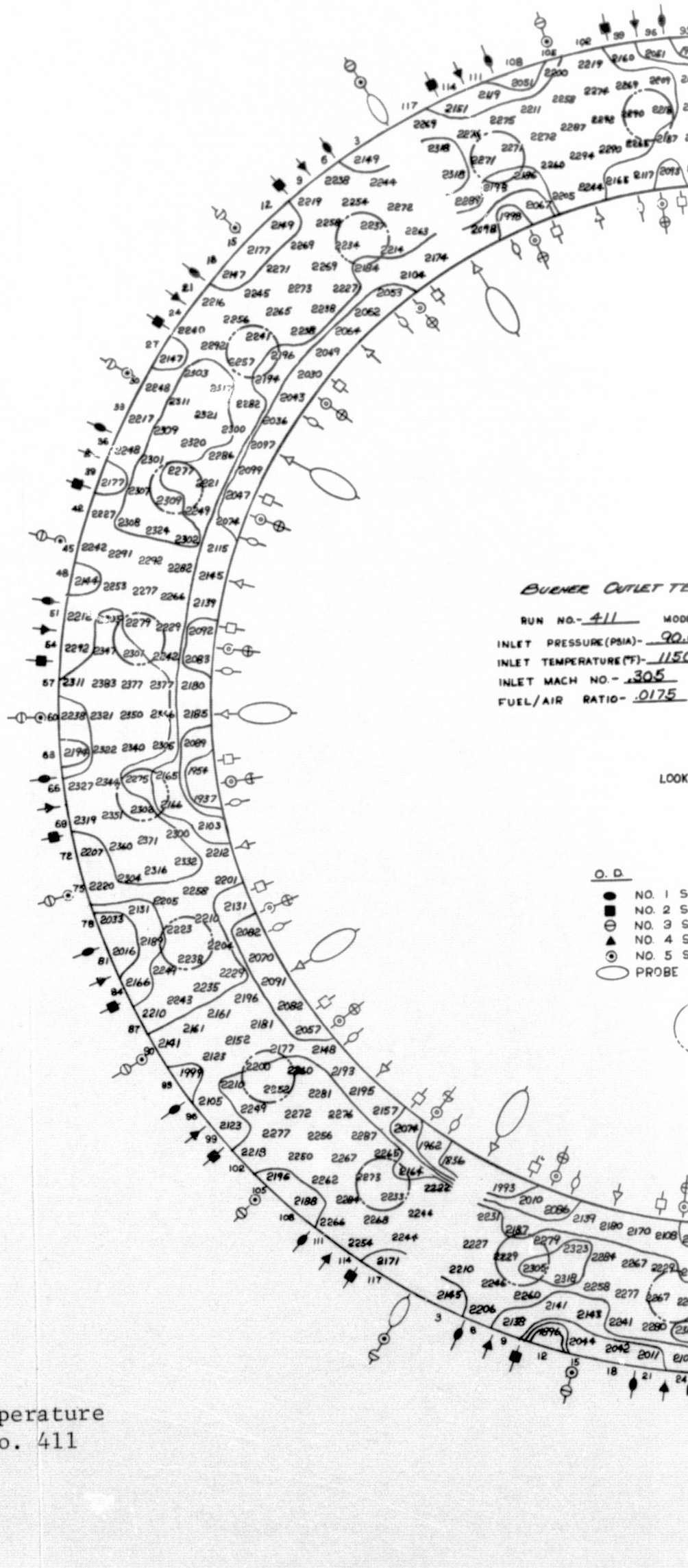

Figure 154. Combustor Outlet Temperature Distribution, Test No. 411

FOLDOUT FRAME /

RE DISTRIBUTION

E DATE - 3-9-68

$T_{max}/\Delta T_{AVG}$ - 1.19

OMBUSTION EFF. - 102.3 %

P/P (%) - 7.18

KIT TEMPERATURE (°F) - 2214

EAM

I. D.

- NO. 1 SCOOP
- NO. 2 SCOOP
- NO. 3 SCOOP
- NO. 4 SCOOP
- NO. 5 SCOOP
- STRUT - DIFFUSER

NOZZLES

FD 24069

2

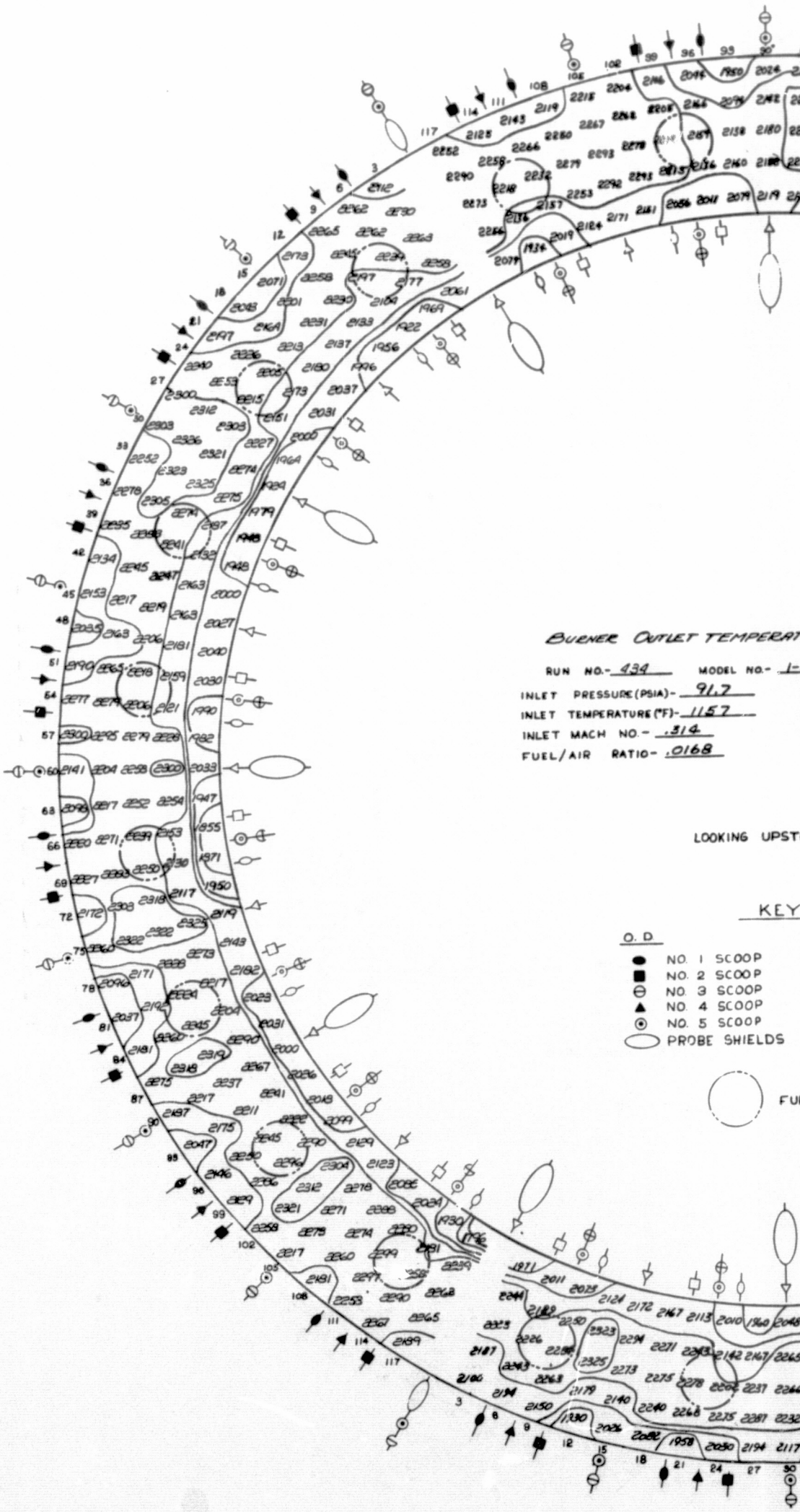

Figure 155. Combustor Outlet Temperature Distribution, Test No. 434

OUTLET FRAME /

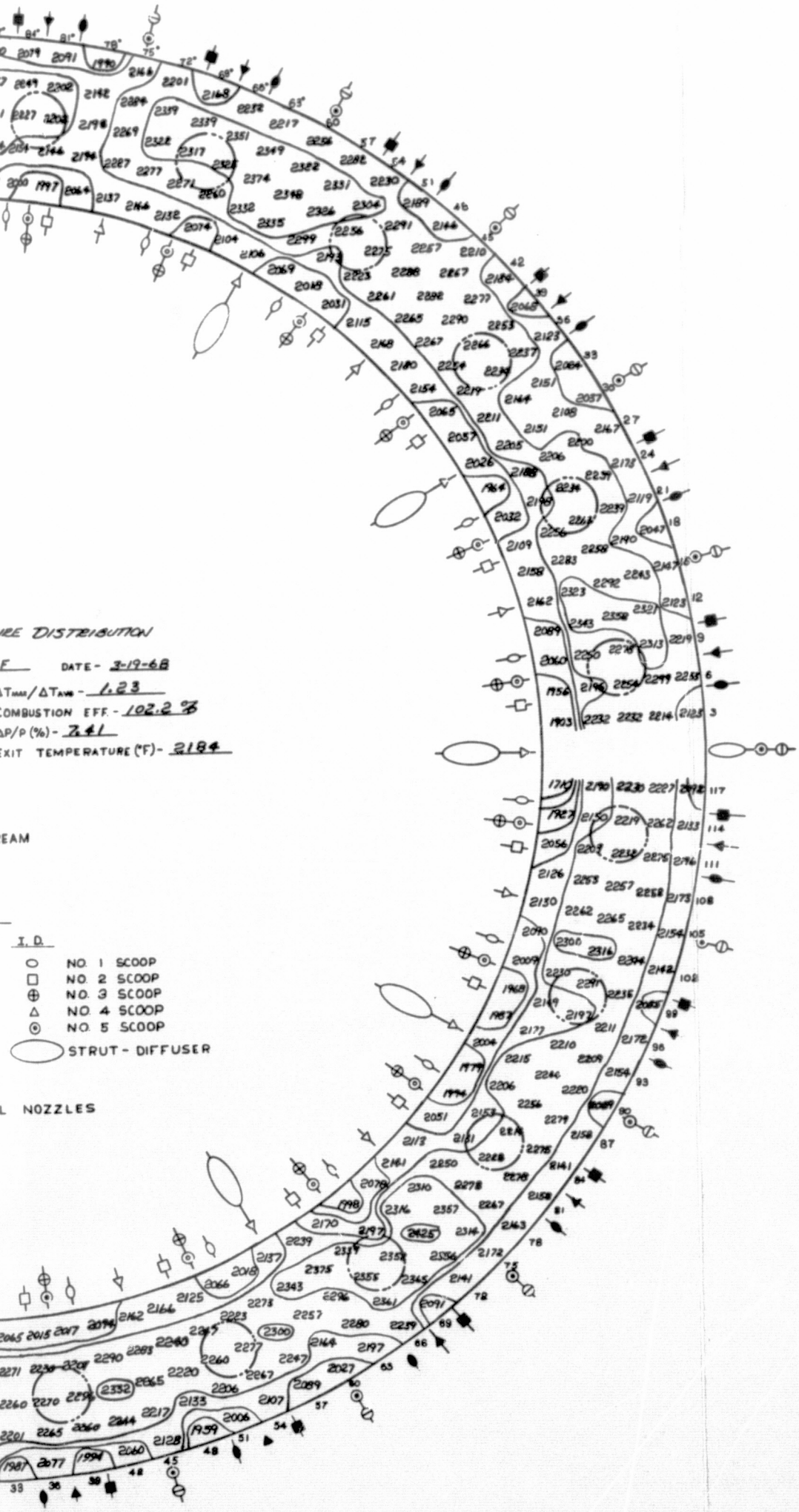
...REE DISTRIBUTION
...F
DATE - 3-19-68
...ΔTmax/ΔTave - 1.23
COMBUSTION EFF. - 102.2 %
ΔP/P (%) - 7.41
EXIT TEMPERATURE (°F) - 2184
...EAM
I. D.
NO. 1 SCOOP
NO. 2 SCOOP
NO. 3 SCOOP
NO. 4 SCOOP
NO. 5 SCOOP
STRUT - DIFFUSER
...L NOZZLES

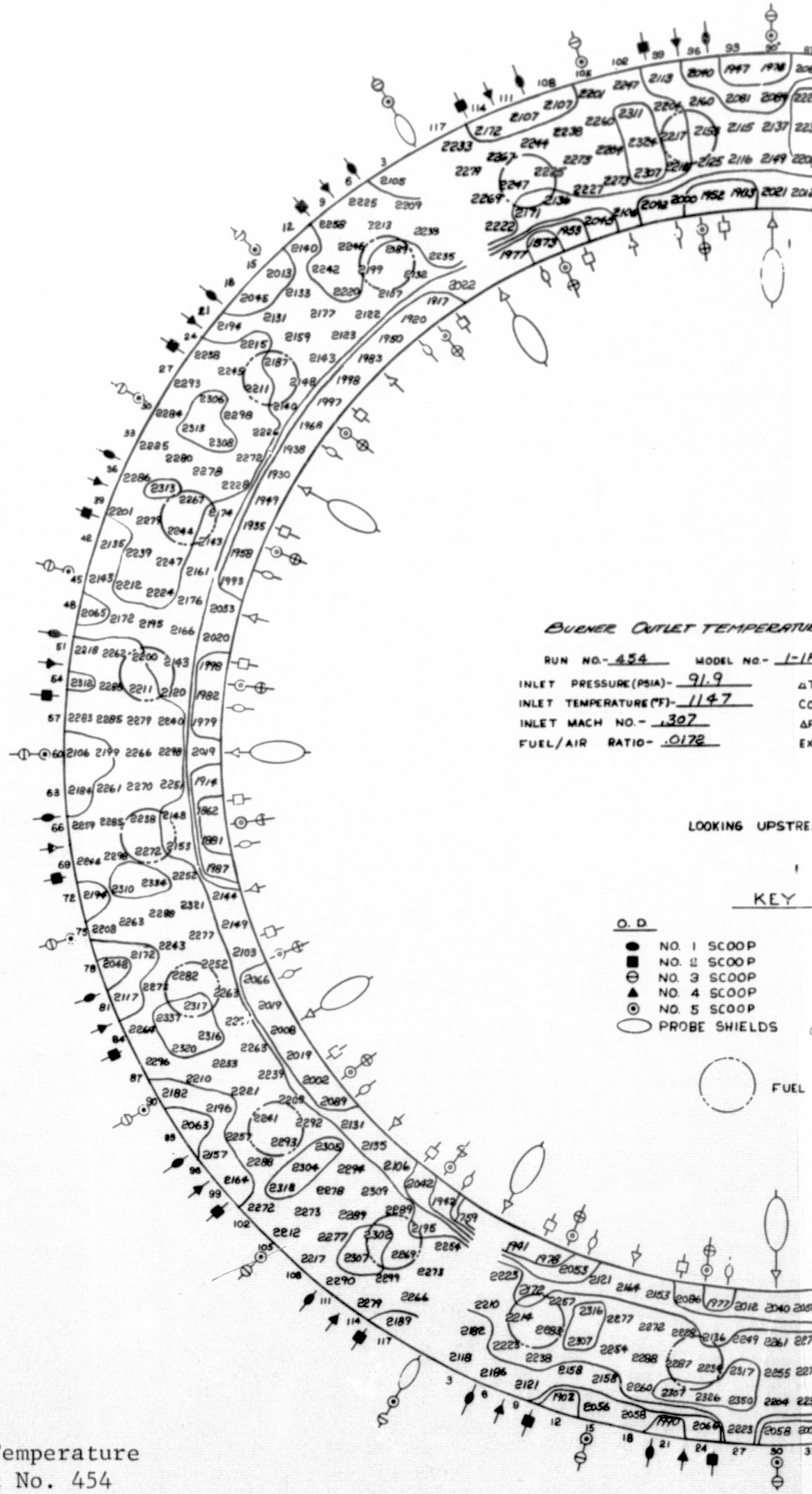

Figure 156. Combustor Outlet Temperature Distribution, Test No. 454

FOLDOUT FRAME 1

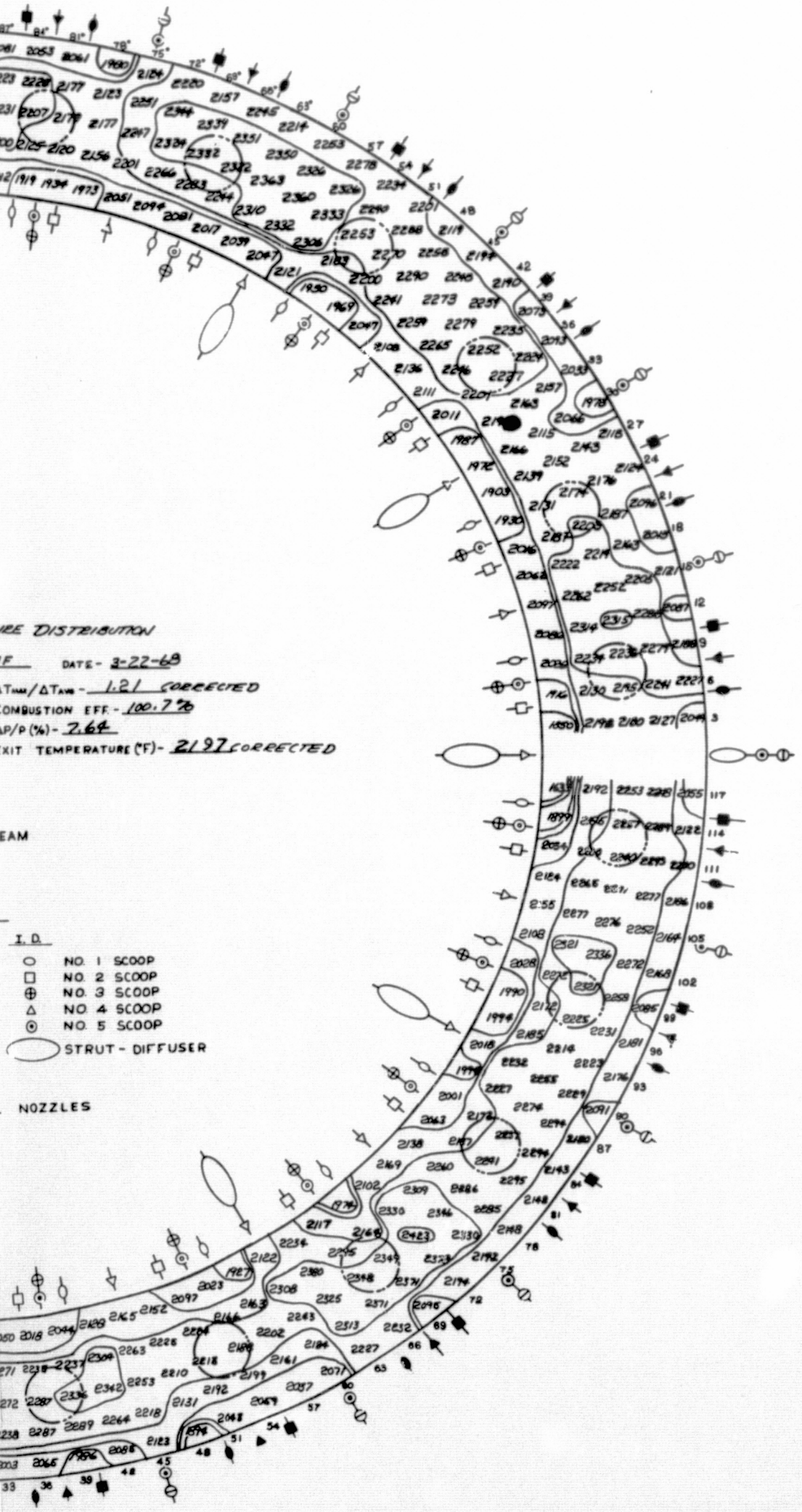

FD 24071

FOLDOUT FRAME 2

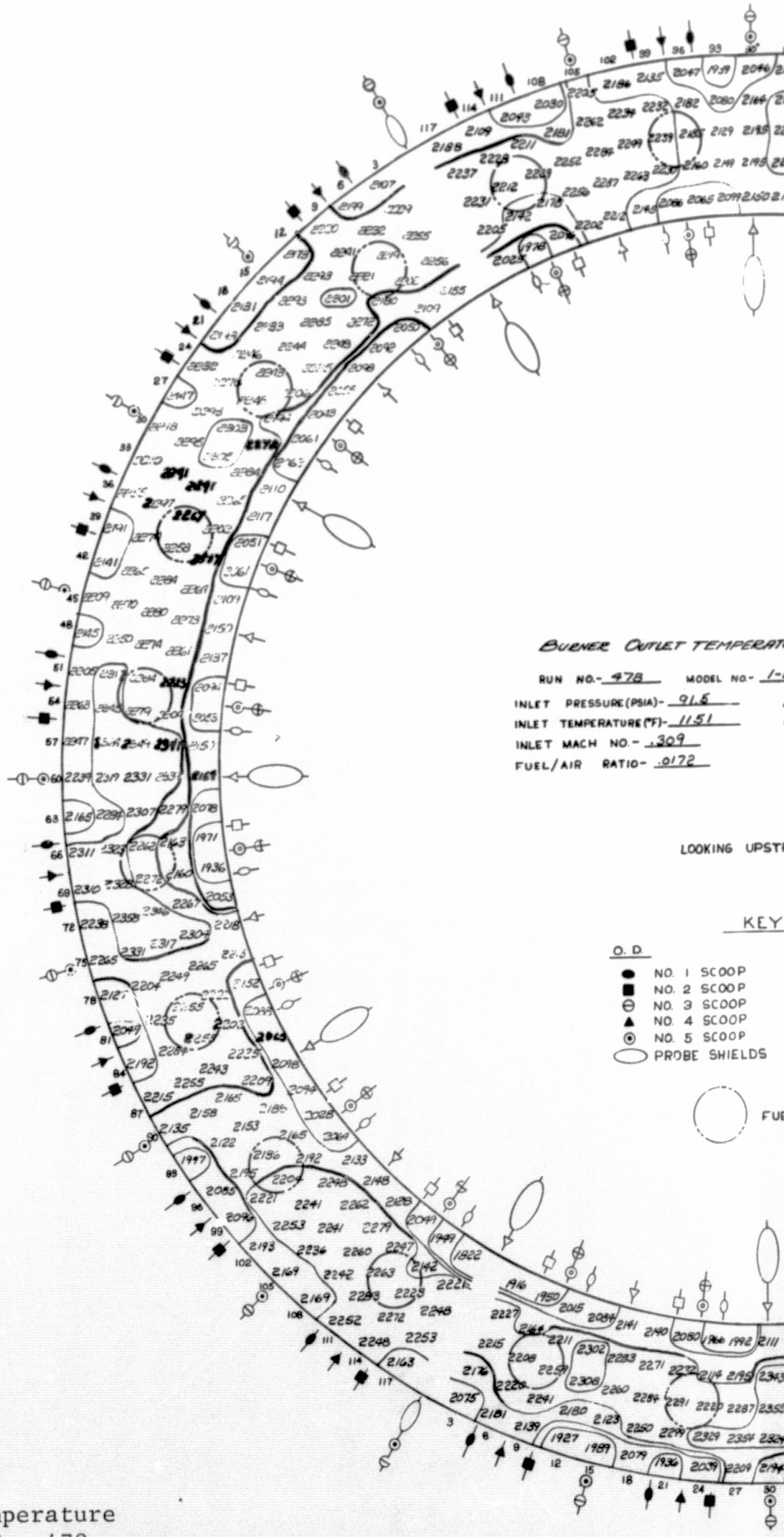

Figure 157. Combustor Outlet Temperature Distribution, Test No. 478

FOLDOUT FRAME 1

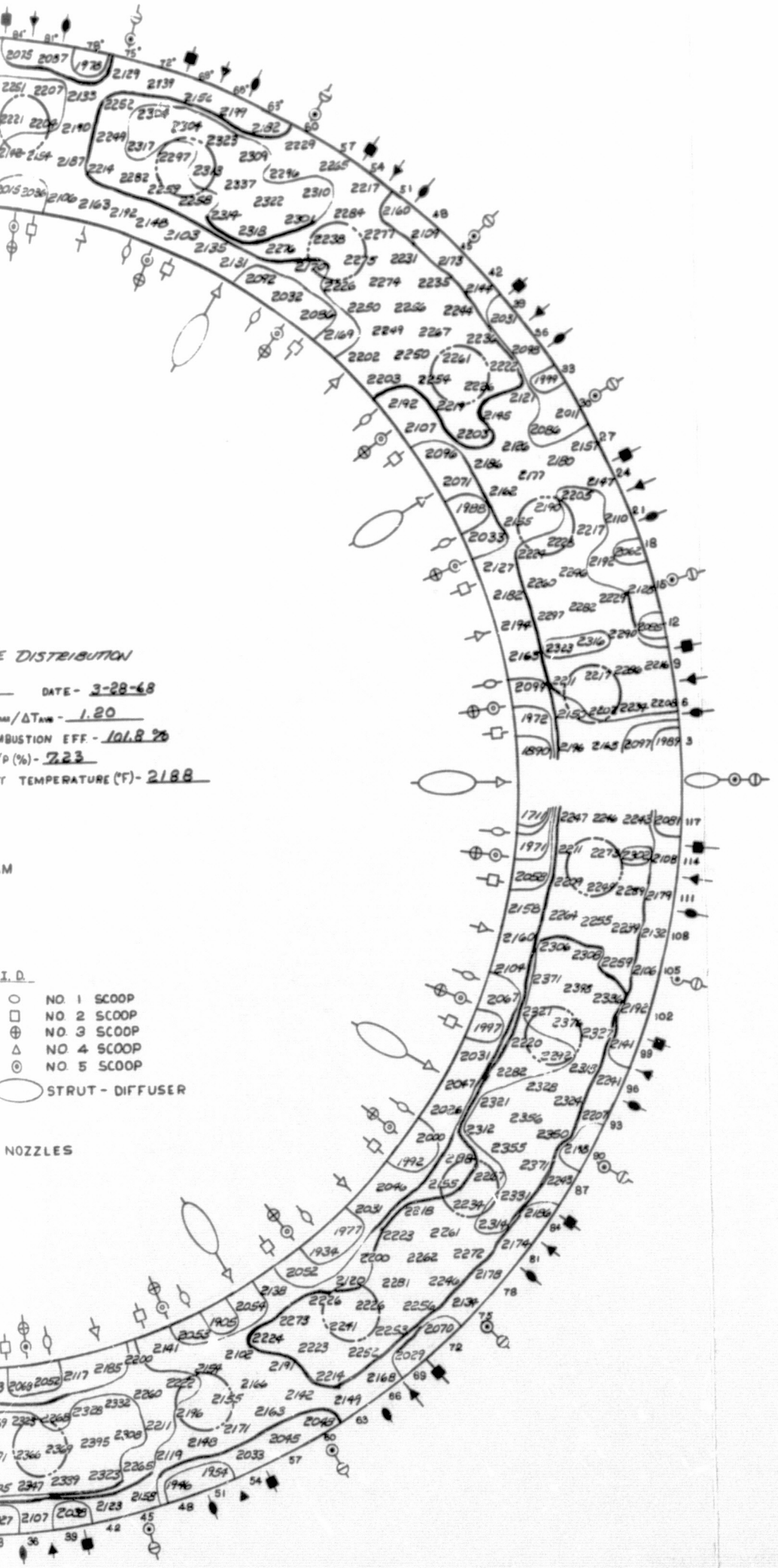

FD 24554

FOLDOUT FRAME 2

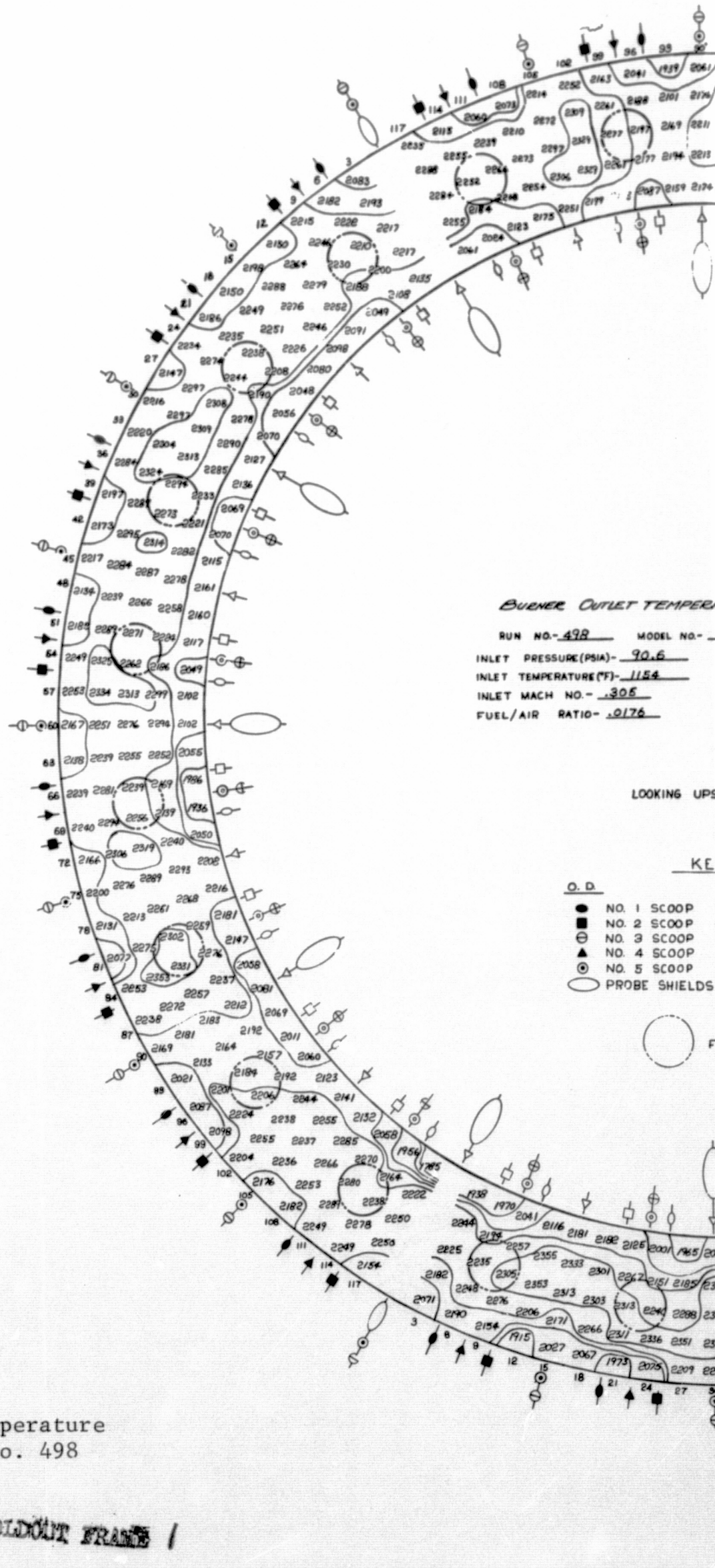

Figure 158. Combustor Outlet Temperature Distribution, Test No. 498

FOLDOUT FRAME 1

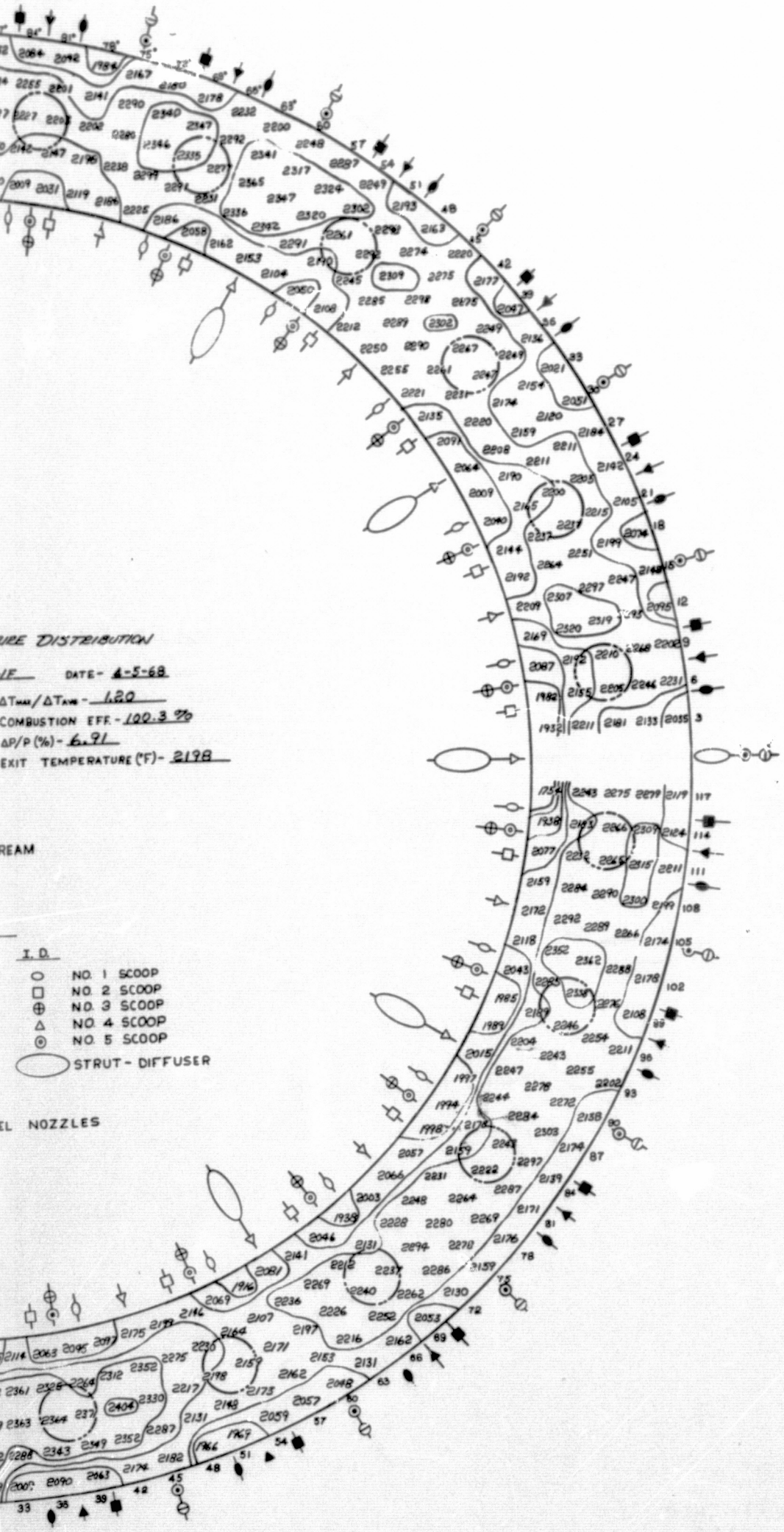

FD 24555

FOLDOUT FRAME 2

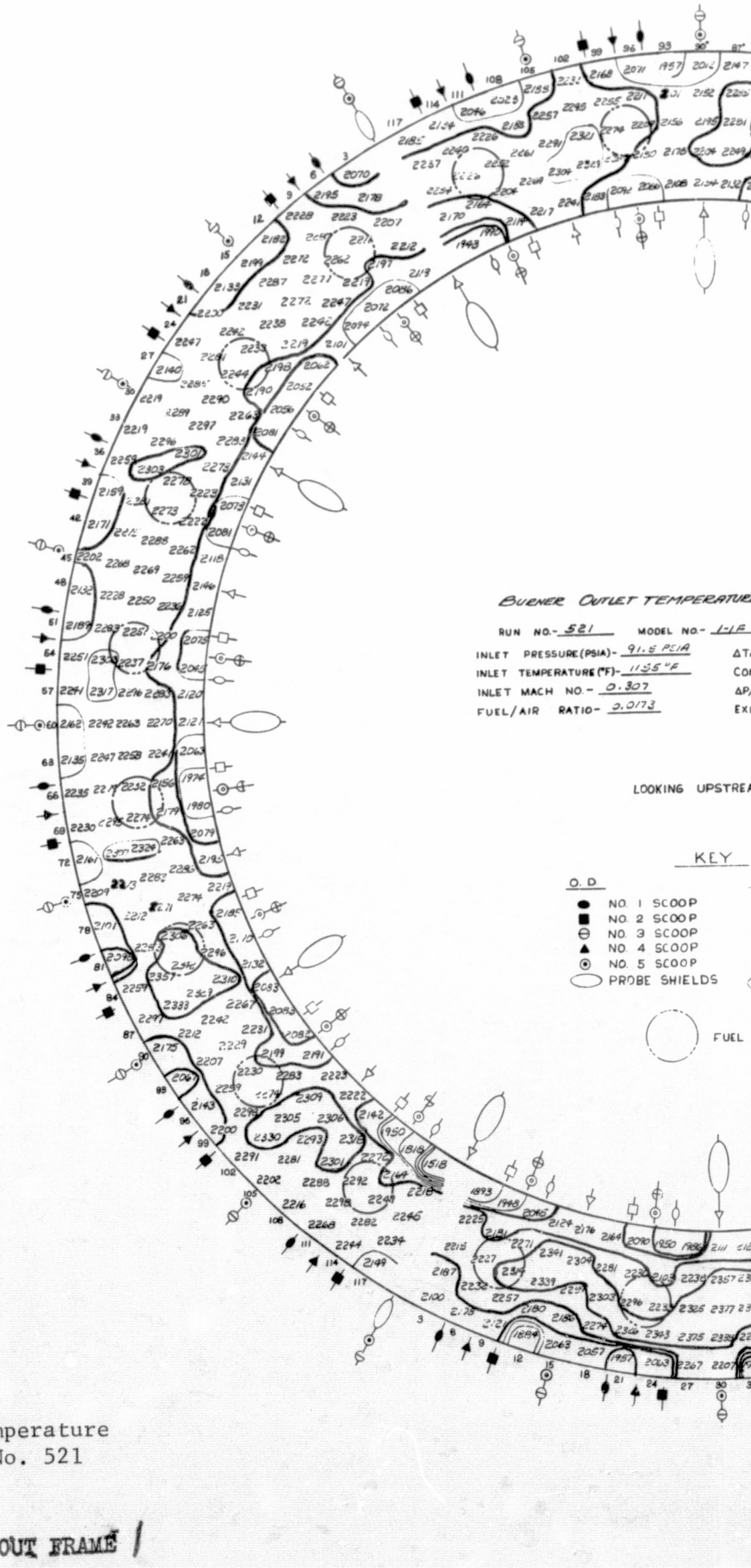

Figure 159. Combustor Outlet Temperature Distribution, Test No. 521

FOLDOUT FRAME 1

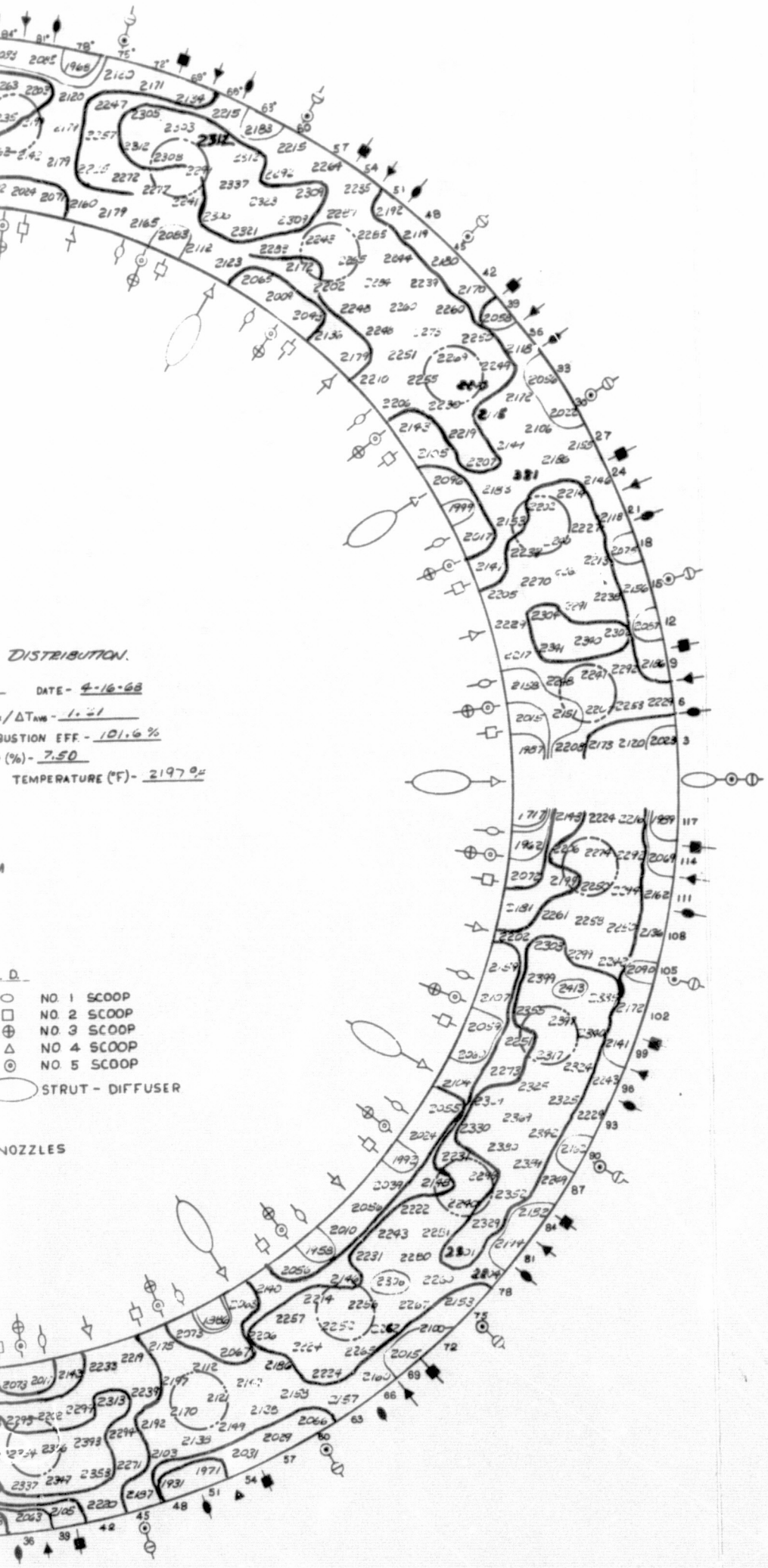

FD 24556

FOLDOUT FRAME 2

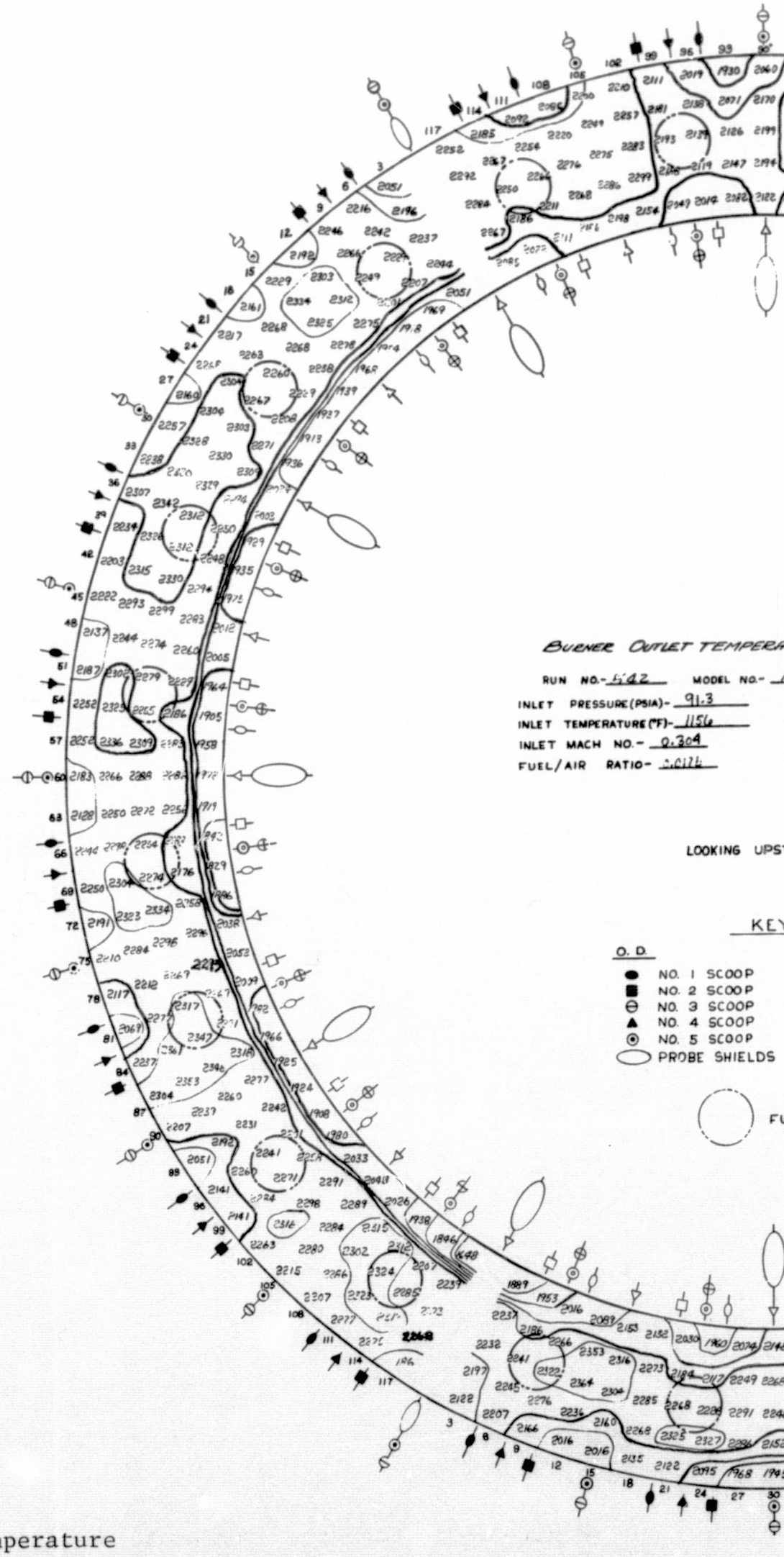

Figure 160. Combustor Outlet Temperature Distribution, Test No. 542

FOLDOUT FRAME 1

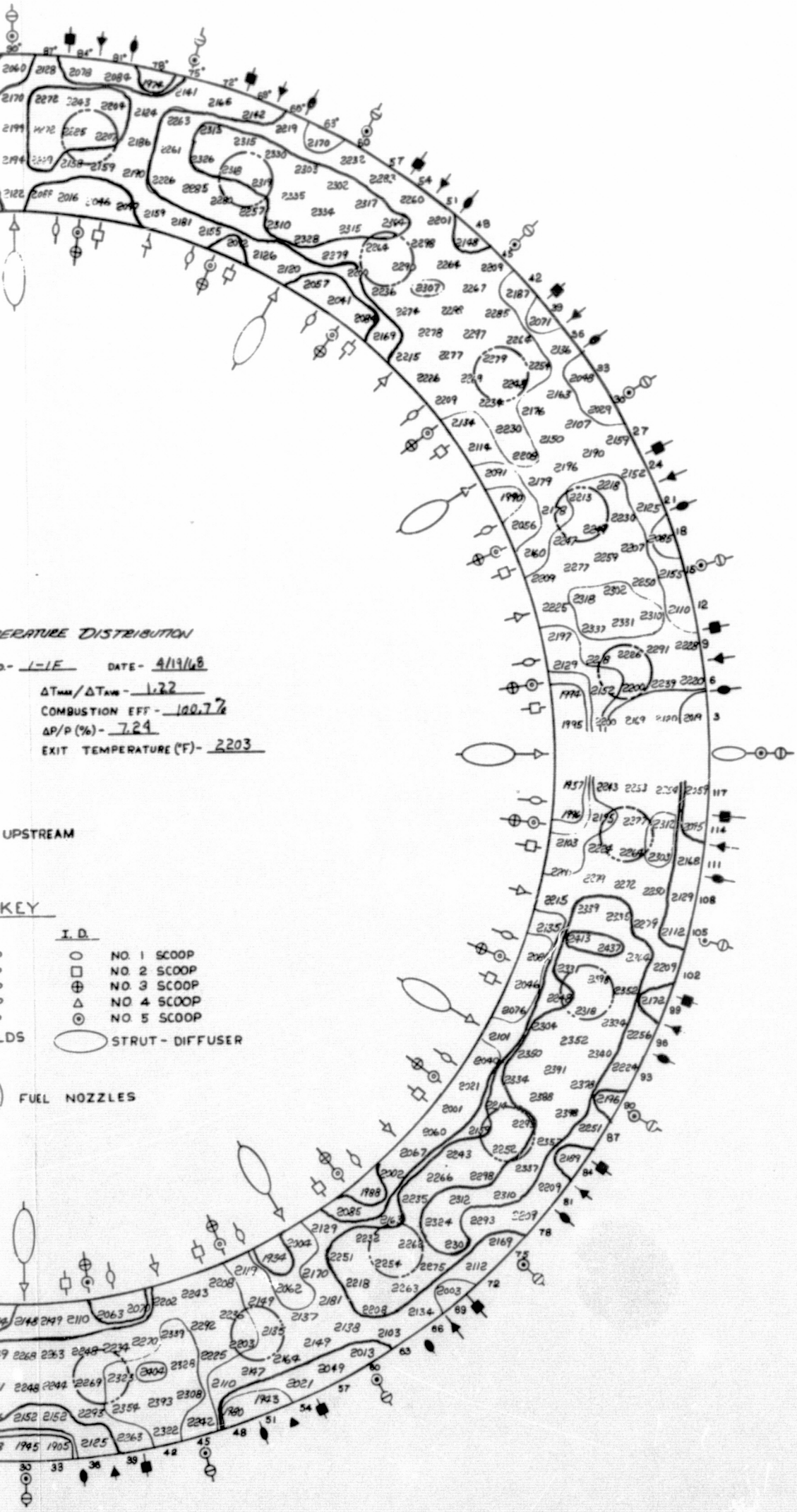

FD 24557

FOLDOUT FRAME 2

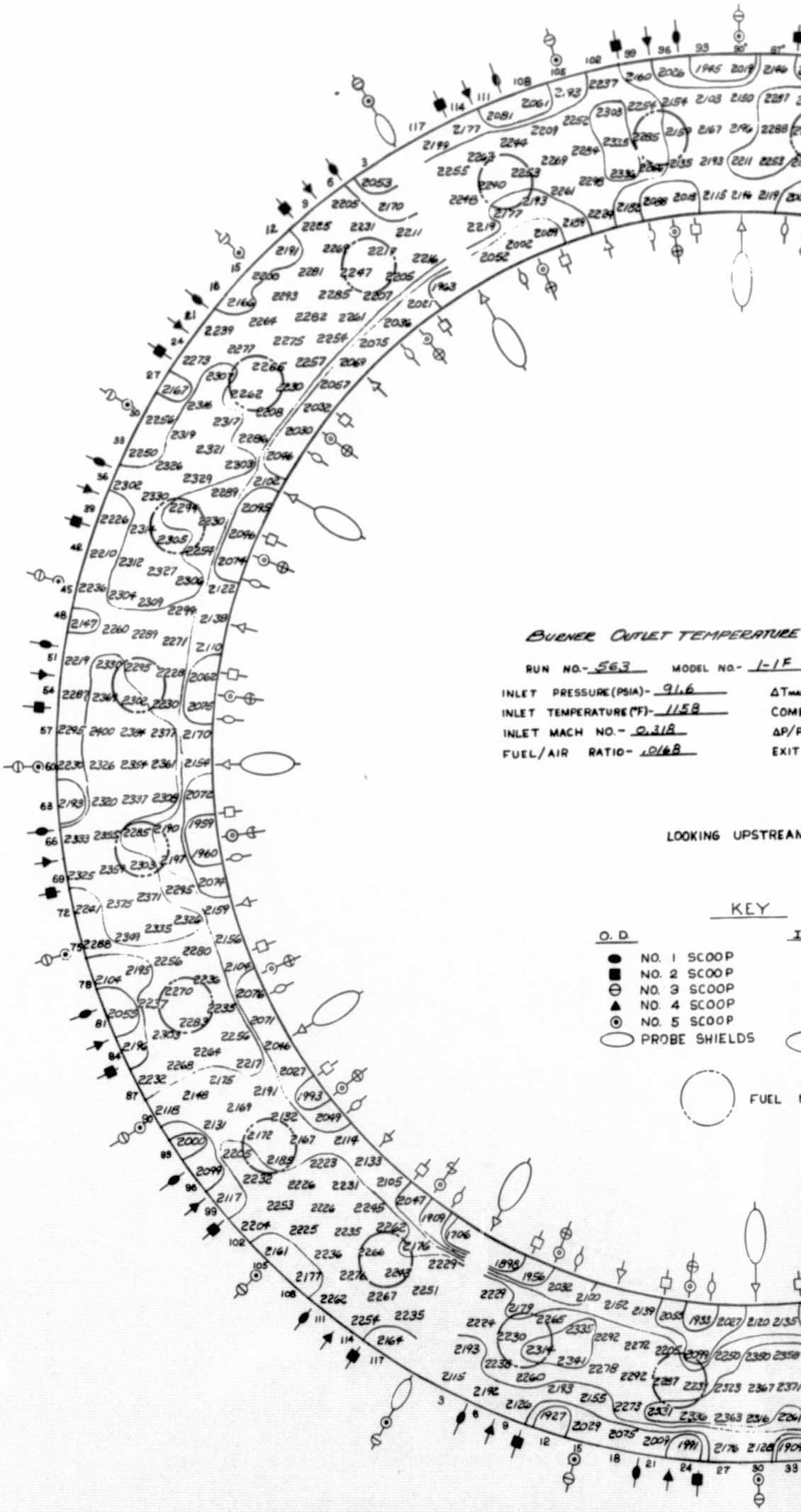

Figure 161. Combustor Outlet Temperature Distribution, Test No. 563

FOLDOUT FRAME

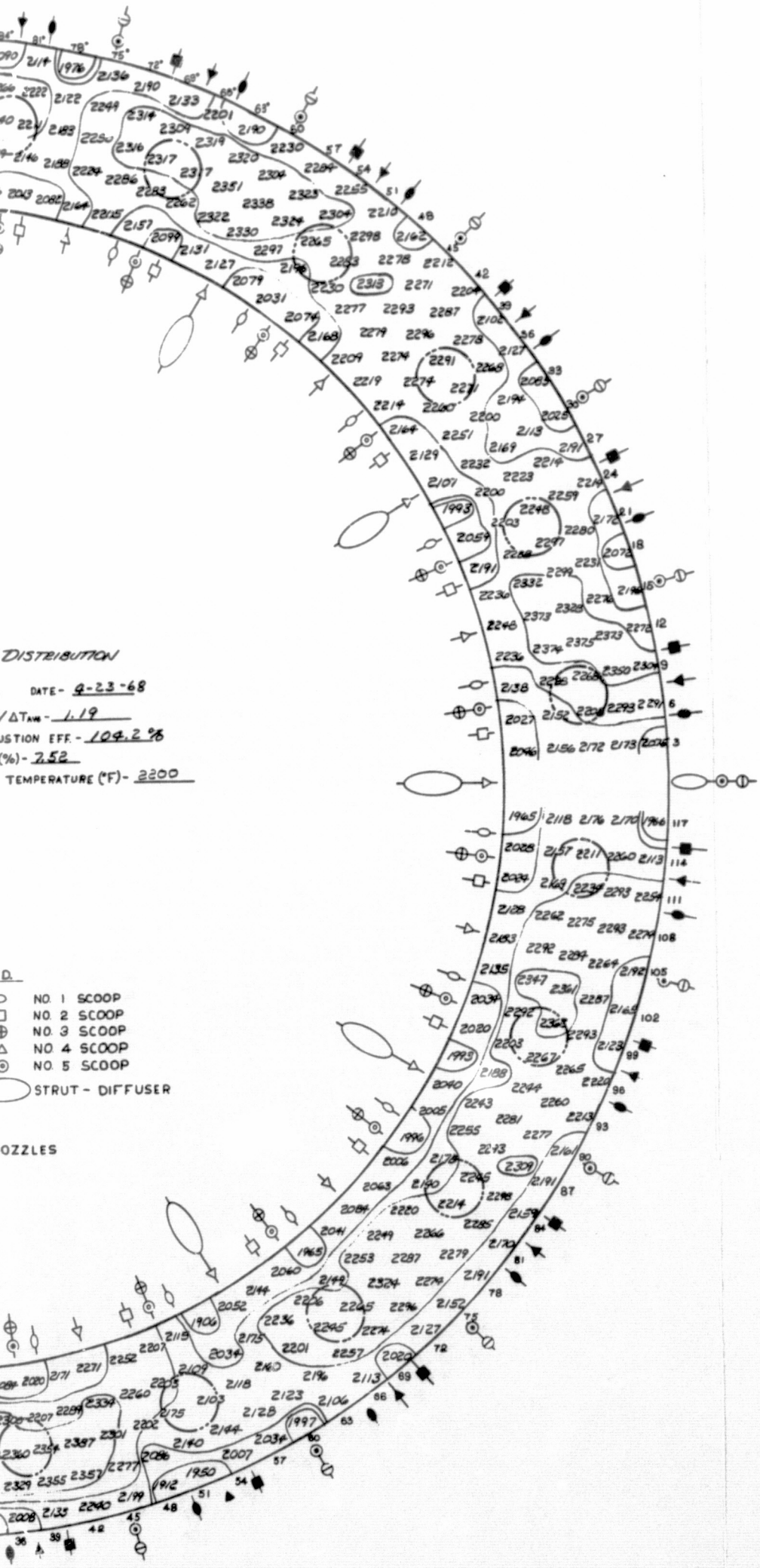

FD 24558

FOLDOUT FRAME 2

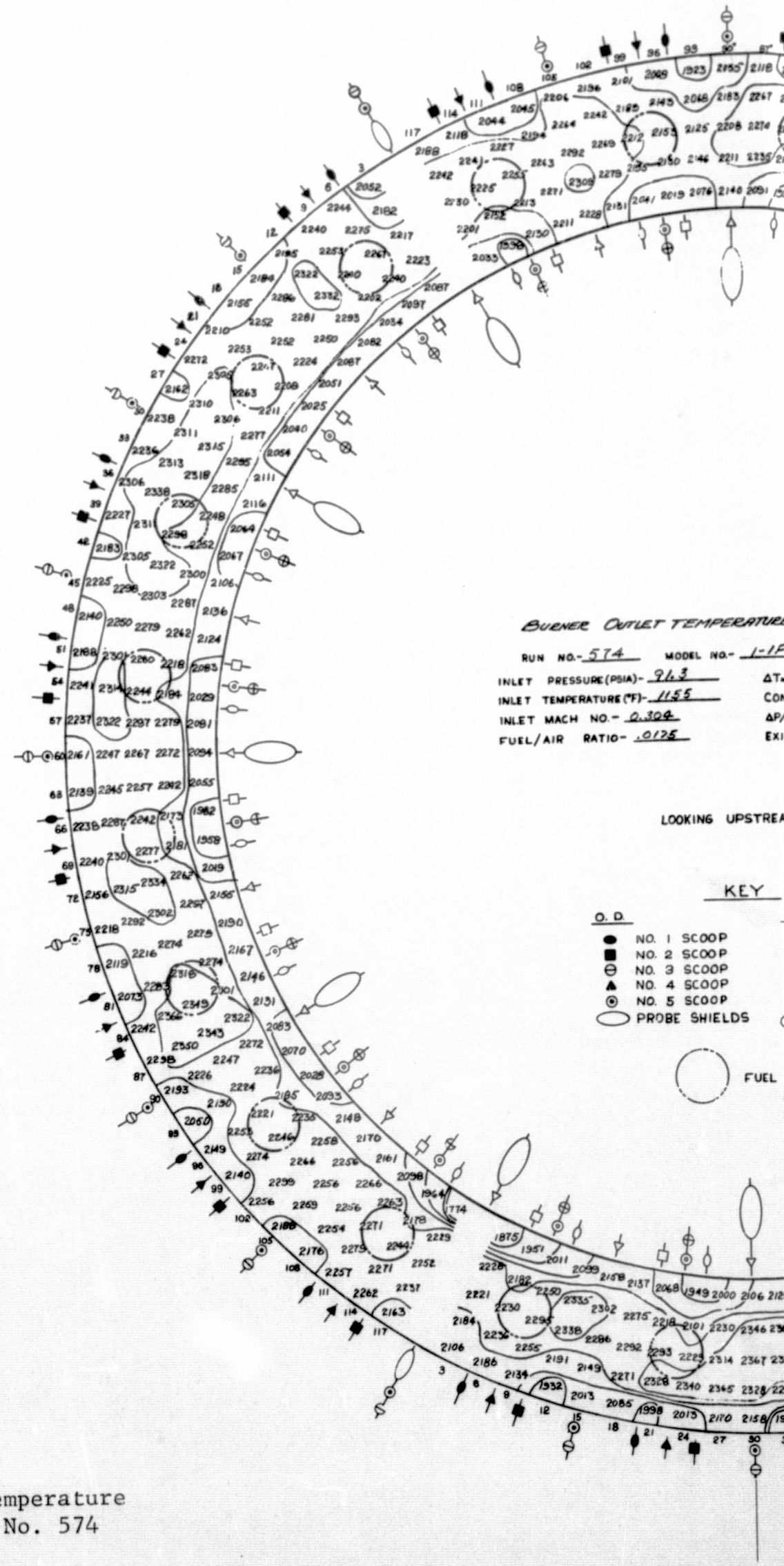

Figure 162. Combustor Outlet Temperature Distribution, Test No. 574

...OUT FRAME

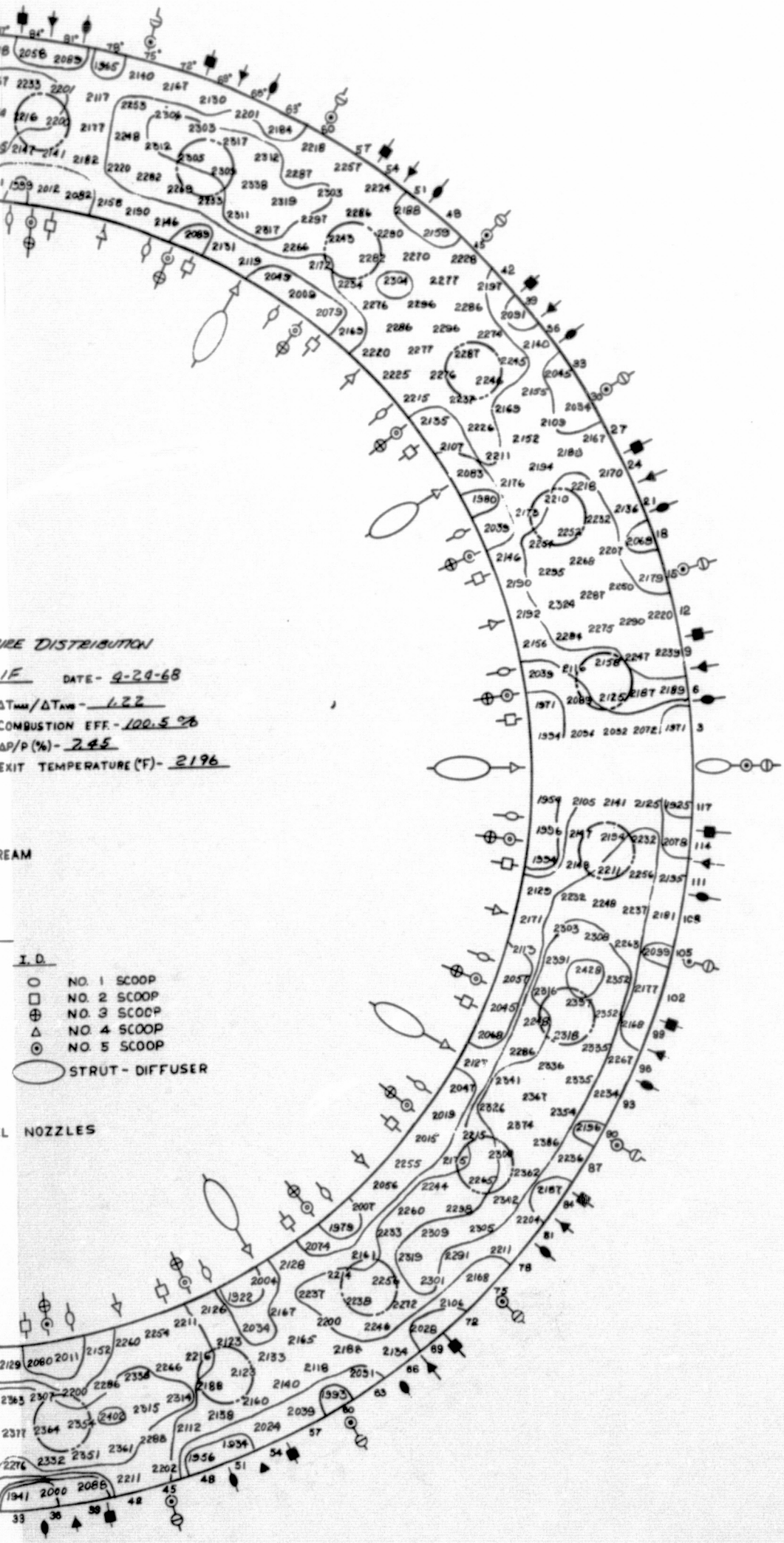

FD 24559

FOLDOUT FRAME 2

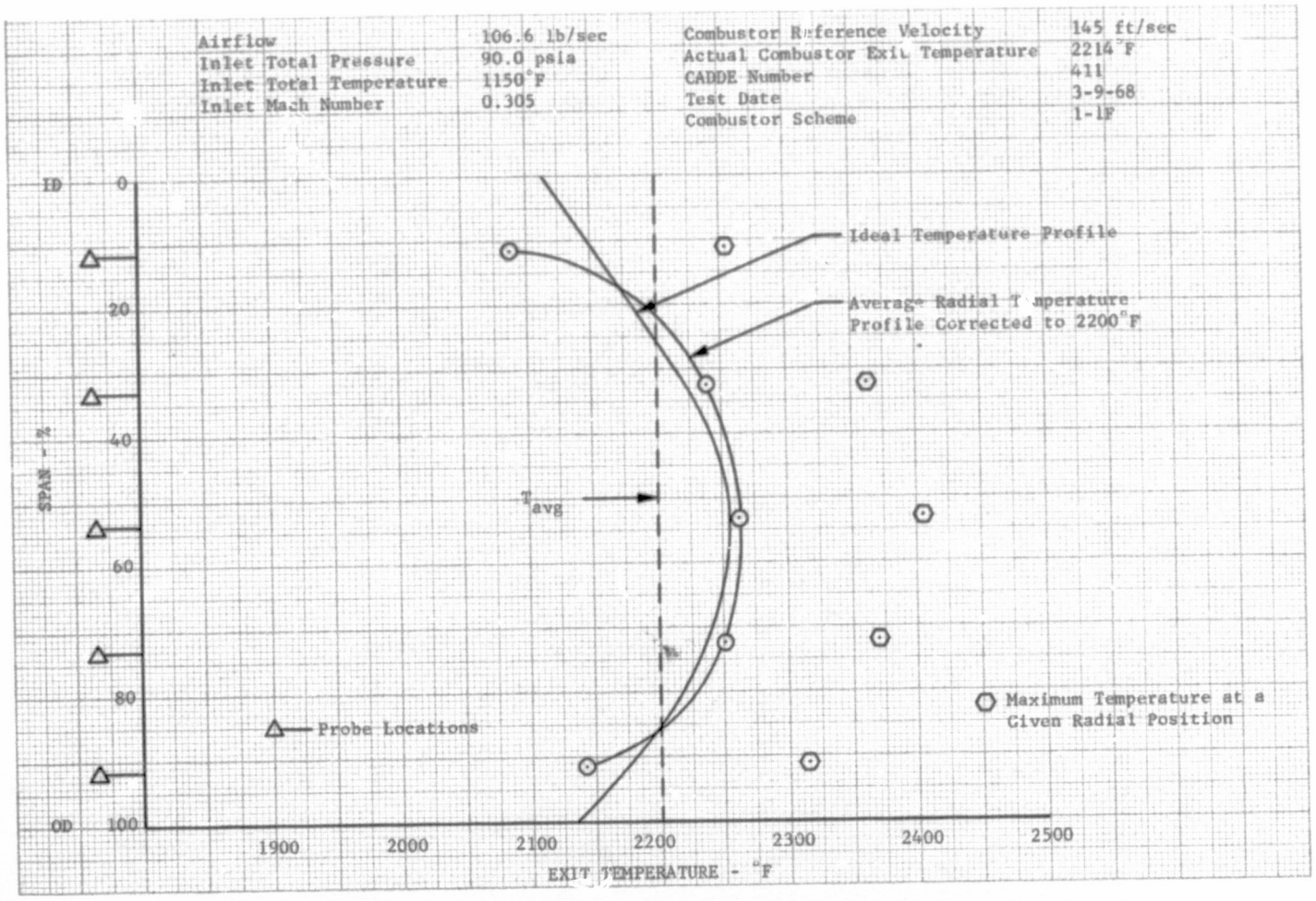

DF 64502

Figure 163. Combustor Average Radial Exit Temperature Profile, Test No. 411

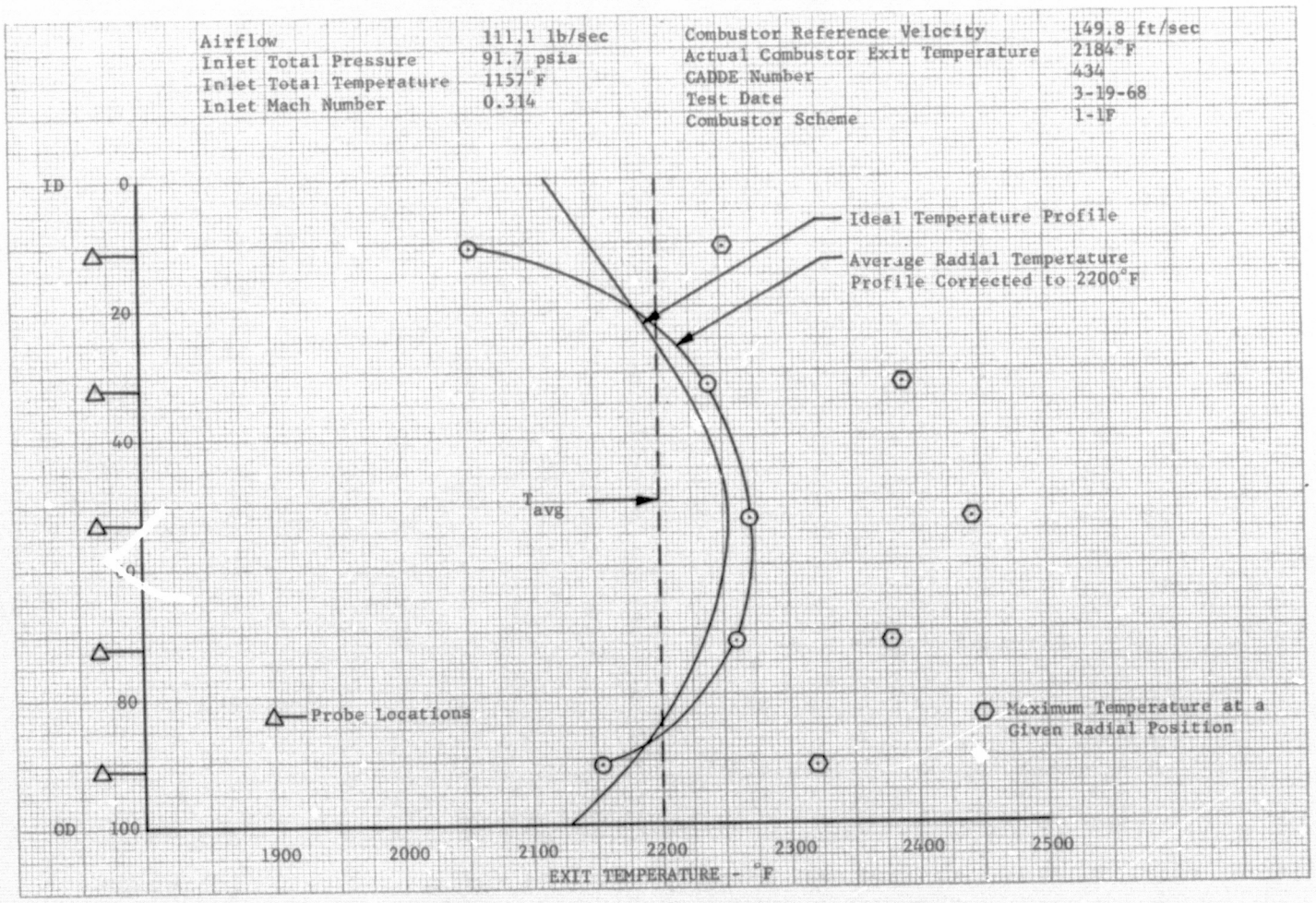

DF 64503

Figure 164. Combustor Average Radial Exit Temperature Profile, Test No. 434

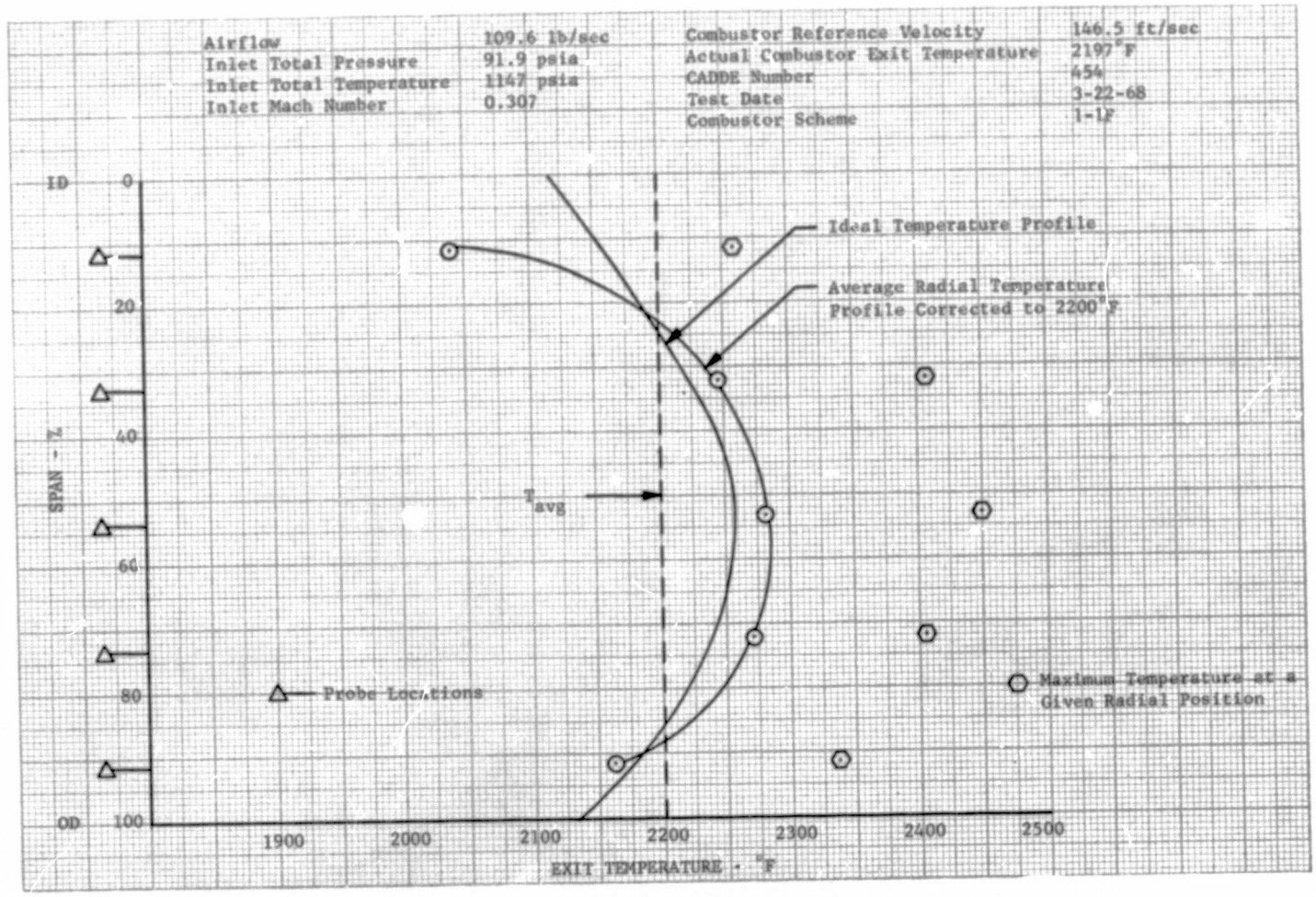

Figure 165. Combustor Average Radial Exit Temperature Profile, Test No. 454

DF 64504

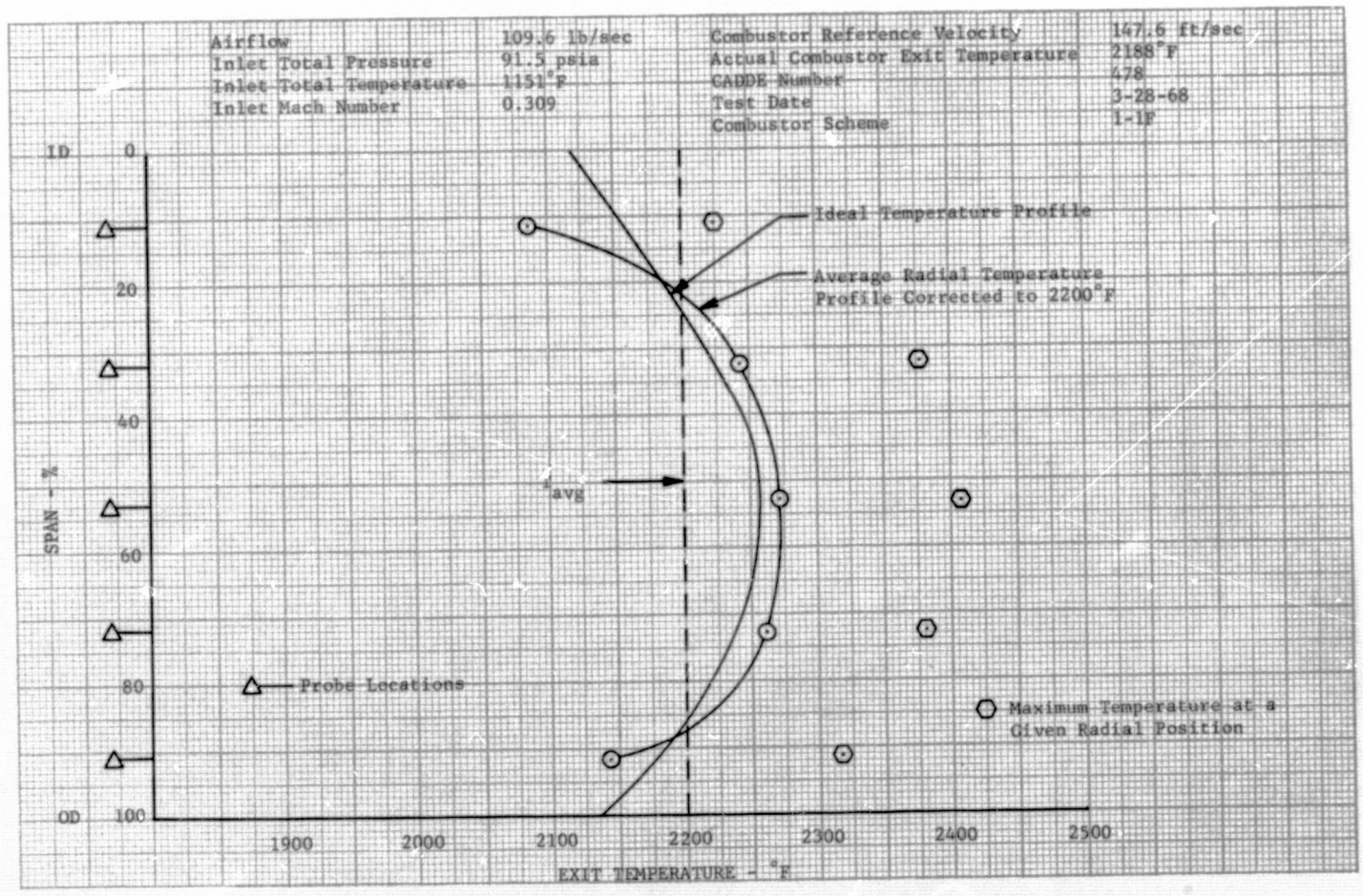

Figure 166. Combustor Average Radial Exit Temperature Profile, Test 478

DF 64505

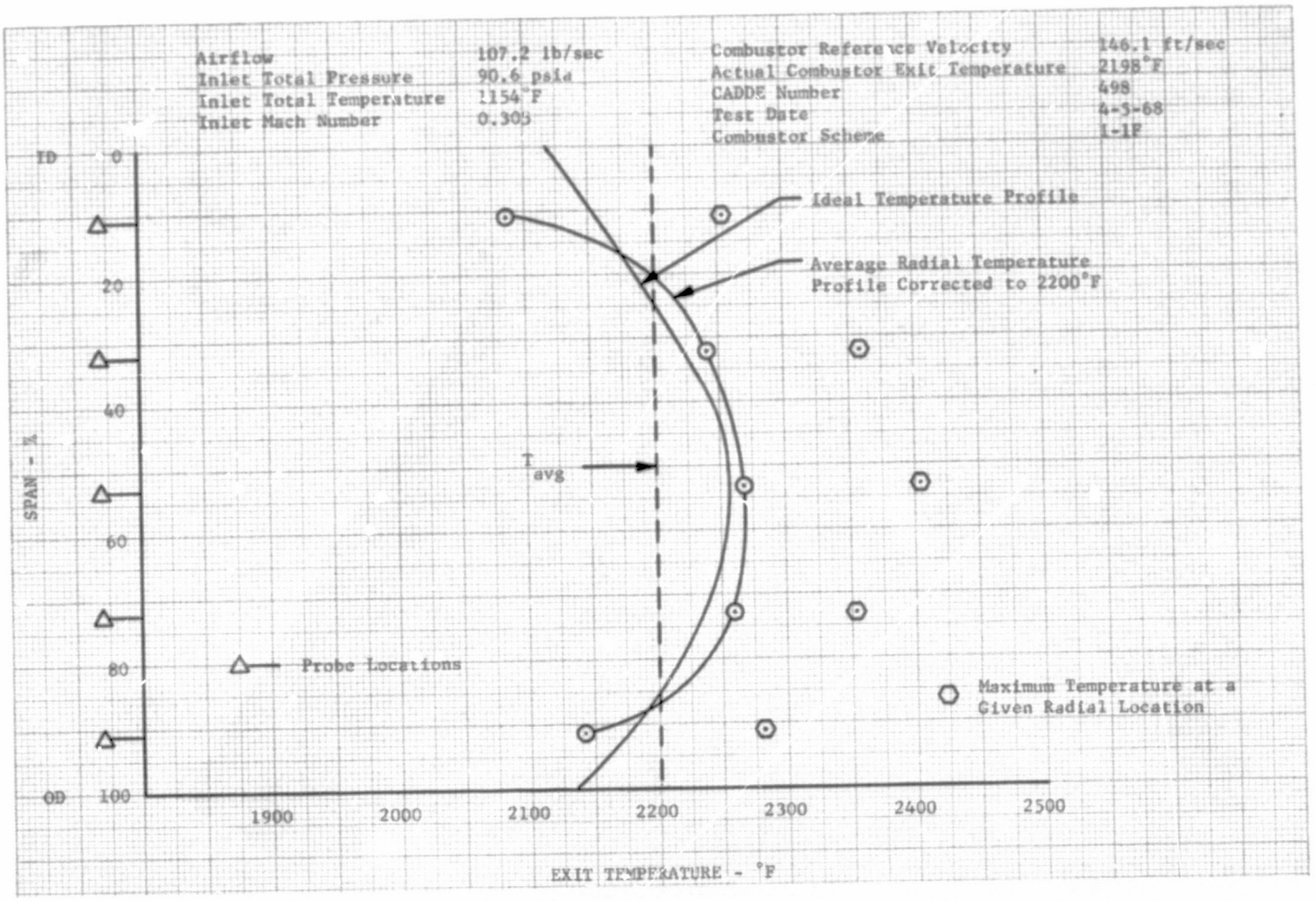

Figure 167. Combustor Average Radial Exit Temperature Profile, Test 498

DF 64506

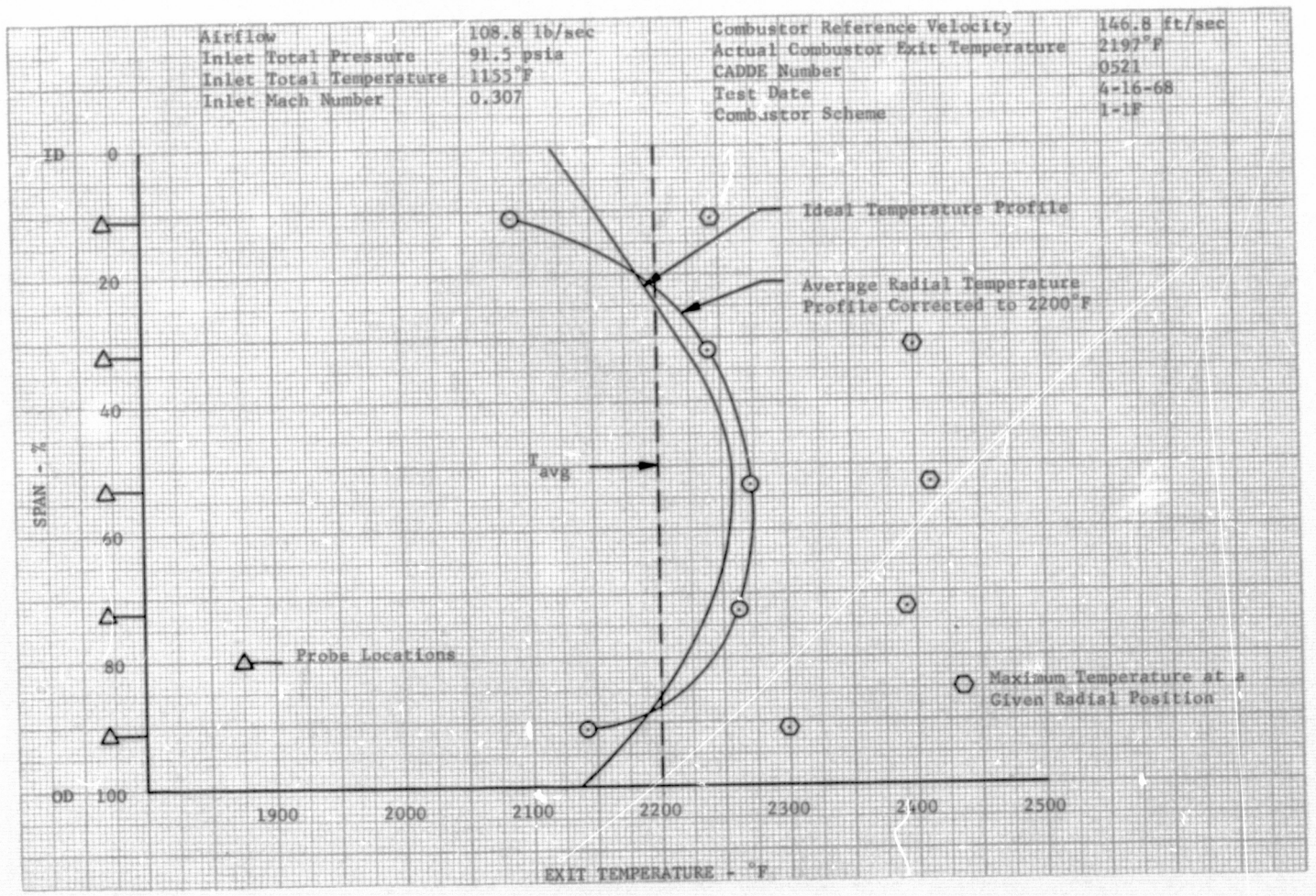

Figure 168. Combustor Average Radial Exit Temperature Profile, Test No. 521

DF 64507

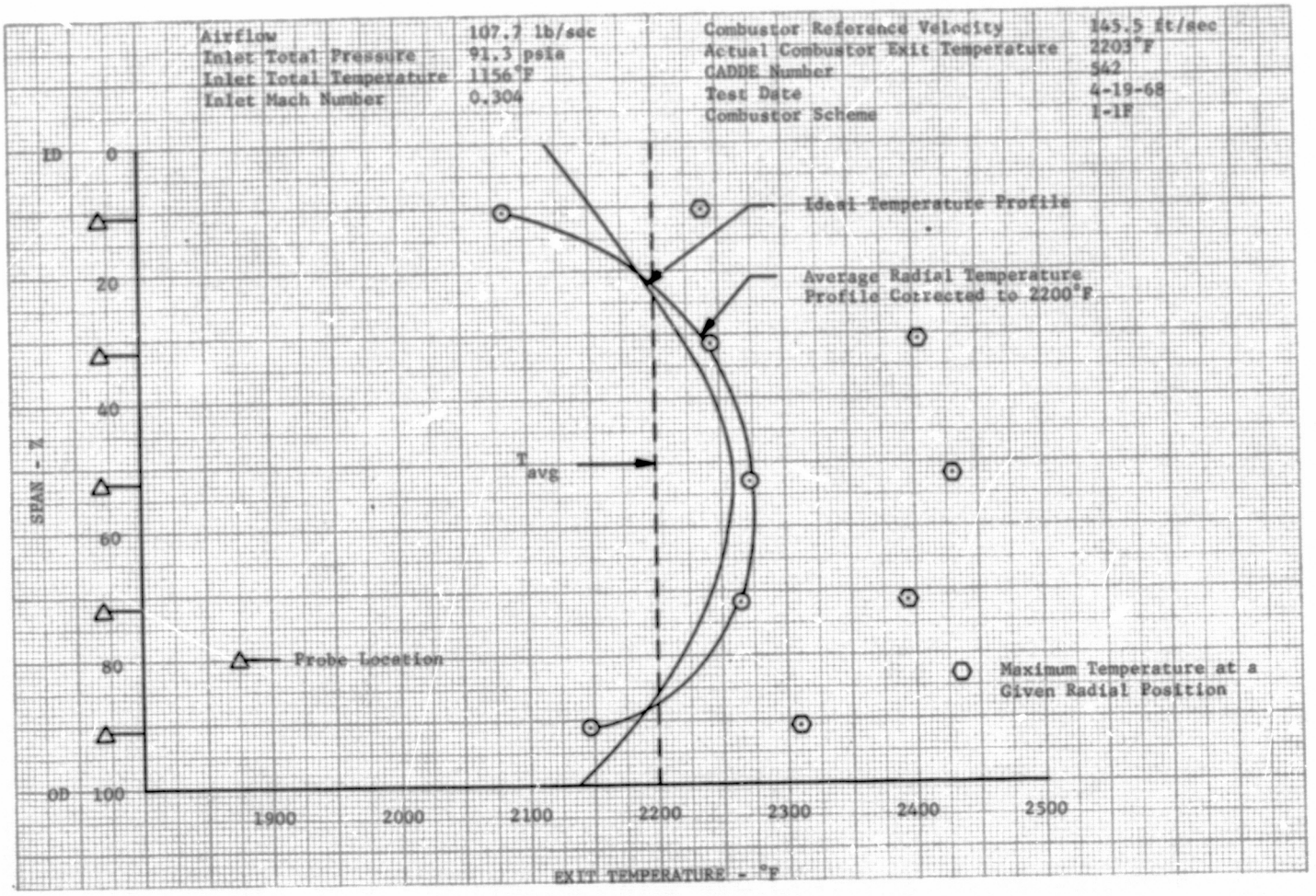

Figure 169. Combustor Average Radial Exit Temperature Profile, Test No. 542

DF 64508

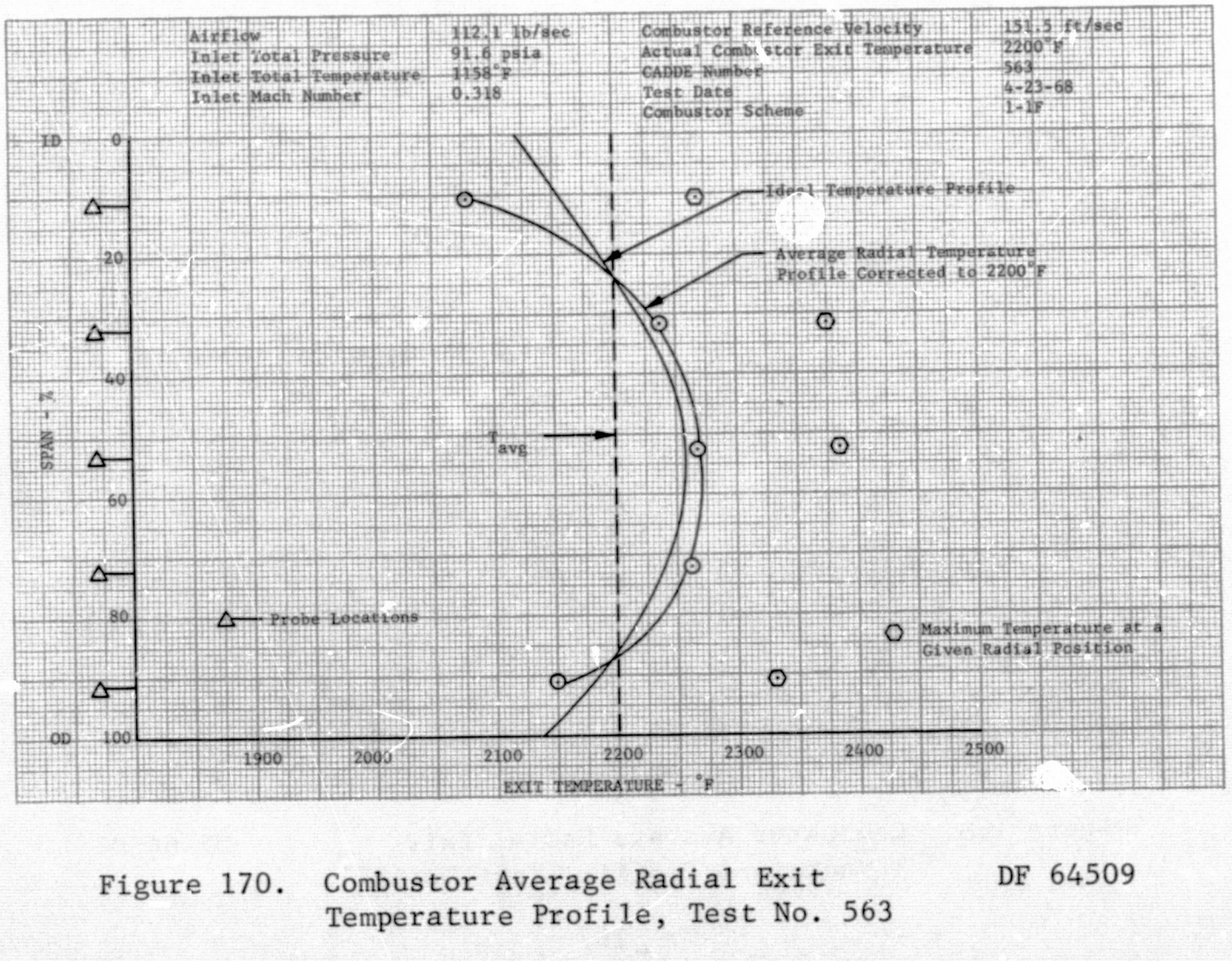

Figure 170. Combustor Average Radial Exit Temperature Profile, Test No. 563

DF 64509

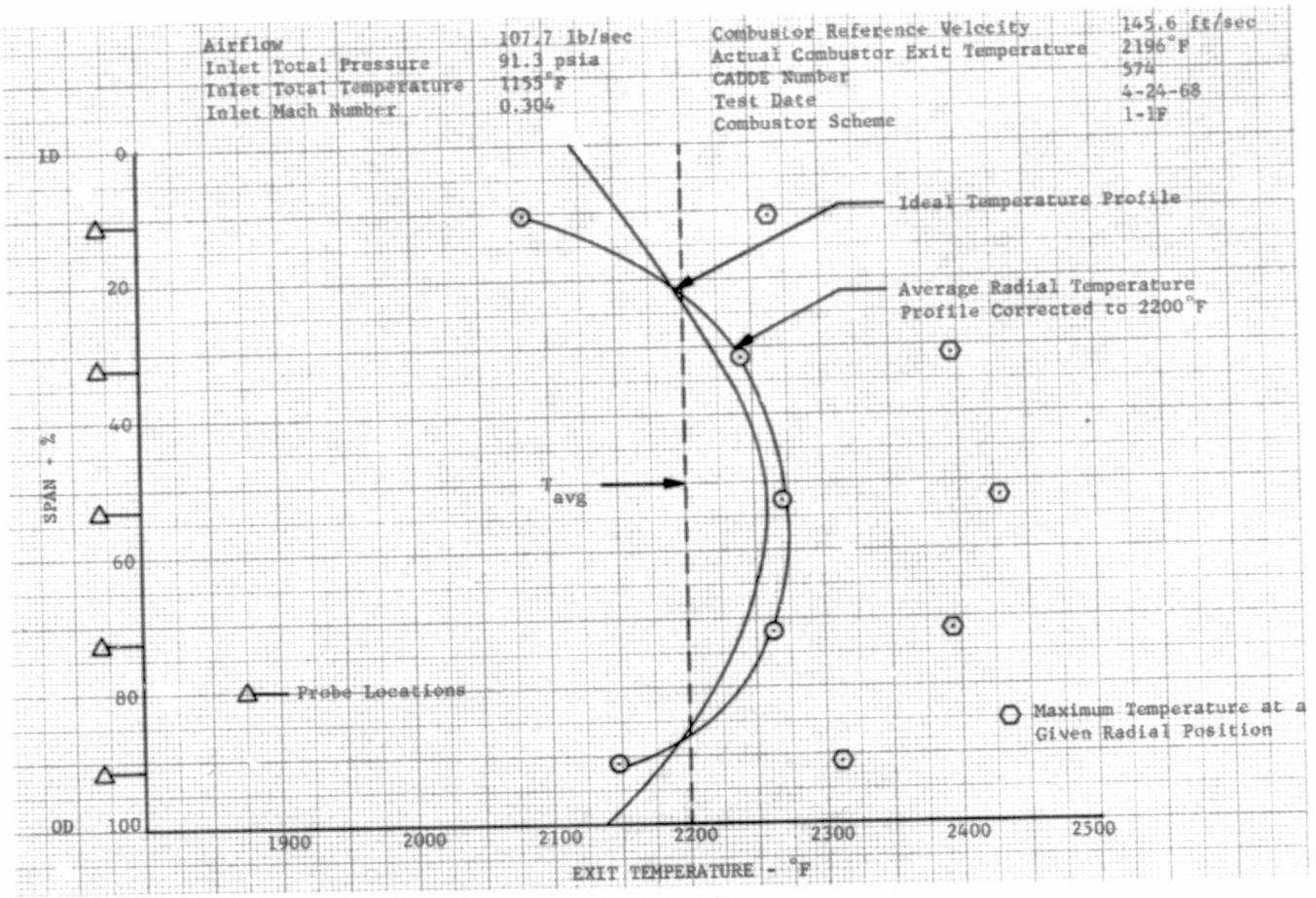

Figure 171. Combustor Average Radial Exit Temperature Profile, Test No. 574

DF 64510

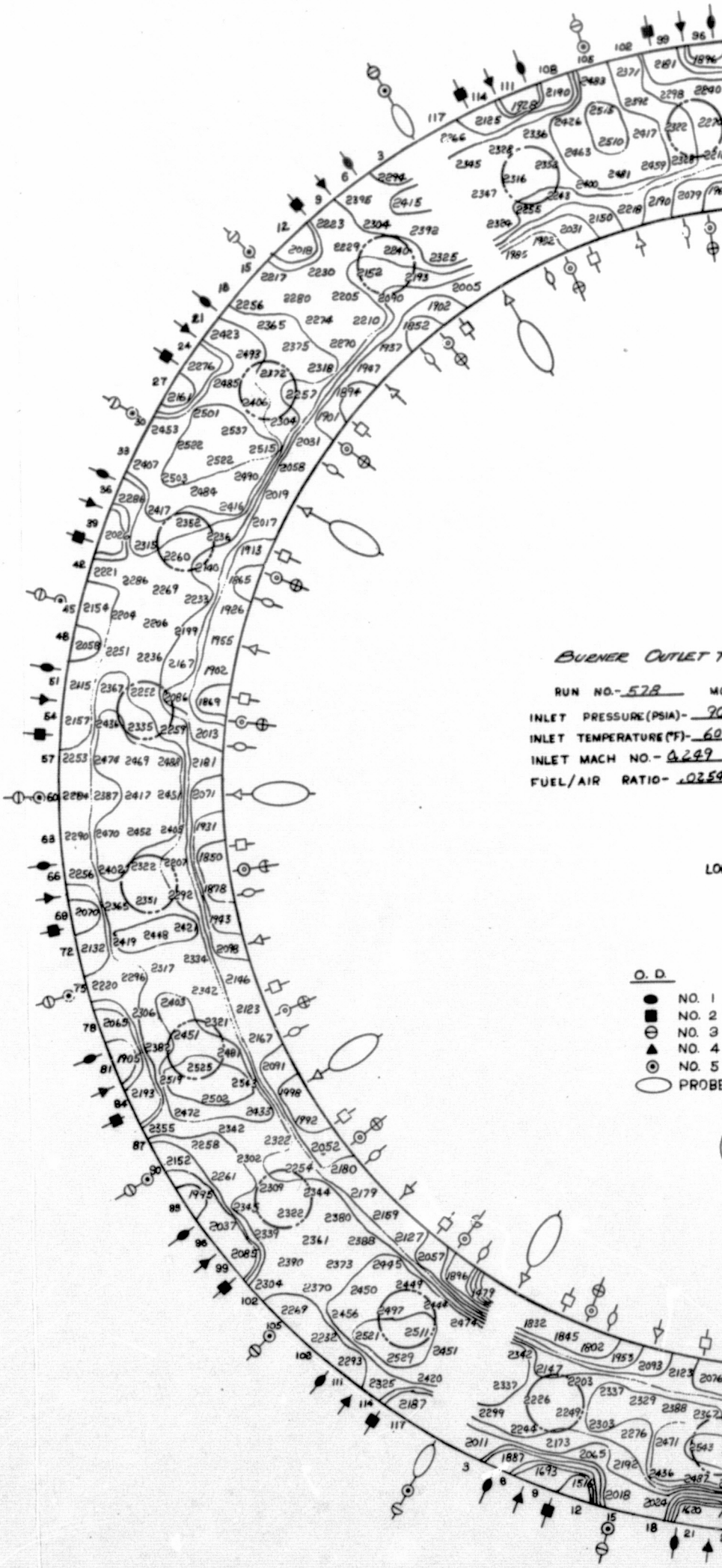

Figure 172. Burner Outlet Temperature Distribution, Test No. 578

FOLDOUT FRAME

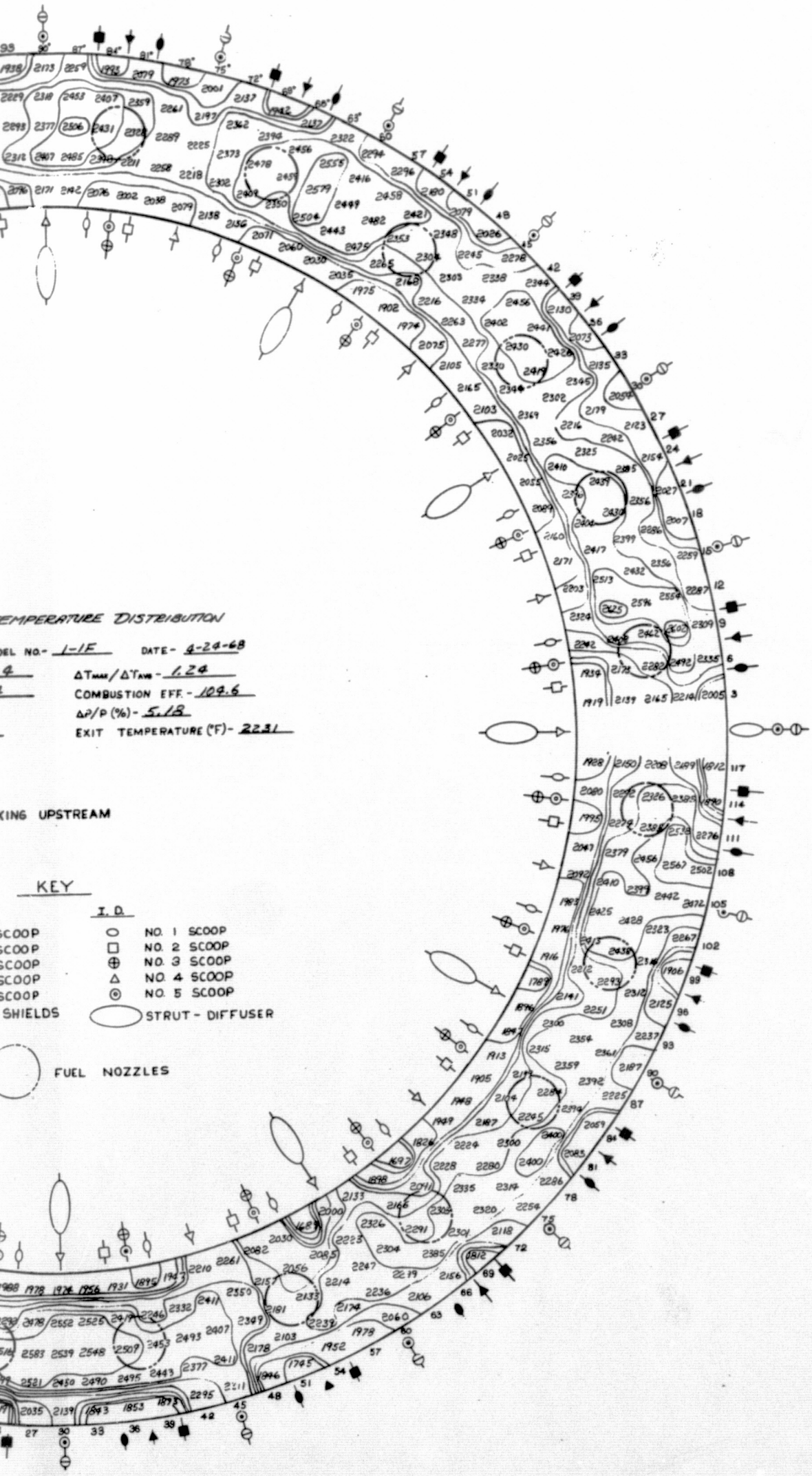

FD 24560

FOLDOUT FRAME 2

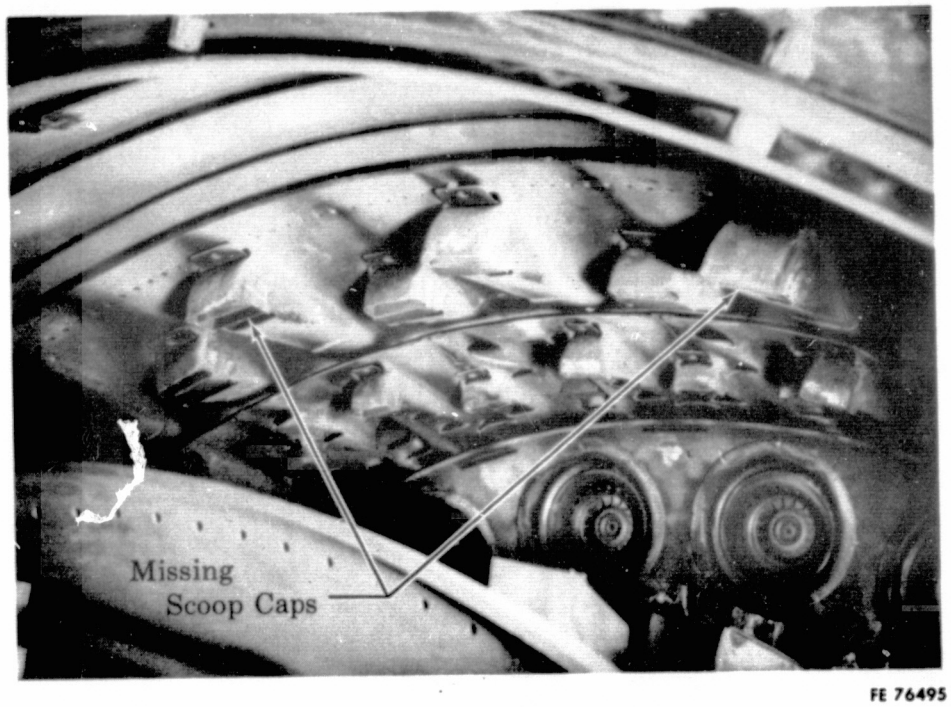

Figure 173. Two No. 5 Scoop Caps Missing FD 24090

Figure 174. No. 5 Scoop Cap Missing FD 24091

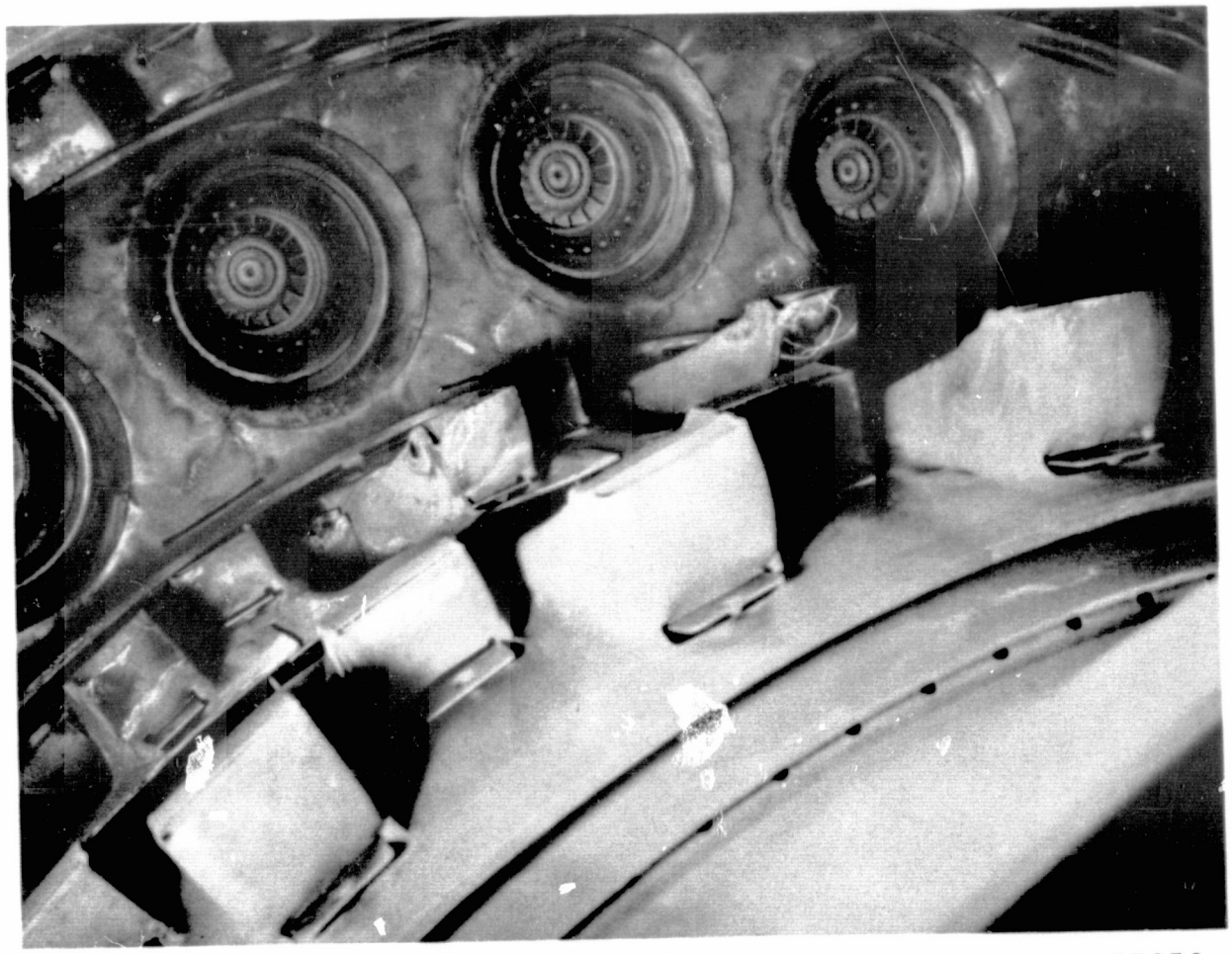

Figure 175. Burned No. 3 Scoops (View 1) FE 77050

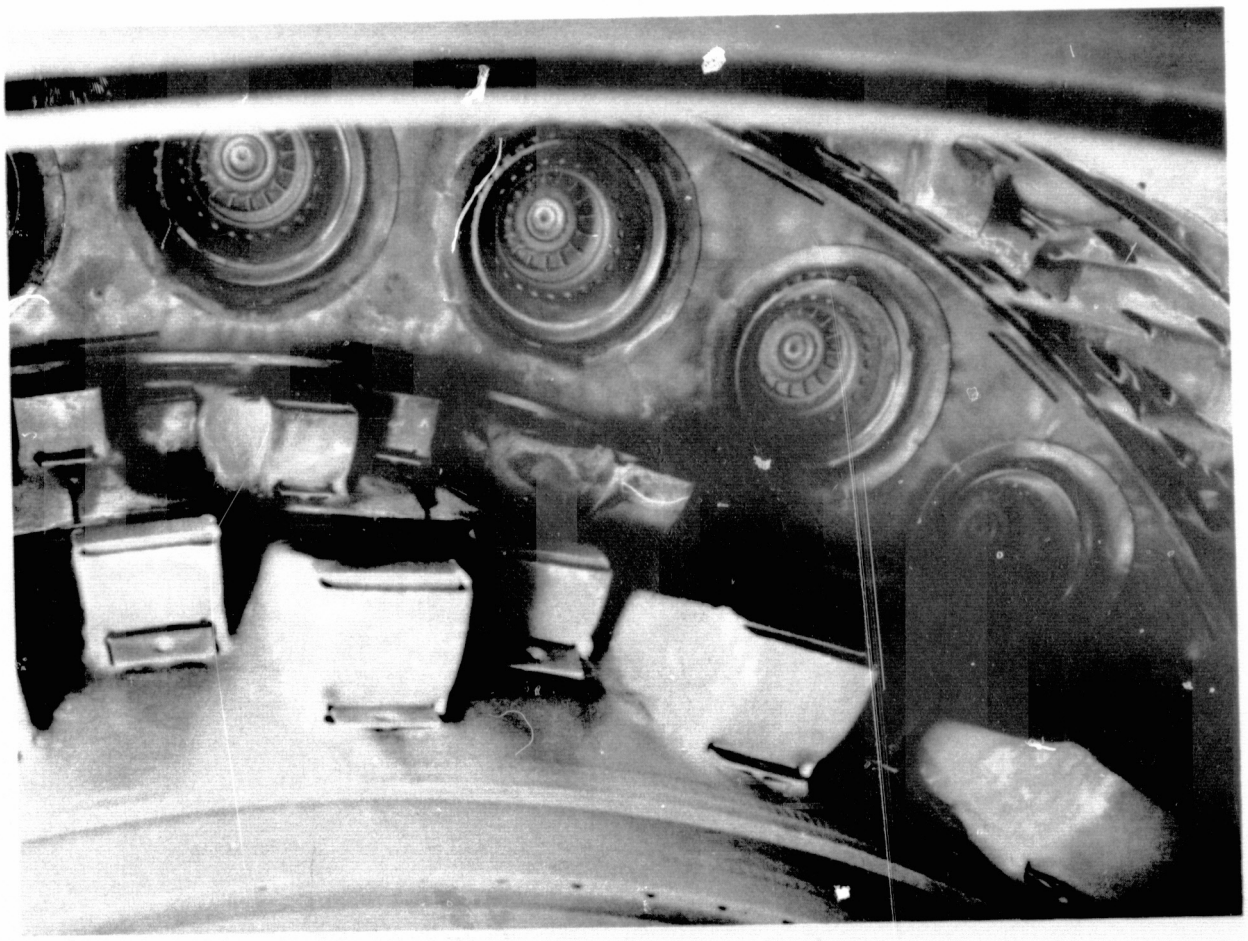

Figure 176. Burned No. 3 Scoops (View 2) FE 77049

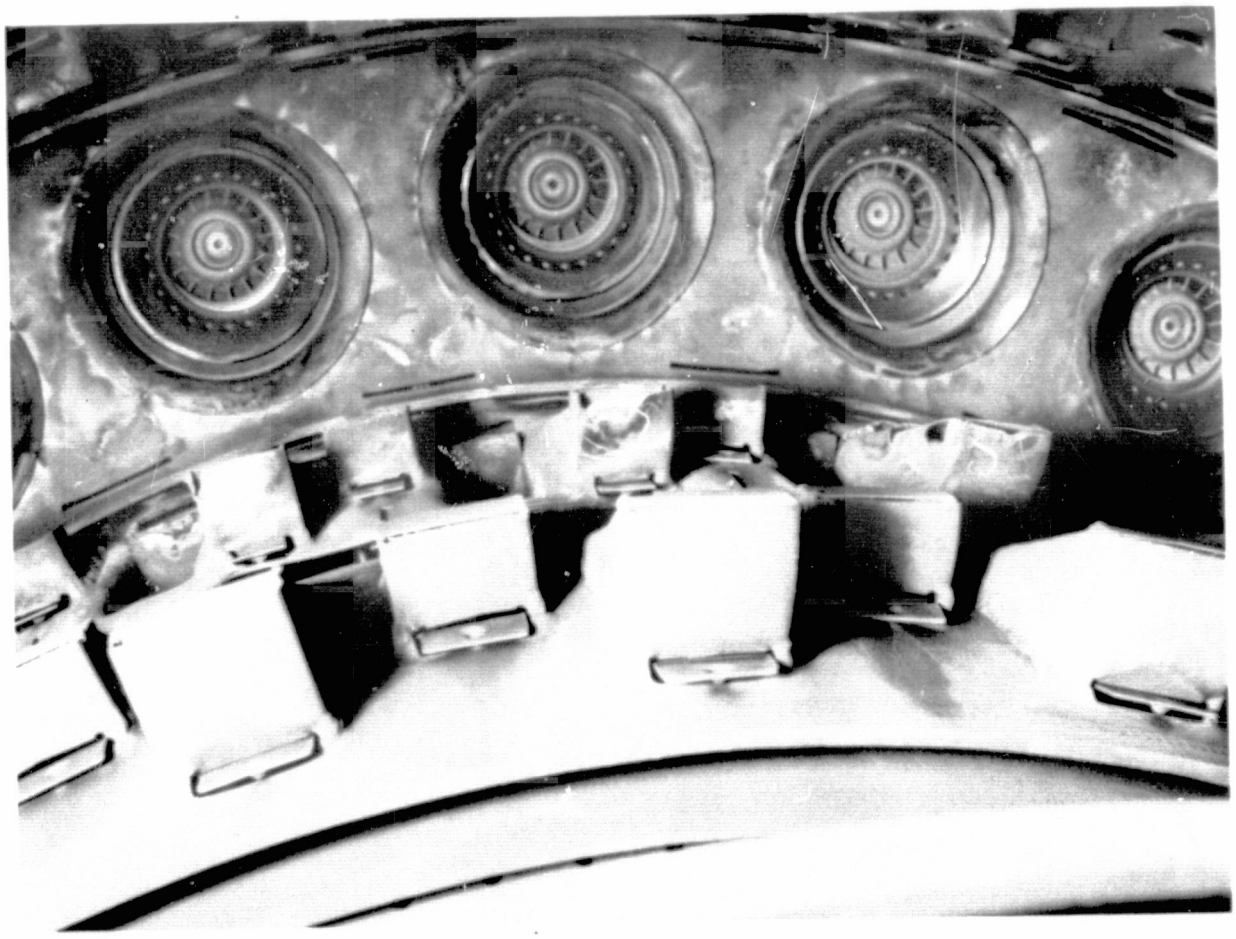

Figure 177. Burned No. 3 Scoops (View 3) FE 77048

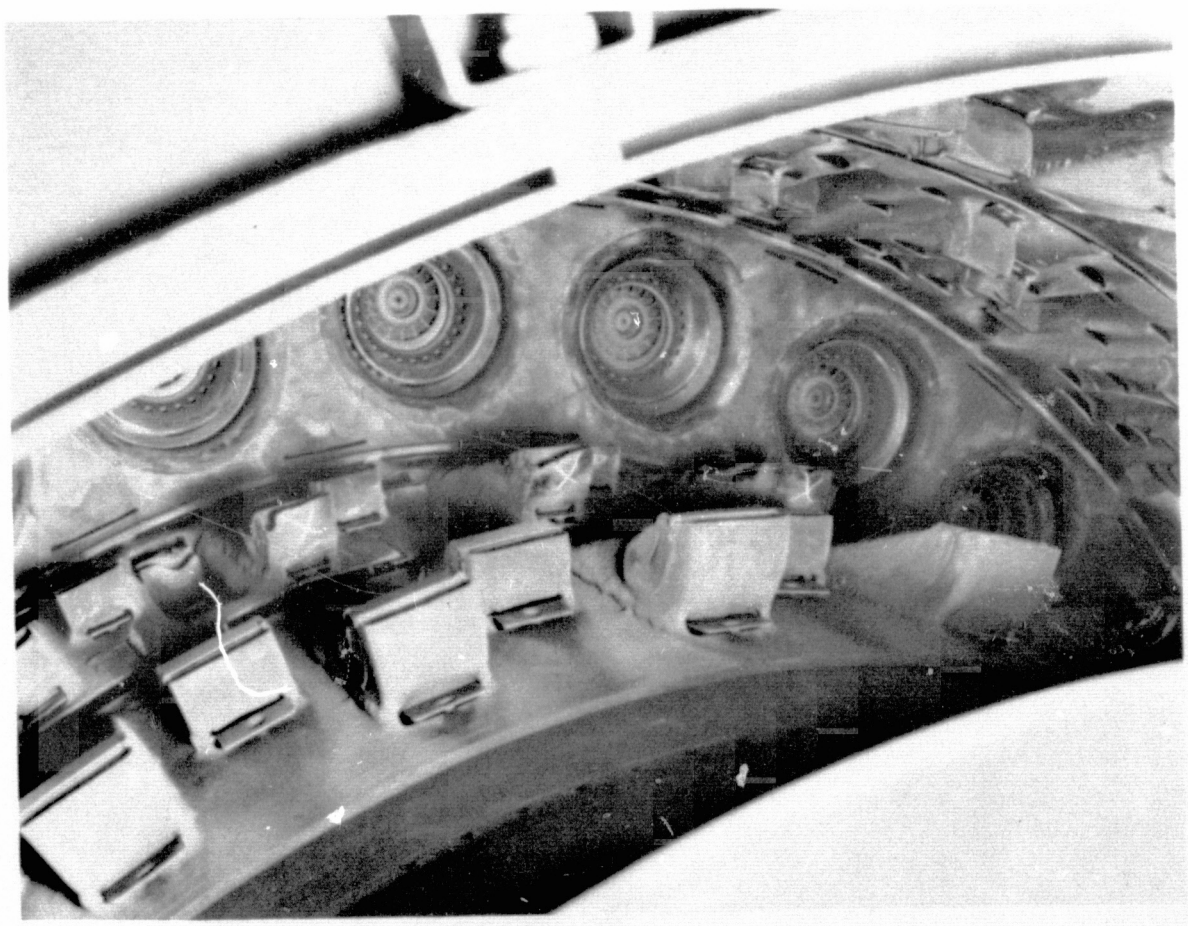

Figure 178. Combustor After 98 Hours of Condition 4 Testing (View 1) FE 77326

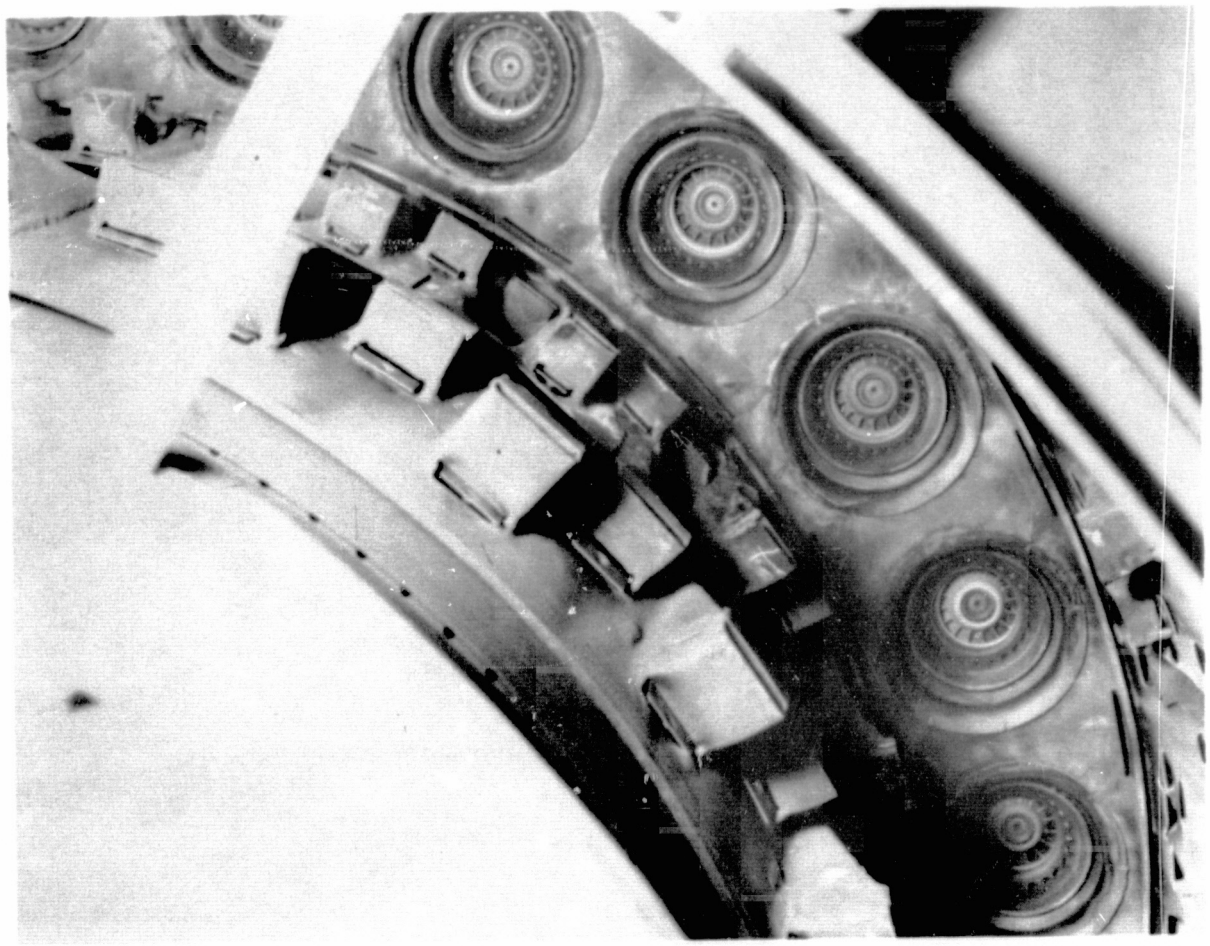

Figure 179. Combustor After 98 Hours of Condition 4 Testing (View 2)

FE 77327

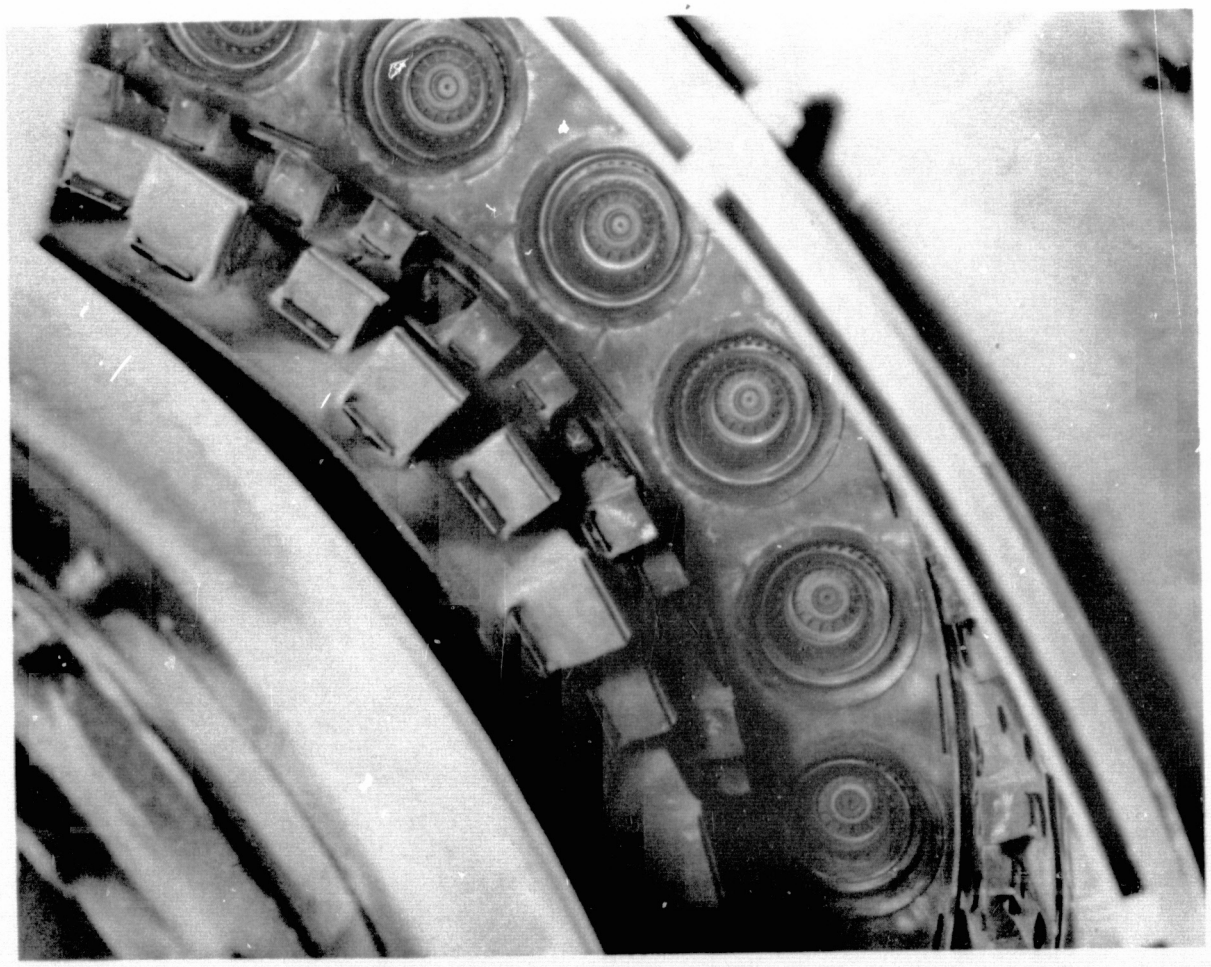

Figure 180. Combustor After 98 Hours of Condition 4 Testing (View 3)

FE 77328

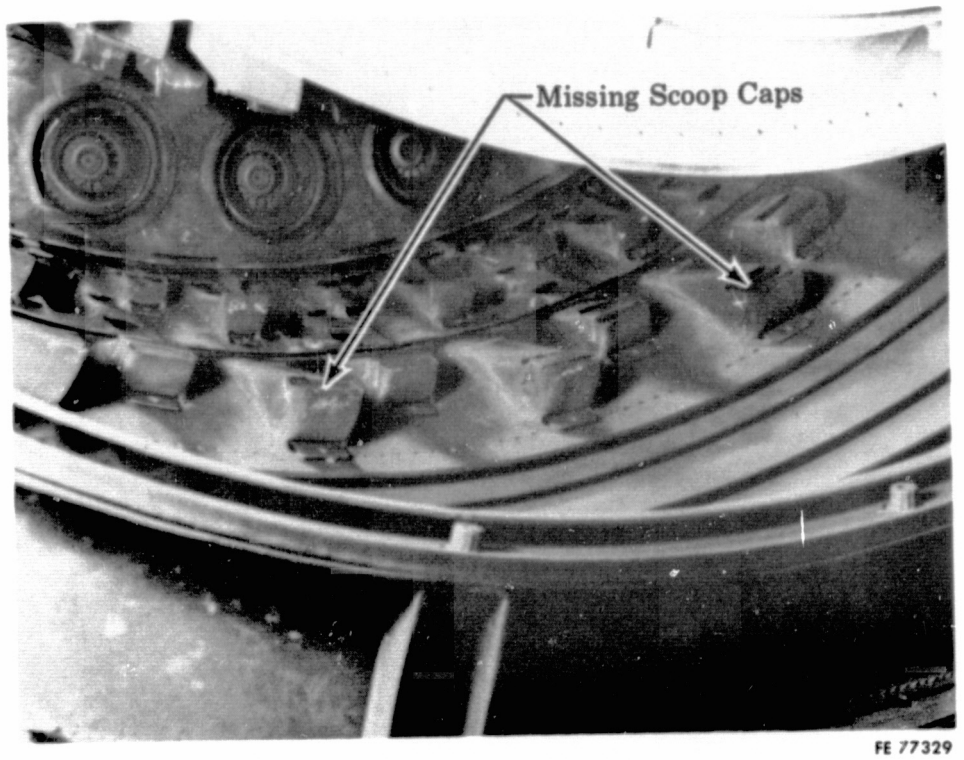

Figure 181. Missing Scoop Caps FD 24655

An inspection of the combustor upon completion of Test Condition 4 testing revealed additional cracks in the combustor, as well as an elongation of some of the previous cracks. The combustor crack surveys taken before, after 45 hours, after 98 hours, and upon completion of Test Condition 4 testing are shown in figures 182 through 185. Extensive burning of several No. 3 ID primary liner scoops, as shown in figures 186 through 194, was also noted. Visual inspection of the heat markings on the combustor liners indicated the No. 3 ID primary scoop burning to be caused by local aspiration of the hot combustion gases through cooling gaps and thermal cracks in the front of the liner. The OD liners and transition liners were in good condition upon completion of testing, as shown in figures 195 through 198. The combustion firewall showed signs of cracking from several of the ID cooling air slots, and on the cooling air deflectors, as shown in figure 199. Some burning of the cooling air deflectors was also noted.

The overall test rig appearance was very good, as shown in figures 200 through 204. The cooling water leakage problems of the rotating traverse drum and ID nozzle section were still apparent at the end of the test program. Modifications and repairs of a more permanent nature will be necessary on these two parts.

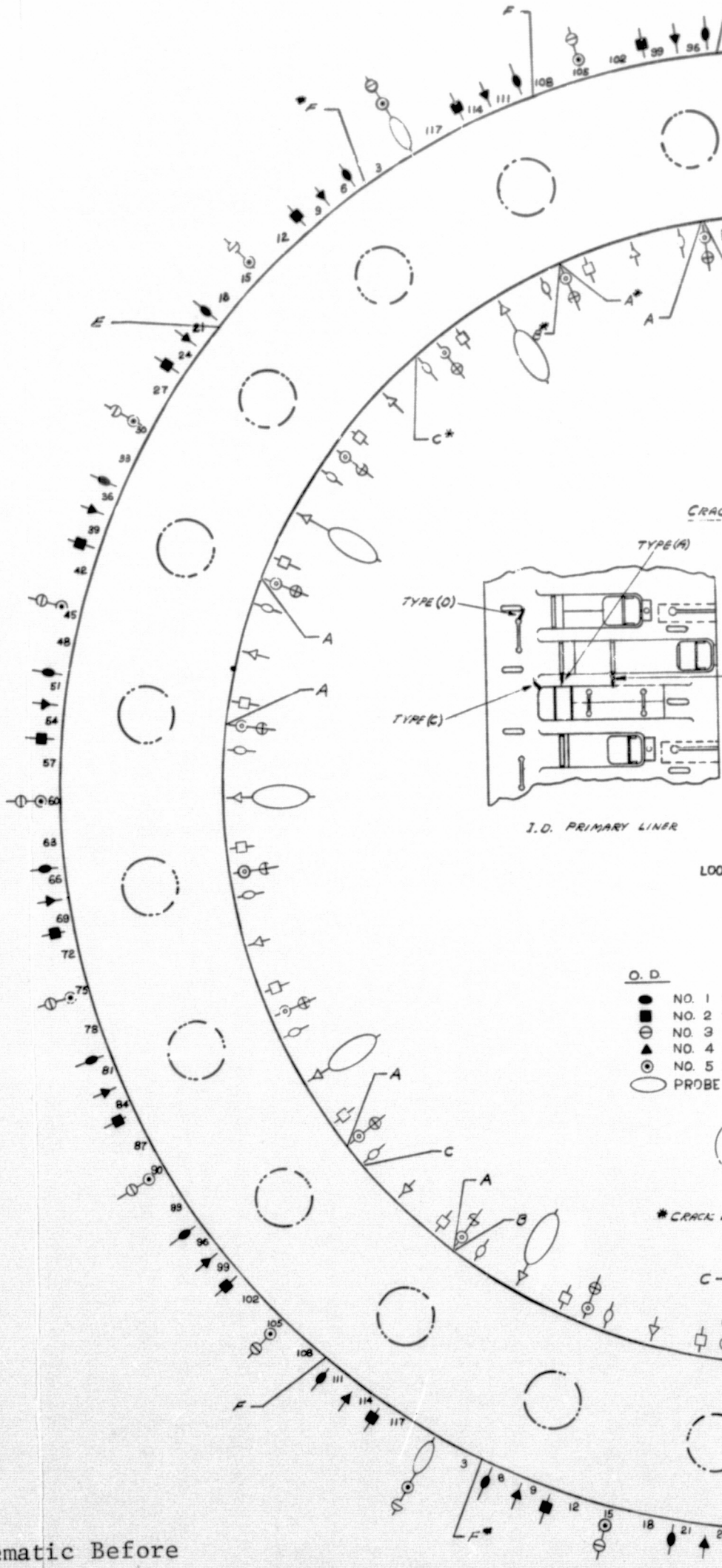

Figure 182. Combustor Crack Schematic Before Condition 4 Testing

FOLDOUT FRAME 1

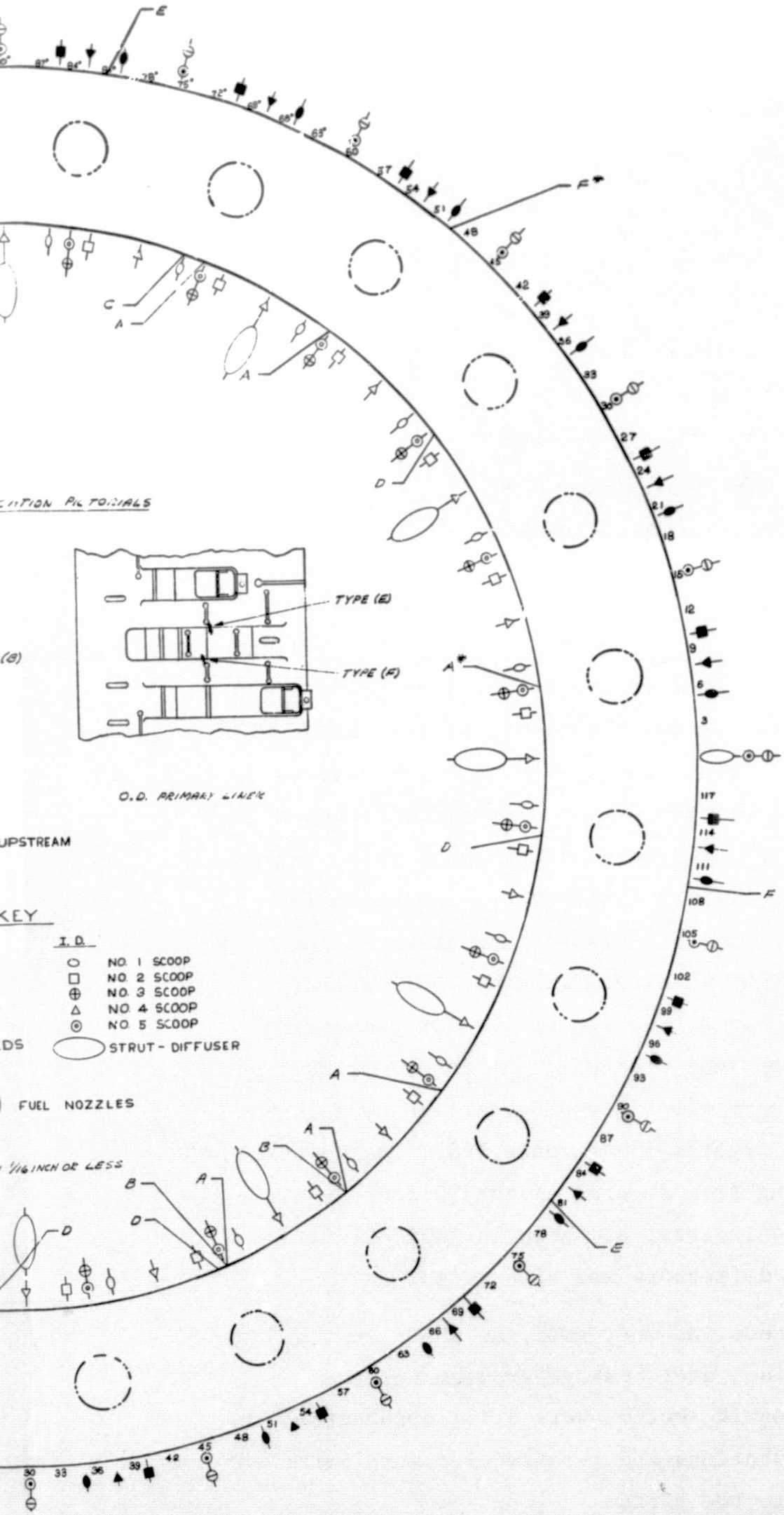

FD 23919

FOLDOUT FRAME 2

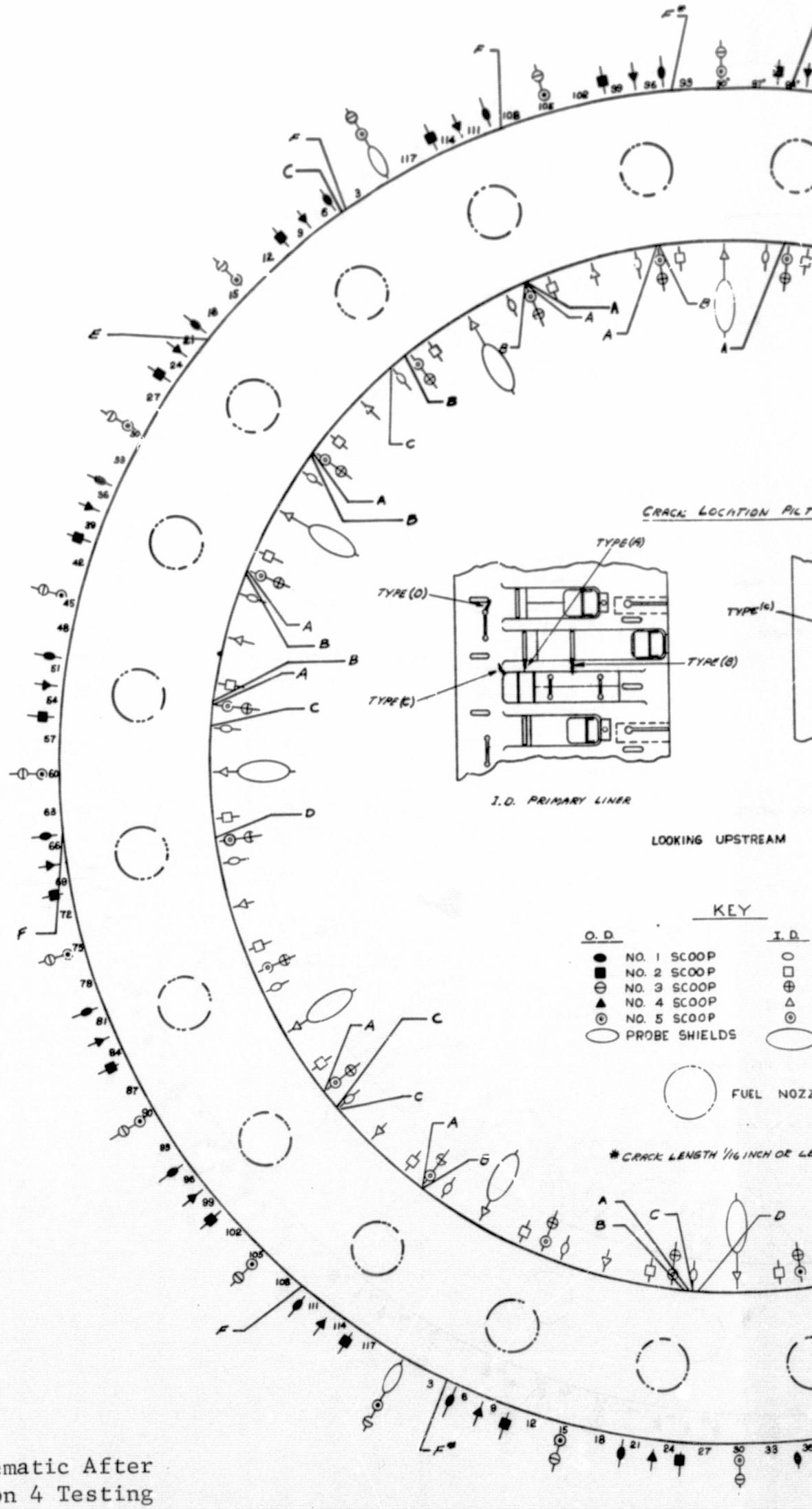

Figure 183. Combustor Crack Schematic After 45 Hours of Condition 4 Testing

FOLDOUT FRAME 1

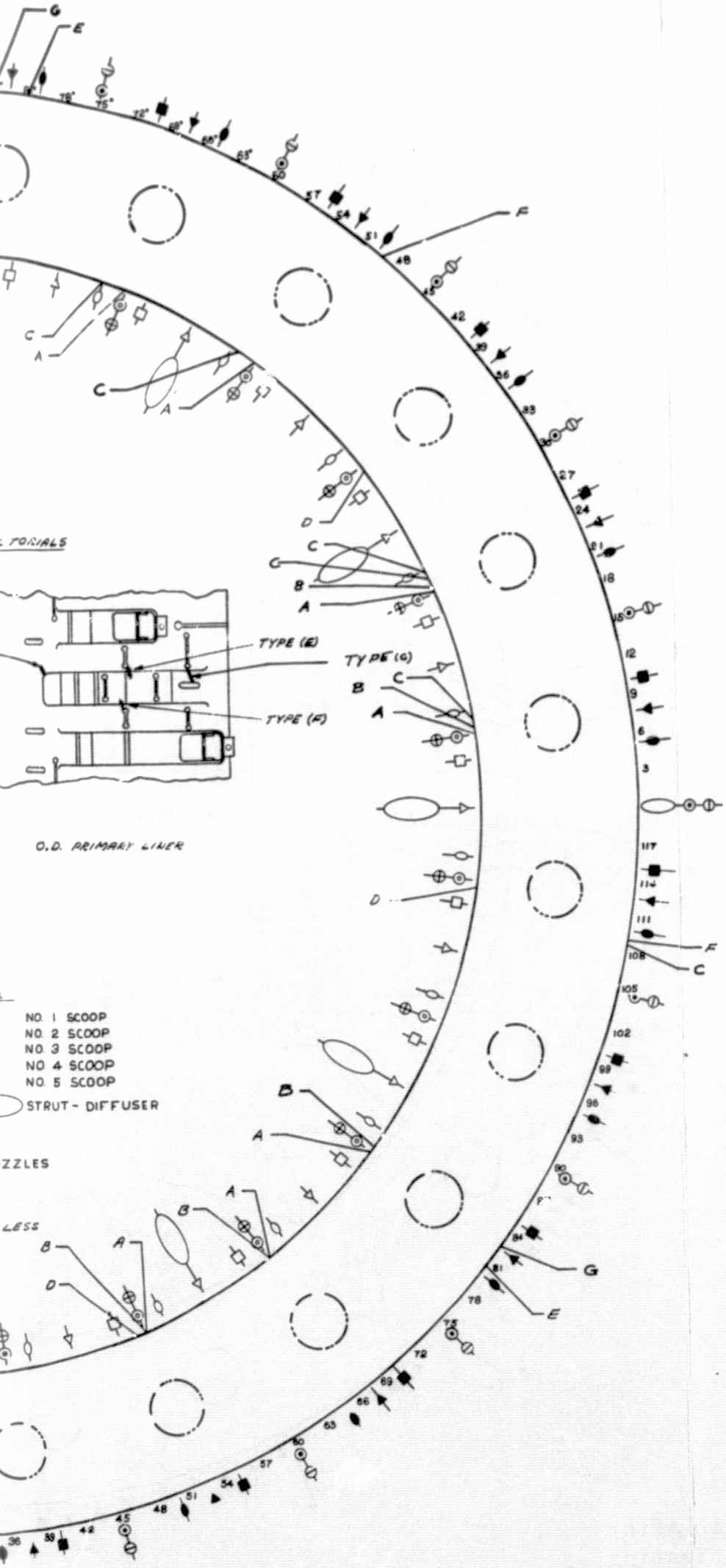

FD 23919A

FOLDOUT FRAME 2

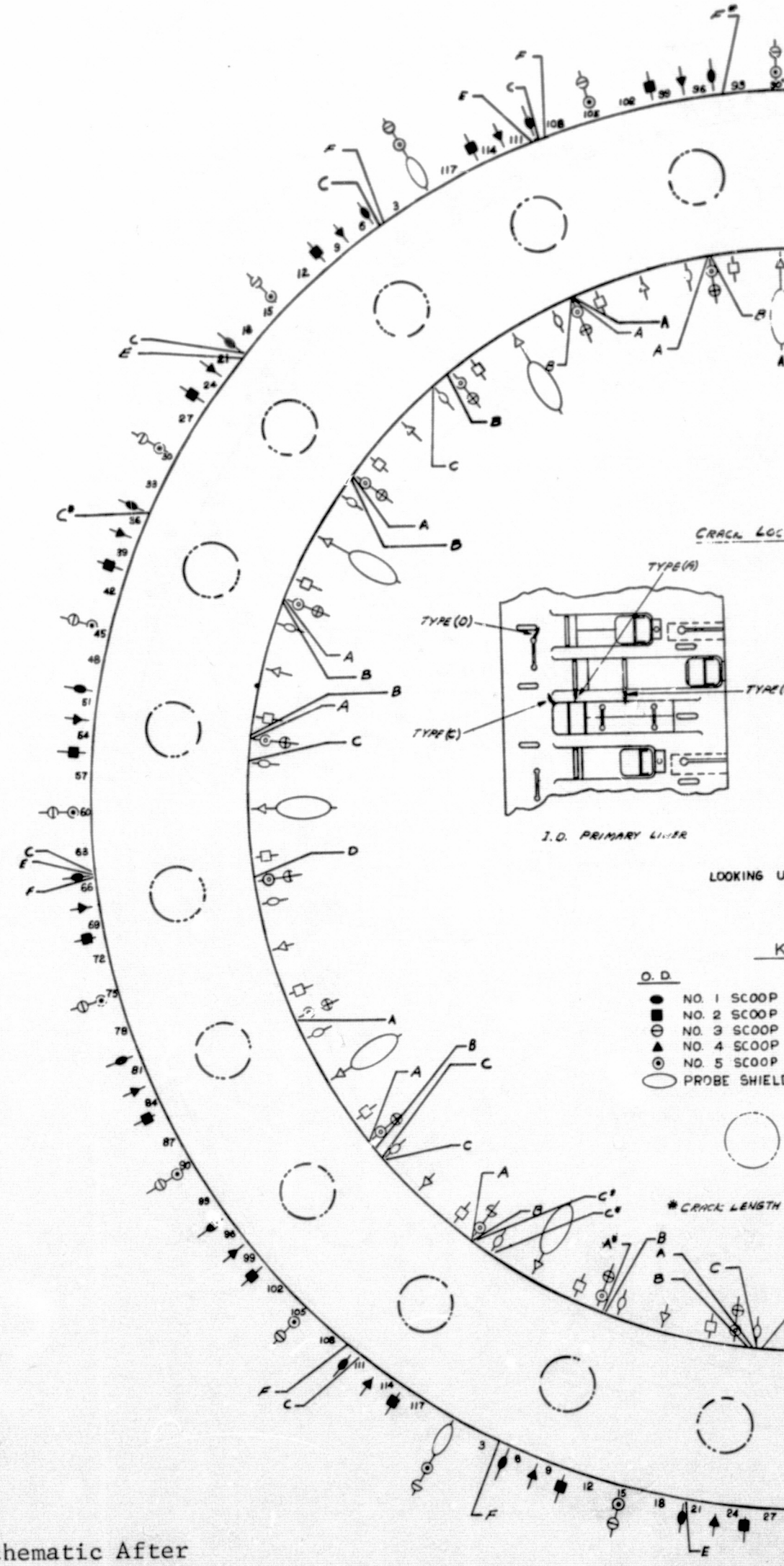

Figure 184. Combustor Crack Schematic After 98 Hours of Condition 4 Testing

FOLDOUT FRAME 1

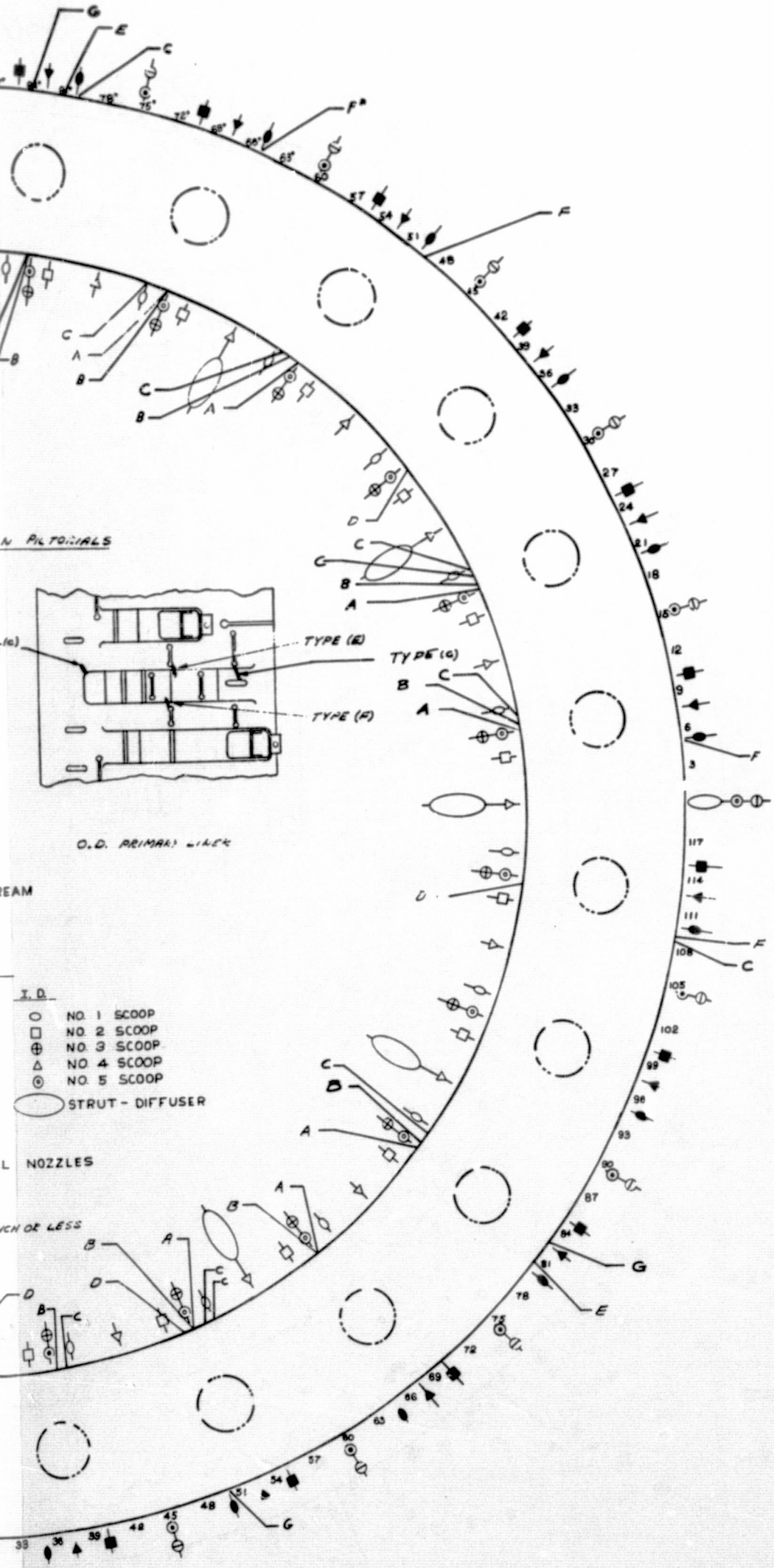

FD 23919B

FOLDOUT FRAME 2

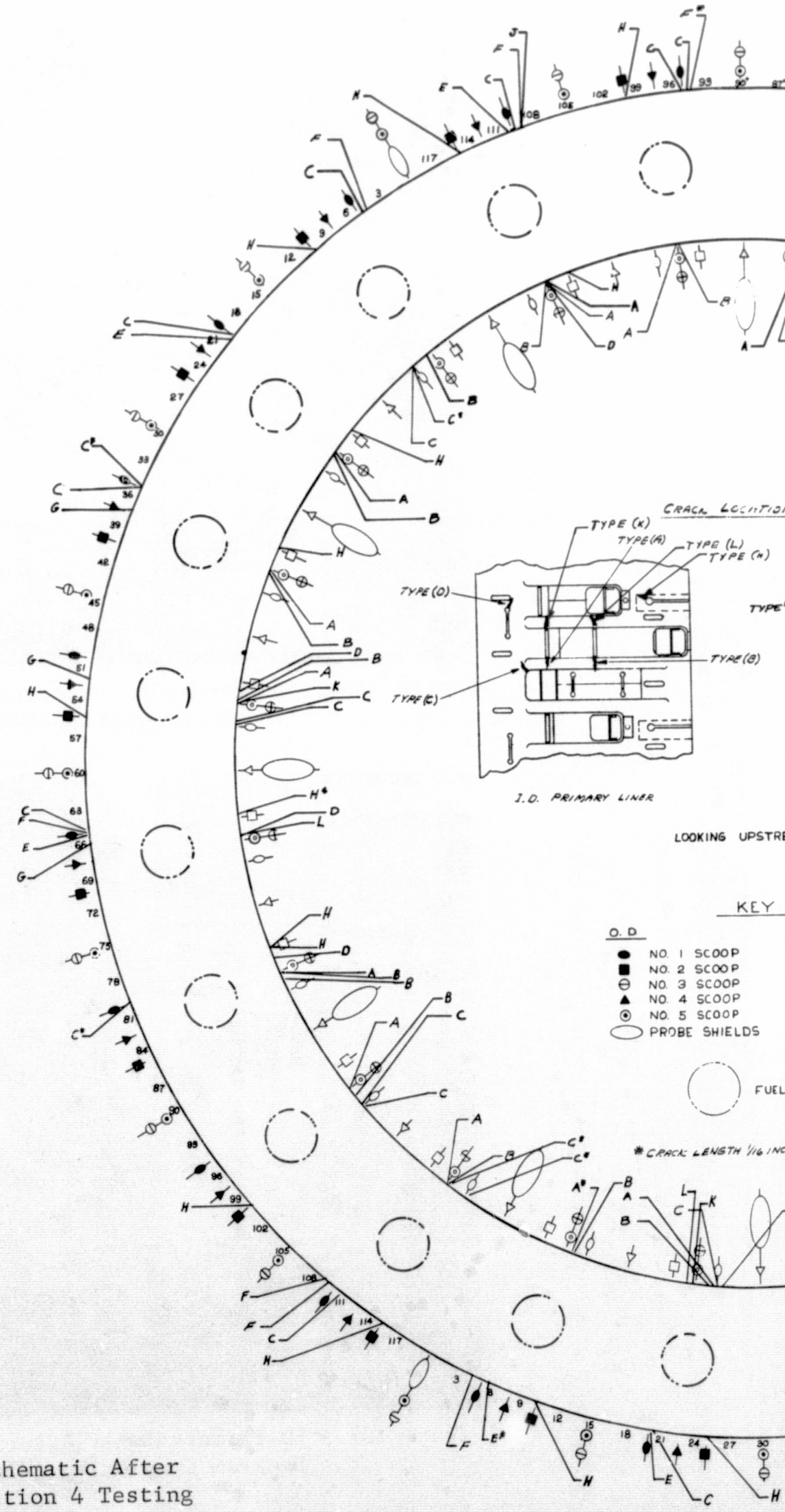

Figure 185. Combustor Crack Schematic After 150 Hours of Condition 4 Testing

FOLDOUT FRAME 1

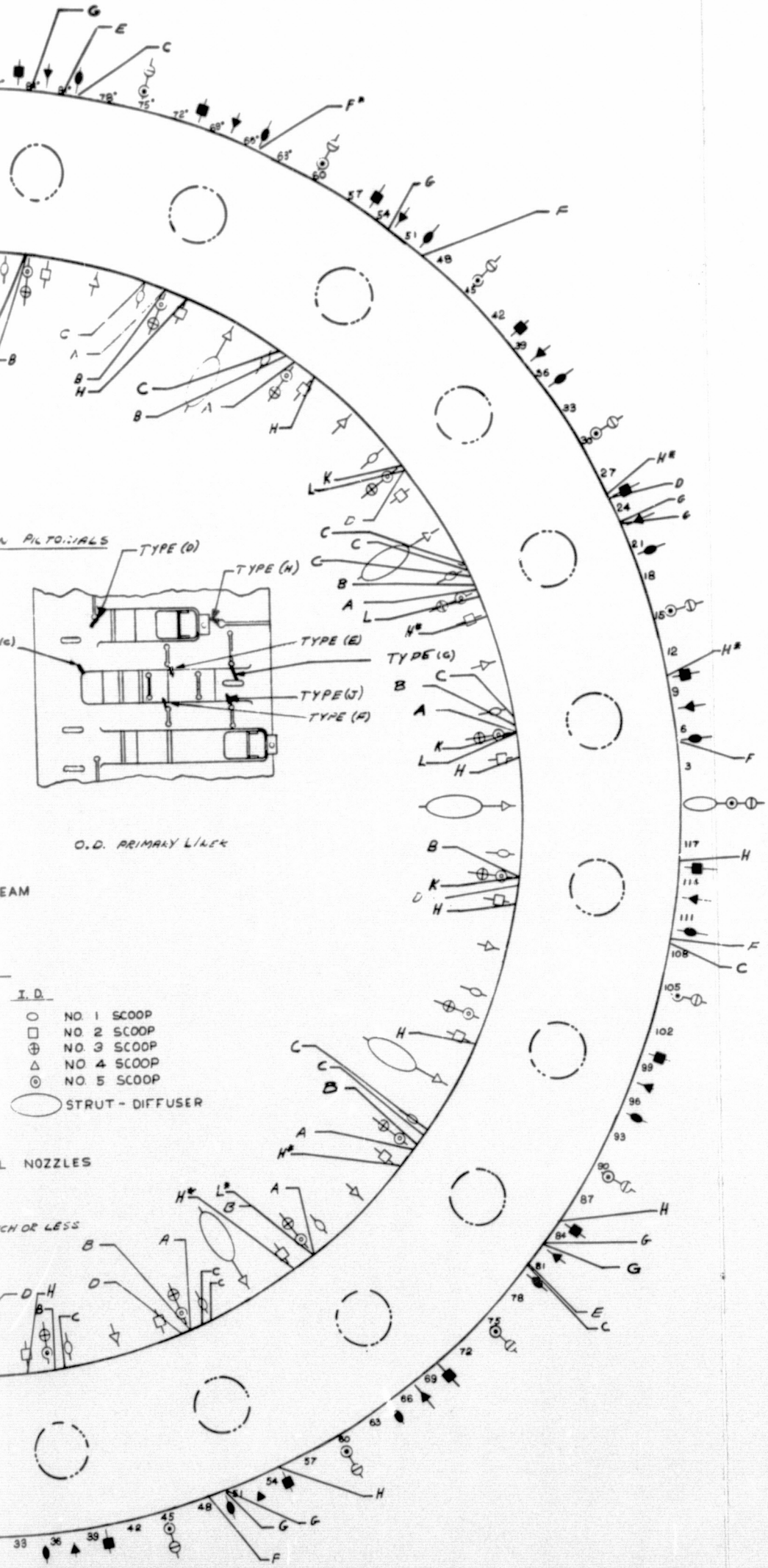

FD 23919C

FOLDOUT FRAME 2

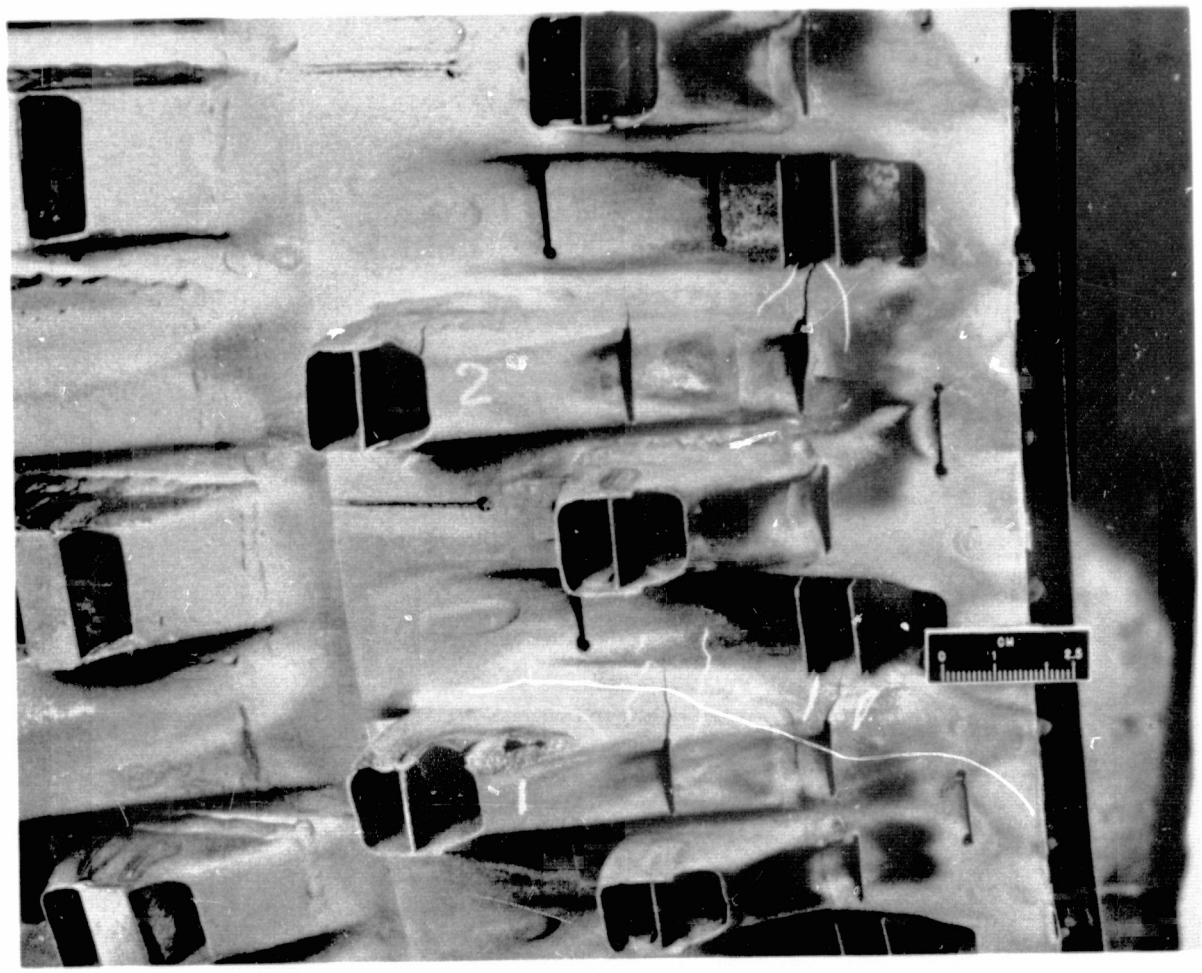

Figure 186. ID Primary Liner After Test Program Completion (View 1)

NASA C-68-1602

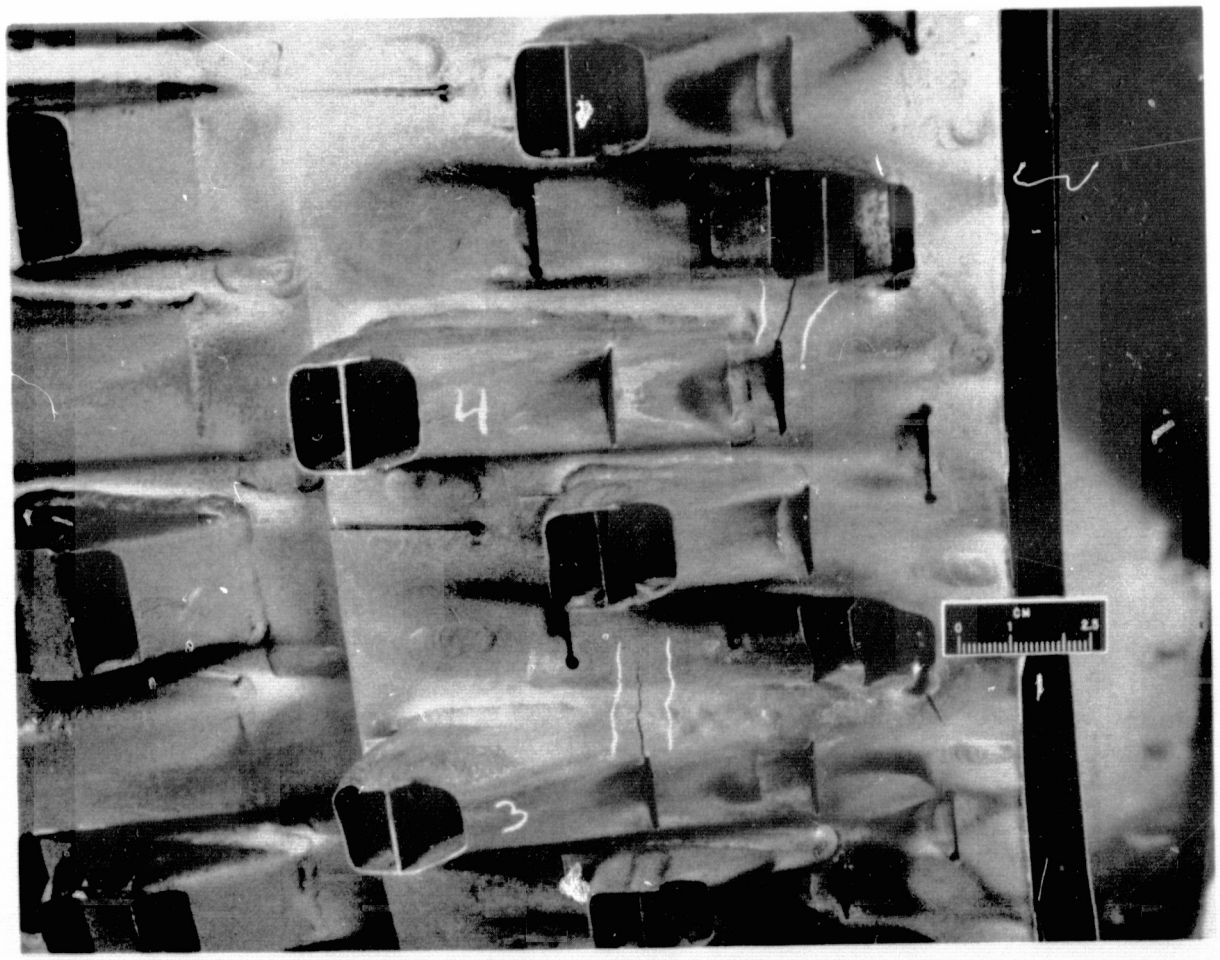

Figure 187. ID Primary Liner After Test Program Completion (View 2)

NASA C-68-1601

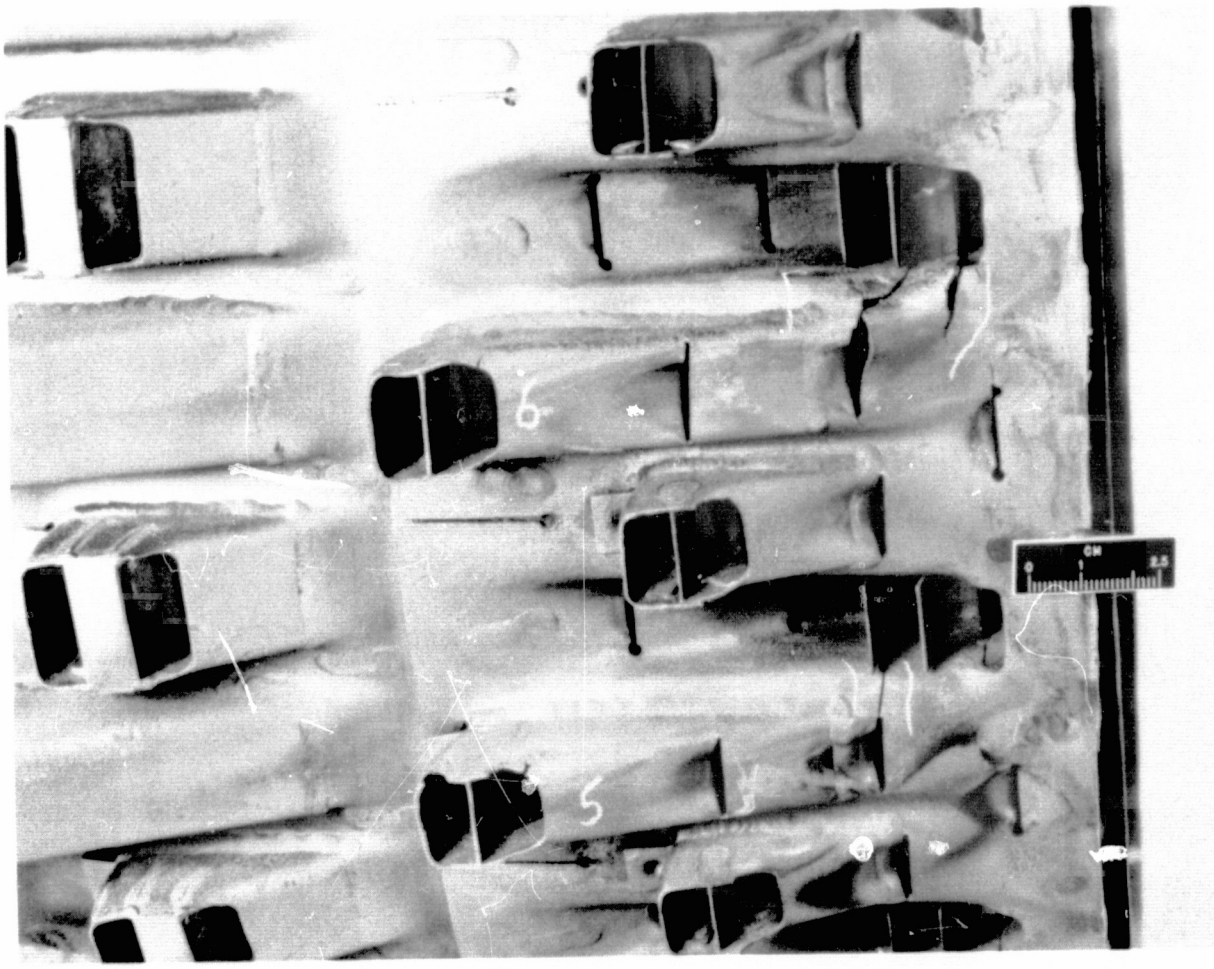

Figure 188. ID Primary Liner After Test Program Completion (View 3)

NASA C-68-1604

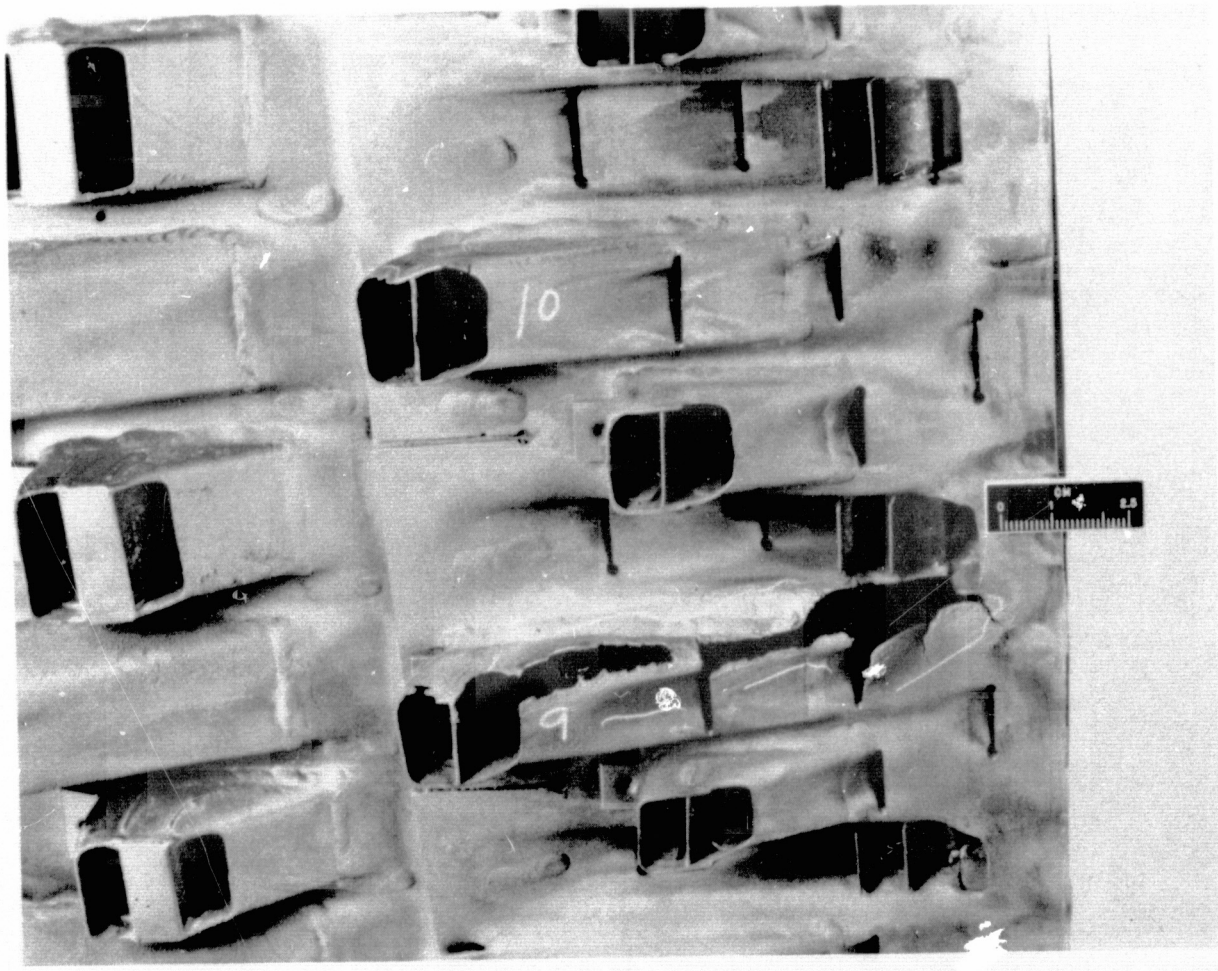

Figure 189. ID Primary Liner After Test Program Completion (View 4)

NASA C-68-1603

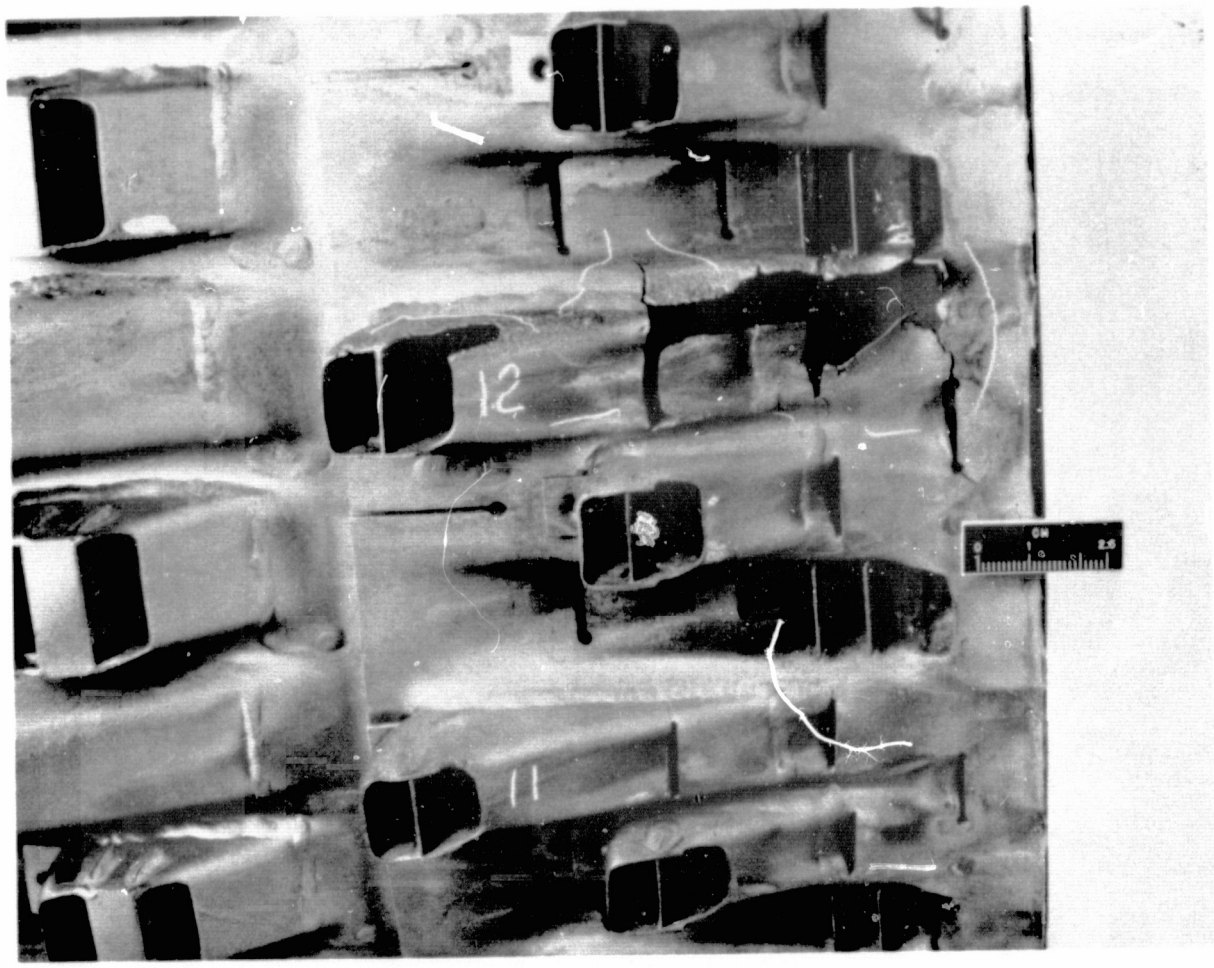

Figure 190. ID Primary Liner After Test Program Completion (View 5)

NASA C-68-1606

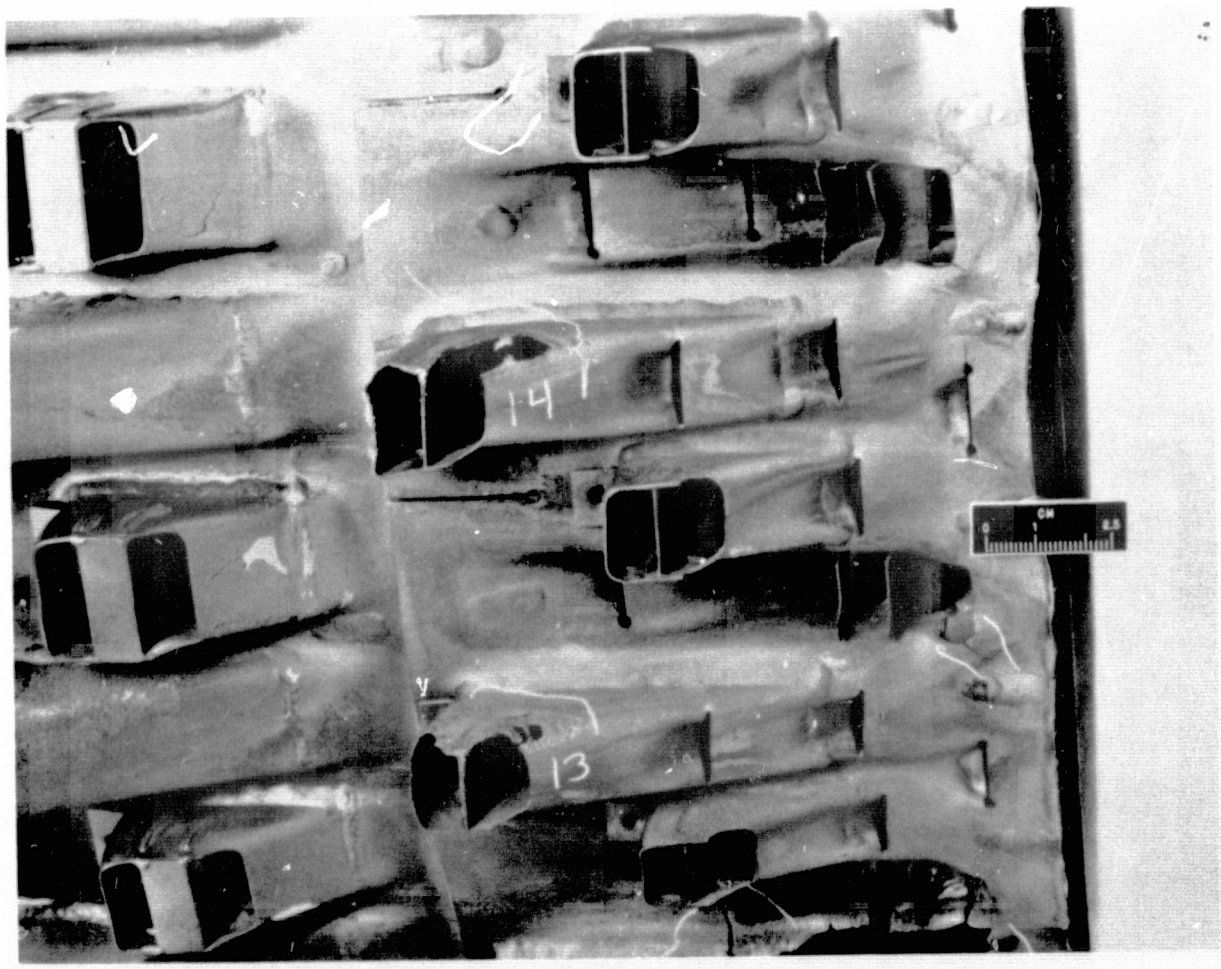

Figure 191. ID Primary Liner After Test Program Completion (View 6)

NASA C-68-1605

Figure 192. ID Primary Liner After Test Program Completion (View 7)

NASA C-68-1608

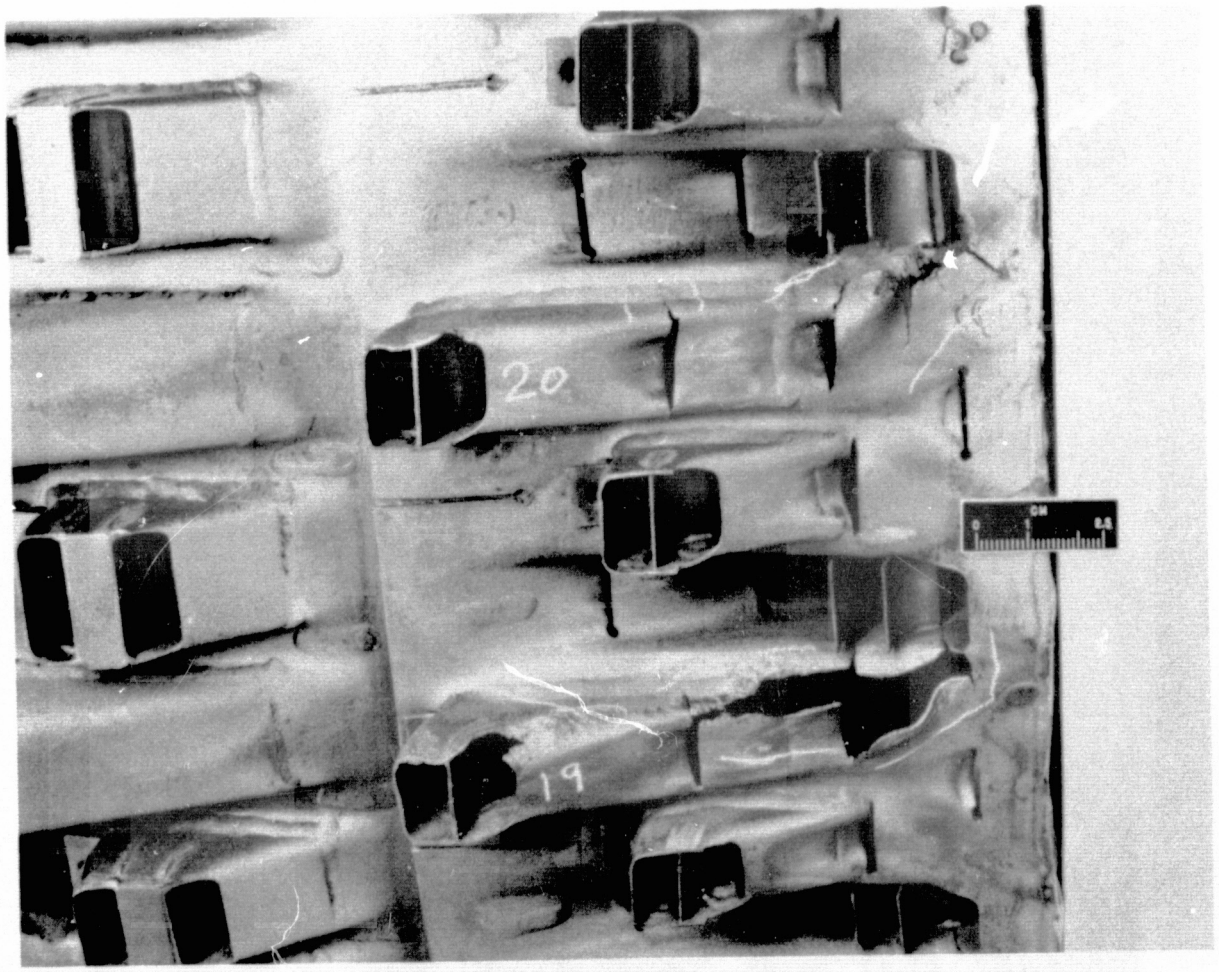

Figure 193. ID Primary Liner After Test Program Completion (View 8)

NASA C-68-1607

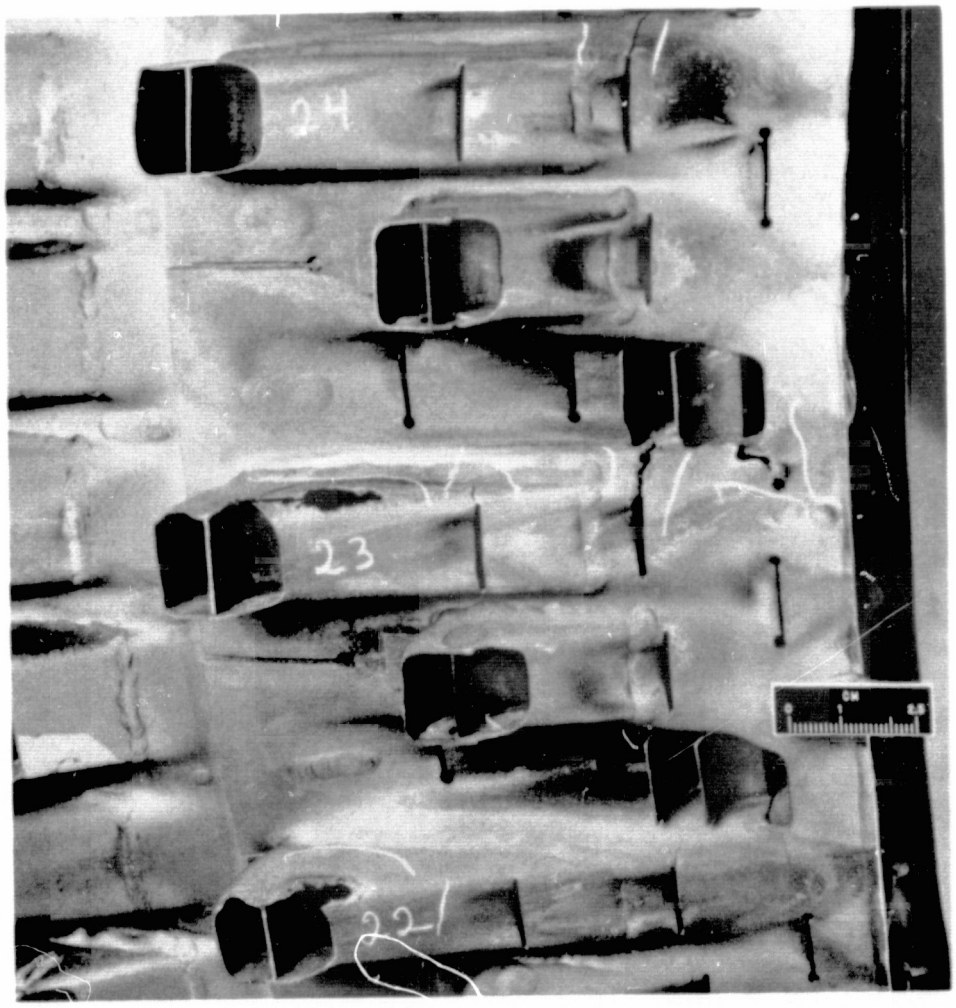

Figure 194. ID Primary Liner After Test Program Completion (View 9)

NASA C-68-1609

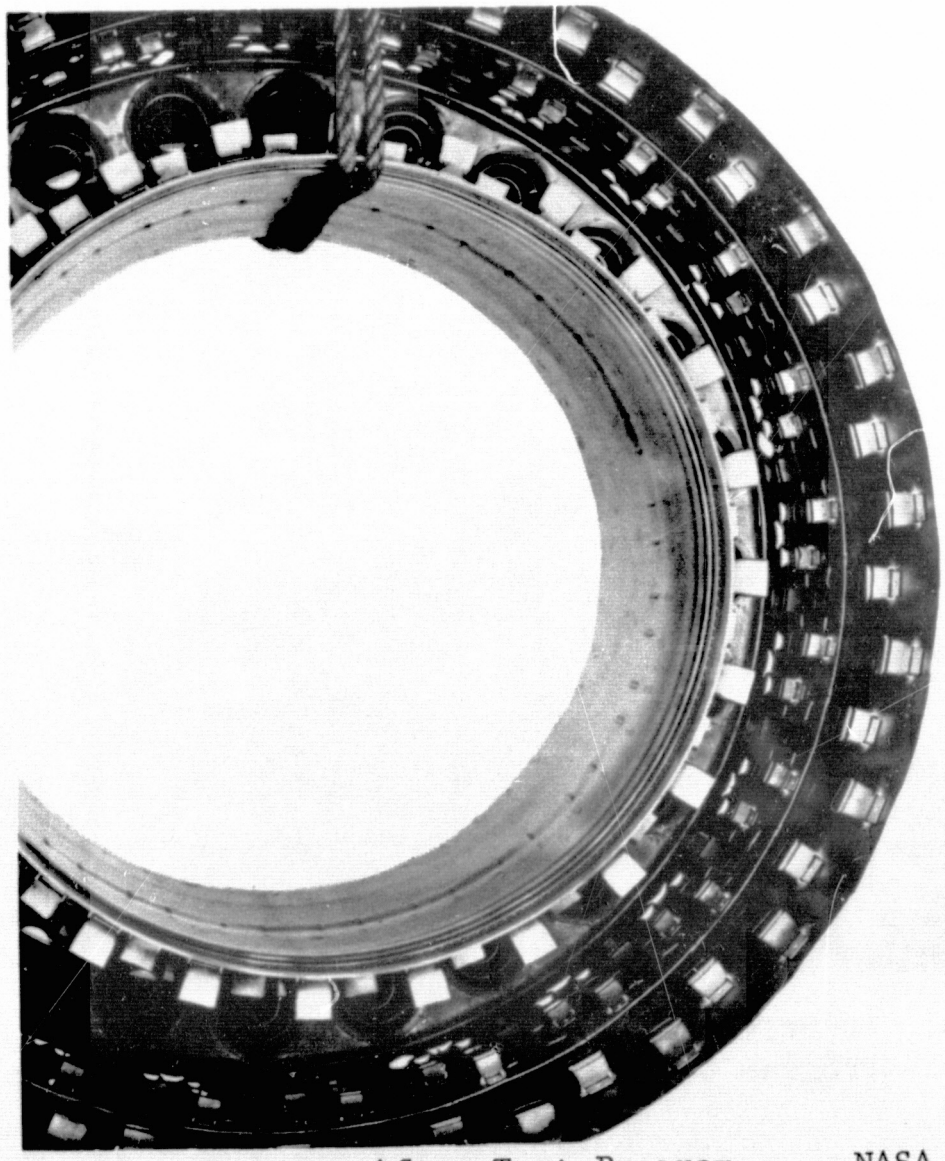

Figure 195. OD Liner After Test Program Completion (View 1)

NASA C-68-1544

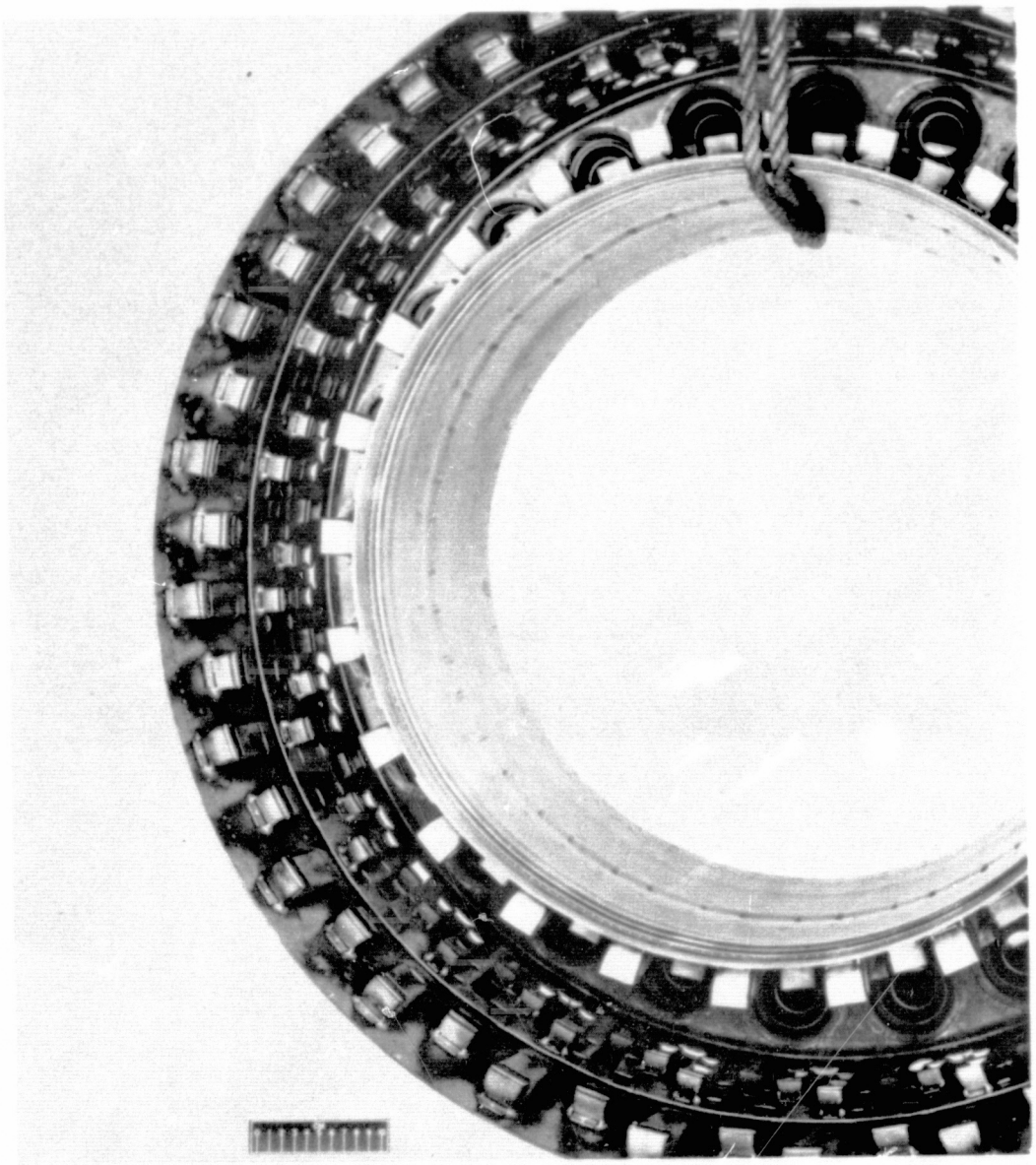

Figure 196. OD Liner After Test Program Completion (View 2) NASA C-68-1543

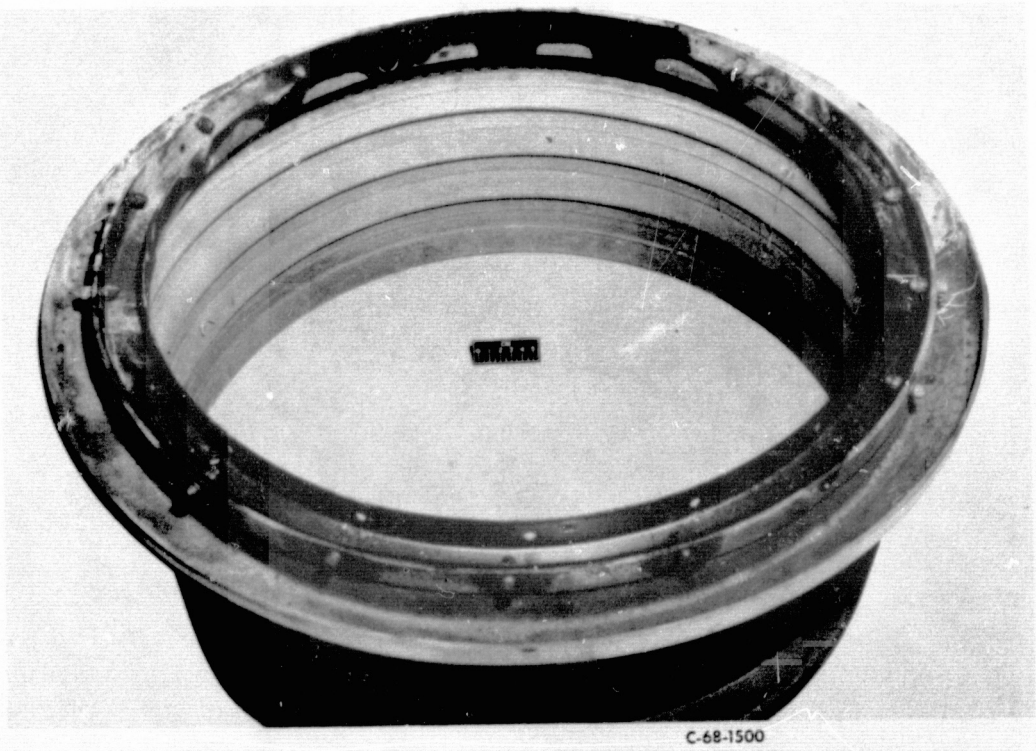

Figure 197. ID Transition Liner After Test Program Completion FD 25891

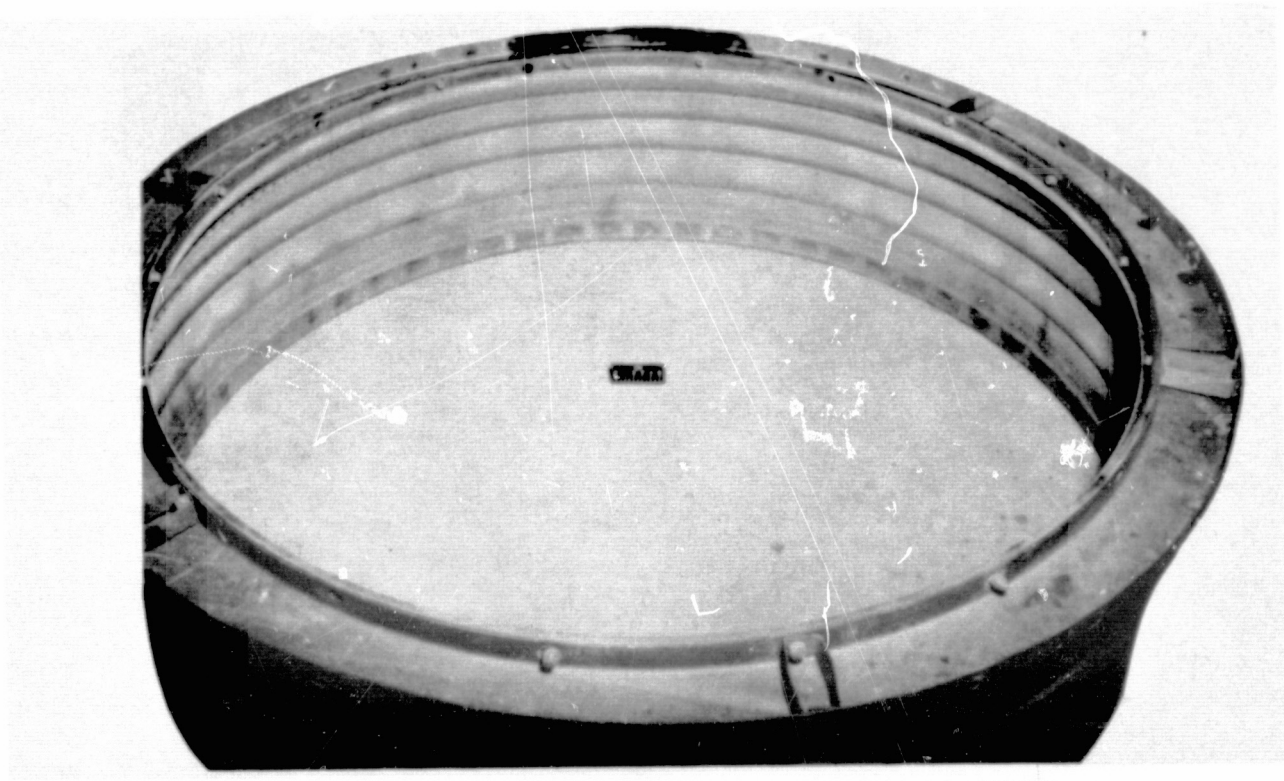

C-68-1503

Figure 198. OD Transition Liner After Test Program Completion FD 2589?

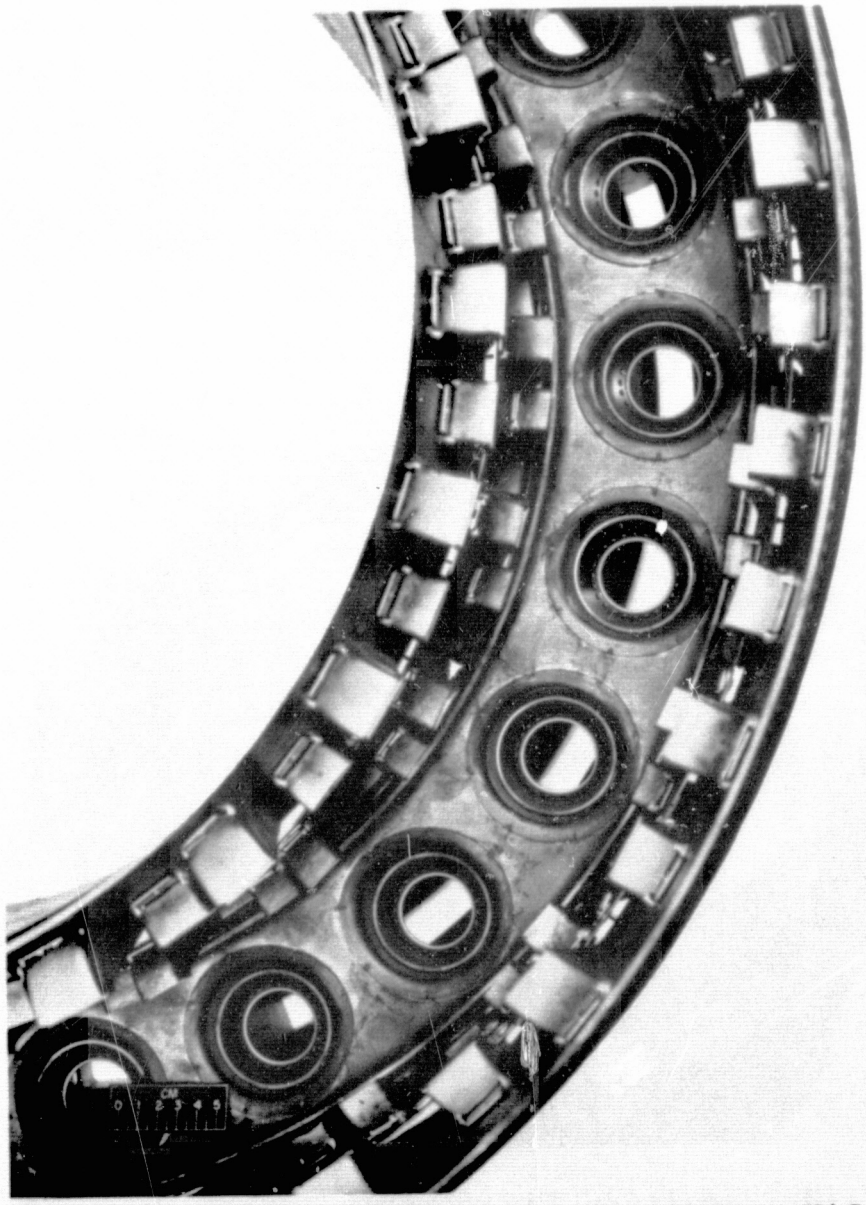

Figure 199. Firewall After Test Program Completion NASA C-68-1545

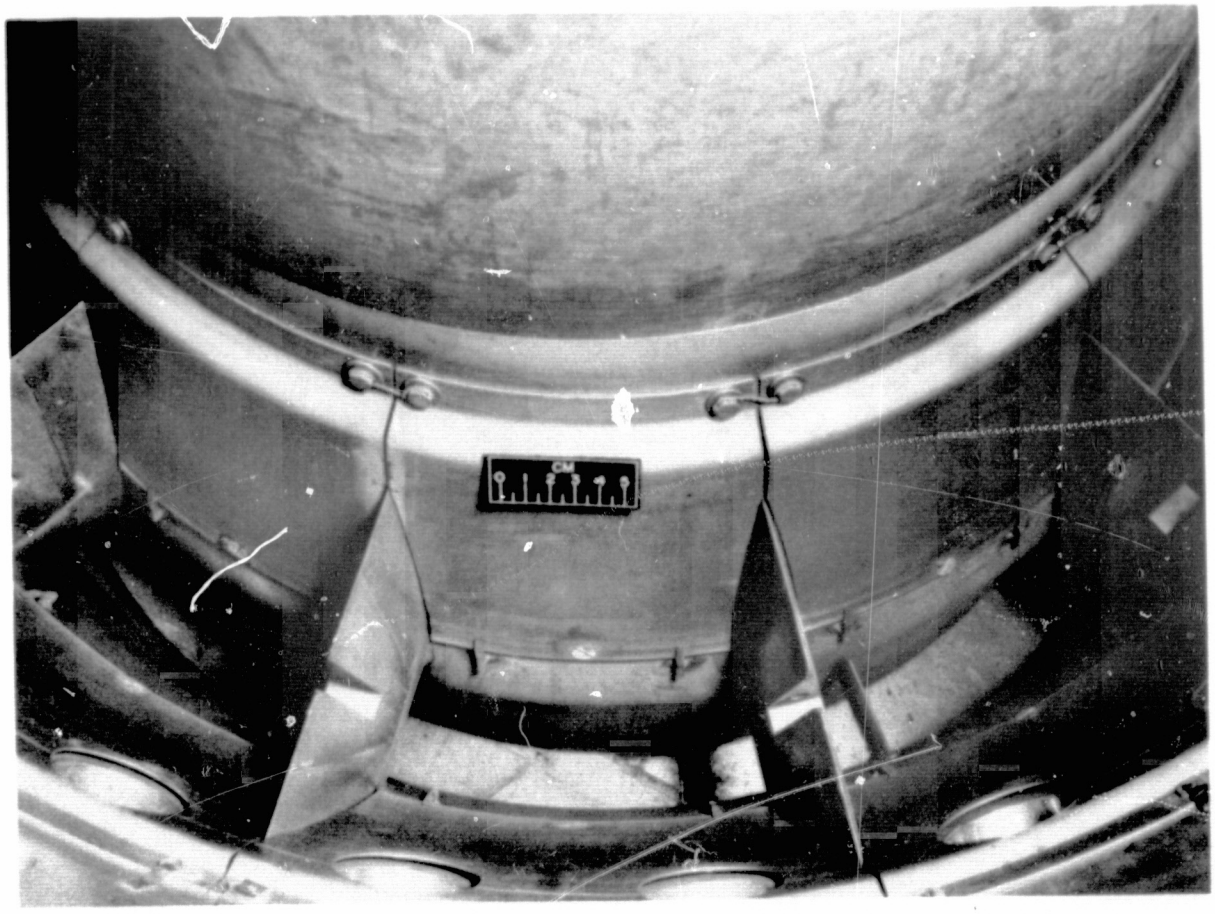

Figure 200. Diffuser After Test Program Completion

NASA C-68-1556

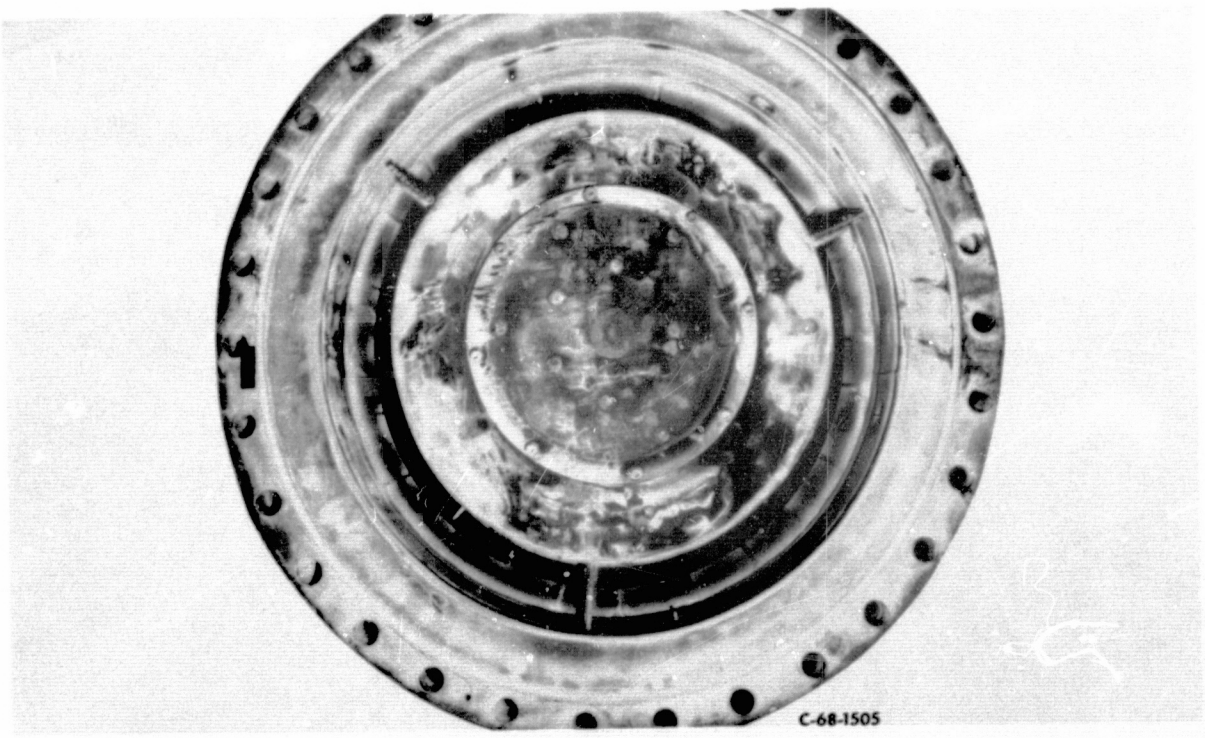

Figure 201. Water-Cooled Exit Assembly After Test Program Completion

FD 25896

V-113

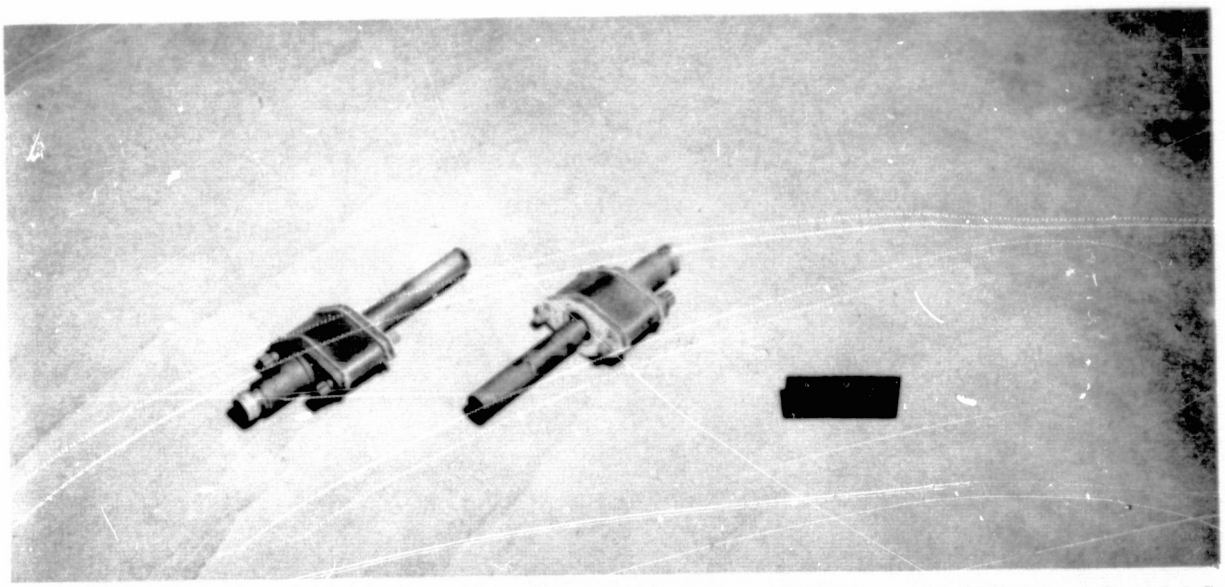

Figure 202. Igniter Plugs After Test Program Completion NASA C-68-1498

V-114

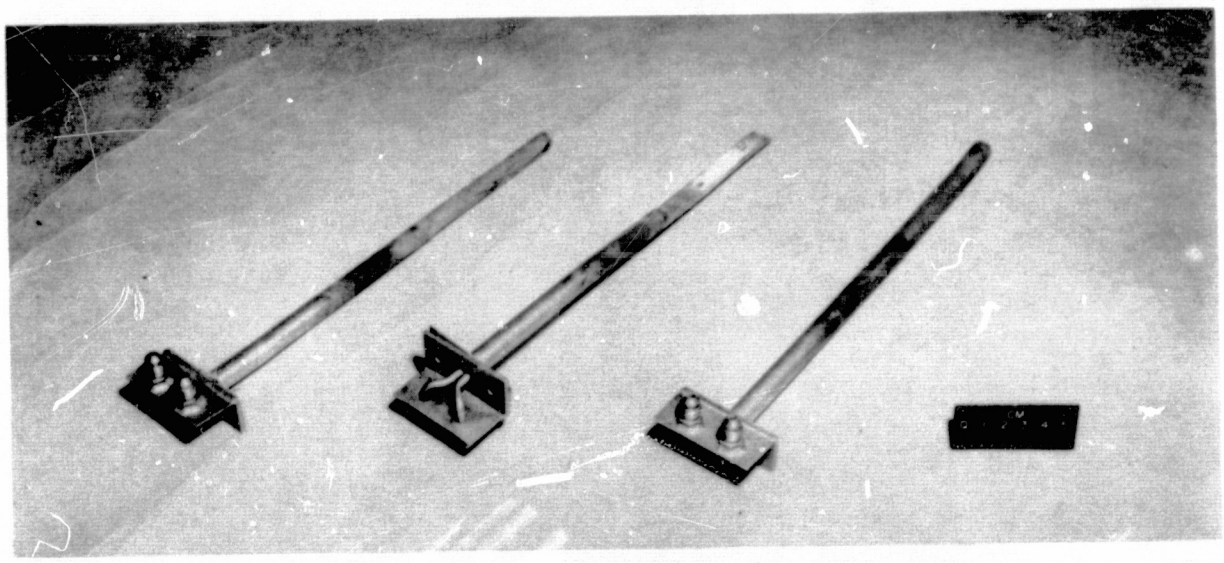

Figure 203. Exit Probe Shield After Test Program Completion NASA C-68-1497

V-115

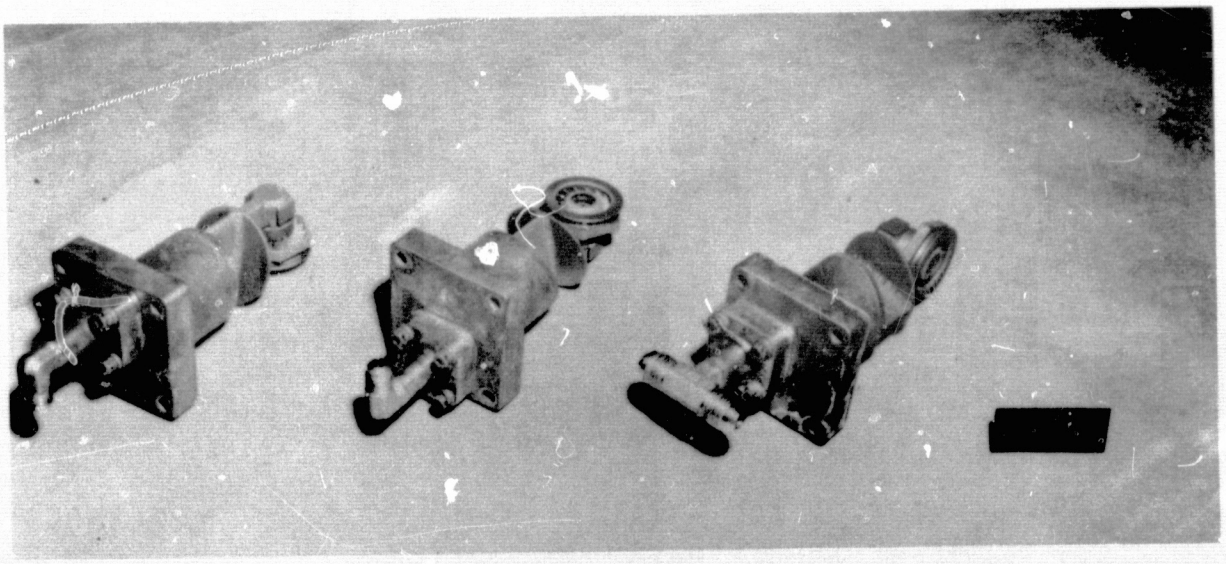

Figure 204. Fuel Struts and Swirlers After Test Program Completion NASA C-68-1499

SECTION VI
CONCLUSIONS AND RECOMMENDATIONS

A. CONCLUSIONS

1. The combustor successfully completed the 325-hour endurance program. Pressure loss, efficiency, and radial exit temperature profile consistently met, or exceeded, contract goals. The combustor exit temperature uniformity did not meet the required goals, but was well within state-of-the-art values.

2. The combustor demonstrated excellent ignition characteristics, consistently igniting at fuel/air ratios as low as 0.007.

3. The hourly thermal cycling of the combustor resulted in extensive cracking of the primary liners, particularly in the corners of the thumbnail scoop cooling louvers.

4. Severe burning of several of the No. 3 ID primary liner scoops was apparently caused by aspiration of the hot combustion gases through cooling gaps and cracks in the front of the liner.

5. No combustion instability occurred throughout the range of operating conditions. No blowouts occurred throughout the test program.

6. The redesign of the primary liner supports and the addition of cooling air deflectors to the combustor dome appear to have corrected the original problems of dome overheating and ID primary liner cooling gap closing.

7. All rig instrumentation, including the actuator mechanism and controls, performed satisfactorily throughout the testing program.

8. All rig parts, with the exception of the ID choke nozzle, rotating traverse drum, and the exit probe shields, were in very good condition upon completion of testing.

B. RECOMMENDATIONS

1. The ram-induction combustor should be considered for future engine designs in which large combustors are required to operate with relatively high reference velocity (150 ft/sec).

2. Additional development effort should be performed to replace the thumbnail scoop cooling louvers with alternate cooling methods. This is needed to eliminate the thermal cracking resulting from the corner stress concentrations inherent in the thumbnail scoop arrangement.

3. The ID primary liner cooling gap should be opened to provide more cooling airflow and reduced metal temperatures in this area.

4. Further development in the area of combustor exit temperature uniformity versus combustor pressure loss should be accomplished.

5. Filters should be installed in the jacket cooling water supply lines to eliminate further clogging problems.

6. The rotating traverse drum and exit nozzle ID section should be modified to prevent further cracking and subsequent water leakage.

APPENDIX
PERFORMANCE PROGRAM FORMULATION

This section presents the theoretical principles and assumptions used in formulating the final and preliminary computer performance programs. Included is a list of symbols, table 11, describing the parameters used in the programs.

The following assumptions were made:

1. The ideal gas equation of state, $P = \rho RT$, is valid over the entire operating range of pressures and temperatures encountered in this contract.
2. The flow is assumed to be isentropic and one-dimensional.
3. The fluid throughout the system is homogeneous and compressible.
4. Combustion is assumed to occur with dry air only and is completed within the combustor. Any water vapor present in the combustor inlet air mixes completely with the dry combustion products before leaving the combustor (see figure 205).

1. FINAL PERFORMANCE PROGRAM

The airflow properties of pressure and temperature are mass weighted to account for the effects of profile peaking on the averages. The general equation for the mass weighted average of any flow property, X, is obtained as follows:

$$X = \frac{\sum_{i=1}^{n} X_i \left(\frac{W_i}{g}\right)}{\sum_{i=1}^{n} \left(\frac{W_i}{g}\right)} = \frac{\sum_{i=1}^{n} X_i W_i}{\sum_{i=1}^{n} W_i}$$

where:

W_i = weight flow in lb/sec

From the equation of continuity and the assumption of one-dimensional flow:

$$\frac{W_i}{A_i} = \rho V$$

Table 11. Nomenclature

SYMBOL	DESCRIPTION	UNITS
AORMT	Arithmetic radial average exit temperature	^{o}F
CPOA	Specific heat of dry air at orifice	btu/lbm^{o}R
CPOW	Specific heat of water vapor at orifice	btu/lbm^{o}R
CP3A	Specific heat of dry air at diffuser inlet	btu/lbm^{o}R
CP3W	Specific heat of water vapor at diffuser inlet	btu/lbm^{o}R
CP5C	Specific heat of dry combustion products at burner exit plane	btu/lbm^{o}R
CPG	Specific heat of dry combustion products returned from Wynne subroutine (equal to CP5C)	btu/lbm^{o}R
CP5W	Specific heat of water vapor at burner exit plane	btu/lbm^{o}R
CPT5	Specific heat of wet combustion products at the burner exit plane	btu/lbm^{o}R
CIN	Speed of sound at diffuser inlet	ft/sec
CGRAV	Specific gravity of fuel	
DPORF	Differential pressure across airflow orifice	lbf/sqin
DTVR	Ratio of maximum temperature rise to the average temperature rise	
DTLOC (J)	Local arithmetic radial average temperature rise	^{o}F
DTCOR1	Temperature rise for a flat exit temperature profile of 2200^{o}F and the actual measured inlet profile	^{o}F
DTCOR2	Temperature rise for a flat exit temperature profile of 1900^{o}F and the actual measured inlet profile	^{o}F
DTAVE	Temperature rise based on arithmetic average of arithmetic radial average exit temperature and the actual measured diffuser inlet temperature	^{o}F
DP/P	Total pressure loss based on percent of inlet total pressure	%
DP/QIN	Total pressure loss based on percent of inlet dynamic pressure	%
DP/QREF	Total pressure loss based on percent of reference dynamic pressure	%
DPLOC (I,J)	Local dynamic pressure at diffuser inlet	lbf/sqin
DPAVG	Average dynamic pressure at diffuser inlet	lbf/sqin

Table 11. Nomenclature (Continued)

SYMBOL	DESCRIPTION	UNITS
DPR (I,J)	Ratio of local inlet dynamic pressure to average inlet dynamic pressure	
EORF	Orifice area multiplier	
EFFMB	Combustion efficiency of the main burner	%
FARAT	Fuel to air mass flowrate ratio	lbm/lbm
GAMOA	Specific heat ratio of dry air at orifice	
GAMOW	Specific heat ratio of water vapor at orifice	
GAMORF	Specific heat ratio of wet air at orifice	
GAM3A	Specific heat ratio of dry air at diffuser inlet	
GAM3W	Specific heat ratio of water vapor at diffuser inlet	
GAM3	Specific heat ratio of wet air at diffuser inlet	
GAM5C	Specific heat ratio of dry combustion products at burner exit	
GAMMAC	Specific heat ratio returned from Wynne sub-routine (equal to GAM5C)	
GAM5W	Specific heat ratio of water vapor at burner exit	
GAM5	Specific heat ratio of wet combustion products at burner exit	
HAIR	Enthalpy of inlet air	btu/lbm
HFUEL	Enthalpy of fuel entering burner	btu/lbm
IFUEL	Heat of formation of fuel entering burner	btu/lbm
KORF	Orifice discharge coefficient	
PS3A	Static pressure at diffuser inlet	psia
PS5A	Static pressure at burner exit	psia
PT3 (I,J)	Local total pressure at diffuser inlet	psia
PT5 (I,J)	Local total pressure at burner exit	psia
PORF	Orifice upstream total pressure	psia
PFUEL	Pressure of fuel entering burner	psia
PT3 (J)	Radially mass weighted average total pressure at diffuser inlet	psia
PT3 (I)	Circumferentially mass weighted average total pressure at diffuser inlet	psia

Table 11. Nomenclature (Continued)

SYMBOL	DESCRIPTION	UNITS
PT3M	Overall mass weighted average total pressure at diffuser inlet	psia
PCHAMB	Theoretical total pressure of combustion input into Wynne subroutine (equal to PS3A)	psia
PT5 (J)	Radially mass weighted average total pressure at burner exit	psia
PT5 (I)	Circumferentially mass weighted average total pressure at burner exit	psia
PT5M	Overall mass weighted average total pressure at burner exit	psia
R3	Gas constant of air at diffuser inlet	ft lbf/lbm ^{o}R
RC5	Gas constant of dry products of combustion at burner exit	ft lbf/lbm ^{o}R
RCHAMB	Gas constant of dry combustion products returned from Wynne subroutine (equal to RC5)	ft lbf/lbm ^{o}R
R5	Gas constant of wet combustion products at burner exit	ft lbf/lbm ^{o}R
TT3A	Total temperature at diffuser inlet	^{o}R
TT5 (I,J)	Local total temperature at burner exit plane	^{o}R
TORF	Total temperature at orifice	^{o}R
TFUEL	Temperature of fuel entering the burner	^{o}R
TS3AG	First guess for static temperature at diffuser inlet	^{o}R
TS3A	Static temperature at diffuser inlet	^{o}R
TT5C	Total temperature of dry combustion products at burner exit	^{o}R
TBRNK	Inlet air total temperature input into Wynne subroutine	^{o}R
TT5X	Theoretical temperature of wet products of combustion at burner exit	^{o}R
TT5M	Mass weighted average total temperature at burner exit	^{o}R
TMAX	Maximum local total temperature of burner exit	^{o}R
TAVE	Arithmetic average total temperature at burner exit	^{o}R
TR	Ratio of overall mass weighted average exit total temperature to diffuser inlet total temperature	

Table 11. Nomenclature (Continued)

SYMBOL	DESCRIPTION	UNITS
TCOR1 (J)	Arithmetic radial average temperature corrected to 2200°F profile	°F
TCOR2 (J)	Arithmetic radial average temperature corrected to 1900°F profile	°F
VREF	Burner reference velocity	ft/sec
WFMB	Fuel flowrate to burner	lbm/sec
WORF	Air mass flowrate measured at orifice	lbm/sec
WA3	Dry air mass flowrate at diffuser inlet	lbm/sec
WW	Water vapor mass flowrate into burner	lbm/sec
WT5	Total mass flowrate at burner exit	lbm/sec
WC5	Mass flowrate of dry combustion products at burner exit	lbm/sec
W3	Total mass flowrate at diffuser inlet	lbm/sec
X	Specific humidity of inlet air	
XM3AT	Diffuser inlet Mach number based on inlet total pressure	
XM3AS	Diffuser inlet Mach number based on inlet static pressure	
XM3	Diffuser inlet Mach number	
XM5	Mach number at burner exit	
XMREF	Reference Mach number	
YORF	Expansion factor, determined from orifice upstream conditions	
Z	Water vapor per pound of dry combustion products	
ZORFA	Compressibility factor of dry air	
ZORFW	Compressibility factor of water vapor	

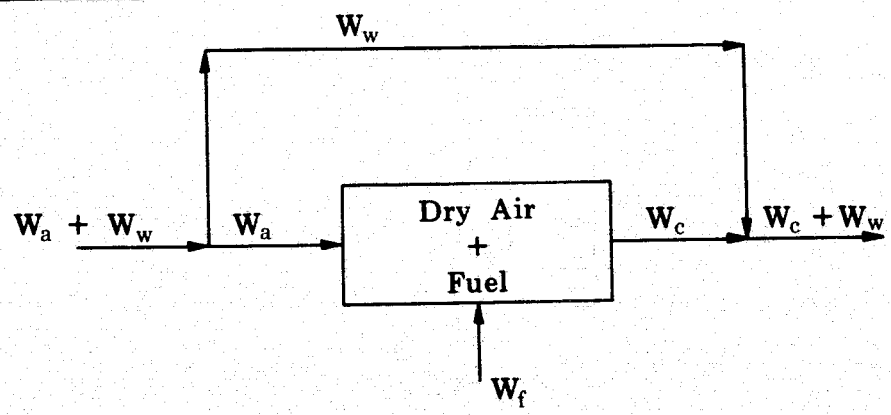

Figure 205. Combustion Model - Main Burner FD 24747A

Since,

$$P_{si} = \rho R T_s \quad \text{(Assumption 1)}$$

$$\frac{W_i}{A_1} = \frac{P_{si}\, V}{R T_{si}}$$

Rearranging the above equation:

$$\frac{W}{A} = \frac{P_{si}\, V}{\sqrt{\gamma R T_{si}}} \sqrt{\frac{\gamma}{R}} \sqrt{\frac{T_{ti}}{T_{si}}} \quad \frac{1}{\sqrt{T_{ti}}}$$

where:

γ = GAM = specific heat ratio

By Assumption 2:

$$\left(\frac{T_{ti}}{T_{si}}\right)^{1/2} = \left[1 + \left(\frac{\gamma - 1}{2}\right) M^2\right]^{1/2}$$

Therefore:

$$\frac{W_i}{A_i} = \sqrt{\frac{\gamma}{R}} \quad \frac{P_{si}}{\sqrt{T_{ti}}} M \sqrt{1 + \frac{\gamma - 1}{2} M^2}$$

By Assumption 2:

$$M^2 = \left[\left(\frac{P_{ti}}{P_{si}}\right)^{\frac{\gamma-1}{\gamma}} - 1\right]\left[\frac{2}{\gamma - 1}\right]$$

or:

$$M = \left\{\left[\left(\frac{P_{ti}}{P_{si}}\right)^{\frac{\gamma-1}{\gamma}} - 1\right]\left[\frac{2}{\gamma - 1}\right]\right\}^{1/2}$$

$$W_i = A_i \sqrt{\frac{2\gamma}{R\,(\gamma - 1)\,T_{ti}}}\, P_{si} \left[\left(\frac{P_{ti}}{P_{si}}\right)^{\frac{2\,(\gamma-1)}{\gamma}} - \left(\frac{P_{ti}}{P_{si}}\right)^{\frac{\gamma-1}{\gamma}}\right]^{1/2}$$

Therefore:

$$X = \frac{\sum_{i=1}^{n} x_i \sqrt{\frac{2\gamma}{R(\gamma-1)}} \frac{A_i P_{si}}{\sqrt{T_{Ti}}} \left[\left(\frac{P_{ti}}{P_{si}} \right)^{\frac{2(\gamma-1)}{\gamma}} - \left(\frac{P_{ti}}{P_{si}} \right)^{\frac{\gamma-1}{\gamma}} \right]^{1/2}}{\sum_{i=1}^{n} \sqrt{\frac{2\gamma}{R(\gamma-1)}} \frac{A_i P_{si}}{\sqrt{T_{Ti}}} \left[\left(\frac{P_{ti}}{P_{si}} \right)^{\frac{2(\gamma-1)}{\gamma}} - \left(\frac{P_{ti}}{P_{si}} \right)^{\frac{\gamma-1}{\gamma}} \right]^{1/2}}$$

If the flow area is divided into equal increments, A_i, and if it is assumed that P_s is constant over the cross section then:

$$X = \frac{\sum_{I=1}^{n} \sum_{J=1}^{k} X_{I,J} \left[\frac{1}{T_{T_{I,J}}} \left\{ \left(\frac{P_{T_{I,J}}}{P_s} \right)^{\frac{2(\gamma-1)}{\gamma}} - \left(\frac{P_{T_{I,J}}}{P_s} \right)^{\frac{\gamma-1}{\gamma}} \right\} \right]^{1/2}}{\sum_{i=1}^{n} \sum_{j=1}^{k} \left[\frac{1}{T_{T_{I,J}}} \left\{ \left(\frac{P_{T_{I,J}}}{P_s} \right)^{\frac{2(\gamma-1)}{\gamma}} - \left(\frac{P_{T_{I,J}}}{P_s} \right)^{\frac{\gamma-1}{\gamma}} \right\} \right]^{1/2}}$$

The double summation over all values of "I" and "J" are made since in tnis program circumferential locations are denoted by "I" and radial locations are denoted by "J."

a. Airflow

The airflow is calculated by the ASME orifice equation as:

$$WORF = 2012.9494\,(KORF)\,(EORF)\,(YORF)\sqrt{\frac{(1 + X)\,(PORF1)\,(DPORF)}{(53.342)\,(TORF)\,(ZORFA) + (85.775)\,(ZORFW)(X)}}$$

Using a 17.875-inch diameter sharp edged orifice, the orifice diameter-to-pipe inner diameter ratio, B, is 0.5069.

b. Diffuser Inlet Airflow Properties

The inlet air specific heat ratio is calculated as:

$$GAM\ 3 = \frac{(GAM\ 3A)\ (GAM\ 3W)\left[CP3A + X\ (CP3W)\right]}{(GAM\ 3W)\ (CP3A) + X\ (GAM\ 3A)\ (CP3W)}$$

At the diffuser inlet there are eight total pressure rakes equally spaced around the circumference with five pressure probes radially located on each rake. Therefore, in mass weighting the inlet total pressure,

"I" varies from 1 to 8 and "J" varies from 1 to 5. Since the inlet total temperature is isothermal, the average mass weighted diffuser inlet total pressure is:

$$PT3M = \frac{\sum_{I=1}^{8} \sum_{J=1}^{5} PT3(I,J) \left[\left(\frac{PT3(I,J)}{PS3A} \right)^{\frac{2(GAM\ 3 - 1)}{GAM\ 3}} - \left(\frac{PT3(I,J)}{PS3A} \right)^{\frac{GAM\ 3 - 1}{GAM\ 3}} \right]^{1/2}}{\sum_{I=1}^{8} \sum_{J=1}^{5} \left[\left(\frac{PT3(I,J)}{PS3A} \right)^{\frac{2(GAM\ 3 - 1)}{GAM\ 3}} - \left(\frac{PT3(I,J)}{PS3A} \right)^{\frac{GAM\ 3 - 1}{GAM\ 3}} \right]^{1/2}}$$

The mass weighted, diffuser inlet, radial total pressure profile is calculated by averaging the corresponding probes ("J" position) on the eight rakes ("I" position), or:

$$PT3(J) = \frac{\sum_{I=1}^{8} PT\ 3(I,J) \left[\left(\frac{PT3(I,J)}{PS3A} \right)^{\frac{2(GAM\ 3 - 1)}{GAM\ 3}} - \left(\frac{PT3(I,J)}{PS3A} \right)^{\frac{GAM\ 3 - 1}{GAM\ 3}} \right]^{1/2}}{\sum_{I=1}^{8} \left[\left(\frac{PT3(I,J)}{PS3A} \right)^{\frac{2(GAM\ 3 - 1)}{GAM\ 3}} - \left(\frac{PT3(I,J)}{PS3A} \right)^{\frac{GAM\ 3 - 1}{GAM\ 3}} \right]^{1/2}}$$

The diffuser inlet Mach number is obtained by:

$$XM3AT = \frac{WORF}{(182.54)(PT3M)} \sqrt{\frac{(53.35)(TT3A)}{(GAM3)(32.174)}} \left[1 + \left(\frac{GAM3-1}{2} \right) (XM3AT)^2 \right]^{\frac{GAM3+1}{2(GAM3-1)}}$$

The inlet total temperature is the arithmetic average of eight inlet total temperature probes spaced equally around the circumference and located just upstream of the diffuser inlet.

c. Combustor Exit Airflow Properties

The temperature and pressure of the combustion products at the combustor exit are measured by a traversing rake (figures 11 and 12) as described in the section on test rig hardware. Since this rake sweeps the full 360° of the exit annulus, except for the three "home" positions, in 3° increments, there are 117 circumferential locations where data are taken. Therefore, at the combustor exit "I" varies from 1 to 117. Also, the sampling probes on the traversing rake are equipped to take data at 5 radial locations. Therefore, at the combustor exit "J" varies from 1 to 5.

The mass weighted total pressure at the combustor exit is then given by:

$$PT5M = \frac{\sum_{I=1}^{117} \sum_{J=1}^{5} PT5\ (I,J) \left[\frac{1}{TT5\ (I,J)} \left(\frac{PT5\ (I,J)}{PS5A} \right)^{\frac{2\ (GAM\ 5\ -\ 1)}{GAM\ 5}} - \left(\frac{PT5(I,J)}{PS5A} \right)^{\frac{GAM\ 5\ -\ 1}{GAM\ 5}} \right]^{1/2}}{\sum_{I=1}^{117} \sum_{J=1}^{5} \left[\frac{1}{TT5\ (I,J)} \left(\frac{PT5\ (I,J)}{PS5A} \right)^{\frac{2\ (GAM\ 5\ -\ 1)}{GAM\ 5}} - \left(\frac{PT5.(I,J)}{PS5A} \right)^{\frac{GAM\ 5\ -\ 1}{GAM\ 5}} \right]^{1/2}}$$

The mass weighted total temperature at the combustor exit is:

$$TT5M = \frac{\sum_{I=1}^{117} \sum_{J=1}^{5} \left\{ TT5\ (I,J) \left[\left(\frac{PT5(I,J)}{PS5A} \right)^{\frac{2\ (GAM\ 5\ -\ 1)}{GAM\ 5}} - \left(\frac{PT5\ (I,J)}{PS5A} \right)^{\frac{GAM\ 5\ -\ 1}{GAM\ 5}} \right] \right\}^{1/2}}{\sum_{I=1}^{117} \sum_{J=1}^{5} \left\{ \frac{1}{TT5\ (I,J)} \left[\left(\frac{PT5(I,J)}{PS5A} \right)^{\frac{2\ (GAM\ 5\ -\ 1)}{GAM\ 5}} - \left(\frac{PT5\ (I,J)}{PS5A} \right)^{\frac{GAM\ 5\ -\ 1}{GAM\ 5}} \right] \right\}^{1/2}}$$

The combustor exit temperature profile is the arithmetic average of each "J" location over the entire circumference, or

$$TT5\ (J) = \frac{\sum_{I=1}^{117} TT5\ (I,J)}{117}$$

This exit radial temperature profile is then corrected to average exit temperatures of 1900°F and 2200°F for comparison to desired profiles at these average exit temperatures.

d. Theoretical Combustion Temperature

Using the airflow properties at the diffuser inlet (the measured fuel flow) and assuming 100 percent combustion, the theoretical exit temperature is calculated by a combustion program which is included as a subroutine in the performance program.

e. Combustor Performance Calculation

The combustor performance is described by the following parameters:

1. ΔTVR is defined as the maximum temperature rise at any location to the average temperature rise, or:

$$\Delta TVR = \frac{TMAX\ -\ TT3A}{TT5M\ -\ TT3A}$$

2. Combustor pressure loss $\Delta P/P$ is defined as the loss in total pressure between the diffuser inlet and the combustor exit

expressed as a percentage of the diffuser inlet total pressure, therefore:

$$\frac{\Delta P}{P} = \frac{PT5M - PT3M}{PT3M} \times (100)$$

3. Combustor efficiency is defined as the ratio of the actual temperature rise as measured by the traversing rake to the theoretical temperature rise. Expressed as a percentage, the combustor efficiency is

$$EFFMB = \frac{TT5M - TT3A}{TT5X - TT3A} \times (100)$$

2. PRELIMINARY PERFORMANCE PROGRAM

In order to make a rapid evaluation of test data and to correct any errors in the data, a preliminary performance program was formulated. The formulation is a simplification of the final performance program previously described.

The primary simplification is the elimination of the calculation for theoretical combustion temperature since that subroutine is very large and complicated. Consequently, the preliminary program does not calculate combustor efficiency.

Other simplifications include:

1. The substitution of arithmetic averages in place of mass weighted averages for the combustor inlet and exit total temperature and total pressure.
2. The elimination of iterative subroutines on the combustor inlet and exit static temperatures and the combustor inlet and exit Mach numbers which are necessary when mass weighting the airflow properties of total temperature and total pressure.
3. The elimination of profile calculations for the combustor inlet total pressure and the combustor exit total temperature and total pressure.

a. Airflow

The orifice airflow equation is the same as that used in the final performance program. The only difference in the calculation is the itera-

tive subroutine on the orifice discharge coefficient, KORF, is replaced with an estimated value of KORF equal to 0.6235. This has proven to be a valid estimation since the airflow values, as calculated by the final performance program and the preliminary performance program, have not differed by more than 1.0%.

b. Performance Calculations

The combustor performance parameters of pressure loss and ΔTVR are calculated by the same equations as used in the final performance program except that arithmetic average values of pressure and temperature are used in place of mass weighted average values.